NOWGONG GIRLS' COLLEGE

Re-Accreditated at A Grade (2nd Cycle) by the
National Assessment and Accreditation Council

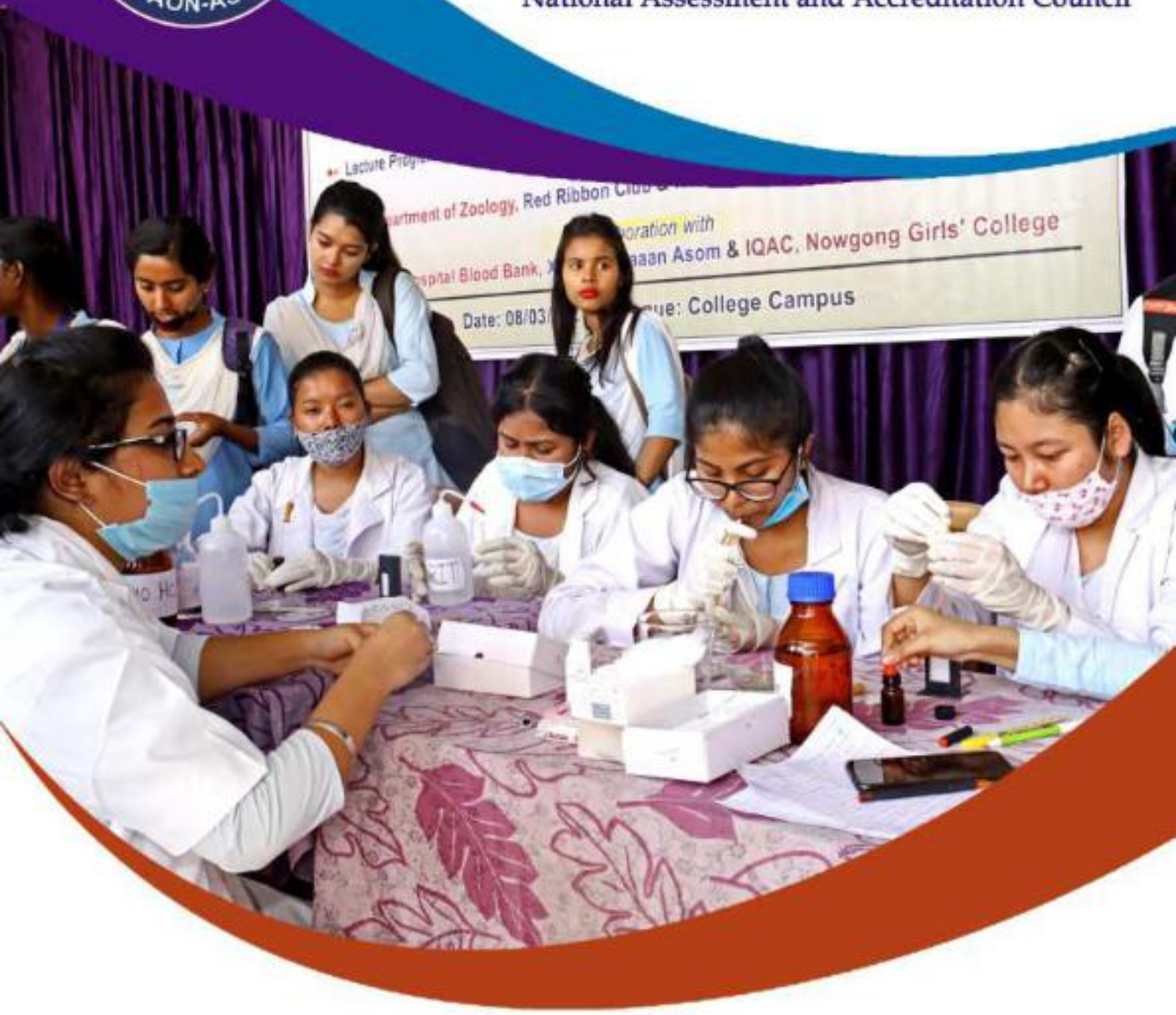

CRITERIA 3: RESEARCH, INNOVATIONS AND EXTENSION

3.3.1: Number of research papers published per teacher in the Journals notified on UGC care list during the last five years

Submitted to
The NAAC for 3rd Cycle of Assessment and Accreditation

Office of the Principal
Nowgong Girls' College
(RE-ACCREDITED AT GRADE 'A' BY NAAC)
Nagaon - 782002 : Assam

✆: 03672 - 220667 (O)
Fax : 03672-220667
e_mail: ngcprincipal2@gmail.com
Website : nowgonggirlscollege.edu.in

Dr. Balin Kumar Bhuyan,M.Sc, Ph.D
Principal & Secretary

Mobile : 94350-63617

Ref. :..... *Date* :.....

DECLARATION

18-12-2022

This is to declare that publications of faculty members prior to 14 June, 2019 are not included in the **UGC CARE** list since the list came into effect on **14 June 2019**.

Nowgong Girls' College ESTD: 1962 Nagaon :: Assam

Principal
Nowgong Girls' College

Principal
Nowgong Girls' College
Nagaon : Assam

Papers published per teacher in the Journals notified on UGC website during the Academic Session: 2017-18

Submitted to the NAAC for 3rd Assessment Cycle of Assessment & Accreditation

NOWGONG GIRLS' COLLEGE

Re-accreditated at A Grade by the NAAC (2nd Cycle)

Sensors & Actuators: B. Chemical 273 (2018) 710–717

Contents lists available at ScienceDirect

Sensors and Actuators B: Chemical

journal homepage: www.elsevier.com/locate/snb

Gold-coated electrospun PVA nanofibers as SERS substrate for detection of pesticides

Nabadweep Chamuah[a], Nabadeep Bhuyan[a], Pranjal Pratim Das[b], Namita Ojah[c], Arup Jyoti Choudhary[c], Tapas Medhi[b], Pabitra Nath[a,*]

[a] Applied Photonics and Nanophotonics Laboratory, Department of Physics, Tezpur University, Napaam, Sonitpur, Assam 784028, India
[b] Department of Molecular Biology And Biotechnology, Tezpur University, Napaam, Sonitpur, Assam 784028, India
[c] Plasma Processing Laboratory, Department of Physics, Tezpur University, Napaam, Sonitpur, Assam 784028, India

ARTICLE INFO

Keywords:
Electrospun
PVA nanofiber
SERS
LSPR
Pesticides

ABSTRACT

Owing to its ability to detect Raman signals from trace amount of Raman active samples, surface enhanced Raman scattering (SERS) substrate has emerged as an interesting field of research for different areas of applications. Herein, we demonstrate a large area with good degree of reproducibility SERS substrate using PVA nanofibers. Gold (Au) coated electrospun PVA nanofibers has been used as SERS substrate in the present study. Using the designed SERS substrate, Raman signal from malachite green (MG) with concentration as low as 10 nM has been measured reliably by the Raman spectrometer. The relative standard deviation (RSD) for signature peaks of this Raman active sample at 420 cm^{-1}, 1188 cm^{-1}, 1378 cm^{-1} and 1618 cm^{-1} were found to be 6.01%, 7.38%, 5.71% and 6.50% respectively. The usability of the designed SERS substrate for detection of three commonly used pesticides namely deltamethrin, quinalphos and thiacloprid has been successfully demonstrated. It has been observed that for concentration well below the maximum residue limit as set in the Global Agricultural Information Network (GAIN) report from United States department of agriculture (USDA) foreign agricultural service, with the proposed SERS substrate one can easily estimate the concentration of the pesticide samples well below the permissible limit.

1. Introduction

Being a surface sensitive technique and its finger printing specificity along with single molecular sensitivity surface enhanced Raman scattering (SERS) has emerged as a promising technique for sensing of biomolecule, chemicals and different gases. Electromagnetic (EM) mechanism dominantly contributes in the enhancement of Raman signal intensity, which is based on coherent collective oscillations of free electrons generating the localized surface plasmon (LSP) field. Due to coupling of the incident electromagnetic field with metal nanostructures a strongly localized field can be felt in the vicinity of the nanostructure. Consequently, when a Raman active sample is brought in the vicinity of the metal nanostructures it scatters intense Raman signal and the intensity of the signal is found to be enhanced by several order with respect to the situation when normal Raman signal is recorded from the bare sample. Along with this, another phenomenon called chemical enhancement (CE) contributes to the enhancement of scattered Raman signal. In CE, surface-absorbed molecule provides higher scattering cross-sections, thus enhancing the Raman signal intensity. However, this process contributes only one or two orders of magnitude higher than that of a plane substrate. To achieve high reproducibility with good enhancement factor (EF) it is important to design proper nanostructures to maximize the LSP field coupling conditions. Therefore, development of best possible SERS substrate with high EF along with good reproducibility characteristics has been a key research interest among the researchers for last few decades.

To develop SERS substrates, primarily two main approaches are adopted - wet-chemical and top-down fabrication process. Metal nanostructures with specific patterns such as nanocubes, nanorods, nanospheres, concave nanocubes, nanostars, porous nanoparticles, etc [1–8]. Using wet-chemical approaches have been demonstrated for different SERS-based sensing studies. These substrates can be developed at low cost with high EF and sensitivity. However, such SERS substrates yield either low or moderate reproducibility. In order to achieve good reproducibility, different lithographic techniques such as electron beam lithography, focused-ion beam lithography, nano-imprint lithography, etc [9–15]. have been used, which would produce a regular patterned nanostructure on the substrate. These approaches, in general are

* Corresponding author.
E-mail address: pnath@tezu.ernet.in (P. Nath).

https://doi.org/10.1016/j.snb.2018.06.079
Received 1 December 2017; Received in revised form 18 May 2018; Accepted 17 June 2018
Available online 25 June 2018
0925-4005/ © 2018 Elsevier B.V. All rights reserved.

Nowgong Girls' College ESTD: 1962 Nagaon :: Assam

Principal
Nowgong Girls' College
Nagaon :: Assam

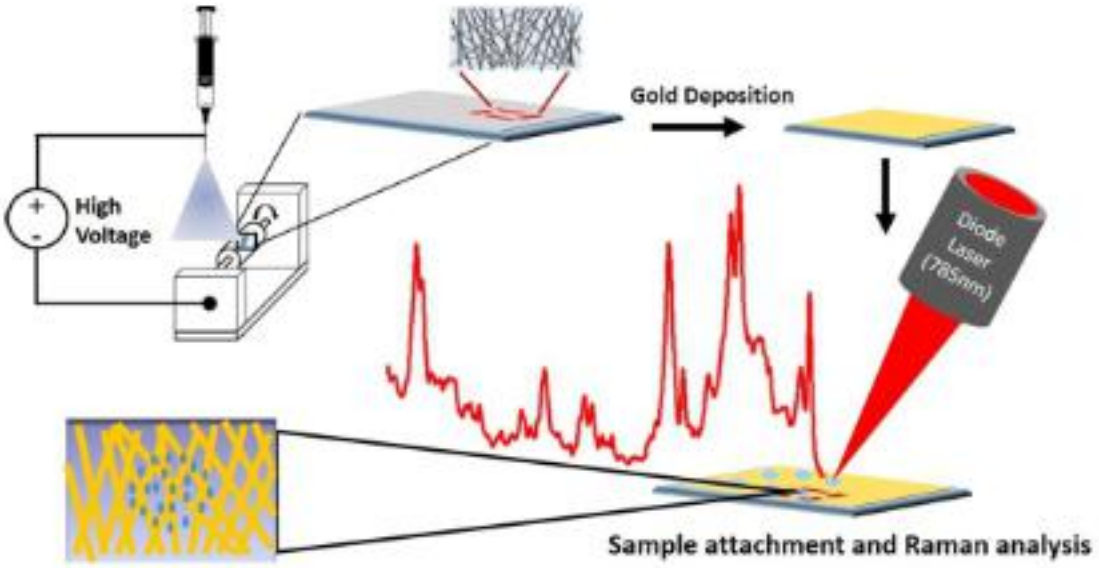

Fig. 1. Schematic representation of fabrication of proposed SERS substrate and its application to measuring of Raman signal from test samples.

expensive and time-consuming and demand sophisticated machines along with sophisticated laboratory set-up for fabrication of the substrates. Keeping these issues in mind, researchers are currently looking for alternative approaches by which SERS substrates can be obtained from naturally available patterned biological samples such as rose petals, diatom frustules, taro leaf, etc [16–26]. The use of diatom as a template for SERS-based investigations has been observed to be cost-effective and time-efficient. Of late, using inkjet printer, metal nanoparticle has been printed on paper and SERS based investigations have been performed on such paper substrate [27–31].

In this work, we demonstrate a technique to develop SERS substrate from Poly(vinyl) alcohol (PVA) nano-fiber where nano-fibers were deposited on glass substrate by electrospining technique. PVA is hydrophilic, nontoxic and biocompatible polymer and exhibits excellent physical properties such as strength, water solubility, gas permeability and thermal stability [32–34]. Using thermal evaporation technique Au nanofilm has been deposited on the crosslinked electrospun PVA nanofiber and the substrate has been used as SERS substrate in the present study. Using the designed substrate Raman signals scattered from different concentrations of MG samples has been successfully measured. For 10μM MG, the RSD of different signature peaks for this sample were found to be varying between 5–8%.

The applicability of the designed SERS substrate for quick and easy detection of some commonly used pesticides well below the permissible limits as set by USDA foreign agricultural service has been demonstrated. Use of pesticides to manage pest problems in the agricultural field has become a common practice around the world. Pesticides are not only used in agricultural fields, but also used in homes, parks, schools, buildings, forests, and roads. Few pesticides have been linked to a wide range of human health hazards, ranging from short-term impacts such as headaches and nausea to chronic impacts like cancer, reproductive harm and endocrine disruption. Acute dangers - such as nerve, skin, eye irritation and damage, headache, dizziness, fatigue and systemic poisoning can sometimes be dramatic, and even occasionally fatal. Issues related to chronic health effects may occur years even after minimal exposure to it in the environment or results from the pesticide residues [35–37]. Thus, reliable detection techniques of pesticides that contained in various food items at an affordable cost would be a re- for healthy and sustainable living style. Three pesticides namely deltamethrin, quinalphos and thiacloprid have been considered as test samples for detection and quantification with the proposed SERS substrate. For the considered pesticide samples, with concentrations well below the permissible level Raman signals scattered from the proposed SERS substrate can be measured reliably by the Raman spectrometer.

2. Materials and methods

2.1. Materials

Gold beads (99.999% purity), Polyvinyl alcohol (PVA) of molecular weight 145,000 and Malachite Green (MG) dye were procured from Sigma-Aldrich, India, deltamethrin, quinalphos and thiacloprid were procured from local agriculture stores. All chemicals were used as received without further processing. For detection and analysis, all the samples were prepared in deionized (DI) water.

2.2. SERS substrate fabrication and Raman signal measurement system

Fig. 1 illustrates the schematic of the experimental setup of the proposed work. The size, shape, alignment and spacing of electrospun PVA nanofibers on glass substrate play the crucial role in determining the characteristics of SERS substrate. To fabricate the SERS substrate, 8 wt% PVA solution was prepared in DI water at 80 °C under vigorous stirring condition. For deposition of PVA nanofibers we have used 1 cm x 1 cm glass slide. Prior to its use, the glass slides were cleaned in ultrasonic acetone bath followed by thorough washing with DI water. The glass slides were then allowed to dry in hot-air oven at 60 °C for 1 h. Using electrospining system (ESPIN-NANO, India) PVA nano-fibers are allowed to deposit on the clean glass substrate for 15 min. During deposition of the fibers we maintained a voltage of 16 kV between the tip of the syringe and the substrate. The flow rate of PVA was set at 0.3 ml/h and the glass slides were mounted on a rotor with its rotational speed was maintained at 1500 rpm. The distance between the tip of the needle and glass slide was kept at 15 cm. Upon completion of this step, the deposited nanofibers were allowed to cross-link at 170 °C for 2 h in the hot-air oven. Using thermal evaporation technique (Hind HiVac BC300), Au nano-film of thickness ~30 nm was allowed to deposit on the cross-linked PVA nano-fibers substrate. Fig. 2(a) shows the FESEM (Carl-Zeiss ΣIGMA VP) image of Au-coated PVA nanofibers deposited on the glass substrate. The diameters of the fibers are found to be varying between 100 nm–190 nm and the spacing among the fibers are varying between 10 nm to several 100 nm. The EDX data shown in Fig. 2(b) confirms the presence of Au in our designed SERS substrate. To study the generation of LSP field in the designed substrate the Au substrate has been illuminated with a broadband optical source (Ocean

Nowgong Girls' College Nagaon :: Assam 1965
Principal Nowgong Girls' College Nagaon :: Assam

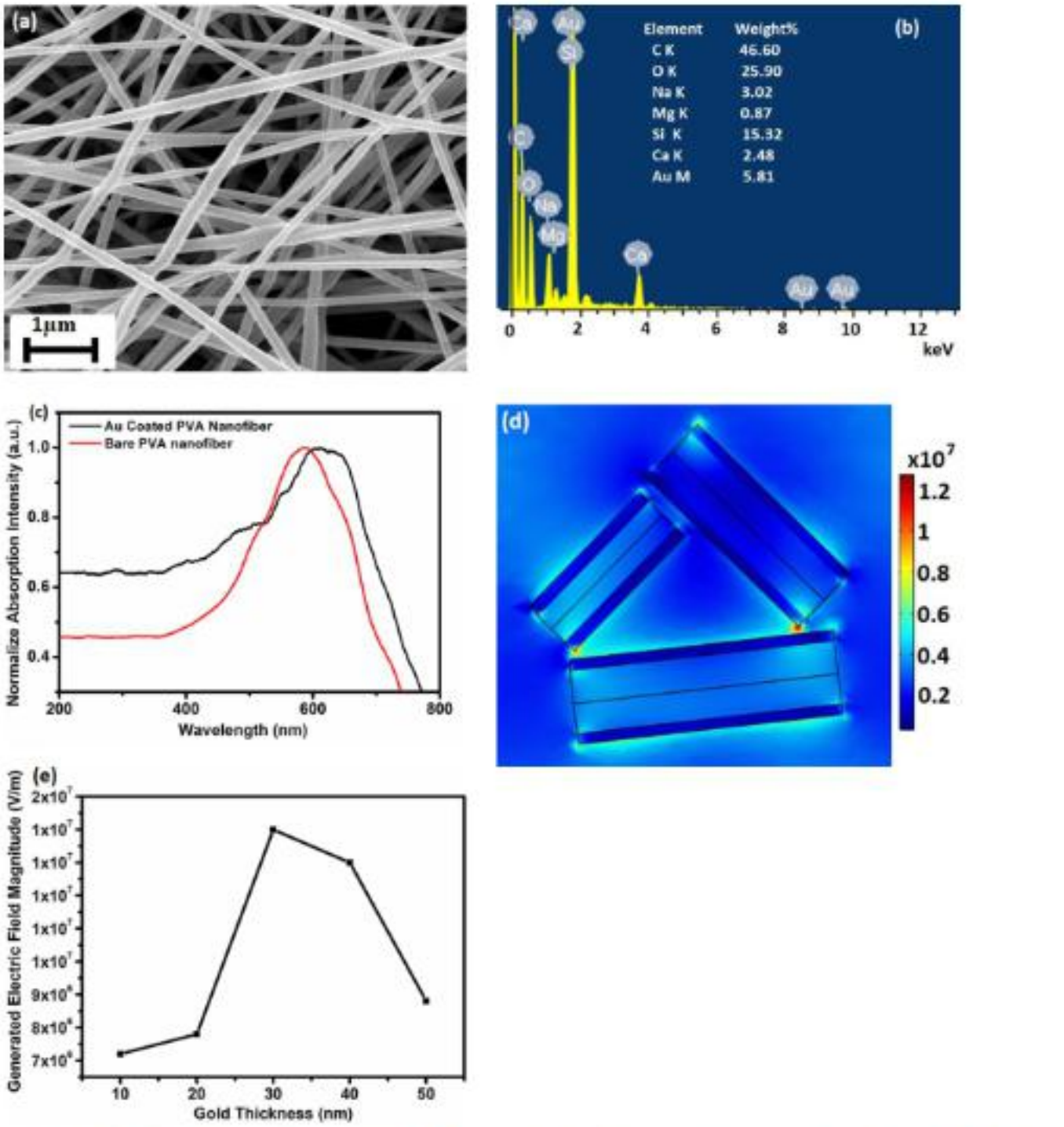

Fig. 2. (a) FESEM image of gold coated PVA nanofibre and (b) EDX data showing the elemental compositions, (c) UV–vis absorption spectra of the developed substrate (d) electromagnetic field distribution around the nanofiber and (e) variation generated electric field magnitude for different gold thickness when 785 nm plane polarized light is allowed to incident normally on the structure.

optics LS-1) and the corresponding absorption spectra of the transmitting modulated signal has been recorded with an optical spectrometer (CCS 200, ThorLabs Inc. USA). Fig. 2c describes the characteristics absorption spectra of the substrate measured by the optical spectrometer. Clearly, the figure indicates that the resonance coupling conditions occurs in the wavelength range from 580 nm to 650 nm. The broad spectrum of resonance condition is attributed to the varying size of PVA nanofibers which subsequently would cause dispersive nature of the resonance coupling condition. The same figure also includes the absorption curve of uncoated PVA substrate. For measurement of Raman signals scattered from Raman active samples, table-top Raman spectrometer (EZ Raman Enwave Optronics, USA) has been used. This spectrometer is equipped with a variable output power (up to 500 mW) a temperature-controlled 785 nm continuous wave diode laser source. The laser light is guided from source to the sample by an optical fiber coupled with a 0.22 NA objective lens. The detector section of the spectrometer is [illegible] with a thermoelectric controlled 2D CCD array with pixel [illegible] cm^{-1} per pixel.

Nowgong Girls' College ESTD: 1962 Nagaon :: Assam
Principal Nowgong Girls' College Nagaon :: Assam

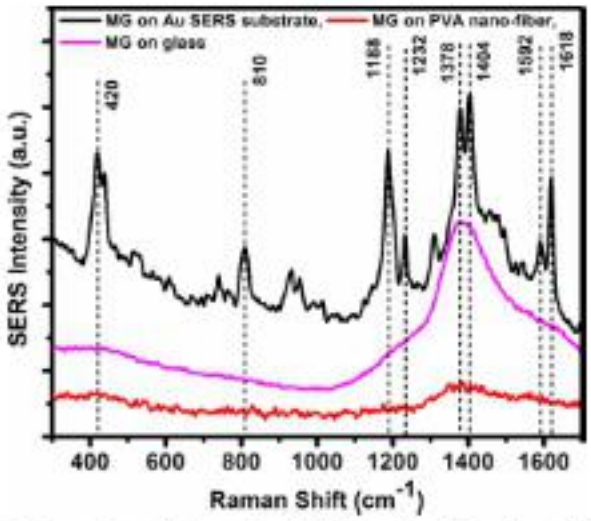

Fig. 3. A comparison of Raman signal of MG scattered from three different substrates namely plane glass substrate, PVA nanofiber coated substrate and gold coated PVA nanofiber substrate.

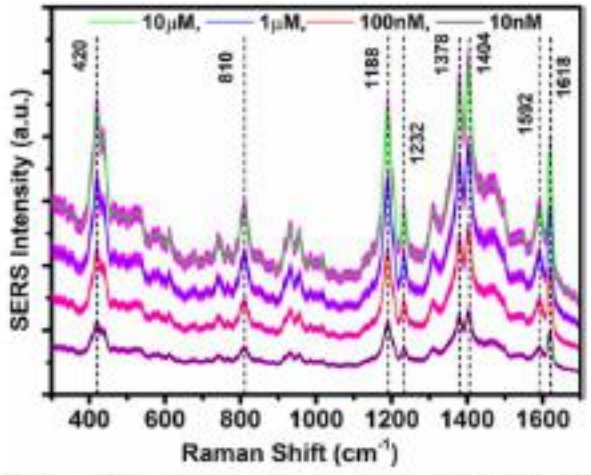

Fig. 4. Raman signal scattered from developed SERS substrate while different concentrations 10μM, 1μM, 100 nM and 10 nM of MG solution were tested.

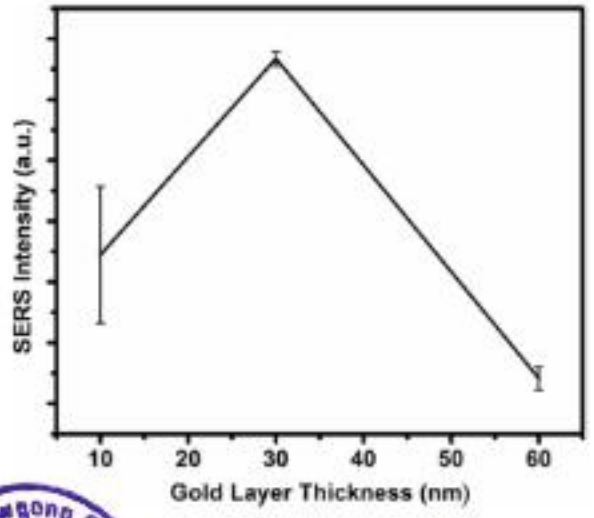

Fig. Characteristics curve of variation of scattered Raman signal intensity of [illegible] and 1188 cm[illegible] with the variation of deposited gold layer thickness.

2.3. Electromagnetic (EM) simulation study

Based on the arrangement of PVA nanofibers laid over the glass substrate we have studied the localized field magnitudes due to coupling of electromagnetic field with the proposed SERS substrate using finite element method (FEM) based simulation tool (COMSOL multiphysics 5.2, wave optic module). In order to minimize the computing time we have carried out the simulation study for three Au-coated PVA fibers. The radius of the fibers are considered to be 35 nm, 40 nm and 50 nm and 30 nm thick of Au film has been coated on the substrate. The length of the PVA fibers are considered to be varying between 700 nm to 1000 nm and oriented in random directions on the glass substrate. A plane polarized light of 785 nm was allowed to incident normally on the structure. The generated EM field magnitude around the fibers is shown in Fig. 2(d). For the designed pattern, we observe a maximum field magnitude of 1.23×10^7 V/m in the structure. To study the effect of Au film thickness on coupling EM field magnitude the Au layer thickness has been varied from 10 nm to 50 nm with a step incremental value of 10 nm. Fig. 2(e) illustrates the maximum field coupling conditions for different Au film thickness on the substrate. These simulation results reveal that with 30 nm thick Au layer, the proposed substrate yields the maximum field coupling condition when it is illuminated with 785 nm laser source.

3. Results and discussions

The performance of the designed SERS substrate has initially been evaluated with one commonly used Raman active sample MG. 10 μM of MG solution has been prepared in the laboratory in DI water and 10 μL of the prepared sample solution has been pipetted on the SERS substrate. The substrate was then allowed to dry in room temperature for 2 h. Upon drying of the sample, it is illuminated with the laser source and the back-scattered Raman signal from the sample has been recorded by the Raman spectrometer. Fig. 3 illustrates the characteristic Raman spectrum of MG scattered from the substrate. The figure also includes the back-scattered signals recorded by the spectrometer for MG treated on a bare PVA nanofibers and from a plane glass substrate. Clearly, it depicts that as compared to plane glass substrate or bare PVA nanofibers, the proposed SERS substrate scatters strong Raman signal. Signature Raman peaks at 420 cm^{-1}, 1188 cm^{-1}, 1378 cm^{-1} and 1618 cm^{-1} have been observed for MG which is attributed to out of plane vibration of phenyl-C-phenyl, in plane vibration of C H ring, N-phenyl stretching and stretching of C C ring respectively [25,38,39]. Medium band at 810 cm^{-1}, 1232 cm^{-1} and 1592 cm^{-1} corresponds to out of plane vibration of C H ring, C H rocking and C C stretching respectively [25,38,39]. The enhancement factor (EF) of our proposed SERS substrate has been calculated using the equation [11]

$$EF = \frac{I_{SERS}}{I_{REF}} \times \frac{N_{REF}}{N_{SERS}} \quad (1)$$

where, I_{SERS} and I_{REF} are Raman signal intensities of the sample from SERS substrate and reference substrate respectively while N_{SERS} and N_{REF} are the number of molecules present within the laser excitation area of the SERS substrate and reference substrate respectively. For the Raman peak at 1188 cm^{-1} I_{SERS} and I_{REF} was observed to be 3321 a.u. and 224 a.u. respectively. N_{REF} is calculated by using $N_{REF} = VcN_A$ where, V is the laser spot excitation volume on reference region, c is the molar concentration of the analyte on the reference region and N_A is Avogadro's number. Considering uniform distribution of analyte molecules over the substrate, N_{REF} is calculated to be 4.4037×10^7 for laser spot size dimension of 4.353 μm. The spot size of the laser has been calculated using the equation $1.22\lambda/NA$ where NA in the numerical aperture of the objective lens. Considering monolayer distribution of MG sample over the substrate, the N_{SERS} is calculated to be 4.4037×10^2. From Eq. (1), the average field EF at 1188 cm^{-1} of MG has been estimated to be 1.48×10^6

Nowgong Girls College ESTD: 1962 Nagaon :: Assam
C.T.C. Principal Nowgong Girls' College Nagaon :: Assam

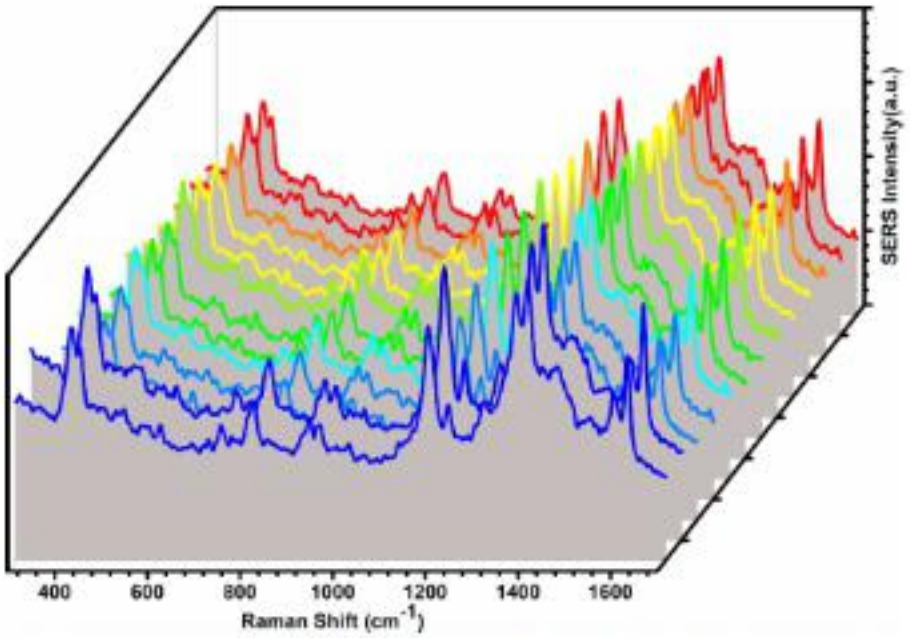

Fig. 6. Back scattered Raman signal intensities of 10 μM MG recorded from 13 different locations of the proposed substrate.

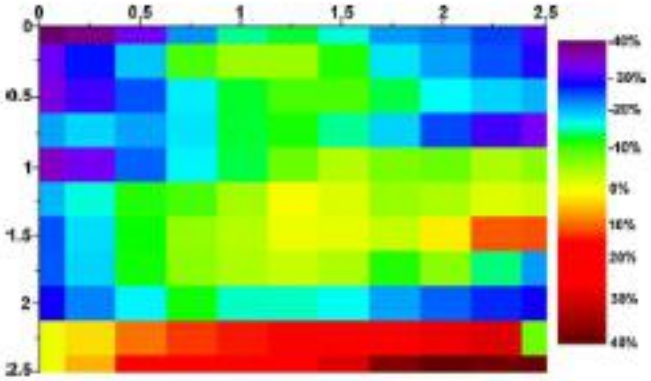

Fig. 7. Raman Signal intensity variation scattered from different locations of the substrate at wavenumber 1214 cm^{-1} when BPE was functionalize with the substrate, the mapping was done over an area of 2.5 mm × 2.5 mm.

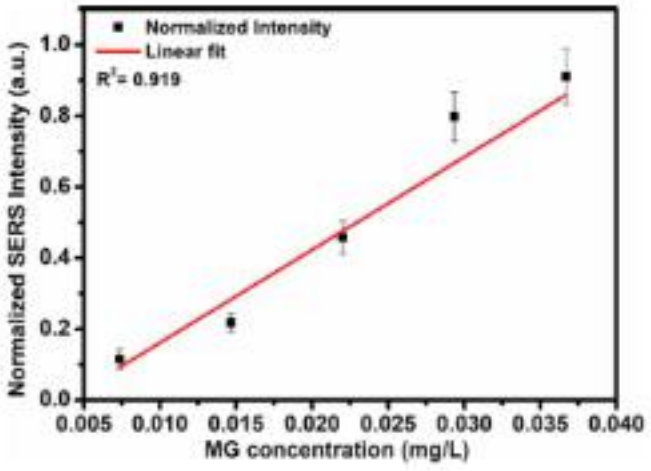

Fig. 8. Normalized SERS signal intensity variation of MG solution corresponding to Raman peak 1188 cm^{-1} for the concentrations 0.00734 mg/L to 0.03669 mg/L.

In the next step, we prepared three more samples of MG with concentrations 1μM, 100 nM and 10 nM by diluting the stock sample with DI water. 10 μL of each sample solution has been treated separately with the proposed SERS substrates. The back-scattered Raman signals of these samples were recorded by the spectrometer. Fig. 4 describes the characteristic Raman signals of different concentration MG samples scattered from the substrates. The figure clearly shows that with decreasing concentration of MG, the intensities of Raman signals decreases gradually. The SERS signal intensities have been recorded from 6 random locations on the substrate for each sample and the fluctuations of the scattered signal for each sample concentrations have been indicated in pink in Fig. 4 and an average intensity fluctuation of 7.62% has been observed corresponding to Raman peak at 1188 cm^{-1} for the considered samples. The minimum concentration that can be reliably detected by the spectrometer was 10 nM. Owing to the fact that MG is highly Raman active, the minimum detectable concentration level for other non-fluorescence Raman active samples may be different with the proposed SERS substrate.

To study the effect of Au thickness on Raman signal intensity variation, we have developed three substrates by depositing 10 nm, 30 nm and 60 nm Au layer on the PVA nanofiber. The substrates were than treated with 10μM MG solution and scattered Raman signals from these substrates have been recorded from 6 different random locations on each substrate. Fig. 5 shows the characteristics Raman signals intensities at 1188 cm^{-1} of MG recorded by the spectrometer for the considered substrates. With 30 nm of Au layer thickness we notice the highest Raman signal intensity from the substrate. This experimental results have been supported by the simulation study discussed in section 2.3.

The reproducibility characteristic of the proposed SERS substrate has been studied. Back scattered Raman signals of 10μM MG from 13 different randomly selected locations of the substrate were recorded by the spectrometer. Fig. 6 depicts the characteristic Raman spectra of the sample measured from these locations. The variations in Raman peaks intensities for MG at 420 cm^{-1}, 1188 cm^{-1}, 1378 cm^{-1} and 1618 cm^{-1} were observed to be 6.01%, 7.38%, 5.71% and 6.50% respectively. The low peak intensity fluctuation of this sample implies that the proposed SERS substrate is highly reproducible. This parameter of the substrate has been studied for two consecutive weeks and we noticed fairly stable readings during this period.

Nowgong Girls' College ESTD: 1962 Nagaon :: Assam

Principal
Nowgong Girls' College
Nagaon :: Assam

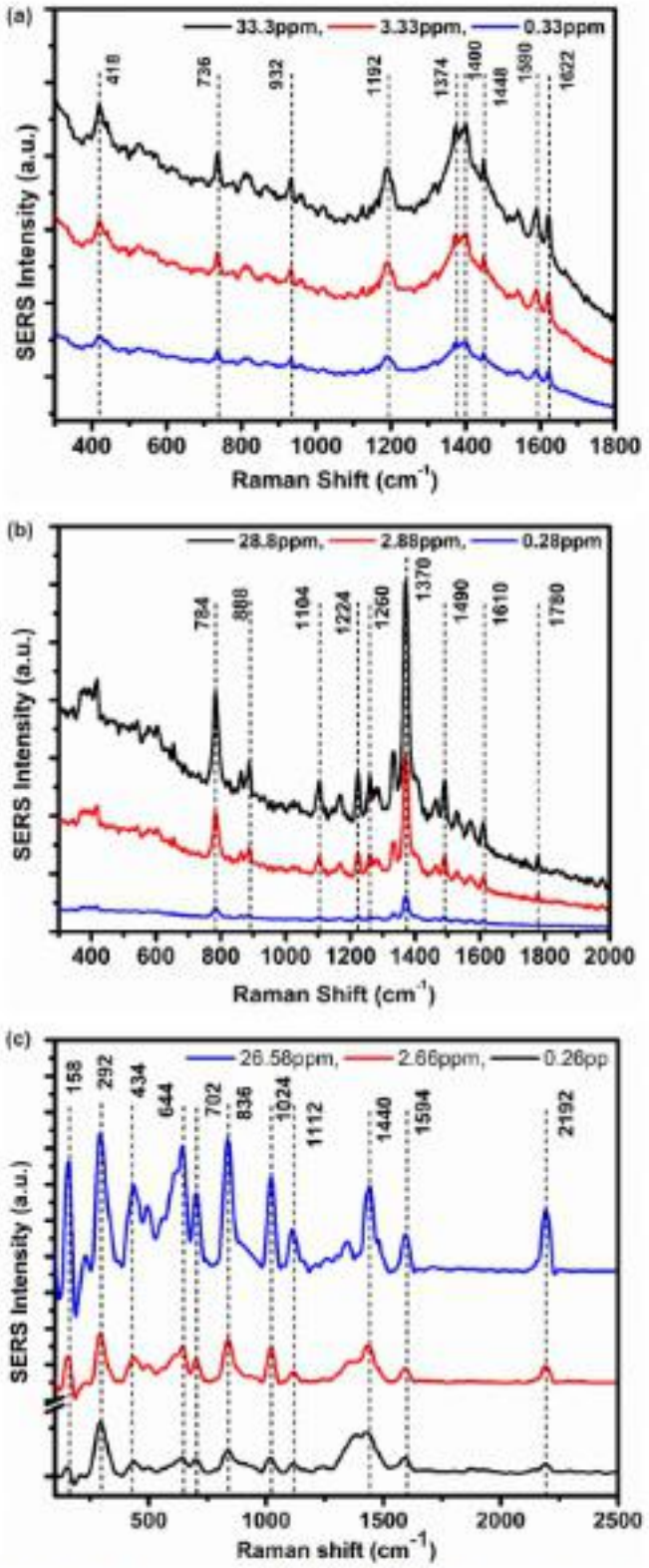

Fig. 9. Raman signal of (a) Deltamethrin, (b) Quinalphos and (c) Thiacloprid at different concentration level scattered from the developed SERS substrate upon functionalization of the pesticides.

To evaluate the spectral uniformity characteristics of the substrate we consider a non-fluorescent Raman active sample- 1,2-bis(4-pyridyl) ethylene (BPE). 1μM of BPE solution was prepared in ethanol medium and then treated with the substrate. Upon drying of the substrate, the scattered Raman signals of BPE were measured. An array of 11 × 11 over an area of 2.5 mm × 2.5 mm on the sensing region of the substrate has been mapped. Fig. 7 shows the intensity variations of Raman signal intensity corresponding to wavenumber 1214 cm^{-1} for BPE. The maximum SERS signal intensity variation was observed to be 40%, however, over 80% of the mapped area, the intensity fluctuation was found to be below 20%. This suggests a good degree of spectral uniformity of the proposed SERS substrate.

In the next step of the present work we estimate the limit of detection (LoD) of the proposed SERS substrate. To evaluate this parameter again we consider 5 different concentration of MG- 20 nM (0.00734 mg/L), 40 nM (0.01467 mg/L), 60 nM (0.02201 mg/L), 80 nM (0.01935 mg/L) and 100 nM (0.03669 mg/L). The samples were then treated separately with the developed substrates and scattered Raman signal intensities were recorded from 7 randomly selected locations on each substrate. The normalized SERS signal intensity variations at 1188cm^{-1} of MG has been indicated in Fig. 8. From this figure the LoD can be calculated using following equation [40].

$$LoD = \frac{3.3\sigma}{S} (2)$$

Where σ is the standard deviation of y-intercepts and S is the slope of the linear fitted line. For MG the LoD of the design substrate is calculated to be 0.01148 mg/L.

In the final step of the present work the applicability of the proposed SERS substrate for detection of three commonly used pesticides- deltamethrine, quinalphos and thiacloprid have been demonstrated. Pesticides residues cause pollution in the environment and are hazardous to human health. We accomplish a series of studies to detect minimum concentration of considered pesticide samples that can be detected by the Raman spectrometer upon its treatment with the proposed SERS substrate. Deltamethrine is generally used in crop, gardens, lawns etc. as an insects repellent. Though there is no reported cases of acute health issue from deltamethrine yet, it is highly toxic for aquatic environment [41–43]. Quinalphos is widely used in several developing and underdeveloped nations for better yield of the crops namely wheat, rice, maize, coffee, sugarcane, cotton etc. Excessive content (more than 0.5 mg/kg body weight) of this chemical in food items may cause toxicity which includes carcinogenicity, reproductive and developmental toxicity, neurotoxicity. It is listed as moderate toxic chemical by world health organization (WHO) and use of this pesticide is restricted in several nations [44]. Again thiacloprid is used in crop fields and gardens also as an insect repellent. Direct exposer of this pesticide may cause skin and eye irritation. The maximum permissible limits of use of these pesticides in agriculture and food materials can be found elsewhere [45].

Three different concentrations of pesticides sample have been prepared in the laboratory and then treated with the SERS substrate separately. The recorded Raman signals for deltamethrine are shown in Fig. 9(a). The characteristics peaks of deltamethrine have been observed at 736, 1192, 1400, 1448, 1590 and 1622 cm^{-1} which correspond to C-Br stretching, C O C stretching of ether group, CH_3 deformation, CH_3 anti-symmetric deformation, aromatic benzene ring stretching and C=O stretch of phenol ether respectively. These characteristic peaks can be clearly visible even after diluting the sample to 0.33 ppm. The SERS spectra for quinalphos is shown in Fig. 8(b). Very sharp and strong peak has been observed at 1370 cm^{-1} which correspond to CH_3 symmetric deformation. Other peaks at 784 cm^{-1}, 1224 cm^{-1}, 1260 cm^{-1}, 1490 cm^{-1} and 1780 cm^{-1} are attributed to CH out of plane deformation, C C N bending, C N stretching, ring stretching and C=O stretching respectively. The Raman signals for this specific pesticide are measurable even when the concentration of the sample has been reduced to 0.288 ppm. Fig. 8(c) illustrates the characteristics SERS spectra of different concentrations of thiacloprid sample. Raman peaks at 434 cm^{-1} and 644 cm^{-1} are correspond to bending of C N C and C S stretching while 702 cm^{-1} and [illegible] correspond to stretching of C-Cl bond. Again 1024 cm^{-1} [illegible] 2 cm^{-1}

Principal
Nowgong Girls' College
Nagaon :: Assam
Nowgong Girls' College
ESTD: 1962
Nagaon :: Assam

Table 1
Comparison between maximum residue limit of the considered pesticides and minimum detectable concentration of developed SERS substrate.

Pesticides	Maximum residue limit (mg/Kg)	Minimum detectable concentration of our developed substrate (mg/Kg)	LoD of other techniques.	Remark
Deltamethrin	10.00	0.33	< 1 ng/mL [46]	Used in rice, wheat, pea, cabbage, broccoli, sweet potato, olive, tea etc. can be detect reliably
Quinalphos	0.50	0.288	5.5 mg/Kg [47]	Used in citrus fruits. Can be detect reliably
Thiacloprid	1.00	0.2658	1.8 ng/mL [48]	Used in mustard seed, tomato, cucumber, berries etc. and can be detected reliably

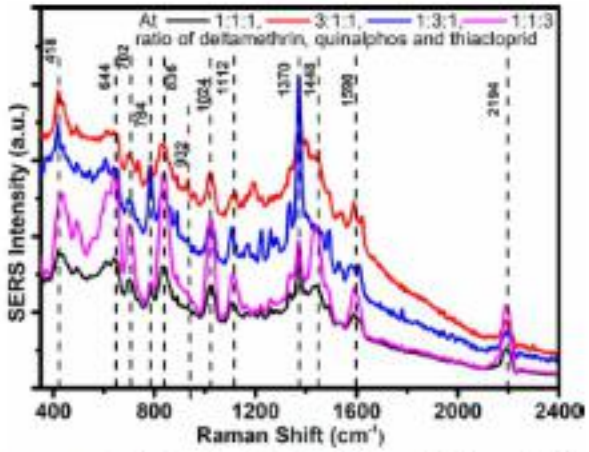

Fig. 10. Raman signal intensity of deltamethrin, quinalphos and thiacloprid mixture when these are mixed at different ratio.

1440 cm^{-1} and1594 cm^{-1} peaks are observed due to ring breathing mode, C N stretching, scissors vibration of CH_2 and C=C stretching respectively. With the designed SERS substrate thiacloprid concentration as low as 0.2658 ppm can be detected reliably. Table 1 summarizes the maximum permissible limit of the above pesticide samples as set by USDA and the minimum concentrations of these samples which can be detected by the present technique. The table also contains the minimum detectable concentrations of these samples as have been reported by other techniques. Clearly, for all the pesticides samples considered in the present study with the proposed SERS substrate one can record the Raman signals of the samples well below the permissible limit.

In order to study the combined effect of the three considered pesticides samples on the Raman signal we have prepared four different samples by mixing deltamethrine: quinalphos: thiacloprid in the ratio 1:1:1, 3:1:1, 1:3:1 and 1:1:3. And the mixtures have been treated separately with the substrates. Fig. 10 shows the characteristics Raman signals for different combination of pesticides samples in the mixture. The figure indicates that when all the pesticides were mixed at equal ratio only the strong characteristics peaks of each pesticides can be observed. For instance when the pesticides were mixed in the ratio we observe the signature Raman peaks at 1590 cm^{-1} for deltamethrin 1370 cm^{-1} for quinalphos and at 836 cm^{-1} for thiacloprid. These characteristics peaks are found to be amplified with the increase in compositions of the respective pesticide in the mixture. This characteristic curve represents the selectivity of the proposed technique while analyzing Raman signals in a mixture.

With 0.22NA objective lens the spot size of the laser source on sensing region of the SERS substrate was calculated to be 4.353 μm. This covers an area of 14.88 μm^2 over the SERS substrate. The relatively wider analyzing area of the sensing region of SERS substrate provides an average Raman signal enhancement information of the sample. Thus, even though the PVA nanofibers were oriented in random directions, due to the consideration of average field enhancement over a relatively large area (which covers tens of nanofibers over the sensing region) yields reasonably good reproducibility of the design substrate. PVA being biocompatible in nature we believe that the proposed SERS substrates can be effectively used to detect and quantify different biomolecular samples without affecting its nature through rigorous chemical processes.

4. Conclusion

In summary, we demonstrate a technique to obtain low-cost, fairly reproducible and sensitive SERS substrate using electrospinning technique. The detection and quantification of MG and spectral uniformity of the designed substrate have been successfully demonstrated in the present work. The practical utility of the proposed SERS substrate for detection and quantification of three commonly used pesticides have been successfully demonstrated. The SERS substrate can be fabricated without the requirement of sophisticated instruments and laboratory facility. We envisioned that the design SERS substrate could potentially emerge as a low-cost Raman signal sensing platform for reliable detection and quantification of other chemicals and biological samples.

Acknowledgements

P. Nath acknowledges SERB-DST, New Delhi, India for financial support vide grant number- SERB/F/5522/2013-14 dated 27.11.2013. Authors gratefully acknowledges Prof. P. P. Sahu, Department of electronics and communication engineering, Tezpur University for allowing us to access his laboratory facility. Authors acknowledge M. Senapati and P. Phukan of Tezpur University for assisting us in gold deposition on the substrate. Authors acknowledge B. Sarmah, IASST, Boragaon, Guwahati, Assam for taking FESEM images and EDX data of the SERS substrate. Authors also thankful to IASST, Boragaon, Guwahati, Assam for allowing to take FESEM imaging of the samples. N. Chamuah gratefully acknowledges the financial support received from UGC, New Delhi, India for awarding National Fellowship for OBC students 2014-15.

References

[1] P.G. Vianna, D. Grasseschi, G.K. Costa, I.C. Carvalho, S.H. Domingues, J. Fontana, et al., Graphene oxide/gold nanorod nanocomposite for stable surface enhanced Raman spectroscopy, ACS Photonics (2016).
[2] J.M. McLellan, Z.-Y. Li, A.R. Siekkinen, Y. Xia, The SERS activity of a supported Ag nanocube strongly depends on its orientation relative to laser polarization, Nano Lett. 7 (2007) 1013–1017.
[3] R. Sanci, M. Volkan, Surface-enhanced Raman scattering (SERS) studies on silver nanorod substrates, Sens. Actuators B: Chem. 139 (2009) 150–155.
[4] X. Wang, Y. Li, H. Wang, Q. Fu, J. Peng, Y. Wang, et al., Gold nanorod-based localized surface plasmon resonance biosensor for sensitive detection of hepatitis B virus in buffer, blood serum and plasma, Biosens. Bioelectron. 26 (2010) 404–410.
[5] L. Wang, X. Zeng, T. Liu, X. Zhang, H. Wei, Y. Huang, et al., Wavelength modulated SERS hot spot distribution in 1D nanostructures on metal film, J. Phys. D Appl. Phys. 49 (2016) p. 425301.
[6] W.H. Park, H. Cheong, Exploring the SERS background using a sandwiched graphene monolayer with gap-plasmon junctions, J. Phys. D Appl. Phys. 49 (2016) p. 105302.
[7] Q. Zhang, N. Large, H. Wang, Gold nanoparticles with tipped [illegible] substrates for single-particle surface-enhanced Raman spectr[illegible] nocubes, nanotetrahedra, and nanostars, ACS Appl. Mat[illegible] 17255–17267.
[8] Q. Zhang, N. Large, P. Nordlander, H. Wang, Porous Au nan[illegible] plasmon resonance and intense field enhancements for sin[illegible]

Principal
Nowgong Girls' College
Nagaon :: Assam
Nowgong Girls' College ESTD 1962 Nagaon :: Assam

Phys. Chem. Lett. 5 (2014) 370–374.
[9] M. Tabatabaei, M. Najiminaini, K. Davieau, B. Kamkaka, M.R. Singh, J.J. Carson, et al., Tunable 3D plasmonic cavity nanosensors for surface-enhanced Raman spectroscopy with sub-femtomolar limit of detection, ACS Photonics 2 (2015) 752–759.
[10] H.Y. Wu, C.J. Choi, B.T. Cunningham, Plasmonic nanogap-enhanced Raman scattering using a resonant nanodome array, Small 8 (2012) 2878–2885.
[11] C.J. Choi, Z. Xu, H.-Y. Wu, G.L. Liu, B.T. Cunningham, Surface-enhanced Raman nanodomes, Nanotechnology 21 (2010) p. 415301.
[12] J. Zhang, M. Irannejad, B. Cui, Bowtie nanoantenna with single-digit nanometer gap for surface-enhanced Raman scattering (SERS), Plasmonics 10 (2015) 831–837.
[13] N. Guillot, H. Shen, B. Frémaux, O. Perot, E. Rinnert, T. Toury, et al., Surface enhanced Raman scattering optimization of gold nanocylinder arrays: influence of the localized surface plasmon resonance and excitation wavelength, Appl. Phys. Lett. 97 (2010) p. 023113.
[14] N. Chamuah, P. Nath, Periodically varying height in metal nano-pillars for enhanced generation of localized surface Plasmon field, Plasmonics 10 (2015) 1367–1372.
[15] N. Chamuah, G.P. Yaklya, A.M. Joseph, P. Nath, Diagonally aligned squared metal nanopillar with increased hotspot density as a highly reproducible SERS substrate, Plasmonics 12 (2017) 1353–1358.
[16] S.-Y. Chou, C.-C. Yu, Y.-T. Yen, K.-T. Lin, H.-L. Chen, W.-F. Su, Romantic story or raman scattering? Rose petals as ecofriendly, low-cost substrates for ultrasensitive surface-enhanced Raman scattering, Anal. Chem. 87 (2015) 6017–6024.
[17] B.B. Xu, Y.L. Zhang, W.Y. Zhang, X.Q. Liu, J.N. Wang, X.L. Zhang, et al., Silver-coated rose petal: green, facile, low-cost and sustainable fabrication of a SERS substrate with unique superhydrophobicity and high efficiency, Adv. Opt. Mater. 1 (2013) 56–60.
[18] J. Yang, L. Zhen, F. Ren, J. Campbell, G.L. Borrer, A.X. Wang, Ultra-sensitive immunoassay biosensors using hybrid plasmonic-biosilica nanostructured materials, J. Biophoton. 8 (2015) 659–667.
[19] N. Kröger, N. Poulsen, Diatoms-from cell wall biogenesis to nanotechnology, Annu. Rev. Genet. 42 (2008) 83–107.
[20] F. Ren, J. Campbell, G.L. Borrer, A.X. Wang, Surface-enhanced Raman spectroscopy sensors from nanobiosilica with self-assembled plasmonic nanoparticles, IEEE J. Sel. Top. Quantum Electron. 20 (2014) 127–132.
[21] F. Ren, J. Campbell, X. Wang, G.L. Borrer, A.X. Wang, Enhancing surface plasmon resonances of metallic nanoparticles by diatom biosilica, Opt. Express 21 (2013) 15308–15313.
[22] M. Pannico, I. Rea, S. Chandrasekaran, P. Musto, N.H. Voelcker, L. De Stefano, Electroless Gold-modified diatoms as surface-enhanced Raman scattering supports, Nanoscale Res. Lett. 11 (2016) 1–6.
[23] Y. Xi, X. Kong, K. Squire, F. LeDuff, G.L. Borrer, A.X. Wang, SERS sensing of sub-nanolitre analyte on diatom biosilica using inkjet printing, SPIE BiOS, (2016) 972406-972406-6.
[24] X. Kong, Y. Xi, F. Leduff, X. Chong, F. Ren, G. Borrer, et al., Ultra-sensitive detection of explosive molecules using multi-functional plasmonic-biosilica, CLEO: Sci. Innov. (2016) p. SF2I. 6.
[25] P. Kumar, R. Khosla, M. Soni, D. Deva, S.K. Sharma, A highly sensitive, flexible SERS sensor for malachite green detection based on Ag decorated microstructured PDMS substrate fabricated from Taro leaf as template, Sens. Actuators B: Chem. 246 (2017) 477–486.
[26] N. Chamuah, L. Chetia, N. Zahan, S. Dutta, G.A. Ahmed, Nath, et al., Naturally occurring diatom frustule as SERS substrate for detection and quantification of chemicals, J. Phys. D Appl. Phys. 50 (2017).
[27] W.Y. Wei, I.M. White, Inkjet printed surface enhanced raman spectroscopy array on cellulose paper, Anal. Chem. 82 (2010) p. 9626.
[28] W.-J. Liao, P.K. Roy, S. Chattopadhyay, An ink-jet printed, surface enhanced raman scattering paper for food screening, RSC Adv. 4 (2014) 40487–40493.
[29] E.P. Huppmann, W.Y. Wei, I.M. White, Highly sensitive and flexible inkjet printed SERS sensors on paper, Methods 63 (2013) 219–224.
[30] N. Chamuah, A. Hazarika, D. Hoffmeyer, Nath, Pabitra, SERS on paper: an extremely low cost technique to measure Raman signal, J. Phys. D Appl. Phys. 50 (2017) pp. 485601.
[31] C. Wang, B. Liu, X. Dou, Silver nanotriangle-loaded filter paper for ultrasensitive SERS detection application benefited by interspacing of sharp edges, Sens. Actuators B: Chem. 231 (2016) 357–364.
[32] T.S. Ganz, A.B. Suksing, M.N. Akhtar, A.A.H. Kadhum, A.B. Mohamad, A.A. Al-Amiery, Properties and applications of polyvinyl alcohol, halloysite nanotubes and their nanocomposites, Molecules 20 (2015) 22833–22847.
[33] C.-K. Kim, B.-S. Kim, F.A. Sheikh, U.-S. Lee, M.-S. Khil, H.-Y. Kim, Amphiphilic poly (vinyl alcohol) hybrids and electrospun nanofibers incorporating polyhedral oligodimethylsiloxane, Macromolecules 40 (2007) 4823–4828.
[34] J.-C. Park, T. Ito, K.-O. Kim, K.-W. Kim, B.-S. Kim, M.-S. Khil, et al., Electrospun poly (vinyl alcohol) nanofibers: effects of degree of hydrolysis and enhanced water stability, Polym. J. 42 (2010) 273–276.
[35] W. Aktar, D. Sengupta, A. Chowdhury, Impact of pesticides use in agriculture: their benefits and hazards, Interdiscipl. Toxicol. 2 (1) (2009) 1–12.
[36] C.A. Damalas, I.G. Eleftherohorinos, Pesticide exposure, safety issues, and risk assessment indicators, Int. J. Environ. Res. Public Health 8 (2011) p. 1402.
[37] **Pesticide residues in food Fact sheet, WHO, 2017 July** http://www.who.int/mediacentre/factsheets/pesticide-residues-food/en/.
[38] S. Lee, J. Choi, L. Chen, B. Park, J.B. Kyong, G.H. Seong, et al., Fast and sensitive trace analysis of malachite green using a surface-enhanced Raman microfluidic sensor, Anal. Chim. Acta 590 (2007) 139–144.
[39] Y. Zhang, Y. Huang, F. Zhai, R. Du, Y. Liu, K. Lai, Analysis of enrofloxacin, furazolidone and malachite green in fish products with surface-enhanced raman spectroscopy, Food Chem. 135 (2012) 845–850.
[40] I.H.T. Guideline, Validation of analytical procedures: text and methodology Q2 (R1), International Conference on Harmonization, Geneva, Switzerland, 2005, pp. 11–12.
[41] T. Bolimi, T. Szegletes, Z. Szegletes, K. Halasy, J. Nemcsok, Biochemical and subcellular changes in carp exposed to the organophosphorus methidathion and the pyrethroid deltamethrin, Aquat. Toxicol. 33 (1995) 279–295.
[42] S. Viran, F.U. Erkoç, H. Polat, O. Kırpık, Investigation of acute toxicity of deltamethrin on guppies (Poecilia reticulata), Ecotoxicol. Environ. Safe 55 (2003) 82–85.
[43] L. Angahar, Investigations of acute toxicity and neurotoxin effects of aqueous extracted pyrethroid (Deltamethrin) from insecticide treated mosquito net on Clarias gariepinus and Heterobranchus bidorsalis, MOJ Biol Med. 1 (4) (2017) 00020.
[44] S. Kegley, B. Hill, S. Orme, A. Choi, PAN pesticide database, Pesticide Act. Netw. (2011).
[45] **USDA foreign agricultural service, GAIN report, CH14019, 2014.** https://gain.fas.usda.gov/Recent%20GAIN%20Publications/Maximum%20Residue%20Limits%20for%20Pesticides%20in%20Food_Beijing_China%20-%20People%20Republic%20of_4-30-2014.pdf.
[46] X. Liu, L. Li, Y.-Q. Liu, X.-B. Shi, W.-J. Li, Y. Yang, et al., Ultrasensitive detection of deltamethrin by immune magnetic nanoparticles separation coupled with surface plasmon resonance sensor, Biosens. Bioelectron. 59 (2014) 328–334.
[47] H. Hu, X. Liu, P. Jiang, X. Yao, X. Cui, A novel chemiluminescence assay of organophosphorus pesticide quinalphos residue in vegetable with luminol detection, Chem. Central J. 4 (2010) p. 13.
[48] Z.J. Liu, X. Wei, H. Xu, M. Li, G.B. Zhu, Y.L. Xue, et al., Sensitive detection of thiacloprid in environmental and food samples by enhanced chemiluminescent enzyme immunoassay, RSC Adv. 6 (2016) 29460–29465.

Nabadweep Chamuah received the M.Sc degree in Electronics and Communication Technology from Gauhati University, Guwahati, Assam, India in 2013 and currently pursuing his PhD degree from Tezpur University, Assam, India. His current research interests include Surface enhanced Raman scattering (SERS), Optical instrumentation.

Nabadeep Bhuyan has completed his master of science (M.Sc) in Physics from Tezpur University, Assam, India in 2017. His current research interests include SERS.

Pranjal Pratim Das is a PhD student at Department of Molecular Biology and Biotechnology, Tezpur University India. He has completed his BSc in Applied Biotechnology, MSc in Molecular Biology and Biotechnology and Post Graduate Diploma in Bioinformatics from SMU in 2009, Tezpur University in 2012 and NIELIT, Govt. of India in 2010 respectively. His area of interest is on insecticide resistance in *Helopeltis theivora* waterhouse.

Namita Ojah is a Ph.D. student at Tezpur University, Assam, India. She also did her M.Sc. from Tezpur University, Assam, India in 2016. Her Research work includes surface modification of some natural polymers like Silk by low temperature Plasma processing for various biomedical applications.

Arup Jyoti Choudhury is a DST INSPIRE faculty at Department of Physics, Tezpur University, Assam, India. He did his masters from Tezpur University and Ph.D. from Gauhati University, Assam, India. He received his post-doctoral award from Yokohama National University, Japan. His Research area includes Experimental Condensed Matter Physics, Experimental Plasma Physics and thin film processing.

Tapas Medhi is an assistant professor at Department of Molecular Biology and Biotechnology, Tezpur University, India. He has completed his Ph.D. from Indian Institute of Technology, Kharagpur (India) on Enzymology in 2004. He was also a postdoctoral Fellow in the Institute of Biochemistry, Faculty of Life Science, Pharmacy and Psychology, Leipzig University, Germany (2004–2006) and former Head of ONGC–CPBT, Tezpur University, India. His research interests are isolation and purification of components of P450 dependent monooxygenase system and their in vitro reconstitution study for cell free reconstitution, elaboration of basic knowledge and conditions for the construction of an enzyme reactor (biosensor), mechanism of insecticide resistance and development of eco-friendly pest control, microbial enhanced oil recovery/bioremediation and psychoneuroimmunological discourse on yogic principles.

Pabitra Nath received the M.Sc degree in Physics from Tezpur University, Napaam, Assam, India, and the Ph.D. degree in electronics science from Gauhati University, Guwahati, Assam, India, in 2000 and 2009, respectively. He is currently an Associate Professor with the Department of Physics, Tezpur University. He has visited Micro and Nano Technology Laboratory (MNTL), Department of Electrical and Computer Engineering, University of Illinois at Urbana Champaign, Urbana, through BOYSCAST fellowship program 2010–2011 sponsored by the Department of Science and Technology, Government of India. His current research interests include fiber optics sensors and system, Smartphone platform sensing systems, SERS and optical bio-sensing systems.

Principal
Nowgong Girls' College
Nagaon :: Assam

Nowgong Girls' College
ESTD 1962
Nagaon :: Assam

International Journal of Biological Macromolecules 114 (2018) 1026–1032

Contents lists available at ScienceDirect

International Journal of Biological Macromolecules

journal homepage: http://www.elsevier.com/locate/ijbiomac

Surface modification of electrospun PVA/chitosan nanofibers by dielectric barrier discharge plasma at atmospheric pressure and studies of their mechanical properties and biocompatibility

Punamshree Das [a], Namita Ojah [a], Raghuram Kandimalla [b], Kiranjyoti Mohan [c], Dolly Gogoi [d], Swapan Kumar Dolui [d], Arup Jyoti Choudhury [a,*]

[a] Department of Physics, Tezpur University, Tezpur 784028, Assam, India
[b] Drug Discovery Laboratory, Institute of Advanced study in Science and Technology, Paschim Boragaon, Guwahati 781035, Assam, India
[c] Central Instruments Facility, Indian Institute of Technology, Guwahati 781039, Assam, India
[d] Department of Chemical Sciences, Tezpur University, Tezpur 784028, Assam, India

ARTICLE INFO

Article history:
Received 7 December 2017
Received in revised form 6 February 2018
Accepted 21 March 2018
Available online 22 March 2018

Keywords:
Poly (vinyl alcohol)
Chitosan
Nanofiber
Plasma modification
Dielectric barrier discharge
Biocompatibility

ABSTRACT

In this paper, surface of electrospun PVA/Cs nanofibers is modified using dielectric barrier discharge (DBD) plasma and the relationship between the observed mechanical properties and biocompatibility of the nanofibers and plasma-induced surface properties is discussed. Plasma treatment of electrospun PVA/Cs nanofibers is carried out with both inert (argon, Ar) and reactive (oxygen, O_2) gases at atmospheric pressure. Incorporation of oxygen-containing polar functional groups on the surface of Ar-plasma treated (PVA/Cs/Ar) and O_2-plasma treated (PVA/Cs/O_2) nanofibers and increase in surface roughness contribute to the improvement of surface wettability and the decrease of contact angle with water of the nanofibers. Both PVA/Cs/Ar and PVA/Cs/O_2 nanofibers show high tensile strength (11.6–15.6%) and Young's modulus (33.8–37.3%) as compared to the untreated one. Experimental results show that in terms of haemolytic activity the PVA/Cs/Ar and PVA/Cs/O_2 nanofibers do not cause structural changes of blood cells and meet the biocompatibility requirements for blood-contacting polymeric materials. MTT cell viability results further reveals improvement in biocompatibility of PVA/Cs nanofibers after Ar and O_2 plasma treatment. The results suggest that DBD plasma treated electrospun PVA/Cs nanofibers have the potential to be used as wound dressing and scaffolds for tissue engineering.

© 2018 Elsevier B.V. All rights reserved.

1. Introduction

Electrospun nanofibers prepared from biodegradable polymers have drawn significant research interest as potential materials for biomedical and biotechnological applications [1–3]. The characteristic features of nanofibers such as large surface area to volume ratio, high porosity and close resemblance to the structure and function of the native extracellular matrix (ECM) of biological systems such as collagen fibers make them suitable materials for controlled drug delivery and tissue engineering [1]. Over the last decade, considerable efforts have been made to explore more advanced applications and sustainable development of electrospun nanofibers in biomedical fields [4–8]. Most of the efforts involve modifying their surfaces to impart certain functionalities such as hydrophilicity, surface energy, adhesion and surface-immobilization of bioactive molecules [4–8].

Various methods have been developed and implemented to modify the surface properties of electrospun nanofibers such as low temperature plasma treatment, wet chemical method, surface graft polymerization, and co-electrospinning of surface active agents and polymers [4]. Among them, low temperature plasma treatment is widely used to modify the surface properties of electrospun nanofibers without affecting their bulk properties [8,9]. It is considered as non-hazardous and environmental-friendly process and has several advantages over other surface modification methods in terms of consumption of energy, processing time and solvent [10]. Through proper selection of plasma source and control of discharge parameters (discharge voltage, working pressure, gas flow rate *etc.*), it is possible to introduce different functional groups on the surface and tailor the surface properties of electrospun nanofibers to facilitate subsequent improvement in biocompatibility of the polymers [8].

Chitosan (Cs), a partially *N*-deacetylated derivative of chitin and one of the most abundant natural polysaccharides, is a promising biomacromolecule for electrospinning, due to its excellent biological properties such as biodegradability, biocompatibility and antibacterial activity and have drawn extensive research interest for applications in controlled drug delivery, wound dressing and tissue engineering [11]. However, chitosan is difficult to electrospin into a nanofibrous

* Corresponding author.
E-mail address: arupjchoudhury@gmail.com. (A.J. Choudhury).

https://doi.org/10.1016/j.ijbiomac.2018.03.115
0141-8130/© 2018 Elsevier B.V. All rights reserved.

Principal
Nowgong Girls' College
Nagaon :: Assam

Nowgong Girls' College
ESTD: 1962
Nagaon :: Assam

membrane due to its limited solubility in most organic solvents, ionic character in dissolved state and three-dimensional networks of strong hydrogen bonds [12]. Therefore Cs is often blended with synthetic polymer like poly(vinyl alcohol) (PVA) to felicitate electrospinning process and achieve uniform nanofibers [12]. PVA is a non-toxic, water-soluble, biocompatible, and biodegradable polymer and has good fiber forming capability in electrospinning process [13]. Several studies report successful fabrication of biocompatible PVA/Cs nanofibers with good mechanical and chemical properties and their potential use in biomedical field [13–15]. However no work has been reported so far on surface modification of PVA/Cs nanofibers by low temperature plasma treatment and subsequent studies of their physico-chemical and mechanical properties and biocompatibility to explore possible biomedical applications.

In this study, surface modification of PVA/Cs nanofibers has been carried out using atmospheric pressure argon (Ar) - and oxygen (O_2) - dielectric barrier discharge (DBD) plasmas at atmospheric pressure with an aim to improve their mechanical strength and biocompatibility for biomedical applications. The effects of plasma treatment on PVA/Cs nanofibers have been investigated using attenuated total reflectance-Fourier transform infrared spectroscopy (ATR-FTIR), field emission scanning electron microscopy (FESEM) and atomic force microscopy (AFM) analyses. In addition, contact angle is measured to assess hydrophillicity changes after plasma treatment while tensiometer is used to evaluate the mechanical strength of both untreated and plasma treated PVA/Cs nanofibers. The study is further involves in carrying out cytotoxicity tests to assess the biocompatibility of the plasma treated PVA/Cs nanofibers *in vitro*.

2. Experimental

2.1. Materials

Chitosan (Cs, low molecular weight, 85% deacetylated) and diiodomethane is purchased from Sigma Aldrich, USA. Polyvinyl alcohol (PVA) (99% hydrolyzed, average Mw = 145 kDa) and glacial acetic acid are purchased from MERCK, India. All materials were used without any further purification.

2.2. Preparation of PVA/Cs nanofibers

PVA is dissolved in distilled water (DW) at a concentration of 7 wt%, and Cs is dissolved in acetic acid (2 wt% v/v) at a concentration of 3 wt%. The prepared solutions, PVA and Cs, are blended together with weight ratio of 80:20 (PVA:Cs). Then the blended polymer solution is fabricated into nanofibers at room temperature using electrospinning unit (ESPIN Nano, Physics Equipment, Channai, India). The polymer solution is placed into a syringe (10 ml) with a 22 gauge stainless steel needle having an inner diameter of 0.413 mm and is dispersed at a rate of 0.5 ml/h. A high voltage of 18 kV is applied across the needle and grounded collector (stainless steel drum) which is covered by aluminum foil at a distant of 15 cm from the tip of needle. The nanofibers are collected on the surface of aluminum foil covering the drum collector at rotation speed of 1100 rpm and finally dried in vacuum oven for 24 h.

2.3. Plasma treatment of electrospun PVA/Cs nanofibers

Surface modification of electrospun PVA/Cs nanofibers is carried out using dielectric barrier discharge (DBD) plasma at atmospheric pressure. A schematic diagram of the DBD set-up is shown in Fig. 1. The discharge is produced between two copper electrodes (thickness = 5 mm, surface area = 25 cm × 25 cm) placed within a cubic enclosure. The upper electrode is covered with glass plate (thickness = 3 mm) and is connected to a high voltage source ((0–40 kV, 50 Hz, Zenoics Systech, India), while the lower electrode is grounded. The discharge chamber is pumped down to 0.5 mbar by a rotary pump (Hena 26, Pfeiffer, Pumping speed: 25 $m^3 h^{-1}$), while a gas flow rate of 2 slpm is passed through the chamber. The gas exhaust, connected to a stop valve, is controlled in such a way that the final working pressure is maintained at 1 bar during the plasma treatment. In this work Ar and O_2 gases are separately used to generate the plasma and each gas flow rate is monitored by digital mass flow controller (Alicat Scintific, USA). The PVA/Cs nanofibers are placed in between the two electrodes with a gap of 6 mm. Surface treatment of the test samples is separately carried out in Ar and O_2 plasmas at applied voltage of 15 KV and treatment time of 30 s. The plasma treated PVA/Cs nanofibers are then taken out of the discharge chamber and placed in vacuum desiccator for further characterizations.

2.4. Characterization techniques

2.4.1. Fourier transform infrared spectroscopy

The plasma treated and untreated PVA/Cs nanofibers are characterized by attenuated total reflectance Fourier transform infrared (ATR-FTIR) spectroscopy (IMPACT 410, NICOLET, USA). The spectra are obtained from a 200 μm diameter sampling area, using an average of 200 scans, at 4 cm^{-1} spectral resolution. Spectra are collected in transmittance mode with spectral region of 4000–650 cm^{-1}.

2.4.2. Contact angle measurement

The wettability of untreated and plasma treated PVA/Cs nanofibers is measured by the contact angle (using the sessile drop method) measurement system (Data Physics OCA 20, Germany). The system is

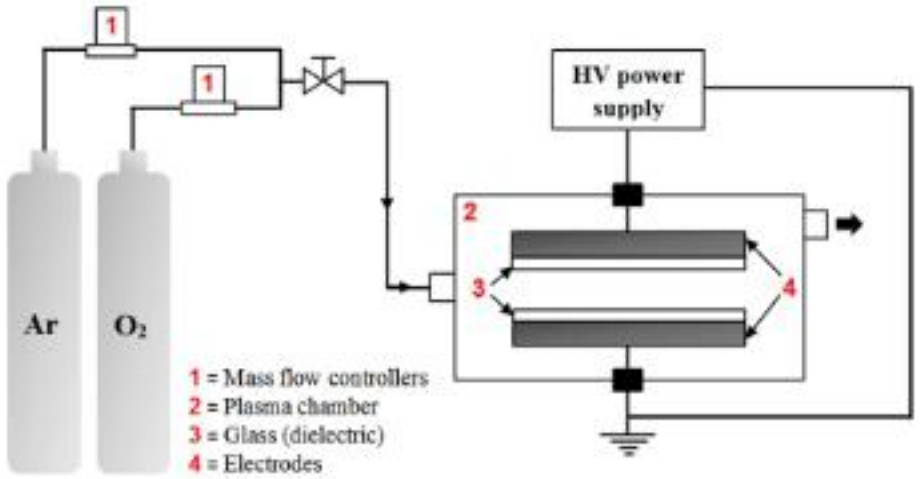

Fig. 1. Schematic of DBD plasma system.

Principal
Nowgong Girls' College
Nagaon :: Assam

Nowgong Girls' College
ESTD: 1962
Nagaon :: Assam

equipped with a software operated high precision liquid dispenser to precisely control the drop size of the used liquid. Small droplets of deionized water and diiodomethane (about 1.8 μl) are dropped on the nanofibers through a computer controlled process and the image is taken immediately. Each image of the drop is then stored *via* a CCD video camera, using a PC based acquisition and data processing system. As the measurement of the contact angle is obtained from the image that is captured immediately, the effect of evaporation on the real measurement can be ignored. In this experiment, five point measurements on each sample are randomly performed and the result is reported as mean ± standard deviation (SD). Surface energy (dispersive (hydrophobic, γ_s^d) and polar (hydrophilic, γ_s^p) components of the surface energy, γ_s) is calculated from the contact angle formed by the drop of liquid (deionized water and diiodomethane) on the surface of the test sample by Owens-Wendt method [16].

2.4.3. Morphological analysis of the surface

Field emission scanning electron microscope (FESEM, SIGMAVP, Carl Zeiss, Germany) is used to observe the surface morphologies of the samples. Prior to SEM examination, the samples are coated with gold/palladium alloy in sputtered coater (SC7620, Emitech) in a low vacuum. Atomic force microscopy (AFM) images are obtained in ambient atmospheric conditions with a digital multimode scanning probe microscope (SPM) (NTEGRA Vita, NT-MDT Spectrum Instruments, Russia) equipped with a nanoscope IVA controller (resolution: horizontal, 0.2 nm and vertical, 0.01 nm). The images are taken in tapping mode at a scanning rate of 1 Hz (scan size: 3 μm × 3 μm). The rms roughness of the PVA/Cs nanofibers is measured by NOVA image analysis software.

2.4.4. Tensile test

The samples are cut into a dumb bell shape according to ASTM D638-10 Type V and the mechanical strength of the samples are evaluated using a universal testing machine (INSTRON 4204) at a constant speed of 10 mm/min with a 10 kN load (temperature: 27 °C and relative humidity: 65%). The specimens are cut into strips of 10 mm × 50 mm (thickness = 0.25 mm) and a gauge length of 20 mm is considered. For each sample, data is taken for five times and the average of Young's modulus of elasticity, tensile strength and elongation at break (%) are evaluated from stress-strain curves. The data are presented as average ± standard deviation (SD).

2.4.5. Hemocompatibility studies

Venous blood is collected from a healthy human volunteer in heparinised tubes, stored at 4 °C and used within a week of collection. The plasma treated and untreated PVA/Cs nanofibers (1 cm^2 of each) are incubated with 10 ml of human blood (1: 9 dilution with 0.9% normal saline) for 1 h at 37 °C. Blood incubated with distilled water without test material is considered as positive control and with 0.9% normal saline is considers as negative control. After 1 h of incubation, the reaction mixture is centrifuged at 1500 rpm for 10 min and supernatant is carefully collected. The free hemoglobin present in the supernatant is measured at 540 nm using UV–visible spectrophotometer. The percentage of hemolysis is calculated using the following relation [17],

$$\text{Hemolysis } (\%) = \frac{(\text{Abs}_{\text{sample}} - \text{Abs}_{-\text{ve control}})}{(\text{Abs}_{+\text{ve control}} - \text{Abs}_{-\text{ve control}})} \times 100 \quad (1)$$

2.4.6. Cytocompatibility studies

The possible cytotoxic effect of plasma treated PVA/Cs nanofibers on mammalian cells are evaluated by MTT cell viability assay and the results are compared with the untreated ones [18]. L929 mouse fibroblast cells are obtained from NCCS, Pune and maintained as per the supplier's guidelines. 1×10^4 cells/well are seeded in a 96 well cell culture plate containing 100 μl DMEM (supplemented with 10% foetal bovine serum) media. At 24 h of post incubation, cultured cells are further incubated with 1 mg of each sample for next 24 h, 48 h and 72 h respectively. After completion of the stipulated time, the culture media is removed from the wells and treated with MTT dye (0.5 mg/ml) and incubated for 4 h at 37 °C. Further, 100 μl DMSO is added to each well to dissolve the blue formazan crystals and the absorbance (570 nm) is accordingly measured. The percentage cell viability is calculated by using the following relation,

$$\text{Cell viability } (\%) = \frac{N_t}{N_c} \times 100 \quad (2)$$

where N_t is the absorbance of the treated cells and N_c is the absorbance of the untreated cells. In this work, the experiments are performed in triplicate and results are reported as mean ± SD.

2.4.7. Statistical analysis

The results are expressed as mean ± SD. The significance of the differences among the experimental groups is determined by one-way analysis of variance (ANOVA) followed by Tukey test for multiple comparisons. A p value <0.05 is considered as significant. Prism version 6.00 (GraphPad Software) is used for statistical analysis.

2.5. Results and discussion

2.5.1. Fourier transform infrared spectroscopy

The ATR-FTIR spectra of PVA/Cs nanofibers before and after plasma (Ar & O_2) treatment are shown in Fig. 2(a). The absorption bands at 1561 cm^{-1}, 1658 cm^{-1} and 1320 cm^{-1} corresponds to amide-II, amide-I and amide-III bands respectively and are characteristic of chitosan [19]. The peaks at 2940 and 2900 cm^{-1} can be assigned to the stretching of $-CH_2-$ and $-CH-$ groups, respectively [20]. The bands at 1376 and 1413 cm^{-1} correspond to CH_3 symmetrical deformation mode [19]. The peak shown at 1700–1725 cm^{-1} is characteristic of carboxylic acid dimers, the presence of which is due to the acetic acid used for dissolving the chitosan [21]. All nanofiber mats show a broad absorption band between 3700 and 3000 cm^{-1} which corresponded to –NH/-OH symmetric stretching vibrations corresponding to chitosan and stretching vibration of hydroxyl (−OH) group from intermolecular and intramolecular hydrogen bonds of PVA [20]. The band is observed to be shifted to higher wavenumber after Ar and O_2 plasma treatment which is attributed to the formation of more of hydrogen bonding in PVA/Cs nanofibers [20,22].

This apparently leads to creation of a highly cross-linked complex structure in the nanofibers induced by Ar and O_2 plasma treatment. The enhanced cross-linked structure of PVA/Cs nanofibers after plasma treatment is further evident from the shifting and subsequent broadening of the absorption bands at 1561 cm^{-1} to higher wavenumber (Ar plasma: 1575 cm^{-1} and O_2 plasma: 1572 cm^{-1}) as seen from Fig. 2 (b)–(d) which depicts the deconvoluted ATR-FTIR spectra of the test samples in the region of interest (1800–1500 cm^{-1}). A schematic illustration of the possible cross-linked chemical structure PVA/Cs nanofibers after Ar and O_2 plasma treatment is shown in Fig. 3. In this simple schematic diagram, the oxygen containing functional groups of PVA is shown to be reacted with hydroxyl and amino groups of chitosan. The proposed cross-linking in plasma treated PVA/Cs nanofibers is facilitated by reactive atomic and molecular species, energetic ions, electrons and UV radiation that transfer energies by impinging on the surface of the nanofibers and subsequently activating the surface layer through formation of free radicals [23,24]. The free radicals produced at the surface of the polymer then either reacts among themselves or with the surface molecules (or both) thereby enabling cross-linking reactions on the surface and eventually resulting in wide range of surface chemistry.

Principal
Nowgong Girls' College
Nagaon :: Assam

Nowgong Girls' College
ESTD: 1962
Nagaon :: Assam

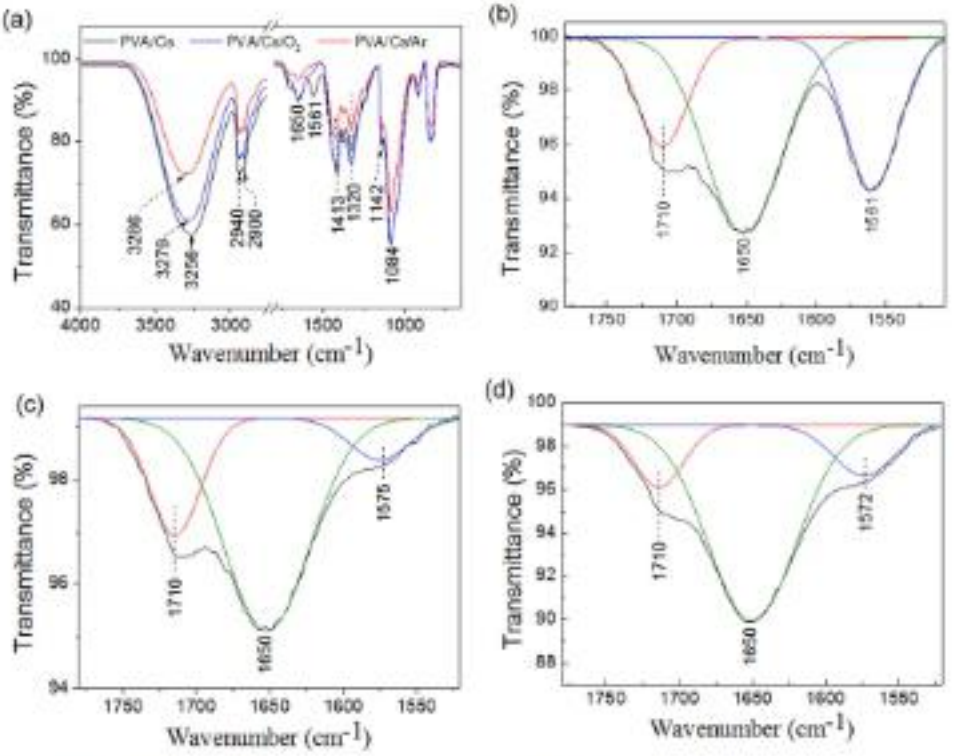

Fig. 2. (a) ATR-FTIR spectra of untreated and plasma (Ar and O_2) treated electrospun PVA/Cs nanofibers. Deconvoluted ATR-FTIR spectra of (b) PVA/Cs and (c) PVA/Cs/Ar and (d) PVA/Cs/O_2 nanofibers in the wavenumber region of interest (1800–1500 cm^{-1}).

2.5.2. Surface morphology analyses

Fig. 4(a)–(c) shows the FESEM micrographs of the non-treated and plasma treated electrospun PVA/Cs nanofibers mats. It is reveals that fibers without defects or beads are obtained and that the average diameter of the fiber is measured to be 167 nm. No visible surface damage is observed during plasma treatment of electrospun PVA/Cs nanofibers. However, AFM images (Fig. 4(d)–(f)) shows an increase in nanometer-scale roughness of the plasma treated electrospun PVA/Cs nanofibers which is attributed to the interaction of energetic ions impinging onto the polymer surfaces during plasma treatment [25]. The degree of surface roughness induced by O_2 plasma on PVA/Cs nanofibers is observed to be relatively higher than that induced by Ar plasma.

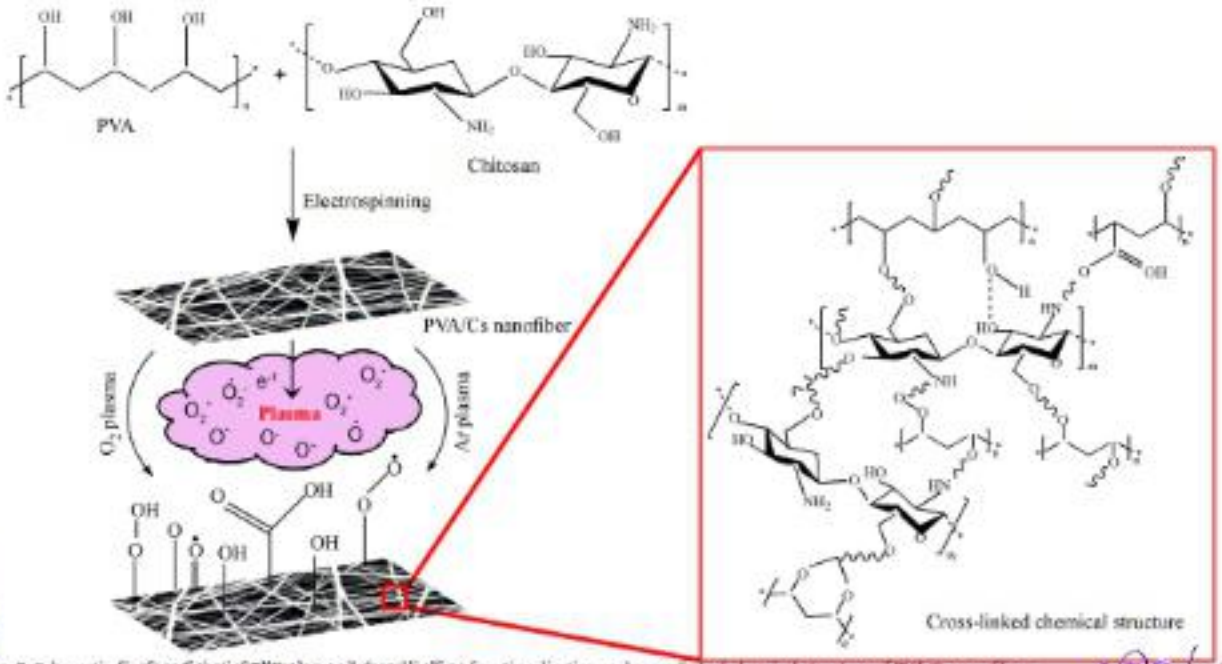

Fig. 3. Schematic [illegible] functionalization and cross-linked chemical structure of PVA/Cs nanofibers.

Nowgong Girls' College ESTD: 1962 Nagaon :: Assam
Principal Nowgong Girls' College Nagaon :: Assam

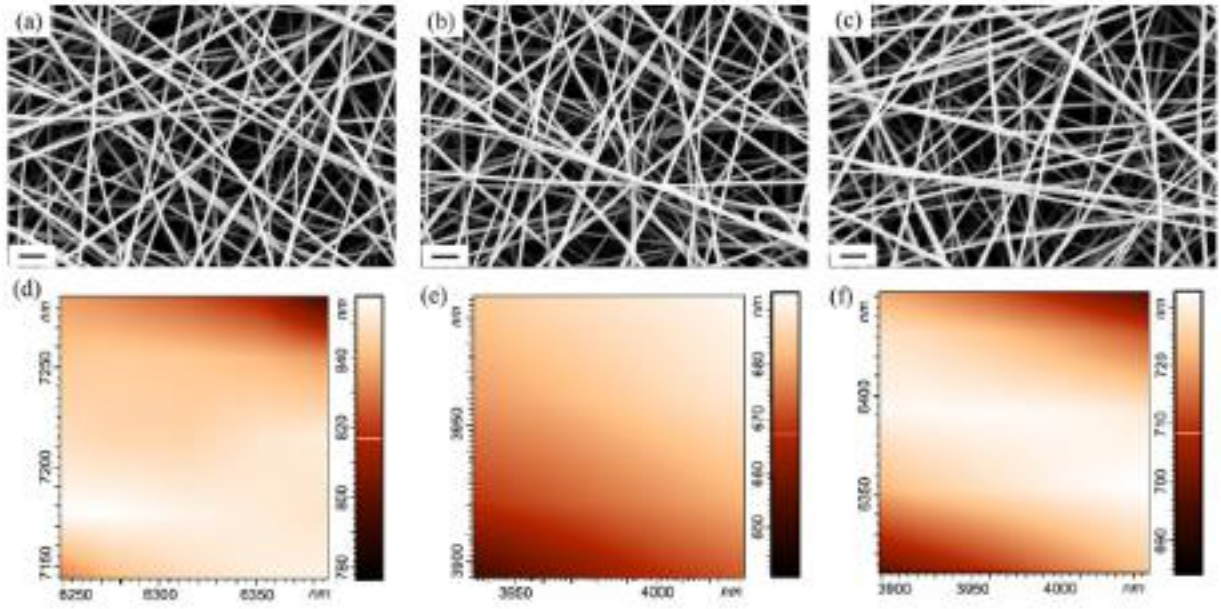

Fig. 4. FESEM images of (a) untreated PVA/Cs nanofibers and PVA/Cs nanofibers treated with DBD plasma with (b) Ar and (c) O_2 gases, respectively. AFM images of PVA/Cs nanofibers: (d) untreated; (e) Ar plasma treated and (f) O_2 plasma treated (FESEM images, scale: 1 μm).

This may be accounted for highly reactive oxygen ions impinging on the surface of PVA/Cs nanofibers which play active role in etching the surface during plasma treatment [25,26]. The inference drawn from above discussion indicates that Ar and O_2 plasma treatment of PVA/Cs nanofibers results in the change of surface topography at the nanoscale without any adverse effect on their bulk physical structure.

2.5.3. Surface wettability studies

The results of water contact angle and the corresponding surface energy measurements of the untreated and plasma treated PVA/Cs nanofibers are presented in Table 1. After Ar and O_2 plasma treatment, the contact angle on PVA/Cs nanofibers is observed to be decreased rapidly. That is attributed to the increasing of surface roughness after the plasma treatment. The wettability increase effect is further related to plasma-induced formation and subsequent incorporation of polar groups on the surface of PVA/Cs nanofibers after Ar and O_2 plasma treatment, as evident from the increase in polar components of the total surface energy. The introduction of polar groups on the surface of PVA/Cs/Ar nanofibers may be accounted for the presence of residual oxygen content in the discharge chamber during Ar plasma treatment at working pressure of 0.5 mbar. In case of PVA/Cs/O_2 nanofibers, a relative increase in water contact angle by 25% and decrease in surface energy by 15% over PVA/Cs/Ar nanofibers can be attributed to high reactivity of oxygen ions which eventually leads to high surface roughness and more incorporation of oxygen containing functional groups on the surface.

2.5.4. Tensile test

The observed mechanical properties in terms of tensile strength, Young's modulus and elongation at break (%) of PVA/Cs nanofibers before and after plasma (Ar and O_2) treatment are presented in Table 2. All of the samples are tested after being conditioned in a laboratory environment (23 °C and 35% relative humidity) for 24 h under identical conditions. It is revealed that Ar and O_2 plasma treatment of PVA/Cs nanofibers results in increase in tensile strength by 11.6% and 15.6% respectively whereas the Young's modulus is increases by 33.8% and 37.3% respectively. Besides, elongation at break (%) is observed to be decreased thereby indicating an increase in stiffness of PVA/Cs/Ar and PVA/Cs/O_2 nanofibers. The increase in tensile strength and Young's modulus coupled with a decrease of elongation at break can be explained by formation of strong hydrogen bonds in PVA/Cs nanofibers matrix induced by Ar and O_2plasma treatment which contributes to high cross-linked density in the nanofibers and causes superior load transfer to the nanofiber matrix [27]. It has been reported that strong interaction occurs between PVA and Cs during blending through formation of intermolecular and intramolecular hydrogen bonds [28]. Ar and O_2 plasma treatments further felicitate the formation of hydrogen bonds in the PVA/Cs nanofibers matrix through interactions between active plasma species and the surface molecules. The interactions result in chain scission and rearrangement of the polymer chains through formation of chemical (intermolecular and intramolecular hydrogen) bonds onto the surface thereby leading to formation of highly cross-linked PVA/Cs nanofibers matrix.

2.5.5. Hemocompatibility studies

The untreated and plasma treated PVA/Cs nanofibers are incubated with blood samples and the results are presented in Fig. 5(a). As negative and positive controls, blood is incubated in saline and distilled water, respectively. It is observed that hemolysis is <0.5% for PVA/Cs nanofibers and does not vary significantly with PVA/Cs/Ar and PVA/Cs/O_2 nanofibers respectively. The observed hemolytic activities of the untreated and plasma treated PVA/Cs nanofibers are thus far below the permissible limit of hemolysis (up to 5%) for biomaterials [29]. The samples subjected to hemolysis studies are further observed under FESEM and the results are shown in Fig. 5(b)–(f). It is evident that

Table 1
Contact angle and surface free energy of untreated and plasma treated (Ar and O_2) electrospun PVA/Cs nanofibers.

Sample	Contact angle (°)		Surface free energy (mJ/m²)		
	Water	Diiodomethane	Dispersive	Polar	Total
PVA/CS	77.23 ± 0.57	46.4 ± 0.65	31.91 ± 0.21	0.44 ± 0.08	38.35 ± 0.34
PVA/CS/Ar	31.03 ± 0.39	19.26 ± 0.31	20.11 ± 0.32	41.60 ± 0.72	61.71 ± 0.74
PVA/CS/O_2	23.10 ± 0.18	12.14 ± 0.14	21.81 ± 0.41	51.09 ± 0.42	72.90 ± 0.80

Nowgong Girls' College ESTD: 1962 Nagaon :: Assam
Principal Nowgong Girls' College Nagaon :: Assam

Table 2
Mechanical properties of untreated and plasma treated (Ar and O_2) electrospun PVA/Cs nanofibers.

Sample	Tensile strength (MPa)	Young modulus (MPa)	Elongation at break (%)
PVA/Cs	20.5 ± 0.35	69.70 ± 0.75	433 ± 1.12
PVA/Cs/Ar	23.2 ± 0.30	105.5 ± 0.84	346 ± 0.90
PVA/Cs/O_2	24.3 ± 0.32	111.3 ± 0.65	326 ± 0.72

there is no effect on RBC morphology induced by PVA/Cs, PVA/Cs/Ar and PVA/Cs/O_2 nanofibers which corroborates the above results. The hemolysis data therefore suggest that all the test samples can meet the hemocompatibility requirements of biomedical materials and can be used as biomaterial without causing any acute hemolysis.

2.5.6. Cytocompatibility studies

The viability of L929 mouse fibroblast is tested on the untreated and plasma treated PVA/Cs nanofibers after culturing for 24, 48 and 72 h respectively (Fig. 6). After 24 h of culture, cell viabilities on PVA/Cs, PVA/Cs/Ar and PVA/Cs/O_2 nanofibers are 93.7 ± 2.71%, 94.2 ± 1.84% and 96.5 ± 1.68%, respectively. Similar results on cell viability are obtained after 48 h of culture. After 72 h, cell viabilities on PVA/Cs, PVA/Cs/Ar and PVA/Cs/O_2 nanofibers are 81.5 ± 2.11%, 84.3 ± 1.73% and 88.6 ± 1.61%, respectively. It is revealed that Ar and O_2 plasma treatment enhances cytocompatibility of PVA/Cs nanofibers up to the observation period of 72 h as compared to untreated one. The improved cytocompatibility can be due to incorporation of polar groups and formation of nano-structured roughness on the surface of AASF which subsequently enhances cell adhesion and proliferation. The more hydrophilicity of PVA/Cs/O_2 nanofibers may further improve its cytocompatible nature over PVA/Cs/Ar nanofibers as observed from the results after 24, 48 and 72 h of culture. These studies clearly confirm that the cells show viability in the presence of the test samples and the plasma treatment does not cause any adverse effect on the cytocompatibility of PVA/Cs nanofibers.

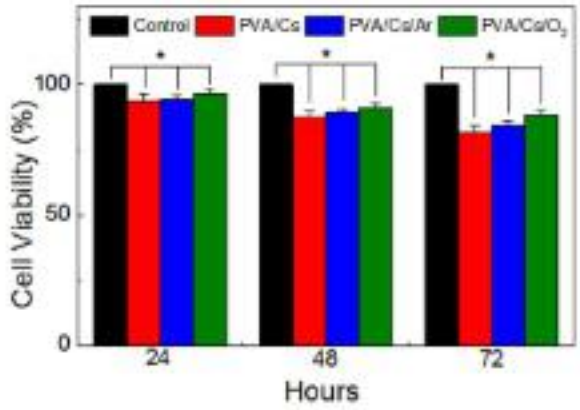

Fig. 6. Viability (%) of L929 mammalian cells at different time points post incubation with PVA/Cs, PVA/Cs/Ar and PVA/Cs/O_2 nanofibers (*$p < 0.05$ compared with control). All the results are expressed in mean ± SD of three batches. Control: Cell with no treatment. (Some error bars are too small to be shown).

3. Conclusion

In this study, surface modification of electrospun PVA/Cs nanofibers is carried out using Ar and O_2 DBD plasmas at atmospheric pressure. Both PVA/Cs/Ar and PVA/Cs/O_2 nanofibers show rapid decrease in contact angle with water as compared to untreated nanofibers, which is attributed to plasma-induced surface roughness and increase in the contents of oxygen and oxygen containing polar functional groups on the surfaces. ATR-FTIR analyses of the PVA/Cs/Ar and PVA/Cs/O_2 nanofibers reveal an increase in the degree of cross-link density which subsequently improves their mechanical properties in terms of increasing tensile strength and Young's modulus. *In vitro* hemolysis assay reveals that Ar and O_2 plasma treatment has no adverse effect on hemocompatibility of PVA/Cs nanofibers. Both PVA/Cs/Ar and PVA/Cs/O_2 nanofibers are observed to exhibit better cytocompatibility than AASF which is attributed to good hydrophilic nature and formation of nano-structured roughness on the surfaces. The DBD plasma surface functionalized PVA/Cs nanofibers may find potential applications with

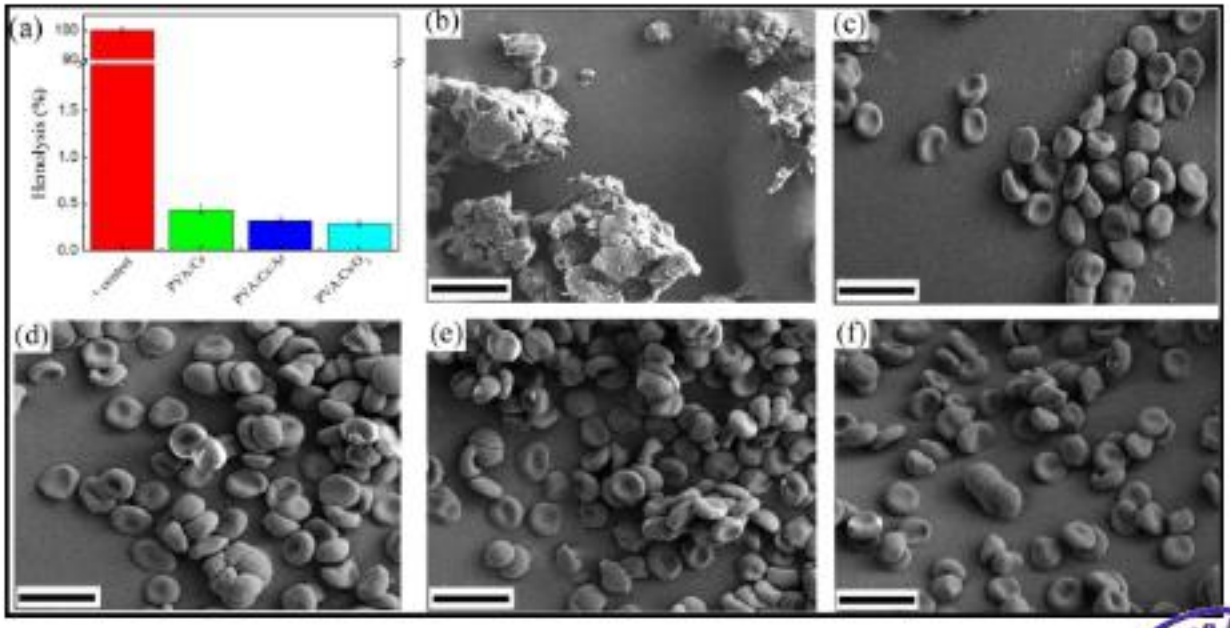

Fig. 5. (a) Hemolysis (%) of human red blood cells after incubation with PVA/Cs, PVA/Cs/Ar and PVA/Cs/O_2 nanofibers. Values represent mean ± SD of three batch[illegible] distilled water. Surface morphologies of RBC subjected to hemolysis test with (b) DW, (c) saline, (d) PVA/Cs and (e) PVA/Cs/Ar and (f) PVA/Cs/O_2 nanofiber[illegible] ved under FE[illegible] images, scale: 10 μm).

Principal
Nowgong Girls' College
Nagaon :: Assam

Nowgong Girls' College
ESTD: 1962
Nagaon :: Assam

improved mechanical strength and biocompatibility as wound dressings and scaffolds for tissue engineering.

Acknowledgment

This research is supported by DST-SERB (Grant No. SR/FTP/PS-147/2012) funded by Department of Science and Technology (DST), India. Arup Jyoti Choudhury expresses gratitude to DST, India for providing financial support through DST-INSPIRE Faculty program (Grant No. IFA14-PH-93) and Tezpur University, Assam, India for hosting the DST-INSPIRE Faculty fellowship. Namita Ojah acknowledges the support provided by DST, India in the form of fellowship under DST-INSPIRE Faculty program.

Conflict of interest

The authors declare no conflict of interest.

References

[1] T. Jiang, E.J. Carbone, K.W.H. Lo, C.T. Laurencin, Electrospinning of polymer nanofibers for tissue regeneration, Prog. Polym. Sci. 46 (2015) 1–24.
[2] H. Li, Y. Xu, H. Xu, J. Chang, Electrospun membranes: control of the structure and structure related applications in tissue regeneration and drug delivery, J. Mater. Chem. B 2 (2014) 5492–5510.
[3] D.I. Braghirolli, D. Steffens, P. Pranke, Electrospinning for regenerative medicine: a review of the main topics, Drug Discov. Today 19 (2014) 743–753.
[4] H.S. Yoo, T.G. Kim, T.G. Park, Surface-functionalized electrospun nanofibers for tissue engineering and drug delivery, Adv. Drug Deliv. Rev. 61 (2009) 1033–1042.
[5] K. Park, Y.M. Ju, J.S. Son, K.D. Ahn, D.K. Han, Surface modification of biodegradable electrospun nanofiber scaffolds and their interaction with fibroblasts, J. Biomater. Sci. Polym. Ed. 18 (2007) 369–382.
[6] F. Yao, L. Xu, B. Lin, G. Fu, Preparation and applications of functional nanofibers based on the combination of electrospinning, controlled radical polymerization and 'Click Chemistry', Nano 2 (2010) 1348–1357.
[7] U. Stachewicz, C.A. Stone, C.R. Willis, A.H. Barber, Charge assisted tailoring of chemical functionality at electrospun nanofiber surfaces, J. Mater. Chem. 22 (2012) 22935–22941.
[8] E. Afshari, S. Mazinani, S. Ranaei-Siadat, H. Ghomi, Surface modification of polyvinyl alcohol/malonic acid nanofibers by gaseous dielectric barrier discharge plasma for glucose oxidase immobilization, Appl. Surf. Sci. 385 (2016) 349–355.
[9] L.A. Can-Herrera, A. Ávila-Ortega, S. de la Rosa-García, A.I. Oliva, J.V. Cauich-Rodríguez, J.M. Cervantes-Uc, Surface modification of electrospun polycaprolactone microfibers by air plasma treatment: effect of plasma power and treatment time, Eur. Polym. J. 84 (2016) 502–513.
[10] D. Gogoi, A.J. Choudhury, J. Chutia, A.R. Pal, N.N. Dass, D. Devi, D.S. Patil, Enhancement of hydrophobicity and tensile strength of muga silk fiber by radiofrequency Ar plasma discharge, Appl. Surf. Sci. 258 (2011) 126–135.
[11] J. Wang, L. Wang, H. Yu, Zain-ul-Abdin, Y. Chen, Q. Chen, W. Zhou, H. Zhang, X. Chen, Recent progress on synthesis, property and application of modified chitosan: an overview, Int. J. Biol. Macromol. 88 (2016) 333–344.
[12] X. Geng, O. Kwon, J. Jang, Electrospinning of chitosan dissolved in concentrated acetic acid solution, Biomaterials 26 (2005) 5427–5432.
[13] S. Fathollahipour, A.A. Mehrizi, A. Ghaee, M. Koosha, Electrospinning of PVA/chitosan nanocomposite nanofibers containing gelatin nanoparticles as a dual drug delivery system, Biomed. Mater. Res. A 103A (2015) 3852–3862.
[14] A. Pangon, S. Saesoo, N. Saengkrit, U. Ruktanonchai, V. Intasanta, Multicarboxylic acids as environment-friendly solvents and in situ crosslinkers for chitosan/PVA nanofibers with tunable physicochemical properties and biocompatibility, Carbohydr. Polym. 138 (2016) 156–165.
[15] S.A. Majd, M.R. Khorasgani, S.J. Moshtaghian, A. Talebi, M. Khezri, Application of chitosan/PVA Nano fiber as a potential wound dressing for streptozotocin-induced diabetic rats, Int. J. Biol. Macromol. 92 (2016) 1102–1108.
[16] D. Owens, R. Wendt, Estimation of the surface free energy of polymers, J. Appl. Polym. Sci. 13 (1969) 1741–1747.
[17] N. Kasoju, R.R. Bhonde, U. Bora, Fabrication of a novel micro–nano fibrous nonwoven scaffold with Antheraea assama silk fibroin for use in tissue engineering, Mater. Lett. 63 (2009) 2406–2409.
[18] S. Kalita, R. Kandimalla, K.K. Sharma, A.C. Kataki, D. Deka, J. Kotoky, Amoxicillin functionalized gold nanoparticles reverts MRSA resistance, Mater. Sci. Eng. C 61 (2016) 720–727.
[19] E.S. Costa-Júnior, E.F. Barbosa-Stancioli, A.A.P. Mansur, W.L. Vasconcelos, H.S. Mansur, Preparation and characterization of chitosan/poly(vinyl alcohol) chemically crosslinked blends for biomedical applications, Carbohydr. Polym. 76 (2009) 472–481.
[20] A. Çay, M. Miraftab, E.P.A. Kumbasar, Characterization and swelling performance of physically stabilized electrospun poly(vinyl alcohol)/chitosan nanofibres, Eur. Polym. J. 61 (2014) 253–262.
[21] T. Wang, M. Turhan, S. Gunasekaran, Selected properties of pH-sensitive, biodegradable chitosan–poly(vinyl alcohol) hydrogel, Polym. Int. 53 (2004) 911–918.
[22] A. Barth, C. Zscherp, What vibrations tell us about proteins, Q. Rev. Biophys. 35 (2002) 369–430.
[23] A. Liguori, A. Bigi, V. Colombo, M.L. Focarete, M. Gherard, C. Gualandi, M.C. Oleari, S. Panzavolta, Atmospheric pressure non-equilibrium plasma as a green tool to crosslink gelatin nanofibers, Sci. Rep. 6 (2016) 38542/1–11.
[24] R.M. France, R.D. Short, Plasma treatment of polymers effects of energytransfer from an argon plasma on the surface chemistry of poly(styrene), low density poly(ethylene), poly(propylene)and poly(ethylene terephthalate), J. Chem. Soc. Faraday Trans. 17 (1997) 3173–3178.
[25] A.J. Choudhury, S.A. Barve, J. Chutia, H. Kakati, A.R. Pal, Jagannath, N. Mithal, R. Kishore, M. Pandey, D.S. Patil, Effect of impinging ion energy on the substrates during deposition of SiO_x films by radiofrequency plasma enhanced chemical vapor deposition process, Thin Solid Films 519 (2011) 7864–7870.
[26] M.R. Sanchis, O. Calvo, O. Fenollar, D. García, R. Balart, Surface modification of a polyurethane film by low pressure glow discharge oxygen plasma treatment, Appl. Surf. Sci. 105 (2007) 1077–1085.
[27] A.R. Kakroodi, S. Cheng, M. Sain, A. Asiri, Mechanical, thermal and morphological properties of nanocomposites based on polyvinyl alcohol and cellulose nanofiber from aloe vera rind, J. Nanomater. 139 (2014) 1–7.
[28] M. Koosha, H. Mirzadeh, Electrospinning, mechanical properties, and cell behavior study of chitosan/PVA nanofibers, J. Biomed. Mater. Res. A 103A (2015) 3081–3093.
[29] N. Sanoj Rejinold, A. Naira, M. Sabithaa, K.P. Chennazhia, H. Tamurab, S.V. Naira, R. Jayakumar, Synthesis, characterization and in vitro cytocompatibility studies of chitin nanogels for biomedical applications, Carbohydr. Polym. 87 (2012) 943–949.

Principal
Nowgong Girls' College
Nagaon :: Assam

Nowgong Girls' College
ESTD: 1962
Nagaon :: Assam

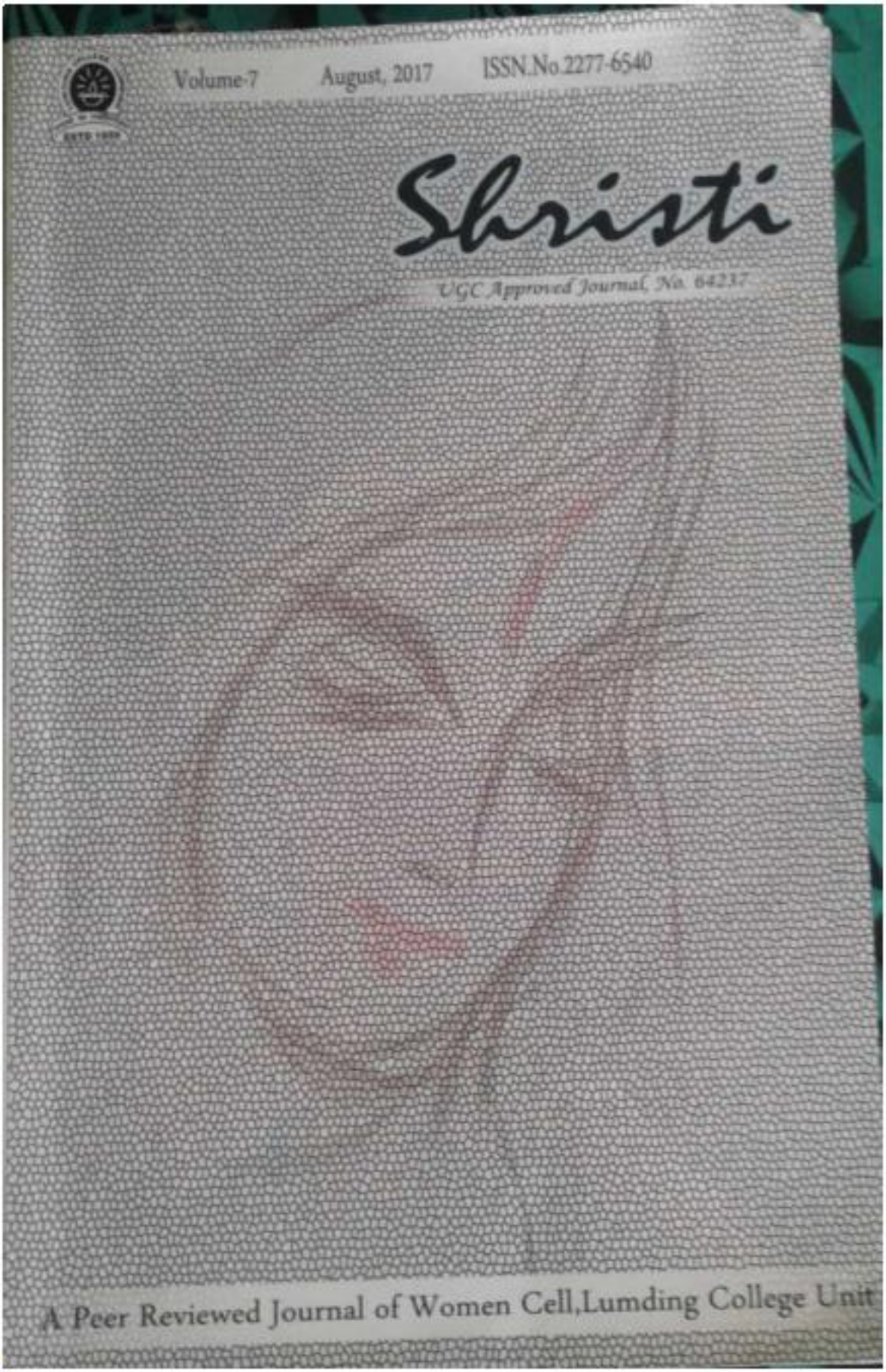

Nowgong Girls' College ESTD: 1962 Nagaon :: Assam

Principal
Nowgong Girls' College
Nagaon :: Assam

A Peer Reviewed Journal of the Women Cell Lumding College Unit
Lumding, Hojai, Assam, 782-447

Patron
Dr. Mrinal Kanti Paul
Principal

Editorial Board

Chief Editor
Dr. Jahnabi Das

Editors
Binita Bhuiyan Onkita Misra

Review Committee

Dr. Dipendu Das, Associate Professor, Deptt. of English, Assam University. Dr. Sima Paul, Associate Professor, Deptt. of Education, Assam University. Dr. Durba Deb, Assistant Professor, Deptt. of Bengali, Assam University. Dr. Sanjay Bhattacharjee, Assistant Professor, Deptt. of Bengali, Gauhati University. Dr. Jitupama Goswami, Assistant Professor, Deptt. of Mathematics, Gauhati University. Dr. Joshodev Arjun, Associate Professor, Deptt. of Zoology, Lumding College. Sri Anjan Kumar Dey, Associate Professor, Deptt. of Physics, Lumding College. Dr. Sanjay Kanti Das, Associate Professor, Deptt. of Commerce, Lumding College. Dr. Gitanjali Nath, Assistant Professor, Deptt. of Assamese, Lumding College. Sri Rajesh Barman, Assistant Professor, Deptt. of Hindi, Lumding College.

© 2017, Women Cell, Lumding College Unit
ISSN 2277-6540

Cover: Concept-Dr. Nibedita Dutta, Dr. Gitanjali Nath
Design-Biswajyoti Purkayastya(Bisu)

Published by Women Cell, Lumding College Unit, Lumding-782 447, Phone: 03674-26364
Fax: 03674-263375, Website :www.lumdingcollege.org

Printed at Rani Publication, Lumding

Nowgong Girls' College ESTD: 1962 Nagaon :: Assam

Principal
Nowgong Girls' College
Nagaon :: Assam

ISSN 2277-6540

A PEER REVIEWED JOURNAL
OF
THE WOMEN CELL, LUMDING COLLEGE UNIT

Vol.7 August 2017

CONTENTS

Section: A Literature

অসমীয়া সাহিত্যৰ 'পৰমাৰ্থী' হেমচন্দ্ৰ গোস্বামী
ড° বহুকান্ত হাজৰিকা ১

লীলা গণ্ডোৰ 'দৈ বৈ যায়' উপন্যাসত জাতীয় উৎসৱ বিহৰ প্ৰতিফলন : এটি চমু আলোচনা
কল্পনী চক্ৰবৰ্তী ৭

ৰবীন্দ্ৰনাথ ও নাৰীবাদ : একটি অনুসন্ধান
শহীদ আতিক-উজ-জামান ১১

নিৰ্বাচিত সাম্প্ৰতিক বাংলা ছোটগল্পে লিঙ্গ-বৈষম্য : তাত্ত্বাত্ত্বিক পৰ্যবেক্ষণ
দেবাৰতি জানা ২১

তুলনামূলক সাহিত্যতত্ত্ব : একটি বিশ্লেষণাত্মক অধ্যয়ন
ড° সন্ধ্যা ভট্টাচার্য ২৯

ড° প্ৰ্যাট্ৰিক্সৰ সংখ্যাতত্ত্ব, সত্যজিতৰ শব্দবিজ্ঞান : প্ৰসঙ্গ 'সমস্কাৰৰ চাৰি'
ড° জাহ্নবী দাশ ৪৫

বাংলা কবিতাৰ শিৰোনামে সময়ৰ চিহ্ন : একটি অনুসন্ধান
মৌসুমী চক্ৰবৰ্তী ৫১

আৱশ্যক ও অৱশ্যৰ অধিকাৰ : একটি তুলনামূলক আলোচনা
নাৰায়ণ দত্ত ৫৭

ৰবীন্দ্ৰনাথ ঠাকুৰৰ 'বিসৰ্জন' ও মামনি ৰয়চম গোস্বামীৰ 'ছিন্নমস্তাৰ মনুহটো' : একটি তুলনামূলক অধ্যয়ন
অঙ্কিতা মিশ্ৰ ৬১

বাংলা সাহিত্য ও ৰামায়ণ : একটি গবেষণামূলক আলোচনা
মৌসুমী কাসেৰপিক ৬৭

তিতাস নদী ও মালো সমাজ : প্ৰসঙ্গ 'তিতাস একটি নদীৰ নাম'
জানকী প্ৰসাদ দেবনাথ ৭১

সুচিত্ৰা ভট্টাচাৰ্যৰ 'কাছের মানুষ' উপন্যাসে প্ৰতিফলিত নাগৰিক জীবন : একটি অধ্যয়ন
অমৃতা সিকিদাৰ ৭৭

পুনৰ্জন্ম : একটি বিশ্লেষণাত্মক অধ্যয়ন
ড° গীতা ৰাণী দে ৮৩

Nowgong Girls' College ESTD: 1962 Nagaon :: Assam

Principal
Nowgong Girls' College
Nagaon :: Assam

Journal Women Cell, Lumding College Unit ISSN-2277-6540
Vol. 7, August - 2017, pp-83-88

পুনর্জন্ম : একটি বিশ্লেষণাত্মক অধ্যয়ন

ড° গীতা রানী দে, সহকারী অধ্যাপক, বাংলা বিভাগ, নগাঁও গার্লস কলেজ

সংক্ষিপ্তসার

পুনর্জন্ম কথাটি শিশুমহলে নিত্যদিন শিহরণ জাগায়। শিশু হারানোর কথা আজকাল প্রায় প্রতিদিন শোনা যায়। খবরের কাগজের প্রথম পাতা এখানকার কথা। বাবা-মায়ের হাতিয়ে যাওয়া কিছুক্ষণ পরেই ফিরিয়ে দেওয়া হয়েছে। হারিয়ে যাওয়া শিশুকে খুব কমই খুঁজে পাওয়া যায়। লক্ষ্মণের গণ্ডিরেখার এই গল্পের সমস্যাটিকে তাই এই গল্পে ভুল দিয়েছেন।

মহিলা এবং সমাজ ওতপ্রোতভাবে একে অপরের সাথে জড়িয়ে আছে। সমাজের বিভিন্ন ঘটনা, কাহিনী ইত্যাদি ভুল পথে পরিচালনা। সমাজের 'অতিরিক্ত' থাকে একটা দৃশ্য প্রচলিত আছে। যার অর্থ হল, পূর্ব জন্মের কথা স্মরণে পড়ে এমন। পরজন্মে সন্তান অন্যান্যদের কথা বলা হয়েছে।

পুনর্জন্ম গল্পে দেখা যায়, একসময় হারিয়ে যাওয়া শিশুকাকে খুঁজে পাওয়া গেছে পরে পরিবারে, নতুন মানুষ-পিতার কাছে। সেই শিশু ফিরতে পারে তার পূর্ব জন্মের মানুষ-পিতা-মাতাদের। এমনকি সে পরিবারে শৈশবের খুন হয়েছিল, সে সন্ধান করতে পারে। লক্ষ্মণের দৃষ্টি পুনর্বিচার বিশ্লেষিত। পরে ঐতিহ্যিক পুনর্জন্মের কথা সম্পূর্ণ ভিন্ন। খুব খুশি নিয়ে আছে একটা বাচ্চাদের কাহিনী একজন শিক্ষক তাদিকে সমাধানে ওনিয়েছে। আছে নিজের জন্মদিনে শিক্ষকের পরিবার থেকে হারিয়ে নিজের কুমারী মাতৃত্বকাল পুনরায় ফেরী পেয়েছে। – এই সমস্ত বিষয়গুলি পুনর্জন্ম : একটি বিশ্লেষণাত্মক অধ্যয়ন শীর্ষক গবেষণা পত্রে আলোচনা করা হবে।

মূল শব্দ : শিশু অপহরণ, শিশু হারা, পুনর্জন্ম, জাতিস্মর, কুমারী মাতৃত্ব।

১. ভূমিকা :

সিদ্ধার্থ সিংহ পুনর্জন্ম (২০১৫) গল্পে পুনর্জন্মের কথা বলেছেন। একবার কোন ব্যক্তির মৃত্যু হওয়ার পর পুনরায় জন্ম হয়, এমন একটা ধর্মীয় বিশ্বাস সমাজে দীর্ঘদিন ধরে চলছে। শাস্ত্রগ্রন্থ সমূহে ধর্মীয় যুক্তি সহকারে পুনর্জন্মের বিষয়ে বিস্তারিত আলোচনা করা হয়েছে। যেমন,- শ্রীমদ্ভাগবদগীতায় বলা হয়েছে,

"বহুনাং জন্মনামন্তে জ্ঞানবান্ মাং প্রপদ্যতে।
বাসুদেবঃ সর্বমিতি স মহাত্মা সুদুর্লভঃ।।"

অর্থাৎ "বহুজন্মের পরে জ্ঞানী আমাকে প্রাপ্ত হন। যারা বিদ্যু আছে সেই সর্বব্যাপী বাসুদেব- এইরূপ জ্ঞানসম্পন্ন মহাত্মা সুদুর্লভ।" এছাড়াও অষ্টম অধ্যায়ের ২১ সংখ্যক , ২২ সংখ্যক, ২৩ সংখ্যক শ্লোকে পুনর্জন্মের কথা বিস্তারিত ভাবে আলোচনা করা হয়েছে। রামায়ণে এবং মহাভারতেও পুনর্জন্মের প্রসঙ্গ আলোচিত হয়েছে। যেমন, রামায়ণে বলা হয়েছে, সীতা পূর্বজন্মে কুশধ্বজের কন্যা বেদবতী ছিলেন।" আবার মহাভারতে বলা হয়েছে, অষ্টবসুর মধ্যে দ্যু-নামক বসু নিজের কর্মফল ভোগ করার জন্য শান্তনুর ঔরসে জন্ম লাভ করেন।" বৌদ্ধ ধর্মাবলম্বীদের একটি গুরুত্বপূর্ণ গ্রন্থ হল, ধম্মপদ। সেখানে বলা হয়েছে,

"পঠবী সমো নো বিরুজ্ঝতি
ইন্দখীলুপমো তাদি সুব্বতো
রহদো ব অপেতকদ্দমো
সংসারা ন ভবন্তি তাদিনো।"

অর্থাৎ- "শীলাজিতত সেই পুরুষ পৃথিবীর ন্যায় সহিষ্ণু, ভদ্র সদৃশ দৃঢ়, কর্দমহীন হ্রদের ন্যায় , তাদৃশের পুনর্জন্ম নাই।" এছাড়াও ১ম অধ্যায় (১২৬ সংখ্যক শ্লোক), ১৮শ অধ্যায় (২৩৮ সংখ্যক শ্লোক), ২০ শ অধ্যায় (৩৩৪ সংখ্যক শ্লোক), ২৮শ অধ্যায়ে (৪২৩ সংখ্যক শ্লোক) পুনর্জন্মের কথা বলা হয়েছে। জাতকের গল্পেও পুনর্জন্মের কথা আছে।

কুমারী মাতার বিষয়ে আলোচনা করতে হলে যাঁর কথা মনে আসে তিনি হলেন, মহাকবি ব্যাসদেব রচিত মহাভারতের পাণ্ডব জননী কুন্তী। তিনি কুমারী অবস্থায় ঋষি দুর্বাসাকে সন্তুষ্ট করে একটি মন্ত্র লাভ করেছিলেন। মন্ত্র প্রদান কালে ঋষি দুর্বাসা তাঁকে বলেছিলেন,

"যং যং দেবং ত্বমেতেন মন্ত্রেণাবাহয়িষ্যসি।
তস্য তস্য প্রসাদাত্ত্বং দেবি পুত্রান্ জনিষ্যসি।।"

Newgong Girls' College ESTD: 1962 Nagaon :: Assam
Principal Newgong Girls' College Nagaon :: Assam

Papers published per teacher in the Journals notified on UGC website during the Academic Session: 2018-19

Submitted to the NAAC for 3rd Assessment Cycle of Assessment & Accreditation

NOWGONG GIRLS' COLLEGE

Re-accreditated at A Grade by the NAAC (2nd Cycle)

Principal
Nowgong Girls' College
Nagaon :: Assam

Nowgong Girls' College
ESTD: 1962
Nagaon :: Assam

संस्कृत साहित्य की आधुनिक प्रासंगिकता : अभिज्ञान शाकुन्तलम् के आलोक में

❑डॉ. मनिका शइकीया❑

भारतीय साहित्य धर्मानुखी साहित्य है। आदि साहित्य वेदों से लेकर परवर्ती समय में लिखित प्रत्येक संस्कृत साहित्य लोक-संपृक्त साहित्य के रूप में परिलक्षित हुए हैं। शायद यही कारण है, हजार-हजार वर्ष पूर्व लिखित ये साहित्य आज भी मनुष्य मात्र को अपनी ओर आकर्षित करने में समर्थ हो रही है। महाकवि भासकृत 'स्वप्नवासवदत्ता' में वर्णित कथांश हो, 'पंचतंत्रम्' की कहानियाँ हो, गीताशास्त्र में निहित सारगर्भित उपदेश हो- सभी काल निर्विशेष ग्रहणयोग्य हैं। संस्कृत के विषय में गदी प्रसाद पंचौलीजी का कहना है- 'संस्कृत भाषा ने ज्ञान को ज्ञान और विज्ञान को विज्ञान की व्याख्या प्रदान की। ज्ञान को इतना उत्कृष्ट बनाया कि वह ब्रह्म का स्वरूप बन गया-, सर्वं ज्ञानमयं ब्रह्म। उसे जीवन का आधार बना दिया- ऋतेज्ञानान्न मुक्तिः। वेद माता हास्तुता सरस्वती वेदमाता। यह मानवता का संविधान है। उसको जीवन में अपनाकर श्रेष्ठ मानव -आर्य बनने का संकल्प साकार किया जाता है। संस्कृत ने विश्वमानुष की धारणा दी। 'वसुधैव कुटुम्बकम्' की भावना उसी का विकास है।

महाकवि कालिदासकृत 'अभिज्ञानशाकुन्तलम्' आज के परिदृश्य में प्रासंगिक क्यों है, इस पर विचार करते समय हमने देखा कि प्रस्तुत नाटक के सभी मूल पात्र, वर्णित प्रसंग तथा संदेश आदि वर्तमान समय में भी उतने ही प्रासंगिक हैं, जितना उस पुरातन समय में थे। सबसे पहले प्रस्तुत नाटक में वर्णित उस वर्णन को ले सकते हैं, कि जब दुर्वासा मुनि आते हैं और शकुंतला अपनी खोई हुई सुखद स्मृतियों में खोई रहती है। शकुंतला अभ्यागत को अनदेखा करती है और दुर्वासा क्रोधित होकर उसे श्राप देते हैं। इस प्रसंग की अवतारणा प्रस्तुत नाटक के लिए कितना महत्वपूर्ण है, प्रत्येक दर्शक, पाठक समझता है। हमारे दृष्टि में प्रस्तुत प्रसंग प्रत्येक मनुष्य का प्रत्येक मनुष्य मात्र के प्रति एक संदेश प्रेषित करता है। अतीत की सुखद स्मृति में लीन रहकर वर्तमान की उपेक्षा करना, अवहेलना करना कदापि क्षम्य, ग्रहणयोग्य नहीं हो सकता। ऐसा व्यवहार भविष्य के लिए हानिकारक सिद्ध हो सकता है। शकुन्तला और राजा दुष्यंत का विवाह, उनका प्रेम, उनका मिलन, गन्धर्व विवाह आदि सम्बन्ध सुखानुभूति प्रदायक अवश्य हैं। किन्तु इसी सुखानुभूतिदायक स्मृतियों में लीन रहकर वर्तमान रूपी दुर्वासा (जिसे कठोर वास्तव मान सकते हैं) की उपेक्षा करने के कारण शकुन्तला को क्षतित होना पड़ा। लेकिन अगर उचित पथ-प्रदर्शक की संगति ही तो भविष्य सुधर सकता है। शकुन्तला के जीवन में सखी अनुसूया और प्रियंवदा ऐसी ही मार्ग-दर्शिका के रूप में आती हैं। ऋषि द्वारा शापित शकुन्तला सम्पूर्ण घटनाक्रम से अनभिज्ञ थी। सखियाँ अपनी प्राणप्रिय सखी का संकटपूर्ण भविष्य के लिए चिंतित हो उठती हैं और दुर्वासा से विनती करके सखी का भविष्य सुधारने का मार्ग खोज लेती हैं। दोनों सखियाँ शकुन्तला को इस विषय चरण के सम्बन्ध में जानकारी न देकर अपने में ही सीमित रखने की बात करती है, क्योंकि वे नवमल्लिका समान कोमल प्रकृति को दुखी देखना नहीं चाहती थी। प्रियंवदा कहती है-

'को नामोष्णोदकेन नवमालिकां सिञ्चति।'

वर्तमान समय में संयुक्त परिवार के स्थान पर एकल परिवार की धारणा बहुत मात्रा में अपनायी जा रही है। संयुक्त परिवार तभी सफल हो सकता है, जब परिवार का प्रत्येक सदस्य हर कदम पर अपना स्थान करने को तैयार रहे, एक दूसरे को

Nowgong Girls' College ESTD: 1962 Nagaon :: Assam
Principal
Nowgong Girls' College
Nagaon :: Assam

ResearchGate

See discussions, stats, and author profiles for this publication at: https://www.researchgate.net/publication/327380730

Arsenic Stress Responses and Tolerance in Rice: Physiological, Cellular and Molecular Approaches

Article in Rice Science · September 2018

DOI: 10.1016/j.rsci.2018.09.007

CITATIONS
66

READS
1,466

4 authors, including:

Jyotirmay Kalita
North Gauhati College
7 PUBLICATIONS 120 CITATIONS
SEE PROFILE

Amit Kumar Pradhan
Gauhati University
18 PUBLICATIONS 155 CITATIONS
SEE PROFILE

Bhaben Tanti
Gauhati University
37 PUBLICATIONS 469 CITATIONS
SEE PROFILE

Some of the authors of this publication are also working on these related projects:

Whitefly-begomovirus interactions View project

C.T.C.
Principal
Nowgong Girls' College
Nagaon :: Assam

All content following this page was uploaded by Jyotirmay Kalita on 04 September 2018.

The user has requested enhancement of the downloaded file.

Available online at www.sciencedirect.com

ScienceDirect

Rice Science, 2018, 25(5): 235–249

Arsenic Stress Responses and Tolerance in Rice: Physiological, Cellular and Molecular Approaches

Jyotirmay KALITA, Amit Kumar PRADHAN, Zina Moni SHANDILYA, Bhaben TANTI

(Department of Botany, Gauhati University, Guwahati 781014, Assam, India)

Abstract: Arsenic (As), a potentially toxic metalloid released in the soil environment as a result of natural as well as anthropogenic processes, is subsequently taken up by crop plants. In rice grains, As has been reported in Asia, North America and Europe, suggesting a future threat to food security and crop production. As^{3+} by dint of its availability, mobility and phytotoxicity, is the most harmful species of As for the rice crop. Specific transporters mediate the transport of different species of As from roots to the aboveground parts of the plant body. Accumulation of As leads to toxic reactions in plants, affecting its growth and productivity. Increase in As uptake leads to oxidative stress and production of antioxidants to counteract this stress. Cultivars tolerant to As stress are efficient in antioxidant metabolism compared to sensitive ones. Iron and selenium are found to have ameliorating effect on the oxidative stress caused by As. Microbes, even many indigenous ones, in the plant rhizosphere are also capable of utilizing As in their metabolism, both independently and in association. Some of these microbes impart tolerance to As-stress in plants grown in As contaminated sites.

Key words: arsenic; rice; phytotoxicity; hyperaccumulator; phytochelatin; antioxidant; mitigation

Arsenic (As), a potentially toxic metalloid, is a naturally occurring element ubiquitous to all soils (Smedley and Kinniburgh, 2002; William et al, 2005). It is the 20th most common element in the earth's crust (Mandal and Suzuki, 2002). Soil contains 1.5–3.0 mg/kg As. As is present in inorganic forms in various minerals in soil, the important ones being realgar, arsenopyrite, etc. From the minerals, As in both inorganic and organic forms, gets mobilized due to natural and human activities, and becomes more readily available to living organisms.

Among the natural sources of mobilization of As, weathering of As-containing minerals (Woolson, 1977; Smedley, 2006) and the activities of microorganisms (Bentley and Chasteen, 2002; Turpeinen et al, 2002) are prominent. On methylation by microbes, As is released as monomethyl arsenate (MMA) or dimethyl arsenate (DMA) (Bentley and Chasteen, 2002). Some microbes utilize As in their metabolism, and release the toxic trimethyl arsine oxide (TMAsO) gas which is subsequently released to the atmosphere (Mandal and Suzuki, 2002).

Human activities that release more As in bio-available forms include application of As pesticides, use of As in paints to be subsequently released by molds and bacteria, mining of metals and heavy extraction of groundwater. Insecticides [calcium arsenate ($Ca_3As_2O_8$) and lead arsenate ($PbHAsO_4$)], herbicide [sodium arsenite ($NaAsO_2$)], rodenticides arsenious oxide (As_2O_3) and sodium arsenite ($NaAsO_2$) contain As (ICAR, 2009). Their residues remain in the soil, get dissolved in the groundwater and become easily available to living organisms. As-containing wallpaper paints, fed upon by molds and bacteria, led to release of the 'Gosio' gas, which was identified to be trimethyl arsine (Woolson, 1977). Metal mining,

Received: 28 February 2018; **Accepted:** 19 June 2018

Corresponding author: Bhaben TANTI (btanti@gauhati.ac.in)

Copyright © 2018, China National Rice Research Institute. Hosting by Elsevier B.V.

This is an open access article under the CC BY-NC-ND license (http://creativecommons.org/licenses/by-nc-nd/4.0/).

Peer review under responsibility of China National Rice Research Institute

https://doi.org/10.1016/j.rsci.2018.06.007

Principal
Nowgong Girls' College
Nagaon :: Assam

Nowgong Girls' College
ESTD: 1962
Nagaon :: Assam

processing of ores and related activities, has contributed to the release of As in the soil and groundwater (Smedley, 2006) in several countries including Thailand, Ghana, Turkey, England, Serbia, Bosnia, Poland, USA and Canada (Barringer and Reilly, 2013).

A very significant means of mobilization of As is the extraction of groundwater from shallow aquifers in various countries, where surface water is contaminated by disease causing microorganisms. Groundwater is generally more vulnerable to As contamination than surface water because of the interaction of groundwater with aquifer minerals and the increased potential in aquifers for the generation of the physicochemical conditions favourable for As release (Smedley, 2006). Groundwater obtained from shallow aquifers is more likely to contain higher amount of As than that obtained from deep aquifers (Smedley, 2006). As contaminated groundwater is found in many countries like Bangladesh, India, China, Argentina, Chile, Vietnam, Hungary and Mexico (Smedley and Kinniburgh, 2002; Smedley, 2006; Chakraborti et al, 2012). Deep aquifers containing high As levels have also been reported in the Mekong Valley, Vietnam, where high amount of groundwater extraction has resulted in subsidence of the land level by almost 3 cm per year as measured by satellite based radar images from 2007 to 2010 (Erban et al, 2013), leading to speculations that similar deep aquifers of groundwater may not remain As free over the years to come.

In soil, As exhibits a number of oxidation states, the common ones being As^{5+}, As^{3+} and As^{3-}. In aerobic soils, As is mainly present in the oxidized form as arsenate (As^{5+}). While in anaerobic environments like paddy soil, it mainly exists in the reduced form as arsenite (As^{3+}) (Takahashi et al, 2004).

With the use of As-contaminated water in irrigation and due to the various processes of its mobilization, the levels of As in soils have escalated, affecting the agricultural system and resulting in the uptake of the element by crop plants. The translocation factor (TF) for As is higher in rice (0.8) compared to the other crops like wheat (0.1) and barley (0.2) (Xu et al, 2008). The amount of As in paddy soil and soil solution stand elevated (Brammer and Ravenscroft, 2009). The scenario is the worst in rice fields in affected areas such as Bangladesh, India, China and Thailand, where rice is the staple food for most of the people (Abedin et al, 2002; Williams et al, 2006; Garnier et al, 2010). Humans also have been exposed to As through drinking of As-contaminated water and consumption of As-contaminated crops. The contaminated groundwater used to cultivate vegetables and rice for human consumption may be an important pathway of As ingestion and exposure to chronic As (Chakraborti et al, 2004). Food imported into the United Kingdom from Bangladesh has a 2- to 100-fold higher As concentration than vegetables cultivated in the United Kingdom and North America (Al Rmalli et al, 2005). In the South Punjab and Sindh provinces of Pakistan, As is a major contaminant of soil, water and fodder, thereby making its way into the food chain of cattle and subsequently the humans (Zubair et al, 2017). Thus, food is an important route of As exposure in some regions and these exposures can have long-term negative health effects in humans. Even, raised air-As concentration, caused by smelter contaminants in Yunnan (China) poisoning incident in 1993, has been found to contaminate crops grown in the area, where 90% of the human As intake is from the food (rice and corn), and only 10% or less from direct inhalation (Mandal and Suzuki, 2002).

The World Health Organization (WHO) certified that the maximum contaminant level (MCL) of As in drinking water is 10 μg/L (reduced from 50 μg/L) in 1993. Regulations in different countries have recommended different values of the MCL (Smedley, 2006; Barringer and Reilly, 2013). Countries like USA, New Zealand, Japan, Argentina, Brazil, Chile and Colombia place 10 μg/L as MCL in drinking water. Australia uses a standard of 7 μg/L. The New Jersey state in USA places 5 μg/L as the MCL. Mexico has adopted a standard of 25 μg/L, whereas some developing countries like Bangladesh have maintained the earlier 50 μg/L MCL standard. In July 2014, the WHO set worldwide guidelines for what it considers to be safe levels of As in rice, suggesting the maximum of 200 μg/kg for white rice and 400 μg/kg for brown rice (Sohn, 2014). Safety measures can be taken for removing As from drinking water (Ghosh and Singh, 2009) by various methods even at household levels (Chaurasia et al, 2012). However, removal of As from food or crop fields after its incorporation is not economically viable.

As is considered to be one of the most highly toxic and carcinogenic elements. According to the US Environmental Protection Agency (EPA) and the International Agency for Research on Cancer (IARC), As and its compounds have been ranked as Group 1 human carcinogen. As present in drinking water or contaminated crops can have severe impact on the

Principal
Nowgong Girls' College
Nagaon :: Assam

Nowgong Girls' College
ESTD. 1962
Nagaon :: Assam

health of human beings as well as other animals (Ng et al, 2003). It has been found to be a fatal carcinogenic element in cases of extreme intake. Several deaths have been reported from areas of high contamination. As is a leading cause of serious health problems such as cancers of the skin, lung, bladder, liver and kidney, as well as adverse effects on cardiovascular, neurological, haematological, renal and respiratory systems (Barringer and Reilly, 2013).

As being taken up from soils, plant roots are the initial tissues to be exposed. The metalloid inhibits the extension and proliferation of roots. Upon its translocation to the shoot, As can inhibit plant growth severely by hindering the expansion and biomass accumulation as well as compromising the plant reproductive capacity through losses in fertility and yield (Rahman et al, 2007, 2008). At sufficiently high concentrations, As interferes with critical physiological and metabolic processes such as cellular membrane damage, and increase in antioxidant mechanisms, which can even lead to the death of the plant (Garg and Singla, 2011).

Occurrence and distribution of arsenic in rice growing areas

Rice, the dietary staple food for half of the world's population, is believed to have originated in Asia (Lahkar and Tanti, 2017), and gradually spread to all the continents. It has an affinity of taking up As from contaminated soil and water and even air to some extent (Abedin et al, 2002; Mandal and Suzuki, 2002). Thus, over the past few decades, with the increase in As content of soil and groundwater, and with the use of contaminated water in irrigation, subsequently, As content in rice grains has also been found to be rising in several parts of the world (Fig. 1).

The rice fields of Bangladesh are heavily irrigated with As contaminated water obtained from millions of shallow tube wells installed by the country's farmers. As a result, in several areas of the country, As content in rice grain has been found to rise to alarming levels which bears threat to food safety and also crop production in future (Williams et al, 2006; Rahman and Hasegawa, 2011). The highest mean As content in rice grains is found in Faridpur (0.95 μg/g), followed by Rajbari (0.76 μg/g), Golapganj (0.57 μg/g), Dinajpur (0.54 μg/g), Srinagar (0.48–0.53 μg/g) and Sonargaon (0.46 μg/g) districts of the country (Williams et al, 2006). Of the overall mean of 0.13 μg/g As in Bangladesh rice grains, about 80% is found to be inorganic, which is more toxic than the organic forms (Williams et al, 2006; Zavala et al, 2008).

In India, As-contaminated rice has been reported in the states of Chattisgarh (Patel et al, 2005) and West

Fig. 1. Map showing the arsenic contaminated groundwater and rice fields.
(Courtesy: British Geological Survey, Natural Environment Research Council (http://www.bgs.ac.uk/arsenic/).

Nowgong Girls' College ESTD: 1962 Nagaon :: Assam
Principal
Nowgong Girls' College
Nagaon :: Assam

Bengal (Santra et al, 2013), and more will potentially be reported in future, with groundwater contamination by As reported in a number of states (Singh, 2004; Chakraborti et al, 2012). In West Bengal, Boro rice varieties (0.451 μg/g) contain more As than Aman ones (0.334 μg/g), while improved high-yielding rice varieties also contain more As than the local ones (Bhattacharya et al, 2010b; Santra et al, 2013). Moreover, on dietary basis, daily As intake is 560 and 393 μg for adults and children, respectively, and the people having poor nutrition are affected more from As toxicity than those having adequate nutrition (Santra et al, 2013). In Chhattisgarh, the concentration of total As in rice samples is 0.018 to 0.446 μg/g (Patel et al, 2005).

In China, mining industries contribute a great deal to As contamination of rice, and the standard threshold for As concertration in food is 0.2 μg/g. As level in brown rice in Guangdong Province of China, which is susceptible to As poisoning from an abandoned tungsten mine (Lianhuashan), is 1.09 μg/g (Liu et al, 2010), which is several times higher than the national safety limit. The total As content in polished rice grains from different production regions of the country ranges from 0.065 to 0.274 μg/g, with an average value of 0.114 μg/g, where inorganic As is predominant, accounting for approximately 72% of the total As with a mean concentration of 0.082 μg/g (Liang et al, 2010). The major role (60%) in exposing the Chinese population to inorganic As is played by rice. Moreover, people from southern China are more prone to acquire cancer from As poisoning than those in the northern part of the country (Li et al, 2011).

Rice from USA contains higher total grain As content compared to rice from counties of Asia and Europe, although the amount of inorganic As (42% ± 5%) is lesser (Williams et al, 2006). Different reports suggest that rice from USA predominantly contains the organic form of As (Meharg et al, 2009), with DMA being a major species (Zavala et al, 2008). Besides these, presence of As in rice has also been reported in several other countries as mentioned in Table 1.

Uptake of arsenic by rice plants

As is available to rice plants in various forms from the soil water. Among the different species of As in soil, the concentration of one often dominates the rest depending upon the various physicochemical parameters in the soil environment. Inorganic As is dominant in soil water over organic (methylated) forms. Under oxidising conditions, the concentration of As^{5+} is the highest, while microbial activity may also lead to accumulation of MMA, DMA or TMAsO, whereas under reducing conditions, As^{3+} is the dominant form in soil (Mandal and Suzuki, 2002). Paddy is grown under waterlogging conditions, which is anaerobic and reducing in nature. The soil water in a paddy field goes on from being As^{5+} dominant to As^{3+} dominant with the passing of time during the cropping season as more and more irrigation water is provided. During the important stages of cropping from panicle development to grain filling, As content of soil water remains high, with the major species being As^{3+}, which is the more toxic form. Therefore, As^{3+} is the most important species of As in soil concerning rice crop growth and yield. Later on, as waterlogging conditions are over, near harvesting period, the soil conditions become oxidising and As^{5+} becomes the major form in the soil (Panaullah et al, 2008).

The uptake of the different species of As from the soil water by rice plants takes place at different rates. The amount of As taken up by rice plants followed the following trend: As^{3+} > MMA > As^{5+} > DMA (Marin et al, 1992). As^{3+} being very easily taken up by plants and also being the dominant one (Mandal and Suzuki, 2002) and one of the most phytotoxic forms (Marin et al, 1992), it is a major hazard for the rice growing and consuming communities of the world.

The transport rates of different As species within the rice plant vary considerably, which leads to variation in their accumulation in different organs of the plant (Fig. 2). Organic As species are more easily transported to the shoots in rice plants than the inorganic species (Marin et al, 1992; Raab et al, 2007; Carey et al, 2010). DMA is readily translocated to the

Table 1. Arsenic (As) found in sampled rice.

Country	Total As (μg/g)	Inorganic As (μg/g)	Reference
China*	0.19–0.76	0.11–0.51	Williams et al, 2006
Thailand	0.11 ± 0.01	0.08	Williams et al, 2006
Thailand	0.127–0.175	0.066–0.114	Torres-Escribano et al, 2008
Canada	0.02–0.11	0.01–0.08	Williams et al, 2006
France*	0.183	0.113	Torres-Escribano et al, 2008
Italy*	0.146–0.273	0.114–0.176	Torres-Escribano et al, 2008
Spain*	0.098–0.406	0.062–0.253	Torres-Escribano et al, 2008
Sweden*	0.20	0.11	Williams et al, 2007

* Samples were obtained from market and samples in China were from Taiwan Province.

Principal
Nowgong Girls' College
Nagaon :: Assam

Nowgong Girls' College
Nagaon :: Assam
1962

shoots. However, the accumulation of the inorganic forms of As do not significantly increase with increase in As concentration in the growth medium (Marin et al, 1992). The majority of the As in rice grains is dominated by As^{3+} and DMA, and the former is retained only in the ovular vascular trace whereas the latter is dispersed throughout the external parts of the grain and up to the endosperm (Carey et al, 2010). This difference in As translocation and accumulation is prevalent in a number of other plant species belonging to several families of both monocots and dicots, suggesting a similarity in the basic mechanism of transport of the respective As species in different plants (Raab et al, 2007).

Different transporters are responsible for the uptake and translocation of different As species in the rice plants (Fig. 2). The uptake and translocation of As^{3+} are mediated by the rice silicic acid transporters Lsi1 (OsNIP2;1), belonging to nodulin26-like intrinsic protein (NIP) family of major intrinsic proteins and Lsi2 belonging to putative anion transporters (Ma et al, 2008). Lsi1 provides the ability to uptake As^{3+} from the medium, whereas Lsi2 helps in translocating As^{3+} to the shoots by regulating its efflux to the xylem. Transporters belonging to the plasma membrane intrinsic proteins (PIP) of rice, viz. OsPIP2;4, OsPIP2;6 and OsPIP2;7, are also observed to play a role in the transport of As^{3+} in heterologous systems (*Arabidopsis thaliana* and *Xenopus laevis* oocytes) by increasing membrane permeability. Among these transporters, OsPIP2;6 has also been demonstrated to efflux As^{3+} to the growth medium in transgenic *A. thaliana* overexpressing OsPIP2;6 during long term experiments, thus providing As^{3+} tolerance to the plant (Mosa et al, 2012). As^{5+} transport is regulated by phosphate transporters in several plants including rice. As^{5+} is an analogue of P, with its uptake being reduced by the presence of higher concentrations of P in the growth medium as determined in the As hyperaccumulator *Pteris vittata* (Wang et al, 2002), or *Brassica carinata* (Irtelli and Navari-Izzo, 2008). In case of rice, OsPHF1 (for phosphate transporter traffic facilitator 1) defective rice mutants uptake less Pi and As^{5+}. Moreover, transgenic rice overexpressing the Pi transporter OsPht1;8 (OsPT8) or those overexpressing the transcription factor OsPHR2 (for phosphate starvation response 2) uptake more Pi and As^{5+} in hydroponic culture, thus raising the maximum influx by three to five times (Carey et al, 2010) suggests strong affinity of Pi transporters for the uptake and translocation of As^{5+} in rice. Among the organic species of As, the methylated forms, MMA and DMA, are taken up by the rice aquaporin Lsi1 (Li et al, 2009).

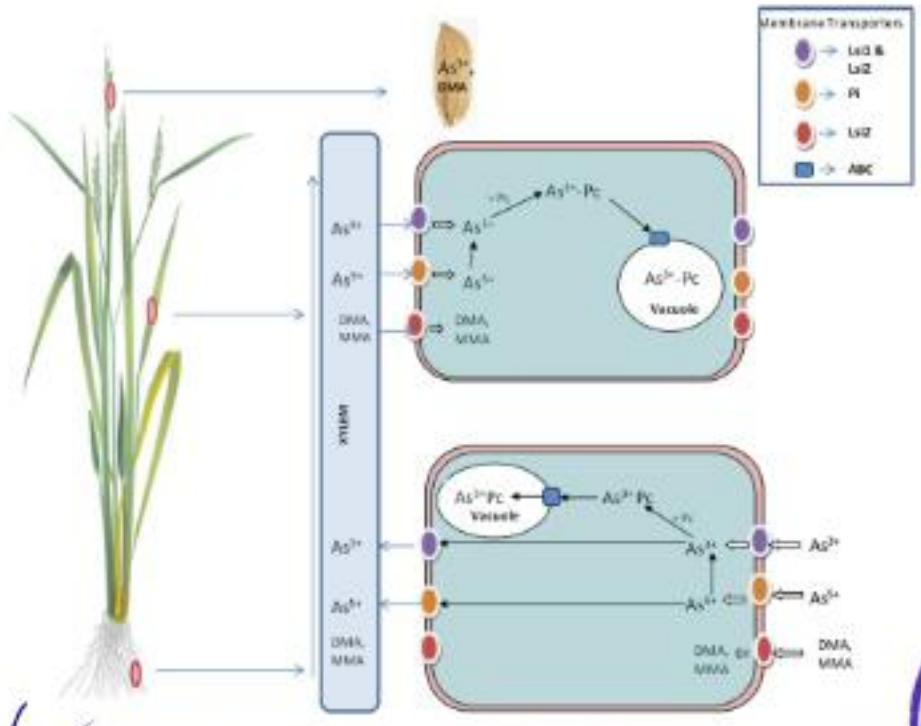

Fig. 2. Transport of arsenic (As) from roots to different parts of rice plants by means of various transporters. DMA, Dimethyl arsenate; MMA, Monomethyl arsenate.

Principal
Nowgong Girls' College
Nagaon :: Assam

Nowgong Girls' College
ESTD: 1962
Nagaon :: Assam

The translocation of DMA within the rice plant takes place at the highest rate among all the species of As (Marin et al, 1992). Along with As^{3+}, DMA forms the major part of As in the rice grains (Carey et al, 2010). However, in reports of As content in grains obtained from various affected countries, rice varieties varying in speciation of grain As content have been found, based on which two major groups of rice varieties can be identified, viz. one with more inorganic As in grains, and the other with more organic As in grains (Zavala et al, 2008). It has been recently shown that higher plants, including rice, are unable to methylate inorganic As (Lomax et al, 2012). However, there is evidence suggesting that organic As can be partially converted to inorganic forms by *Sinapis alba* (Jedynak et al, 2010). The exact mechanisms responsible for variation of the major As species in rice grains remain to be worked out.

Arsenic accumulation and toxicity

The amount of As accumulated in different parts of rice plants follows the order: straw > husk > grain (Abedin et al, 2002; Bhattacharya et al, 2010c). Abedin et al (2002) also showed that the concentrations of As in root and straw do not vary too much, suggesting that translocation from roots to straw takes place readily. However, its concentration decreases considerably in husk and yet further in grains.

From what evidence is present regarding transportation of different As species in rice plants, it can be seen that As^{3+} is the most easily taken up by roots, and DMA is the most easily translocated within the rice plants. As^{3+} and DMA are the two most prominent species of As that are translocated to the grains. However, a considerable amount of As^{5+} is also being taken up from the soil by the rice roots, and its concentration in the aboveground tissues of the plant is affected by mechanisms associated with As-tolerance response such as the presence of different arsenate reductases in rice, like OsHAC1;1, OsHAC1;2 and OsHAC4, which regulate the conversion of arsenate to arsenite. These genes are expressed mainly in the roots, and catalyse the reaction in the outer cell layer of root, thereby, facilitating arsenite efflux from the root to soil (Xu et al, 2017). A significant amount of As^{5+} is reduced to As^{3+} in root tissues of plants such as Indian mustard (Pickering et al, 2000), tomato and rice (Xu et al, 2007). Two ACR2-like genes, *OsACR2.1* and *OsACR2.2*, similar to the yeast *ACR2* genes responsible for arsenate reduction are identified in the rice genome, with the former being much active than the latter (Duan et al, 2007). Mutation of such genes led to decreased arsenate reduction in root, decreased arsenite efflux and increased As accumulation in root and grain. However, Chao et al (2014) demonstrated that *ACR2*-like genes are only found to reduce As^{5+} to As^{3+} *in vitro* and not in living plants. Moreover, the sequences of the yeast *ACR2* and *HAC1* genes found in plants are similar, and it is only the *HAC1* gene rather than the *ACR2*-like genes that takes part in arsenate reduction and arsenite efflux in plants. *HAC1* can therefore be an important candidate gene, which can reduce the accumulation of As in aboveground tissues due to its role in As^{3+} efflux mechanism.

Accumulation of As in rice varies according to the genotype of the plant (Norton et al, 2010) and its mobilization and intake is controlled by different factors such as As speciation, soil texture, pH and organic matter present (Mitra et al, 2017). The variation in accumulation may be due to the difference in presence of As in irrigation water, soils and the genetic makeup. The root characteristics also play a major role in As accumulation, which includes the root aeration, porosity (Wu et al, 2011), rhizosphere interactions (Dasgupta et al, 2004) and Fe-plaque formation on the root surfaces (Liu et al, 2004b). The solubility of As in the soils and its bioavailability to the rice plants is controlled by the soil texture and pH (Quazi et al, 2011). Silt and clayey soils with the fine texture provide large surface area for As scavenging compared to the sandy and loamy soils mainly based on the presence of Fe-oxides. Soil pH [both low (< 5.0) and high (> 8.5)] greatly affects As uptake and accumulation in the rice plants. The soils with low pH (< 5) provide higher As binding species such as Fe-oxyhydroxide compounds and enhance As uptake by plants. Under high pH, the negative surface charge is increased, giving rise to increase in hydroxyl ions, thus facilitating desorption of As from Fe-oxides and resulting in As transport in root vicinity and accumulation in the plant (Bhattacharya et al, 2010a; Ahmed et al, 2011). Organic matter has a greater affinity for As adsorption due to the formation of an organo-As complex, thereby reducing As availability to plants (Mitra et al, 2017).

Accumulation of As by rice plants results in various toxic reactions and affects the growth, morphological and physiological processes of the plant (Gupta et al,

Principal
Nowgong Girls' College
Nagaon :: Assam

2018). Increasing As content of growing medium or increased accumulation reduces chlorophyll content of the rice plants, the extent of reduction varying slightly among different varieties. This results in reduction in the rate of photosynthesis, leading to reduction in root and shoot growth and grain yield (Rahman et al, 2007; Halim et al, 2014). Yield reduction has also been observed with the increase in As content in soils in subsequent cropping years due to retention of As from previous years' contaminated irrigation water in the soils (Panaullah et al, 2008). A physiological disease called straight head is also attributed to As toxicity (Rahman et al, 2008). The symptoms of this disease include reduction in the sterility of florets/spikelets, desreased grain yield, and in severe cases, non-formation of the panicles or heads.

The level of sensitivity to As toxicity varies in different rice genotypes (Chaturvedi, 2013). Moreover, all the As species cause dissimilar levels of toxicity in rice plants. DMA is the least toxic form of As as determined by its effect on plant dry mass, and its application in low concentrations has only resulted in increased dry mass, while high concentration leads to no changes at all. Application of As^{3+} causes no significant change in dry mass. However, As^{3+} and MMA are highly toxic to plants, with the effect of MMA being greater than As^{3+} (Marin et al, 1992).

Arsenic hyperaccumulation and tolerance

It is well established that As accumulation leads to various toxic reactions in plants. However, some plants are tolerant to elevated levels of As and accumulate high levels of the metalloid in their bodies. The fern *Pteris vittata* is the first reported As hyperaccumulator whose fronds contain high amounts of mostly the toxic inorganic forms of As (Ma et al, 2001). *Sarcosphaera coronaria*, an ectomycorrhizal ascomycetous fungus, also accumulates very high amounts of As (mostly in the form of methylarsonic acid) in its fruit bodies (Falandysz and Borovička, 2013). The yeast ACR3 arsenite effluxer provides As tolerance on its heterologous expression in *Arabidopsis thaliana* (Ali et al, 2012). Two genes from *P. vittata*, *PvACR3* and *PvACR3;1*, similar to the yeast ACR3 arsenite effluxer, have been isolated. Of these, *PvACR3* has a definite role in As tolerance in the plant (Indriolo et al, 2010). ACR3 is a membrane protein. Once taken up by the roots, As^{5+} gets reduced to As^{3+}. *PvACR3* effluxes As^{3+} into the vacuole for sequestration. *ACR3* gene is absent in angiosperms. However, when *PvACR3* is expressed in transgenic *A. thaliana*, its tolerance to As is increased. *PvACR3* transgenic seeds of *A. thaliana* could even germinate in very high concentrations of As that are potentially lethal for wild type plants (Chen et al, 2013). *P. vittata* has been demonstrated to help in phytoremediation by removing As from soil. Rice cultivated in soils where *P. vittata* is grown previously has been found to accumulate less As in straw and grains (Ye et al, 2011).

QTLs for As accumulation in shoots have been identified in a doubled haploid population obtained from anther culture of F_1 plants generated from a cross between rice cultivars CJ06 (*japonica*) and TN1 (*indica*). The QTLs, *AsS*, *AsSe1* and *AsSe2*, are located on chromosomes 2, 6 and 8, respectively (Zhang et al, 2008). *AsSe2* collocates with the QTL for P accumulation in shoots at the seedling stage, having LOD value of 4.97.

Dasgupta et al (2004) found that in general *indica* rice varieties are more tolerant to As stress than *japonica* ones. In their experiments, CO39 is the most tolerant whereas Dawn is the most susceptible. They identified an As tolerance gene *AsTol* on chromosome 6 between markers RZ516 and RG213. Three tolerance genes in the rice genome play a part in As susceptibility or tolerance, and two are located on chromosome 6 whereas the other on chromosome 10. The genes, *AsTol6.1*, *AsTol6.2* and *AsTol10.1*, are epistatic in action with tolerance resulting in plants having inherited a minimum of two of the three genes from a tolerant parent (Norton et al, 2008). Plasma membrane intrinsic proteins from rice, OsPIP2;4, OsPIP2;6 and OsPIP2;7, when overexpressed in transgenic *Arabidopsis*, are found to increase As^{3+} tolerance in the plants during short term exposure (Mosa et al, 2012). These transporters might as well play important roles in rice tolerance to As. *Arabidopsis* plants mutant for auxin transporters have been found to be more sensitive to As^{3+} stress. Providing exogenous auxin improves As^{3+} tolerance in such mutants (Krishnamurthy and Rathinasabapathi, 2013). This hints at a possible role of auxin in ameliorating As stress in rice, however, the molecular basis of the mechanism need to be tested.

Phytochelatins in arsenic metabolism

Phytochelatins (PC) are thiol-rich peptides having the general formula $\gamma(\text{Glu-Cys})_n\text{-Gly}$, where n ranges from 2 to 11 (called accordingly as PC_2, PC_3, PC_4, etc.), produced in plants in response to stress from

Principal
Nowgong Girls' College
Nagaon :: Assam

Nowgong Girls' College
Estd. 1962
Nagaon :: Assam

heavy metals and metalloids including As (Hartley-Whitaker et al, 2001a). These are synthesized from glutathione by a specific γ-glutamylcysteine dipeptidyl transpeptidase known as phytochelatin synthase (PCS) (Grill et al, 1989). PCs help in As detoxification by sequestrating it in the vacuoles. PCs bind As^{3+}, forming As-PC complexes which are then transported to vacuoles (Verbruggen et al, 2009). As^{5+} in plants is also reduced to As^{3+} (Pickering et al, 2000; Xu et al, 2007), which can be subsequently bound by PC and transported to the vacuoles. The transport of As-PC complexes to the vacuoles is mediated by the AtABCC1 and AtABCC2 transporters in *A. thaliana* (Song et al, 2010). Such ABC type transporters are supposed to help in transport of As-PC complexes in different plant species.

PC production in response to As stress has been demonstrated in plants like *Holcus lanatus*, *Agropyron repens*, *Glecoma hederacea*, *Leonurus marrubi-Astrum*, *Lolium perenne*, *Urtica dioica* and *Zea mays* (Hartley-Whitaker et al, 2001a, b; Schulz et al, 2007). In *A. thaliana*, overexpressing the phytochelatin synthase AtPCS1, tolerance to As stress, is increased (Li et al, 2004). In *H. lanatus*, concentration of PC increases with increasing As concentration in medium in case of tolerant and partially tolerant clones. However, in non-tolerant clones, PC production decreases at higher As^{3+} concentration in medium (Hartley-Whitaker et al, 2001a, b). The findings of Schulz et al (2007) and Hartley-Whitaker et al (2001b) agree on the dominant forms of PC in tolerant and non-tolerant plants. The dominant form of PC found in tolerant plants is PC_2 while in the non-tolerant plants it is PC_3. In intermediate tolerant clones of *H. lanatus*, PC_2 and PC_3 concentrations are approximately equal, while PC_4 is in lesser amounts in all clones. However, Schulz et al (2007) and Srivastava et al (2007) have shown that not all As is bound by PCs. After 4 d of treatment, the amount of As chelates by PCs in As^{3+} treated plants is 39%, while in As^{5+} treated plants, it is 35% (Srivastava et al, 2007). In the As hyperaccumulator fern *P. vittata*, only PC_2 is detected on As treatment. The concentration of PCs correlates significantly with As concentration. However, only a small portion of the As (1%–3%) is chelated with the PCs (Zhao et al, 2003). This suggest that PCs have a limited role in the tolerance of this fern to As stress.

In rice plants exposed to As stress, PCs belonging to the groups: PC [γ(Glu-Cys)$_n$-Gly, *n* ranges from 2 to 4], Ser-PCs [γ(Glu-Cys)$_n$-Ser, *n* ranges from 2 to 4], Des-PCs [γ(Glu-Cys)$_n$, *n* ranges from 2 to 3] and Glu-PCs, [γ(Glu-Cys)$_n$-Glu, *n* ranges from 2 to 3] are produced. The concentration of PCs correlates with the concentration of i-As in the roots (Batista et al, 2014). As-PC complexation in rice leaves leads to reduction in the translocation of As^{3+} to grains (Duan et al, 2007). However, the role of As-PC complexation in reducing grain As content is specific to certain varieties, while in others, different mechanisms such as As-PC release and transport seem to be decisive (Batista et al, 2014).

Oxidative response to arsenic stress

Intake of toxic metals leads to synthesis of reactive oxygen species (ROS) such as H_2O_2 in plants. These ROS cause oxidative injury in plants (Sarma et al, 2016), and plants resist this injury by various antioxidant metabolism reactions (Chutia et al, 2012). Plants may be tolerant or sensitive to metal toxicity. Tolerant plants often demonstrate a much competent antioxidant defence system than sensitive ones (Fig. 3).

As stress has also been found to induce oxidative response in plants. Polyamines involved in protection of plant structures against damage by ROS have been detected in red clover shoots after As treatment (Mascher et al, 2002). Moreover, the activities of superoxide dismutase (SOD) and peroxidase (POD) are detected in As-treated red clover shoots. The presence of three different SOD isoenzymes, Mn-SOD, Cu/Zn-SOD I and Cu/Zn-SOD II, have been determined. There is a tendency of antioxidant activity to increase with increasing concentration of As in culture when As concentration is low. However, their activities get inhibited at high metal concentration (Mascher et al,

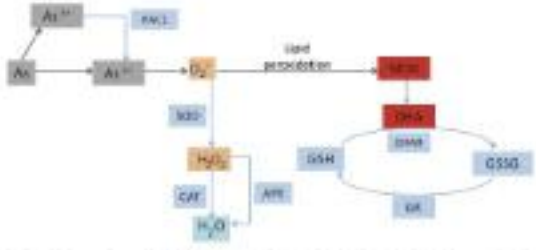

Fig. 3. Roles of antioxidants SOD, CAT, APX, GSH and GR in plants response to arsenic stress induced reactive oxygen species formation.

As, Arsenic; SOD, Superoxide dismutase; CAT, Catalase; APX, Ascorbate peroxidase; GSH, Glutathione; GR, Glutathione reductase; GSSG, Glutathione disulphide; MDA, Malondialdehyde; DHA, Dehydroascorbate; DHAR, Dehydroascorbate reductase; HAGI, High As content 1.

Principal
Nowgong Girls' College
Nagaon :: Assam

2002). Malondialdehyde (MDA) is an indicator of the occurrence of lipid peroxidation due to oxidative damage, which is detected in spinach leaves when grown in presence of As (Srivastava and Sharma, 2013; Hore et al, 2017; Nahar et al, 2018). Variation in the level of antioxidant activity is detected on comparison of tolerant and susceptible plant species. The As hyperaccumulator *Pteris vittata*, which is tolerant to much higher concentration of As, shows better resistance to oxidative injury than the non-hyperaccumulator *Pteris ensiformis*. *P. vittata* shows much less H_2O_2 concentration and lipid peroxidation as indicated by thiobarbituric acid-reactive substances (TBARS) formation as compared to *P. ensiformis*. Moreover, antioxidant defence is more competent in *P. vittata* than in *P. ensiformis* as indicated by ascorbate and glutathione pools. The ratios of reduced to oxidized forms of both ascorbate (AsA/DAsA) and glutathione (GSH/GSSG) are higher in *P. vittata* than in *P. ensiformis* under all treatments (Singh et al, 2006). In comparison of *Pisum sativum* and *Pennisetum typhoides*, it has been found that H_2O_2 concentration and lipid peroxidation are much higher in *P. sativum* than in *P. typhoides*. Moreover, concentrations of thiols, SOD activity, catalase (CAT) activity and ascorbate peroxidase (APX) activity indicate a much better antioxidant defence mechanism in *P. typhoides* than in *P. sativum*. This suggests that *P. typhoides* is the tolerant species whereas *P. sativum* is the sensitive one in response to As induced oxidative stress (Sharma, 2013). In tolerant plants, antioxidant activity is enhanced at high metal concentration and with the passing of time. However, it has been observed that, although antioxidant activity is enhanced with increasing metal accumulation initially, it gradually gets inhibited after a few days and the plants succumb to oxidative damage.

In rice, H_2O_2 concentration and lipid peroxidation level as indicated by MDA concentration increase with the accumulation of As. However, iron supplemented with As in the growth medium results in decrease of ROS concentration in the rice plants. Antioxidants CAT, SOD, AsA and glutathione (GSH) levels are also considerably high in only As^{5+} treated rice plants as compared to Fe supplemented ones (Nath et al, 2014). Fe plaque formation on root surface acts as a buffer, leading to the lowering of As translocation to shoots (Liu et al, 2004a, b). Thus, reducing As stress leads to reduction of ROS concentration and levels of antioxidants in rice plants. This suggests the activity of an antioxidant defence mechanism against As stress in rice plants. The variation of this defence mechanism in different varieties of rice plants need to be worked out in order to identify varieties tolerant to As in the growth medium.

Selenium (Se) has an ameliorating effect on As-induced oxidative stress measured in terms of H_2O_2 concentration, lipoxygenase (LOX) activity, lipid peroxidation as determined by estimation of MDA, and ion leakage measured in terms of electrical conductivity. Oxidative damage is found to decrease on supplementation of Se with As in the medium. The activities of CAT, APX and glutathione peroxidase (GPX) decrease under As treatment, but increase when As in the medium is supplemented with Se, indicating that Se boosts antioxidant activities and prevents any damage from oxidative stress (Kumar et al, 2015).

Role of rhizosphere microorganisms in arsenic stress

Soil rhizospheric microbial activity can affect As adsorption/desorption, solubility, bioavailability, mobility, and soil-plant transfer by altering the chemical speciation of As in soil (Ayangbenro and Babalola, 2017). Microorganisms can interconvert As^{3+} and As^{5+} and thus are capable of either solubilizing or immobilizing As in the soil-plant system (Suhadolnik et al, 2017). These microbially induced biotransformations of As play important roles in the biogeochemical behavior of As and are key in risk assessment and remediation studies (Anguita et al, 2017).

Arbuscular mycorrhizal fungi (AMF) associations can enhance resistance to As stress in plants. AMF such as *Glomus mosseae* and *G. caledonium* have been shown to reduce the uptake of As^{5+} by host *Holcus lanatus* plants, which are resistant to As (Gonzalez-Chavez et al, 2002). Moreover, AMF from contaminated sites are resistant to As stress compared to those from non-contaminated sites. However, both resistant and non-resistant AMF reduce the uptake of As by host plants. In a number of non-resistant plants including soybean and maize, mycorrhizal associations have proven to be beneficial for the host plants in resisting stress due to As (Bai et al, 2008; Spagnoletti and Lavado, 2015; Nahar et al, 2016).

Other microbes in the rhizosphere soil such as some fungi and bacteria also play important roles in determining the level of As toxicity on plants. The ectomychorrizal fungus *Sarcodontia setosa* (*Hydnellum aurantiacum*) accumulates high levels of As in its fruiting bodies

Principal
Nowgong Girls' College
Nagaon :: Assam

Nowgong Girls' College ★ Nagaon :: Assam ★ ESTD 1962

(Falandysz and Borovička, 2013). Other microbes have the capacity to transform As species in the soil, with great potential for increasing plant tolerance to As stress, and playing roles in bioremediation of As-contaminated soil and groundwater. Many rhizospheric N_2 fixing symbiotic microbes (eg. rhizobacteria) tolerate high metal concentration (Jaiswal, 2011). NT-26 strain of *Agrobacterium* / Rhizobium branch of α-Proteobacteria, strains MNZ1 (homologous to Enterobacter sp.), strains MNZ4 and MNZ6 (both homologous to *Klebsiella pneumoniae*) have been reported to oxidize As^{3+} to As^{5+} (Santini et al, 2000; Abbas et al, 2014). In natural environments a variety of As^{3+} oxidizers exist some autotrophic and others heterotrophic. They may further be aerobic and anaerobic. Mechanisms of As^{3+} oxidization varies among different groups, as indicated by the variation in gene and amino acid sequences of the arsenite oxidases (Rhine et al, 2007). This variation can be useful in isolation of useful microbial species that confers As stress resistance to plants in a variety of environments. Of particular importance in paddy cultivation can be the three strains, DAO1 (*Azoarcus* sp.), DAO10 (*Sinorhizobium* sp.) and MLHE-1 (*Alkalilimnicola ehrlichei*), which can oxidize As^{3+} in anaerobic conditions similar to those in submerged paddy cultivation. Furthermore, there are also strains that can reduce As^{5+} to As^{3+} such as *Desulfovibrio* strain Ben-RA and *Desulfomicrobium* strain Ben-RB (Macy et al, 2000). Indigenous microbes found in As contaminated environments are capable of transforming As. Both As^{5+} reducing and As^{3+} oxidising microbes often coexist and are supposed to be common in As contaminated sites (Macy et al, 2000). As^{3+} oxidising bacteria are also found to be effective in improving the bioremediation of As^{3+} contaminated sites by *Pteris vittata*. These microbes can potentially reduce the toxic effect of As on the growth of plants. In case of rice plants, microbes capable of transforming As^{3+} in anaerobic environment might be useful in promoting plant growth in As contaminated sites.

Agronomic mitigation of arsenic accumulation in rice

Different agronomic methods may be adopted to mitigate the effects of As accumulation in rice, which includes soil aeration by water management and preventing the reduction of As; creating the condition

Fig. 4. Aspects of arsenic (As) stress in rice, and possible ways to deal with the problem.

that forms the precipitation of insoluble As in soil; and decreasing As uptake and translocation in rice plants by augmenting mineral nutrients in soils that competes with As uptake (Fig. 4).

Supplementation of soil with mineral nutrients (S, P, Fe and Si) can significantly decrease the accumulation of As in the food grains by minimizing its uptake and transport in food crops. Fe plaque plays an important role in diminution of As absorption around the roots of rice plants (Bakhat et al, 2017). P and Si which are complementary in nature to As competes for the intake by the rice plant through the transporter, thus the external application of P and Si reduces the chances of As intake from the soil.

Management of irrigation system or development of water saving mechanism maintains the redox level of soil and aggrandises the oxidation state that consequently hinders the reduction of As^{5+} to As^{3+}: which has prominently higher solubility, plant availability and toxicity (Takahashi et al, 2004). Thus, a water-saving regime has been reported to be an immediate and sustainable solution to decrease As content in rice (Arao et al, 2009). It has been reported that under aerobic water management practices, rice takes up less As (0.23–0.26 mg/kg) than under anaerobic practices (0.60–0.67 mg/kg) (Talukder et al, 2011).

Bioremediation strategies such as increase in number of soil microbes improved the mineral content of the soil through immobilization and mineralization thus affecting the availability and transport of As in the environment (Huang, 2014). [illegible] controlling the expression of transport mediator genes like *OsLsi1* and *OsLsi2* by AMF (Chen et al, 20[illegible] also helps in mitigation of As toxicity.

Principal
Nowgong Girls' College
Nagaon :: Assam
Nowgong Girls' College :: Assam ★ ESTD: 1962

CONCLUSIONS

The problem of As in rice has two dimensions, human health hazard due to incorporation of As in the food chain, and threat to the crop and sustainable agriculture due to the resulting stress.

Different transporters are involved in the uptake and translocation of As in rice plants. With the translocation rates of different As species varying with their respective transporters, rate of uptake and translocation of As in rice plants could be reduced by working out the underlying mechanisms. The cause of variation of the major As species in American and Asian rice need to be identified. The reason could be either genotypic, or due to difference in soil conditions and agricultural practices. If any difference at a molecular level exists between these varieties, it could be worked out to ensure incorporation of lesser inorganic As in rice grains. As efflux genes such as *HAC1* can be important in developing rice containing low grain As content.

Rice varieties have shown difference in tolerance to As, with the identification of mechanisms of tolerance such as As^{3+} efflux, vacuole sequestration or thiol complexation, and also genes for tolerance being detected, there is scope for traditional breeding approaches to develop tolerance to As among high yielding or traditional varieties. With phytohormone auxin being connected to As tolerance in *Arabidopsis* plants, such phenomenon in rice can be investigated. Hormone treatment of rice seedlings can be tried out to assess any change in tolerance to As stress.

Phytoremediation and land reclamation processes can make use of As-hyperaccumulators such as *Pteris vittata*. Bioremediation using As accumulating rhizosphere bacteria is also a feasible way to reduce the impact of As stress on rice. Elements that ameliorate the impact of As stress are useful when present in As contaminated soils. The formulation of optimum levels of these elements for extrogenous application, depending upon the soil type can alleviate As stress in rice plants. Moreover, management of irrigation is also important in limiting the soil arsenic levels, thereby reducing As uptake and accumulation in rice plants.

REFERENCES

Rafatullah M. 2014. Isolation and characterization of arsenic resistant bacteria from wastewater. *Braz J Microbiol*, **45**(4): 1309–1315.

Abbas G, Murtaza B, Bibi I, Shahid M, Niazi N K, Khan M I, Amjad M, Hussain M, Natasha. 2018. Arsenic uptake, toxicity, detoxification, and speciation in plants: Physiological, biochemical, and molecular aspects. *Int J Environ Res Public Health*, **15**(1): 59.

Abedin M J, Feldmann J, Meharg A A. 2002. Uptake kinetics of arsenic species in rice plants. *Plant Physiol*, **128**: 1120–1128.

Ahmed Z U, Panaullah G M, Gauch Jr H, McCouch S R, Ytagi W, Kabir M S, Duxbury J M. 2011. Genotype and environment effect rice (*Oryza sativa* L.) grain arsenic concentration in Bangladesh. *Plant Soil*, **338**: 367–382.

Al Rmalli S W, Haris P I, Harrington C F, Ayub M. 2005. A survey of arsenic in foodstuffs on sale in the United Kingdom and imported from Bangladesh. *Sci Total Environ*, **337**: 23–30.

Ali W, Isner J C, Isayenkov S V, Liu W, Zhao F J, Maathuis F J M. 2012. Heterologous expression of the yeast arsenite efflux system ACR3 improves *Arabidopsis thaliana* tolerance to arsenic stress. *New Phytol*, **194**(3): 716–723.

Anguita J M, Rojas C, Pastén P A, Vargas I T. 2017. A new aerobic chemolithoautotrophic arsenic oxidizing microorganism isolated from a high Andean watershed. *Biodegradation*, **29**(1): 59–69.

Arao T, Kawasaki A, Baba K, Mori S, Matsumoto S. 2009. Effects of water management on cadmium and arsenic accumulation and dimethylarsinic acid concentrations in Japanese rice. *Environ Sci Technol*, **43**: 9361–9367.

Ayangbenro A S, Babalola O O. 2017. A new strategy for heavy metal polluted environments: A review of microbial biosorbents. *Int J Environ Res Public Health*, **14**(1): 94.

Bai J F, Lin X G, Yin R, Zhang H Y, Wang J H, Chen X M, Luo Y M. 2008. The influence of arbuscular mycorrhizal fungi on As and P uptake by maize (*Zea mays* L.) from As-contaminated soils. *Appl Soil Ecol*, **38**(2): 137–145.

Bakhat H F, Zia Z, Fahad S, Abbas S, Hammad H M, Shahzad A N, Abbas F, Alharby H, Shahid M. 2017. Arsenic uptake, accumulation and toxicity in rice plants: Possible remedies for its detoxification: A review. *Environ Sci Pollut Res*, **24**(10): 9142–9158.

Barringer J L, Reilly P A. 2013. Arsenic in groundwater: A summary of sources and the biogeochemical and hydrogeologic factors affecting As occurrence and mobility. *In*: Current Perspectives in Contaminant Hydrology and Water Resources Sustainability. IntechOpen: 4.

Batista B L, Nigar M, Mestrot A, Rocha B A, Júnior F B, Price A H, Raab A, Feldmann J. 2014. Identification and quantification of phytochelatins in roots of rice to long-term exposure: Evidence of individual role on As accumulation and translocation. *J Exp Bot*, **65**(6): 1467–1479.

Bentley R, Chasteen T G. 2002. Microbial methylation of metalloids: Arsenic, antimony, and bismuth. *Microbiol Mol Biol Rev*, **66**: 250–271.

Bhattacharya P, Samal A C, Majumdar J, Santra S C. 2010a. Accumulation of arsenic and its distribution in rice plant (*Oryza*

C.T.C.
Principal
Nowgong Girls' College
Nagaon :: Assam

Nowgong Girls' College ★ Nagaon :: Assam ★ ESTD 1962

sativa L.) in gangetic West Bengal, India. *Paddy Water Environ*, **8**(1): 63–70.

Bhattacharya P, Samal A C, Majumdar J, Santra S C. 2010b. Arsenic contamination in rice, wheat, pulses, and vegetables: A study in an arsenic affected area of West Bengal, India. *Water Air Soil Pollut*, **213**(1): 3–13.

Bhattacharya P, Samal A C, Majumdar J, Santra S C. 2010c. Uptake of arsenic in rice plant varieties cultivated with arsenic rich groundwater. *Environ Asia*, **3**(2): 34–37.

Brammer H, Ravenscroft P. 2009. Arsenic in groundwater: A threat to sustainable agriculture in South and South-east Asia. *Environ Int*, **35**(3): 647–654.

Carey A M, Scheckel K G, Lombi E, Newville M, Choi Y, Norton G J, Charnock J M, Feldmann J, Price A H, Meharg A A. 2010. Grain unloading of arsenic species in rice. *Plant Physiol*, **152**(1): 309–319.

Chakraborti D, Sengupta M K, Rahman M M, Ahamed S, Chowdhury U K, Hossain M A, Mukherjee S C, Pati S, Saha K C, Dutta R N, Quamruzzaman Q. 2004. Groundwater arsenic contamination and its health effects in the Ganga-Meghna-Brahmaputra plain. *J Environ Monit*, **6**(6): 74–83.

Chakraborti D, Singh E J, Das B, Shah B A, Hossain M A, Nayak B, Ahamed S, Singh N R. 2012. Groundwater arsenic contamination in Manipur, one of the seven North-Eastern Hill states of India: A future danger. *Environ Earth Sci*, **56**(2): 381–390.

Chao D Y, Chen Y, Chen J G, Shi S L, Chen Z R, Wang C C, Danku J M, Zhao F J, Salt D E. 2014. Genome-wide association mapping identifies a new arsenate reductase enzyme critical for limiting arsenic accumulation in plants. *PLoS Biol*, **12**(12): e1002009.

Chaturvedi I. 2013. Genotypic differences in effects of arsenic on growth, and concentration of As in rice (*Oryza sativa*) genotypes. *Res J Recent Sci*, **2**(3): 49–52.

Chaurasia S C, Sahayam A C, Venkateswarlu G, Dhavile S M, Thangavel S, Rastogi L. 2012. Groundwater contamination problems in rural India: Detection and remediation at the household level. *BARC Newsl*, **324**: 39–45.

Chen X W, Li H, Chan W F, Wu C, Wu F Y, Wu S C, Wong M H. 2012. Arsenite transporters expression in rice (*Oryza sativa* L.) associated with arbuscular mycorrhizal fungi (AMF) colonization under different levels of arsenite stress. *Chemosphere*, **89**(10): 1248–1254.

Chen Y S, Xu W Z, Shen H L, Yan H L, Xu W X, He Z Y, Ma M. 2013. Engineering As tolerance and hyperaccumulation in plants for phytoremediation by a PvACR3 transgenic approach. *Environ Sci Technol*, **47**(16): 9355–9362.

Chutia J, Borah S P, Tanti B. 2012. Effect of drought stress on protein and proline metabolism in seven traditional rice (*Oryza sativa* Linn.) genotypes of Assam, India. *J Res Biol*, **2**(3): 206–214.

Dasgupta T, Hossain S A, Meharg A A, Price A H. 2004. An arsenate tolerance gene on chromosome 6 of rice. *New Phytol*, **163**(1): 43–49.

Duan G L, Zhou Y, Tong Y P, Mukhopadhyay R, Rosen B P, Zhu Y G. 2007. A CDC25 homologue from rice functions as an arsenate reductase. *New Phytol*, **174**(2): 311–321.

Erban L E, Gorelick S M, Zebker H A, Fendorf S. 2013. Release of arsenic to deep groundwater in the Mekong Delta, Vietnam, linked to pumping-induced land subsidence. *Proc Natl Acad Sci USA*, **110**(34): 13751–13756.

Falandysz J, Borovička J. 2013. Macro and trace mineral constituents and radionuclides in mushrooms: Health benefits and risks. *Appl Microbiol Biotechnol*, **97**(2): 477–501.

Garg N, Singla P. 2011. Arsenic toxicity in crop plants: Physiological effects and tolerance mechanisms. *Environ Chem Lett*, **9**(3): 303–321.

Garnier J M, Travassac F, Lenoble V, Rose J, Zheng Y, Hossain M S, Chowdhury S H, Biswas A K, Ahmed K M, Cheng Z, van Geen A. 2010. Temporal variations in arsenic uptake by rice plants in Bangladesh: The role of iron plaque in paddy fields irrigated with groundwater. *Sci Total Environ*, **408**(19): 4185–4193.

Ghosh N C, Singh R D. 2009. Groundwater Arsenic Contamination in India: Vulnerability and Scope for Remedy. Roorkee, Uttarakhand, India: National Institute of Hydrology.

Gonzalez-Chavez C, Harris P J, Dodd J, Meharg A A. 2002. Arbuscular mycorrhizal fungi confer enhanced arsenate resistance on *Holcus lanatus*. *New Phytol*, **155**(1): 163–171.

Grill E, Löffler S, Winnacker E L, Zenk M H. 1989. Phytochelatins, the heavy-metal-binding peptides of plants, are synthesized from glutathione by a specific γ-glutamylcysteine dipeptidyl transpeptidase (phytochelatin synthase). *Biochemistry*, **86**(18): 6838–6842.

Halim M A, Nigar M, Ghosh M, Akhter N, Hossain F. 2014. Interaction effects of arsenic and phosphorus on seedling growth, leaf pigments and leaf protein of rice cultivars under hydroponic culture. *J Asiat Soc Bangl*, **40**(1): 141–150.

Hartley-Whitaker J, Ainsworth G, Meharg A A. 2001a. Copper and arsenate-induced oxidative stress in *Holcus lanatus* L. clones with differential sensitivity. *Plant Cell Environ*, **24**(7): 713–722.

Hartley-Whitaker J, Ainsworth G, Vooijs R, Bookum W T, Schat H, Meharg A A. 2001b. Phytochelatins are involved in differential arsenate tolerance in *Holcus lanatus*. *Plant Physiol*, **126**(1): 299–306.

Hore P, Nahar S, Hasampura M, Tanti B. 2017. Phylogenetic analysis and homology modelling of betaine aldehyde dehydrogenase: An aroma producing protein in rice (*Oryza sativa* L.). *Int J Multidiscip Approach Stud*, **4**(3): 139–148.

Huang J H, Hu K N, Decker B. 2011. Organic arsenic in the soil environment: Speciation, occurrence, transformation, and adsorption behaviour. *Water Air Soil Pollut*, **219**: 401–415.

Huang J H. 2014. Impact of microorganisms on arsenic biogeochemistry: A review. *Water Air Soil Pollut*, **225**: 1848.

Indian Council of Agricultural Research (ICAR). 2009. Classification of pesticides based on their chemical nature. *Handbook Agric*, **6**: 716–719.

Indriolo E, Na G, Ellis D, Salt D E, Banks J A. 2010. A vacuolar arsenite transporter necessary for arsenic tolerance in the arsenic hyperaccumulating fern *Pteris vittata* is missing in flowering plants. *Plant Cell*, **22**: 2045–2057.

Irtelli B, Navari-Izzo F. 2008. Uptake kinetics of different arsenic species by *Brassica carinata*. *Plant Soil*, **30**[illegible]105–113.

Jaiswal S. 2011. Role of rhizobacteria in reduction of arsenic uptake

Principal
Nowgong Girls' College
Nagaon :: Assam

Nowgong Girls' College ★ ESTD 1962 ★ Nagaon :: Assam

by plants: A review. *J Bioremed Biodegrad*, **2**: 4.

Jedynak L, Kowalska J, Kossykowska M, Golimowski J. 2010. Studies on the uptake of different arsenic forms and the influence of sample pretreatment on arsenic speciation in white mustard (*Sinapis alba*). *Microchem J*, **94**(2): 125–129.

Jorhem L, Astrand C, Sundström B, Baxter M, Stokes P, Lewis J, Grawé K P. 2007. Elements in rice on the Swedish market: I. Cadmium, lead and arsenic (total and inorganic). *Food Add Contam: Part A*, **25**(3): 284–292.

Krishnamurthy A, Rathinasabapathi B. 2013. Auxin and its transport play a role in plant tolerance to arsenite-induced oxidative stress in *Arabidopsis thaliana*. *Plant Cell Environ*, **36**(10): 1838–1849.

Kumar S, Dubey R S, Tripathi R D, Chakrabarty D, Trivedi P K. 2015. Omics and biotechnology of arsenic stress and detoxification in plants: Current updates and prospective. *Environ Int*, **74**: 221–230.

Lahkar L, Tanti B. 2017. Study of morphological diversity of traditional aromatic rice landraces (*Oryza sativa* L.) collected from Assam, India. *Ann Plant Sci*, **6**(12): 1855–1861.

Li G, Sun G X, Williams P N, Nunes L, Zhu Y G. 2011. Inorganic arsenic in Chinese food and its cancer risk. *Environ Int*, **37**(7): 1219–1225.

Li R Y, Ago Y, Liu W J, Mitani N, Feldmann J, McGrath S P, Ma J F, Zhao F J. 2009. The rice aquaporin Lsi1 mediates uptake of methylated arsenic species. *Plant Physiol*, **150**(4): 2071–2080.

Li Y, Dhankher O P, Carreira L, Lee D, Chen A, Schroeder J I, Balish R S, Meagher R B. 2004. Overexpression of phytochelatin synthase in *Arabidopsis* leads to enhanced arsenic tolerance and cadmium hypersensitivity. *Plant Cell Physiol*, **45**(12): 1787–1797.

Liang F, Li Y, Zhang G L, Tan M G, Lin J, Liu W, Li Y, Lu W. 2010. Total and speciated arsenic levels in rice from China. *Food Addit Contam: Part A*, **27**(6): 810–816.

Liu C P, Luo C L, Gao Y, Li F B, Lin L W, Wu C A, Li X D. 2010. Arsenic contamination and potential health risk implications at an abandoned tungsten mine, southern China. *Environ Pollut*, **158**(3): 820–826.

Liu W J, Zhu Y G, Smith F A, Smith S E. 2004a. Do phosphorus nutrition and iron plaque alter arsenate (As) uptake by rice seedlings in hydroponic culture. *New Phytol*, **162**(2): 481–488.

Liu W J, Zhu Y G, Smith F A, Smith S E. 2004b. Do iron plaque and genotypes affect arsenate uptake and translocation by rice seedlings (*Oryza sativa* L.) grown in solution culture. *J Exp Bot*, **55**: 1707–1713.

Lomax C, Liu W J, Wu L Y, Xue K, Xiong J B, Zhou J Z, McGrath S P, Meharg A A, Miller A J, Zhao F J. 2012. Methylated arsenic species in plants originate from soil microorganisms. *New Phytol*, **193**(3): 665–672.

Ma J F, Yamaji N, Mitani N, Xu X Y, Su Y H, McGrath S P, Zhao F J. 2008. Transporters of arsenite in rice and their role in As accumulation in rice grain. *Proc Natl Acad Sci USA*, **105**(29): 9931–9935.

Ma L Q, Komar K M, Tu C, Zhang W, Cai Y, Kennelley E D. 2001. A fern that hyperaccumulates arsenic. *Nature*, **409**: 579.

Meharg A A, Williams P N, Adomako E, Lawgali Y Y, Deacon C, Villada A, Cambell R C J, Sun G, Zhu Y G, Feldmann J, Raab A, Zhao F J, Islam R, Hossain S, Yanai J. 2009. Geographical variation in total and inorganic arsenic content of polished (white) rice. *Environ Sci Technol*, **43**(5): 1612–1617.

Mitra A, Chatterjee S, Moogouei R, Gupta D K. 2017. Arsenic accumulation in rice and probable mitigation approaches: A review. *Agronomy*, **7**(4): 67.

Mosa K A, Kumar K, Chhikara S, McDermott J, Liu Z, Musante C, White J C, Dhankher O P. 2012. Members of rice plasma membrane intrinsic proteins subfamily are involved in arsenite permeability and tolerance in plants. *Transg Res*, **21**(6): 1265–1277.

Nahar S, Kalita J, Sahoo L, Tanti B. 2016. Morphophysiological and molecular effects of drought stress in rice. *Ann Plant Sci*, **5**(9): 1409–1416.

Nahar S, Vemireddy L R, Sahoo L, Tanti B. 2018. Antioxidant protection mechanisms reveal significant response in drought-induced oxidative stress in some traditional rice of Assam, India. *Rice Sci*, **25**(4): 185–196.

Nath S, Panda P, Mishra S, Dey M, Choudhury S, Sahoo L, Panda S K. 2014. Arsenic stress in rice: Redox consequences and regulation by iron. *Plant Physiol Biochem*, **80**: 203–210.

Ng J C, Wang J P, Shraim A. 2003. A global health problem caused by arsenic from natural sources. *Chemosphere*, **52**(9): 1353–1359.

Norton G J, Nigar M, Williams P N, Dasgupta T, Meharg A A, Price A H. 2008. Rice-arsenate interactions in hydroponics: A three-gene model for tolerance. *J Exp Bot*, **59**(8): 2277–2284.

Norton G J, Deacon C M, Xiong L Z, Huang S Y, Meharg A A, Price A H. 2010. Genetic mapping of the rice ionome in leaves and grain: Identification of QTLs for 17 elements including arsenic, cadmium, iron and selenium. *Plant Soil*, **329**: 139–153.

Panaullah G M, Alam T, Hossain M B, Loeppert R H, Lauren J G, Meisner C A, Ahmed Z U, Duxbury J M. 2008. Arsenic toxicity to rice (*Oryza sativa* L.) in Bangladesh. *Plant Soil*, **317**(1): 31–39.

Patel K S, Shrivas K, Brandt R, Jakubowski N, Corns W, Hoffmann P. 2005. Arsenic contamination in water, soil, sediment and rice of central India. *Environ Geochem Health*, **27**(2): 131–145.

Pickering I J, Prince R C, George M J, Smith R D, George G N, Salt D E. 2000. Reduction and coordination of arsenic in Indian Mustard. *Plant Physiol*, **122**(4): 1171–1177.

Quazi S, Datta R, Sarkar D. 2011. Effect of soil [illegible] and [illegible] arsenical pesticide on rice growth and develo[illegible]. *Int J Environ Sci Technol*, **8**(3): 450–460.

Raab A, Williams P N, Meharg A, Feldman[illegible] 2007. Uptake and

Principal
Nowgong Girls' College
Nagaon :: Assam

Nowgong Girls' College ★ ESTD 1962 ★ Assam

translocation of inorganic and methylated arsenic species by plants. *Environ Chem*, **4**: 197–203.

Rahman M A, Hasegawa H, Rahman M M, Islam M N, Miah M A M, Tasmin A. 2007. Effect of arsenic on photosynthesis, growth and yield of five widely cultivated rice (*Oryza sativa* L.) varieties in Bangladesh. *Chemosphere*, **67**(6): 1072–1079.

Rahman M A, Hasegawa H, Rahman M M, Miah M A M, Tasmin A. 2008. Straighthead disease of rice (*Oryza sativa* L.) induced by arsenic toxicity. *Environ Exp Bot*, **62**(1): 54–59.

Rahman M A, Hasegawa H. 2011. High levels of inorganic arsenic in rice in areas where arsenic contaminated water is used for irrigation and cooking. *Sci Total Environ*, **409**(22): 4645–4655.

Rhine E D, Ni Chadhain S M, Zylstra G J, Young L Y. 2007. The arsenite oxidase genes (aroAB) in novel chemoautotrophic arsenite oxidizers. *Biochem Biophys Res Commun*, **354**(3): 662–667.

Santini J M, Sly L I, Schnagl R D, Macy J M. 2000. A new chemolithoautotrophic arsenite-oxidizing bacterium isolated from a gold mine: Phylogenetic, physiological, and preliminary biochemical studies. *Appl Environ Microbiol*, **66**(1): 92–97.

Santra S C, Samal A C, Bhattacharya P, Banerjee S, Biswas A, Majumdar J. 2013. Arsenic in foodchain and community health risk: A study in Gangetic West Bengal. *Proced Environ Sci*, **18**: 2–13.

Sarma B, Basumatary N R, Nahar S, Tanti B. 2016. Effect of drought stress on morpho-physiological traits in some traditional rice cultivars of Kokrajhar district, Assam, India. *Ann Plant Sci*, **5**(8): 1402–1408.

Schulz H, Härtling S, Tanneberg H. 2007. The identification and quantification of arsenic-induced phytochelatins comparison between plants with varying arsenic sensitivities. *Plant Soil*, **303**: 275–287.

Sharma I. 2013. Arsenic-induced oxidative stress and antioxidant defense system of *Pisum sativum* and *Pennisetum typhoides*: A comparative study. *Res J Biotechnol*, **8**(4): 48–56.

Singh A K. 2004. Arsenic Contamination in Groundwater of North Eastern India. *In*: Proceedings of National seminar on Hydrology with focal theme on Water Quality. Roorkee, India: National Institute of Hydrology: 255–262.

Singh N, Ma L Q, Srivastava M, Rathinasabapathi B. 2006. Metabolic adaptations to arsenic-induced oxidative stress in *Pteris vittata* L. and *Pteris ensiformis* L. *Plant Sci*, **170**(2): 274–282.

Smedley P L, Kinniburgh D G. 2002. A review of the source, behaviour and distribution of arsenic in natural waters. *Appl Geochem*, **17**(5): 517–568.

Smedley P L. 2006. Sources and distribution of arsenic in groundwater and aquifers. *In*: Proceedings in Seminar: Arsenic in Groundwater: A World Problem. Utrecht.

Sohn E. 2014. Contamination: The toxic side of rice. *Nature*, **514**: 62–63.

Song W Y, Park J, Mendoza-Cózatl D G, Suter-Grotemeyer M, Shim D, Hörtensteiner S, Geisler M, Weder B, Rea P A, Rentsch D, Schroeder J I, Lee Y, Martinoia E. 2010. Arsenic tolerance in *Arabidopsis* is mediated by two ABCC-type phytochelatin transporters. *Proc Natl Acad Sci USA*, **107**: 21187–21192.

Spagnoletti F, Lavado R S. 2015. The arbuscular mycorrhiza rhizophagus intraradices reduces the negative effects of arsenic on soybean plants. *Agron J*, **5**(2): 188–199.

Srivastava S, Mishra S, Tripathi R D, Dwivedi S, Trivedi P K, Tandon P K. 2007. Phytochelatins and antioxidant systems respond differentially during arsenite and arsenate stress in *Hydrilla verticillata* (L.f.) Royle. *Environ Sci Technol*, **41**(8): 2930–2936.

Srivastava S, Sharma Y K. 2013. Altered growth, photosynthetic machinery and induced oxidative stress in spinach in response to arsenic stress. *J Plant Physiol Pathol*, **1**: 4.

Suhadolnik M L S, Salgado A P C, Scholte L L S, Bleicher L, Costa P S, Reis M P, Dias M F, Avila M P, Barbosa F A R, Chartone-Souza E, Nascimento A M A. 2017. Novel arsenic-transforming bacteria and the diversity of their arsenic-related genes and enzymes arising from arsenic-polluted freshwater sediment. *Sci Rep*, **7**(1): 1–17.

Takahashi Y, Minamikawa R, Hattori K H, Kurishima K, Kihou N, Yuita K. 2004. Arsenic behaviour in paddy fields during the cycle of flooded and non-flooded periods. *Environ Sci Technol*, **38**(4): 1038–1044.

Talukder A S M H M, Meisner C A, Sarkar M A R, Islam M S. 2011. Effect of water management, tillage options and phosphorus status on arsenic uptake in rice. *Ecotoxicol Environ Safety*, **74**(4): 834–839.

Torres-Escribano S, Leal M, Vélez D, Montoro R. 2008. Total and inorganic arsenic concentrations in rice sold in Spain, effect of cooking, and risk assessments. *Environ Sci Technol*, **42**(10): 3867–3872.

Turpeinen R, Pantsar-Kallio M, Kairesalo T. 2002. Role of microbes in controlling the speciation of arsenic and production of arsines in contaminated soils. *Sci Total Environ*, **285**: 133–145.

Verbruggen N, Hermans C, Schat H. 2009. Mechanisms to cope with arsenic or cadmium excess in plants. *Curr Opin Plant Biol*, **12**(3): 364–372.

Wang J R, Zhao F J, Meharg A A, Raab A, Feldmann, McGrath S P. 2002. Mechanisms of arsenic hyperaccumulation in *Pteris vittata*: Uptake kinetics, interactions with phosphate, and arsenic speciation. *Plant Physiol*, **130**(3): 1552–1561.

Williams P N, Price A H, Raab A, Hossain S A, Feldmann J, Meharg A A. 2005. Variation in arsenic speciation and concentration in paddy rice related to dietary exposure. *Environ Sci Technol*, **39**(15): 5531–5540.

Williams P N, Islam M R, Adomako E E, Raab A, Hossain S A, Zhu Y G, Feldman J, Meharg A A. 2006. Increase in rice grain arsenic for regions of Bangladesh irrigating paddies with elevated arsenic in groundwaters. *Environ Sci Technol*, **40**: 4903–4908.

Woolson E A. 1977. Fate of arsenicals in different environmental substrates. *Environ Health Perspect*, **19**: 73–81.

Wu Z C, Ren H Y, McGrath S P, Wu P, Zhao F J. 2011. Investigating the contribution of the phosphate transport pathway to arsenic accumulation in rice. *Plant Physiol*, **157**(1): 498–508.

Xu J M, Shi S L, Wang L, Tang Z, Lv T T, Zhang L, Ding Y M, Wang Y F, Zhao F J, Wu Z C. 2017. OsHAC4 is critical for

Principal
Nowgong Girls' College
Nagaon :: Assam

Nowgong Girls' College ★ Assam ★ ESTD: 1962

arsenate tolerance and regulates arsenic accumulation in rice. *New Phytol*, **215**(3): 1090–1101.

Xu X Y, McGrath S P, Zhao F J. 2007. Rapid reduction of arsenate in the medium mediated by plant roots. *New Phytol*, **176**(3): 590–599.

Xu X Y, McGrath S P, Meharg A A, Zhao F J. 2008. Growing rice aerobically markedly decreases arsenic accumulation. *Environ Sci Technol*, **42**(15): 5574–5579.

Ye W L, Khan M A, McGrath S P, Zhao F J. 2011. Phytoremediation of arsenic contaminated paddy soils with *Pteris vittata* markedly reduces arsenic uptake by rice. *Environ Pollut*, **159**(12): 3739–3743.

Zavala Y J, Gerads R, Gürleyük H, Duxbury J M. 2008. Arsenic in Rice: II. Arsenic speciation in USA grain and implications for human health. *Environ Sci Technol*, **42**(10): 3861–3866.

Zhang J, Zhu Y G, Zeng D L, Cheng W D, Qian Q, Duan G L. 2008. Mapping quantitative trait loci associated with arsenic accumulation in rice (*Oryza sativa*). *New Phytol*, **177**(2): 350–355.

Zhao F J, Wang J R, Barker J H A, Schat H, Bleeker P M, McGrath S P. 2003. The role of phytochelatins in arsenic tolerance in the hyperaccumulator *Pteris vittata*. *New Phytol*, **159**(2): 403–410.

Zubair M, Martyniuk C J, Shaheen A. 2017. Rising level of arsenic in water and fodder: A growing threat to livestock and human populations in Pakistan. *Toxin Rev*: 1–11.

(Managing Editor: LI Guan)

Principal
Nowgong Girls' College
Nagaon :: Assam

Nowgong Girls' College ★ Nagaon :: Assam ★ ESTD: 1962

ChemPubSoc Europe

DOI: 10.1002/slct.201803000

Chemistry SELECT Full Papers

Catalysis

Selective and Green Sulfoxidation in Water using a New Chitosan Supported Mo(VI) Complex as Heterogeneous Catalyst

Kabirun Ahmed, Gangutri Saikia, Pakiza Begum, Sandhya Rani Gogoi, Mitu Sharma, Hiya Talukdar, and Nashreen S. Islam*[a]

Immobilization of oxo-peroxo molybdenum(VI) species on natural biopolymer, chitosan led to the development of a new heterogeneous catalyst which displayed excellent activity, stability and chemoselectivity for the oxidation of a wide variety of sulfides to the respective sulfoxides by H_2O_2 in water, at ambient temperature. The catalyst has been comprehensively characterized by elemental analysis, spectral studies (FTIR, Raman, solid-state ^{13}C NMR and diffuse reflectance UV-Vis), PXRD, Brunauer-Emmett-Teller (BET), SEM, EDX and TGA-DTG analysis. The density functional theory (DFT) method has been employed to study the structure of the synthesized chitosan peroxomolybdenum complex (**PMoCh**). In addition to water, the catalyst is also highly compatible with a variety of safer organic solvents like methanol and acetonitrile. Apart from being high yielding and operationally simple, the developed catalytic protocol is environmentally clean and safe as it is absolutely free from halogenated organic solvent. Other significant green attributes of the methodology include its ready scalability, high H_2O_2 efficiency and easy recyclability of the catalyst for several catalytic cycles with consistent activity/selectivity profile.

Introduction

Immobilization of catalytically active transition metal complexes on insoluble polymer supports often leads to heterogenised catalysts that offer the advantages of ease of separation and recovery of the catalyst by enhancing the catalyst stability within the polymer.[1] Apart from improving the overall productivity and cost effectiveness of the process, the catalyst recycling minimizes the environmental impact of a chemical transformation, thereby contributing to the sustainability of the process.[1] In recent years, natural polymers such as cellulose, chitin and chitosan have been attracting considerable attention as promising green support materials for heterogenisation of metal catalysts.[1a,2] Chitosan, the deacetylated derivative of chitin, is one of the most abundant biopolymers in nature.[3] The unique features of chitosan such as their non-toxicity, biodegradability, biocompatibility and easy accessibility make it vastly attractive for a wide variety of potential applications in areas ranging from therapeutics, cosmetics, food processing to environmental applications.[2,3]

Moreover, owing to the high thermal stability, durability, facile functionalization of chitosan and its derivatives, this class of biopolymers are increasingly being recognized as highly efficient solid support ideal for catalytic application.[4] Due to the presence of active amino group along with the hydroxyl group in the polymer, it has the potential to bind with transition metals through chelation or ion exchange method facilitating chitosan metal complexes to be thermally stable and leaching resistant.[4] There has been plethora of reports demonstrating heterogenized chitosan metal complexes as catalysts in diverse organic transformations such as hydrogenation,[5] condensation,[4a,6] water splitting reaction,[7] coupling reaction,[8] polymerization,[9] hydroxylation,[10] Suzuki and Hecks reactions[11] etc. However, a survey of literature revealed that data concerning heterogeneous catalytic oxidation with chitosan immobilized metal complexes are still very limited.[1e,3a]

Selective oxidation of thioethers to the corresponding sulfoxide is one of the most fundamentally and industrially important transformations in organic synthesis as sulfoxides serve as significant intermediates for generating a range of fine chemicals and biologically active molecules, including therapeutic agents and chiral auxiliaries.[12] Since the first successful synthesis of sulfoxides by Maercker in 1865,[13] multitude of interesting and promising methodologies based on transition metal catalysts, including titanium,[14] vanadium,[15] molybdenum,[16] niobium,[17] iron,[15c,18] tungsten,[4c,15d,16e,19] systems have been developed for oxidation of sulfides using H_2O_2 as an eco-friendly oxidant.[20] Nevertheless, the important criterion of ecological sustainability concerning the selective oxidation of sulfides is still a challenging issue to address. Many of the available otherwise efficient oxidation protocols still rely upon

[a] K. Ahmed, G. Saikia, Dr. P. Begum, S. R. Gogoi, M. Sharma, H. Talukdar, Prof. N. S. Islam
Department of Chemical Sciences
Tezpur University
Napaam, Tezpur-784028, Assam, India
Phone: +91-9435380222 (Off.)
Phone: +91-3712-267007
Fax: +91-3712-267006
E-mail: ...@tezu.ernet.in
nashreen.islam@rediffmail.com

Supporting information for this article is available on the WWW under https://doi.org/10.1002/slct.201803000

© 2018 Wiley-VCH Verlag GmbH & Co. KGaA, Weinheim

Nowgong Girls' College Nagaon :: Assam STD 1962

Principal
Nowgong Girls' College
Nagaon :: Assam

NJC

PAPER

View Article Online
View Journal | View Issue

Check for updates

Cite this: New J. Chem., 2018, 42, 5142

Vanadium-based polyoxometalate complex as a new and efficient catalyst for phenol hydroxylation under mild conditions†

Mitu Sharma,[a] Gangutri Saikia,[a] Kabirun Ahmed,[a] Sandhya Rani Gogoi,[a] Vedavati G. Puranik[b] and Nashreen S. Islam *[a]

Received 15th November 2017,
Accepted 12th February 2018

DOI: 10.1039/c7nj04433j

rsc.li/njc

An eco-compatible catalytic protocol for H_2O_2 induced hydroxylation of phenol (PH) to catechol (CT) and hydroquinone (HQ) in aqueous medium, using a polyoxovanadate (POV) complex as the catalyst, is described. The synthesis of the POV catalyst, with a new type of three dimensional framework, $Na_6(H_2O)_{22}(V_{10}O_{28})\cdot 2H_2O$ (**1**) was accomplished by establishing a non-hydrothermal one-step methodology under mild conditions. The catalyst was characterized by elemental analysis, spectral studies, single crystal X-ray diffraction studies, and Brunauer–Emmett–Teller (BET) and TGA analysis. Under optimum conditions of reaction, conducted at ambient temperature, the phenol conversion reached up to 55.4% providing a TON of 138. The catalyst could be recovered easily and recycled at least up to three cycles without significant change in activity. The developed methodology is operationally simple and free from halogenated solvents or any other hazardous additives.

Introduction

Oxidation of phenol (PH) into dihydroxybenzenes (DHBs) such as catechol (CT) and hydroquinone (HQ) represents one of the most fundamentally and industrially important processes in organic synthesis.[1] Catechol and hydroquinone are known to serve as significant intermediates for obtaining a wide range of fine chemicals[2] and biologically active molecules[1a,3] including pharmaceuticals, agrochemicals, perfumes, flavors, antioxidants and polymerization inhibitors.[1a,2] Moreover, with phenol being largely present as a highly toxic, carcinogenic and poorly biodegradable waste[4] in chemical industry wastewaters,[4b,5] oxidation of phenol to high-value chemical products is gaining importance from environmental perspectives as well.

A large number of promising catalytic strategies for phenol oxidation have been developed over the years using H_2O_2 as a green oxidant,[3a,b,6–8] including transition metal based nano-catalysts,[9a–c] layered double hydroxides,[9d] modified zeolite catalysts,[9e,f] hydroxyl porphyrins[9h] and metal organic frameworks.[9g] Many of the available methods, however, still rely on the use of toxic and volatile organic solvents as the reaction medium, or are associated with one or more limitations such as high cost, complicated catalyst preparation, difficulty in regeneration of the catalyst, requirements of high temperature *etc.*[4b,9g] Thus, the search for newer alternative catalysts and oxidation protocols that use safer green reagents as well as benign non-polluting reaction media continues unabated.[10] With water being the ultimate green natural solvent,[11] there has been a recent upsurge in interest in aqueous phase organic reactions. This also necessitated the development of water-tolerant catalysts and water soluble ligands to support such transformations.[11a,c,12a] However, reports on water-based metal-catalysed phenol hydroxylation processes in aqueous medium are still very limited.[2,3a,9j,13]

In the recent past, we have developed a number of new homogeneous as well as heterogeneous catalysts and eco-compatible catalytic protocols based on peroxo compounds of d^0 metal ions, *viz.*, V(v), Nb(v), Mo(vi) and W(vi), for a variety of oxidative organic transformations including sulfide oxidation and oxidative bromination.[12] Significantly, a few of these systems proved to be excellent recoverable catalysts for clean and selective oxidation of sulfides with 30% H_2O_2 in neat water.[12a,c]

As a direct sequel to our efforts to develop convenient and sustainable methodologies and catalysts to accomplish organic oxidations, in the present work we have focused on exploring the scope of using a sodium decavanadate (V_{10}) complex as the catalyst, to achieve phenol hydroxylation in aqueous medium. Polyoxovanadates (POVs) have been recognized as an important

[a] Department of Chemical Sciences, Tezpur University, Tezpur 784 028, Assam, India. E-mail: nsi@tezu.ernet.in, nashreen.islam@redf@mail.com; Tel: +91 9435380222
[b] Materials Characterisation, National Chemical Laboratory,

† Electronic supplementary information (ESI) available: PSD curve, crystal diagrams, [illegible] efficiency calculation, FTIR and ^{51}V-NMR spectra for the recyclability of the catalyst. CCDC 1523627. For ESI and crystallographic data in CIF or other electronic format see DOI: 10.1039/c7nj04433j

Principal
Nowgong Girls' College
Nagaon :: Assam

 This journal is © The Royal Society of Chemistry and the Centre National de la Recherche Scientifique 2018

Published on 13 February 2018. Downloaded by Tezpur University on 10/23/2018 6:48:39 AM.

This is an open access article published under an ACS AuthorChoice License, which permits copying and redistribution of the article or any adaptations for non-commercial purposes.

ACS OMEGA

Perspective

Cite This: ACS Omega 2018, 3, 9462−9475

http://pubs.acs.org/journal/acsodf

Lanthanide(III)-Based Single-Ion Magnets

Atanu Dey,[†] Pankaj Kalita,[‡] and Vadapalli Chandrasekhar*[,†,§]

[†]Tata Institute of Fundamental Research Hyderabad, Hyderabad 500107, India

[‡]School of Chemical Sciences, National Institute of Science Education and Research, HBNI, Bhubaneswar 752050, India

[§]Department of Chemistry, Indian Institute of Technology Kanpur, Kanpur 208016, India

Supporting Information

ABSTRACT: Mononuclear lanthanide-based single-ion magnets (SIMs) are known since 2003 with the discovery of SIM properties in a bis-(phthalocyaninato)lanthanide complex. A recent report on $[Dy(Cp^{ttt})_2][BC_8F_5]$ indicating that it exhibits the highest known blocking temperature (60 K) has spurred fresh interest in this area. In this article, we discuss about the various requirements of lanthanide-based SIMs along with representative examples. Specifically, we describe the complexes whose coordination numbers vary from 2 to 8. We also discuss the representative examples of organometallic lanthanide complexes that can function as molecular magnets.

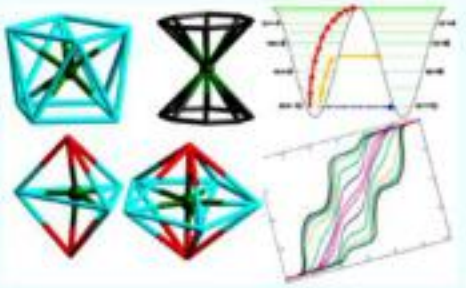

1. INTRODUCTION

The discovery of single-molecule magnetism in the dodecanuclear mixed-valent (Mn^{IV}/Mn^{III}) complex, $[Mn^{III}_6Mn^{IV}_6O_{12}(O_2CMe)_{16}(H_2O)_4]$ (hereafter $Mn_{12}Ac$) (**1**),[1] heralded the birth of an interdisciplinary field involving the study of molecular magnets.[2] Such systems have attracted the attention of chemists, physicists, and materials scientists for several reasons. These include the challenges involved in their design and syntheses, understanding their physics, and harnessing their applications in many new technologically relevant areas.[3] The latter include high-energy density storage,[4] molecular spintronics,[4b,c,5] quantum computation,[4a,c,d,6] molecular refrigeration,[7] and so forth.

Single-molecule magnets (SMMs) are characterized by an energy barrier, U_{eff}, which has to be overcome for spin reversal. Several mechanisms for the relaxation of the magnetization of SMMs are now known; these are discussed briefly vide infra. Another important parameter that can attest to the quality of an SMM is the so-called blocking temperature, T_B, below which the magnetization of the system is blocked, allowing it to function as an SMM. Although the value of T_B depends on the manner in which the experiment is carried out (the frequency of measurement in an ac susceptibility experiment or the rate of sweep of magnetic field in an M vs H experiment), it is still a useful parameter for comparing various SMMs.[8] The highest T_B (60 K) observed till date is for the complex, $[Dy(Cp^{ttt})_2][BC_8F_5]$ ($Cp^{ttt} = C_5H_2{}^tBu_3$-1,2,4) (**2**).[9]

The field of SMMs was initially dominated by polynuclear transition metal clusters not only because of the inspiration of $Mn_{12}Ac$ but also because of the understanding gained in the subject that the U_{eff} for such SMMs qualitatively equals $|D|(S^2 - 1/4)$ for half-integer spins and $|D|S^2$ for integer spins [D = zero-field splitting parameter related to the Ising-type magnetic anisotropy of the system; S = total spin of the system].[8] After a flurry of activity involving several polynuclear transition-metal complexes, it was soon realized that a linear increase of S does not lead to an increase in U_{eff} and that the factors that would enable the enhancement of magnetic anisotropy are more important.[10] This realization was also coincident with the discovery that lanthanide-based mononuclear complexes $(Bu_4N)[Ln^{III}Pc_2]$ [Ln = Tb (**3**), Dy (**4**); Pc = phthalocyaninato] were SMMs.[11] This report slowly shifted the focus of research from polynuclear complexes to mononuclear complexes as systems suitable for the SMM behavior. Such systems are also now known as single-ion magnets (SIMs). Although both transition-metal[12] and lanthanide[13]/actinide[13g,h,14] SIMs are now known, this review will focus on lanthanide-based SIMs. Most lanthanide ions except La^{III}, Gd^{III}, and Lu^{III} show a strong spin−orbit coupling (SOC) because of the large unquenched orbital angular momentum. Because of this, in lanthanide complexes, Ln^{III} ions show a larger SOC energy ($\Delta E = 10^4$ to 10^3 cm^{-1}) in comparison to the crystal field (CF) splitting ($\Delta E = 10^3$ to 10^2 cm^{-1}). The reverse is true for the 3d metal-ion complexes where the CF splitting is found to be significantly larger compared to SOC ($\Delta E = 10^3$ cm^{-1} and $\Delta E = 10$ cm^{-1}, respectively).[15] On the basis of the current understanding, the key factors needed to maximize U_{eff} in the lanthanide-based SMMs and SIMs can be summarized as follows: (i) the ground $\pm m_J$ states should be degenerate with the highest m_J value (as expected for Kramers ions, to achieve magnetic bistability),[16]

Received: June 1, 2018
Accepted: August 3, 2018
Published: August 20, 2018

 © 2018 American Chemical Society

DOI: 10.1021/acsomega.8b01304
ACS Omega 2018, 3, 9462−9475

Pankaj Kalita

Nowgong Girls' College ★ ESTD: 1962 ★ Nagaon :: Assam

C.T.C.
Principal
Nowgong Girls' College
Nagaon :: Assam

NGJI, An International Refereed Journal
(NGSI-BHU, ISSN: 0027-9374/2018/1650)
Vol. 64, No. 1-2, March-June, 2018

Estimation of soil loss sensitivity in the Jinari river basin using the Universal Soil Loss Equation

Nilotpal Kalita[1], Akangsha Borgohain[2], Dhrubajyoti Sahariah[3] and Siddhinath Sarma[4]

Abstract

Soil erosion hazard is an environmental problem in diverse geographical areas and oftentimes has repercussions that are felt in downstream areas. This study assesses various aspects of soil erosion in the Jinari River basin in Assam, India using the Universal Soil Loss Equation (USLE) in a GIS environment. The average rainfall erosivity index is found as 165.2 MJ mm/ha/yr and soil erodability factor K varies between 0.56 - 0.43. The LS factor was computed using Digital Elevation Model (DEM) data, while the C factor was computed from Normalized Difference Vegetative Index (NDVI) values derived from Landsat TM data. In the Jinari River basin no supporting practice was observed, thus the value of 'P' has been taken as 1. The average annual soil loss estimated in the watershed using USLE was 1.76 ton/ha/yr and 0.95 ton/ha/yr for 2007 and 2011 respectively.

Keynote: *USLE, soil loss, river basin management*

Introduction

Soil erosion is the result of the interplay of several complex parameters such as slope, rock type, relief, rainfall, as well as land use and land cover. It is a phenomenon which consists of detachments of individual soil particles from the soil mass and their transportation by erosive agents like running water and wind. Soil loss is the net mass of sediment removed from a particular portion of the slope (Kalita & Sarmah, 2016). Soil loss can be an environmental problem when it happens due to the strong force of water action. Several studies have used Universal Soil Loss Equation (USLE) and Revised Universal Soil Loss Equation (RUSLE) models to identify soil loss sensitivity zones (Sen et al., 2001; Wang et al., 2003; Dabral et al., 2008; Karaburun, 2010; Prasannakumar et al., 2011; Ghosh et al., 2013; Farhan et al., 2013; Jaiswal et al. 2014).

Jinari River and its environment

The Jinari River is a south bank tributary of the Brahmaputra River, Assam. It lies in between the East Garo Hills district of Meghalaya

1. Assistant Professor, Department of Geography, Gossaigaon College, Gossaigaon
2. Research Scholar, Department of Geography, Gauhati University, Guwahati
3. Associate Professor, Department of Geography, Gauhati University, Guwahati
4. Associate Professor, Department of Geography, Goalpara College, Goalpara

C.T.C.
Principal
Nowgong Girls' College
Nagaon :: Assam

Nowgong Girls' College ★ Nagaon :: Assam ★ ESTD: 1962

and Goalpara district of Assam. The locational extent of the basin is 900 20/ 0 // E - 90 0 42 / 30// E longitude to 260 8/ 30// N - 250 44/ 0 // N latitude. It is surrounded by Dudhnoi-Krishnai sub basin on the east and south and the Jinjiram sub basin on the West and by the Brahmaputra to the north. The river basin covers an area of 432.9 km2. The catchment areas that lie within the state of Meghalaya are mostly hilly barring a few narrow floodplains along its course. In the Goalpara district of Assam, the catchment is mostly along level lowland stretches barring a few hill sections portion on the south of the National Highway No -37.

On October 7 of the year 2004, a flash flood in Jinari river of Assam was triggered by a cloudburst over Meghalaya that caused great havoc in the downstream areas in Assam. This sudden event wiped out about 20 villages over an area of about 4 sq. km, killing 250 people. A similar cloudburst occurred in 2014 killing 40 people (Report, 2017). As the shape of the Jinari basin is elongated therefore surface flow has a low lag time, thereby creating flash flood in the downstream areas. However, due to lack of rain gauges inside the basin, proper documentation of the cloud burst events are missing. The Jinari basin has a long history of climatic and geomorphic disaster and therefore understanding the physical parameters is necessary. This present study aims to quantify the nature of soil loss in the basin with the help of proven model USLE.

Data and Methods

USLE has been used in the study area to investigate the long term average soil loss of concerned field area for the year 2007 and 2011 using Landsat TM data to identify the specific crop-cover management practices that underlie the erosion processes.

The general USLE model is as follows:

$$A = R*K*LS*C*P$$

where, A is average annual soil loss (t ha?1y?1); R is the rainfall and runoff erosivity

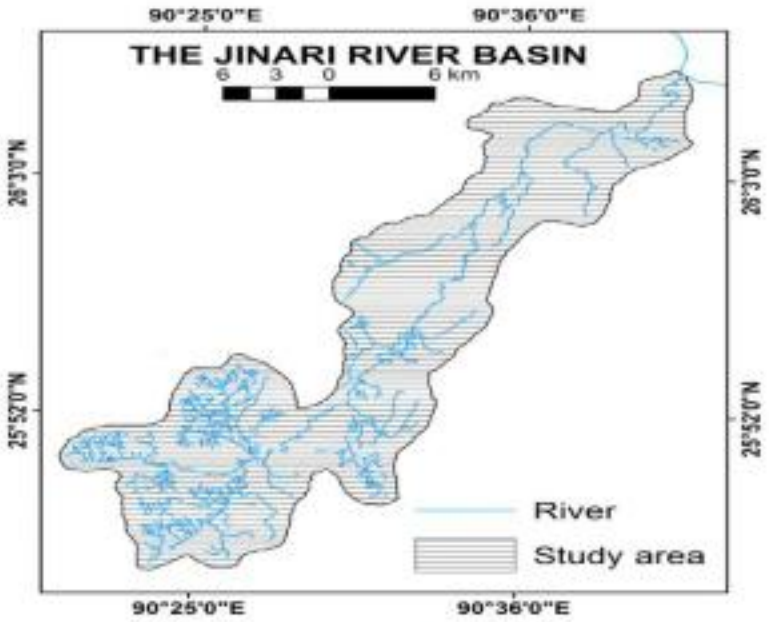

Fig. 1: Location of the study area

Principal
Nowgong Girls' College
Nagaon :: Assam

Nowgong Girls' College ★ Nagaon :: Assam ★ ESTD: 1962

index (in MJ mm ha-1hr-1); K is the soil erodibility factor (in ton/MJ/mm); LS is the slope and length of slope factor; C is the crop-cover management factor; P is the is the supporting conservation practice factor. For the calculation of these factors, the data were collected from various sources. The rainfall data was obtained from the Water Resource Department, Government of Assam; the soil data for the calculation of K was collected from Agricultural Department, Government of Assam; while a Cartosat Digital Elevation Model (DEM) was used to generate terrain data in the area of interest and finally Landsat TM satellite imagery of 2011 was downloaded from the USGS website. The following is a schema of the workflow employed in the present analysis (Fig. 2):

Rainfall and runoff erosivity factor (R)

The rainfall-runoff erosivity factor (R) quantifies the effect of raindrop impact and reflects the amount and rate of runoff likely to be associated with rain. It is a numerical description of the ability of rainfall to erode soil (Wischmeier and Smith, 1978). The R values can also be obtained by 'iso erodent' maps, tables as well as historic data of the area concerned (Renard et al., 1997). The following equation is used in estimating the R factor in the Indian context which is given by Singh et al (1981).

$$R = 79 + 0.363 * P$$

Here, R is the annual R factor; P is the average annual rainfall in mm.

Soil erodability factor (K)

The soil erodibility (K) values are computed from the soil map data prepared by the Department of Agriculture, Government of Assam. Since, K factor value is mainly related to soil texture, thus in computing soil erodibility factor soil properties that were collected from the technical bulletin on soil series of Assam as well as soil samples collected through field investigation were used.

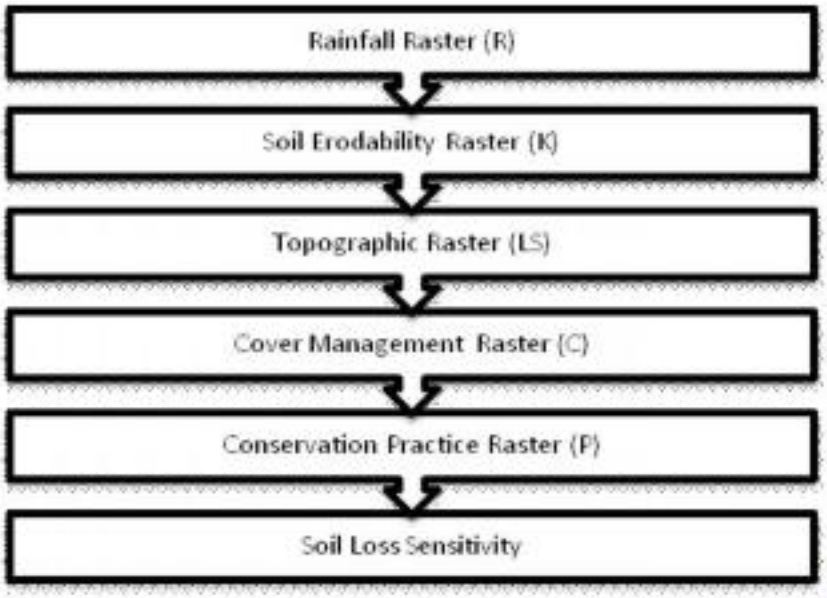

Fig. 2: Flow chart of steps followed in the soil loss sensitivity assessment

Principal
Nowgong Girls' College
Nagaon :: Assam

Nowgong Girls' College ★ Nagaon :: Assam ★ ESTD: 1962

Table 1: Values of erodability factor based on soil types and per cent organic matter content in soil (Foster et al. 1981)

Textural class	K based on % organic matter content in soil		
	0.5%	2%	4%
Fine sand	0.36	0.31	0.22
Very fine sand	0.94	0.81	0.63
Loamy sand	0.27	0.22	0.18
Loamy very fine sand	0.98	0.85	0.67
Sandy loam	0.60	0.54	0.42
Very fine sandy loam	1.05	0.92	0.74
Silt loam	1.07	0.94	0.74
Clay loam	0.63	0.56	0.47
Silt clay loam	0.83	0.72	0.58
Silt clay	0.56	0.51	0.43

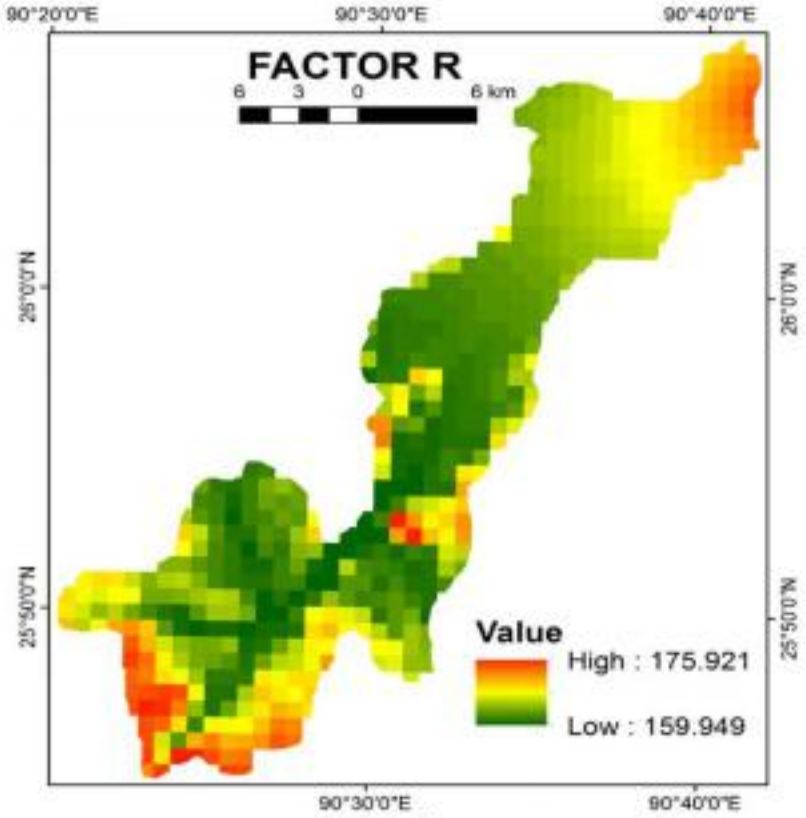

Fig. 2: Rainfall-runoff erosivity factor (R)

Principal
Nowgong Girls' College
Nagaon :: Assam

Nowgong Girls' College ★ ESTD: 1962 ★ Nagaon :: Assam

Table 2: Calculated K values on the basis of textural classes

Soil code	Soil Textural Class	Calculated k values
AS 57 (Typic Udifluvents)	fine loamy (clay loam)	0.56
AS 55 (Typic Fluvaquents)	Fine silty clay	0.43
AS 80 (typic haplaquepts)	fine loamy	0.56
Aquic eutrochepts	Fine loamy	0.56
Typic haplaquepts	Silt loam	0.51
Typic kandiudults	Fine loamy (clay loam)	0.56
Dystric eutrochrepts	Fine loamy (clay loam)	0.56
Umbric dystrpchrepts	Fine loamy (clay loam)	0.56
Typic udorthens	Coarse loamy (sandy loam)	0.54
Dystric eutrochrepts	Fine loamy	0.56

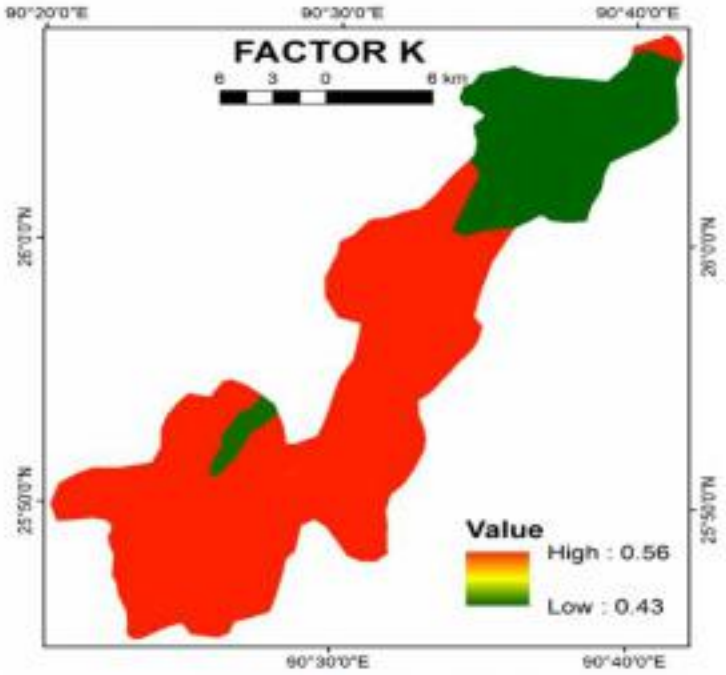

Fig. 4: Soil erodibility factor (K)

Topographic factor (LS)

In the present study the LS factor is computed with the help of a DEM. The DEM of the study area is of 9 meter resolution and the slope layer was derived from the former. The formula used for calculation of LS factor was proposed by Moore and Burch (1986) , Zeng et al. (2009) and Silva et al.(2012).

LS=(v/22.13)0.4 (Sin ?/0.0896)1.3

Here, LS is slope length and slope steepness factor, V is the product of flow accumulation and cell size, ? is the slope in degree (Silva et al. 2012)

Principal
Nowgong Girls' College
Nagaon :: Assam

Nowgong Girls' College ★ ESTD: 1962 ★ Nagaon :: Assam

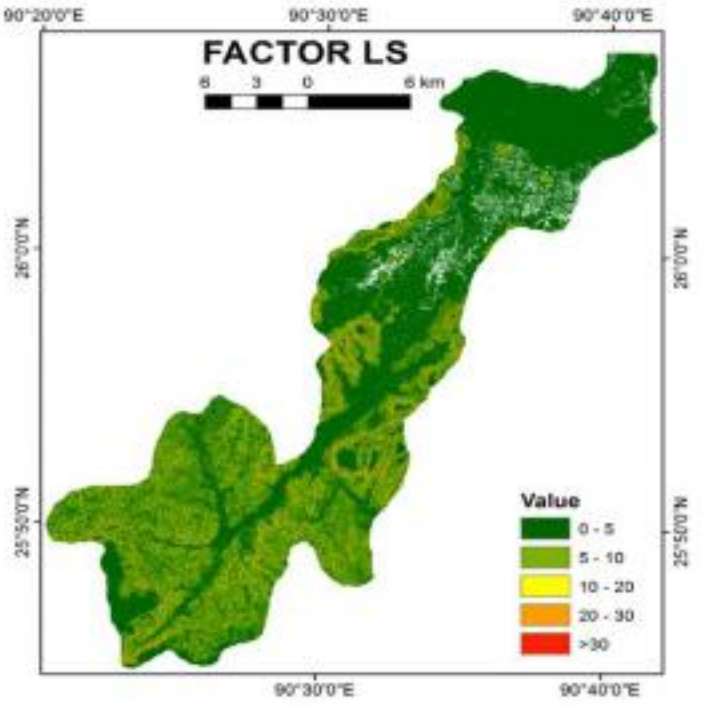

Fig. 5: Length and steepness factor

Cropping management factor (C)

This represents the effect of soil-disturbing activities, plants, crop sequence and productivity level, soil cover and subsurface bio-mass on soil erosion (Prasannakumar et al., 2012). The C factor reflects the effect of cropping and management practice on soil erosion rates, and is the factor used most often to compare the relative impacts of vegetation cover and management options on conservation tactics (Renard et al., 1997). This C factor has a close connection to land use and land cover types and also anthropogenic interventions on the soil erosion processes (Jaiswal et al., 2014). Currently, due to the variety of land cover patterns with spatial and temporal variations, satellite remote sensing data sets were used for the assessment of C-factor (Karydas et al., 2009; Tian et al., 2009).

Conservation practice factor (P)

In the study area of Jinari River basin no supporting practice such as strip cropping , terracing, contouring etc are witnessed thus the value of 'P' taken as 1.

Results and discussion

The river basin is characterised by both lowland and hill topography and erosion is equally significant in both types of terrain. This is possibly since erosion depends not only upon the action of fluvial processes but also results from the action of splash erosion. The average annual soil loss estimated in the watershed using USLE was 1.76 ton/ha/yr and 0.95 ton/ha/yr for the years 2007 and 2011 respectively (Fig 7, Table 3. & Table 4.). In 2007 the tropical dense forest areas had high erosion rates and it accounted for 36.1 percent of total erosion of the basin. On the other hand in 2011 the settlement classes had the maximum erosion rates accounting for 49.4 percent of total erosion. This is due to the conversion of dense forest areas into settlement

C.T.C.
Principal
Nowgong Girls' College
Nagaon :: Assam

Nowgong Girls' College
ESTD: 1962
Nagaon :: Assam

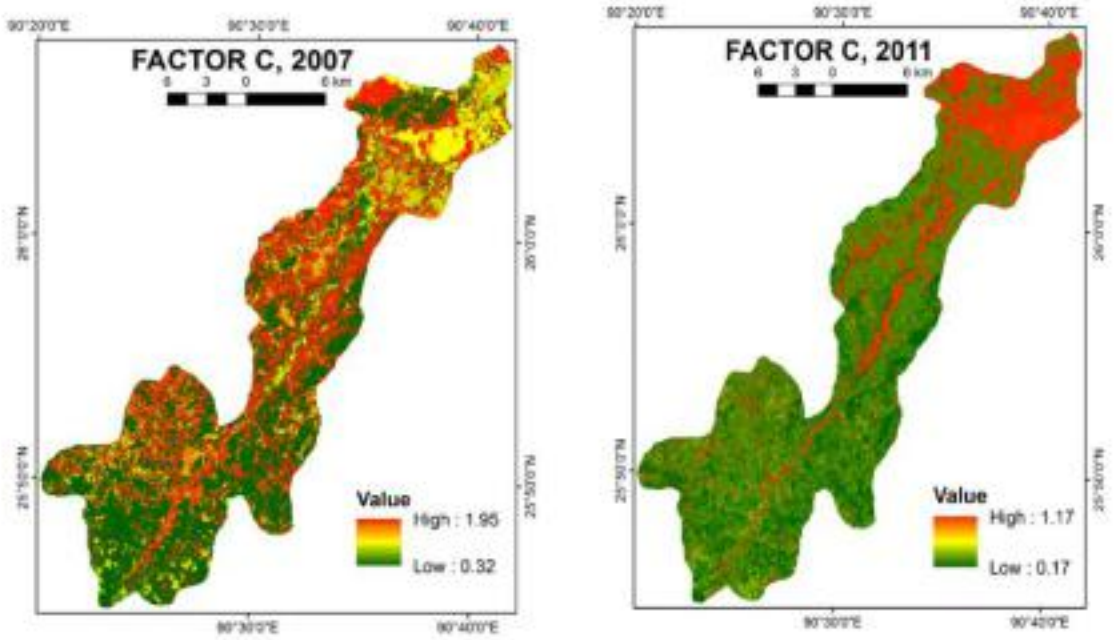

Fig. 6: Cropping management factor of 2007 and 2011

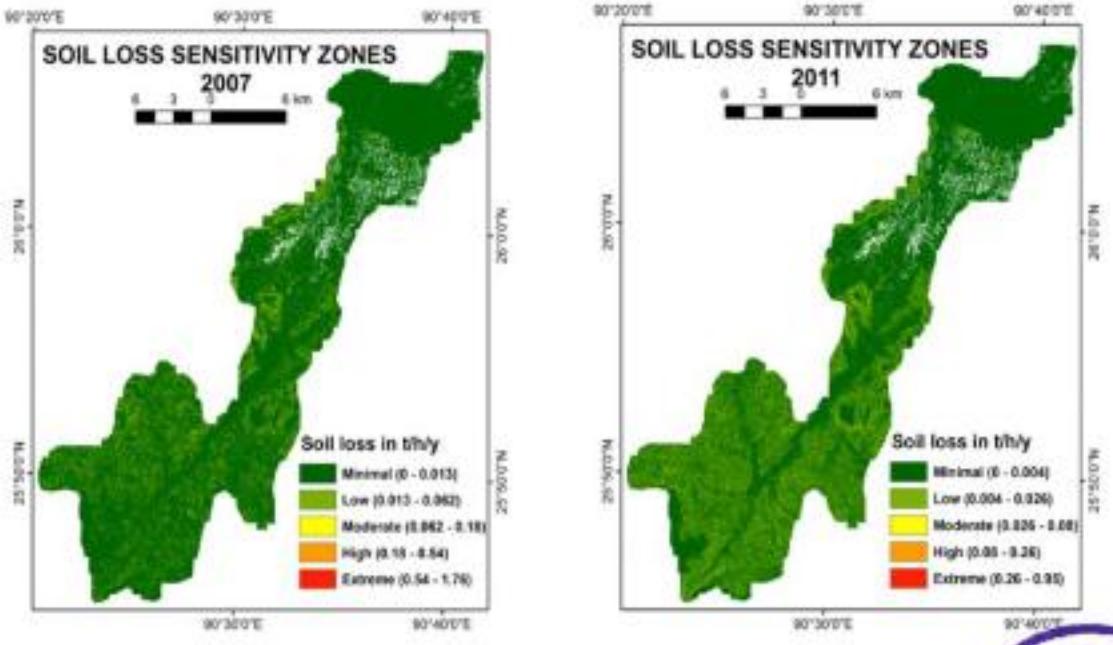

Fig. 7: Soil loss sensitivity classes of 2007 and 2011

Principal
Nowgong Girls' College
Nagaon :: Assam

Nowgong Girls' College
ESTD: 1962
Nagaon :: Assam

areas and because of that the amount of splash erosion is relatively high in such areas. The basin experiences more or less similar rainfall conditions and thus the soil loss of the area is dependent upon the LS, K and C factors.

Table 3: Soil loss sensitivity classes, 2007

Soil loss (t/h/y)	Soil erosion sensitivity zone	Area (sq. km)	Percentage
0- 0.013	Minimal	357.15	89.57549
0.013 - 0.062	Low	36.18	9.074173
0.062 - 0.18	Moderate	04.88	1.223935
0.18 - 0.54	High	00.48	0.120387
0.54 - 1.76	Extreme	0.024	0.006019

Table 4: Soil loss sensitivity classes, 2011

Soil loss (t/h/y)	Soil erosion sensitivity zone	Area (sq. km)	Percentage
0 - 0.004	Minimal	310.85	77.99836
0.004 - 0.026	Low	83.45	20.93924
0.026 - 0.08	Moderate	3.92	0.983605
0.08 - 0.26	High	0.29	0.072767
0.26 - 0.95	Extreme	0.024	0.006022

The soil loss data recorded in the table 3 & 4 revealed that although erosion in the basin has increased considerably, yet it is hard to relate it with the nature of disaster in the basin. However increasing clearance of the dense forest for other land use has triggered soil erosion in the basin. It is interesting to note that tropical dense forest and degraded forest category contribute significantly to the total estimated soil loss in the basin (Table 5).

When compared the average annual soil loss data with Belsiri basin records (Kalita and Sarmah, 2016) it was found higher soil loss rates existed in the Jinari river basin. The catastrophic

Table 5: Percentage distribution of land use and statistical of soil loss using USLE during 2007

Landuse	Area		Estimated soil loss (ton)		
	sq. km	%	Maximum	Mean	SD
Agricultural Land	20.5	4.7	14351	0.2	27.5
Tropical Dense Forest	156.1	36.1	16969	64.3	207.4
Mixed Vegetation	37.8	8.7	8277	3.1	47.7
Degraded Forest	65.5	15.1	23033	27.5	190.5
Barren Land	4.1	0.9	14389	4.2	84.1
Water body	34.8	8.0	41329	12.7	204.7
Settlement	113.8	26.3	76292	166.4	758

Principal
Nowgong Girls' College
Nagaon :: Assam

Nowgong Girls' College
ESTD: 1962
Nagaon :: Assam

Table 6: Percentage distribution of land use and statistical of soil loss using USLE during 2011

Landuse	Area		Estimated soil loss (in ton)		
	Km2	%	Maximum	Mean	SD
Agricultural Land	12.5	2.8	1774	0.05	4.3
Tropical Dense Forest	26.4	6.1	6988	8.0	58.7
Mixed Vegetation	84.6	19.5	8932	26.6	117.8
Degraded Forest	47.0	10.8	28247	14.4	167.5
Barren Land	16.5	3.8	10985	8.7	81.9
Waterbody	31.7	7.3	41329	8.1	166.3
Settlement	213.8	49.4	19090	56.8	197.9

flood occurrences of the basin are inextricably linked to unusually high soil and water discharge rates of the basin. To formulate a realistic and effective disaster management plan for the basin it is imperative to take into account the soil loss specifics that are at work, as evidenced by this analysis.

Conclusion

USLE are useful in assessing soil loss parameters in a given area. In the Jinari river basin in Assam, India a unique set of factors are at work in shaping and influencing soil loss and rapid land-use/land-cover changes have accentuated soil loss. Unfortunately, this aspect is often lost sight of by planners and governmental stakeholders. However, in order to minimize future loss of lives and property the factors underlying high soil losses need to be factored in.

References

Assam State Action Plan on Climate Change, (2017): Department of Environment & Forest, Government of Assam

Dabral, P. P., Baithuri, N., & Pandey, A. (2008). *Soil erosion assessment in a hilly catchment of North Eastern India using USLE, GIS and remote sensing*. Water Resources Management, 22(12), 1783-1798.

Farhan, Y., Zregat, D., & Farhan, I. (2013). *Spatial estimation of soil erosion risk using RUSLE approach, RS, and GIS techniques: a case study of Kufranja Watershed,* Northern Jordan. *Journal of Water Resource and Protection*, 5(12), 1247.

Foster, G. R., D. K. McCool, K. G. Renard, and W. C. Moldenhauer. "*Conversion of the universal soil loss equation to SI metric units.*" *Journal of Soil and Water Conservation*, 36, no. 6 (1981): 355-359.

Ghosh, K., De, S. K., Bandyopadhyay, S., & Saha, S. (2013). *Assessment of soil loss of the Dhalai river basin, Tripura, India using USLE*. International Journal of Geosciences, 4(01), 11.

Jaiswal, M. K., Thakuria, G., Borah, A. C., & Saikia, R. (2014). *Evaluation of parametic impact on soil loss of Panchnoi river basin, North-east India, using revised universal soil loss equation* (rusle). The Clarion, 3(1), 51-60.

Kalita, N. and Sarmah, R. (2016) *Soil loss sensitivity in the Belsiri river basin using Universal Soill loss Equation in GIS*, International Journal of Current Research, Vol. 8, Issue, 03, pp.28831-28838, March, 2016

Karaburun, A. (2010). Estimation of C factor for soil erosion modeling using NDVI in Buyukcekmece watershed. *Ozean Journal of applied sciences*, 3(1), 77-85.

Karydas, C. G., Sekuloska, T., & Silleos, G. N. (2

Principal
Nowgong Girls' College
Nagaon :: Assam

Nowgong Girls' College
ESTD: 1962
Nagaon :: Assam

Quantification and site-specification of the support practice factor when mapping soil erosion risk associated with olive plantations in the Mediterranean island of Crete. Environmental Monitoring and Assessment, 149(1-4), 19-28.

Moore, I. D., & Burch, G. J. (1986). *Physical Basis of the Length-slope Factor in the Universal Soil Loss Equation* 1. Soil Science Society of America Journal, 50(5), 1294-1298.

Prasannakumar, V., Shiny, R., Geetha, N., & Vijith, H. (2011). *Spatial prediction of soil erosion risk by remote sensing, GIS and RUSLE approach: a case study of Siruvani river watershed in Attapady valley*, Kerala, India. Environmental Earth Sciences, 64(4), 965-972.

Prasannakumar, V., Vijith, H., Abinod, S., & Geetha, N. (2012). *Estimation of soil erosion risk within a small mountainous sub-watershed in Kerala, India, using Revised Universal Soil Loss Equation (RUSLE) and geo-information technology*. Geoscience Frontiers, 3(2), 209-215.

Renard, K. G., Foster, G. R., Weesies, G. A., McCool, D. K., & Yoder, D. C. (1997). *Predicting soil erosion by water: a guide to conservation planning with the Revised Universal Soil Loss Equation (RUSLE) (Vol. 703)*. Washington, DC: United States Department of Agriculture.

Sen, T. K., Murali, S., Dubey, P. N., & Velayutham, M. (2001). *Soil erodibility of Jorhat and Sibsagardistricts of Assam*. Agropedology, 11, 29-36.

Singh, G. , Rambabu V. V. and Chandra S. (1981), *"Soil Loss Prediction Research in India,"* ICAR Bullet, T12/D9, CS WCTRI, Dehradun

Da Silva, R. M., Montenegro, S. M. G. L., & Santos, C. A. G. *(2012). Integration of GIS and remote sensing for estimation of soil loss and prioritization of critical sub-catchments: a case study of Tapacurá catchment*. Natural Hazards, 62(3), 953-970.

Tian, Y. C., Zhou, Y. M., Wu, B. F., & Zhou, W. F. (2009). *Risk assessment of water soil erosion in upper basin of Miyun Reservoir, Beijing*, China. Environmental Geology, 57(4), 937-942.

Wang, G., Gertner, G., Fang, S., & Anderson, A. B. (2003). *Mapping multiple variables for predicting soil loss by geostatistical methods with TM images and a slope map*. Photogrammetric Engineering & Remote Sensing, 69(8), 889-898.

Wischmeier, W. H., & Smith, D. D. (1978). *Predicting rainfall erosion losses-a guide to conservation planning. Predicting rainfall erosion losses-a guide to conservation planning*.

Zhang, Y., Degroote, J., Wolter, C., & Sugumaran, R. (2009). *Integration of Modified Universal Soil Loss Equation (MUSLE) into a GIS framework to assess soil erosion risk*. Land Degradation & Development, 20(1), 84-91.

●●●

Principal
Nowgong Girls' College
Nagaon :: Assam

Nowgong Girls' College
ESTD: 1962
Nagaon :: Assam

ChemPubSoc Europe

DOI: 10.1002/ejic.201801049

EurJIC Full Paper

Single-Molecule Magnets

Homodinuclear $\{Ln^{III}_2\}$ (Ln^{III} = Gd^{III}, Tb^{III}, Ho^{III}, and Dy^{III}) Complexes: Field-Induced SMM Behavior of the Dy^{III} and Tb^{III} Analogues

Pankaj Kalita,[a] Joydeb Goura,[a,b] Juan Manuel Herrera Martínez,[c] Enrique Colacio,*[c] and Vadapalli Chandrasekhar*[b,d]

Abstract: A family of four dinuclear complexes, $[NHEt_3]_2[Ln_2(\mu\text{-}NO_3)_2(NO_3)_2(HL)_2]$ [Ln = Gd^{III} (**1**), Tb^{III} (**2**), Ho^{III} (**3**), Dy^{III} (**4**)], were synthesized by the reaction of an enolizable multidentate Schiff base ligand H_3L (H_3L = *N'*-(2-hydroxy-3-methoxy-5-nitrobenzylidene)-2-(hydroxyimino)propanehydrazide) with hydrated lanthanide nitrates in the presence of NEt_3. The molecular structure of complexes **1**–**4** was confirmed by single-crystal XRD analysis. All of the centrosymmetric complexes are dianionic, isostructural and each of the Ln^{III} centers is nine-coordinate and adopts a muffin like coordination geometry as indicated by SHAPE analysis. The dynamic magnetization studies revealed that the compounds **2** and **4** are field-induced single-molecule magnets with effective energy barriers U_{eff} = 34(2) K (for **2**) and 80(3) K (for **4**) and pre-exponential factors, $\tau_0 = 1.1 \times 10^{-8}$ s (for **2**) and 1.15×10^{-7} s (for **4**).

Introduction

Single-molecule magnets based on lanthanide complexes are of considerable interest in view of the unquenched spin-orbit angular momentum present among lanthanide ions leading to an inherent magnetic anisotropy in many of them particularly in ions such as Dy^{III}, Tb^{III}, Ho^{III}, Er^{III} etc.[1–4] Various types of lanthanide complexes containing diverse features such as varying nuclearity and structural topology have been investigated revealing a rich magnetochemistry.[5–11] Among all the lanthanide ion-containing single molecule magnets investigated thus far, the complex $[(Cp^{ttt})_2Dy(Cp^*)][BK_6F_{24}]$ possesses the highest blocking temperature, 80 K, below which the complex once magnetized retains its magnetization for long periods of time.[12] While such single ion magnets are certainly of considerable interest there is also substantial interest in dinuclear complexes because of several reasons. One, such complexes serve as the simplest models to understand inter-lanthanide interactions mediated through ligands.[13–16] Second, the pioneering work of Long and co-workers has revealed that having appropriate bridging ligands between the lanthanide centers allows a favorable electronic communication between them.[17] Thus, the complex, $[K(18\text{-crown-6})(THF)_2]$ $[\{(Me_3Si)_2N\}_2(THF)Tb]_2(\mu\text{-}\eta^2{:}\eta^2\text{-}N_2)]$, where the lanthanide centers are connected to each other by the radical ligand $(N_2)^{3-}$ shows an effective barrier for magnetization reversal U_{eff} = 227 cm^{-1} and a blocking temperature of 14 K.[17] Spurred by this exciting result there have been many efforts to study dinuclear complexes.[18–24] While a large number of ligands have been used for assembling such complexes, ligand design that can lead to the exclusive isolation of dinuclear complexes still is an important issue. Oxo-ligand systems have been shown to be quite effective in the synthesis of such complexes, besides providing an opportunity to effect slight structural variations which in turn can bring a change in the magnetic interaction between the lanthanide centers.[15,25,26] Also, studies on dinuclear lanthanide complexes reveal that a number of strategies can be employed to enhance the energy barriers of magnetization reversal. The commonly employed methods are tuning terminal ligands,[27] tuning local coordination geometries[28] and tuning ligand fields.[14]

We have been utilizing multidentate hydrazone ligands, for some time, to assemble lanthanide complexes.[29–31] In this context, we wished to explore a *o*-vanillin-supported multidentate ligand, *N'*-(2-hydroxy-3-methoxy-5-nitrobenzylidene)-2-(hydroxyamino) propanehydrazide (H_3L) to prepare dinuclear Ln^{III} complexes. Based on our previous understanding of such ligand systems we intuited that keto-enol tautomerism would allow H_3L to be present in an enol form and when de-protonated the enolate oxygen can be profitably used to bridge two lanthanide ions. Accordingly, we have isolated a family of dinuclear Ln^{III}_2

[a] School of Chemical Sciences, National Institute of Science Education and Research, NBW,
Bhubaneswar Jatni, Khurda - 752050, Odisha, India
[b] Department of Chemistry, Indian Institute of Technology Kanpur,
Kanpur 208016, India
E-mail: vc@iitk.ac.in
[c] Departamento de Química Inorgánica, Facultad de Ciencias,
Universidad de Granada,
Avenida de Fuentenueva s/n, 18071 Granada, Spain
E-mail: ecolacio@ugr.es
[d] Tata Institute of Fundamental Research,
Gopanpally, Hyderabad - 500 107, India
E-mail: vc@tifrh.res.in

Supporting information and ORCID(s) from the author(s) for this article are available on the WWW under https://doi.org/10.1002/ejic.201801049.

© 2019 Wiley-VCH Verlag GmbH & Co. KGaA, Weinheim

Pankaj Kalita

C.T.C.
Principal
Nowgong Girls' College
Nagaon :: Assam

Nowgong Girls' College
ESTD: 1962
Nagaon :: Assam

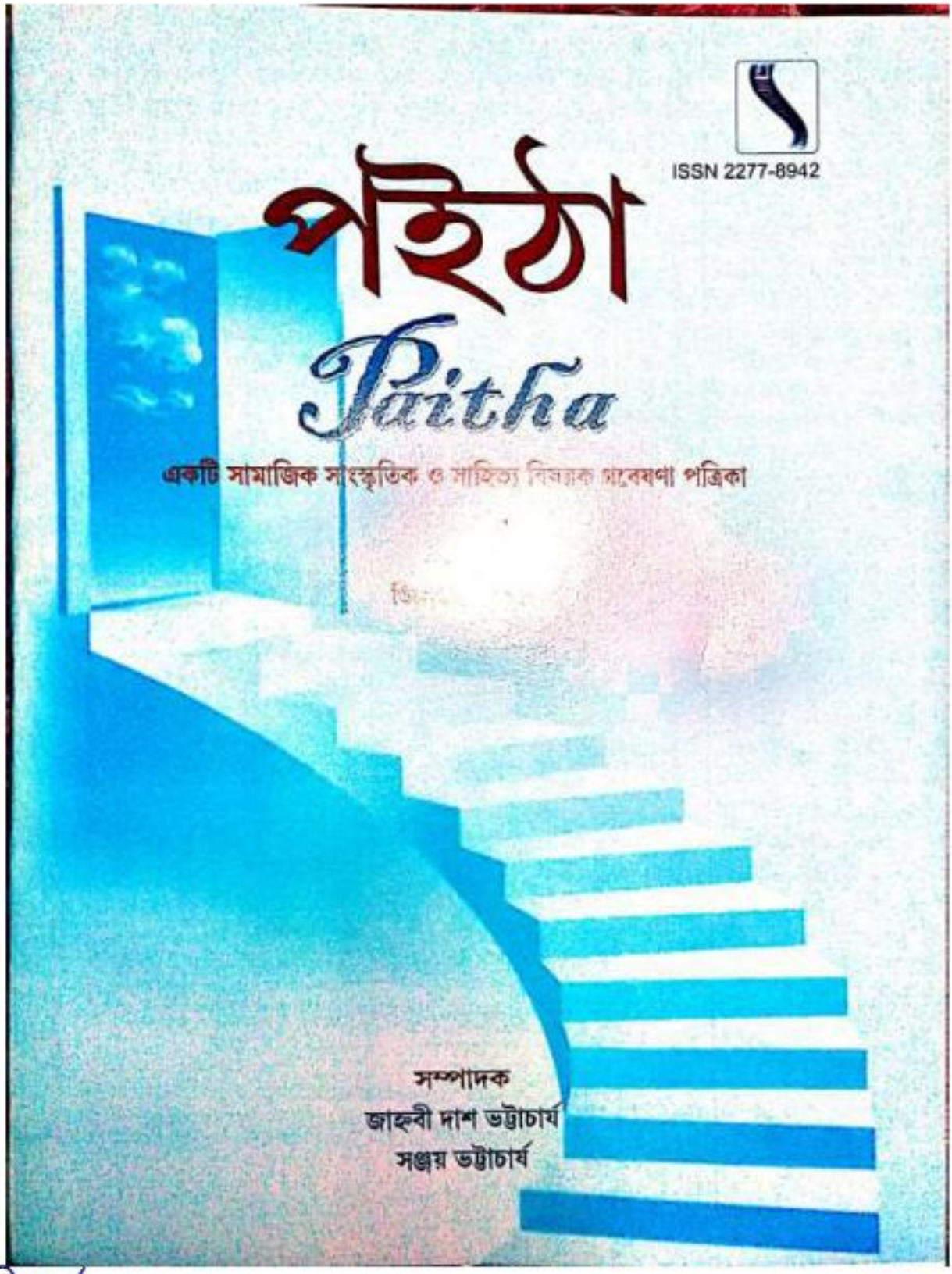

C.T.C.

Principal
Nowgong Girls' College
Nagaon :: Assam

Nowgong Girls' College ESTD: 1962 Nagaon :: Assam

ISSN No. 2277-8942

পইঠা

Paitha

একটি সামাজিক সাংস্কৃতিক ও সাহিত্য বিষয়ক গবেষণা পত্রিকা

নবম বর্ষ
ডিসেম্বর, ২০১৮

সম্পাদক
জাহ্নবী দাশ ভট্টাচার্য
সঞ্জয় ভট্টাচার্য

C.T.C.
Principal
Nowgong Girls' College
Nagaon :: Assam

Nowgong Girls' College
ESTD: 1962
Nagaon :: Assam

ISSN No. 2277-8942

বর্ষ ঃ নবম ডিসেম্বর ২০১৮

সূচি

'মা' উপন্যাসে জননী চরিত্র : একটি বিশ্লেষণাত্মক অধ্যয়ন

রীতা রাণী দে ১

শোণিতপুর জেলার করম উৎসব ঃ একটি পর্যালোচনা

বাপন দাস ১২

পুরাণপথের পুণর্জাগরণ ও বর্তমান জীবন-মানস ঃ বুদ্ধদেব বসুর 'প্রথম পাঠ' ও সুনীল গঙ্গোপাধ্যায়ের 'নন্দন কাননে দ্রৌপদী'

প্রাণজিৎ সরকার ২০

'আনপুটডাউনেবল' সত্যজিৎ ঃ প্রসঙ্গ 'রয়েল বেঙ্গল রহস্য'

জাহ্নবী দাশ ৩৯

প্রথম যুগের বাংলা নাটকে চলতি গদ্যের ব্যবহার ঃ একটি সংক্ষিপ্ত অধ্যয়ন

সঞ্জয় ভট্টাচার্য ৫১

C.T.C.

Principal
Nowgong Girls' College
Nagaon :: Assam

Nowgong Girls' College ESTD: 1962 Nagaon :: Assam

পইঠা
নবম বর্ষ
ডিসেম্বর, ২০১৮
ISSN 2277-8942

'মা' উপন্যাসে জননী চরিত্র : একটি বিশ্লেষণাত্মক অধ্যয়ন

রীতা রাণী দে, সহকারী অধ্যাপক, নগাঁও গার্লস কলেজ

সংক্ষিপ্তসার

বাংলা ঔপন্যাসিকরা তাঁদের উপন্যাসে অনেক অসাধারণ জননী চরিত্র অঙ্কন করেছেন। ঔপন্যাসিক অনুরূপা দেবী তাঁদের মধ্যে একজন। তাঁর 'মা' উপন্যাসে বেশ কয়েকজন জননীর দেখা পাওয়া যায়। সেকালের সমাজের প্রতিনিধি স্থানীয়া বহু জননী চরিত্র অংকন করেছেন অনুরূপা দেবী। আলোচ্য গবেষণাপত্রে আমরা সেদিকেই আলোকপাত করার চেষ্টা করেছি।

বীজ-শব্দ : জননী, কন্যা, সমাজ, পুত্রবধূ, বিবাহিতা।

১. ভূমিকা :

জননীরূপে আমাদের দেশে নারীকে পুজো করা হয়। শাস্ত্র থেকে সমাজে এই ধারণা বদ্ধমূল। শাস্ত্রকার মনু বলেছেন,

"প্রজনার্থং মহাভাগাঃ পূজার্হা গৃহদীপ্তয়ঃ।
স্ত্রিয়ঃ শ্রিয়শ্চ গেহেষু ন বিশেষোঽস্তি কশ্চন।।"[১]

-অর্থাৎ "সন্তানের হেতু স্ত্রীলোকেরা বহুকল্যাণভাজন, (বস্ত্রালংকারাদি দ্বারা) পূজনীয়া, গৃহশোভাকারিণী; গৃহে স্ত্রীলোক ও শ্রী (লক্ষ্মী) তে কোন ভেদ নেই।"[২] শাস্ত্রকার মনু আরো একটি শ্লোকে বলেছেন,

"উপাধ্যায়ান্ দশাচার্য আচার্যাণাং শতং পিতা।
সহস্রন্তু পিতৃন্মাতা গৌরবেণাতিরিচ্যতে।।"[৩]

–অর্থাৎ গৌরবে আচার্য দশ উপাধ্যায়কে অতিক্রম করেন, পিতা অতিক্রম করেন একশত আচার্যকে এবং মাতা এক সহস্র পিতাকে অতিক্রম করেন। ভারতবর্ষে মাতার আসন সর্বকালেই যথেষ্ট শ্রদ্ধার এবং সম্মানের। মাতা পরিবারের কেন্দ্রে থেকে স্নেহ-প্রেমে-মমতায় পুরো পরিবারকে বেষ্টন করে রাখেন। আমাদের ধর্মসাধনার কেন্দ্র ভূমিতে রয়েছে মাতৃ মহিমা। বিখ্যাত সমালোচক বলেছেন, "বিশেষতঃ, 'মা' নামে এমন একটা মন্ত্র-শক্তি নিহিত আছে, যাহার প্রভাব কেবলমাত্র আমাদের

Principal
Nowgong Girls' College
Nagaon :: Assam

Nowgong Girls' College
ESTD: 1962
Nagaon :: Assam

GNOSIS

An International Refereed Journal of English Language and Literature

Included in the UGC Approved list of Journals with journal number 48815

Vol. 4 – No. 4 July 2018

Abstracting and Indexing:

Index Copernicus, SJIF, Citefactor.org, IIJIF, DAIJ, ESJI, DRJI, Google Scholar, Academia.edu, Researchgate

Editor

Dr. Saikat Banerjee
Department of English
Dr. K.N. Modi University,
Newai, Jaipur
Rajasthan, India
Mobile: +91-9529386461
E-mail: gnosisprintjournal@gmail.com
Website: www.thegnosisjournal.com

Principal
Nowgong Girls' College
Nagaon :: Assam

Publisher

Yking Books
G-13, S.S. Tower, Dhamani Street, Chaura Rasta,
Jaipur - 302003, Rajasthan, India
Phone No. + 91-141-4020251, M.: 9414056846
E-mail: ykingbooks@gmail.com
Website: www.ykingbooks.com

Nowgong Girls' College
ESTD: 1962
Nagaon :: Assam

DISCLAIMER: Articles and views published in this journal DO NOT necessarily reflect the views or policies of the Editorial Board.

© **COPYRIGHT:** Reproduction of the contents of GNOSIS in whole or in part without the prior permission of the Editor is prohibited.

All disputes concerning the journal are subject to Jaipur Jurisdiction.

Principal
Nowgong Girls' College
Nagaon :: Assam

Nowgong Girls' College
ESTD: 1962
Nagaon :: Assam

Table of Contents

Editorial 7

Articles

Baudelaire's Quest for 'New' in *The Flowers of Evil*
—Amitabh Roy

Dickensian Echoes in D.H. Lawrence: A Study in Comparison
—Richa Bhardwaj

A Critical Assessment of the Epistemology of a Queer Hero
—Mohd. Ahmar Alvi

Bankimchandra Chattopadhyay's *Prachina ebong Nabina*
—Anavisha Banerjee

Nineteenth century Victorian India through
the Eyes of a Woman Traveler Mary Carpenter
—Amrita Bhattacharyya

Nation as Identity in Amitav Ghosh's
The Circle of Reason and *The Shadow Lines*
—Rekha Tiwari

Food Metaphors in Chitra Banerjee Divakaruni's
The Mistress Of Spices and *Sister Of My Heart*
—Manreet Dhaliwal

Wide Sargasso Sea: A Journey from
Identity Creation to Identity Destruction
—Vipan Kumar

Liberating Lesbian Bonds in
Manju Kapur's *A Married Woman*
—Shalini Sharma

Trauma: Dimensions, Politics and Representability
—Dona Elizabeth Sam

Principal
Nowgong Girls' College
Nagaon :: Assam

Nowgong Girls' College
ESTD: 1952
Nagaon :: Assam

The Language of Negation in *The Madness of the Day*

—Nisarga Bhattacharjee, Ananya Chatterjee

(Re)reading the Subjugated History of the Subcontinent through the Bangla Magic Realist Novel *Khowabnama*

—Somrwita Ghosh

Stature of Women in U.R. Ananthamurthy's *Samskara*

—Vidhi Yadav, Manoj Kumar Vidyalankara

"How to Tell a Shattered Story": Reading Ecofeminism in *The Ministry of Utmost Happiness*

—Sarita Dubey

(Un)Womanliness and Masculinity on Trial:
A Gendered Study of George Eliot's *The Lifted Veil*

—Riya Maji

Tale of Two Families: A Representation of Aussie Identity by reworking the Matrix of Australian Family in Tim Winton's *Cloudstreet*

—Midhu Mirian Alex

Man's Entrapment within the Construct of Masculinity:
An Analysis of Strindberg's *The Dance of Death*

**—Brahmacharimayum Samita Devi,
Paonam Sudeep Mangang**

South Asian women writers and Partition:
A Psychoanalytic study of *The Skeleton* and *Cracking India*

—Himani Sharma, Bhavya, Shweta Saroha

History and the Other: Writing Pain and Marginality in J. M. Coetzee's *Disgrace*

—Surojit Kayal

Investigating the Interface between Organ Trading and Cyberculture in Manjula Padmanabhan's *Harvest*

—Abhisek Ghosal

Religious Persecution of Christians from the Tribal Communities and Dalits in Orissa: The Politics of Accusation and Huntington's 'Clash of Civilizations'

—Recho Benjamin Teron

Principal
Nowgong Girls' College
Nagaon :: Assam

Nowgong Girls' College
ESTD: 1960
Nagaon :: Assam

GNOSIS: Vol. 4, No. 4 July-2018
ISSN 2394-0131; pp. 128-134

"How to Tell a Shattered Story": Reading Ecofeminism in *The Ministry of Utmost Happiness*

Sarita Dubey

Submitted: , Revised: , Accepted:

Abstract: Ecofeminism combines two very important words within its purview-'ecology' and 'feminism'. Both the concepts play a major role in the human existence. Ecofeminism is an inclusive theory that is developing a multi-system approach to understanding the interconnected forces that operate to oppress women and environment. It extends familiar feminist critiques of social isms of domination, for e.g., sexism, racism, classicism, heterosexism, ageism, to nature, i.e. naturism. The paper will analyze what are the problems it address, how it arise, and how it is concerned with the future of women and ecology of India and what best framework ecofeminism can provide to analyze them. Arundhati Roy is a strong voice against environmental degradation and gender exploitation. Her novels The God of Small Things and The Ministry of Utmost Happiness acknowledge that world is not what it should be. The Ministry of Utmost Happiness deals with lives of queers, racism, sexism, regionalism, speciesism, terrorism, rape, animal exploitation and pollution. Ecofeminism is knowledge and value based theory and its strength is dependent on flexibility, inconclusiveness and reflexibility of the community in which it is generated. The critical study of the characters and natural settings of the novel will point out the current situation of Indian women and nature and how this theory supports India towards planetary health, global justice and future of earth.

Keywords: Ecofeminism, Religion, Women, Ecology, Arundhati Roy, India.

Introduction

The term 'Ecofeminism' was first used by the French feminist author and civil rights activist Francoise d' Eaubonne in her work *Le Fe' minisme ou la Mort* (Feminism or Death), 1974. This book intended to create the awareness against the parallelism drawn between the women and nature for their subordination by the patriarchy. Ecofeminism

Principal
Nowgong Girls' College
Nagaon :: Assam

Nowgong Girls' College
ESTD: 1962
Nagaon :: Assam

GNOSIS: Vol. 4, No. 4 July-2018
ISSN 2394-0131; pp. 193-201

Religious Persecution of Christians from the Tribal Communities and Dalits in Orissa: The Politics of Accusation and Huntington's 'Clash of Civilizations'

Recho Benjamin Teron

Submitted: , Revised: , Accepted:

Abstract: Religious persecution in Orissa is a burning issue and the roots of this violence can be discerned in the light of Huntington's 'Clash of Civilizations' theory. As the causes of this persecution is studied, the underlying politics of accusation by religious leaders play a big part in flaming up of the mob frenzy. It is observed in the continuous violence committed against native Christians, especially in the persecution in Kandhamal that affected thousands of Christians. This paper studies this persecution in that state and its roots and causes.

Keywords: Religious persecution, Christians, Huntington, clash of civilizations.

> "Blessed are you when they revile you and persecute you.. for My sake"
>
> (Matthew 5:11, The Holy Bible, NKJV)

In the beatitudes that Jesus proclaimed, he predicted that his followers' persecution and being the perfect example, he himself underwent the fiery accusations and was crucified. Later on, almost all of his twelve apostles were martyred with tradition saying that St. Thomas was martyred in India around AD 52. So the history of this persecution in India can be traced to first century Christianity. My aim through this research article is to highlight the politics of accusation by Hindutva factions is responsible for persecution on Christian converts from the tribal communities and Dalits in Orissa in the past decades.

Samuel P. Huntington, American political scientist, adviser and academic, in his famous essay "The Clash of Civilizations?" said that

> "The great divisions among humankind and the dominating source of conflict will be cultural".

Principal
Nowgong Girls' College
Nagaon :: Assam

Nowgong Girls' College
ESTD: 1962
Nagaon :: Assam

22

THE SOCIAL CONSTRUCT OF AN IDEAL WIFE ACCORDING TO THE BIBLE

Recho Benjamin Teron, *Research Scholar, Department of English, University of Delhi, India*

Abstract:

The study of the picture of an ideal wife as prescribed by social structures also relates to the broader field of discourse of the study of the institution of marriage and the role of the patriarchy, religion and capitalism in creating idealistic roles for individuals in the society. In this paper, there will be the study of the idea of a noble and virtuous wife and what constitutes her qualities and characteristics according to the Holy Bible. The pursuit of an ideal spouse in marriage for an ideal married life has always been given a lot of importance and this leads to certain social constructs of the ideal nature of a wife as seen in the Bible. Primary sources will be Proverbs 31:10-31, (Old Testament, Holy Bible), Ephesians 5:22-33, Colossians 3:18, 1 Peter 3 (New Testament, Holy Bible). To critically analyze the study the secondary sources will be Theodor Adorno's Minima Moralia: Reflections from a damaged Life (1951), J.S. Mill & Harriet Taylor's Early Essays on Marriage and Divorce, (1951) Genesis 24 (Old Testament, Holy Bible) Thomas Hardy's Far From the Madding Crowd (1874). The description of the virtuous wife in the Bible doesn't necessarily restrict women in their dignity, importance and socio-economic contributions to society but in the family structure, women are to be second to the man to maintain the hierarchical structure for the semblance of order.

> By all means marry; if you get a good wife, you'll be happy. If you get a bad one, you'll become a philosopher.

The study of the picture of an ideal wife as prescribed by social structures also relates to the broader field of discourse of the study of the institution of marriage and the role of the patriarchy, religion and capitalism in creating idealistic roles for individuals in the society. The institution of marriage has been one of the most important social pillars that has been fundamental to the fabric of any society. The social system has prescribed the rules for marriage and has also defined ideal roles for the husband and the wife in the confines of marriage and the family, mainly for the purpose of order and smooth functioning of the society. The pursuit of an ideal spouse in marriage for an ideal married life has always been given a lot of importance and this leads to certain social constructs of the ideal nature of a wife.

> A marriage is not a concrete reality that necessarily reveals itself to husband and wife in the same form. It is a history of actions and interactions, combined with mutual expectations based on that history and on broader cultural norms and values (Ross, Catherine E., 281).

These broader cultural norms and values go a long way in determining the mutual expectations one has in marriage and form the construct of the institution of marriage. The wife and the husband perform roles in the marriage and these roles are fixed by the broader societal spectrum, roles that have been gradually formulated since the time when humans started the family structures.

In order to understand the position of a wife in society at the present times and to fully grasp the changes that have come about in our worldviews regarding marriage we would have to look at how the position of a wife was constructed from ancient times in the sphere of authority and religion. It is important to examine and analyze the concept of an ideal wife as found in the Bible and critique it in the light of the position and situation of the woman in the hierarchy of the society.

C.T.C.
Principal
Nowgong Girls' College
Nagaon :: Assam

Nowgong Girls' College
ESTD: 1962
Nagaon :: Assam

An excellent wife *is* the crown of her husband,
But she who causes shame *is* like rottenness in his bones (Holy Bible, NKJV, Proverbs 12: 4)

A wife of noble character is praised profusely in the Bible; a woman who is excellent to the husband is like a reward to him, while the wife who brings shame is like a disease to her husband. The Biblical society has constructed the wife to be someone who should adhere to the moral latitudes laid down by the Bible and also to be a woman who lives by society's standards of an honourable woman. In this way, the wife is like a 'crown', that is, like a reward or a trophy that he wins, in front of the people and as the wife is noticed by all to be noble, the praises for her character flows to the husband in being fortunate to be the spouse of such a noble wife.

The same exaltation is of an excellent wife right from the Biblical is still carried over to this 21st century in certain urban terms such as 'wife material'. 'Wifey material' is described as "a phrase often used to describe a girl whom you feel possesses certain qualities that qualifies her to be a model wife for you" (urbandictionary.com) and the qualities that such a woman is supposed to be kind, caring, sweet, compassionate etc.. Thus, the social construct of an ideal wife has been prevalent in society from the earliest times till the present day.

We can further find what an excellent or noble wife is like in the Bible's description of the virtuous wife and in its instructions to the wife and husband. The description of the virtuous wife in the Bible doesn't necessarily restrict women in their dignity, importance and socioeconomic contributions to society but in the family structure, women are to be submissive to the man to maintain the hierarchical structure for the semblance of order.

The description of the virtuous wife is found in the book of Proverbs in the Bible in chapter 31 from the verses 10 to 31 and it begins with these lines:

Who can find a virtuous wife?
For her worth is far above rubies.
The heart of her husband safely trusts her;
So he will have no lack of gain
(Holy Bible, NKJV, Proverbs 31: 10-11).

These lines extol the worth of finding a virtuous wife, lifting her above the average woman. The virtuous wife is a woman who brings 'gain' to her husband, her worth seems to be 'far above rubies'. Thus, the ideal wife would be someone who would bring gain to the husband and the family at all areas, be it economically, emotionally and socially. It is to be considered extremely fortunate and a blessing from God if one were to be married to a woman who fits the bill of the virtuous wife in Proverbs 31. She is supposed to be a rare breed, treasured and valued way above the average and the search for her is supposed to be elusive. As we go through Proverbs 31, we find the example of a virtuous wife being described. She is not only a diligent caretaker of the house, taking care of the domestic needs of everyone in the house and excelling in womanly work like weaving, cooking etc., but she is also a clever businesswoman who earns through her intelligent dealings with merchants and in the fields. She is also wise and hardworking, "strength and honour are her clothing", she is a God-fearing woman who helps the poor and the needy; she is praised by everyone and her husband becomes a very respectable man. The verses end with the famous lines:

Charm is deceitful and beauty is passing,
But a woman who fears the Lord, she shall be praised.
Give her of the fruit of her hands,
And let her own works praise her in the gates.
(Holy Bible, NKJV, Proverbs 31:30-31)

Thus, the qualities and the great advantages that the virtuous wife brings, makes someone like her a

C.T.C. Principal Nowgong Girls' College Nagaon :: Assam

Nowgong Girls' College Estd. 1962 Nagaon :: Assam

a very prized catch and she is sought after by every eligible bachelor. Every marriageable man would dream of finding someone who comes as close to her likeness. This concept of a finding a virtuous wife could be because of the need for self-preservation and satisfaction of the man in having an able partner to help him to a better life and catapult his family above the social ladder. Theodor Adorno, in his Minima Moralia, reflects on the concept of modern day marriage and says, "Marriage, living on as an abject parody in a time that has removed the basis of its human justification, usually serves today as a trick of self-preservation" (Adorno, Theodor, 30).

Adorno could never have been truer in echoing the real reason of a man to be in the pursuit of an ideal wife- the so called virtuous wife of Proverbs 31, the reason being mainly the 'trick of self-preservation' that compels the patriarchy to define the social construct of an ideal wife and to aspire to get her for himself. The extolling of the quality of a virtuous wife can be understood in diametrically opposite directions. In one, like Adorno says, it can be a trick of self-preservation where the ideal wife is created and sought after for selfish motives by the patriarchy. In this direction, there is no freedom for the wife, no equality or elevation of position over the husband in the family, but it is just a business transaction where having the qualities of an ideal wife will land her in a good marriage that will give her some amount of respect in society and free her from the taboo of being an unmarried woman. The social construct of an ideal wife can be a means of subjugating women by pressurizing them to fulfil certain criteria to get a groom for herself, failing which she has to face the social stigma of being rejected for marriage and crossing the marriageable age without being hitched, thus facing shame and being stigmatized in the eyes of the society. J.S. Mill in his essay on marriage says,

> A single woman therefore is felt both by herself and others as a kind of excrescence on the surface of society, having no use or function or office there (Mill, J.S. Mill, Harriet Taylor, 4).

Thus, the social construct of the ideal wife can be used as a means of creating a profitable capital of women by forcing them to conform to the ideals set up for them and failing which, they are left in a position of disgrace. The ideals set up in such a system where failure meant stigmatization, would only be achieved by women to appease the patriarchy and will not in any way help in their individual growth as a person who is free to take their own courses in life and choose their own dreams of being happy and shake off the shackles of the patriarchy.

Thus, there could be a gradual degradation of the situation and position of women as their individual liberties stand to be curbed through the impositions of a patriarchal society and the virtuous wife would no longer be the independent woman who stood on an equal footing with her husband, but would be someone who stands to fulfill only her husband's wishes and the standards set by a judgmental society. This direction would also gradually lead to the removal of the amount of independence of the virtuous wife and would lower her standards after the equal footing is removed. The stigmatization of independent women who aren't married would naturally lead to the inferiority of the wife in the realms of marriage and the subsequent domination of the husband over the wife.

The same ideal of the virtuous wife, when taken in the opposite direction, in a positively women-centric way, would mean a whole world of good for the woman in the society. Proper ideals are always a good thing to strive for through one's own desire, without being forced upon by a powerful extra entity. The ideals of the virtuous wife can also be the ideal of a virtuous husband. The description of the virtuous wife in Proverbs 31 gives a lot of power to the woman as she is seen not only as an able manager of the household but also as a clever manager of the estate that she buys with her own money; furthermore, she becomes a wealthy merchant outside the confines of her house. Thus, she is very progressive in the socio-economic sphere and this virtuous wife can be a great role model to empower girls to stand on her own feet on equal footing with men and then continue to do so even after marriage. As a praise to this amazing woman the Bible says, "Strength and honour are her clothing" (Holy Bible, NKJV, Proverbs 31:25) giving her the

Principal Nowgong Girls' College Nagaon :: Assam

Nowgong Girls' College ESTD: 1962 Nagaon :: Assam

qualities that normally would be ascribed to a man, that of having the stereo-typically masculine possession of 'strength' and also the 'honour' that comes from the people due to her extraordinary feats. She can be seen as an independent woman who has free reign of her works and she might be more admired than her husband for her virtue that is praised all over the town. The picture of the virtuous wife would also help men to see that women do not lack behind in any qualities and skills but that they can do better than men when they are given the right environment to bloom and that they are to be treasured invaluably for their virtues in the house as well as the outside world. In a world where women are seen as the 'weaker' sex, it is important to remove the inequality that has prevailed and it can only be done by realizing that women are equal before God, having equal dignity and honour and abilities, not lagging behind in any good work and are not just child-bearers and domestic helps. It is important for the patriarchy to realize that women can possess all the virtues that any man can possess that of strength, honour, wisdom and many others and should be given free rein in order for their virtues to come forth. Adorno in his Minima Moralia says,

> The only decent marriage would be one allowing each partner to lead an independent life, in which, instead of a fusion derived from an enforced community of economic interests, both freely accepted mutual responsibility (Adorno, Theodor, 31).

Adorno is signifying the importance of independence for an ideal marriage, which respects the interests of both the husband and the wife. However, the Biblical view of the ideal wife as seen in the New Testament calls for the submission of the wife to the husband. It can be seen in Ephesians 5:22-24

> Wives, submit to your own husbands, as to the Lord. For the husband is head of the wife, as also Christ is head of the church; and He is the Savior of the body. Therefore, just as the church is subject to Christ, so let the wives be to their own husbands in everything. Husbands, love your wives like Christ also loved the church and gave Himself for her (Holy Bible, NKJV)

Also in Colossians 3:18- 19,

> Wives, submit to your own husbands, as is fitting in the Lord.
> Husbands, love your wives and do not be bitter toward them
> (Holy Bible, NKJV, Col 3:18-19)

And in 1 Peter 3: 1-4,

"Wives, likewise, be submissive to your own husbands, that even if some do not obey the word, they, without a word, may be won by the conduct of their wives, when they observe your chaste conduct accompanied by fear. Do not let your adornment be merely outward-arranging the hair, wearing gold, or putting on fine apparel- rather let it be the hidden person of the heart, with the incorruptible beauty of a gentle and quiet spirit, which is very precious in the sight of God (Holy Bible, NKJV, 1 Peter 3:1-4).

It can be seen in all these verses that submission to the headship of the husband is the quality of an ideal wife. The Bible equates the submitting of the wife to the husband as the church being subject to Christ. Does it contradict the freedom and the position of the woman that can be seen in the Old Testament in the Proverbs 31 example of a virtuous wife? One cannot say that these views contradict, that the man and woman are unequal beings, but that in the family, for the semblance of order, the husband is supposed to be the head of the family by default. This cannot be construed to the fact that it demeans the worth of the woman in any means. Of course this command for submission can be taken to its illogical ends, that of dominating the woman and considering her as being of lesser worth and being inferior to the man. But the text in no way justifies that. The succeeding verses ask the husband to love the wife as Christ has loved the church, and in Ephesians 5:24 its written "So husbands are to love their wives as their own bodies; he who loves his wife loves himself", the analogy of submission is as the submission and love of the church for Christ and the sacrifice of Christ in His love for the church to be His bride. The question of who is supposed to be in headship and not the wife is going to be a fiercely debatable topic which long drawn battle to topple the patriarchy and feminists would take the fight to remove the instruction for submission.

Certified
Principal
Nowgong Girls' College
Nagaon :: Assam

Nowgong Girls' College
ESTD: 1962
Nagaon :: Assam

arguing that making the woman second to the man in the question of authority and headship as a tyrannical order and violates the position of equality of the woman. The critics on the other side of the camp would argue that this was given so that there be order in the family leading to order in the society if this was followed with proper context; they would argue that submission is necessary for love to exist and for anarchy to be contained.

> In speaking of marriage, it is easy to fall into the habit of thinking of it as a concrete entity with features as readily observable as any three-dimensional object with volume, density and a visible surface. However, a marriage is actually a relationship between two people, not a concrete object. It is a dynamic system that emerges from the actions and interactions of people
> (Ross, Catherine E., 282).

Marriage is not just a concretely observable entity, it is a relationship between two people and their interactions and in this abstract nature of marriage lies the individual personal values, emotions and personalities that are a large part of the psychological nature of the family. A mutual respect and love between spouses would lead to a happy marriage full of happy individuals, while a marriage without those equations is likely to be an unsuccessful one.

J.S. Mill and Harriet Taylor in their essay on marriage writes, "It may be assumed, as one of those presuppositions which would almost be made weaker by anything so ridiculous as attempting to prove them, that men and women ought to be perfectly coequal: that a woman ought not to be dependent on a man, more than a man on a woman, except so far as their affections make them so, by a voluntary surrender, renewed and renewing at each instant by free and spontaneous choice. But this perfect independence of each other for all save affection, cannot be, if there be dependence in pecuniary circumstances; a dependence which in the immense majority of cases must exist, if the woman be not capable, as well as the man, of gaining her own subsistence." (Mill, J.S. Mill, Harriet Taylor, 5)

Here, Mill and Taylor acknowledge the need for independence as well as mutual submission for the marriage. The Biblical virtuous wife does not in any way lack in this regard, she is not dependent on her husband for her subsistence, however she is submissive due to her affection. There is no diminishing of her worth but she is second to the man in terms of the hierarchy of the family order for the semblance of order. The quality of submission in the virtuous wife will always be questioned by people from the sceptical brigade, but the other camp would point out that if love humility are virtues to be sought after, then submission is also a good virtue.

The social construct of an ideal wife according to the Bible, lays down some ideals for women to aspire to in the realms of marriage and it definitely gives worth and value to the woman in all spheres. However, the Biblical virtuous wife is supposed to be submissive to her husband in the context of marriage and she is under the husband in the hierarchy of the family, but this position in no way diminishes her individual worth, respect and importance in the wider society.

Works Cited

1. *Holy Bible*. New King James Version, Nashville: Thomas Nelson Publishers, 1982: Print
2. Adorno, Theodor. *Minima Moralia: Reflections of a Damaged Mind*. Trans. E.F.N. Jephcott. New York: Verso, New Left Books, 2005: Print.
3. Mill, J.S. and Mill, Harriet Taylor. *Essays on Sex Equality*. Chicago: University of Chicago Press, 1970: Print.
4. Ross, Catherine E. and Mirowsky, John. *Sociological Perspectives* Vol. 27, No. 3, pp. 281-300, New York: Sage Publications, Inc, 1984: Print
5. Palmer, "Wifey Material", 23 March 2005 https://www.urbandictionary.com/define.php?term=Wifey%20Material

Principal Nowgong Girls' College Nagaon :: Assam

Nowgong Girls' College ★ ESTD: 1962 ★ Nagaon :: Assam

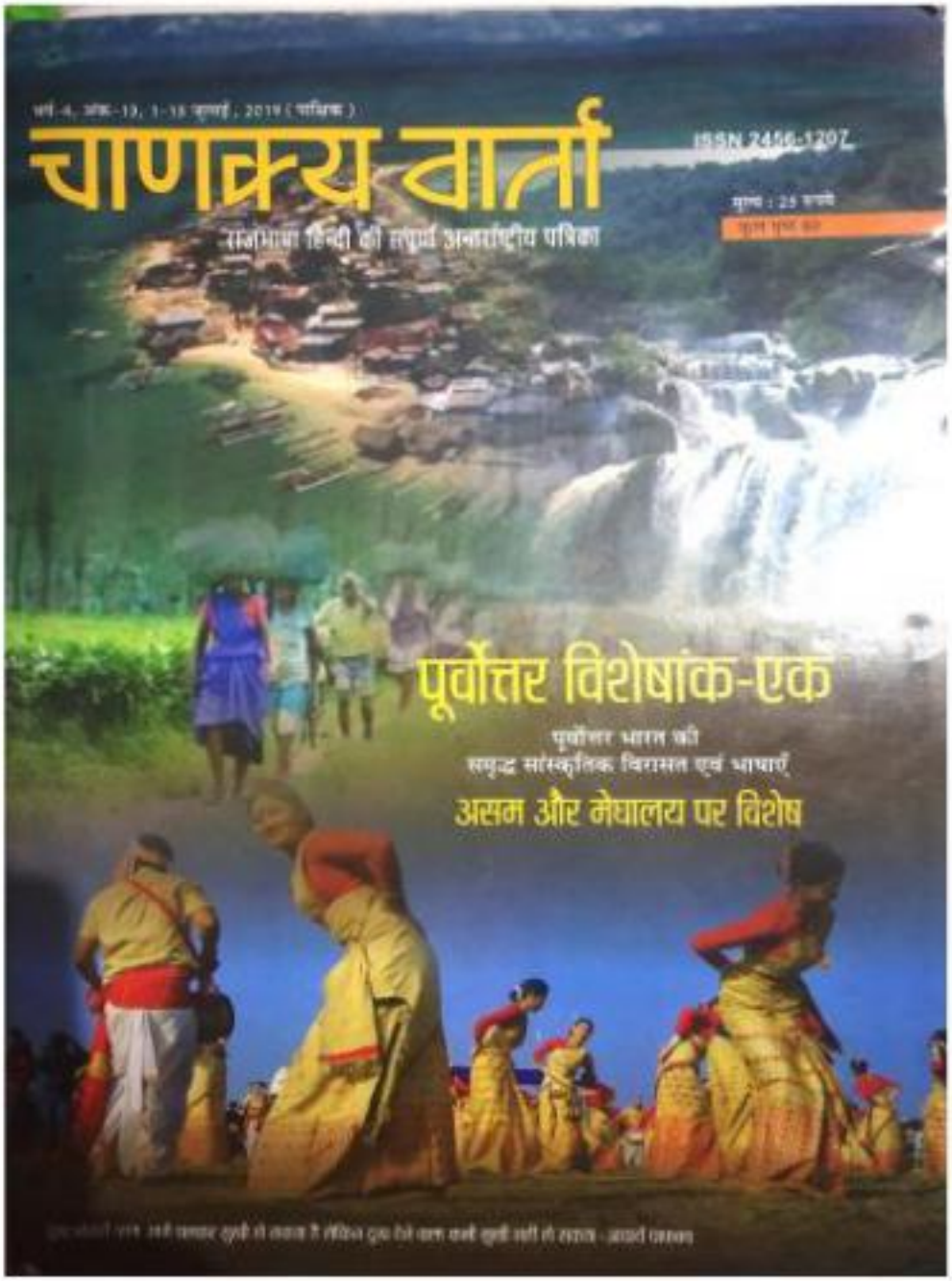

Principal
Nowgong Girls' College
Nagaon :: Assam

Nowgong Girls' College
ESTD: 1962
Nagaon :: Assam

मुखा भाउना : पौराणिक आख्यानों की कलात्मक अभिव्यक्ति

मुखा एक आवरण है जिसके परिप्रेक्ष्य का प्रमुख रूप मुखौटा है। अपने प्रमुख रूप को मुखौटा से मुखा का किसी मुखौटे के रूप को पहनना या किसी खास सिद्धि के लिए मुखौटा का प्रयोग आदिम काल से ही चला आ रहा है। किंतु मुखौटा केवल मुख को ही नहीं छिपाता। नाटक के संदर्भ में मुखौटा पहनकर अभिनेता दर्शकों को सच के करीब ही ले जाता है। अभिव्यक्ति की सशक्त और कलात्मक की मांग का ख्याल रखते हुए मुखौटों को भिन्न-भिन्न तरीके से प्रस्तुत किया जाता है। कुछ मुखौटा सिर से लेकर पैर तक अभिनेता के शरीर से बंधा होता है तो कुछ मुखौटा अभिनेता के केवल चेहरे के आगे सिर से बंधा होता है तो कुछ उसे अपने सिर से थामे खड़ा होता है।

मुखौटा आवरण के लिए नयी संकल्पना नहीं है। विश्व के अन्य प्रान्तों की भांति प्राचीन काल से ही असम में भी मुखौटा का प्रयोग आवश्यकता अनुसार होता रहा है। स्थानीय लोगों द्वारा लौकी, खपरा, मिट्टी के बर्तन आदि में किए गए कारीगरी में मुखौटा का प्राचीन स्वरूप देखने को मिलता है। असम में मुखौटा मूलतः बांस से ही बनाया जाता है। काठ से भी मुखौटा बनाने का प्रावधान है। कई सभों में काठ से बना प्राचीन मुखौटा उपलब्ध है, परंतु जनश्रियता बांस से बने मुखौटों की ही अधिक है। असम में मुखौटा निर्माण अत्यन्त धैर्य वाले कार्य वाले सुलझे व्यक्तियों से होता है। इसके लिए धान, जूट, बनपाट, बालाह, गोबर और 'कुमार माटि' की आवश्यकता होती है। मुखौटा निर्माण के तीन चरण हैं—

प्रथम चरण- इसमें बांस को काटकर चार-पांच दिन के लिए पानी में भीगोकर रखा जाता है। ऐसा करने से बांस जल्दी खराब नहीं होता है। उसके बाद इन टुकड़ों से मुखौटों की कार्यशैला तैयार किया जाता है। आवश्यकता अनुसार 'डाका खरि' पोखरा उससे मुखौटा के ऊपर रखकर सूखने के लिए धूप में रख दिया जाता है।

द्वितीय चरण- द्वितीय चरण में गोबर और 'कुमार माटि' को एक साथ हाथ से मिलाकर मुखौटा के ऊपर से लगाया जाता है और फिर से धूप में सूखाया जाता है।

तृतीय चरण- इसमें मुखौटा को रंगों के साथ सजाते हुए मुखौटा निर्माण में लगे 'लाहकार'

> "मुखौटा असम के लिए नयी संकल्पना नहीं है। विश्व के अन्य प्रान्तों की भांति प्राचीन काल से ही असम में भी मुखौटा का प्रयोग आवश्यकता अनुसार होता रहा है। स्थानीय लोगों द्वारा लौकी, खपरा, मिट्टी के बर्तन आदि में किए गए कारीगरी में मुखौटा का प्राचीन स्वरूप देखने को मिलता है। असम में मुखौटा मूलतः बांस से ही बनाया जाता है। काठ से भी मुखौटा बनाने का प्रावधान है। कई सभों में काठ से बना प्राचीन मुखौटा उपलब्ध है, परंतु जनश्रियता बांस से बने मुखौटों की ही अधिक है।"

'शंकुड़' आदि गोंदे का प्रयोग किया जाता था। परंतु इन गोंदे को उत्पादकता की दिशि बहुत अधिक और समयसाध्यी है। इसी कारण अब सभों में काठ से आसानी से उपलब्ध कुलिम गोंदे का ही प्रयोग किया जाता है।

मुखौटे में तीन प्रकार के मुखौटा का निर्माण होता है—बनमुखा, लोटोवाई और मुख-मुखा। बनमुखा सामान्य मुखा से बहुत बड़ा होता है। मुखौटा का सिर और चेहरा भाग आलग-आलग बनाया जाता है। चेहरा बनते समय सिर के भाग को अतिरिक्त सिर में और चेहरा भाग को शरीर में पहना लेता है। लोटोवाई मुखौटा भी बनमुखा जैसा ही होता है, केवल इसका धड़ छोटा होता है। मुख-मुखा में केवल अभिनेता के सिर भाग के लिए मुखौटा बनाया जाता है।

एक विशिष्ट कला के रूप में मुखौटा का सर्वप्रथम प्रयोग श्रीमंत शंकरदेव ने ही किया। शंकरदेव के द्वारा स्थापित राजा के साथ में स्थापित 'सिद्धनाथ थानम' में सो साल पहले मुखौटा का उपयोग किया गया था। भाओना का मुकुल श्रीमंतशंकर शंकरदेव ने ही किया। भाओना नाट्य का ही एक रूप है। सूत्रधान इसका मुख्य अंग है। यह नकल भी है, प्रहसन भी है तथा विचारधारा भी। यह भाओना के पात्रों को दर्शकों से परिचय कराता है, उनके आगमन और प्रस्थान की सूचना देता है। सूत्रधार संपूर्ण भाओना के पूरी को एक सूत्र में बांधे रखता है। मंच की प्रारंभिक पात्रों के आगमन के साथ ही खोल्ल बजने लगता है और पात्र खोल्ल के ताल में ताल मिलाकर नियंत्रित ढंग से चलते हैं और अपने प्रदर्शन दिखाते हैं। भाओना में विभिन्न पात्रों का अभिनय भी मुखौटा के किया करते हैं।

बहुरूपी, गायनरा, महाबाहु और अन्य अभिनेता भी इसी प्रकार के मुखौटे का ही प्रयोग किया जाता है। इसी मुख देने अभिनेता का मानसिक भाव होते हैं जिसके कारण कलाकार के लिए मुखौटा को अत्यधिकार होती है। जैसे कि

C.T.C.
Principal
Nowgong Girls' College
Nagaon :: Assam

Nowgong Girls' College
ESTD: 1962
Nagaon :: Assam

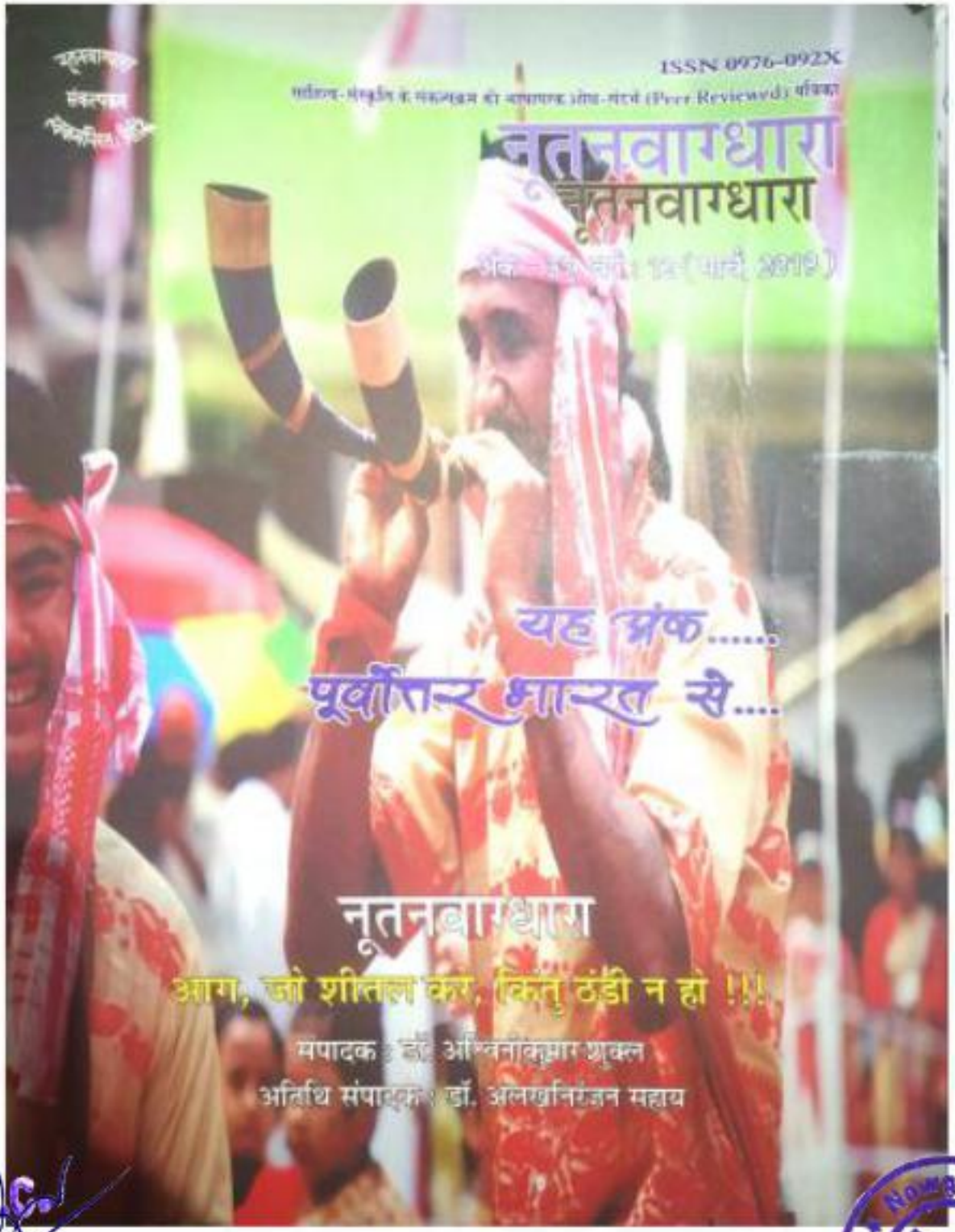

Principal
Nowgong Girls' College
Nagaon :: Assam

Nowgong Girls' College
ESTD: 1962
Nagaon :: Assam

आलोड़न-विलोड़न

1. असमीया कथा-साहित्य के तीन दशक : कतिपय विशिष्ट्य / डॉ.मुर्धकांत त्रिपाठी / 87
2. त्रिपुरी लोकनृत्य : एक परिचय / डॉ. बीना देवबर्मा / 89
3. असमीया बाल-साहित्य : दशा एवं दिशा / डॉ. मनिका शईकिया / 92
4. पूर्वोत्तर में हिंदी तथा भाषाई मीडिया की चुनौतियाँ / रविशंकर रवि / 95
5. पूर्वोत्तर में हिंदी-शिक्षण की चुनौतियाँ और समाधान/ तिनत बोरा / 97
6. भाषिक-सांस्कृतिक विविधता का राज्य नगालैंड / डॉ. चन्द्रशेखर चौबे / 99
7. बुरी-भूत बुलाते : अपति, विकास एवं आयोजन / डॉ. जमुना बीनी तादर / 103
8. 'जोंके' जनजाति और उनके लोकगीत / डॉ. अरुण कुमार पांडेय / 105
9. पूर्वोत्तर भारत : जीवन-शैली एवं लोकसाहित्य / डॉ. सी. एस. मेरेजा / 109
10. भूपेन हाजारिका के गीतों में प्रकृति-चित्रण / डॉ. जोमाली कलिता / 112
11. अरुणाचलप्रदेश के नानो जनजातीय समाज की एक झलक / सुकेन रिगु / 115
12. पूर्वोत्तर की सात बहनें / अंचल कुमारी राय / 117
13. असमीया संस्कृति का बदलता परिदृश्य / हिमी दत्त / 120
14. अरुणाचलप्रदेश के आदिवासियों की मृत्यु-विषयक अवधारणा / वीरेंद्र परमार / 122
15. सनातन आलोक धर्म : अतीत से वर्तमान तक / बेबी बिश्वकर्मा / 125
16. पेड़-पौधों पर आधारित मणिपुरी मुहावरों का सार, हिंदी अनुवाद एवं विश्लेषण / तेलकुचम सतोम्बा सिंह / 127
17. अरुण राज्य को लेकर कही-अनकही बातें (संस्मरण) / तिया लखपति / 129
18. डॉ. भूपेन हाजारिका के गीतों में समन्वय के स्वर / पुलह प्रसाद डोलकोटय / 130

कहानी-प्रवाह

1. पहचान / तिनत बोरा / 133

अंजलि-निधि

1. मोरी मनोरंजु (मुल असमीया- धीरेन चंद्र तमुली) / अनुवाद- डॉ. रमाकांत त्रिपाठी / 137
2. सागर देखा है? (मूल असमीया- देवकांत बरुवा) / अनुवाद- डॉ. रमाकांत त्रिपाठी / 137
3. तीन असमीया गीत / डॉ. अरुण प्रभात / 147

अतीत के गलियारे

1. पहाड़न की हत्या / डॉ. अग्निशेखर / 139
2. पहाड़ों की स्मृतियाँ / डॉ. सुरेन्द्र कुमार अग्निहोत्री / 141
3. क्या जीड़ न्यूशी घाटी है / अरुण कुमार त्रिपाठी / 146
4. चिट्ठी, चिराग, कंघा, गाजरें ...न जाने क्या-क्या... / कवीर कुमार सुमन / 149

समीक्षा

1. सीमांतिक समाज का दर्पण के 50 वर्ष की अनिवार्यता : कोरकी / डॉ. सुनील कुमार शर्मा / 143

C.T.C.
Principal
Nowgong Girls' College
Nagaon :: Assam

Nowgong Girls' College
ESTD: 1962
Nagaon :: Assam

लुप्तप्राय आहोम धर्म : अतीत से वर्तमान तक

बेबी बिश्वकर्मा*

असम भिन्न-भिन्न सामाजिक, सांस्कृतिक, धार्मिक विशेषता से संपन्न राज्य समूहों का समावेशन रहा है। उसी श्रेणी के पूर्वोत्तर में आहोम अन्यतम थे आए और बुरंजर आमोलगा जाति, भाषा एवं संस्कृति को गढ़ने में आहोम जातियों को विभाजन इनकी अपनी प्रकृति और विशेषताएँ हैं, जो इनकी विलक्षणता को चित्रित करता है।

आहोम धर्म मूलतः एकेश्वरवादी है, परंतु इसमें बहु-ईश्वरवाद के भी तत्व मिलते हैं। आहोम एक विशेषज्ञ पराशक्ति पर विश्वास रखते हैं, जो इस विश्व-ब्रह्माण्ड का निर्माता है, प्रतिपालक है और संहारक भी है। यह धर्म प्रकृति के अत्यंत निकट है। प्रकृति के भिन्न-भिन्न तत्वों (अग्नि, वायु, वनों, पेड़) में बसे निर्गुण देवताओं की पूजा के द्वारा प्रकृति भी ही पूजा की जाती है।

निर्गुण ईश्वर की आराधना के कारण इस धर्म में मूर्तिपूजा का विधान नहीं है। किसी भी देवी या देवता की प्रतिमा इस धर्म में उपलब्ध नहीं है, सिवाय 'चुम देव' के। ऐसा माना जाता है कि चुम देव पवित्रता एवं को अभिलाषित धन, ऐश्वर्य और शक्ति का प्रदान देते हैं। आहोम स्वर्ग को लेंगदन (स्वर्ग के देवता) के संबंध होने के कारण आहोम राजा अपने राज्य के आगे 'स्वर्गदेव' (स्वर्ग के देवता) की उपाधि लगाते थे। आहोम-कालीन इतिहास में यह उल्लेख है कि जब लेंगदन के पोते सुए लुंग और सुए लाइ वर्ग में शासन के उद्देश्य से आए, तब लेंगदन ने चुम देव की मूर्ति उन्हें भेंट में दी। इसी कारण राजनीतिक के अवसर पर चुम देव की पूजा करना अनिवार्य माना जाता था। अचंभे की बात यह है कि चुम देव की मूर्ति का स्वरूप किसी नहीं है। आहोम के इस राजकीय देवता की प्रतिमा के संदर्भ में लोगों के किसी का मानना है कि इसका स्वरूप बाघ का है, तो कभी कहा जाता है कि यह एक पेटी में सहेजकर रखा गया अमूल्य धन है।

राह आहोम धर्म में किसी भी देवी देवता के लिए मठ-मंदिर बनने की संकल्पना नहीं की, परंतु स्थानीय आती 'डबजाति के निवासस्थान 'चेंग घर' बनाने की प्रथा की आहोम धर्म ने अपना लिया था। फिर तो प्रत्येक देवी-देवता के लिए भिन्न-भिन्न स्थान बना है, परंतु इसके निर्गत 'देवघर' आराधना के लिए निर्दिष्ट किया गया एक पवित्र स्थान है।

मृत पूर्वजों की पूजा आहोम धर्म की सर्वोत्कृष्ट विशेषता है। आहोम यह मानते थे कि मृत्यु के पश्चात उनके पूर्वज 'ग्राम देवता' बन जाते हैं, एवं परिवार की सुख-शांति, धन-ऐश्वर्य की देखभाल पूर्वजों की आत्मा करती है। इसी कारण 'ग्राम पिः' अनुष्ठान के जरिये इन सभी उनकी पूजा करना, उन्हें संतुष्ट रखना आवश्यक है। लोकविश्वास के अनुसार-

अर अमाई साथ देवताए हाबाय / साक लागे थाकबाय, बाघे थाकाय, आमेर थाकबाके नहीं // (जिसके साथ ग्राम देवता का आशीर्वाद है, उसे साँप नहीं काटता, बाघ नहीं खाता, शत्रु भी उसे नहीं ले जा सकता)

आहोम धर्म में मृत व्यक्ति की अंतिम क्रिया अत्यन्त नहीं, बल्कि 'मेताम' में संस्कार करते थे। यदि मेताम शरीर का दो तीन प्रकार एक मूर्तिया बना दी जाती थी, क्योंकि ऐसा माना जाता था कि मृत्यु के 21 दिन तक, जब तक मृतक सम्पत्ति संबंधी सभी रस्में सम्पन्न नहीं हो जाती, मृतक की आत्मा नहीं रहती है। अभी भी शिवसागर जिले के चराइदेउ में स्थित इन चरम राजसी मैदानों को देखा जा सकता है।

आहोम धर्म में मृतक वर्ग की उपस्थिति भी बीभत्स थी। धार्मिक रीति-नीति एवं अनुष्ठानों के संपन्न प्रतिपादन का दायित्व पुरोहित के तीन वर्गों- बोहाग (पोहान), चेंगमाय (देउधाइ) और सालेकोए (बाइनुर) होताओं को थे एवं भाषा और लिपि के ज्ञाता थे सभी दाह क्रियाओं में तिन्हें मंत्रों का उच्चारण करते हुए पूजा की विधि का पालन करते थे। विवाह में मिले दाह धर्म और चालना को ये आज तक संरक्षण देते आए हैं।

C.T.C.
Principal
Nowgong Girls' College
Nagaon :: Assam

Nowgong Girls' College
ESTD: 1962
Nagaon :: Assam

Shikshan Sanshodhan : Journal of Arts, Humanities and Social Sciences ISSN: 2581-6241 Volume - 2, Issue - 5, Sept-Oct – 2019
Bi-Monthly, Peer-Reviewed, Refereed, Indexed Journal Impact Factor: 1.847
Received on : 03/10/2019 Accepted on : 14/10/2019 Publication Date: 30/10/2019

तीसरी ताली : तृतीय लिंगी समाज का यथार्थ

बेबी विश्वकर्मा

शोधार्थी, हिन्दी विभाग, राजीव गांधी केन्द्रीय विश्वविद्यालय, अरुणाचल प्रदेश, दोइमुख-791112

Email- biswakarmababy95@gmail.com

शोध सार : साहित्य और समाज का संबंध अन्योनाश्रित है। साहित्य मात्र कल्पना की उड़ान नहीं है। साहित्यकार अपने समय की सारी रूढ़ियों, परिस्थितियों, समाज का बदलता स्वरूप, समाज में हो रहे उथल-उथल सभी का कलात्मक अभिव्यक्ति कुछ इस प्रकार करता है कि वह पाठक के मर्मस्थल को भेद जाता है। आज बहुत से साहित्यकार एवं बुद्धिजीवी किन्नरों के अस्तित्व के संघर्ष में योगदान दे रहे हैं तथा 'किन्नर विमर्श' नाम से एक साहित्यिक विमर्श ही चल पड़ा है। प्रदीप सौरभ इन्हीं साहित्यकारों में से एक हैं, जिनके उपन्यास 'तीसरी ताली' ने हिन्दी साहित्य जगत में हलचल मचा दिया। लेखक ने प्रस्तुत उपन्यास के माध्यम से अवहेलित वर्ग के अनछुए अंधकार पहलुओं को प्रकाश में लाया है।

बीज शब्द : किन्नर, शोषण, उपेक्षा, लैंगिक भिन्नता, हाशिए।

शोध उद्देश्य :

1. भारतीय समाज में किन्नरों की स्थिति एवं उनके संघर्ष पर प्रकाश डालना।
2. 'तीसरी ताली' में अभिव्यक्त किन्नर के जीवन से जुड़े समस्याओं एवं चुनौतियों का विश्लेषण करना।

शोध प्रविधि : प्रस्तुत शोध-कार्य में निम्नलिखित शोध प्रविधियों का प्रयोग किया गया है –

1. पुस्तकालय में प्राप्त ग्रन्थों एवं पत्रिकाओं में प्रकाशित सामग्रियों का अध्ययन।
2. इंटरनेट पर उपलब्ध संबन्धित शोध सामग्रियों का अध्ययन।

प्रस्तावना :

भारतीय जन किन्नरों से शुभाशीष की मांग तो कर लेता है परंतु बदले में थोड़ी-सी सहानुभूति और संवेदनशीलता का प्रदर्शन नहीं कर पाता। इस वर्ग के प्रति हमारे समाज में एक अजीब-सा डर, घृणा, शंका और अवज्ञा का माहोल है। किन्नर अपने शारीरिक बनावट के कारण न तो पूर्णतः स्त्री बन पाये और न ही पुरुष। इसीकारण समाज ने उन्हें पूर्ण व्यक्ति के रूप में देने से ही इनकार कर दिया। लैंगीक भिन्नता के कारण किन्नर समुदाय हाशिये के [illegible] के लिए अभिशप्त है। आधुनिक और प्रगतिशील कहलानेवाला हमारा समाज आज भी उदारतापूर्वक उन्हें अपना नहीं पाया है। प्रदीप सौरभ का उपन्यास 'तीसरी ताली' तथाकथित सभ्य समाज की इसी संवेदनहीनता, क्रूरता, विकृत सोच

Principal
Nowgong Girls' College
Nagaon :: Assam

की त्रासदी, शारीरिक शोषण, सामाजिक पारिवारिक उपेक्षा, मुख्यधारा में शामिल न हो पाने के कारण जीविका के चाह में दर-बदर भटकते और वेश्या-वृत्ति के गर्त में धकेले गए किन्नर समुदाय की व्यथा-कथा है।

किन्नरों की ताली से या तो यह समाज आतंकित होता है या फिर विरक्त। उन तालियों के अनगुंज के पीछे छिपे दर्द की गहराई तक उनकी संवेदना नहीं उतर पाती। एक किन्नर का सम्पूर्ण जीवन उपेक्षा, घृणा, अवज्ञा, शर्मिंदगी, तिरस्कार और अवज्ञा से भरा होता है। उनके परिवारवालें, यहाँ तक कि उनके माता-पिता भी यह बताने से कतराते हैं कि वह उनके परिवार का हिस्सा है। कितनी दुख की बात है कि दूसरों के जन्म अवसर पर बधाई देनेवाले, नाच-गान कर झूमनेवाले किन्नरों के जन्म पर केवल शोक ही मनाया जाता है। जन्मोपरांत या तो उसे लावारिस छोड़ दिया जाता है या फिर सदा के लिए त्याग कर किन्नर समुदाय को सौप देते हैं। इसके विपरीत यदि कोई परिवार उन्हे अपने सिने से लगाए रखना चाहता है, अच्छी परवरिश देना चाहता है, तब यह समाज उस परिवार को भी उत्पीड़ित कर उसके आत्मविश्वास को चकनाचूर कर देता है। ऐसी ही हालत सिधार्थ एनक्लेव के गौतम साहब का भी था- "गौतम साहब की चाल में जो अकड़ आई थी, वह ढीली पड़ने लगी। मोटे चश्मे के पीछे चमकनेवाली आँखें भी झुक गयी। वे हमेशा झुंझलाए-झुंझलाए से दिखते। अजीब तरह की चिंता उनके माथे पर दिखती।... बेतरतीबी ऐसी की गौतम साहब कभी मोजा पहनना भूल जाते तो कभी उनकी कमीज पीछे से निकली होती या फिर आगे से"।[i] गौतम साहब विनीत के पालन-पोषण में कोई कमी नहीं रहने देना चाहते थे परंतु समाज उनकी मनःशक्ति को शनैः शनैः क्षीण करती जा रही थी। समाज की सारी मानवीय विशेषताएँ किन्नरों की यौनिक भिन्नता के समक्ष आकर धूल हो जाती है। केवल और केवल लिंग के धरातल पर यह समाज उसे मुख्यधारा से बेदर्दी से बाहर फेंक देना चाहता है। शिक्षा, रोजगार, सामाजिक प्रतिष्ठा इन सभी से समाज उन्हे वंचित रखना चाहता है। शिक्षा संस्थाओं को भारतीय समाज विद्या का पवित्र मंदिर मानता है। परंतु यहाँ भी किन्नरों को अपमानित ही होना पड़ता है। छठी कक्षा के बाद निकिता को स्कूल में केवल इसीलिए दाखिला नहीं मिल पाता क्योंकि वह एक किन्नर है। निकिता कभी अपने किन्नर अस्तित्व को स्वीकार नहीं पायी। अपना अधूरापन उसे खलता था। सामान्य जीवन व्यतीत न कर पाने की छटपटाहट से मुक्ति के लिए वह आत्महनन का पथ चुनती है। ऐसे न जाने कितने की किन्नर हैं जो समाज के उपेक्षा और संवेदनहीनता के कारण हीनता से भरकर आत्महत्या कर लेते हैं। आर्थिक दुर्दशा, अशिक्षा, हर क्षेत्र पर समाज से मिलते दुत्कार, अज्ञानता तथा तकनीकी अकुशलता इन्हे पारंपरिक नाच-गान के धंधों में उलझा रखता है अथवा देह व्यवसाय के लिए बाध्य करता है।

जिस प्रकार स्त्री को महिमामंडित कर उसका शोषण किया जाता है ठीक उसी प्रकार किन्नरों को भी महिमामंडित कर लिंगधारी समाज उन्हे छलावे में रखता है। कोई उन्हे अरवाण का वंशज मानता है तो कोई उन्हे कृष्ण का मोहिनी अवतार। ईश्वर का हवाला देकर यह तक भी कहा जाता है कि किन्नरों को श्री राम का वरदान है जिसकारण ये अपना घर परित्याग कर नाच-गान कर बधाई देते फिरते हैं। इसी छलावे में आकर डिम्पल जैसे किन्नर परंपरागत पेशों में ही अपने को सीमित रखना चाहती है। हिजड़े हमारे आस-पास मौजूद हैं फिर भी हम उनके सामाजिक संरचना से अनजान हैं। उनके नाचते-गाते या फिर बस, ट्रेन आदि में गालियाँ बरसाती छवि ही जनमानस के मन में सामान्यतः उभरती है। परंतु हिजड़ों की अन्तर्मन की हल-चल को यह समाज भाँप नहीं पाता। सभ्य समाज का दोमुंहापन देखिए- एक तरफ हिजड़ों को रामवरदानी कहता है तो दूसरी ओर उनकी अंतिम यात्रा तक देखना आम जनों के लिए अशुभ माना जाता है। "भोपाल

CTC
Principal
Nowgong Girls' College
Nagaon :: Assam
Nowgong Girls' College Estd. 1962 Nagaon

में मशहूर है कि ऐसी ही जिन्न की सवारी आजादी से पहले पाँच पुलिसवालों ने देखी थी, तो वे पागल हो गए थे। जिन्नों की सवारी शलभ ने भी देख ली थी। अब शायद उसकी पागल होने की बारी थी।...क्रास पर सुरैया का शव लटका था। यह उसकी अंतिम यात्रा थी। उसे पुराने कब्रिस्तान में ले जाया जा रहा था लोगों की नज़रों से बचा कर ताकि कोई तीसरी योनि की अशुभ यात्रा न देख सके...इस योनि के अमंगल की छाया किसी पर न पड़े।"[ii] हिजड़ों की अस्तित्व एवं उनके समाज को लेकर आशंका, अजनबीपन एवं अंधविश्वास भरे माहौल को बनाए रखने के पीछे व्यवस्था का प्रपंच काम कर रही है ताकि वे मुख्यधारा के समाज से सदेव अलग-थलग रहें।

समाज की अवज्ञा के साथ साथ किन्नरों की अज्ञानता भी उनकी दुर्दशा के लिए दायी है। 'तीसरी ताली' उपन्यास में लेखक किन्नरों की परंपरा से बंधे रहने की इस रूढ़िवादिता की ओर संकेत करते हैं। अमेरिकी मोबाइल कंपनी द्वारा मिले नौकरी के प्रस्ताव को ठुकराते हुए नीलम, रीना और डिम्पल के डेरों के किन्नर कहती हैं- "साहब हम अपने नाच-गाने से ही खुश हैं। हमें आपकी नौकरी नहीं करनी। हम तो भगवान राम के आदेश पर सदियों से नाच-गाकर अपनी रोटी कमा रहे हैं। हमें भी एकदिन ऊपर उनके पास जाना है। वहाँ जाकर हम क्या जवाब देंगे"।[iii] किन्नर समाज का बहुत बड़ा अंश अभी भी अपने अधिकारों के प्रति उदासीन है। महत्वकांक्षा और जागृति की कमी ने उन्हे यथास्थिति में जकड़े रखा है।

किन्नरों की जीवन कथा अत्यंत करुण है। जिंदगी भर वे निर्वासित, शापित जीवन काटते हैं। बुनियादी सुविधाओं के लिए भी उन्हे पल-पल संघर्ष करना पड़ता है। मुख्यधारा के पूर्ण व्यक्ति होने के गर्व से गर्वित सदस्य इतना अधम और हवसी है कि जिस किन्नर को लेंगीक रूप से विकलांग मान दरकिनार करता है अवसर मिलने पर उसी किन्नर का शारीरिक शोषण भी कर लेता है। 'तीसरी ताली' के मणि कुमार जैसे कई पात्र असल जिंदगी में भी मौजूद हैं जो दुर्भाग्यवश तथाकथित सभ्य समाज के हवस का शिकार बन जाते हैं। किन्नरों की पहचान ही उनके लिए अभिशाप साबित होती है। कैसी विडंबना है कि एक तरफ अस्तित्व रक्षा की अनेक आंदोलन चल रही है तो दूसरी ओर किन्नर अपने अस्तित्व से ही परेशान है। उनका पहचान ही उनका दुश्मन है, जिससे वे भागना चाहते हैं। विजय भी ऐसा ही एक पात्र है जो अपने फोटोग्राफी केरियर में कामयाब होने के लिए अपने किन्नर होने के सच को दुनिया से छुपाए रखता है क्योंकि वह जानता है यह समाज किन्नर को सदा पैरों तले रौंदता आया है। जो वर्ग समाज के जेंडर-नियमों के सीमा में नहीं समाता, उसे प्रताड़ना के अलावा कुछ भी नहीं मिलता।

निष्कर्ष :

मुख्यधारा समाज के लिए 'हिजड़ा' शब्द एक भद्दी गाली है जो उनके वीरता पर प्रश्न खड़ा करता है। चूंकि किन्नर प्रजनन में अक्षम हैं संभवतः इसीलिए उन्हे मुख्यधारा से वंचित कर दिया गया था क्योंकि प्राचीन काल में पुरा वृद्धि मानव जीवन का अंतिम महत्वपूर्ण लक्ष्य था। परंतु अब समस्या प्रजनन की रह नहीं गयी है। विज्ञान इतना आगे बढ़ चुका है कि कृत्रिम साधनों से भी प्रजनन संभव हो चुका है। जनसंख्या विस्फोट तो अब एक वैश्विक समस्या बन चुकी है। अतः अनावश्यकीय मान्यताओं को सदेव के लिए ढोये रखने का कोई औचित्य नहीं है। गर्भावस्था में हुए लेंगीक भेद के कारण मनुष्य के एक वर्ग को इस प्रकार शापित जीवन जीने के लिए बाध्य कर देना कतई उचित नहीं है। किन्नर मानसिक

CTC Principal Nowgong Girls' College Nagaon :: Assam
Nowgong Girls' College EST 1968 Nagaon :: Assam

एवं शारीरिक तौर पर पूरी तरह से स्वस्थ हैं। यदि उन्हे व्यक्तित्व विकास का समुचित अवसर दिया जाए तो वे अपने सामर्थ्य को सिद्ध करने में सक्षम हैं। इस बात की पुष्टि प्रदीप जी भी विनीता, सुप्रिया कपूर जैसे पात्रों द्वारा करते हैं जो अनेक बाधाओं को लांघते हुए कामयाबी का मुकाम हासिल करते हैं। हिजड़ों को कानूनी अधिकार तो प्राप्त है परंतु सामाजिक स्वीकृति प्राप्त नहीं है। जिस कारण वे शोषण का शिकार बनते हैं। समाज की संकुचित मानसिकता, अपमानजनक व्यवहार हिजड़ों की व्यक्तित्व विकास की संभावनाओं को अवरोधित करता है। जब तक समाज की मानसिकता परिष्कार नहीं होगी, किन्नरों की मुक्ति पूर्णतः संभव नहीं है।

संदर्भ सूची :

[i] सौरभ प्रदीप, तीसरी ताली, वाणी प्रकाशन, नई दिल्ली, आवृत्ति 2018, पृ 40

[ii] वही, पृ 149

[iii] वही, पृ 180

iv मेहरा, दिलीप, हिन्दी साहित्य में किन्नर जीवन, वाणी प्रकाशन, नई दिल्ली, 2009.

C.T.C.
Principal
Nowgong Girls' College
Nagaon :: Assam

Nowgong Girls' College ★ ESTD: 1962 ★ Nagaon :: Assam

Acta Agrobotanica

DOI: 10.5586/aa.1793

Publication history
Received: 2019-04-19
Accepted: 2019-09-03
Published: 2019-11-26

Handling editor
Barbara Hawrylak-Nowak, Faculty of Environmental Biology, University of Life Sciences in Lublin, Poland

Authors' contributions
ZMS carried out all the experiments, analyzed the data, and prepared the manuscript; BT designed the experiment, supervised the task, and gave the inputs to finalize the manuscript

Funding
This research was financed from the fellowship obtained the from Department of Science and Technology – Innovation in Science Pursuit for Inspired Research (DST-INSPIRE), Government of India, No. DST/INSPIRE Fellowship/2016/160744 dated 2018-02-12.

Competing interests
No competing interests have been declared.

Copyright notice
© The Author(s) 2019. This is an Open Access article distributed under the terms of the Creative Commons Attribution License, which permits redistribution, commercial and noncommercial, provided that the article is properly cited.

Citation
Shandilya ZM, Tanti B. Hydroponic screening of traditional rice varieties in Assam, India to estimate their potential resistance to Al toxicity under P deficiency. Acta Agrobot. 2019;72(4):1793. https://doi.org/10.5586/aa.1793

ORIGINAL RESEARCH PAPER

Hydroponic screening of traditional rice varieties in Assam, India to estimate their potential resistance to Al toxicity under P deficiency

Zina Moni Shandilya, Bhaben Tanti*

Plant Molecular Biology Laboratory, Department of Botany, Gauhati University, Guwahati 781014, Assam, India

* Corresponding author. Email: btanti@gauhati.ac.in

Abstract

Acid soils encompass nearly one-third of the available terrestrial land surface worldwide. Acidic soil is one of the major abiotic constraints for agricultural practices by potentially creating aluminum (Al) toxicity and/or phosphorous (P) deficiency. Assam, being an agricultural state of India, has the majority of its area covered by acidic soils due to the varied terrain in the region. Soil acidification increases the solubility of Al present in the soil from its nontoxic silicate or oxide forms into highly phytotoxic ionic Al (mainly the trivalent cation Al^{3+}). Ionic Al can form complexes with the available phosphorous leading to plant nutrient deficiency. In the present investigation, screening of traditional rice varieties from Assam was conducted for tolerance to combined Al toxicity and P deficiency. Seedlings of 41 rice landraces from various agro-climatic locations were subjected to three different concentrations of Al (0, 50, 100 µM) for 24, 48, and 72 h under P deficiency in static nutrient culture to identify the extent of their resistance to these stressed conditions. Different morpho-physiological parameters (root and shoot lengths, fresh and dry weight yields, chlorophyll and relative water content) were evaluated after stress treatment. All the experiments were conducted in a randomized block design with three replicates. Based on the overall morphological characters, total stress response index (TSRI) was calculated which showed a variation ranging from 18 to 23. Accordingly, the varieties were classified into different groups of resistance. Varieties 'Moti' and 'Baismuthi' were found to be the least resistant, whereas 'Holpuna', 'Beto', and 'Soria Sali' were identified as most tolerant varieties to Al toxicity under P deficiency. The findings of the present investigation could be exploited for developing promising varieties in future rice breeding programs.

Keywords
aluminium toxicity; phosphorus deficiency; morpho-physiological parameters; *Oryza sativa* L.; total stress tolerance index

Introduction

Aluminum (Al) is one of the most abundant metals comprising approximately 7% in the Earth's crust. The chemical stability of Al depends upon the [illegible] soil. At a neutral pH, Al minerals exist in an almost insoluble state. However, in acidic conditions Al is oxidized to Al^{3+}, which is toxic to most of the cultivated crops including rice [1–3]. As such, Al^{3+} binds to soluble phosphorous (P), limiting the plant-available P. Therefore, the adverse effect of an acidic soil on plant growth is strongly related to both the toxicity of Al^{3+} and P deficiency.

C.T.C.
Principal
Nowgong Girls' College
Nagaon :: Assam

Nowgong Girls' College
ESTD 1962
Nagaon :: Assam

Very little free Al^{3+} in the soil solution causes damage to plant systems. Soluble forms of Al inhibit root growth as well as the development of root hairs. This results in poor nutrient uptake and assimilation and thereby leads to shoot nutrient deficiencies and a reduction of productivity [1,4]. This inhibition of root growth is one of the significant symptoms of Al toxicity, which occurs due to the interaction between Al^{3+} ions and root cells and their components [5–7].

Plants have a wide range of adaptability to tolerate the soluble form of Al^{3+}; some species can tolerate >1 mg L^{-1}, whereas most will show an adverse effect even at concentrations <0.5 mg L^{-1}. A large proportion of soil Al is locked up in soil minerals such as aluminosilicates, with much smaller fractions appearing in soluble forms that are capable of influencing biological systems [8].

Deficiency of P is one of the major limiting factors for rice growth and yield [9]. In upland conditions, P deficiency commonly occurs due to the strong binding affinity of P, which predominantly reacts with Al and iron (Fe) in acidic soils, whereas it reacts with calcium (Ca) in neutral to alkaline conditions and consequently forms partially soluble complexes [10]. As compared to other macronutrients, P is found to be one of the least mobile and available elements in the soil. Phosphorus in the soils occurring in both organic and inorganic forms and P availability is a prime limiting criterion for plant growth and development.

The alarming increase in human population demands the necessity to accelerate agricultural productivity. Hence, it is a challenge for the agricultural community to fulfil the increasing demands for future food supply across the globe. In this context, it is equally important to think about soil health status, which is being impacted due to various abiotic factors caused by climatic changes. Efforts are being made to understand the complex processes of agro-ecosystems and the various interactions governing the sustainability of agricultural lands [11]. However, it is becoming clear that conventional agricultural practices cannot sustain the production base to maintain a healthy plant/soil system indefinitely and, as such, augment crop productivity. Currently, agronomists depend heavily on chemical fertilizers. In this context, P is the next most limiting essential nutrient after nitrogen (N), restricting crop growth and productivity. In the global context of soil status, most tropical and subtropical soils are acidic in nature and are thus often P deficient [12].

Acid soils are a serious problem in Assam and most of the areas of Northeast India and Southeast Asia, including Myanmar, Bangladesh, and parts of China. The low pH of Assam soils adversely affects crop productivity, notably of rice [13]. As rice is widely cultivated in Assam, it is therefore imperative for plant biologists to identify promising rice varieties that can thrive under Al toxicity and P-deficient soil conditions. With this in mind, the present study was conducted to explore the potential of some traditional rice landraces from Assam and to identify tolerant varieties to be used in future rice breeding programs.

Material and methods

Plant material and growth conditions

Seeds of 41 traditional rice (*Oryza sativa* L.) varieties were collected from different agro-climatic zones of Assam, India. The collected rice samples with their vernacular names were: 'Baismuthi', 'Rupohi', 'Anjana', 'Kartik', 'Hung bora', 'Moti', 'Maguribao', 'Sokbonglong', 'Jahingia', 'Basful', 'Bejilahi', 'Adoliya', 'Sornosab', 'Kekuabao', 'Lucky', 'Batisali', 'Moinagiri', 'Boradhan', 'Bokulbora', 'Kolabora', 'Moinaxali', 'Guntibora', 'Chokuwa', 'Biyoisali', 'Soriasali', 'Kolajoha', 'Bhugpuri joha', 'Bor joha', 'Betguti', 'Lotasali', 'Malsora', 'Halda', 'Nalbora', 'Lauguti', 'Suwagmoni', 'Tilbora', 'Beto', 'Fulpakhri', 'Hoipuma', 'Nania', and 'Prasad bhog'.

Seeds were surface-sterilized with 0.1% $HgCl_2$ for 15 minutes and washed three four times with sterile distilled water to remove the residues of previous treatments. Germination was carried out on paper film and sterile moistened cotton in a growth chamber at 25–28°C for 72 h. Twenty seedlings of almost equal size were transplanted into transparent plastic vessels and allowed to grow in Hoagland's nutrient solution

C.T.C.
Principal
Nowgong Girls' College
Nagaon :: Assam

Nowgong Girls' College
Nagaon :: Assam

[14] in the growth chamber under white light with a photon flux density of 220 µmol $m^{-2} s^{-1}$ (PAR) over a 14-h photoperiod. The nutrient solution was replaced after 5 days. Nine-day old seedlings were subjected to a 500 µM $CaCl_2$ (pH 4.5) pretreatment for 24 h in order to maintain homeostasis, followed by treatment with $AlCl_3$ at different concentrations (0, 50, and 100 µM) for 24, 48, and 72 h in a modified Hoagland's solution where $NH_4H_2PO_4$ was replaced by NH_4Cl to maintain the P-deficient conditions. Plants grown in regular Hoagland's medium without P deficiency and Al stress were considered as the controls. Three biological replicates were maintained and cultures were placed in a randomized block design in the growth chamber.

Measurement of plant growth and biomass

Plant growth was measured in terms of shoot and root length, fresh weights, dry weights, relative water content (RWC), and chlorophyll content. For each treatment, three replicates consisting of 20 seedlings were considered, and from each replicate five plants were chosen randomly for the measurement of shoot and root lengths. Again, three plants from each replicate were randomly selected for measurement of fresh and dry biomass. Then shoot and root tissues were dried at 80°C for 48 h and weighed to obtain dry biomass.

To determine the relative water content (RWC), the fresh weight was initially measured, then the seedlings were placed in distilled H_2O for 4 h in diffuse light. When a shoot became fully turgid, it was reweighed. The dry weight was taken after drying for 72 h and the shoot RWC was then calculated [15].

Determination of chlorophyll concentration

For chlorophyll *a*, *b*, and total chlorophyll concentrations, fresh leaf samples of 300 mg were crushed in mortar and pestle with 5 mL of 80% acetone. The absorbance was measured at 663 nm and 645 nm using an UV-Vis spectrophotometer (Eppendorf Bio-Spectrophotometer Basic-603873) against 80% acetone as reference, and total chlorophyll was calculated by using a standard formula [15].

Determination of total stress response index

Total stress response index (TSRI) was calculated for the maximum stress duration (72 h) by using the established formula with modifications [16]. Calculation was carried out by dividing the average stress from the average control value for each variety at both Al concentrations (50 µM and 100 µM) for all the parameters determined individually. Summation of all the parameters was made to obtain the datasets for both Al concentrations. Finally, the mean tolerance values of both data sets were calculated to determine the TSRI. A dendrogram was generated by Ward's linkage method based on similarity in total tolerance indices.

Statistical analysis

As the experiments were conducted with a completely randomized design, summarized data were calculated as treatment means ±*SE* for three replicates. Pearson's correlation coefficient analysis was carried out using the MS Excel data set and statistical significance was considered at p values <0.05. Data were analyzed using the XLSTAT 2017 statistical package [17]. A cluster analysis of the 41 rice varieties was carried out based on the TSRI data.

C.T.C.
Principal
Nowgong Girls' College
Nagaon :: Assam

Nowgong Girls' College
ESTD: 1962
Nagaon :: Assam

Results

Morpho-physiological parameters under Al treatment and P deficiency

Shoot and root length. The growth of the rice seedlings in Hoagland's solution under Al treatment and P deficiency was measured in terms of shoot and root lengths and revealed that the growth of most of the varieties was impacted. The shoot length of all the 41 traditional rice varieties ranged from 15.9 to 46.1 cm at 50 µM Al and from 15.6 to 26.6 cm at 100 µM Al after 24 h of the stress treatment. Forty-eight h of stress resulted in a range of shoot lengths between 15.0 and 40.8 cm at 50 µM Al and between 15.8 and 25.1 cm in the 100 µM Al treatment. After 72 h at this Al concentration, a range of 15.1–23.6 cm at 50 µM Al and 15.2–26.4 cm was noted. Variety 'Suwagmoni' produced the maximum shoot length (46.1 cm), whereas 'Sokbonglong' showed the lowest (15.9 cm) at 50 µM Al. Variety 'Lauguti' emerged as most tolerant at 100 µM Al concentration after 24 h stress duration. However, after 48 h, 'Sokbonglong' had the lowest (15.0 cm) and 'Bhugpuri joha' the greatest (40.8 cm) shoot lengths. With 72 h Al exposure, 'Sokbonglong' showed the lowest (15.1 cm) and 'Maguri bao' the highest (23.6 cm) shoot lengths in the 50 µM Al treatment, whereas 'Sornosab' showed the lowest (15.2 cm) and 'Kartik' the highest (26.4 cm) shoot lengths at 100 µM Al (Fig. 1).

In the case of the roots, lengths ranged from 4.4–11.9 cm at 50 µM Al to 4.7–11.5 cm at 100 µM Al after 24 h. After 48 h, root lengths did not show marked differences at both the Al concentrations used. After 72 h, the root lengths ranged from 4.2 to 11.5 cm at 50 µM Al and from 4.3 to 11.1 cm at 100 µM Al. Variety 'Bhugpuri joha' showed the lowest (4.4 cm) and 'Moinagiri' was characterized by the highest (11.9 cm) root length at 50 µM Al. Varieties 'Kola joha' and 'Moinagiri' were the lowest (4.7 cm) and the highest (11.5 cm), respectively, at 100 µM Al after 24-h exposure. After 48 h, the lowest and highest root lengths at 50 µM Al were found in 'Bhugpuri joha' (4.4 cm) and 'Moinagiri' (11.9 cm), respectively, and at 100 µM Al in 'Sokbonglong' (4.3 cm) and 'Moinagiri' (11.5 cm), respectively. With an increased stress exposure time to 72 h, 'Sokbonglong' showed the lowest (11.5 cm) and 'Moinagiri' the highest (15.1 cm) root lengths at 50 µM Al, whilst at 100 µM Al, 'Sokbonglong' produced the lowest (4.3 cm) and 'Kartik' the highest (11.1 cm) root lengths (Fig. 2).

Root and shoot fresh weights. The root fresh weights ranged from 0.04 to 0.13 g at 50 µM Al and from 0.04 to 0.17 g at 100 µM Al after 24 h of exposure. After 48 h, they ranged from 0.05 to 0.13 g at 50 µM Al and from 0.05 to 0.14 g under 100 µM Al treatment, respectively. After 72 h, they ranged from 0.04 to 0.15 g at both Al concentrations used. After 24 h of treatment, 'Bhugpuri joha' showed the lowest root fresh weights (0.04 g) at both Al concentrations, whereas 'Bora dhan' showed the highest (0.12 g) root fresh weights at 50 µM Al and 'Baismuthi' emerged as tolerant at 100 µM Al (0.17 g). However, after 48 h of stress, 'Bhugpuri joha' had the lowest (0.05 g) and 'Bora dhan' the highest (0.13 g) root fresh weights at 50 µM Al and Fulpakhri the lowest (0.04 g) and 'Bora dhan' the highest (0.13 g) root fresh weights in 100 µM Al. After 72 h exposure, 'Bhugpuri joha' produced the lowest (0.04 g) and 'Rupohi' the highest (0.15 g) root biomass at 50 µM Al. Varieties 'Nalbora' and 'Basful' had the lowest (0.05 g) and the highest (0.15 g) root fresh weights, respectively, at 100 µM Al (Fig. 3).

The fresh weight of shoots ranged from 0.09–0.31 g at 50 µM Al to 0.18–0.31 g at 100 µM Al after 24 h. However, after 48 h they ranged between 0.16 and 0.30 g at 50 µM Al and between 0.18 and 0.38 g in the 100 µM Al treatment. After 72 h, a range of 0.15–0.29 g in 50 µM Al and 0.15–0.34 g in the 100 µM Al treatment was noted. Variety 'Kola bora' produced the lowest shoot fresh weights (0.09 g) at 50 µM Al and 'Kola joha' the lowest (0.18 g) at 100 µM Al. Variety 'Lauguti' showed the highest shoot fresh weights (0.31 g) in both the Al treatments after 24 h. However, after 48 h, 'Bhugpuri joha' showed the lowest (0.16 g) and 'Lauguti' the highest shoot fresh weights (0.30 g) in 50 µM Al. Simultaneously, 'Moti' produced the lowest (0.18 g) and Kowaisan the highest (0.30 g) shoot fresh weights at 100 µM Al. After 72 h of Al exposure, 'Bhugpuri joha' demonstrated the lowest shoot fresh weights (0.15 g) in both the Al treatments used and 'Adoliya' showed the highest (0.29 g) at 50 µM Al. 'Kartik' had the greatest shoot fresh weights (0.34 g) at 100 µM Al (Fig. 4).

C.T.C.
Principal
Nowgong Girls' College
Nagaon :: Assam

Nowgong Girls' College
Nagaon :: Assam
ESD: 1962

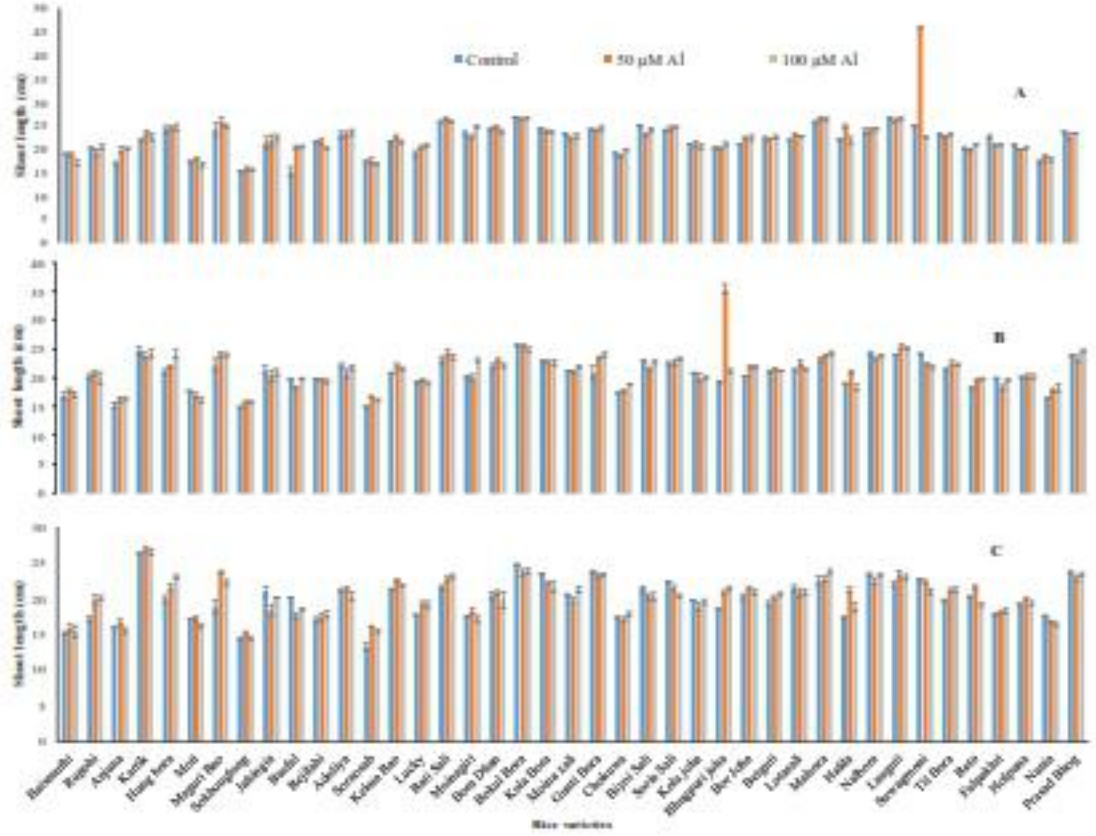

Fig. 1 The length of rice shoots under Al toxicity and P deficiency after 24 h (**A**), 48 h (**B**), and 72 h (**C**) of Al stress exposure (data presented as means ±*SE*, $n = 3$, where n indicates the number of replicates).

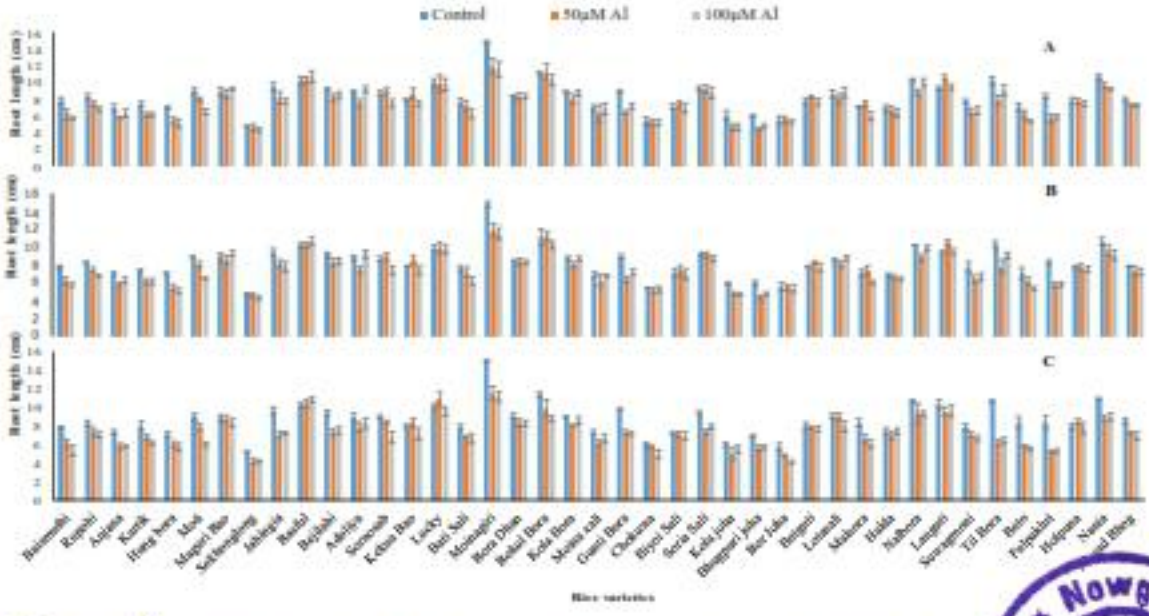

Fig. 2 The root lengths under Al toxicity and P deficiency after 24 h (**A**), 48 h (**B**), and 72 h (**C**) of Al stress exposure (data presented as means ±*SE*, $n = 3$, where n indicates the number of replicates).

Principal
Nowgong Girls' College
Nagaon :: Assam

Nowgong Girls' College
Nagaon :: Assam
ESTD: 1962

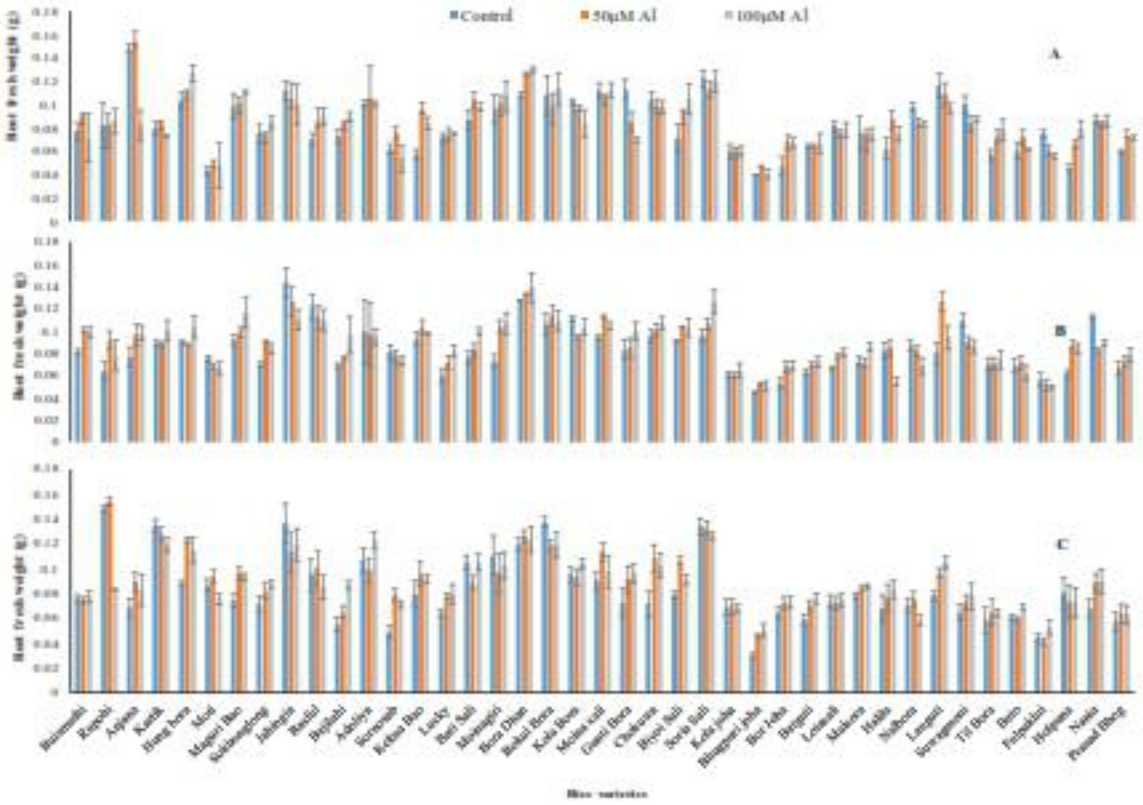

Fig. 3 The root fresh weights under Al toxicity and P deficiency after 24 h (**A**), 48 h (**B**), and 72 h (**C**) of Al stress exposure (data presented as means ±*SE*, $n = 3$, where n indicates the number of replicates).

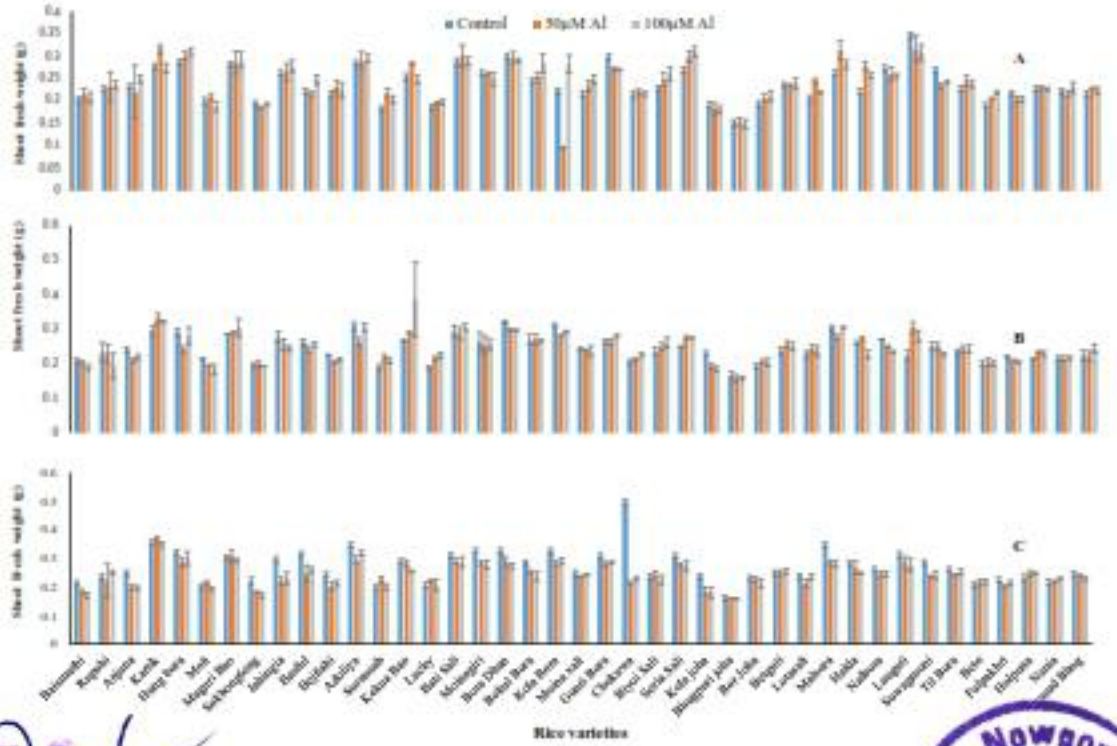

Fig. 4 The shoot fresh weights under Al toxicity and P deficiency after 24 h (**A**), 48 h (**B**), and [illegible] of Al stress exposure (data presented as means ±*SE*, $n = 3$, where n indicates the number of replicates).

Principal
Nowgong Girls' College
Nagaon :: Assam

Nowgong Girls' College
Nagaon :: Assam
ESTD: 1962

Root and shoot dry weights. Root dry weights ranged from 4 to 10 mg at 50 µM Al and from 3 to 17 mg at 100 µM Al after 24 h in the stress treatments. After 48 hours, the dry weights ranged from between 3 and 58 mg at 50 µM Al and between 3 and 50 mg at 100 µM Al and after 72 h, a range of 3–10 mg in 50 µM Al and 3–9 mg in the 100 µM Al concentrations were found. With all the times of stress duration, 'Bhugpuri joha' showed the lowest root dry weights (3 mg) at both the Al concentrations used. 'Bora dhan' had the highest root dry weights (10 mg) at 50 µM Al, whilst 'Rupohi' emerged as tolerant (17 mg) in 100 µM Al after 24 h. However, after 48 h, 'Baismuthi' revealed the highest root dry weights (50 mg) in both Al treatments. After 72 h, 'Bhugpuri joha' demonstrated the lowest (4 mg) and 'Rupohi' and 'Kartik' the highest (10 mg) root dry weights at 50 µM and 100 µM Al, respectively (Fig. 5).

After 24 h, the shoot dry weights ranged from 18 to 80 mg in the 50 and 100 µM Al treatments, respectively. After 48 h, they ranged from between 17 and 90 mg at 50 µM Al and between 10 and 70 mg at 100 µM Al. After 72 h, a range of 18–50 mg for 50 µM Al and 19–60 mg for 100 µM Al was noted. With 24-h treatment, varieties 'Lucky' and 'Bhugpuri joha' produced by the lowest shoot dry weights at 50 µM Al and 100 µM Al, respectively. 'Rupohi' was seen to have highest (80 mg) shoot dry weights. However, after 48 h, 'Bhugpuri joha' showed the lowest shoot dry weights (17 mg) at both Al concentrations and 'Anjana' the highest shoot fresh weights (90 mg) at 50 µM Al and 'Kartik' showed the highest shoot dry weights (70 mg) at 100 µM Al. Again, after 72-h stress treatment, 'Bhugpuri joha' showed the lowest shoot dry weights (18 mg) in both the Al concentrations and 'Rupohi' the highest shoot fresh weights (56 mg) at 50 µM Al. Variety 'Anjana' produced the highest shoot dry weights (60 mg) in 100 µM Al (Fig. 6).

Relative water content (RWC). To understand the effect of Al stress, relative water content (RWC) of the leaves was monitored in both control and treated plants. RWC showed significant differences in both the Al stress regimes. Varieties 'Jahingia' and 'Moti' showed higher RWCs at 24 h, 'Bati Sali' and 'Hung bora' at 48 h, and 'Betguti' and 'Bor joha' showed higher RWCs after 72 h. Varieties 'Nal bora' and 'Prasad bhog' showed the lowest RWCs at 24 h and 48 h, whereas at 72 h, a significant reduction in RWC was found in 'Anjana' at 50 µM Al and in 'Baismuthi' at 100 µM Al (Fig. 7).

Chlorophyll concentration. All the rice varieties tested revealed variations in total chlorophyll content in the Al-treated plants compared to the control. The total chlorophyll concentrations ranged from 5.2 to 23.3 mg mL^{-1} at 50 µM Al and from 3.9 to 21 mg mL^{-1} at 100 µM Al after 24 h. After 48 h of treatment, ranges of 3.9–11.8 mg mL^{-1} at 50 µM Al and 3.8–11.56 mg mL^{-1} at 100 µM Al were determined. After 72 h, the ranges were 5.8–12.1 mg mL^{-1} for 50 µM Al and 5.3–10.6 mg mL^{-1} for 100 µM Al. Among all the rice varieties, 'Anjana' showed a significantly highest total chlorophyll concentration, whereas 'Moti', 'Maguri bao', and 'Basful' showed lower chlorophyll concentrations over the respective time frames (Fig. 8).

Correlation between the different morpho-physiological parameters of rice grown under Al toxicity and P deficiency

Pearson's correlation coefficients for comparisons between different morphological and physiological parameters are tabulated in Tab. 1. These showed significant positive relationships between shoot fresh weight (SFW) and shoot length (SL) ($r = 0.64$) at 24 h of Al treatment, 0.55 at 48-h exposure, and 0.59 after 72 h. Shoot fresh weight showed significantly positive correlations with shoot length ($p < 0.05$) at all durations of treatment. Similarly, a significant positive was revealed between root fresh weight (RFW) and SFW, and shoot dry weight (SDW) and root dry weight (RDW) for all Al treatment durations. After 72-h treatment, other significant positive correlations were observed: RDW–SFW, RDW–RFW, and RDW–SDW.

C.T.C.
Principal
Nowgong Girls' College
Nagaon :: Assam

Nowgong Girls' College ★ Nagaon :: Assam ★ ESTD: 1962

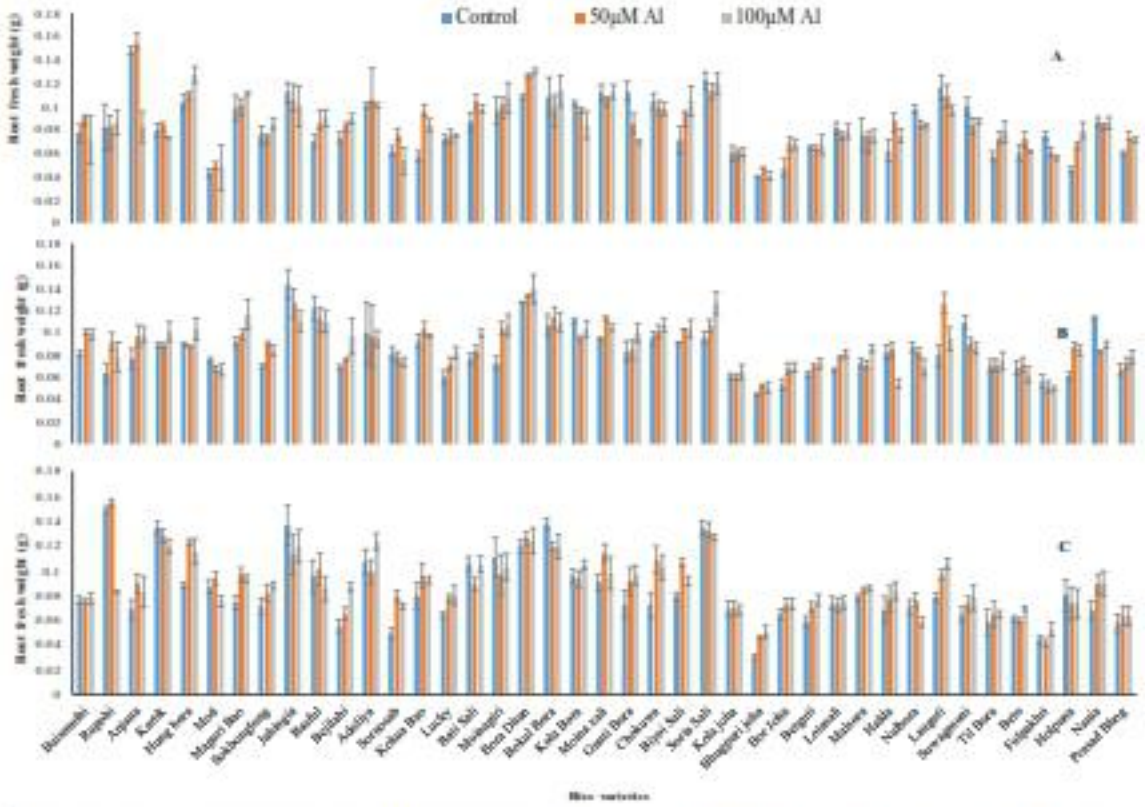

Fig. 5 The root dry weights under Al toxicity and P deficiency after 24 h (**A**), 48 h (**B**), and 72 h (**C**) of Al stress exposure (data presented as means ±*SE*, $n = 3$, where n indicates the number of replicates).

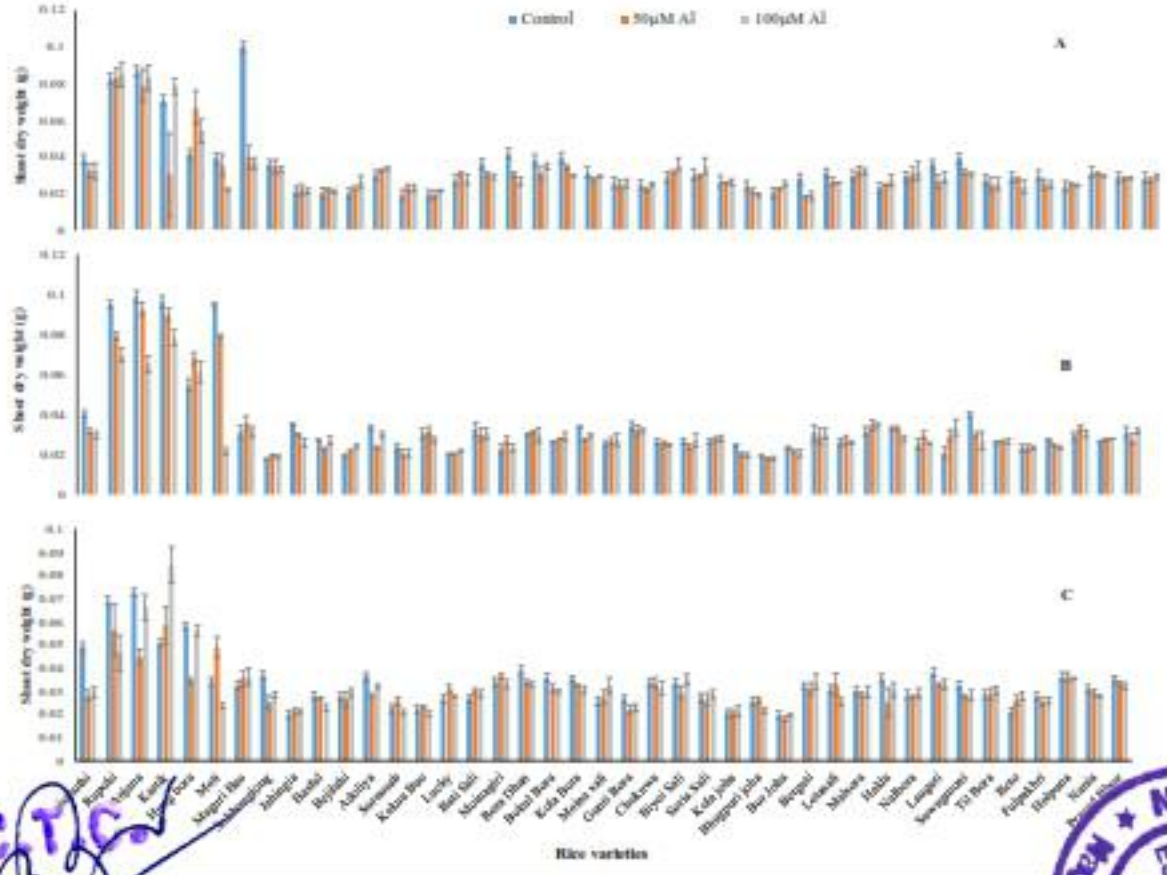

Fig. 6 The shoot dry weights under Al toxicity and P deficiency after 24 h (**A**), 48 h (**B**), and 72 h (**C**) of Al stress exposure (data presented as means ±*SE*, $n = 3$, where n indicates the number of replicates).

C.T.C.
Principal
Nowgong Girls' College
Nagaon :: Assam
Nowgong Girls' College ★ Nagaon :: Assam ★ ESTD: 1962

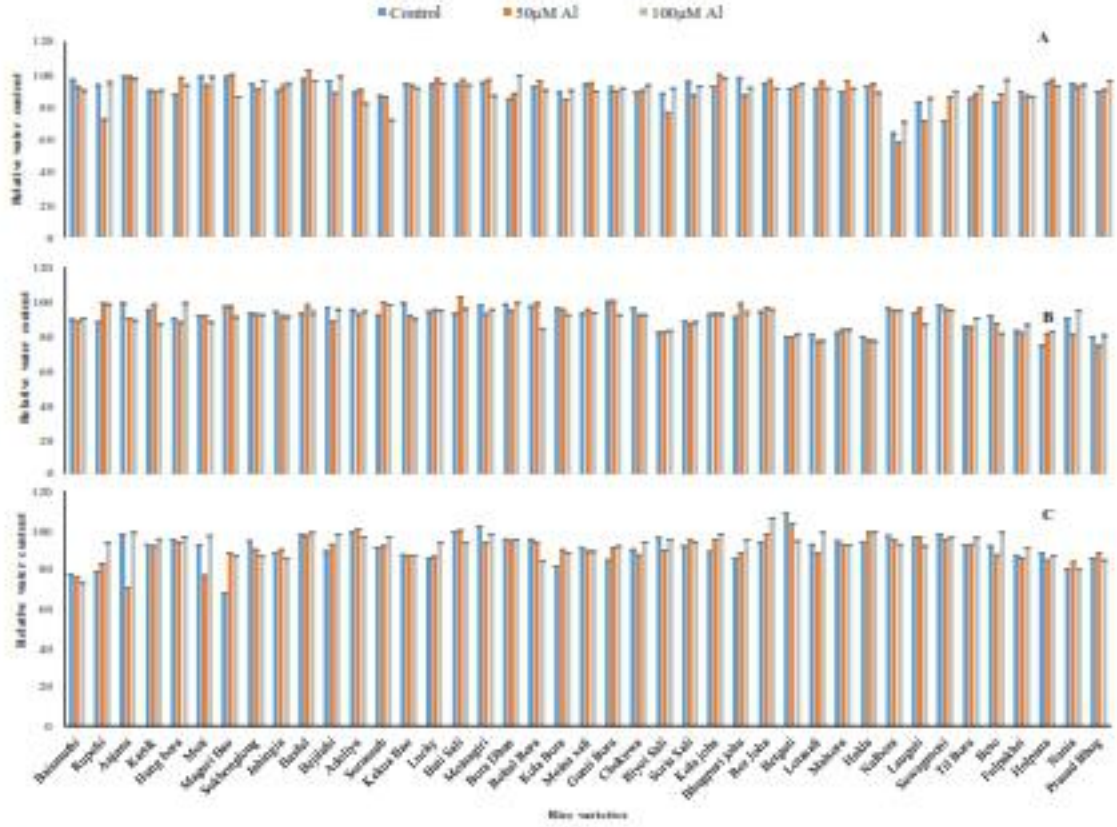

Fig. 7 Relative water content under Al toxicity and P deficiency after 24 h (**A**), 48 h (**B**), and 72 h (**C**) of Al stress exposure (data presented as means ±*SE*, $n = 3$, where n indicates the number of replicates).

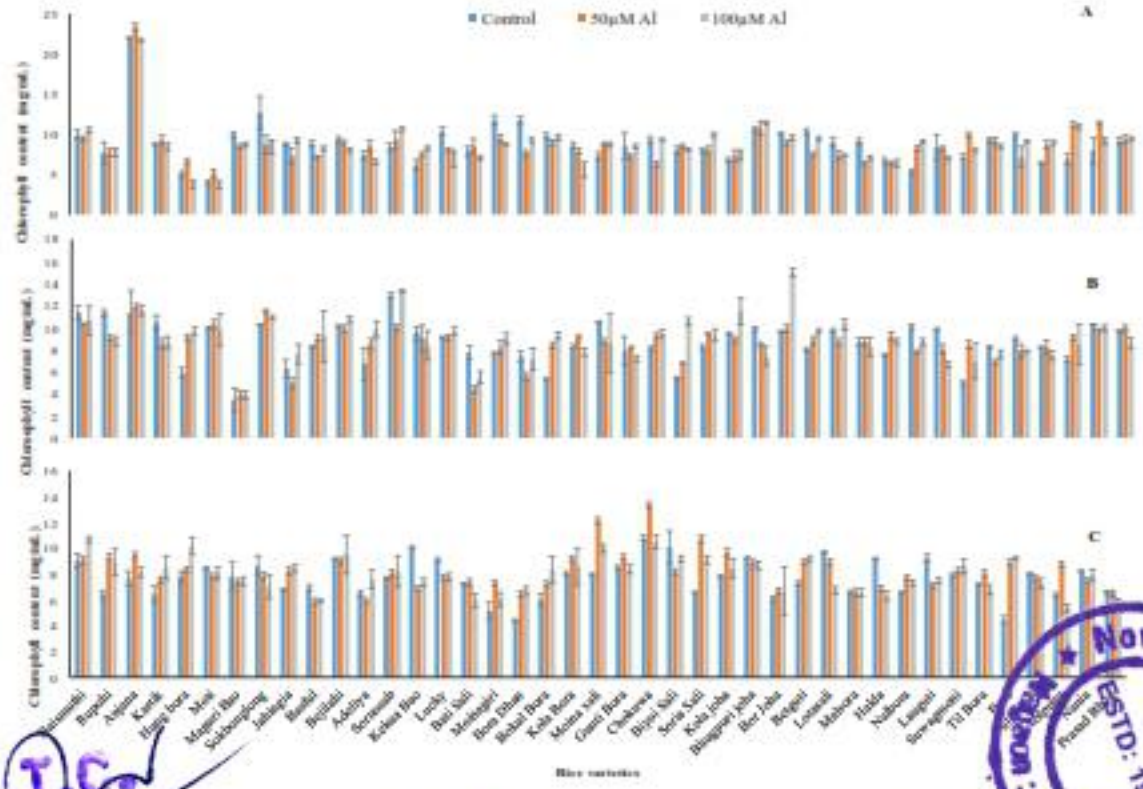

Fig. 8 Total chlorophyll concentration under Al toxicity and P deficiency after 24 h (**A**), 48 h (**B**), and [illegible] of treatment (data presented as means ±*SE*, $n = 3$, where n indicates the number of replicates).

C.T.C.
Principal
Nowgong Girls' College
Nagaon :: Assam
Nowgong Girls' College ESTD: 1962 Nagaon :: Assam

Tab. 1 Pearson's correlation coefficients for different morpho-physiological rice parameters after 24-h, 48-h, and 72-h Al treatment.

Parameters	SL	RL	SFW	RFW	SDW	RDW	CHL	RWC
24 h								
SL	1							
RL	0.213	1						
SFW	0.644*	0.335	1					
RFW	0.389	0.288	0.668*	1				
SDW	0.023	−0.089	0.314	0.397	1			
RDW	−0.169	−0.037	0.060	0.177	0.576*	1		
CHL	−0.218	−0.068	−0.150	0.265	0.412	0.136	1	
RWC	−0.316	−0.157	−0.215	−0.062	0.084	−0.013	0.201	1
48 h								
SL	1							
RL	0.189	1						
SFW	0.550*	0.336	1					
RFW	0.140	0.388	0.603*	1				
SDW	−0.075	−0.161	0.182	0.061	1			
RDW	−0.228	−0.097	−0.163	0.068	0.321	1		
CHL	−0.583	−0.232	−0.554	−0.367	0.144	0.209	1	
RWC	0.022	0.103	0.130	0.349	0.087	0.056	−0.049	1
72 h								
SL	1							
RL	0.143	1						
SFW	0.594*	0.284	1					
RFW	0.293	0.264	0.624*	1				
SDW	0.221	−0.021	0.371	0.502*	1			
RDW	0.244	0.220	0.555*	0.717*	0.737*	1		
CHL	−0.248	−0.377	−0.199	−0.057	−0.056	−0.226	1	
RWC	0.234	0.067	0.300	0.052	−0.140	−0.179	−0.293	1

Level of significance: * $p < 0.05$ (two-tailed). RL – root length; SL – shoot length; RFW – root fresh weight; RDW – root dry weight; SFW – shoot fresh weight; SDW – shoot dry weight; RWC – relative water content; CHL – chlorophyll concentration.

Total stress response index (TSRI)

All the morpho-physiological parameters were statistically analyzed and based on these results, TSRI was calculated which clearly illustrated the differences in plant resistance to Al toxicity under P deficiency between the rice varieties. Based on its TSRI value, variety 'Holpuna' could be identified as the most resistant, 'Soria Sali' and 'Beto' as moderately resistant, whilst 'Baismuthi' and 'Moti' are the most sensitive (Fig. 9). On the basis of the differences of all the TSRI values, the varieties can be classified into four groups: highly resistant (≥4.0), moderately resistant (3–4), susceptible (2–3), and highly susceptible (≤2.0) to Al toxicity under P deficiency.

Clustering based on morpho-physiological parameters of rice grown under Al toxicity and P deficiency

A dendrogram was constructed and a cluster analysis performed based on distance matrices which revealed two major clusters. Cluster I comprised 18 rice varieties and Cluster II 13 varieties. Additionally, Cluster I was further divided into two groups and

C.T.C.
Principal
Nowgong Girls' College
Nagaon :: Assam

Nowgong Girls' College ★ Nagaon ★ Assam ESTD 1962

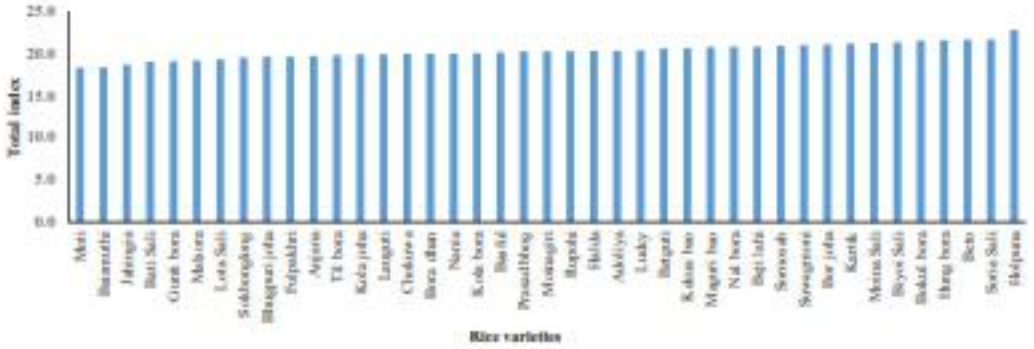

Fig. 9 Total stress response indices based on morpho-physiological parameters of different rice varieties grown under Al toxicity and P deficiency.

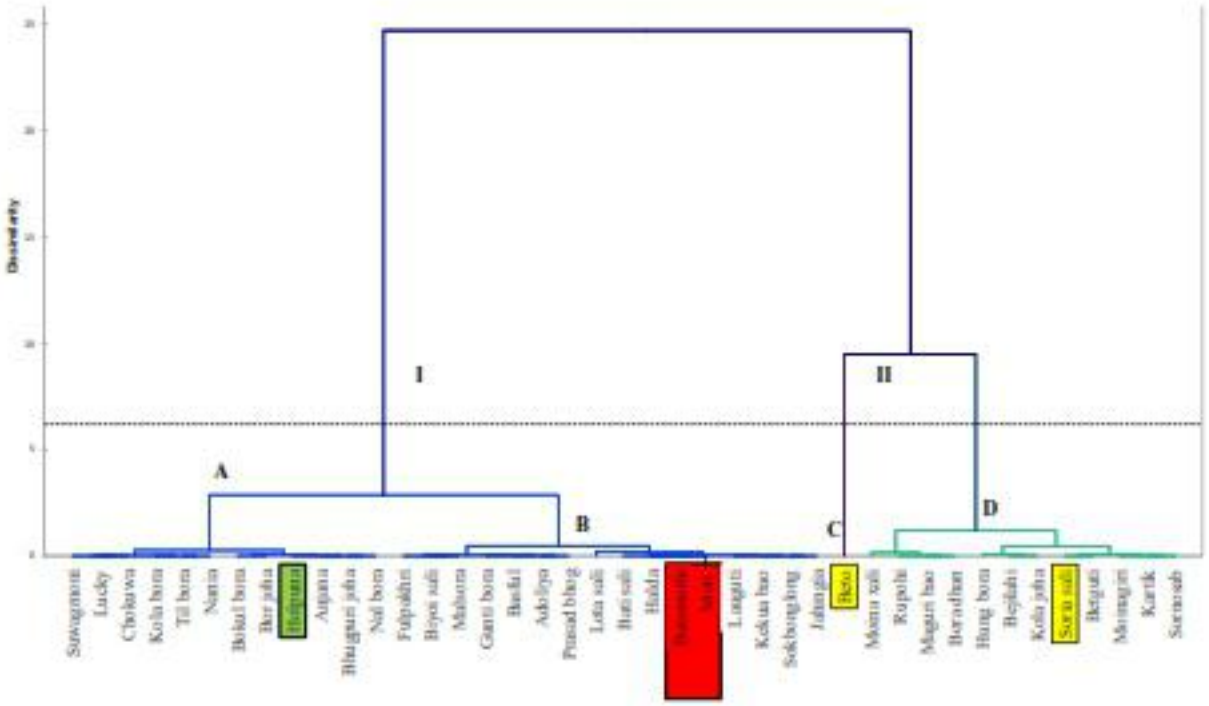

Fig. 10 Dendrogram showing a correlation cluster analysis of all the rice varieties based on the total stress response index.

Cluster II formed two major groups (C, D). Group D could be further divided into three subgroups. The selected susceptible varieties 'Moti' and 'Baismuthi' clustered together revealing their similarity in Al response. Varieties 'Soria sali' and 'Beto' clustered together again suggesting moderate similarity, whereas the highly tolerant 'Holpuna' emerged in a different cluster justifying our conclusions on the basis of morpho-physiological parameters under Al toxicity and P deficiency (Fig. 10).

Discussion

It has been demonstrated in previous works that P supply can ameliorate Al toxicity possibly through precipitation of Al in the rhizosphere. There arises a relative ranking of Al tolerance in plants and the probable cause is due to P and Al interactions which exist in acidic soils. Under P-limiting conditions, it was observed that P-efficient genotypes acquire more P from soils and transport more P to the root tips resulting in an increase in Al tolerance [18]. Adaptation to low-P acidic soils might involve a superior ability to tolerate Al and utilize organic P efficiently. Keeping this in mind,

C.T.C.
Principal
Nowgong Girls' College
Nagaon :: Assam

Nowgong Girls' College
ESTD 1962

the present experimental model was designed with modification in composition from the basal Hoagland's nutrient solution. It is necessary to lower the P concentration in the growth medium to enable a conclusive comment on the effect of the applied Al concentration. In Hoagland's medium, NH_4PO_4 is the P source and therefore, in our experimental growth medium, NH_4PO_4 was substituted by NH_4Cl to create P-deficient conditions [19].

Here, the tolerance to different concentrations of Al (50 µM or 100 µM) in the growth medium of the 41 rice cultivars collected from various agroclimatic zones of Assam, India was evaluated and the effect of Al^{3+} ions on different growth parameters was determined. Inhibition of root growth parameters such as root length and root fresh or dry weights was prominent in presence of the concentrations of Al employed in the growth medium. The roots showed the classical symptoms of Al toxicity, notably a reduction in root growth and the development of lateral roots. Stunted root growth was observed in almost all the experimental rice varieties under stress exposure and became more apparent with its duration. Root growth was reduced at both the Al concentrations and for all durations, and there was a distinct reduction at 100 µM Al for 72 h. This observed reduced root growth behavior was similar to earlier reports by other authors [20–22].

Severe reduction of fresh and dry weight and relative water content of roots and shoots were observed in the Al treatments. A decrease in RWC and chlorophyll content was also observed to some extent. The effect was generally greater at the higher concentration of Al (100 µM). These observations also agree with previous results of other researchers [23–27].

Determination of correlations between various morpho-physiological parameters of rice would be useful to select the best combinations of attributes for experimental rice varieties when screening their resistance to Al stress under P deficiency. Correlations between all the eight parameters measured here were calculated which showed significant interaction ($p < 0.05$) among the different traits. Shoot and root biomass were found to show a significant positive correlation in the presence of Al^{3+} ions in the growth medium.

Based upon our observations, we believe that the stress tolerance index can be considered as a suitable marker for screening of a large number of rice varieties to determine the tolerance to a particular environmental stress. In our experiment, this index was useful to differentiate all the screened rice varieties for their tolerance to Al stress and P-deficient conditions. This finding was also supported by the cluster analysis which was found to agree with earlier reports [16,28].

Conclusion

In this experiment, only a few rice varieties were found to show higher resistance than others when exposed to Al stress under P deficiency. Root fresh weight, dry weight, and relative water content were all significantly decreased in the sensitive varieties. The effect of Al^{3+} ions was mostly shown by varietes 'Baismuthi' and 'Moti'. Based on the studies of several parameters, it was shown that variety 'Holpuna' is a comparatively resistant variety, whereas 'Moti' is the most susceptible of the 41 cultivars screened. 'Holpuna' can therefore be recommended for Assam farmers. The screening approach we used has also paved a way for further selection of rice varieties which can be used to study the mechanism of enhanced Al tolerance under P deficiency. It can also be beneficial for breeding programs to produce resistant genotypes or to determine gene regulation patterns, and then for producing a genetically-engineered Al tolerant variety.

Principal
Nowgong Girls' College
Nagaon :: Assam

Nowgong Girls' College ★ Nagaon :: Assam ★ ESTD: 1962

Acknowledgments

The authors are thankful to the DST-FIST and UGC-SAP (DRS-I), Government of India for using the infrastructures in the Botany Department, Gauhati University, Assam, India.

References

1. Kochian LV, Piñeros MA, Liu J, Magalhaes JV. Plant adaptation to acid soils: the molecular basis for crop aluminum resistance. Annu Rev Plant Biol. 2015;66:571–598. https://doi.org/10.1146/annurev-arplant-043014-114822
2. Amonette JE, Russell CK, Carosino KA, Robinson NL, Ho JT. Toxicity of Al to *Desulfovibrio desulfuricans*. Appl Environ Microbiol. 2003;69:4057–4066. https://doi.org/10.1128/AEM.69.7.4057-4066.2003
3. Zhang J, Jia W, Yang J, Ismail AM. Role of ABA in integrating plant responses to drought and salt stresses. Field Crops Res. 2006;97(1):111–119. https://doi.org/10.1016/j.fcr.2005.08.018
4. Taylor GJ, McDonald-Stephens JL, Hunter DB, Bertsch PM, Elmore D, Rengel Z, et al. Direct measurement of aluminum uptake and distribution in single cells of *Chara corallina*. Plant Physiol. 2000;123:987–996. https://doi.org/10.1104/pp.123.3.987
5. Horst WJ, Wang Y, Eticha D. The role of the root apoplast in aluminium-induced inhibition of root elongation and in aluminium resistance of plants: a review. Ann Bot. 2010;106(1):185–197. https://doi.org/10.1093/aob/mcq053
6. Ma JF. Role of organic acids in detoxification of aluminum in higher plants. Plant Cell Physiol. 2000;41(4):383–390. https://doi.org/10.1093/pcp/41.4.383
7. Wang J, Raman H, Zhou M, Ryan PR, Delhaize E, Hebb DM, et al. High-resolution mapping of the *Alp* locus and identification of a candidate gene *HvMATE* controlling aluminium tolerance in barley (*Hordeum vulgare* L.). Theor Appl Genet. 2007;115(2):265–276. https://doi.org/10.1007/s00122-007-0562-9
8. Guodao YJLL. Research on soil acidification and acidic soil's melioration. Journal of South China University of Tropical Agriculture. 2006;1:001–004.
9. Cakmak I, Horst WJ. Effect of aluminium on net efflux of nitrate and potassium from root tips of soybean (*Glycine max* L.). J Plant Physiol. 1991;138(4):400–403. https://doi.org/10.1016/S0176-1617(11)80513-4
10. Holford ICR. Soil phosphorus: its measurement, and its uptake by plants. Soil Res. 1997;35(2):227–240. https://doi.org/10.1071/S96047
11. Pradhan AK, Shandilya ZM, Lahkar L, Hasnu S, Kalita J, Borgohain D, et al. Comparative metabolomics approach towards understanding chemical variation in rice under abiotic stress. In: Hasanuzzaman M, Fujita M, Nahar K, Biswas JK, editors. Advances in rice research for abiotic stress. Duxford: Woodhead Publishing; 2019. p. 537–550. https://doi.org/10.1016/B978-0-12-814332-2.00026-5
12. Gaume A, Mächler F, Frossard E. Aluminum resistance in two cultivars of *Zea mays* L.: root exudation of organic acids and influence of phosphorus nutrition. Plant Soil. 2001;234(1):73–81. https://doi.org/10.1023/A:1010535132296
13. Kalita J, Pradhan AK, Shandilya ZM, Tanti B. Arsenic stress responses and tolerance in rice: physiological, cellular and molecular approaches. Rice Sci. 2018;25(5):235–249. https://doi.org/10.1016/j.rsci.2018.06.007
14. Kapoor N, Pande V. Effect of salt stress on growth parameters, moisture content, relative water content and photosynthetic pigments of fenugreek variety RMt-1. Journal of Plant Sciences. 2015;10(6):210–221. https://doi.org/10.3923/jps.2015.210.221
15. Hoagland DR, Arnon DI. The water-culture method for growing plants without soil. Berkeley, CA: University of California; 1950. [Circular (California Agricultural Experiment Station); vol 347].
16. Singh B, Reddy KR, Redona ED, Walker, T. Screening of rice cultivars for morpho-physiological responses to early-season soil moisture stress. Rice Sci. 2017;24(6):322–335. https://doi.org/10.1016/j.rsci.2017.10.001
17. Lahkar L, Tanti B. Study of morphological diversity of traditional aromatic rice landraces (*Oryza sativa* L.) collected from Assam, India. Annals of Plant Science. 2017;6(12):1856–1861. https://doi.org/10.21746/aps.2017.6.12.9
18. Zheng SJ, Yang JL, He YF, Yu XH, Zhang L, You JF, et al. Immobilization of aluminum with phosphorus in roots is associated with high aluminum resistance in buckwheat. Plant Physiol. 2005;138:297–303. https://doi.org/10.1104/pp.105.059626

C.T.C.
Principal
Nowgong Girls' College
Nagaon :: Assam

Nowgong Girls' College ★ ESTD: 1962 ★ Nagaon :: Assam

19. Yu-Mei Du, Jiang Tian, Hong Liao, Chang-Jun Bai, Xiao-Long Yan, Guo-Dao Liu. Aluminium tolerance and high phosphorus efficiency helps *Stylosanthes* better adapt to low-P acid soils. Ann Bot. 2009;103:1239–1247. https://doi.org/10.1093/aob/mcp074

20. Hore P, Nahar S, Hasampura M, Tanti B. Phylogenetic analysis and homology modelling of betaine aldehyde dehydrogenase – an aroma producing protein in rice (*Oryza sativa* L.). International Journal of Multidisciplinary Approach and Studies. 2017;4(3):139–148.

21. Lahkar L, Tanti B. Morpho-physicochemical and cooking characteristics of traditional aromatic Joha rice (*Oryza sativa* L.) of Assam, India. Biocatal Agric Biotechnol. 2018;16:644–654. https://doi.org/10.1016/j.bcab.2018.10.001

22. Nahar S, Kalita J, Sahoo L, Tanti B. Morphophysiological and molecular effects of drought stress in rice. Annals of Plant Science. 2016;5(9):1409–1416. https://doi.org/10.21746/aps.2016.09.001

23. Nahar S, Vemireddy LR, Sahoo L, Tanti B. Antioxidant protection mechanisms reveal significant response in drought-induced oxidative stress in some traditional rice of Assam, India. Rice Sci. 2018;25(4):185–196. https://doi.org/10.1016/j.rsci.2018.06.002

24. Chutia J, Borah SP, Tanti B. Effect of drought stress on protein and proline metabolism in seven traditional rice (*Oryza sativa* L.) genotypes of Assam, India. Journal of Research in Biology. 2012;2(3):206–214.

25. Alvim MN, Ramos FT, Oliveira DC, Isaias RM, Franca MG. Aluminium localization and toxicity symptoms related to root growth inhibition in rice (*Oryza sativa* L.) seedlings. J Biosci. 2012;37(1):1079–1088. https://doi.org/10.1007/s12038-012-9275-6

26. Pandey P, Srivastava RK, Dubey RS. Salicylic acid alleviates aluminum toxicity in rice seedlings better than magnesium and calcium by reducing aluminum uptake, suppressing oxidative damage and increasing antioxidative defense. Ecotoxicology. 2013;22(4):656–670. https://doi.org/10.1007/s10646-013-1058-9

27. Awasthi, JP, Saha B, Regon P, Sahoo S, Chowra U, Pradhan A, et al. Morpho-physiological analysis of tolerance to aluminum toxicity in rice varieties of North East India. PloS One. 2017;12(4):e0176357. https://doi.org/10.1371/journal.pone.0176357

28. Nahar S, Sahoo L, Tanti B. Screening of drought tolerant rice through morpho-physiological and biochemical approaches. Biocatal Agric Biotechnol. 2018;15:150–159. https://doi.org/10.1016/j.bcab.2018.06.002

Selekcja tradycyjnych odmian ryżu w celu oszacowania ich potencjalnej odporności na toksyczność glinu (Al) w warunkach niedoboru fosforu

Streszczenie

Gleby kwaśne zajmują prawie jedną trzecią dostępnych gleb uprawnych na świecie. Gleba kwaśna stanowi jedno z głównych ograniczeń abiotycznych dla praktyk rolniczych, które wywołuje toksyczność glinu (Al) i niedobór fosforu (P). Assam jest rolniczym regionem Indii, a na większości obszaru występują gleby kwaśne. Zakwaszenie gleby zwiększa rozpuszczalność obecnego w glebie Al z jego nietoksycznych form krzemianowych lub tlenków w wysoce fitotoksyczne formy jonowe (głównie trójwartościowy jon Al^{3+}). Jonowa forma Al tworzy ponadto kompleksy z dostępnym fosforem, co prowadzi do niedoborów niezbędnych składników mineralnych dla roślin. W prezentowanych badaniach przeprowadzono selekcję tradycyjnych odmian ryżu z rejonu Assam pod kątem ich tolerancji na toksyczność Al i niedobór P. Czterdzieści jeden lokalnych odmian ryżu pochodzących z różnych lokalizacji agroklimatycznych poddano działaniu trzech różnych stężeń Al (0, 50, 100 μM) przez 24, 48 lub 72 godziny w warunkach niedoboru P, aby określić zakres ich odporności na tego typu warunki stresowe. Po oddziaływaniu stresu oceniono różne parametry morfofizjologiczne roślin, tj. długość korzenia i pędu, świeżą i suchą masę, zawartość chlorofilu i względną zawartość wody (RWC). Wszystkie eksperymenty przeprowadzono w układzie zrandomizowanym blokowym z trzema powtórzeniami. W oparciu o ogólne cechy morfologiczne roślin obliczono wskaźnik całkowitej reakcji na stres (TSRI), który wahał się w zakresie od 18,2 do 22,73. Stosownie do jego wartości odmiany zostały zaklasyfikowane do różnych grup odporności. Odmiany 'Moti' i 'Baismuthi' okazały się najmniej odporne, podczas gdy 'Holpuna', 'Beto' i 'Soria' zostały zidentyfikowane jako odmiany najbardziej odporne na toksyczność Al w warunkach niedoboru P. Wyniki przeprowadzonych badań można wykorzystać do opracowania obiecujących odmian w przyszłych programach hodowli ryżu.

C.T.C.
Principal
Nowgong Girls' College
Nagaon :: Assam

Nowgong Girls' College ★ ESTD: 1962 ★ Nagaon :: Assam

Polyhedron 159 (2019) 192–205

Contents lists available at ScienceDirect

Polyhedron

journal homepage: www.elsevier.com/locate/poly

A chitosan supported peroxidovanadium(V) complex: Synthesis, characterization and application as an eco-compatible heterogeneous catalyst for selective sulfoxidation in water

Gangutri Saikia, Kabirun Ahmed, Sandhya Rani Gogoi, Mitu Sharma, Hiya Talukdar, Nashreen S. Islam *

Department of Chemical Sciences, Tezpur University, Tezpur 784028, Assam, India

ARTICLE INFO

Article history:
Received 14 September 2018
Accepted 8 November 2018
Available online 29 November 2018

Keywords:
Peroxidovanadium(V) complex
Chitosan immobilized vanadium(V)
Heterogeneous catalysis
Green oxidation catalyst
Aqueous sulfide oxidation

ABSTRACT

Anchoring of peroxidovanadium(V) (pV) species to chitosan, a natural chelating polymer, afforded a new and structurally defined immobilized complex, $VO(O_2)_2(NH_2)$-chitosan (**ChpV**) which was comprehensively characterized by elemental analysis (CHN, ICP-OES, energy dispersive X-ray spectroscopy), spectral studies (FT-IR, Raman, ^{13}C NMR, diffuse reflectance UV–Vis and XPS), SEM, XRD, Brunauer–Emmett–Teller (BET) and thermogravimetric analysis (TGA). Apart from being thermally stable, the compound is water-tolerant and non-hygroscopic. The compound effectively facilitated chemoselective oxidation of thioethers with H_2O_2 in aqueous medium to the respective high purity sulfoxide, in impressive yield (TOF 5628 h^{-1}) and with high H_2O_2 efficiency, under mild reaction condition. In addition to water, the heterogeneous catalyst is highly compatible in a variety of organic solvents and is recyclable for several catalytic cycles without significant loss in selectivity. The catalytic procedure is amenable to ready scalability and is free from halogen, co-catalyst and acidic or any other hazardous additive.

© 2018 Elsevier Ltd. All rights reserved.

1. Introduction

Currently, with an ever increasing emphasis on the development of cleaner and sustainable chemical processes, efforts towards heterogenization of homogenous catalysts by immobilization of active transition metal complexes on insoluble polymer supports appear to have intensified. Various advantages associated with such systems, including their enhanced stability, specific site selectivity, ease of handling of toxic materials, facile separation and recovery of the catalysts etc., ultimately contributes toward enhancing the overall sustainability of a chemical transformation by minimizing its environmental impact [1].

Apart from cross-linked synthetic organic polymers, natural materials, *viz.* cellulose, chitin and chitosan, are receiving tremendous contemporary interest as potential polymer supports for immobilization and heterogenization of metal catalysts [1e,2]. Chitosan, the copolymer of 2-amino-2-deoxy-D-glucopyranose and 2-acetamido-2-deoxy-D-glucopyranose, [3] with amino and hydroxyl groups in its structure, exhibits an enormous ability to form metal complexes and has been extensively used in the extraction of metallic ions from wastewater [4]. Moreover, owing to its attractive physical and mechanical properties, chitosan is also becoming increasingly relevant in a wide variety of applications, including biomedical products [4b,c,5], cosmetics [4b,6], food processing [4b,c,7] etc. Some of the unique features of chitosan and its derivatives which boost their applicability as green supports for heterogenization of metal complexes [2b,3b,4d,8] include: (i) biocompatibility and biodegradability, (ii) non-toxicity, (iii) low cost and eco-friendly, (iv) high metal dispersion on the surface of chitosan, (v) high thermal stability and durability, (vi) physical and chemical versatility, and (vii) insolubility in organic solvents [1e,2b,3b,4d,8]. Several studies have demonstrated chitosan-metal complexes as catalysts in wide range of organic transformations, including C—C bond formation reactions [1e,4d], hydration [1e,4d,9], polymerization [1e], water splitting reactions [9] etc. Nevertheless, reports dealing with the application of chitosan immobilized metal complexes as heterogeneous catalysts in the field of organic oxidation appear to be still scarce [10–12].

It is pertinent to mention here that our group has developed in recent years a series of novel polymer immobilized peroxidometal complexes using d^0 metal ions belonging to group 5 and 6, *viz.* vanadium [13], niobium [14], molybdenum [15] and tungsten [15c,16], which display excellent activity in a variety of organic oxidations, including phenol hydroxylation [13a], oxidative bromination [13b,c,16a] and sulfide oxidation [14,15a,16b,c],

* Corresponding author at: Dept. of Chemical Sciences, Tezpur University, Napaam, Tezpur 784028, Assam, India. Fax: +91 3712 267006.
E-mail address: nsi@tezu.ernet.in (N.S. Islam).

https://doi.org/10.1016/j.poly.2018.11.028
0277-5387/© 2018 Elsevier Ltd. All rights reserved.

Nowgong Girls' College ESTD. 1962 Nagaon Assam

Principal
Nowgong Girls' College
Nagaon :: Assam

Dalton Transactions

PAPER

View Article Online
View Journal | View Issue

Check for updates

Cite this: Dalton Trans., 2019, 48, 4857

Mononuclear lanthanide complexes assembled from a tridentate NNO donor ligand: design of a Dy^{III} single-ion magnet†

Pankaj Kalita,[a] Amit Malakar,[a,d] Joydeb Goura,[a,c] Subhashree Nayak,[a] Juan Manuel Herrera,[b] Enrique Colacio *[b] and Vadapalli Chandrasekhar *[a,c,d]

Received 1st February 2019,
Accepted 8th March 2019

DOI: 10.1039/c9dt00504h

rsc.li/dalton

The reaction of a tridentate NNO donor ligand, 4-nitro-2-((2-(pyridine-2-yl)hydrazono)methyl)phenol (HL) with lanthanide(III) nitrates in the presence of triethylamine afforded a new family of neutral mononuclear Ln^{III} complexes $[Ln(NO_3)(L)_2(HOCH_3)]$ (Ln = Gd; (**1**) Tb; (**2**), Dy; (**3**), and Ho (**4**). The mononuclear complexes were structurally characterized by single crystal X-ray diffraction studies which revealed a spherical tricapped trigonal prism geometry with a *pseudo* D_{3h} symmetry around the Ln^{III} centre. Static (dc) and dynamic (ac) magnetic studies have been performed on these complexes. Field-induced single-ion magnet behaviour was observed in the Dy^{III} analogue with an effective energy barrier and an pre-exponential factor of Δ/k_B = 68(2) K and $\tau_0 = 1.8 \times 10^{-7}$ s, respectively.

Introduction

The observation of single-molecule magnet (SMM) behaviour in the lanthanide bis-phthalocyanine double-decker complexes, $[LnPc_2]^-$ (Ln = Dy^{III} and Tb^{III}; Pc = phthalocyanine)[1] has spurred interest in utilizing complexes containing 4f metal ions in molecular magnets.[2] A deeper analysis of the role of 4f metal ions in the field of molecular magnetism has revealed that the inherent unquenched spin-orbital angular momentum present in lanthanide ions can allow, particularly, ions such as Dy^{III}, Tb^{III}, Er^{III} and Ho^{III} to have large magnetic anisotropy, an important criterion in promoting SMM behaviour.[3] Although crystal field effects are dominated by spin–orbit coupling in lanthanide complexes the former play a crucial and important role in perturbing the energy levels in the resultant complexes as shown by Ishikawa in his pioneering work and as subsequently analysed by others.[3b,4]

A seminal insight was provided by Long and co-workers who argued that the oblate electron density around Dy^{III} and Tb^{III} would need an axial crystal field to harness and maximize the magnetic anisotropy while Er^{III} and Ho^{III} having a prolate electron density would need an equatorial crystal field.[5] A further qualitative analysis revealing that complexes possessing high axial symmetries such as $C_{\infty v}$, D_{4h}, S_{8}, D_{5h}, D_{6h}, and D_{8h} etc. would be good candidates as molecular magnets has allowed rational design to take precedence over serendipity in preparing potential SMMs.[3c,6] These developments have led to a spurt in the growth of mononuclear lanthanide complexes with an aim to achieve high blocking temperatures (T_B) and high energies of barrier (U_{eff}) for magnetization reversal. Recent reports on mononuclear Ln^{III} complexes show that large energy barriers for magnetization reversal and high blocking temperatures can be achieved by employing strong axial ligand fields with the Ising-type anisotropic lanthanides such as Dy^{III}.[7] Till date, the mononuclear dysprosium complex, $[(Cp^{ttt})Dy(Cp^*)][B(C_6F_5)_4]$ has the highest blocking temperature of 80 K, among all other reported lanthanide based single-molecule magnets.[8] Also there are some interesting reports on air-stable mononuclear lanthanide-based single molecule magnets having high energy barriers of magnetization reversal.[9] These recent advancements have triggered a fresh interest in utilizing the 4f-ions in molecular magnetism.

We have been utilizing polydentate ligands for preparation of hetero- (3d/4f) and homometallic lanthanide complexes as molecular magnets.[10] In the latter we were able to tune the nuclearity of complexes from the lowest possible to a highest of 21.[11] Recently, utilizing a rigid ligand that enforces an equatorial geometry we prepared a heptacoordinate lanthanide

[a]School of Chemical Sciences, National Institute of Science Education and Research Bhubaneswar, HBNI, Jatni, Khurda – 752050, Odisha, India. E-mail: pankajkalita14@niser.ac.in, amitchem.27@gmail.com, joydebgoura@gmail.com, subhashree.nayak@niser.ac.in
[b]Departamento de Química Inorgánica, Facultad de Ciencias, Universidad de Granada, Avenida de Fuentenueva s/n, 18071 Granada, Spain. E-mail: ecolacio@ugr.es, jmherrera@ugr.es
[c]Department of Chemistry, Indian Institute of Technology Kanpur, Kanpur-208016, India. E-mail: vc@iitk.ac.in, vc@iitk.res.in
[d]Tata Institute of Fundamental Research Hyderabad, Gopanpally, Hyderabad-500107, India

†Electronic supplementary information (ESI) available: CCDC 1891541, 1891542, 1891553 and 1891560. For ESI and crystallographic data in CIF or other electronic format see DOI: 10.1039/c9dt00504h

Principal
Nowgong Girls' College
Nagaon :: Assam

Pankaj Kalita

Nowgong Girls' College ★ Nagaon :: Assam ★ ESTD: 1962

Accepted Manuscript

Kinetics of inactivation of peroxidase and polyphenol oxidase in tender coconut water by dielectric barrier discharge plasma

Hemanta Chutia, Dipankar Kalita, Charu Lata Mahanta, Namita Ojah, Arup Jyoti Choudhury

PII: S0023-6438(18)31032-6

DOI: https://doi.org/10.1016/j.lwt.2018.11.071

Reference: YFSTL 7635

To appear in: *LWT - Food Science and Technology*

Received Date: 10 October 2018

Revised Date: 21 November 2018

Accepted Date: 22 November 2018

Please cite this article as: Chutia, H., Kalita, D., Mahanta, C.L., Ojah, N., Choudhury, A.J., Kinetics of inactivation of peroxidase and polyphenol oxidase in tender coconut water by dielectric barrier discharge plasma, *LWT - Food Science and Technology* (2018), doi: https://doi.org/10.1016/j.lwt.2018.11.071.

This is a PDF file of an unedited manuscript that has been accepted for publication. As a service to our customers we are providing this early version of the manuscript. The manuscript will undergo copyediting, typesetting, and review of the resulting proof before it is published in its final form. Please note that during the production process errors may be discovered which could affect the content, and all legal disclaimers that apply to the journal pertain.

Principal
Nowgong Girls' College
Nagaon :: Assam

Nowgong Girls' College ★ ESTD: 1962 ★ Nagaon :: Assam

ACCEPTED MANUSCRIPT

Kinetics of inactivation of peroxidase and polyphenol oxidase in tender coconut water by dielectric barrier discharge plasma

Hemanta Chutia[1], Dipankar Kalita[1], Charu Lata Mahanta[1*], Namita Ojah[2], Arup Jyoti Choudhury[2]

Running title: Effect of cold plasma on tender coconut water

[1] Department of Food Engineering & Technology, Tezpur University, Tezpur, Assam, India

[2] Department of Physics, Tezpur University, Tezpur University, Tezpur, Assam, India

[*]Corresponding author: Tel: +91-3712-275702, Fax: +91-3712-267005

Email address: charu@tezu.ernet.in

ABSTRACT

The spoilage enzymes in tender coconut water were inactivated by atmospheric cold plasma technology. The kinetics of peroxidase (POD) and polyphenol oxidase (PPO) inactivation was studied at voltage levels varying between 18 and 28 kV dielectric barrier discharge plasma treatments (DBD) at atmospheric air. The time of treatment and applied voltage were significant factors for inactivation of the enzymes. POD was more resistant than PPO. The experimentally observed data were fitted to establish different kinetics models and model parameters were evaluated. The sigmoidal logistic was the best fitting model to explain the kinetics of browning enzymes inactivation based on high RMSE values. The time required for half maximal activity values for POD was 0.84, 1.67 and 2.53 min at 18 kV, 23 kV and 28 kV, respectively which was higher than PPO with half maximal activity values of 0.67, 1.18 and 1.35 min, respectively. This indicates that POD is more resistant to cold plasma than PPO and its inactivation in tender coconut water by cold plasma can be considered as a [illegible]

CTC
Principal
Nowgong Girls' College
Nagaon :: Assam

Nowgong Girls' College ★ ESTD: 1962 ★ Nagaon :: Assam

quality parameter. DBD generated cold plasma can therefore be used to process fruits and vegetables juices where in enzymes activity is one of the quality deterioration parameters.

Keywords: Cold plasma, peroxidase, polyphenol oxidase, tender coconut water, inactivation model

1. Introduction

Tender coconut *(Cocos nucifera L.)* water is a widely consumed refreshing beverage. Its unique flavour and presence of all essential nutrients makes it very popular among consumers (Mahnot et al., 2014). The beverage is useful for health and medicinal purposes due to its significant antioxidant, anti-ageing, anti-carcinogenic, anti-thrombotic effects and balanced electrolytes (Jean et al., 2009).

Among the various intrinsic enzymes, POD and PPO being more stable are more responsible for spoilage through biochemical reactions and are taken as indicators of effectiveness of thermal processing (Matsui et al., 2007; Robinson, 1991). These enzymes are known to adversely change the sensory, nutritional and textural properties (Matsui et al., 2007; Misra et al., 2016). PPO is responsible for browning and discoloration (McEvily et al., 1992), whilst POD catalyses peroxidation reaction wherein the generated end products give off-flavour in food products (Pankaj et al., 2013).

Heat treatment is conventionally used for inactivation of the enzymes (Anthon & Barrett, 2002); however adversely affects sensory and nutritional qualities of food products. Researchers are therefore, interested in novel nonthermal technologies for enzyme inactivation like high pressure processing (Bermejo-Prada at al., 2014), gamma irradiation (Jha et al., 2013), pulsed electric fields (Samaranayake & Sastry, 2016), ultraviolet light (Augusto et al., 2015) and sonication (Cao et al., 2018). Many of these non thermal technologies are complex, expensive and difficult for commercial scaling up (Pankaj et al., 2013).

Principal
Nowgong Girls' College
Nagaon :: Assam

Nowgong Girls' College ★ Nagaon :: Assam ★ ESTD: 1962

ACCEPTED MANUSCRIPT

Cold plasma is a nonconventional technology found to be effective for decontaminating foods. Surowsky et al. (2014) inactivated *Citrobacter freundii* in apple juice using cold plasma and found that Weibull model was not good for low amount of *Citrobacter freundii*. Cold plasma was found to stabilise wheat germ by inactivating lipase and lipoxygenase which is desirable for extending the shelf life (Tolouie et al., 2018). Pankaj et al. (2013) reported the effects of cold plasma from DBD to inactivate tomato POD and also studied the kinetics of tomato POD inactivation at different voltages (30, 40 and 50 kV) for different time intervals (15 s to 5 min). The authors found logistic model to properly describe tomato POD inactivation. Up to 45% reduction in PPO activity as compared to the control in cold plasma treated fresh cut samples (Tappi et al., 2014) and up to 17% reduction in POD in cold plasma treated fresh cut melon (Tappi et al., 2016) have been reported. Vukic et al. (2017) studied the color changes of orange and carrot juice blend due to atmospheric air DBD plasma treatment and they reported that the DBD reduces cloud loss and can cause minor degradation of color attributes. Segat et al. (2016) reported that dielectric barrier discharge-atmospheric cold plasma treatment at high voltages (40, 50 and 60 kV) for durations ranging between 15 s and 5 min had significantly inactivated alkaline phosphatase enzyme and the enzyme inactivation kinetics was best described by Weibull method.

The effects as well as the kinetics of PPO and POD activity in tender coconut water using DBD at cold atmospheric pressure and modelling of the inactivation have not been reported. This study was undertaken (i) to investigate the parameters involved in the inactivation of POD and PPO in tender coconut water, (ii) to model kinetics of enzymes activity, and (iii) to compare the kinetics of activity of POD and PPO.

2. Materials and methods

2.1. Materials

CSTC
Principal
Nowgong Girls' College
Nagaon :: Assam

Nowgong Girls' College ★ Nagaon :: Assam ★ ESTD: 1962

ACCEPTED MANUSCRIPT

Fresh tender coconut (*Cocos nucifera L.*) was harvested from plants grown in a nearby area of Tezpur University, Assam, India. Tender coconut water had a pH of 5.20 ± 0.2, (pH meter model PB 11, Sartorius), and soluble solids content of 3.95 ± 0.25 °Brix (refractometer model Erma, Tokyo, Japan).

2.2. Preparation of sample

The water from the coconut was collected following the method of Mahnot et al, (2014) with slight modification. Two days before processing, formaldehyde and potassium chromate were used to clean the working area to prevent contamination of coconut water. The nuts were thoroughly rinsed with tap water and sanitized by dipping in 300 mg/l sodium hypochlorite solution. The processing equipment were sterilized in an autoclave before use.

2.3. Cold plasma treatment

In the experimental setup as shown in Fig. 1, the DBD plasma system comprised of two square copper plate electrodes, with an area of 225 cm^2 and thickness of 5 mm and was covered with glass dielectric plate (2 mm thickness). A high voltage power supply (0-50 kV, 50 Hz, Zenoics Systech, India) gave power to the upper electrode and the lower electrode was grounded. An uncovered Petri plate (90 mm diameter) containing coconut water (15 ml per plate) was placed between the two dielectric plates with a gap of 15 mm. Stable and uniform air plasma discharge was obtained across the discharge gap at atmospheric pressure (1 bar) and at different applied voltages (Break down voltage for the current set-up was above 12 kV) of 18 kV, 23 kV and 28 kV. All treatment processes were carried out at relative humidity (RH) of 58% and temperature of 27°C using a humidity-temperature probe (Testo 176T2, UK).

2.4. Enzyme activity and inactivation kinetics

Principal
Nowgong Girls' College
Nagaon :: Assam

Nowgong Girls' College
ESTD: 1962
Nagaon :: Assam

POD and PPO activities were measured using the modified spectrophotometric method described by Purkayastha et al. (2012). Inactivation kinetics of POD and PPO reported by Pankaj et al. (2013) was followed.

2.5. Statistical analysis

The data obtained were statistically analysed by ANOVA test in SPSS 24.0 (SPPS Inc., Chicago, IL, USA). The model parameters for all equations were estimated by non-linear least squares regression using Microsoft Excel Solver (Microsoft office, USA). The goodness of fit was determined from adjusted coefficient of determination, R^2 (adj) and the adequacy of the model fittings was indicated by root mean squared error (RMSE). Higher R^2_{adj} value and lower RMSE value indicated that the model was best fitted.

3. Results and Discussion

3.1. Effect of treatment time and voltage on activity of POD and PPO

Significant reduction in enzyme activity after treatment with DBD plasma was observed (P<0.05). A rise in temperature by 5°C only was recorded by infrared thermometer (Maplin Electronics, UK) in all the experiments. It was observed that temperature required for inactivation of enzymes was not reached. Both treatment times and voltage significantly reduced the activity of POD and PPO ($P \leq 0.05$). All three applied voltages showed significant difference in residual activity ($P \leq 0.05$). Also, voltage was found to significantly ($P \leq 0.05$) interact with time.

3.2. First order kinetics model

Kp, the inactivation rate constant for first order kinetic model of POD and PPO was calculated from the slope of the lines. The values of Kp and R^2 for the kinetic model at the different voltage levels studied are given in Table 1. Even though the R^2 values were quite high (0.8[illegible] 0.99[illegible] for both enzymes, satisfactory RMSE values were not obtained, being in the range of 2.7[illegible] 8.61 for POD and 2.81 to 8.59 for PPO. Therefore, the residual activity of

Principal
Nowgong Girls' College
Nagaon :: Assam

Nowgong Girls' College
Nagaon :: Assam
ESTD: 1962

both PPO and POD was not satisfactorily described by the first-order model as can be seen from Figs. 2a and 2b for POD and PPO, respectively. This may be due to the complex structure of the enzyme and difference in the mechanism of disruption of a single bond or structure (Pankaj et al., 2013). The proposed first-order kinetics model in the inactivation of enzymes appeared to be exceedingly simple. However, this model showed that inactivation kinetics of PPO was slightly higher as compared to POD.

3.3. Weibull distribution model

Experimental data were taken to determine scale parameter (α) and shape parameter (Y) of the Weibull model. The values of α and Y along with R^2 values for POD and PPO are summarised in Table 1. Weibull model could strongly predict residual activity for both POD and PPO after DBD plasma treatments as seen from the high R^2 value ($R^2 \geq 0.99$) obtained for the different voltage levels taken for study.

The scale parameter for POD ranged from 1.18 to 2.22 and for PPO it ranged from 0.76 to 1.95. Voltage levels inversely influenced the activity of the enzymes as lower applied voltage level showed higher scale parameter. The shape parameter for both POD and PPO ranged from 0.79 to 1.43 and 0.73 to 1.35, respectively. Figs. 3a and 3b show the fitted curves of the Weibull model for POD and PPO, respectively at different voltage levels. The figures revealed tailing effect at 23 kV treatment voltage that could not be accounted for by Weibull fit. The higher RMSE value at 23 kV treatment voltage as given in Table 1(4.55 and 6.29 for POD and PPO, respectively) also suggested the inadequacy of Weibull model. Even though $R^2 \geq 0.99$, the RMSE values were higher especially for 23 kV indicating that Weibull distribution model was not sufficient.

3.4. Logistic Model

The curves for both POD and PPO inactivation that were fitted using logistic model are shown in Figs. 4a and 4b, respectively. From the R^2 values, it can be said that this model

Principal
Nowgong Girls' College
Nagaon :: Assam

Nowgong Girls' College
ESTD: 1962
Nagaon :: Assam

147 explained ≥ 99 % of the variability in residual activity of the enzymes. Tailing effect for POD
148 and PPO for 18 kV treatments was explained by the A^a_{min} values (6.39 ± 0.56 for POD and
149 8.06±0.99 for PPO). The t^a_{50} values for both POD and POD indicated the rapid inactivation
150 for both POD and PPO at 28 kV compared to 23 kV and 18 kV treatments. The R^2 values
151 were very high (≥ 0.99). RMSE values for both enzymes were very low ranging from 0.6 to
152 0.99 for POD and 0.2 to 1.02 for PPO. Thus, it can be inferred that the POD inactivation was
153 sigmoidal, which was adequately supported by the logistic type model. Table 1 also shows
154 that at same voltage and time treatments, the t^a_{50} values for POD were 0.84, 1.67 and 2.53
155 min which were higher than PPO showing values of 0.67, 1.18 and 1.35 min at 18 kV, 23 kV
156 and 28 kV respectively. The values indicate that POD is more stable than PPO in terms of
157 cold plasma treatment. Surowsky et al. (2013) also reported that cold plasma is effective in
158 reducing the activity of both PPO and POD in a model food system. There was 90%
159 reduction in PPO activity after cold plasma treatment for 180 s and 85% reduction of POD
160 activity after 240 s of treatment. There is no reported study on effects of cold plasma from
161 DBD on the activity of enzymes in tender coconut, mainly POD and PPO.

162 Inactivation by cold plasma can be attributed to the reaction between plasma
163 generated reactive species and chemically reactive side-chain of the amino acids in the
164 enzyme (Pankaj et al. 2013; Surowsky et al., 2013; Takai et al., 2012;). Superoxide anion
165 radicals, hydroxyl radicals, hydrogen peroxide radicals and oxide of nitrogen are the well
166 known reactive species and the reactive amino acid side chains are cysteine, aromatic rings of
167 phenylalanine, tyrosine, and tryptophan and their reaction causes modifications in the
168 secondary structure of the proteins (Attri & Venkatesu, 2017; Pankaj et al. 2013; Surowsky et
169 al., 2013; Takai et al., 2012). Segat et al. (2016) also observed that the inactivation of alkaline
170 phosphatase enzyme was attributed to the loss of α- helical and β-sheet secondary structures

Principal
Nowgong Girls' College
Nagaon :: Assam

Nowgong Girls' College
ESTD: 1962
Nagaon :: Assam

of the proteins. The decomposition of bonds in protein (C–H, C–N and N–H) may also cause enzyme inactivation (Hayashi et al. 2009).

4. Conclusion

This study for the first time reports the effect of atmospheric cold plasma from DBD on POD and PPO activity in tender coconut water. POD and PPO inactivation increased with voltage and time of plasma treatment and POD was more resistant than PPO. Logistic model best described the inactivation of both enzymes. Further, voltage and time were noted to be important parameters that influenced the rate of inactivation and determined the shape of enzyme inactivation curve. These results indicated that cold plasma has the ability to inactivate enzymes in addition to microbial inactivation that has been widely reported. Further work can be done to study the mechanism of enzyme inactivation by cold plasma.

ACKNOWLEDGMENTS

The authors thank DST-FIST and AICTE-NEQIP for providing instrument facility for the work.

DECLARATION OF CONFLICTING INTERESTS

The authors have no conflict of interest to declare.

References

Anthon, G. E., & Barrett, D. M. (2002). Kinetic parameters for the thermal inactivation of quality-related enzymes in carrots and potatoes. *Journal of Agricultural and Food Chemistry*, 50(14), 4119–4125.

Attri, P., Venkatesu, P., Kaushik, N., Han, Y., Nam, C., Choi, E., & Kim, K. (2012). Effects of atmospheric-pressure non-thermal plasma jets on enzyme solutions. Journal of the Korean Physical Society, 60, 959-964.

Principal
Nowgong Girls' College
Nagaon :: Assam

Nowgong Girls' College
ESTD: 1962
Nagaon :: Assam

Augusto, P. E., Ibarz, R., Garvín, A., & Ibarz, A. (2015). Peroxidase (POD) and polyphenol oxidase (PPO) photo-inactivation in a coconut water model solution using ultraviolet (UV). *Food Research International*, 74, 151-159.

Bermejo-Prada, A., Van Buggenhout, S., Otero, L., Houben, K., Van Loey, A., & Hendrickx, M. E. (2014). Kinetics of thermal and high-pressure inactivation of avocado polygalacturonase. *Innovative Food Science & Emerging Technologies*, 26, 51-58.

Cao, X., Cai, C., Wang, Y., & Zheng, X. (2018). The inactivation kinetics of polyphenol oxidase and peroxidase in bayberry juice during thermal and ultrasound treatments. *Innovative Food Science & Emerging Technologies*, 45, 169-178

Hayashi, N., Kawaguchi, R., & Liu, H. (2009). Treatment of protein using oxygen plasma produced by RF discharge. *Journal of Plasma and Fusion Research Series*, 8, 552–555.

Jean, W. H., Yong, L. G., Yan F. N., & Swee, N.T. (2009). Review: The Chemical Composition and Biological Properties of Coconut *(Cocos nucifera L)* Water. *Journal of Molecules*, 14, 5144-5164.

Jha, P. K., Kudachikar, V. B., & Kumar, S. (2013). Lipase inactivation in wheat germ by gamma irradiation. *Radiation Physics and Chemistry*, 86, 136-139.

Mahnot, N. K., Kalita, D., Mahanta, C. L., & Chaudhuri, M.K. (2014). Effect of additives on the quality of tender coconut water processed by nonthermal two stage microfiltration technique. *LWT - Food Science and Technology*, 59, 1191-1195.

Matsui, K. N., Granado, L. M., Oliveirac, P. V., & Tadini, C. C. (2007). Peroxidase and polyphenol oxidase thermal inactivation by microwaves in green coconut water simulated solutions. *LWT- Food Science and Technology*, 40, 852–859.

C.T.C.
Principal
Nowgong Girls' College
Nagaon :: Assam

Nowgong Girls' College
ESTD: 1962
Nagaon :: Assam

ACCEPTED MANUSCRIPT

McEvily, A. J., Iyengar, R., & Otwell, W. S. (1992). Review: Inhibition of enzymatic browning in foods and beverages. *Critical Reviews in Food Science and Nutrition*, 32(3), 253–273.

Misra, N. N., Pankaj, S.K., Segat, A., & Ishikawa, K. (2016). Review: Cold plasma interactions with enzymes in foods and model systems. *Trends in Food Science & Technology*, 55, 39-47.

Pankaj, S.K.,Misra, N.N., and Cullen, P.J. (2013). Kinetics of tomato peroxidase inactivation by atmospheric pressure cold plasma based on dielectric barrier discharge. *Innovative Food Science and Emerging Technologies*, 19,153–157.

Purkayastha, M. D., Kalita, D., Mahnot, N. K., Mahanta, C. L., Mandal, M., & Chaudhuri,M.K. (2012). Effect of L-ascorbic acid addition on the quality attributes of micro-filtered coconut water stored at 4 °C. *Innovative Food Science and Emerging Technologies*, 16, 69–79.

Robinson, D. S. (1991). Peroxidases and catalases in foods. In D. S. Robinson, & N. A. M. Eskin (Eds.), Oxidative enzymes in foods. New York: *Elsevier Applied Science*, (pp. 1–45).

Samaranayake, C. P., & Sastry, S. K. (2016). Effect of moderate electric fields on inactivation kinetics of pectin methylesterase in tomatoes: The roles of electric field strength and temperature. *Journal of Food Engineering*, 186, 17-26.

Segat, A., Misra, N. N., Cullen, P. J., & Innocente, N. (2016). Effect of atmospheric pressure cold plasma (ACP) on activity and structure of alkaline phosphatase. Food and Bioproducts Processing, 98, 181-188.

Surowsky, B., Fischer, A., Schlueter, O., & Knorr, D. (2013). Cold plasma effects on enzyme activity in a model food system. Innovative Food Science & Emerging Technologies, 19, 146-152.

C.T.C.
Principal
Nowgong Girls' College
Nagaon :: Assam

Nowgong Girls' College
ESTD: 1962
Nagaon :: Assam

Surowsky, B., Fröhling, A., Gottschalk, N., Schlüter, O., & Knorr, D. (2014). Impact of cold plasma on Citrobacter freundii in apple juice: Inactivation kinetics and mechanisms. *International Journal of Food Microbiology*, 174, 63–71.

Takai, E., Kitano, K., Kuwabara, J., & Shiraki, K. (2012). Protein Inactivation by Low temperature atmospheric pressure plasma in aqueous solution. *Plasma Processes and Polymers*, 9(1), 77–82.

Tappi, S., Berardinelli, A., Ragni, L., Dalla Rosa, M., Guarnieri, A., & Rocculi, P. (2014).Atmospheric gas plasma treatment of fresh-cut apples.Innovative Food Science & EmergingTechnologies, 21, 114-122.

Tappi, S., Gozzi, G., Vannini, L., Berardinelli, A., Romani, S., Ragni, L., & Rocculi, P. (2016). Cold plasma treatment for fresh-cut melon stabilization. Innovative Food Science & Emerging Technologies, 33, 225-233.

Tolouie,H., Amin, M., Ghomi, M.H., Yaghoubi,A.S., Hashemi, M. (2018).The impact of atmospheric cold plasma treatment on inactivation of lipase and lipoxygenase of wheat germs. Innovative Food Science & Emerging Technologies, 47, 346-352.

Vukic, M., Vujadinovic, D., Lvanovic, M.,Gojkovic, V.& Grujic, R. (2017). Color change of orange and carrot juice blend treated by non-thermal atmospheric plasma. *Food Processing and Preservation*. 10.1111/jfpp.1352

Figure legends

Fig. 1. Schematic of the experimental setup for DBD plasma system.

Fig 2. First order model curve fitting at different voltage levels for residual activity of (a) POD and (b) PPO.

Fig 3. Weibull model curve fitting at different voltage levels for residual activity of (a) POD and (b) PPO.

Principal
Nowgong Girls' College
Nagaon :: Assam

Nowgong Girls' College
ESTD: 1962
Nagaon :: Assam

ACCEPTED MANUSCRIPT

Fig 4. Logistic model curve fitting at different voltage levels for residual activity of (a) POD and (b) PPO.

ACCEPTED MANUSCRIPT

Principal
Nowgong Girls' College
Nagaon :: Assam

Nowgong Girls' College
ESTD: 1962
Nagaon :: Assam

ACCEPTED MANUSCRIPT

Table1

Results on the parameters of the models fitted to inactivation kinetics of PPO and POD enzymes

Model	Parameters	POD			PPO		
		18 kV	23 kV	28 kV	18 kV	23 kV	28 kV
First Order	K_F (Min)	0.49±0.06	0.57±0.05	0.73± 0.07	0.59± 0.08	0.73±0.06	1.01±.05
	R^2	0.93	0.95	0.99	0.93	0.96	0.99
	RMSE	8.61	6.79	2.7	7.72	8.59	2.81
Weibull	α (min)^a	2.22±0.06	1.84±.05	1.18 ± 0.03	1.95±0.05	1.46±0.02	0.76±0.03
	Y^a	1.43±0.2	1.17±0.16	0.79±0.008	1.35±0.13	1.19±0.09	0.73±0.06
	R^2	0.99	0.99	0.99	0.99	0.99	0.99
	RMSE	2.87	4.55	1.95	2.99	6.29	1.38
Logistic	A^a_{min}	6.39±0.56	11.02±.99	6.82±0.89	8.06±0.99	5.67±0.89	2.63±0.51
	t^a_{50}	2.53±0.02	1.67±0.03	0.84±0.05	1.35±0.023	1.18±0.016	0.67±0.09
	P^a	1.59±0.09	2.85±0.16	2.07± 0.3	2.78±0.56	3.24±0.15	2.02±0.21
	R^2	0.99	0.99	0.99	0.99	0.99	0.99
	RMSE	0.08	0.01	0.95	1.02	0.08	0.02

R^2 = regression coefficient; a = value ± standard error

ACCEPTED MANUSCRIPT

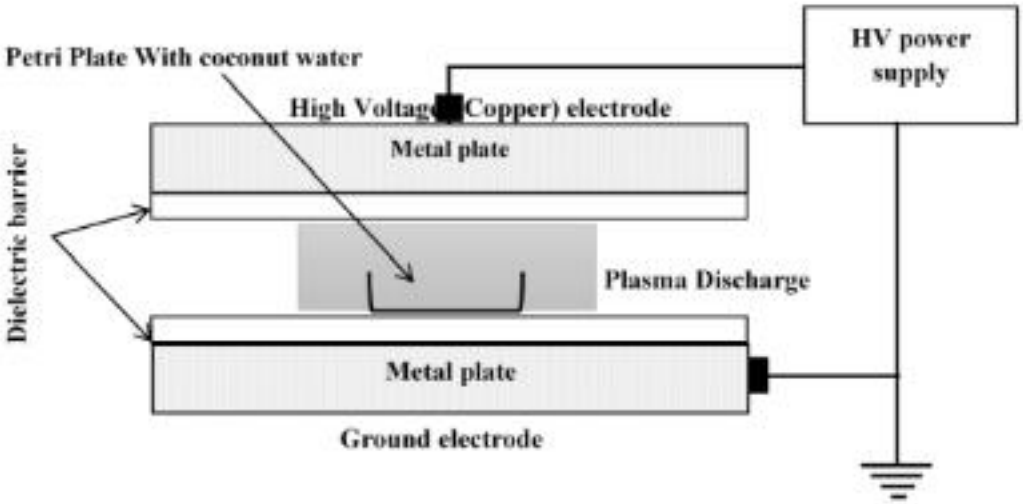

Fig. 1.

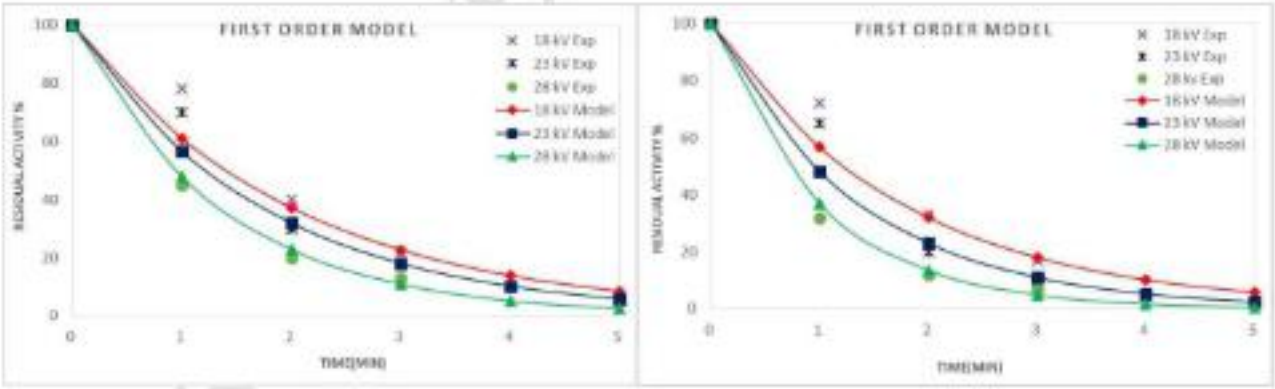

(a) (b)

Fig 2.

Principal
Nowgong Girls' College
Nagaon :: Assam

Nowgong Girls' College
ESTD: 1962
Nagaon :: Assam

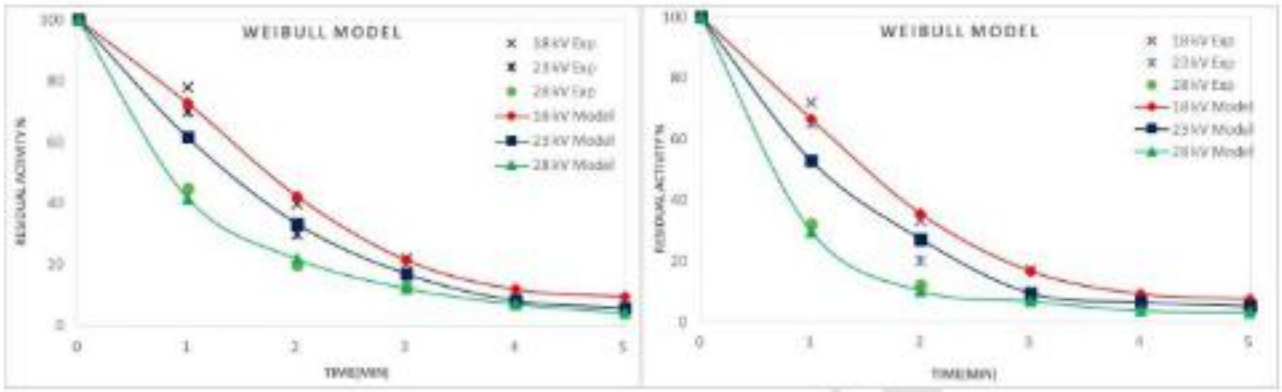

(a) (b)

Fig 3.

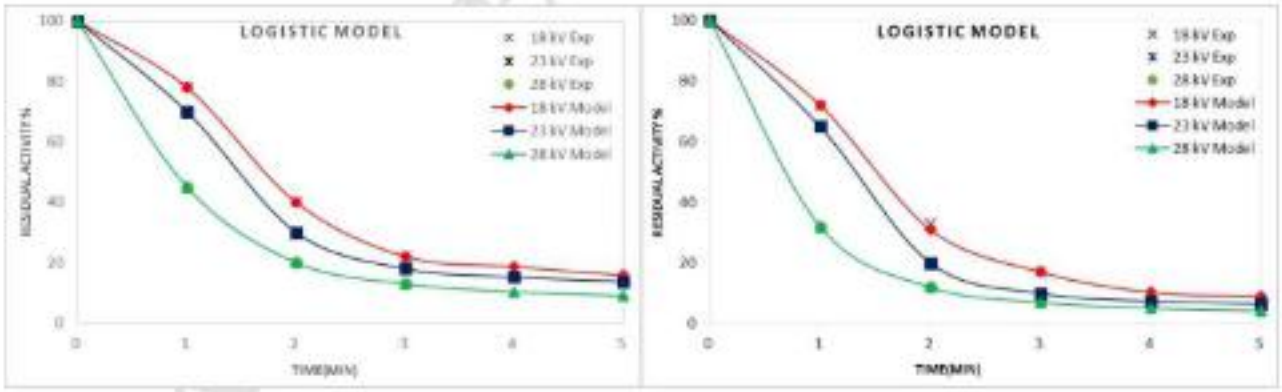

(a) (b)

Fig 4.

Principal
Nowgong Girls' College
Nagaon :: Assam

Nowgong Girls' College
ESTD: 1962
Nagaon :: Assam

- DBD cold plasma used to inactivate POD and PPO in tender coconut water
- Treatment time and applied voltage showed significant inactivation
- POD was more resistant than PPO to DBD cold plasma
- Sigmoidal shaped Logistic model adequately described the enzymes inhibition
- DBD cold plasma can be used as a quality indicator for enzymatically spoiled foods

ACCEPTED MANUSCRIPT

Principal
Nowgong Girls' College
Nagaon :: Assam

Nowgong Girls' College
ESTD: 1962
Nagaon :: Assam

Applied Surface Science 475 (2019) 219–229

Contents lists available at ScienceDirect

Applied Surface Science

journal homepage: www.elsevier.com/locate/apsusc

Full Length Article

Surface modification of core-shell silk/PVA nanofibers by oxygen dielectric barrier discharge plasma: Studies of physico-chemical properties and drug release behavior

Namita Ojah[a], Diana Saikia[a], Dolly Gogoi[b], Pitambar Baishya[c], Gazi Ameen Ahmed[a], Anand Ramteke[c], Arup Jyoti Choudhury[a,*]

[a] Laboratory for Plasma Processing of Materials, Department of Physics, Tezpur University, Tezpur 784028, Assam, India
[b] Central Instrument Facility, Indian Institute of Technology, Guwahati 781039, Assam, India
[c] Department of Molecular Biology and Biotechnology, Tezpur University, Tezpur 784028, Assam, India

ARTICLE INFO

Keywords:
Bombyx mori silk fibroin
Core-shell nanofibers
Dielectric barrier discharge plasma
Surface modification
Mechanical properties
Drug delivery

ABSTRACT

Bombyx mori silk fibroin (BMSF), a natural protein polymer, has increasingly gained research interest as promising biomaterial in drug delivery application due to its excellent biological and physiochemical properties. In this study, antibiotic loaded silk/PVA core-shell nanofibers has been prepared followed by surface modification using homogeneous oxygen (O_2) dielectric barrier discharge (DBD) plasma at atmospheric pressure. Polyvinyl alcohol (PVA) is used as the shell material whereas amoxicillin trihydrate is loaded into the silk solution (AMOX-BMSF) and the mixture is used as core material for fabricating core-shell nanofibers. O_2 DBD plasma treatment induces surface hydrophilicity in AMOX-BMSF/PVA nanofibers due to incorporation of polar functional groups onto the surface as revealed from X-ray photoelectron spectroscopy (XPS) analyses. The O_2 DBD plasma treatment facilitates formation of hydrogen bonds on the surface of the nanofibers resulting in better mechanical behavior of the nanofibers. The DBD plasma treated nanofibers show relatively faster biphasic drug profile than the untreated nanofibers with prolonged antibacterial activities against Gram-negative *Escherichia coli* and Gram-positive *Staphylococcus aureus* bacteria. The results demonstrate that O_2 DBD plasma surface modified AMOX-BMSF/PVA nanofibers can be explored as mechanically enhanced wound dressing in treatment of skin and wound infections.

1. Introduction

Controlled release systems for drug delivery have emerged as promising approach for applications in biotechnology, medicine and modern healthcare [1,2]. Significant research interest has been focussed on design and development of these drug delivery systems into drug-loaded wound dressings [3–5]. These wound dressings can accelerate the wound healing process by delivering the drug directly to the targeted site, thereby improving bioavailability and maintenance of drug concentration within the therapeutic window [6,7]. The major advantage of local drug delivery is its ability to achieve maximum and sustained local concentrations of drug without large systemic doses, thus minimizing systemic toxicity [7]. Drug loaded wound dressings have been developed from both natural and synthetic polymers and successfully used in skin wound healing. Among various available drug-loaded wound dressings, core-shell polymeric nanofibers with excellent drug release behavior are considered as promising materials due to their high mechanical strength and drug-encapsulation efficiency, good pH and thermoresponsive behaviors, ability to reduce the burst release and maintain sustain release of drug thereby preventing bacterial contamination to the infected site or a prolong period of time and promote rapid wound healing [8–10].

Core-shell nanofibers are prepared by coaxial electrospinning technique in which two different polymer solutions are spanned simultaneously [8]. The major advantage of coaxial electrospinning is its ability to use an electrospinnable polymer as a carrier (shell) to produce nanofibers with core material comprising either non-electrospinnable polymer or material of low molecular weight such as drugs or a mixture of both [8,10]. The shell protects the drug from sudden and uncontrolled burst release and with proper selection of shell material and/or its thickness it is possible to control the release rate thereby facilitating sustained release of drug to the targeted site till the wound

* Corresponding author.
E-mail address: arupjchoudhury@gmail.com (A.J. Choudhury).

https://doi.org/10.1016/j.apsusc.2018.12.270
Received 5 September 2018; Received in revised form 6 December 2018; Accepted 7 December 2018
Available online 29 December 2018
0169-4332/ © 2018 Elsevier B.V. All rights reserved.

C.T.C.
Principal
Nowgong Girls' College
Nagaon :: Assam

Nowgong Girls' College
ESTD: 1962
Nagaon :: Assam

healing process is completed.

Surface modification of polymeric biomaterials to tailor drug loading and release behavior by cold atmospheric pressure plasma (CAPP) treatment has drawn considerable research interest over the past few years due to their promising clinical applications [11,12]. Plasma is a partially ionized gas composed of electrons, ions, excited gas molecules, atoms, free radicals and photons [13]. This environment-friendly technique can modify the surface properties and surface chemistry of polymers without affecting their bulk characteristics [13]. In addition, CAPP surface modification enables prompt processing of polymers with shorter treatment time as compared to wet surface modification and elimination of sophisticated and expensive vacuum systems [11]. CAPP treatment introduces various functional groups on the polymer surface that improve biocompatibility or allow immobilization of various drugs and bioactive molecules onto the treated surface. Such physico-chemical modifications by CAPP treatment influence the rate of water penetration and/or molecular chain mobility of the drug loaded polymer matrix, which eventually controls the drug release from the polymer [7,11–13].

The aim of this present study is to investigate the influence of oxygen (O_2) dielectric barrier discharge (DBD) plasma treatment on surface chemistry of core-shell nanofibers prepared from amoxicillin trihydrate-loaded silk fibroin (used as the core solution) and PVA (used as the shell solution) via coaxial electrospinning process and their *in vitro* drug release behavior. Silk fibroin is a fibrous protein derived from the *Bombyx mori* silkworm and has amphiphilic characteristics, comprising hydrophilic, amorphous regions and hydrophobic, crystalline domains that form a β-sheet secondary structure. *Bombyx mori* silk fibroin (BMSF) possesses good mechanical strength, elasticity, biocompatibility, and controllable biodegradability which make it an attractive biomaterial for tissue engineering and drug delivery applications [14,15]. On the other hand, PVA, a synthetic water soluble biopolymer, has attracted considerable attention in biomedical applications due to its biodegradability, biocompatibility, non-toxicity, good chemical stability and excellent film/fiber forming properties [16]. The effect of O_2 DBD plasma and O_2 DBD plasma-emitted UV radiation on the crystalline structure of BMSF/PVA nanofibers is studied in this work. Moreover, the drug release behavior of both the O_2 DBD plasma treated and untreated core-shell AMOX-BMSF/PVA nanofibers are investigated and the results are correlated with surface chemistry and surface properties. The antimicrobial activities of the core-shell AMOX-BMSF/PVA nanofibers, before and after O_2 DBD plasma treatment, are further evaluated against both Gram-negative *Escherichia coli* and Gram-positive *Staphylococcus aureus* bacteria.

2. Materials and methods

2.1. Materials

Silk cocoons from domesticated *Bombyx mori* silk are supplied by Central Silk Board, Guwahati, India. Fully hydrolyzed polyvinyl alcohol (PVA) has been purchased from Merck, India. (Mw = 145 kDa). Sodium bicarbonate ($NaHCO_3$, ≥99%), Dulbecco's modified eagle's medium (DMEM), dimethyl sulfoxide (DMSO, ≥99%), Acetic acid (glacial, ≥99%) and phosphate buffered saline (PBS) are supplied by Sigma-Aldrich, USA. Amoxicillin hydrochloride trihydrate (AMOX) and Lithium Bromide (LiBr, ≥99%) are purchased from BR Biochem Life Sciences, India and Tokyo Chemical Industries, Japan, respectively. Dialysis membrane (12–14 kDa molecular weight cut off) is supplied by Himedia, India. All chemical reagents are analytical reagent grade and used as received. A Millipore Milli-Q system (USA) is used to produce ultrapure distilled water.

2.2. Methods

2.2.1. Preparation of precursors solution

The raw *Bombyx mori* silk cocoons are cut into small pieces and degummed for 30 min by boiling in 0.2 M aqueous solution of $NaHCO_3$ followed by thorough rinsing with de-ionized distilled water and air dried at room temperature [14]. The BMSF, as obtained after degumming process, is then dissolved in 9.3 M aqueous LiBr solution with mass to liquid ratio 1:4 (BMSF:LiBr) and kept in an oven at 60 °C for 4 h. The silk solution is then dialyzed against deionized distilled water using 12–14 kDa molecular weight cut off cellulose membrane for 72 h followed by centrifugation (5000 rpm). The final protein concentration of the dialyzed silk solution is calculated to be 6.7% (w/v). AMOX is then slowly added to the silk solution at a concentration 2000 μg/ml with mild stirring for 15 min. The AMOX loaded BMSF (BMSF-AMOX) solution is then stored at 4 °C till further use. A 10% (w/v) PVA aqueous solution is prepared by stirring PVA powder in water at 80 °C for 3 h. The solution is allowed to stand overnight at room temperature to remove air bubbles before electrospinning.

2.2.2. Electrospinning of core-shell nanofibers

Core-shell AMOX-BMSF/PVA nanofibers are fabricated from the above precursors solution via coaxial electrospinning process as shown in the (Fig. 1(A)). The 10% (w/v) PVA solution is added to a 10 ml syringe, which is connected to the outer 20 G needle (inner diameter: 0.41 mm, outer diameter: 0.71 mm) and AMOX-BMSF solution is filled with another 10 ml syringe connected to the inner 24 G needle (inner diameter: 0.31 mm, outer diameter: 0.56 mm). Each syringe is placed in separate syringe pumps which permit adjustment and control of solution flow rate. The syringe pumps deliver PVA and AMOX-BMSF solutions at controlled flow rates of 0.4 ml/h and 0.1 ml/h, respectively. A high voltage of 22 kV is applied across the outer needle via an alligator clip and the electrospinning solution is drawn out from spinneret and forms a compound Taylor cone with a core-shell nanostructure of coaxial jet. A square stainless steel plate (150 mm × 150 mm) covered with aluminum foil is used as a static collector and connected to the ground. The core-shell nanofibers are collected on the aluminum foil at a tip-to-collector distance of 150 mm under the ambient conditions (temperature: 25 °C and relative humidity: 50%). The prepared nanofibers are kept in a vacuum desiccator for further characterization.

2.2.3. DBD plasma treatment

The DBD system operating at atmospheric pressure under ambient conditions (temperature: 25 °C and relative humidity: 50%) is presented schematically in Fig. 1(B). The discharge is produced between two copper electrodes (250 mm × 250 mm), placed within a square enclosure. The upper electrode is connected to a high voltage source (0–40 kV, 50 Hz, Zenoics Systech, India), while the lower electrode is connected to earth. Both the electrodes are covered with quartz plates (thickness = 2 mm, surface area = 250 mm × 250 mm) and the grounded electrode can be adjusted vertically to change the discharge gap. The O_2 (Assam Air Products, purity > 99.99%) gas is allowed to enter the discharge chamber and the gas flow rate is controlled by a digital mass flow controller (Alicat Scientific, USA). The samples are placed on the lower electrode, while O_2 gas (flow rate: 2 slpm) flows between the electrodes. In this work, discharge uniformity in the O_2 DBD plasma is monitored using a digital single-lens reflex camera (DSLR, Nikon D7200) with the exposure time of 1/8000 s mounted on a stable optical platform. The plasma discharge is observed from the side view of the discharge chamber. Optical images obtained at applied voltage of 15 kV, discharge gap of 6 mm and different interval of time (0 s, 10 s, 20 s) is shown in Fig. 1(C). It is observed that under these discharge conditions, stable homogeneous DBD without filaments is obtained at atmospheric pressure and the discharge spreads uniformly in the gap and covers the entire surface cross section of the quartz plates [17–19].

Nowgong Girls' College ESTD. 1962 Nagaon :: Assam
CERTIFIED TRUE COPY Principal Nowgong Girls College Nagaon :: Assam

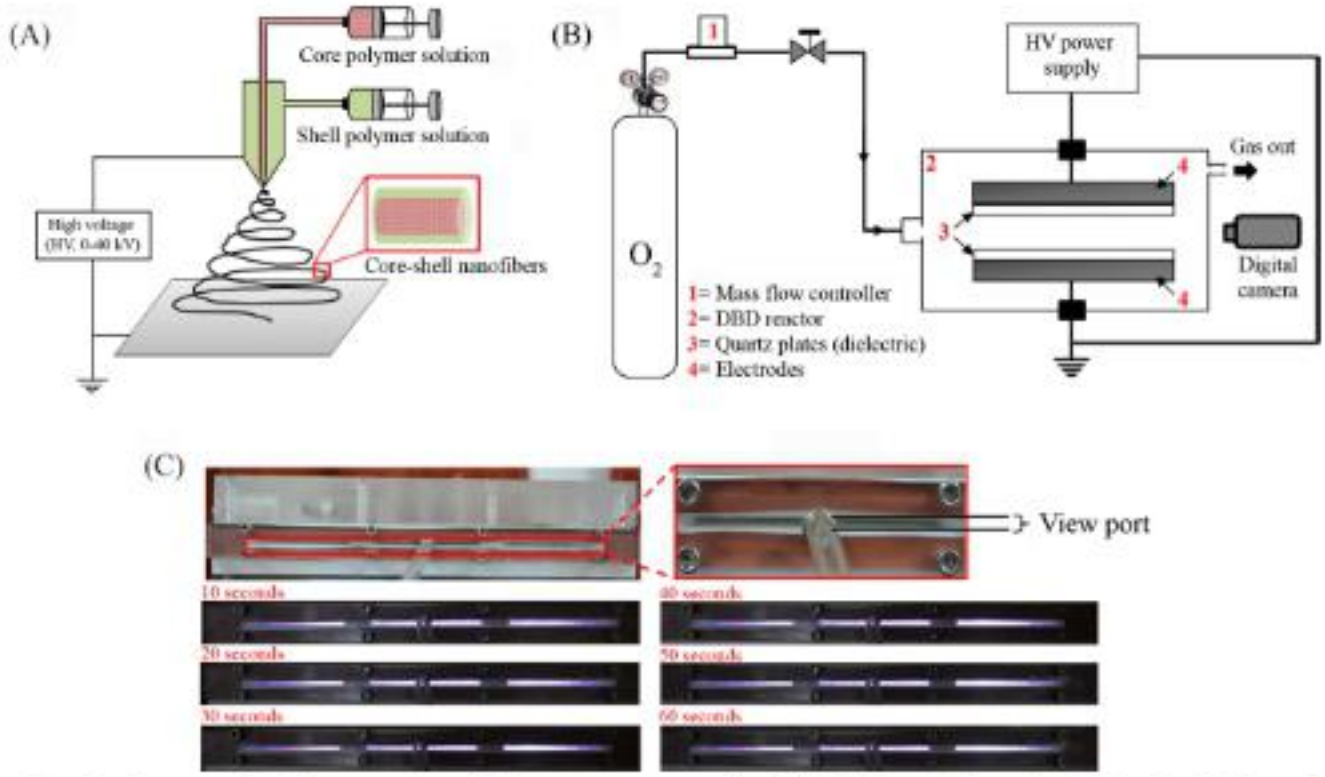

Fig. 1. (A) Schematic representation of the process for core-shell AMOX-BMSF/PVA nanofibers fabrication by coaxial electrospinning. (B) Schematic diagram of DBD system. (C) Discharge images (exposure time: 1/8000 s) of O_2 DBD plasma at different observation periods (10–60 s).

2.2.4. Characterization techniques

The surface morphologies of the AMOX-BMSF/PVA nanofibers, before and after O_2 DBD plasma treatment, are observed by field emission scanning electron microscope (FESEM, Zeiss, Sigma, Germany), transmission electron microscope (TEM, JEOL 2100, USA) and atomic force microscope (AFM, NTEGRA Vita, NT-MDT Spectrum Instruments, Russia). For FESEM observation, the samples are cut from electrospun mat collected on aluminum foil and sputter-coated by an ultrathin layer of gold/palladium alloy (SC7620, Emitech) in a low vacuum. The average diameter of the nanofibers is determined by measuring 150 nanofibers selected randomly from the FESEM images using ImageJ software. To confirm formation of the core-shell structure, the nanofibers are observed using TEM in ultrahigh vacuum condition with a resolution of 0.2 nm. For TEM observation, the nanofibers are directly deposited onto carbon-coated Cu grid. The AFM images are obtained by digital multimode scanning probe microscope (SPM) equipped with a nanoscope IVA controller (resolution: horizontal, 0.2 nm and vertical, 0.01 nm). The images are taken in tapping mode at a scanning rate of 1 Hz (scan size: 3 μm × 3 μm). The rms roughness of the nanofibers is measured by NOVA image analysis software.

The chemical compositions of AMOX-BMSF/PVA and AMOX-BMSF/PVA/O_2 nanofibers are analyzed using attenuated total reflectance Fourier transform infrared (ATR-FTIR) spectroscopy (IMPACT 410, NICOLET, USA). The spectra are obtained from a 200 μm diameter sampling area, using an average of 200 scans, at 4 cm^{-1} spectral resolution. Spectra are collected in transmittance mode with spectral region of 4000–650 cm^{-1}. The elemental compositions on the surface of nanofibers are characterized by X-ray photoelectron spectroscopy (XPS) (VG ESCA spectrometer system with Mg X-ray source, Gmbh, Germany). With Mg K_α line (1253.6 eV), detailed spectra are collected followed by high-resolution scan of relevant core level and valence level photoemission peaks of all the main elements.

The mechanical strength of AMOX-BMSF/PVA and AMOX-BMSF/PVA/O_2 nanofibers are evaluated using a universal testing machine (INSTRON 4204) at a constant speed of 10 mm min^{-1} with a 10 kN load (temperature: 25 °C and relative humidity: 50%). The specimens are cut into strips of 10 mm × 50 mm (thickness = 0.25 mm) and a gauge length of 20 mm is considered. For each sample, data is taken for five times and the average of Young's modulus of elasticity; tensile strength and elongation at break (%) are evaluated from stress-strain curves. The data are presented as average ± standard deviation (SD).

The wettability of AMOX-BMSF/PVA and AMOX-BMSF/PVA/O_2 nanofibers is measured by contact angle (using the sessile drop method) measurement system (Data Physics OCA 20, Germany). The system is equipped with a software operated high precision liquid dispenser to precisely control the drop size of the used liquid. Small droplets of deionized water and diiodomethane (1 μl) are dropped on the nanofibers through a computer controlled process and the image is taken immediately. Each image of the drop is then stored via a CCD video camera, using a PC based acquisition and data processing system. As the measurement of the contact angle is obtained from the image that is captured immediately, the effect of evaporation on the real measurement can be ignored. In this experiment, five point measurements on each sample are randomly performed and the result is reported as mean ± standard deviation (SD).

Surface energy (γ_s) of AMOX-BMSF/PVA and AMOX-BMSF/PVA/O_2 nanofibers is calculated by OWRK method using the following equation [20],

$$\gamma_s = \gamma_s^p + \gamma_s^d \quad (1)$$

where γ_s^p and γ_s^d are polar and dispersive components of the surface energy, γ_s respectively. To determine them, the contact angles corresponding to two liquids, deionized water (polar liquid) and diiodomethane (dispersion liquid) are first evaluated and then the polar and dispersive components are calculated from the following set of equations [20]:

Principal
Nowgong Girls' College
Nagaon :: Assam
Nowgong Girls College
ESTD. 1962
Nagaon :: Assam

$$\left.\begin{aligned}(\gamma_s^d)^{0.5} + 1.53(\gamma_s^p)^{0.5} &= 7.80(1 + \cos\theta_W)\\ (\gamma_s^d)^{0.5} + 0.22(\gamma_s^p)^{0.5} &= 3.65(1 + \cos\theta_D)\end{aligned}\right\} \quad (2)$$

where θ_D and θ_W are the contact angles obtained from diiodemethane and deionized water respectively.

2.2.5. Drug release study

The AMOX release profile from AMOX-BMSF/PVA and AMOX-BMSF/PVA/O_2 nanofibers is investigated by immersing specific amount of the sample in 10 ml phosphate-buffered saline (PBS, pH = 7.4) at 37 °C. After certain interval of time, 1 ml aliquots are collected and replaced with equal volume of fresh PBS to maintain sink conditions. The amount of drug released to the PBS medium is determined from a calibration curve of AMOX in PBS by measuring the UV absorbance of the removed aliquots (UV–visible spectrophotometer, Shimadzu, UV 1800, Japan) at a wavelength of 273 nm. The percentage drug release from the test sample is calculated from the following relation,

$$\text{Amount of drug release}\,(\%) = \frac{m_t}{m_0} \times 100 \quad (3)$$

where m_t is the amount of AMOX released at specific time t and m_0 is the total amount of drug loaded in the test sample. Three replicates are performed in this experiment and the results are presented as the mean ± standard deviation (SD).

To investigate the release kinetics of AMOX from AMOX-BMSF/PVA/O_2 nanofibers, the experimental results are fitted with different mathematical models specifically zeroth order, first order, second order, Korsmeyer-Peppas and Weibull method and the best fit is determined against highest value of correlation coefficient, R^2. In this work, the following Weibull model is selected to be the best fitted model with highest R^2 value for both AMOX-BMSF/PVA and AMOX-BMSF/PVA/O_2 nanofibers. This mathematical model is also suitable for describing drug release from polymer matrix [22],

$$F = 1 - e^{-\frac{t^b}{K_H}} \quad (4)$$

where F is the fraction of drug released to the PBS medium at specific time t, b describes the shape of the drug release curve and $K_H = \frac{1}{a}$ denotes the release rate constant.

2.2.6. Antibacterial study

The antibacterial activities of the O_2 DBD plasma treated and untreated AMOX-BMSF/PVA nanofibers are evaluated using agar disk diffusion method with strain of Gram positive *S. aureus* (ATCC 6633) and Gram negative *E. coli* (ATCC 25922) bacteria. The bacteria are first inoculated into Luria Bertani (LB) nutrient broth (1% peptone, 0.5% yeast extract, 0.5% NaCl, pH 7.0) and kept in an incubator at 37 °C. Bacterial cultures are prepared on solidified Mueller-Hinton agar (MHA) dispensed into sterile Petri dishes with proper care to ensure uniform growth throughout the dish. The samples, each having the dimension of 10 mm × 10 mm, are placed on agar plates and pressed lightly against the surface of the agar using a sterilized forceps. After incubation in a bacteriological oven at 37 °C for 24 h, the growth inhibition is quantified by calculating the size of each sample inhibition zone. The experiment is carried out in triplicate and repeated thrice and the result is reported as mean ± standard deviation (SD).

3. Results and discussion

3.1. Surface morphological analyses

The effect of O_2 DBD plasma treatment on AMOX-BMSF/PVA nanofibers morphology is investigated and analyzed using FESEM images and the results are shown in Fig. 1. The nanofibers with their diameters are in the nanoscale range are observed to be randomly oriented. Besides, uniform and bead-free morphology of AMOX-BMSF/PVA and AMOX-BMSF/PVA/O_2 nanofibers are observed and there are no obvious changes to the nanofiber surfaces after O_2 DBD plasma treatment. The average diameter of AMOX-BMSF/PVA and AMOX-BMSF/PVA/O_2 nanofibers is calculated to be 348 ± 2 nm and 349 ± 1 nm, respectively. It is evident that O_2 DBD plasma treatment does not induce significant changes in the topological structure of the nanofibers.

To verify the formation of core–shell structure of AMOX-BMSF/PVA nanofibers and observe the morphologies of the nanofibers, before and after O_2 DBD plasma treatment, TEM images are obtained and shown as insets in Fig. 2(A) and (B). The sharp contrast at the vicinity of the core and shell confirms the formation of the core/shell fibers where the inner dark region corresponds to AMOX-BMSF and the outer light region is recognized as PVA. The TEM images further confirm that AMOX is successfully incorporated and confined into the core region and does not diffuse into PVA during electrospinning process. The average diameter of AMOX-BMSF/PVA nanofibers shown in the TEM image is evaluated at 349 ± 2 nm with a core diameter of 233 ± 1 nm. For AMOX-BMSF/PVA/O_2 nanofibers, no significant change in the diameter is observed as a result of O_2 DBD plasma treatment and the average diameter is evaluated at 350 ± 2 nm with a core diameter of 234 ± 1 nm.

The AFM images and surface roughness profiles of AMOX-BMSF/PVA and AMOX-BMSF/PVA/O_2 nanofibers are further presented in Fig. 2(C)–(F). AFM image analyses reveal root mean square (rms) roughness values of 4.0 ± 0.2 nm and 10.0 ± 0.2 nm for AMOX-BMSF/PVA and AMOX-BMSF/PVA/O_2 nanofibers, respectively. The increase in surface roughness after O_2 plasma treatment is further confirmed through surface profile analyses of AMOX-BMSF/PVA and AMOX-BMSF/PVA/O_2 nanofibers (Fig. 2(E) and (F)). The higher surface roughness of AMOX-BMSF/PVA/O_2 nanofibers can be attributed to the etching of the surface by reactive oxygen ions that are generated in the discharge chamber during O_2 DBD plasma treatment. The increase in surface roughness is expected to provide high surface area for better wettability and stronger interfacial bonding for AMOX-BMSF/PVA/O_2 nanofibers.

3.2. Contact angle measurements

The wettability of polymer surface can be described by intermolecular interaction with the liquid phase that characterizes the degree of wetting of a solid surface by a liquid droplet and is controlled by its chemical structure and surface topography or roughness [23]. Surface wettability can directly influence the interactions of polymers with cells in terms of adhesion, proliferation, viability and differentiation thereby eventually affecting their biocompatibility [24]. The water contact angle on AMOX-BMSF/PVA and AMOX-BMSF/PVA/O_2 nanofibers and the corresponding surface energy results are shown in Fig. 3(A) and (B). It is evident that O_2 DBD plasma treatment significantly improves wettability of AMOX-BMSF/PVA/O_2 nanofibers by lowering the value of water contact angle from 73° ± 2° to 25° ± 2° and subsequently increasing surface energy from 47 ± 2 mJ/m^2 to 68 ± 2 mJ/m^2 respectively. The observation clearly indicates incorporation of oxygenated functional groups that are generated during O_2 plasma treatment onto the surface of AMOX-BMSF/PVA/O_2 nanofibers. These polar functional groups then strongly interact with water molecules resulting in a decrease in contact angle as depicted in the schematic (inset) in Fig. 3(A) [25–27]. The improvement in surface wettability of AMOX-BMSF/PVA/O_2 nanofibers can be further associated with surface roughness which is expected to be increased after O_2 DBD plasma treatment as revealed from AFM analyses [23].

3.3. Chemical analyses

The ATR-FTIR spectra of AMOX, BMSF, PVA and AMOX-BMSF/PVA nanofibers are shown in Fig. 4(A). The ATR-FTIR spectrum of AMOX

C.T.C. Principal Nowgong Girls College Nagaon :: Assam

Nowgong Girls College ESTD: 1962 Nagaon :: Assam

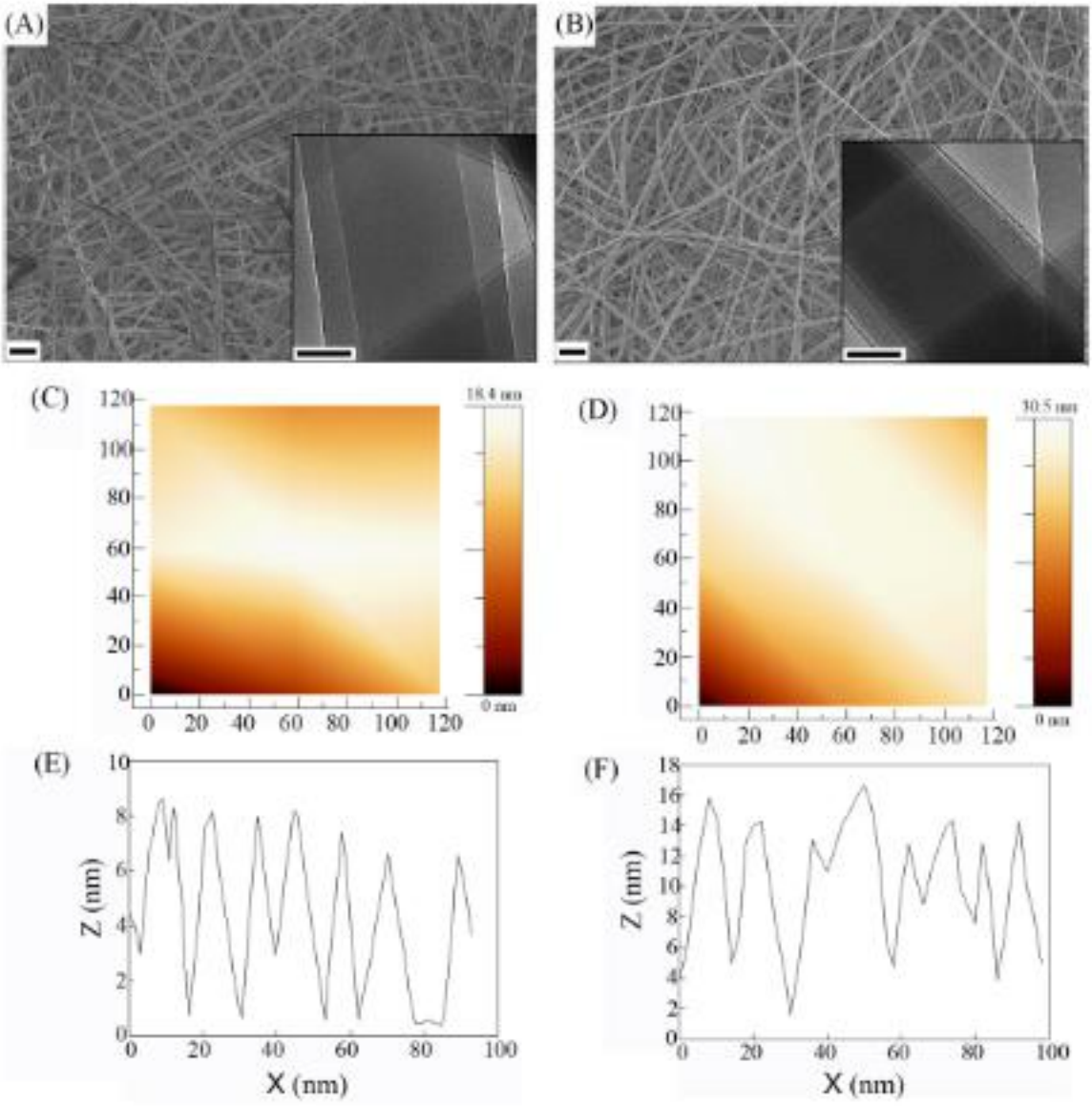

Fig. 2. FESEM images of (A) AMOX-BMSF/PVA and (B) AMOX-BMSF/PVA/O_2 nanofibers. The insets show the TEM images of AMOX-BMSF/PVA and AMOX-BMSF/PVA/O_2 nanofibers, respectively. (C) and (D) AFM topography images and (E) and (F) surface roughness profiles of AMOX-BMSF/PVA and AMOX-BMSF/PVA/O_2 nanofibers (FESEM image, scale: 1 μm; TEM image, scale: 100 nm).

shows absorption bands at 3412 cm^{-1}, 3167 cm^{-1} and 3033 cm^{-1} which correspond to hydrogen-bonded OH stretching, N H stretching of secondary amines/OH stretching and CH stretching of aromatic ring [28]. The peak at 2972 cm^{-1} is assigned to asymmetric CH stretching vibration of alkyl groups [28]. The absorption peak at 1776 cm^{-1} is characteristic of β-lactum ring of AMOX and corresponds to C=O stretching vibration [29,30]. The C=O stretching vibration (amide I), N H bending of the secondary amine/C=C stretching of aromatic ring and C N stretching of primary amine are assigned to the absorption peaks at 1688 cm^{-1}, 1482 cm^{-1} and 1250 cm^{-1}, respectively [31]. The peaks at 1572 cm^{-1} and 1398 cm^{-1} are attributed to asymmetrical and symmetrical stretching vibration of carboxylate (COO^-) groups, respectively [31]. The ATR-FTIR spectrum of BMSF shows absorption band centered at 3287 cm^{-1} which arises due to the overlapping of N H and O H stretching vibrations of the primary amino groups and O H stretching vibrations (H-bonded) of hydroxyl groups [31]. The characteristic peaks of BMSF corresponding to amide I, amide II and amide III are observed at 1657 cm^{-1}, 1517 cm^{-1} and 1224 cm^{-1}, respectively [32]. For better comparison, the ATR-FTIR spectrum of PVA is further included in Fig. 4(A). The broad peak centered at 3296 cm^{-1} is attributed to stretching vibrations of OH from the intramolecular and intermolecular hydrogen bonds in PVA [33]. The peaks observed at 2941 cm^{-1} and 2910 cm^{-1} are assigned to the symmetric and asymmetric CH stretching vibration of alkyl groups, respectively [33–35]. The characteristic vibration bands of carbonyl groups are found at 1735 cm^{-1} (C=O stretching vibration), 1657 cm^{-1} (C O stretching vibration) and 1564 cm^{-1} (C=C stretching vibration) whereas the peaks observed at 1427 cm^{-1}, 1375 cm^{-1}, 1325 cm^{-1}, 1245 cm^{-1} and 1092 cm^{-1} are assigned to the CH_2 bending vibration, CH stretching, CH deformation vibration, CH wagging and C O stretching of acetyl groups, respectively [33–35]. The presence of carbonyl group (C=O) at 1735 cm^{-1} is related to the residual acetate groups that remains after the manufacture of PVA from the hydrolysis of polyvinyl acetate [36]. The vibrational modes of C C stretching and CH_2 wagging are observed at 947 cm^{-1} and 848 cm^{-1} [34]. These characteristic absorption bands/peaks of PVA nanofibers are observed in the ATR-FTIR spectrum of AMOX-BMSF/PVA nanofibers whereas those corresponding to BMSF and AMOX are found to be absent as revealed from Fig. 4(A). These findings thus confirm the successful formation of AMOX-BMSF/PVA nanofibers with AMOX-BMSF as the core and PVA as shell material.

Principal Nowgong Girls' College Nagaon :: Assam
Nowgong Girls' College ESTD. 1962 Nagaon :: Assam

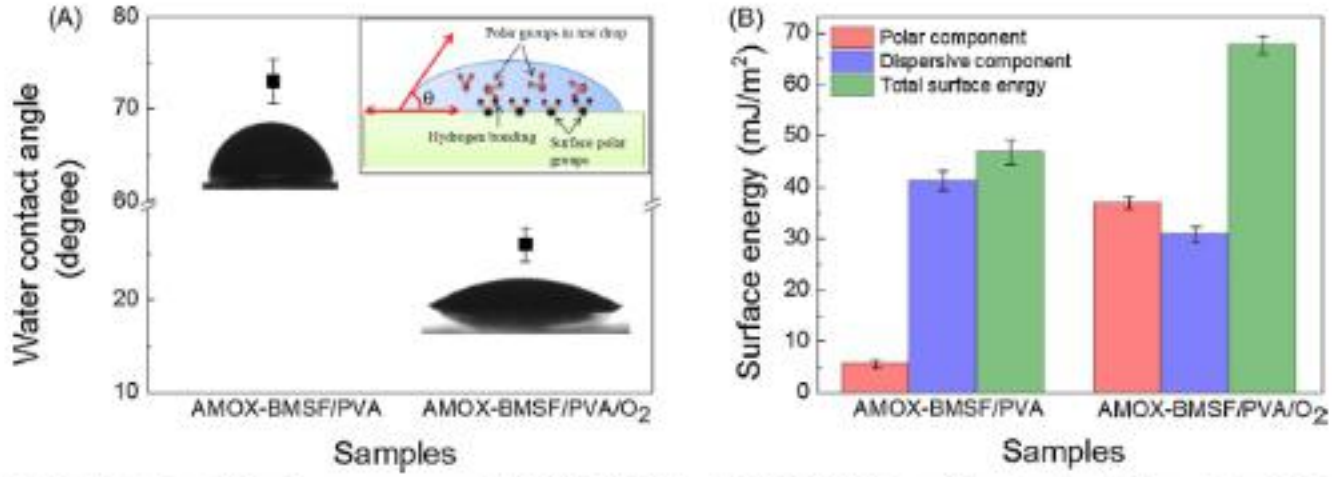

Fig. 3. (A) Contact angle and (B) surface energy measurement of AMOX-BMSF/PVA and AMOX-BMSF/PVA/O_2 nanofibers. The schematic diagram shown in the inset of (A) depicts the interactions among the polar groups present on the surfaces of AMOX-BMSF/PVA/O_2 nanofibers and water molecules. θ is the measured contact angle with respect to the surface as shown in the inset.

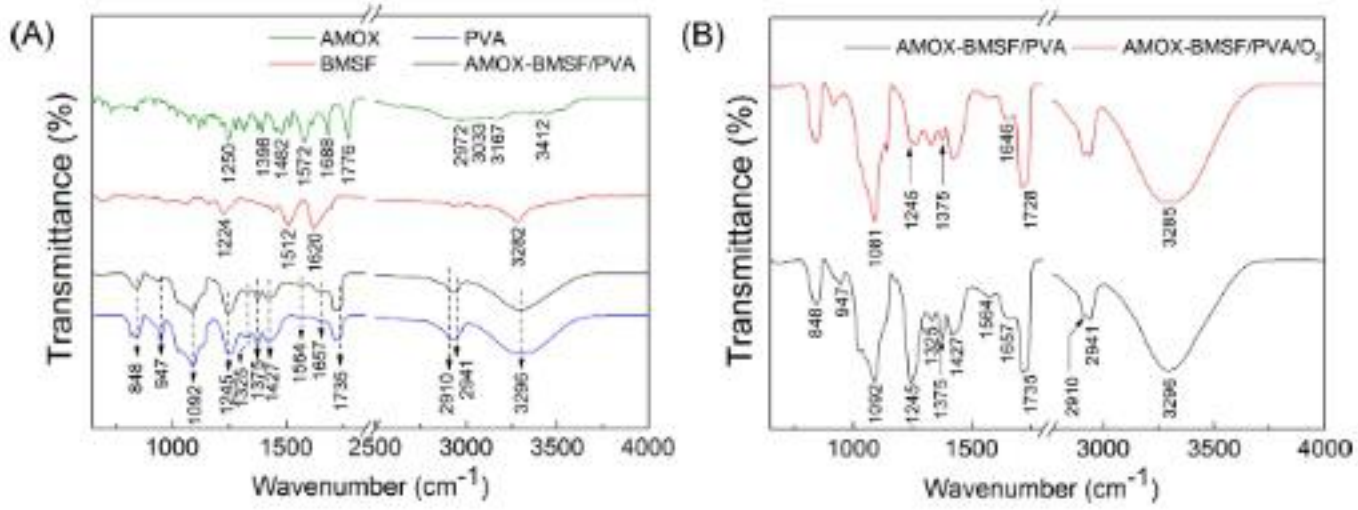

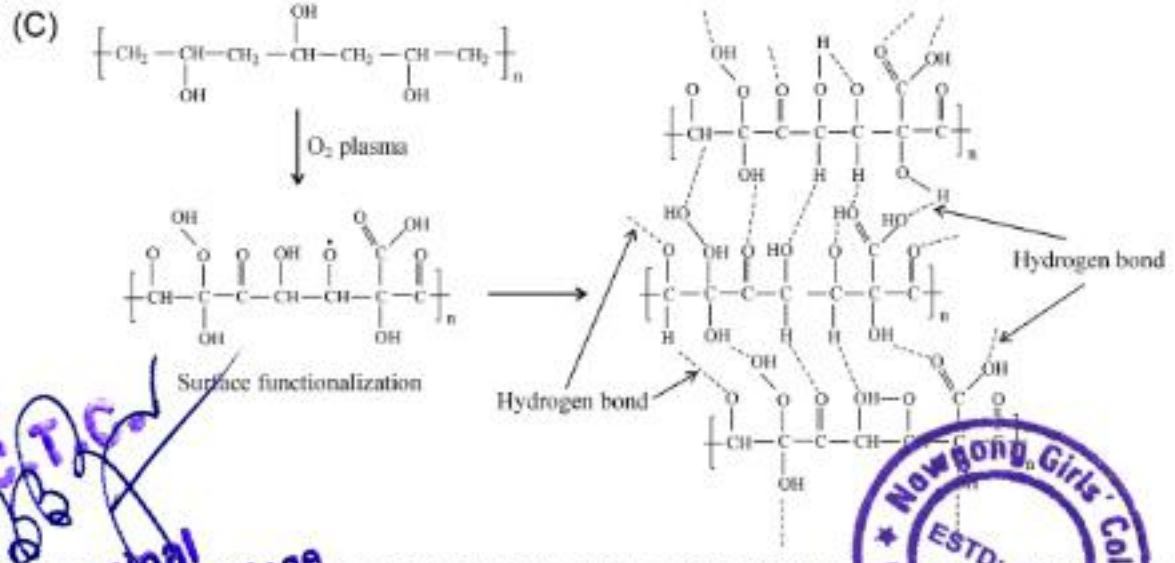

Fig. 4. ATR-FTIR spectra of (A) AMOX, PVA and AMOX-BMSF/PVA nanofibers and (B) AMOX-BMSF/PVA and AMOX-BMSF/PVA/O_2 nanofibers. (C) Schematic diagram illustrates surface functionalization of PVA by O_2 DBD plasma that results in formation of different polar groups and subsequent interaction of the polar groups among themselves and with the molecular chains of PVA though hydrogen bonds.

C.T.C.
Principal
Nowgong Girls' College
Nagaon :: Assam
Nowgong Girls' College
ESTD: 1962
Nagaon :: Assam

The effect of O_2 DBD plasma treatment on surface chemistry of AMOX-BMSF/PVA nanofibers is further investigated and the results are presented in Fig. 4(B). In ATR-FTIR spectrum of AMOX-BMSF/PVA/O_2 nanofibers, the OH stretching absorption band is observed to be broadened and shifted towards lower wavenumber (3285 cm^{-1}) which indicates incorporation of polar functional groups and formation of hydrogen bonding on the surface of PVA after O_2 DBD plasma treatment. It has been reported that OH stretching vibration is sensitive to hydrogen bonding and the formation of hydrogen bond is usually accompanied by shifting of the hydroxyl absorption band (3650–3000 cm^{-1}) towards lower wavenumber [37,38]. The intensities of the absorption peaks at 1375 cm^{-1} and 1245 cm^{-1} are found to be significantly reduced which may be accounted for abstraction of hydrogen from alkyl groups by reactive oxygen species (O, O_2, O_2^- etc.) [39]. These species are generated during O_2 plasma treatment and interact chemically with PVA thereby causing hydrogen abstraction and formation of oxygen-containing (polar) functional groups at the surface. A schematic illustration of surface functionalization of PVA through formation of polar groups by O_2 plasma and subsequent interaction of the functional groups among themselves and with PVA molecular chains though hydrogen bonding is shown in Fig. 4(C). The incorporation of oxygen-rich functional groups at the surface of AMOX-BMSF/PVA/O_2 nanofibers is further evident by observing a shift in absorption band corresponding to C=O and C–O stretching vibrations towards lower wavenumbers, i.e. 1728 cm^{-1}, 1646 cm^{-1} and 1081 cm^{-1}, respectively. These observations clearly show that O_2 DBD plasma treatment facilitates formation of more hydrogen bonds in AMOX-BMSF/PVA/O_2 nanofibers though incorporation of oxygen containing functional groups onto the surface.

The surface chemistry of AMOX-BMSF/PVA and AMOX-BMSF/PVA/O_2 nanofibers is further analyzed by XPS. The variation of atomic compositions and the oxygen/carbon (O/C) ratio of the nanofibers are presented in Table 1. It is observed that O_2 DBD plasma treatment results in an increase in oxygen content and subsequent decrease in carbon content on the surface of AMOX-BMSF/PVA/O_2 nanofibers. Also, O/C ratio for AMOX-BMSF/PVA/O_2 is observed to be higher as compared to AMOX-BMSF/PVA nanofibers. The results confirm that oxygen-containing functional groups are incorporated onto the surface of AMOX-BMSF/PVA/O_2 nanofibers after O_2 DBD plasma treatment.

To gain more insight into the surface chemistry of AMOX-BMSF/PVA and AMOX-BMSF/PVA/O_2 nanofibers, the high resolution C_{1s} and O_{1s} XPS spectra of the samples are fitted in different peaks (Fig. 5(A)–(D)). As seen from Fig. 5(A), the C_{1s} spectrum is resolved and fitted into three components corresponding to the peaks at 283.5 eV (C–C), 284.8 eV (C–H) and 286.6 eV (C–O), respectively while two new components corresponding to the peaks at 287.3 eV (C=O) and 288.2 eV (O–C=O), respectively are observed for AMOX-BMSF/PVA/O_2 nanofibers. On the other hand, the O_{1s} spectrum of AMOX-BMSF/PVA nanofibers shows the presence of one component corresponding to the peak at 531.4 eV (C–O) whereas the resolved O_{1s} spectrum of AMOX-BMSF/PVA/O_2 nanofibers reveals presence of two additional peaks at 530.2 eV (C=O) and 533.8 eV (O–C=O), respectively. The relative percentage concentration of components of the resolved C_{1s} and O_{1s} spectra is shown in Table 2. It is evident that O_2 DBD plasma treatment indeed results in incorporation of oxygen containing functional groups (C=O and O–C=O) onto the surface of AMOX-BMSF/PVA/O_2 nanofibers. Besides, due to the effect of O_2 plasma etching, the reactive oxygen ions abstract hydrogen from alkyl group leading to subsequent decrease in the relative percentage of C–C and C–H components on the surface of AMOX-BMSF/PVA/O_2 nanofibers.

Table 1
Atomic concentration and the oxygen/carbon (O/C) ratio of the deconvoluted C1s and O1s high resolution XPS spectra of AMOX-BMSF/PVA and AMOX-BMSF/PVA/O_2 nanofibers (mean ± standard deviation (SD)).

Sample	C	O	O/C
BMSF/AMOX/PVA	55.0	45.0	0.8
BMSF/AMOX/PVA/O_2	43.0	57.0	1.3

Nowgong Girls' College ESTD: 1962 Nagaon :: Assam

3.4. Structural analyses

The XRD analyses of BMSF/PVA nanofibers are carried out to investigate the effect of O_2 DBD plasma and O_2 DBD plasma-emitted UV radiation on the crystal structure of the nanofibers. For this purpose, The BMSF/PVA nanofibers are completely covered with magnesium fluoride (MgF_2) window (Edmond optics, USA, spectral range: 120–400 nm, diameter: 20 mm, thickness: 2 mm) as shown in Fig. 6(A). This arrangement allows the UV radiation to pass through the MgF_2 window but prevents the plasma species (electrons, ions, excited molecules etc.) from interacting with the nanofibers. The BMSF/PVA nanofibers covered with MgF_2 window are then exposed to O_2 plasma at the same discharge conditions as described earlier. The XRD curves of BMSF/PVA and BMSF/PVA/O_2 nanofibers and UV radiation treated BMSF/PVA (BMSF/PVA/UV) nanofibers are shown in Fig. 6(B). The XRD curves show two broad peaks at around 13° and 21°, respectively. The first peak corresponds to the crystalline structure of PVA whereas the second peak arises due to the overlapping of β-sheet crystalline structure of BMSF and PVA. It is evident that UV radiation treatment does not induce any structural change in BMSF/PVA nanofibers. Moreover, no remarkable differences in the crystalline structure of BMSF/PVA nanofibers could be observed after O_2 plasma treatment thereby underlining the merit of low temperature plasma in surface modification process where plasma treatment only tailors the surface chemistry without affecting inherent physical structure of the polymer. The results show that UV radiation plays an insignificant role in affecting the crystalline structure of BMSF/PVA nanofibers and suggest that UV radiation emitted by DBD plasma is most likely to be absorbed by O_2 molecules at atmospheric pressure which may subsequently result in generation of oxygen containing functional groups, as revealed from XPS spectra analyses. It has been reported that non-thermal atmospheric-pressure plasmas are typically not very effective sources of high-energy UV radiation below 290 nm [40]. Even in sterilization process, in the case of low temperature atmospheric plasmas, it is the highly reactive species such as O, OH, and NO_2 that play the most crucial role in the destruction of microorganisms whereas the effect of UV radiation and heat is minimal [41,42]. However, Low-pressure plasma discharges can provide significant UV radiation in the range of wavelengths (200–290 nm) effective not only in sterilization but also in surface modification of polymers [40,43,44].

3.5. Mechanical properties

In this study, the tensile strength, Young's modulus and elongation at break (%) of AMOX-BMSF/PVA nanofibers are measured before and after O_2 DBD plasma treatment and the results are summarized in Fig. 7(A) and (B). Fig. 7(A) shows the typical stress-strain curves for AMOX-BMSF/PVA and AMOX-BMSF/PVA/O_2 nanofibers. From the results shown in Fig. 7(B) the tensile strength increases from 5.0 ± 0.2 MPa for AMOX-BMSF/PVA nanofibers to 6.0 ± 0.2 MPa for AMOX-BMSF/PVA/O_2 nanofibers. Besides, O_2 DBD plasma treatment results in an increase in Young's modulus of the nanofibers from 12.0 ± 1.4 MPa to 47.0 ± 2.0 MPa. The remarkable improvement in the mechanical properties of AMOX-BMSF/PVA/O_2 nanofibers is attributed to the hydrogen bond interactions among different polar groups and [illegible] between the polar groups and PVA molecular chains thereby leading to enhanced interfacial interaction and efficient load transfer in the nanofibers [47]. However, elongation at break (%) is observed to be decreased from 38% to 8% thereby indicating an increase in stiffness and rigidity in molecular chains within AMOX-BMSF/PVA/O_2 nanofiber mat.

Principal Nowgong Girls' College Nagaon :: Assam

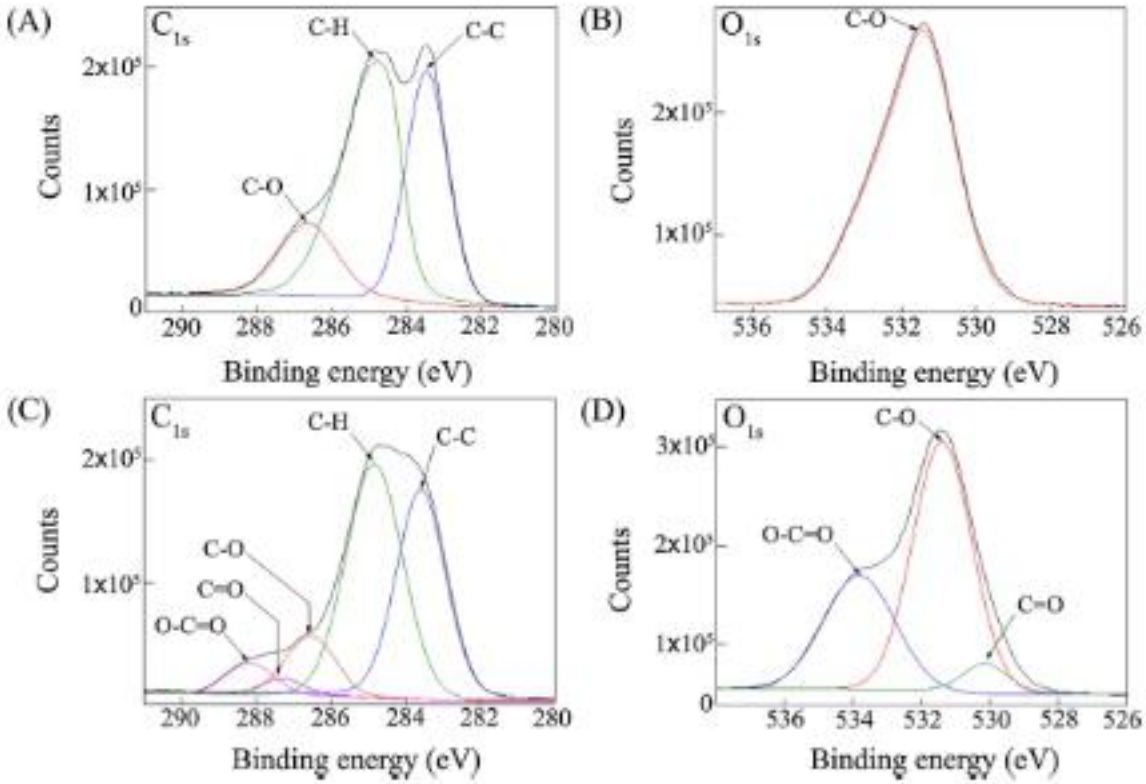

Fig. 5. Deconvoluted C_{1s} and O_{1s} high resolution XPS spectra of (A), (B) AMOX-BMSF/PVA and (C), (D) AMOX-BMSF/PVA/O_2 nanofibers, respectively.

3.6. Drug release study

The drug release profiles of AMOX-BMSF/PVA and AMOX-BMSF/PVA/O_2 nanofibers have been studied in PBS and the results are shown in Fig. 8(A). It is observed that AMOX-BMSF/PVA and AMOX-BMSF/PVA/O_2 nanofibers show drug release up to 40% and 24% respectively, after 24 h of immersion in PBS. The release profile of each nanofibers is also fitted with Weibull model to investigate the release kinetics of AMOX. The drug release rate constant (K_H) as determined by fitting the experimental data with the kinetic drug model is found to be 1.0 h^{-1} and 1.2 h^{-1} respectively corresponding to AMOX-BMSF/PVA and AMOX-BMSF/PVA/O_2 nanofibers. The results thus predict faster release of AMOX from AMOX-BMSF/PVA/O_2 nanofibers as compared to AMOX-BMSF/PVA nanofibers. The AMOX release profile from AMOX-BMSF/PVA nanofibers shows a continuous and steady rise of drug release (60%) up to the observation period of 200 h after which a plateau is reached. On the other hand, for AMOX-BMSF/PVA/O_2 nanofibers, the release profile shows a relatively rapid drug release (54%) as compared to AMOX-BMSF/PVA nanofibers after 55 h of immersion followed by a sustained release (62%) up to the observation period of 120 h and finally a plateau is reached. The observed fast release of drug can be explained in terms of enhanced surface hydrophilicity of AMOX-BMSF/PVA/O_2 nanofibers and higher rate of degradation of PVA in PBS medium. As a result, more release of drug takes place in PBS medium from the surface of BMSF. To confirm increase in degradation of PVA after O_2 DBD plasma treatment, degradation behavior of both AMOX-BMSF/PVA and AMOX-BMSF/PVA/O_2 nanofibers are investigated in PBS medium. As revealed from the results shown in Fig. 8(B), AMOX-BMSF/PVA/O_2 nanofibers show higher degree of degradation as compared to AMOX-BMSF/PVA nanofibers therefore corroborating the above observations. The sustain release of drug from both AMOX-BMSF/PVA and AMOX-BMSF/PVA/O_2 nanofibers up to the observation period of 314 h can be attributed to the swelling of BMSF in PBS medium thereby allowing penetration of PBS and subsequent diffusion of AMOX from silk matrix.

3.7. Antimicrobial test

The antibacterial activities of AMOX-BMSF/PVA and AMOX-BMSF/PVA/O_2 nanofibers are revealed by clearly visible zone of inhibition (I.) against bacterial (*E. coli* and *S. aureus*) growth after 24 h of observation period as shown in Fig. 9(A)–(D). The results show that O_2 DBD plasma treatment improves antibacterial activities of AMOX-BMSF/PVA/O_2 nanofibers against *E. coli* and *S. aureus*. The high antibacterial activities of AMOX-BMSF/PVA/O_2 nanofibers may be attributed to the enhanced surface hydrophilicity induced by O_2 DBD plasma treatment which

Table 2
Relative concentration (%) of components of the deconvoluted C_{1s} and O_{1s} high resolution XPS spectra of AMOX-BMSF/PVA and AMOX-BMSF/PVA/O_2 nanofibers (means ± standard deviation (SD)).

Sample	Relative concentration (%)								
	C_{1s}					O_{1s}			
	283.5 eV (C–C)	284.8 eV (C–H)	286.6 eV (C–O)	287.3 eV (C=O)	288.2 eV (O–C=O)	530.2 eV (C=O)	531.8 eV (C–O)	533.8 eV (O–C=O)	
BMSF/AMOX/PVA	38	48	11	–	–	–	100		
BMSF/AMOX/PVA/O_2	38	43	9	3	7	7	60	33	

Nowgong Girls' College ESTD: 1962 Nagaon :: Assam
C.T.C.
Principal
Nowgong Girls' College
Nagaon :: Assam

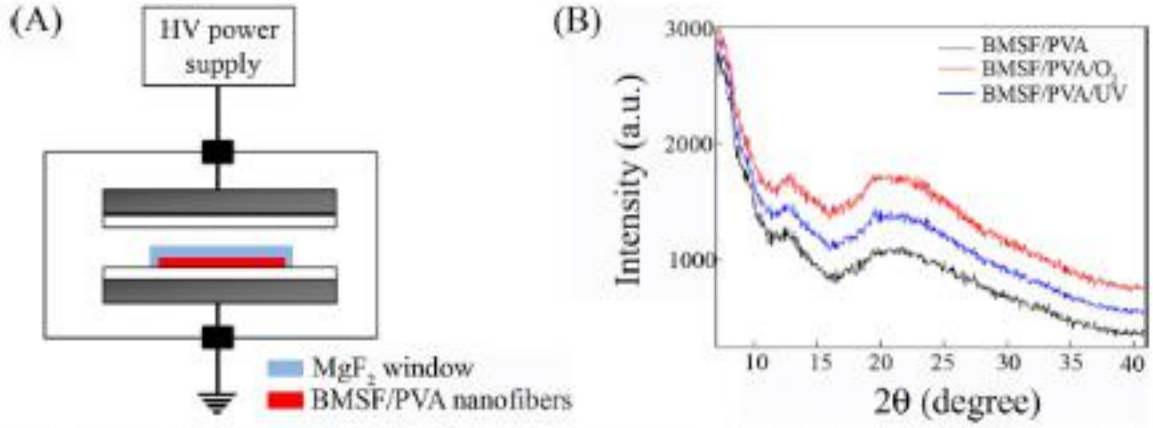

Fig. 6. (A) Experimental arrangements to observe the effect of UV radiation on BMSF/PVA nanofibers in DBD system. (B) XRD spectra of BMSF/PVA, BMSF/PVA/O_2 and BMSF/PVA/UV nanofibers.

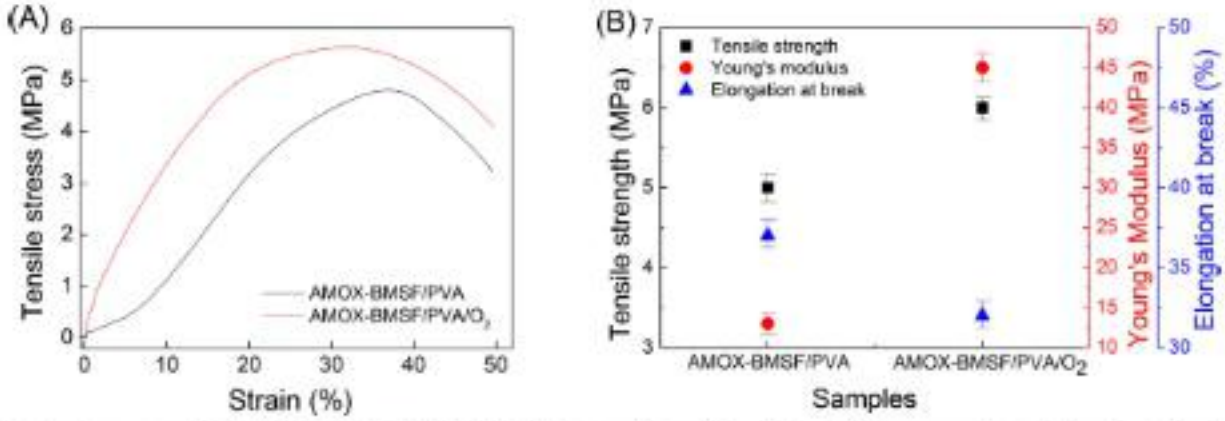

Fig. 7. (A) Strain-stress curves of AMOX-BMSF/PVA and AMOX-BMSF/PVA/O_2 nanofibers. (B) Tensile strength, Young's modulus and elongation at break of AMOX-BMSF/PVA and AMOX-BMSF/PVA/O_2 nanofibers.

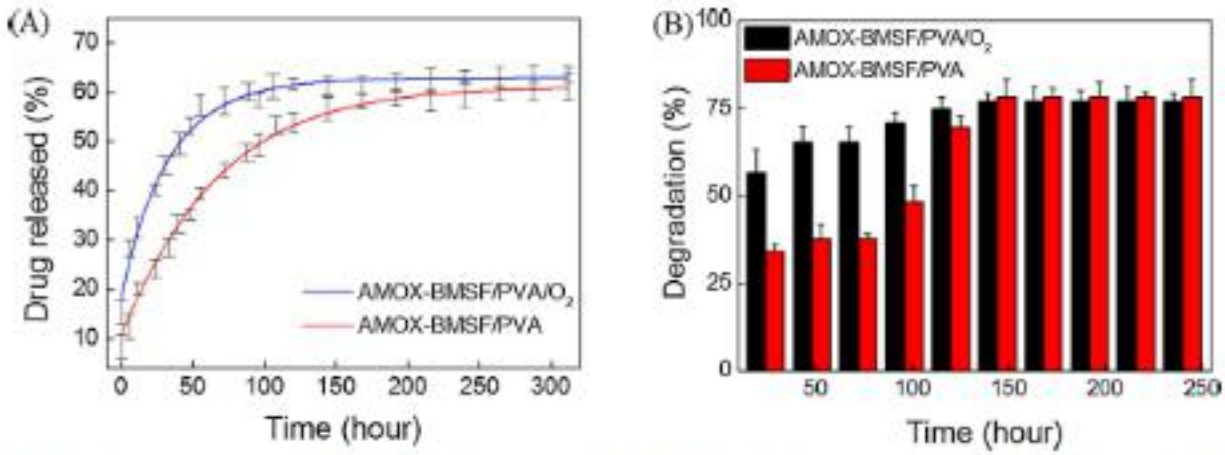

Fig. 8. (A) Variation of AMOX release (%) in PBS medium as a function of observation time. (B) Variation of degradation (%) of AMOX-BMSF/PVA and AMOX-BMSF/PVA/O_2 nanofibers in PBS medium as a function of observation time. Values represent mean ± SD of 3 batches.

causes faster release of AMOX as compared to AMOX-BMSF/PVA nanofibers. The experimental results further show that the AMOX-BMSF/PVA/O_2 nanofibers maintain similar zone of inhibition against both the bacteria up to 48 h followed by a regular decrease in the size of zone of inhibition up to 240 h and after that complete bacterial growth is observed on the nanofibers (Fig. 9(E) and (F)). However, during the entire period of observation (220 h), AMOX-BMSF/PVA/O_2 nanofibers show higher zone of inhibition against *E. coli* and *S. aureus* bacteria as compared to that observed for AMOX-BMSF/PVA nanofibers. The prolonged antibacterial activities of AMOX-BMSF/PVA and AMOX-BMSF/PVA/O_2 nanofibers against both *E. coli* and *S. aureus* bacteria are attributed to the sustained release of AMOX from the silk matrix as evident from earlier discussion. The results suggest that AMOX-BMSF/PVA/O_2 nanofibers can be more effective to inhibit the bacterial growth and subsequently prevent bacterial infection at the incised skin through controlled release of AMOX to the targeted site.

CERTIFIED
Principal
Nowgong Girls' College
Nagaon :: Assam
Nowgong Girls' College
ESTD 1962
Nagaon :: Assam

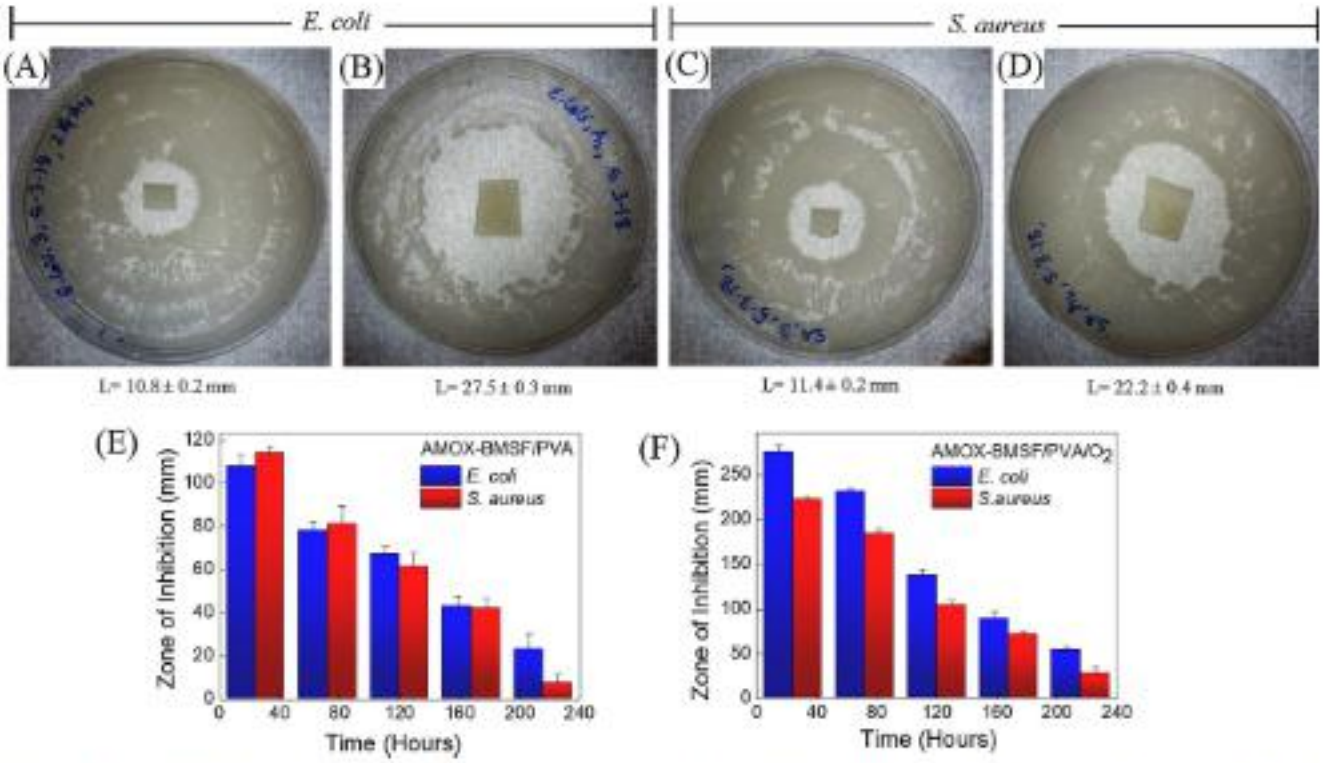

Fig. 9. Antibacterial activities of AMOX-BMSF/PVA and AMOX-BMSF/PVA/O_2 nanofibers against (A), (B) *E. coli* and (C), (D) *S. aureus*, respectively. Variation of zone of inhibition of (E) AMOX-BMSF/PVA and (F) AMOX-BMSF/PVA/O_2 nanofibers against *E. coli* and *S. aureus* as a function of observation time. Values represent mean ± SD of three batches.

4. Conclusion

The fabrication of core-shell AMOX-BMSF/PVA nanofibers followed by surface modification using homogeneous O_2 DBD plasma at atmospheric pressure has been carried out. O_2 DBD plasma treatment induces hydrophilicity to AMOX-BMSF/PVA/O_2 nanofibers due to incorporation of polar functional groups at the surface. The strong hydrogen bond interactions among polar groups and also between polar groups and PVA molecular chains enhances interfacial interaction and subsequently results in improving the mechanical properties of AMOX-BMSF/PVA/O_2 nanofibers. O_2 plasma and O_2 plasma-emitted UV radiation do not seemed to induce any crystalline structural change in AMOX-BMSF/PVA nanofibers. This study demonstrates that O_2 DBD plasma treatment is an effective and favorable approach to alter the surface chemistry of AMOX-BMSF/PVA/O_2 nanofibers which allows fast release of AMOX from the nanofibers mat and improve its antibacterial activities against both Gram-negative (*E. coli*) and Gram-positive (*S. aureus*) bacteria. These mechanically strong AMOX-BMSF/PVA/O_2 nanofibers can be explored as promising drug-release wound dressings with excellent antibacterial activity for preventing bacterial infection at the incised skin.

Acknowledgement

This research work is supported by DST-SERB (Grant No. SR/FTP/PS-147/2012 and EMR/2016/000140). Funded by Department of Science and Technology (DST), India. Dip[illegible] Choudhury expresses his gratitude to the DST-INSPIRE Faculty Fellowship (Grant No. IFA14-PH-93) for the financial support to carry out this research work and the Tezpur University, Assam, India for awarding the fellowship. Namita Ojah acknowledges the support provided by DST, India in the form of fellowship under DST-INSPIRE Faculty program. The assistance of Debolina Sarmah, Department of Physics, Tezpur University, Kiranjyoti Mohan, Department of Chemical Sciences, Tezpur University and Saurav Haloi, Department of Molecular biology and biotechnology, Tezpur University in carrying out contact angle and Tensile strength measurement and antibacterial activity test is gratefully acknowledged. The authors would like to thank Prof. Swapan Kumar Dolui, Department of Chemical Sciences, Tezpur University and Dr. Tapas Medhi, Department of Molecular biology and biotechnology, Tezpur University for providing the necessary laboratory facility for performing Tensile strength measurement and antibacterial activity test.

References

[1] Y. Kim, Y. Tabata, Dual-controlled release system of drugs for bone regeneration, Adv. Drug Deliv. Rev. 94 (2015) 28–40.
[2] J.R. Weiser, W.M. Saltzman, Controlled release for local delivery of drugs: barriers and models, J. Control. Release 190 (2014) 664–673.
[3] Y. Mayet, S. Hribernik, T. Mohan, D.M. Sterbe, U. Maver, K. Stana-Kleinschek, Functional wound dressing materials with highly tunable drug release properties, RSC Adv. 5 (2015) 77875–77884.
[4] Y. Ma, L. Xin, H. Tan, M. Fan, J. Li, Y. Jia, Z. Ling, Y. Chen, X. Hu, Chitosan membrane dressings toughened by glycerol to load antibacterial drugs for wound healing, Mater. Sci. Eng., C 81 (2017) 522–531.
[5] S. Soghrandeh, C. Rinoldi, M. Schot, S.S. Kashef, F. Sharifi, E. Jalilian, K.N.G. Gianniki, P. Mostafalu, H. Derakhshandeh, K. Yue, W. Swieszkowski, A. Memic, A. Tamayol, A. Khademhosseini, Drug delivery systems and materials for wound healing applications, Adv. Drug Deliv. Rev. 127 (2018) 138–166.
[6] F. Yamashita, M. Hashida, Pharmacokinetic considerations for targeted drug delivery, Adv. Drug Deliv. Rev. 65 (2013) 139–147.
[7] A.J. Chowdhury, D. Gogoi, J. Chutia, R. Kandimalla, S. Kalita, J. Konkey, Y.B. Chaudhuri, M.R. Khan, K. Kalita, Controlled antibiotic-releasing *Antheraea assama* silk fibroin sutures for infection prevention and fast wound healing, Surgery 159 (2016) 539–[illegible]
[8] Y. Cao, F. Li, [illegible] D. Gao, Y. Gao, F. Li, Z. Wang, H. Ran, Drug release from core-shell PVA/silk fibroin nanofibers fabricated by one-step electrospraying, [illegible] (2017) [illegible]
[9] R. Sedghi, [illegible] Electrospun biocompatible core/shell polymer-free core structured [illegible] with superior [illegible] antibiotic potency against multi drug resistant [illegible], Polymer 101 (2016) 145–157.
[10] S. Zupančič, [illegible] Simões, J. Kristl, A.L. Yarin, Controlled release of ciprofloxacin from core–shell nanofibers with monolithic or blended core, Mol. Pharm. [illegible] 1393–1402.
[11] D.G. Pe[illegible] Plasma treatment as an efficient

Principal
Nowgong Girls' College
Nagaon :: Assam
Nowgong Girls College
ESTD. 1962
Nagaon :: Assam

tool for controlled drug release from polymeric materials: a review, J. Control. Release 266 (2017) 57–74.
[12] C. Canal, M. Modic, U. Cvelbar, M.P. Ginebra, Regulating the antibiotic drug release from β-tricalcium phosphate ceramics by atmospheric plasma surface engineering, Biomater. Sci. 4 (2016) 1454–1461.
[13] F.E. Chu, J.Y. Chen, L.F. Wang, N. Huang, Plasma-surface modification of biomaterials, Mater. Sci. Eng., R 36 (2002) 143–206.
[14] D.N. Rockwood, R.C. Preda, T. Yücel, X. Wang, M.L. Lovett, D.L. Kaplan, Materials fabrication from *Bombyx mori* silk fibroin, Nat. Protoc. 6 (2011) 1612–1631.
[15] S. Mehrotra, S.K. Nandi, B.B. Mandal, Stacked silk-cell monolayers as a biomimetic three dimensional construct for cardiac tissue reconstruction, J. Mater. Chem. B 5 (2017) 6325–6338.
[16] P. Das, N. Ojah, B. Kandimalla, R. Mohan, D. Gogoi, S.K. Dolui, A.J. Choudhury, Surface modification of electrospun PVA/chitosan nanofibers by dielectric barrier discharge plasma at atmospheric pressure and studies of their mechanical properties and biocompatibility, Int. J. Biol. Macromol. 114 (2018) 1026–1032.
[17] A.A. Garamoon, D.M. El-aseer, Atmospheric pressure glow discharge plasma in air at frequency 50 Hz, Plasma Sources Sci. Technol. 18 (2009) 1–8.
[18] J. Ran, C. Li, D. Ma, H. Luo, X. Li, Homogeneous dielectric barrier discharges in atmospheric air and its influencing factor, Phys. Plasmas 25 (2018) 1–5.
[19] Y.S. Golubovskii, V.A. Maiorov, J.F. Behnke, J. Tepper, M. Lindmayer, Study of the homogeneous glow-like discharge in nitrogen at atmospheric pressure, J. Phys. D Appl. Phys. 37 (2004) 1346–1356.
[20] D.K. Owens, R.C. Wendt, J. Appl. Polym. Sci. 13 (1969) 1741–1747.
[21] R. Scaffaro, F. Lopresti, A. Sutera, L. Botta, R.M. Pontarelli, G. Gallo, Plasma modified PLA electrospun membranes for actinorhodin production intensification in *Streptomyces coelicolor* immobilized-cell cultivations, Colloids Surf. B 157 (2017) 233–241.
[22] S. Dash, P.N. Murthy, L. Nath, P. Chowdhury, Kinetic modeling on drug release from controlled drug delivery systems, Acta Pol. Pharm. 67 (2010) 217–223.
[23] I. Yilgor, S. Bilgin, M. Isik, E. Yilgor, Tunable wetting of polymer surfaces, Langmuir 28 (2012) 14809–14814.
[24] S. de Valence, J. Tille, C. Chaabane, R. Gurny, M. Bochaton-Piallat, B.H. Walpoth, M. Moller, Plasma treatment for improving cell biocompatibility of a biodegradable polymer scaffold for vascular graft applications, Eur. J. Pharm. Biopharm. 85 (2013) 78–86.
[25] K.G. Kostov, T.M.C. Nishime, A.H.R. Castro, A. Toth, L.R.O. Hein, Surface modification of polymeric materials by cold atmospheric plasma jet, Appl. Surf. Sci. 314 (2014) 367–375.
[26] A. Kuzminova, M. Vandrovcová, A. Shelemin, O. Kylián, A. Choukourov, J. Hanuš, L. Bačáková, D. Slavínska, H. Biederman, Treatment of poly(ethylene terephthalate) foils by atmospheric pressure air dielectric barrier discharge and its influence on cell growth, Appl. Surf. Sci. 357 (2015) 689–695.
[27] K.G. Kostov, T.M.C. Nishime, L.R.O. Hein, A. Toth, Study of polypropylene surface modification by air dielectric barrier discharge operated at two different frequencies, Eur. Conf. Tech. 234 (2013) 60–66.
[28] D.L. Pavia, G.M. Lampman, G.S. Kriz, Introduction to Spectroscopy, fourth ed., Harcourt College Publishers, New York, 2001.
[29] T. Kupinski, β-Lactam antibiotics. Spectroscopy and molecular orbital (MO) calculations: part I. IR studies of complexation in penicillin-transition metal ion systems and semi-empirical PM3 calculations on simple model compounds, Spectrochim. Acta A 53 (1997) 2649–2658.
[30] C. Bisson-Boutelliez, S. Fontanay, C. Finance, F. Kadirvelraj, Preparation and physicochemical characterization of amoxicillin β-cyclodextrin complexes, AAPS PharmSciTech. 11 (2010) 574–581.
[31] S. Ling, Z. Qi, B. Watts, Z. Shao, X. Chen, Structural determination of protein-based polymer blends with a promising tool: combination of FTIR and STXM spectromicroscopic imaging, Phys. Chem. Chem. Phys. 16 (2014) 7741–7748.
[32] Y.P. Singh, N. Bhardwaj, B.B. Mandal, Potential of agarose/silk fibroin blended hydrogel for in vitro cartilage tissue engineering, ACS Appl. Mater. Interfaces 8 (2016) 21236–21249.
[33] H.S. Mansur, C.M. Sadahira, A.N. Souza, A.A.P. Mansur, FTIR spectroscopy characterization of poly (vinyl alcohol) hydrogel with different hydrolysis degree and chemically crosslinked with glutaraldehyde, Mater. Sci. Eng., C 28 (2008) 539–548.
[34] P. Bhattacharjee, B. Kundu, D. Naskar, T.K. Maiti, D. Bhattacharya, S.C. Kundu, Nanofibrous mammalian silk/PVA scaffold for osteoinduction and osseointegration, Biopolymers 103 (2015) 271–284.
[35] U. Habiba, T.C. Joca, T.A. Siddiquee, A. Salleha, B.C. Ang, A.M. Afifi, Effect of degree of deacetylation of chitosan on adsorption capacity and reusability of chitosan/polyvinyl alcohol/TiO_2 nano composite, Int. J. Biol. Macromol. 104 (2017) 1133–1142.
[36] L.I. Atanase, S. Binac, G. Riess, Effect of poly(vinyl alcohol-co-vinyl acetate) copolymer blockiness on the dynamic interfacial tension and dilatational viscoelasticity of polymer-anionic surfactant complex at the water-1-chlorobutane interface, Soft Matter 7 (2015) 2665–2672.
[37] A. Fridman, Plasma Chemistry, Cambridge University Press, Cambridge, 2008.
[38] J.H. Choi, I. Han, H.K. Baik, M.H. Lee, D.W. Han, J.C. Park, I.S. Lee, K.M. Song, Y.S. Lim, Analysis of sterilization effect by pulsed dielectric barrier discharge, J. Electrostat. 3 (2006) 17–22.
[39] G. Fridman, A. Gutsol, A.B. Shekhter, V.N. Vasilets, A. Fridman, Applied plasma medicine, Plasma Process Polym. 3 (2008) 503–533.
[40] N. Munakata, E. Hieda, K. Kobayashi, A. Ito, T. Ito, Action spectra in ultraviolet wavelengths (150–250 nm) for inactivation and mutagenesis of *Bacillus subtilis* spores obtained with synchrotron radiation, Photochem. Photobiol. 3 (1986) 385–390.
[41] D. Zhang, E.M. Dougal, M.S. Yeganeh, Effects of UV irradiation and plasma treatment on a polystyrene surface studied by IR-visible sum frequency generation spectroscopy, Langmuir 16 (2000) 4528–4532.
[42] A. Barth, Infrared spectroscopy of proteins, Biochim. Biophys. Acta 1767 (2007) 1073–1101.
[43] X. Qi, X. Yao, S. Deng, T. Zhou, Q. Fu, Water-induced shape memory effect of graphene oxide reinforced polyvinyl alcohol nanocomposites, J. Mater. Chem. A 2 (2014) 2240–2249.
[44] J. He, Y.T. Zhang, Modeling study on the generation of reactive oxygen species in atmospheric radio-frequency helium-oxygen discharges, Plasma Process. Polym. 9 (2012) 919–928.
[45] X. Hu, Z. Xu, C. Gao, Multifunctional, supramolecular, continuous artificial nacre fibres, Sci. Rep. 2 (2012) 1–8.
[46] C. Bao, Y. Guo, L. Song, Y. Hu, Poly(vinyl alcohol) nanocomposites based on graphene and graphite oxide: a comparative investigation of property and mechanism, J. Mater. Chem. 21 (2011) 13942–13950.

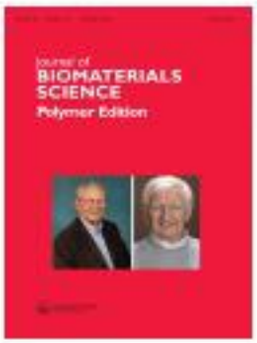

Journal of Biomaterials Science, Polymer Edition

ISSN: 0920-5063 (Print) 1568-5624 (Online) Journal homepage: https://www.tandfonline.com/loi/tbsp20

Chitosan coated silk fibroin surface modified by atmospheric dielectric-barrier discharge (DBD) plasma: a mechanically robust drug release system

Namita Ojah, Jyotishikha Deka, Saurav Haloi, Raghuram Kandimalla, Dolly Gogoi, Tapas Medhi, Manabendra Mandal, Gazi Ameen Ahmed & Arup Jyoti Choudhury

To cite this article: Namita Ojah, Jyotishikha Deka, Saurav Haloi, Raghuram Kandimalla, Dolly Gogoi, Tapas Medhi, Manabendra Mandal, Gazi Ameen Ahmed & Arup Jyoti Choudhury (2019) Chitosan coated silk fibroin surface modified by atmospheric dielectric-barrier discharge (DBD) plasma: a mechanically robust drug release system, Journal of Biomaterials Science, Polymer Edition, 30:13, 1142-1160, DOI: 10.1080/09205063.2019.1622844

To link to this article: https://doi.org/10.1080/09205063.2019.1622844

Accepted author version posted online: 21 May 2019.
Published online: 03 Jun 2019.

Submit your article to this journal

Article views: 31

View Crossmark data

Principal
Nowgong Girls' College
Nagaon :: Assam

Full Terms & Conditions of access and use can be found at
https://www.tandfonline.com/action/journalInformation?journalCode=tbsp20

Nowgong Girls' College ★ ESTD: 1962 ★ Nagaon :: Assam

JOURNAL OF BIOMATERIALS SCIENCE, POLYMER EDITION
2019, VOL. 30, NO. 13, 1142–1160
https://doi.org/10.1080/09205063.2019.1622844

Taylor & Francis
Taylor & Francis Group

Check for updates

Chitosan coated silk fibroin surface modified by atmospheric dielectric-barrier discharge (DBD) plasma: a mechanically robust drug release system

Namita Ojah[a], Jyotishikha Deka[a], Saurav Haloi[b], Raghuram Kandimalla[c], Dolly Gogoi[d], Tapas Medhi[b], Manabendra Mandal[b], Gazi Ameen Ahmed[a] and Arup Jyoti Choudhury[a]

[a]Laboratory for Plasma Processing of Materials, Department of Physics, Tezpur University, Tezpur, Assam, India; [b]Department of Molecular Biology and Biotechnology, Tezpur University, Tezpur, Assam, India; [c]Drug Discovery Laboratory, Institute of Advanced study in Science and Technology, Guwahati, Assam, India; [d]Central Instruments Facility, Indian Institute of Technology, Guwahati, Assam, India

ABSTRACT

The current study is designed to develop mechanically strong chitosan (Cs) coated silk based drug delivery system loaded with amoxicillin trihydrate (AMOX). For this purpose, surface modification of *Antherarea assama* silk fibroin (AASF) yarn is carried out using dielectric barrier discharge (DBD) oxygen (O_2) plasma at atmospheric pressure followed by coating with drug incorporated Cs (AASF/O_2/Cs-AMOX). It is observed that O_2 plasma treatment results in altering surface chemistry and morphology of silk fibroin surface which subsequently improves mechanical properties of AASF/O_2/Cs-AMOX yarn. The AASF/O_2/Cs-AMOX yarn exhibits strong antibacterial activities against gram-positive *Staphylococcus aureus* and gram-negative *Escherichia coli* bacteria. *In vitro* drug release profile reveals biphasic release behavior of AASF/O_2/Cs-AMOX yarn consisting of immediate followed by controlled and sustained release of AMOX up to the observation period of 168 hours. MTT cell viability study further reveals that O_2 plasma treatment and incorporation of AMOX do not have any adverse effect on cytocompatibility of AASF/O_2/Cs-AMOX yarn. Together, all these results suggest that AASF/O_2/Cs-AMOX yarn can be explored in treatment of bacterial infected wounds as potential surgical suture.

ARTICLE HISTORY
Received 6 February 2019
Accepted 21 May 2019

KEYWORDS
Chitosan; *Antherarea assama* silk fibroin; dielectric barrier discharge; oxygen plasma; drug delivery; antibacterial activity

Introduction

Polymer-based drug delivery systems (PDDSs) are promising technology for biomaterials engineering, clinical and healthcare applications due to their ability to enhance bioavailability of drugs, maximize the therapeutic efficacy of drug with minimum side-effects, control drug release rate, reduce systemic toxicity and facilitate rapid wound healing [1–3].

CONTACT Arup Jyoti Choudhury arupjchoudhury@gmail.com Laboratory for Plasma Processing of Materials, Department of Physics, Tezpur University, Tezpur, Assam, 784028, India.

© 2019 Informa UK Limited, trading as Taylor & Francis Group

Principal
Nowgong Girls' College
Nagaon :: Assam

Nowgong Girls' College ★ Nagaon ★ Assam ★ ESTD: 1962

With rapid development of materials engineering and processing technology, PDDSs have been developed into various forms, such as fibers/yarn, nano/micro-particles, microspheres, micelles, and hydrogels [1, 4]. In PDDSs, selection of polymer acting as a drug carrier with desirable properties such as non-toxicity, biocompatibility, biodegradability, and physico-chemical and thermal stability is very essential as it eventually plays critical role in determining the encapsulation efficacy, drug release profile and release mechanism of the drug delivery system [1, 3]. Development of novel and smart PDDSs comprising appropriate polymer carrier and therapeutic molecules can significantly improve their pharmacokinetic and pharmacodynamic properties as well as enhance targeted and sustained drug release kinetics [5].

Naturally derived polymers such as chitosan and silk fibroin display excellent biocompatibility, mechanical strength, non-cytotoxicity and non-inflammatory, biodegradability and physico-chemical properties which make them promising biomaterials for applications in tissue engineering, drug delivery and regenerative medicine [1, 3]. Chitosan is a natural polycationic linear polysaccharide and exhibits mucoadhesive, permeation enhancing, in situ gelling, and efflux pump inhibitory properties [6]. On the other hand, *Antheraea assama* silk fibroin (AASF), obtained from wild silkworms, has drawn considerable research interest due to its excellent mechanical properties, outstanding structural integrity, non-toxicity, slow biodegradability and biocompatibility [7]. However, AASF offers poor resistance against microbial growth and proliferation leading to biofilm formation on the surface which makes it a poor choice of material having a high risk of surgical site bacterial infections and as a result the prospect of clinical applications of AASF is far less explored.

Low temperature plasma is widely used in developing silk fibroin for various biomedical applications due to its efficacy in tailoring surface chemistry and morphology by controlling plasma kinetics and -surface interactions without affecting the bulk properties [8–13]. Plasma treatment has been proven to be extremely efficient in inducing surface activation and wettability of silk fibroin for improving bioadhesion and drug-loading efficiency [7, 9, 10]. It has been reported that argon plasma treatment can successfully immobilize drug onto silk fibroin nanofibrous scaffold thereby enhancing the osteogenic potential of silk fibroin nanofibers [11]. Another report shows that air plasma treatment enhances *in vivo* bone regenerative capacity of silk fibroin-based biomaterials [12]. Due to ability to modulate cell adhesion and proliferation behaviour, the fluorocarbon plasma treated silk fibroin nanofibrous membranes has been shown to be useful for biomedical applications such as a guided bone regeneration [13].

In this work, surface modification of AASF yarn is carried out using dielectric barrier discharge oxygen (O_2) plasma at atmospheric pressure followed by coating with drug-incorporated chitosan (Cs) with an aim of developing AASF/O_2/Cs-AMOX yarn as drug delivery system with enhanced mechanical properties. The mechanical properties, antibacterial activity and *in vitro* biocompatibility of AASF, AASF/O_2, AASF/Cs, AASF/O_2/Cs and AASF/O_2/Cs-AMOX yarns are evaluated and the results are correlated with surface chemistry and morphology. Additionally, drug release profile of AASF/O_2/Cs-AMOX yarn is also investigated *in vitro*. These investigations are conducted to explore the clinical applications of this novel AASF/O_2/Cs-AMOX yarn as suture mater

Principal
Nowgong Girls' College
Nagaon :: Assam
Nowgong Girls' College ★ ESD: 1962 ★ Assam

Experimental section

Materials

Antheraea assama silk fibroin (AASF) in the form of multifilament yarn of average diameter 400 μm is obtained from Central Silk Board, Guwahati, Assam, India. Prior to use, AASF yarn is rinsed three times in deionized water, dried in ambient environment (temperature: 25 °C; relative humidity: 50%) and stored in a desiccator. Amoxicillin trihydrate (AMOX), chitosan (Cs, low molecular weight; ~75–85% deacetylated), Dulbecco's modified eagle's medium (DMEM) and dimethyl sulfoxide (DMSO) are purchased from Sigma Aldrich. Acetic acid (glacial) and phosphate buffered saline (PBS) are purchased from Merck. All chemical reagents are analytical reagent grade and used as received. A Millipore Milli Q system (USA) is used to produce ultrapure distilled water.

Methods

Plasma treatment

Surface functionalization of AASF yarn has been carried out using dielectric barrier discharge (DBD) O_2 plasma. The experimental details of the DBD set-up have been reported elsewhere [14]. Briefly, the DBD discharge chamber comprises two copper electrodes (thickness = 5 mm, surface area = 25 cm × 25 cm) that are placed within a cubic enclosure. Both the electrodes are covered with glass plates (thickness = 3 mm) and the plasma is generated at a discharge gap of 6 mm between the two glass plates. The upper electrode is connected to a high voltage source (0–40 kV, 50 Hz, Zenoics Systech, India), while the lower electrode is grounded. The O_2 (Assam Air Products, purity > 99.99%) gas is allowed to enter the discharge chamber and the gas flow rate (standard liter per minute, slpm) is controlled by a digital mass flow controller (Alicat Scintific, USA). The surface treatment of AASF yarn is carried out for 60 seconds and after that the sample is taken out of the discharge chamber and placed in a vacuum desiccator for further characterizations.

The plasma treatment induces surface hydrophilicity to AASF/O_2 yarn, as the contact angle of water on AASF and AASF/O_2 yarns is measured to be 96.2° ± 2.1° and 29.3° ± 1.1° respectively. The surface wettability of the samples is assessed by dynamic contact angle measurement using tensiometer (Data physics, DCAT-11, Germany). The hydrophilic nature of AASF/O_2 yarn remains stable in air (temperature: 25 °C; relative humidity: 50%) up to 6 days and after that it shows mild hydrophobic recovery due to increase in contact angle of water. Based on these observations, the surface characterization of AASF/O_2 yarn is completed well before 2–3 days of O_2 plasma post-treatment.

Optimization of plasma discharge conditions

The discharge conditions (applied voltage and O_2 flow rate) are optimized to obtain homogeneous and stable O_2 plasma at atmospheric pressure. The O_2 plasma discharge is obtained at different values of discharge voltage ranging from 10 to 16 kV (at regular interval of 2 kV) and O_2 flow rate ranging from 0.5 to 3

Principal
Nowgong Girls' College
Nagaon :: Assam

Nowgong Girls' College
Nagaon :: Assam
ESTD 1962

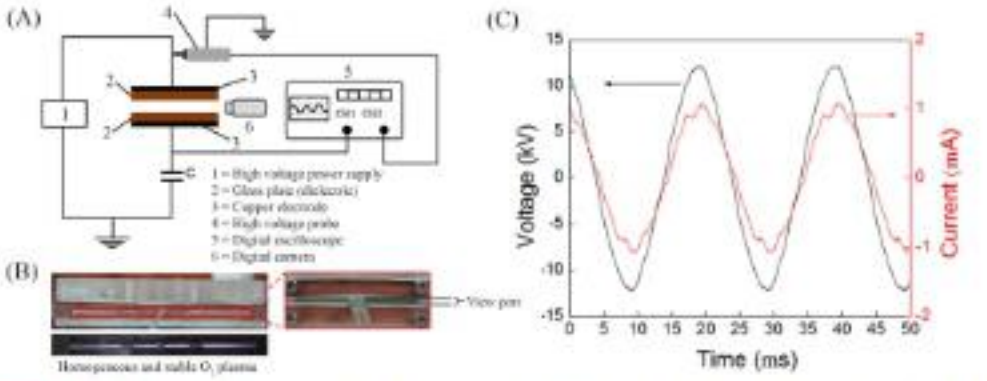

Figure 1. (A) Schematic representation of experimental arrangement for measurement of applied voltage and discharge current. (B) Discharge image and (C) applied voltage and discharge current waveforms of stable homogeneous O_2 plasma.

slpm (at regular interval of 0.5 slpm), respectively. The discharge homogeneity in O_2 plasma is monitored using a digital single-lens reflex camera (DSLR, Nikon D7200, Japan) with the exposure time of 1/8000 s mounted on a stable optical platform and the discharge characteristics (voltage and current waveforms) are studied using a high voltage probe (Tetronix, P6015A, 1000:1) and a digital oscilloscope (Tetronix, TPS2024B, 200 MHz). The plasma discharge is observed from the side view of the discharge chamber. The voltage and current waveforms are recorded by the digital oscilloscope. The experimental arrangement to study the waveforms of the applied voltage and discharge current is shown in Figure 1A. The voltage applied to the upper electrode is measured via the high voltage probe whereas the discharge current is measured by placing a 2 nF capacitor (C) between the bottom electrode and the ground, respectively. At applied voltage of 12 kV and O_2 flow rate of 2 slpm, homogeneous and stable O_2 plasma is obtained, as revealed from image of the discharge (Figure 1B) and also characterized by a single current pulse per half-cycle of the applied voltage with the same periodicity (Figure 1C) [15, 16]. The AASF yarn is placed in between the two electrodes and after that surface modification is performed at the above optimized discharge conditions. The homogeneity of the DBD discharge further ensures uniform surface treatment of AASF yarn exposed to O_2 plasma.

Preparation of Cs-AMOX coated AASF/O_2 yarn

A solution of Cs is prepared by dissolving Cs in 10% (v/v) glacial acetic acid at a concentration of 3 mg/ml. To this solution, AMOX (25% (w/w) of Cs dissolved in acetic acid) is added and the mixture is stirred for 15 minutes (200 rpm) at ambient environment (temperature: 25 °C and relative humidity: 50%). The addition of this specific amount of AMOX to Cs solution is based on its minimum inhibitory concentration (MIC) values against *E. coli* (37 µg/ml) and *S. aureus* (39 µg/ml), respectively. After plasma treatment, AASF/O_2 yarn is immediately taken out of the discharge chamber and placed in a container filled with Cs-AMOX mixture in order to evaluate any possible effect of air or humidity on its surface properties. Afterwards the AASF/O_2 yarn

Principal
Nowgong Girls' College
Nagaon :: Assam
Nowgong Girls' College
Nagaon :: Assam

is passed across two Teflon rollers to ensure uniform coating onto the surface with good repeatability and reproducibility. The gap between the rollers is adjusted mechanically so as to control the coating thickness and exert pressure on the yarn thereby enabling more drug-incorporated Cs (Cs-AMOX) to spread through the spaces among the inner fibers. Coating repetitions of the yarn are conducted thrice and after that the Cs-AMOX coated AASF/O_2 (AASF/O_2/Cs-AMOX) yarn is dried in vacuum at room temperature (25 °C) and placed in a vacuum desiccator. In this work, the average thickness of Cs layer coated on AASF/O_2 yarn is measured to be 14.54 ± 0.84 µm.

Characterization techniques

Field emission scanning electron microscope (FESEM, SIGMAVP, Carl Zeiss, Germany) is used to observe the surface morphologies of the test samples (AASF, AASF/O_2, AASF/O_2/Cs and AASF/O_2/Cs-AMOX yarns). Prior to FESEM examination, the samples are coated with gold/palladium alloy in sputtered coater (SC7620, Emitech) in a low vacuum (2×10^{-2} mbar).

The chemical composition of the test samples is investigated using attenuated total reflectance Fourier transform infrared (ATR-FTIR) spectroscopy (IMPACT 410, NICOLET, USA). The spectra are obtained from a 200 µm diameter sampling area, using an average of 32 scans, at 4 cm^{-1} spectral resolution. Spectra are collected in transmittance mode with spectral region of 4000–650 cm^{-1}.

The surface chemistry of the test samples is further investigated by X-ray photoelectron spectroscopy (XPS, Omicron, Germany). The XPS studies are conducted in a UHV chamber (base pressure $< 2 \times 10^{-10}$ mbar) using a VG make, CLAM-2 model hemispherical analyzer with a non-monochromatic twin Mg X-ray source. With Mg K_α line (1253.6 eV), detailed spectra are collected followed by high-resolution scan of relevant core level and valence level photoemission peaks of all the main elements. The binding energy (BE) scale is calibrated using the peaks of Au $4f_{7/2}$ (BE = 84.0 eV) and Ag $3d_{5/2}$ (BE = 368.2 eV) from polycrystalline gold and silver foils, respectively. The binding energy of the hydrocarbon component of the C_{1s} spectrum at 285.0 eV, corresponding to organic/polymeric materials, is used as a calibration to compensate for charging effects [17]. The XPS peak fitting is performed by using XPSPEAK 4.1 software.

The mechanical properties of the test samples are evaluated using a universal testing machine (INSTRON 4204, USA) at a constant speed of 10 mm min^{-1} with a 10 kN load (temperature: 25 °C and relative humidity: 50%). The specimens are cut into strips of 10 mm × 50 mm (thickness = 0.25 mm) and a gauge length of 20 mm is considered. For each sample, data is taken for five times and the average values of Young's modulus, tensile strength and elongation at break (%) are evaluated from stress-strain curves. The data are presented as mean ± standard deviation (SD).

Antibacterial test

The antibacterial activities of AASF, AASF/O_2, AASF/O_2/Cs and AASF/O_2/Cs-AMOX yarns are evaluated against gram-positive *S. aureus* (ATCC 25923) and gram-negative *E. coli* (ATCC 25922) bacteria using standard agar disk diffusion method. The bacteria are

Principal Nowgong Girls' College Nagaon :: Assam
Nowgong Girls' College ★ 1962 ★ Nagaon :: Assam

first inoculated into Luria Bertani (LB) nutrient broth (1% peptone, 0.5% yeast extract, 0.5% NaCl, pH 7.0) and kept in an incubator at 37 °C. Bacterial cultures are prepared on solidified Mueller-Hinton agar (MHA) dispensed into sterile Petri dishes with proper care to ensure uniform growth throughout the dish. The samples are carefully placed and pressed lightly against the surface of the agar using a sterilized forceps. After incubation in a bacteriological oven at 37 °C for 24 hours, the growth inhibition is quantified by calculating the diameter of each sample inhibition zone. The experiment is carried out in triplicate and repeated thrice and the result is reported as mean ± standard deviation (SD).

Swelling behaviour

The swelling behavior of AASF/O_2/Cs yarn is studied by immersing specific amount of the dried sample in 10 mL of phosphate buffered saline (PBS, pH = 7.4) at 37 °C until swelling equilibrium is achieved. The samples are taken out at regular intervals of time and weighed after removing the excess surface water by blotting with filter paper and then placed in the same bath. The degree of swelling (Q) is then calculated from the following equation,

$$Q = \frac{W_w - W_d}{W_d} \tag{1}$$

where W_w and W_d are the weights of swollen and dry sample, respectively. The experiment is conducted in triplicate and the result is reported as mean ± standard deviation (SD).

Drug release study

The AMOX release profile from AASF/O_2/Cs-AMOX yarn is investigated by immersing specific amount of the sample in 10 ml phosphate-buffered saline (PBS, pH = 7.4) at 37 °C. After certain intervals of time, 1 ml aliquots are collected for measurements and replaced with equal volume of fresh PBS to maintain sink conditions. The amount of drug released to the PBS medium is determined from a calibration curve of AMOX in PBS by measuring the UV absorbance of the removed aliquots (UV-visible spectrophotometer, Shimadzu, UV 1800) at a wavelength of 273 nm. The percentage drug releases from AASF/O_2/Cs-AMOX yarn is calculated from the following relation,

$$\text{Amount of drug release } (\%) = \frac{m_t}{m_0} \times 100 \tag{2}$$

where m_t is the amount of AMOX released at specific time t and m_0 is the total amount of drug loaded in AASF/O_2/Cs-AMOX yarn. Three replicates are performed in this experiment and the results are presented as the mean ± standard deviation (SD).

To investigate the release kinetics of AMOX from AASF/O_2/Cs-AMOX yarn, the experimental results have been fitted with the following Weibull model which is suitable for describing drug release from polymer matrix [18],

$$F = 1 - e^{-\frac{t}{\tau}} \tag{3}$$

Principal
Nowgong Girls' College
Nagaon :: Assam

Nowgong Girls' College ★ Nagaon :: Assam ★ ESTD: 1962

where F is the fraction of drug released to the PBS medium at specific time t, b describes the shape of the drug release curve and $K_H = \frac{1}{a}$ denotes the release rate constant [18].

In vitro cytotoxicity

The possible cytotoxic effect of AASF, AASF/O_2, AASF/O_2/Cs and AASF/O_2/Cs-AMOX yarns are evaluated by the MTT (3-[4,5-dimethylthiazole-2-yl]-2,5-diphenyltetrazolium bromide) cell viability assay in L929 mouse fibroblast cells. 1×10^4 cells/well are seeded in a 96 well cell culture plate containing 100 µl DMEM supplemented with 10% fetal bovine serum and incubated for 72 hours at 37 °C. After 24, 48 and 72 hours of incubation, the supernatant of each well is replaced with MTT diluted in serum-free medium and the plates are incubated for another 4 hours at 37 °C. Further, 100 µl DMSO is added to each well to dissolve the blue formazan crystals and the absorbance (570 nm) is accordingly measured using a UV-visible spectrophotometer (Shimadzu, UV 1800, Japan). The percentage cell viability is calculated by using the following relation,

$$\text{Cell viability } (\%) = \frac{N_t}{N_c} \times 100 \tag{4}$$

where N_t is the absorbance of the treated cells and N_c is the absorbance of the untreated cells. All experiments are performed three times with three replicates for each sample and control and the results are reported as mean ± standard deviation (SD).

Statistical analysis

The statistical analyses are performed using one-way ANOVA with post-hoc Tukey analysis (GraphPad Prism 7). The data are represented as mean ± standard deviation (SD). The data in the figures are marked by an asterisk (*) for $p < 0.05$ and double asterisks (**) for $p < 0.01$.

Results and discussion

Surface morphological analysis

The surface morphology of AASF, AASF/O_2, AASF/O_2/Cs and AASF/O_2/Cs-AMOX yarns are characterized by FESEM. Figure 2A–D show typical FESEM images of the test samples. As seen from Figure 2A, surface morphology of AASF is observed as smooth, compact, and without any crack or pores. However, O_2 plasma treatment results in formation of nano-structured roughness on the surface of AASF which is attributed to the etching of the silk fibroin surface by reactive oxygen species (O, O^*, O^-, O_2^- etc.) that are generated in the discharge chamber (Figure 2B) [19]. The FESEM image of AASF/O_2/Cs yarn (Figure 2C) reveals uniform and smooth surface of Cs coated onto AASF/O_2. However, incorporation of AMOX in Cs solution and subsequent coating of AASF/O_2 with Cs-AMOX mixture results in introducing roughness on the surface AASF/O_2/Cs-AMOX yarn (Figure 2D). The presence of

Certified
Principal
Nowgong Girls' College
Nagaon :: Assam
Nowgong Girls' College
ESTD: 1962
Nagaon :: Assam

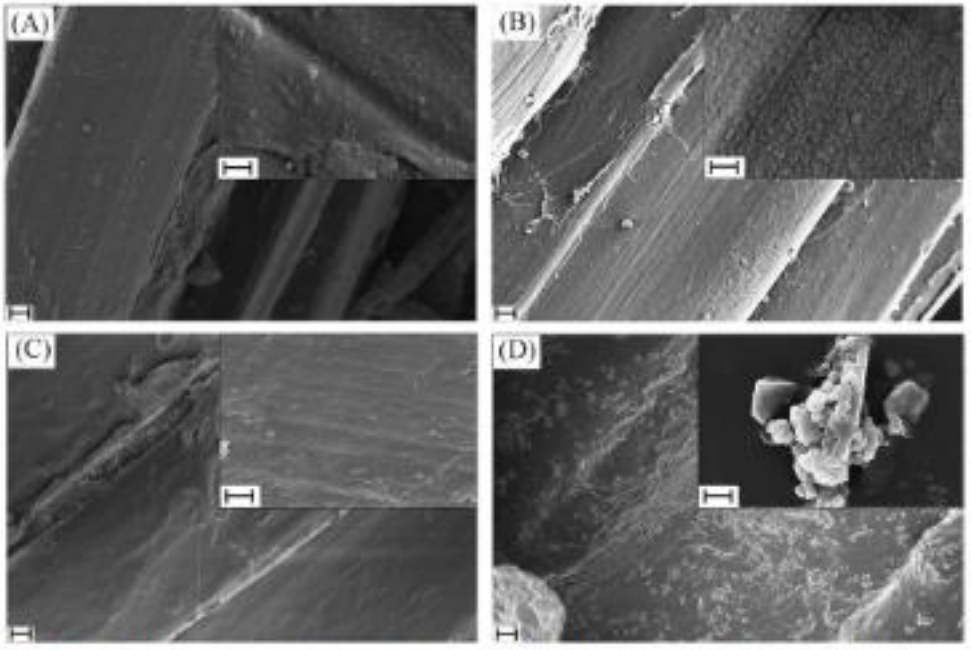

Figure 2. FESEM images of (A) AASF, (B) AASF/O_2, (C) AASF/O_2/Cs and (D) AASF/O_2/Cs-AMOX yarns (scale bar represents 2 μm). The inset of each corresponding yarn shows the high magnification FESEM image (scale bar represents 100 nm).

AMOX is observed on the surface of AASF/O_2/Cs-AMOX yarn where the drug molecules are adhered to the Cs matrix.

Chemical and structural analyses

The ATR-FTIR spectra of AASF yarn, AMOX, Cs and AASF/O_2/Cs-AMOX yarn are shown in Figure 3A. The infrared absorption spectrum of AASF reveals characteristic absorption peaks of amide I (C=O stretching vibration), amide II (N–H bending vibration) and amide III (C=O bending/C–N stretching vibration) at 1621 cm^{-1}, 1515 cm^{-1} and 1231 cm^{-1}, respectively corresponding to β-sheet structure [20]. The broad absorption band in the range of 3100–3700 cm^{-1} is due to the OH stretching vibration that overlapped with the NH bands of amine and amide of AASF and similar band can be observed in the spectrum of Cs [21]. The spectrum of AMOX shows absorption bands in the range of 3100–3700 cm^{-1} which is attributed to NH and OH stretching of the primary amino groups [21]. In addition, the spectrum shows absorption peaks at 2972 cm^{-1} and 2914 cm^{-1}, referring to the symmetric and asymmetric CH stretching vibration of alkyl groups, characteristic absorption peak at 1776 cm^{-1} due to β-lactum ring, and peaks at 1688 cm^{-1}, 1482 cm^{-1} and 1260 cm^{-1}, corresponding to the C=O stretching vibration (amide I), N-H bending of the secondary amine/C=C stretching of aromatic ring and C-N stretching of primary amine, respectively [22, 23]. The peaks at 1586 cm^{-1} and 1398 cm^{-1} which correspond to N-H bending vibration of primary amide (amide II) and symmetrical stretching vibration of carboxylate (COO^-) groups, are also observed [21]. As seen from the

Principal
Nowgong Girls' College
Nagaon :: Assam
Nowgong Girls' College
ESTD: 1962
Assam

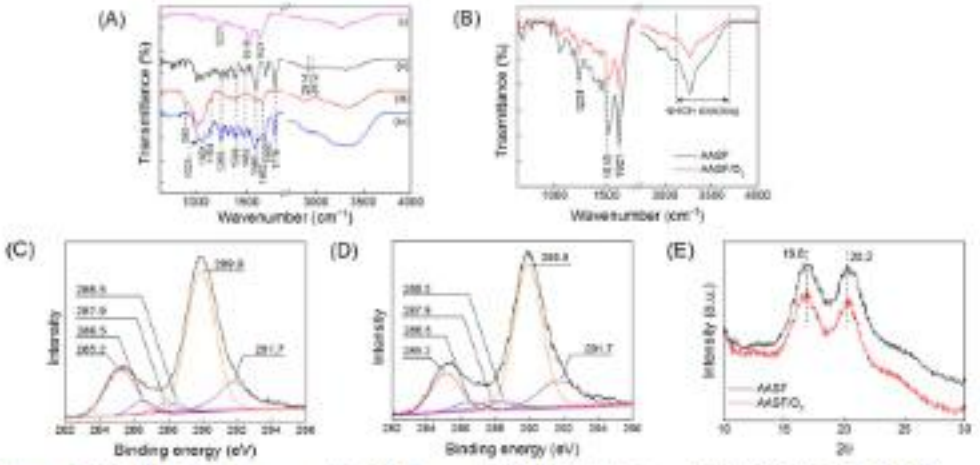

Figure 3. (A) ATR-FTIR spectra of (i) AASF yarn, (ii) AMOX, (iii) Cs and (iv) AASF/O_2/Cs-AMOX yarn. (B) ATR-FTIR spectra of AASF and AASF/O_2 yarns. Deconvoluted C_{1s} peaks of (C) AASF and (D) AASF/O_2 yarns. (E) XRD spectra of AASF and AASF/O_2 yarns.

spectrum of Cs, the absorption peaks at 1652 cm^{-1}, 1586 cm^{-1} and 1260 cm^{-1} are characteristic of Cs and are assigned to amide I, amide II and amide III, respectively [21]. In addition, the absorption peaks at 1154 cm^{-1}, 1061 cm^{-1}, 1023 cm^{-1} and 893 cm^{-1} are characteristic of chitosan's saccharide structure [24]. Analysis of the spectrum of AASF/O_2/Cs-AMOX yarn reveals the presence of characteristic absorption peaks/bands corresponding to both Cs and AMOX. Besides, the absence of characteristic peaks of AASF in the spectrum of AASF/O_2/Cs-AMOX yarn may indicate uniform coating of Cs on the surface of AASF/O_2.

To investigate the effect of O_2 plasma treatment on the surface chemistry of AASF, the ATR-FTIR spectra of AASF and AASF/O_2 are shown in Figure 3B. The results show that O_2 plasma does not seem to induce any kind of conformational changes in protein structure of AASF as no shift in the peak position of amide I, amide II and amide III is observed. However, in the higher wavenumber region (3100–4000 cm^{-1}) O_2 plasma treatment resulted in broadening of the band corresponding to hydrogen-bonded OH group and shifting towards lower wavenumber which indicates incorporation of polar functional groups on to the surface of AASF. This finding is accounted for generation of different reactive oxygen species during O_2 plasma treatment and their strong interaction with AASF thereby leading to formation of oxygen-containing (polar) functional groups at the surface. To confirm incorporation of polar groups on to surface of AASF/O_2, surface analysis of AASF and AASF/O_2 is further carried out by XPS. Table 1 presents the surface composition determined from XPS analysis. It is observed that after O_2 plasma treatment, the oxygen (O) content (at %) on the surface of AASF/O_2 is increased by ~ 4% whereas the carbon (C) content (at %) decreases by ~ 4.5%. The variation in the percentage of nitrogen (N) remains more or less unchanged. Also, O/C ratio for AASF/O_2 is found to be higher than observed for AASF. These data indicate that O_2 plasma treatment increases incorporation of oxygen-containing functional groups onto the surface of AASF. For better understanding the chemical environment at the surface of AASF and AASF/O_2

Principal
Nowgong Girls' College
Nagaon :: Assam
Nowgong Girls' College
ESD 1962
Nagaon :: Assam

Principal
Nowgong Girls' College
Nagaon :: Assam

Table 1. Elemental composition (atomic %) and relative concentration (%) of components of the resolved C_{1s} spectra of AASF and AASF/O_2 yarns determined by XPS (mean ± standard deviation (SD)).

	Atomic composition (at %)					Relative concentration (%)					
Sample	C	O	N	O/C	N/C	285.2 eV (C-C/C-H)	286.5 eV (C-O/C-O-C)	287.9 eV (C=O)	288.5 eV (O-C-O)	289.9 eV (O-C=O)	291.7 eV (O-CO=O)
AASF	89.20 ± 2.85	8.10 ± 1.02	2.70 ± 0.66	0.09	0.03	19.38 ± 0.84	3.77 ± 0.51	3.67 ± 0.63	2.90 ± 0.47	54.41 ± 1.01	15.87 ± 0.76
AASF/O_2	84.69 ± 3.21	12.21 ± 1.96	3.10 ± 0.87	0.15	0.04	14.09 ± 1.11	5.04 ± 0.71	4.47 ± 0.52	4.02 ± 0.61	55.34 ± 1.14	17.04 ± 1.04

Nowgong Girls' College
ESTD: 1962
Nagaon :: Assam

the high resolution C_{1s} spectra of the samples are fitted in different peaks (Figure 3C and D). The deconvoluted C_{1s} spectra show the presence of five components corresponding to the peaks at 285.2 eV (C-C/C-H), 286.5 eV (C-O/C-O-C), 287.9 eV (C = O), 288.5 eV (O-C-O), 289.9 eV (O-C = O) and 291.7 eV (O-CO = O), respectively [25]. The relative percentage concentration of components of the resolved C_{1s} spectra is shown in Table 1. The results reveal that the relative percentage of the oxygen-containing components that are present on the surface of AASF/O_2 is higher as compared to AASF. This is attributed to the surface oxidation of AASF by O_2 plasma which results in abstraction of hydrogen from alkyl group and subsequent decrease in the relative percentage of C-C/C-H component on the surface of AASF/O_2 [26, 27].

To further study the crystal structure, XRD analysis of AASF and AASF/O_2 is performed (Figure 3E). The XRD curve of AASF shows two broad peaks at 16.8° and the second peak at 20.2° which are characteristics of β-sheet secondary conformation and β-sheet crystalline structure [28]. No change in the crystal structure of AASF is observed after O_2 plasma treatment thereby underlining the merit of low temperature plasma in surface modification process where plasma treatment only tailors the surface chemistry without affecting the inherent physical structure of polymer.

Mechanical properties

The mechanical properties play crucial role to the performance of polymeric biomaterials in medical and clinical applications. In this work, tensile strength, Young's modulus and elongation at break (%) of AASF, AASF/O_2, AASF/Cs and AASF/O_2/Cs yarn are evaluated, and the results are presented in Table 2. As revealed from Table 2, the tensile strength and Young's modulus for AASF/O_2 yarn are higher as compared to AASF which is attributed to the hydrogen bonding interaction between polar groups and silk fibroin surface leading to efficient load transfer in the yarn. The formation of hydrogen bond is attributed to the presence of oxygen containing functional groups which are incorporated onto the surface of AASF through generation of active plasma species during O_2 plasma treatment. However, the elongation at break has been observed to be decreased after plasma treatment which indicates an increase in stiffness of AASF/O_2 yarn. The observed increase in tensile strength and Young's modulus in AASF/O_2/Cs yarn, as compared to AASF/Cs yarn, also indicates strong hydrogen bonding interactions between silk fibroin surface and Cs molecules induced by O_2 plasma [14]. A schematic of hydrogen bonding interaction between polar groups present on silk fibroin surface and Cs molecules leading to improved mechanical properties of AASF/O_2/Cs yarn is presented in Figure 4.

Table 2. Mechanical properties of AASF, AASF/O_2, AASF/Cs and AASF/O_2/Cs yarns.

Sample	Tensile strength (GPa)	Young's Modulus (GPa)	Elongation at [illegible]
AASF	2.61 ± 0.24	19.58 ± 1.27	56.7[illegible]
AASF/O_2	2.83 ± 0.21	35.46 ± 2.20	54.[illegible]
AASF/Cs	2.89 ± 0.31	38.20 ± 3.10	51.[illegible]74
AASF/O_2/Cs	3.66 ± 0.23	45.08 ± 2.11	48.[illegible]10

C.T.C.
Principal
Nowgong Girls' College
Nagaon :: Assam
Nowgong Girls' College
ESTD: 1962
Nagaon :: Assam

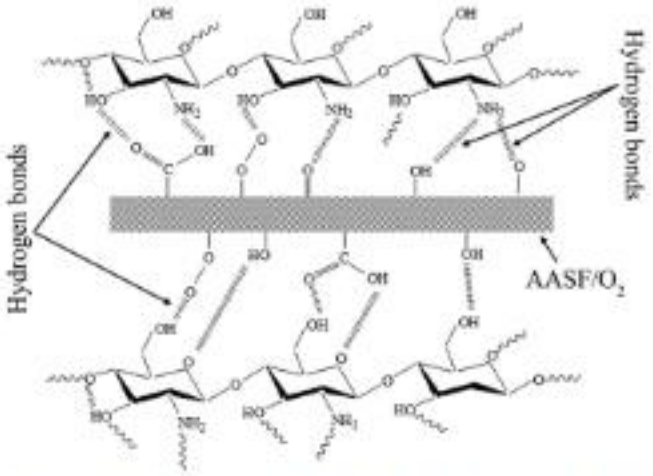

Figure 4. Schematic showing hydrogen bonding interaction between polar groups present on AASF/O_2 surface and Cs molecules.

Moreover, it has been observed that O_2 plasma treatment induces nanoscale pattern surface roughness in AASF/O_2 yarn [29]. The formation of surface roughness results in high degree of friction between fiber to fiber thereby leading to higher mechanical properties of AASF/O_2 as compared to AASF yarn. Besides, during Cs coating process, Cs solution penetrates the available spaces among the fibers and spread throughout the surface of the fibers comprising AASF. In case of AASF/O_2, the observed surface roughness provides better mechanical interlocking between the fibers as well as fiber and Cs matrix which subsequently enhances mechanical performance of AASF/O_2/Cs over AASF/Cs yarn [30, 31].

Antimicrobial test

The AASF, AASF/O_2, AASF/O_2/Cs and AASF/O_2/Cs-AMOX yarns are subjected to the antibacterial activity studies with the selected microorganisms and the results are shown in Figure 5A–P. The FESEM image corresponding to each sample is also presented in Figure 5A–P for better understanding. It is evident that both the microorganisms grow and proliferate around AASF and AASF/O_2/Cs yarn after observation period of 24 hours. Besides, O_2 plasma treatment does not seemed to improve the antibacterial activity of AASF yarn. In contrast, antibacterial activity of AASF/O_2/Cs-AMOX yarn is demonstrated by the formation of the zone of inhibition in the agar plate against the microorganisms. It is observed that AASF/O_2/Cs-AMOX yarn shows comparatively higher inhibition activity against *E. coli* than *S. aureus* as clearly indicated by the size of zone of inhibition. The results indicate that AMOX, which is a broad-spectrum antibiotic, is highly effective against both gram-positive and gram-negative bacteria as compared to penicillin which is more sensitive to gram-positive than gram-negative bacteria, as reported in the literature [32].

The antibacterial activity of AASF/O_2/Cs-AMOX yarn is further assessed at different time interval against *E. coli* (Figure 5Q) and *S. aureus* (Figure 5R) respectively. It is observed that the AASF/O_2/Cs-AMOX yarn shows measurable zone of inhibition

Principal
Nowgong Girls' College
Nagaon :: Assam
Nowgong Girls' College ESTD: 1962 Assam

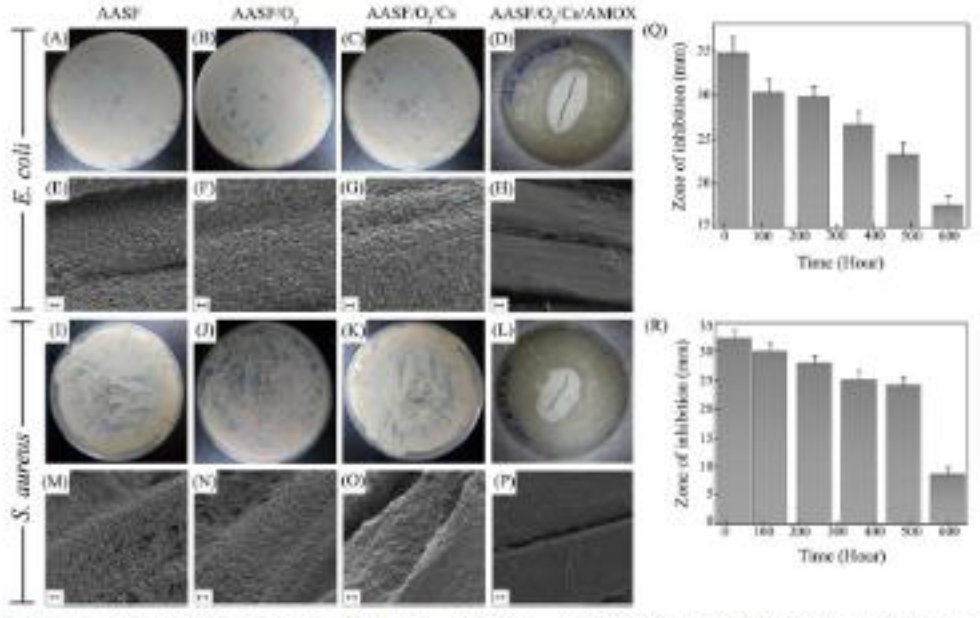

Figure 5. Antibacterial activities of AASF, AASF/O_2, AASF/O_2/Cs and AASF/O_2/Cs-AMOX yarns against (A)-(D) *E. coli* and (I)-(L) *S. aureus* respectively. Typical FESEM images show surface morphologies of AASF, AASF/O_2, AASF/O_2/Cs and AASF/O_2/Cs-AMOX yarns against (E)-(H) *E. coli* and (M)-(P) *S. aureus*, respectively (scale bar represents 2 μm). The variation of zone of inhibition of AASF/O_2/Cs-AMOX yarn against (Q) *E. coli* and (R) *S. aureus* as a function of observation time. Values represent mean ± SD of three batches.

against both the bacteria up to 600 hours (25 days) and finally bacterial growth begins to occur on the yarn after 26 days. The prolonged antibacterial activities of AASF/O_2/Cs-AMOX yarn against both *E. coli* and *S. aureus* bacteria are attributed to the sustained drug release from the Cs matrix. Several studies report on similar surgical sutures where the antibacterial zones of inhibition are observed to be smaller than that shown by AASF/O_2/Cs-AMOX yarn and the zones vanishes within 10 days of incubation period [33–35]. It is therefore evident that AASF/O_2/Cs-AMOX yarn can be very effective in preventing bacterial infection of surgical site in situations where longer treatment time is required.

In vitro drug release study

In vitro drug release profile of AASF/O_2/Cs-AMOX yarn is shown in Figure 6A. The inset of Figure 6A shows the calibration curve of AMOX in PBS medium (pH = 7.4) at 37 °C. The AMOX release profile from AASF/O_2/Cs-AMOX yarn is characterized by a biphasic pattern showing an initial burst release within 24 hours of immersion reaching around 55% followed by a sustained release (76%) up to the observation period of 168 hours. After 192 hours of observation period, the release of AMOX becomes slow and reaches 78% up to 336 hours after which a plateau is attained. The drug release behavior is related to the distribution of AMOX in both at the outer and inner surface of Cs during blending and subsequent coating on AASF/O_2 yarn. The

Principal
Nowgong Girls' College
Nagaon :: Assam
Nowgong Girls' College
ESTD: 1962
Nagaon :: Assam

Nowgong Girls' College * Nagaon :: Assam * ESTD: 1962
Principal
Nowgong Girls' College
Nagaon :: Assam

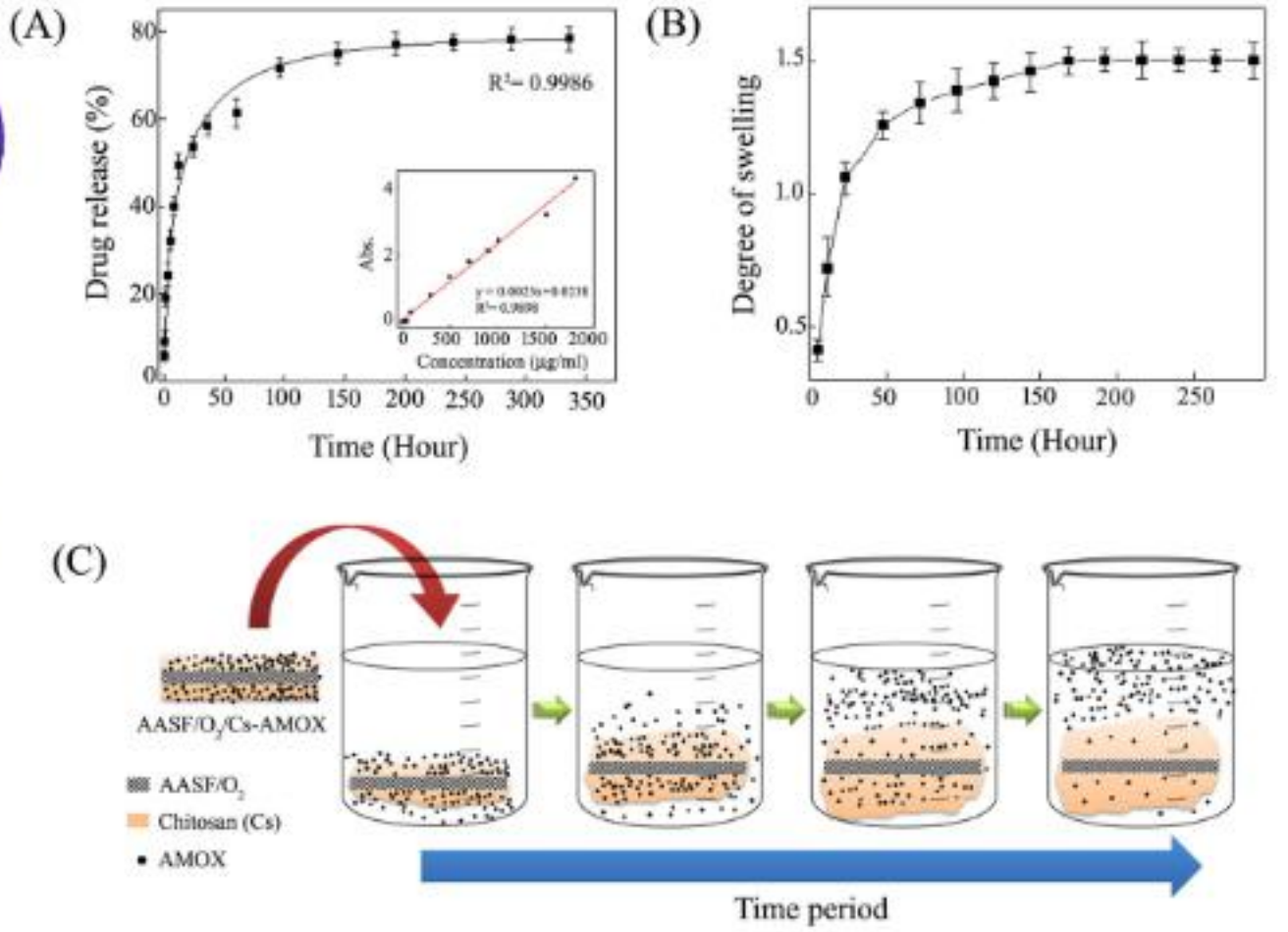

Figure 6. (A) Variation of AMOX release (%) in PBS medium as a function of time. Inset shows the calibration curve of AMOX concentration in PBS medium. (B) Variation of degree of swelling of Cs in PBS medium as a function of time. Values represent mean ± SD of 3 batches. (C) Schematic showing swelling of Cs in PBS medium resulting in release of AMOX from AASF/O_2/Cs-AMOX yarn.

rapid initial burst release is therefore attributed to desorption of AMOX which is weakly bound to the relatively large surface of Cs. In contrast, diffusion of AMOX through the Cs matrix is the determining factor in the observed sustained release characteristic of AASF/O_2/Cs-AMOX yarn. From the drug release profile, the concentration of AMOX released to PBS medium at observation period of 24 hours is evaluated to be 38.4 µg/ml which is found to be closed to the respective MIC value of AMOX against *E. coli* (37 µg/ml) and *S. aureus* (39 µg/ml). This finding can further be corroborated with the results shown in Figure 5Q and R where maximum value of zone of inhibition, corresponding to AASF/O_2/Cs-AMOX yarn, can be observed after 24 hours of incubation against *E. coli* and *S. aureus*, respectively.

The diffusion of AMOX from Cs matrix is ascribed to the swelling of Cs in PBS medium. It has been reported that when Cs is immersed in PBS, the glass transition temperature of Cs starts decreasing with time and become equal to the temperature of the medium. During the transition process the molecular chains of chitosan also begin to relax and PBS starts penetrating the Cs matrix thereby resulting in swelling of Cs [36–38]. The swelling of Cs gradually increases and eventually saturates with incubation time thereby resulting in slow but sustained release of drug over an extended period of time. To validate the observation, the assessment of the swelling ability of Cs coated AASF/O_2 yarn is carried out in this work. Figure 6B shows the variation of degree of swelling (Q) in AASF/O_2/Cs yarn as a function of time. The Q value for AASF/O_2/Cs yarn increases with time and reaches equilibrium within 200 hours. During the experimental period no weight loss of Cs is observed which is attributed to its rigid crystalline structure that makes it insoluble in aqueous medium (pH > 6–6.5). These findings suggest that the sustained release of AMOX from AASF/O_2/Cs-AMOX yarn indeed depends on swelling behavior Cs in PBS medium. A schematic showing the release of AMOX from AASF/O_2/Cs-AMOX yarn at various time of observation is shown in Figure 6C.

The release profile of AASF/O_2/Cs-AMOX yarn is further investigated to understand the release kinetics of AMOX from the yarn. For this purpose, the release profile in Figure 6A is best fitted with the Weibull model which is used to analyze the release profile of matrix-type drug delivery system. The drug release rate constant (K_H) as determined by fitting the experimental data with the kinetic drug model is found to be 0.052 h^{-1}. From the fitted mathematical model, the value of b is found to be close to 1.04 which reveals that the release profile of AASF/O_2/Cs-AMOX yarn follows the exponential release kinetics of drug from polymer-matrix by obeying Fick's first law of diffusion.

Cytotoxicity assay

The *in vitro* cytocompatibilities of AASF, AASF/O_2, AASF/O_2/Cs and AASF/O_2/Cs-AMOX yarns against L929 mouse fibroblast cells are evaluated using MTT assay. As shown in Figure 7, the cell viabilities after 24 hours are over 95% for all test samples, indicating the non-toxicities and good biocompatibilities of the yarns toward cells. After 48 hours of culture, cell viability on AASF/O_2 yarn (95.1 ± 1.82%) is slightly higher than AASF (93.4 ± 1.77%), AASF/O_2/Cs (92.3 ± 1.85%) and AASF/O_2/Cs-

Nowgong Girls' College ESTD: 1962 Nagaon :: Assam
Principal
Nowgong Girls' College
Nagaon :: Assam

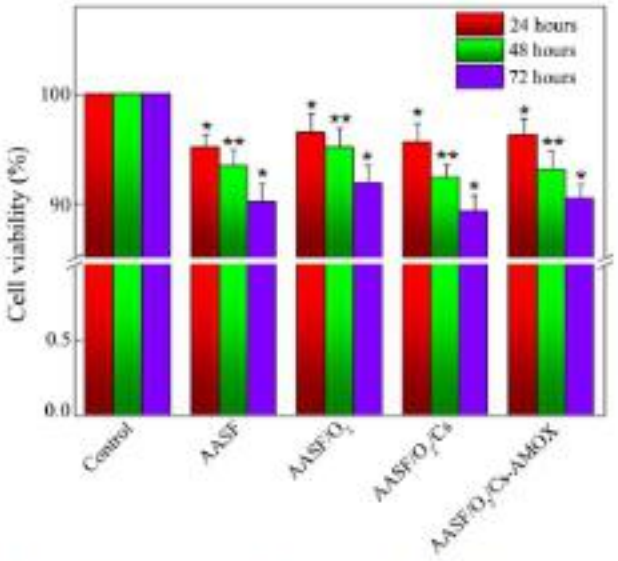

Figure 7. Viability (%) of L929 mammalian cells at different time points post incubation with AASF, AASF/O_2, AASF/O_2/Cs and AASF/O_2/Cs-AMOX yarns (** and * show significant differences from control at $p < 0.01$ and $p < 0.05$, respectively). Values represent mean ± SD of three batches. Control: cell with no treatment.

AMOX (93.1 ± 1.76%) yarns. The improved cytocompatibility of AASF/O_2 yarn could be attributed to the incorporation of polar functional groups onto the surface, due to O_2 plasma treatment, which subsequently enhances cell growth, proliferation and attachment. After 72 hours of incubation, the cell viabilities on all the samples are observed to be around 89–91%. In case of AASF/O_2/Cs yarn, the high degree of deacetylation and presence of amino group are the key factors favoring the interactions between Cs and cells. These studies clearly demonstrate that O_2 plasma treatment and incorporation of drug does not cause any adverse effect on the cytocompatibility of AASF/O_2/Cs-AMOX yarn.

Conclusions

In this study a potential controlled drug delivery system of Cs-AMOX coated AASF yarn modified by DBD O_2 plasma at atmospheric pressure has been successfully developed. Results obtained from XPS, ATR-FTIR and FESEM analyses indicate that O_2 plasma treatment influences surface chemistry and morphology of AASF by increasing the concentrations of oxygen containing functional (polar) groups onto the surface as well as forming nano-structured surface roughness. Due to hydrogen bonding between silk fibroin surface and Cs molecules facilitated by surface polar groups and mechanical interlocking, AASF/O_2/Cs-AMOX yarn shows higher tensile strength and Young's modulus as compared to both AASF and AASF/Cs yarns. The AASF/O_2/Cs-AMOX yarn exhibits excellent bactericidal activities against *S. aureus* and *E. coli* bacteria and retains its antibacterial activities for prolonged period of time (2000 hours) due to sustained release of drug from Cs matrix. *In vitro* drug release

Principal
Nowgong Girls' College
Nagaon :: Assam
Nowgong Girls' College ★ Nagaon :: Assam ★ ESTD: 1962

study shows that the AASF/O_2/Cs-AMOX yarn exhibits biphasic drug release profile i.e., the drug release from the surface as well as from the bulk of Cs matrix following a Fickian diffusion mechanism. O_2 plasma treatment and incorporation of antibiotic drug do not have any adverse effect on cytocompatibility of AASF/O_2/Cs-AMOX yarn, as confirmed by *in vitro* cytotoxicity test toward L929 fibroblasts. These results thus demonstrate that AASF/O_2/Cs-AMOX yarn with excellent mechanical strength and controlled drug release behavior can be considered a promising biomaterial for application as surgical suture.

Acknowledgments

This research work is supported by DST-SERB (Grant No. SR/FTP/PS-147/2012, IFA14-PH-93 and EMR/2016/006146) funded by Department of Science and Technology (DST), India. Arup Jyoti Choudhury expresses his gratitude to the DST-INSPIRE Faculty Fellowship (Grant No. IFA14-PH-93) for the financial support to carry out this research work and Tezpur University, Assam, India for hosting the fellowship. Namita Ojah acknowledges the support provided by DST-INSPIRE and DST-SERB in the form of fellowship.

Disclosure statement

No potential conflict of interest was reported by the authors.

References

[1] Liechty WB, Kryscio DR, Slaughter BV, et al. Polymers for drug delivery systems. Annu Rev Chem Biomol Eng. 2010;1:149–173.
[2] Das D, Pal S. Modified biopolymer-dextrin based crosslinked hydrogels: application in controlled drug delivery. RSC Adv. 2015;5:25014–25050.
[3] Bernkop-Schnürch A, Dünnhaupt S. Chitosan-based drug delivery systems. Eur J Pharm Biopharm. 2012;81:463–469.
[4] Zhang Y, Sun T, Jiang C. Biomacromolecules as carriers in drug delivery and tissue engineering. Acta Pharm Sin B. 2018;8:34–50.
[5] Senapati S, Mahanta AK, Kumar S, et al. Controlled drug delivery vehicles for cancer treatment and their performance. Signal Transduct Target Ther. 2018;3:1–19.
[6] Elgadir MA, Uddin MS, Ferdosh S, et al. Impact of chitosan composites and chitosan nanoparticle composites on various drug delivery systems: a review. J Food Drug Anal. 2015;23:619–629.
[7] Choudhury AJ, Gogoi D, Chutia J, et al. Controlled antibiotic-releasing Antheraea assama silk fibroin suture for infection prevention and fast wound healing. Surgery. 2016;159:539–547.
[8] Kondyurin A, Lau K, Tang F, et al. Plasma ion implantation of silk biomaterials enabling direct covalent immobilization of bioactive agents for enhanced cellular responses. ACS Appl Mater Interfaces. 2018;10:17605–17616.
[9] Jeong L, Yeo IS, Kim HN, et al. Plasma-treated silk fibroin nanofibers for skin regeneration. Int J Biol Macromol. 2009;44:222–228.
[10] Ribeiro VP, Almeida LR, Martins AR, et al. Influence of different surface modification treatments on silk biotextiles for tissue engineering applications. J Biomed Mater Res. 2016;104:496–507.
[11] Kalani MM, Nourmohammadi J, Negahdari B. Osteogenic potential of Resuvastatin immobilized on silk fibroin nanofibers using argon plasma treatment. Biomed Mater. 2019;14:1–14.

Principal
Nowgong Girls' College
Nagaon :: Assam
Nowgong Girls' College 1962 Assam

[12] Zhang Q, Ma L, Zheng S, et al. Air-plasma treatment promotes bone-like nano-hydroxylapatite formation on protein films for enhanced in vivo osteogenesis. Biomater Sci. 2019;

[13] Lee M, Ko YG, Lee JB, et al. Hydrophobization of silk fibroin nanofibrous membranes by fluorocarbon plasma treatment to modulate cell adhesion and proliferation behaviour. Macromol Res. 2014;22:746–752.

[14] Das P, Ojah N, Kandimalla R, et al. Surface modification of electrospun PVA/chitosan nanofibers by dielectric barrier discharge plasma at atmospheric pressure and studies of their mechanical properties and biocompatibility. Int J Biol Macromol. 2018;14: 1026–1032.

[15] Srivastava AK, Prasad G. Characteristics of parallel-plate and planar-surface dielectric barrier discharge at atmospheric pressure. J Electrostat. 2014;72:140–146.

[16] Fang Z, Xie X, Li J, et al. Comparison of surface modification of polypropylene film by filamentary DBD at atmospheric pressure and homogeneous DBD at medium pressure in air. J Phys D: Appl Phys. 2009;42:1–9.

[17] Beamson G, Briggs D. High resolution XPS of organic polymers: the Scienta ESCA 300 database. Chichester (UK): John Wiley & Sons; 1992.

[18] Dash S, Murthy PN, Nath L, et al. Kinetic modeling on drug release from controlled drug delivery systems. Acta Pol Pharm. 2010;67:217–223.

[19] Chai J, Lu F, Li B, et al. Wettability interpretation of oxygen plasma modified poly (methyl methacrylate). Langmuir. 2004;20:10919–10927.

[20] Singh YP, Bhardwaj N, Mandal BB. Potential of agarose/silk fibroin blended hydrogel for in vitro cartilage tissue engineering. ACS Appl Mater Interfaces. 2016;8: 21236–21249.

[21] Pavia DL, Lampman GM, Kriz GS, et al. Introduction to spectroscopy. 5th ed. Boston (MA): Cengage Learning; 2008.

[22] Bisson-Boutelliez C, Fontanay S, Finance C, et al. Preparation and physicochemical characterization of amoxicillin β-cyclodextrin complexes. Aaps Pharmscitech. 2010;11: 574–581.

[23] Wijesena RN, Tissera N, Kannangara YY, et al. A method for top down preparation of chitosan nanoparticles and nanofibers. Carbohy Polym. 2015;17:731–738.

[24] Homayoni H, Ravandi SAH, Valizadeh M. Electrospinning of chitosan nanofibers: processing optimization. Carbohy Polym. 2009;77:656–661.

[25] Amornsudthiwat P, Mongkolnavin R, Kanokpanont S, et al. Improvement of early cell adhesion on Thai silk fibroin surface by low energy plasma. Colloids Surf B Biointerfaces. 2013;111:579–586.

[26] Theapsak S, Watthanaphanit A, Rujiravanit R. Preparation of chitosan-coated polyethylene packaging films by DBD plasma treatment. ACS Appl Mater Interfaces. 2012;4: 2474–2482.

[27] López-Pérez PM, Marques AP, da Silva RM, et al. Effect of chitosan membrane surface modification via plasma induced polymerization on the adhesion of osteoblast-like cells. J Mater Chem. 2007;17:4064–4071.

[28] Bhardwaj N, Singh YP, Devi D, et al. Potential of silk fibroin/chondrocyte constructs of muga silkworm Antheraea assamensis for cartilage tissue engineering. J Mater Chem B. 2016;4:3670–3684.

[29] Jeon HJ, Lee JY, Lee H, et al. Nanostructured surface of electrospun PCL/dECM fibres treated with oxygen plasma for tissue engineering. RSC Adv. 2016;6:32887–32896.

[30] Xie J, Xin D, Cao H, et al. Improving carbon fiber adhesion to polyimide with atmospheric pressure plasma treatment. Surf Coat Technol. 2011;206:191–201.

[31] Ma K, Chen P, Wang B, et al. A Study of the effect of oxygen plasma treatment on the interfacial properties of carbon fiber/epoxy composites. J Appl Polym Sci. 2010;118: 1606–1614.

CTC
Principal
Nowgong Girls' College
Nagaon :: Assam

Nowgong Girls' College
ESTD: 1962
Assam

[32] Choudhury AJ, Gogoi D, Kandimalla R, et al. Penicillin impregnation on oxygen plasma surface functionalized chitosan/Antheraea assama silk fibroin: studies of antibacterial activity and antithrombogenic property. Mater Sci Eng C. 2016;60:475–484.

[33] Obermeier A, Schneider J, Wehner S, et al. Novel high efficient coatings for anti-microbial surgical sutures using chlorhexidine in fatty acid slow-release carrier systems. PLoS One. 2014;9:1–7.

[34] Gupta B, Anjum N, Gulrez SKH, et al. Development of antimicrobial polypropylene sutures by graft copolymerization. II. Evaluation of physical properties, drug release, and antimicrobial activity. J Appl Polym Sci. 2007;103:3534–3538.

[35] Chen X, Hou D, Wang L, et al. Antibacterial surgical silk sutures using a high-performance slow-release carrier coating system. ACS Appl Mater Interfaces. 2015;7:22394–22403.

[36] Kim SJ, Yoon SG, Lee YM, et al. Water sorption of poly (vinyl alcohol)/poly (diallyldimethylammonium chloride) interpenetrating polymer network hydrogels. J Appl Polym Sci. 2003;90:1389–1392.

[37] Sami AJ, Khalid M, Jamil T, et al. Formulation of novel chitosan guargum based hydrogels for sustained drug release of paracetamol. Int J Bio Macromol. 2018;1058:324–332.

[38] Ghori MU, Conway BR. Hydrophilic matrices for oral control drug delivery. Am J Pharmacol Sci. 2015;3:103–109.

Principal
Nowgong Girls' College
Nagaon :: Assam

Nowgong Girls' College
ESTD: 1962
Nagaon :: Assam

North Eastern Geographer, Vol. 40, No. 1 & 2, 2019, pp. 101-112
ISSN 0973-0915 © NEIGS

SOME ASPECTS OF FLOW BEHAVIOUR OF THE BELSIRI RIVER, ASSAM

Nilotpal Kalita[1], Rana Sarmah[2] *and* ***Ashok Kumar Bora[3]***

[1]Depatment of Geography, Gossaigaon College
[2]Depatment of Geography, Pandu College
[3]Department of Geography, Gauhati University
Email : nilotpalkalita4@gmail.com

Abstract : The Belsiri river of Assam is a right bank tributary of the Brahmaputra river and located in the Tezpur Subdivision of the Sonitpur District, Assam. Based on the stage- discharge data collected from Water Resource Department of the Government of Assam for the period 1991-2015 an attempt is made here to examine the flow behaviour of the river. During the study period, maximum discharge was 171 m3s-l recorded on 20 June 1993 corresponding to the highest water level of 73m for the same day. The minimum discharge was 0.27 m3s-l recorded on 24 May 1998 corresponding to the lowest water level of 71m for the same day. The average discharge was calculated to be 20 m3s-l. The average discharges of monsoon and non-monsoon seasons are calculated at 34 m3s-l and 6 m3s-l respectively. The stage-discharge hydrographs constructed for the monsoon season shows variable nature of flow behavior. In the hydrographs of monsoon and non-monsoon seasons, most of the peaks of the discharge and water level are coincided. Non-coincidence of peaks is noticed in some locations which may be because of the changes in channel morphology such as bank erosion, channel widening, etc. The rating curve of the Belsiri River constructed between discharge and sediment transport rates using logarithmic power function equation indicates strong positive correlation (+0.77). The correlation coefficients for the monsoon and non monsoon periods are +0.68 and +0.53 respectively. The higher removal of sediments from the catchment, bed and banks by the rainfed water during monsoon months is reflected in high positive correlation between discharge and suspended sediment load.

Key words: Stage, Discharge, Flow behavior, Sediment transport.

Introduction

Study of flow behavior of river is a prime concern of research in fluvial geomorphology as it marks the influences of surficial processes responsible for development of fluvial landforms. Development of landforms is closely associated with the flow behaviour of rivers located in the wet tropical region as that of the present study area. Besides, the ways of life of peoples living in such region

Principal
Nowgong Girls' College
Nagaon :: Assam

Nowgong Girls' College ★ ESTD: 1962 ★ Nagaon :: Assam

are strongly regulated by the flow behavior of the river concerned. In general, common fluvial events and processes associated with the flow behaviour of river such as flood, flood inundation, bank erosion, sedimentation, channel shifting etc are very short periodic events but have far reaching consequences in land and economy of the people. Several works have been done on flow behaviour of rivers across the globe in general and in the Brahmaputra river system in particular. The works of Agarwal and Mishra (1987), Brice (1974), Bristow (1987), Dietrich and Smith (1983), Goswami (1985a, 1992), Gottesfeld, et.al. (1990), Hill (1973), Hooke (1980), Leopold and Wolman (1957), Lewin,et.al. (1977), Lyons and Beschta (1983), Mosley (1975), Schmidt et. al., (1990), Schumn (1960, 1969), Slaa, et. al. (1994), Wolman (1957, 1959), Wolman and Leopold (1970), World Bank (1990) are worth mentioning.

Studies on the Brahmaputra river system pertaining to different aspects of channel behaviour are mostly found in the works of Bora (1990, 2003), Coleman (1969, Duarah (1999), Goswami (1985, 1992, 1998), Hazarika ((2003), Kar (1994), Mahanta (1995), Mukhopadhyay (1982), Sarma (1980), Sarmah (2001, 2003, 2006-2007, 2012a, 2012b). The present study, despite the constraints of inadequate database is an attempt to study on some aspect of flow behaviour of the Belsiri river in Assam.

The Belsiri river and its environment

Assam part of the Belsiri river basin is taken-up as the study area. The Belsiri river, a right bank tributary of the Brahmaputra river Assam (INDIA), is located in the north-eastern part of India and its basin extends from 26°36/N lat. to 27005/N lat. and 92°20/ E longitude to 92040/E longitude (Fig. 1.1). Belsiri river flows through the territories of the west Kameng District of the state of Arunachal Pradesh and the western part of the Sonitpur District of the state of Assam. The Belsiri basin occupies a total area of 496 km2 sharing 154 km2 (31%) and 342 km2 (69%) in the territories of the states of Arunachal Pradesh and Assam in India.

The Belsiri river basin is too small compared to the other river basins of India like the Ganges, the Brahmaputra, the Godavari, the Krishna rivers. The Belsiri river is a middle category river of the Brahmaputra systems. The similar tributary rivers in the central part of the northern bank of the Brahmaputra are Tangani river, Gelabil river, Panchnoi river, Ghiladhari river. However, the overall basin morphological characteristics of the Belsiri river basin are similar with that of the other tributary basins of the Brahmaputra system. The basin exhibits an elongated shape with wider extent in the plains than that in the hills. The basin perimeter measures 158 km with a maximum length and width of 57 km and 15 km respectively.

The Belsiri River is located in the Tezpur Sub-division of the Sonitpur District in Assam (Fig.1). Being a right bank tributary of the Brahmaputra river in Assam it originates at a place called Pankmala of the West Kameng District of Arunachal Pradesh where it is known as the Bichrikho river of Arunachal Himalaya and traverses a total length of 90km towards south through the territories of

Principal
Nowgong Girls' College
Nagaon :: Assam

Nowgong Girls' College ★ Nagaon :: Assam ★ ESTD: 1962

Arunachal Pradesh and Assam before falling in the Brahmaputra river. After crossing the steep hilly terrain, the river flows in the south-eastern direction through the Sonai-Rupai Reserve Forest in Assam. The Belsiri river gets its name 'Belsiri' in Assam while traversing through the piedmont and alluvial plains. After taking a sinuous course in the hilly terrain, the Belsiri river flows for a distance of about 53 km towards south-east direction through the piedmont plain upto the Belsiri Railway station. From this point, it flows almost straight for more than 1.4 km and meets a tributary river called Mejangjuli river in its left bank. The Belsiri River proceeds further south-west direction and flows 3.6 km to meet another tributary known as Baiganajuli river on its right bank. It continues to flow in the same direction for 10 km and meets one another tributary river called Chapai river on right bank. From this point the Belsiri river further traverses for 2 km south east and meets with the river Garjuli river. Garjului river is known as Dhekiajuli river in its upper course. After travelling 1.6 km from the confluence of the Garjuli River, it crosses the North Trunk Road-52 at Keherukhanda village. From this point, the river continues to flow in south-south-west direction for 17.4 km from the North Trunk Road-52 crossing point and empties into the Brahmaputra river.

The climate of the study area enjoys tropical to sub-topical monsoon climate of warm-humid summer and cool-dry winter. The average annual precipitation varies from 1500 mm to 1960 mm. The summertime temperature shows variations from 25oc to 35oc and most of the rainfall occurs in this time of the year. The southwest monsoon strikes in the beginning of the May and continues till October.

Data source and methodology

Study on flow behaviour of river require longer time-span database for reliable understanding and decision making. This study uses daily flow data for the period 1991 to 2015 which were collected from the Water Resource Department of the Government of Assam (India). Data on suspended sediment load were available for the period 1977 to 1983 and are used in this study. All these data are observed in N.T.Road crossing point

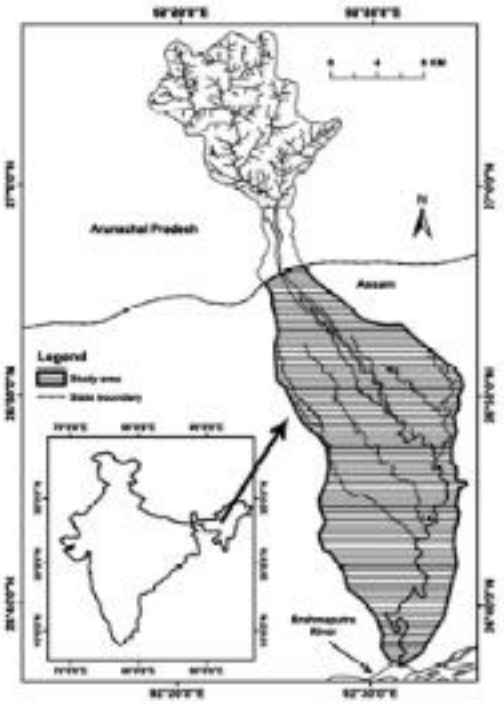

Fig. 1: Location of the study area

Principal
Nowgong Girls' College
Nagaon :: Assam

Nowgong Girls' College ★ Nagaon :: Assam ★ ESTD: 1962

of the Belsiri river. Common statistical plot methods of flow analysis such as construction of stage- discharge hydrograph, stage-discharge rating curve, sediment rating curve are used to study the flow behaviour of the river. These graphs are constructed for monsoon and non-monsoon periods of flow as there are significant seasonal variations in rainfall and temperature parameters.

Results and discussion

Characteristics of flow of water in rivers vary with time and magnitude and directly depend on the precipitation regimes. Components of natural flow regime can be understood using various time series (e.g., Fourier and wavelet), and probability analyses, for example, extremely high or low flows, or of the entire range of flows expressed as average daily discharge. River flow regimes show regional patterns that are determined largely by river size and by geographic variation in climate, geology, topography, and vegetative cover. Belsiri River originates in the Himalayan foothills and gets bankful during wet season mostly July and August. It is observed that the maximum discharge during the study period (1991-2015) was 171 m3s-l recorded on 20 June 1993 corresponding to the highest water level of 73 m for the same day. The minimum discharge was 0.27 m3s-l recorded on 24 May 1998 corresponding to the lowest water level of 71 m for the same day. The average daily discharge was calculated to be 20 m3s-l for the entire twenty years period. The average discharges of monsoon (May to October) and non-monsoon (November to April) seasons are calculated to be 34 m3s-l and 6 m3s-l respectively.

The stage-discharge hydrograph of the river at N-T Road crossing for the period 1991-2015 is presented in fig.2. It is observed in the stage discharge hydrograph that the water discharges are excessively high during the monsoon period (May to October) compared to non-monsoon period. This is evident in the stage discharge hydrograph (Fig.2) reflecting the variable nature of flow behavior. In the hydrographs of monsoon and non-monsoon seasons, most of the peaks of the discharge and water level are coincident. Non-coincidence of peaks is noticed in some locations which may be because of the changes in channel morphology such as bank erosion, channel widening, etc. Peak flows vary from 35 m3s-l to 175 m3s-l. It is evident in the hydrograph that in most of the years there are sudden rise of the peak flows demonstrating the severe nature of flood. It is also evident that these peak flows do not continue for long and mostly confined to two to three days period. The stage discharge hydrographs constructed for the monsoon and non-monsoon season and presented in figure 3 and figure 4 also show variable nature of flow behavior. It is found that 70% of the time flow was below the average. Out of the total time of flows, flow above the danger level was only 3% of time.

Relationship between stage and discharge is also examined by constructing stage-discharge rating curve and presented in figure 6. It is seen in the graph that high concentrations of points are within the

C.T.C.
Principal
Nowgong Girls' College
Nagaon :: Assam

Nowgong Girls' College ★ Nagaon :: Assam ★ ESTD: 1962

discharge range of 0 - 80 m3s-l and water level range of 71.5-72.50 m. This demonstrates magnitude of flow in the river is not very high to bring about considerable fluvial activity. In fact, the river is a middle category river in respect of basin size among the tributary rivers of the Brahmaputra system of rivers. The correlation coefficient between stage and discharge is calculated to be +0.75 which indicates the strong role of monsoon rainfall regime of the study region. This correlation coefficient values for the monsoon and non-monsoon seasons are calculated to be +0.66 and +0.48 respectively and these values also signify the strong role of monsoon rainfall regime of the study area.

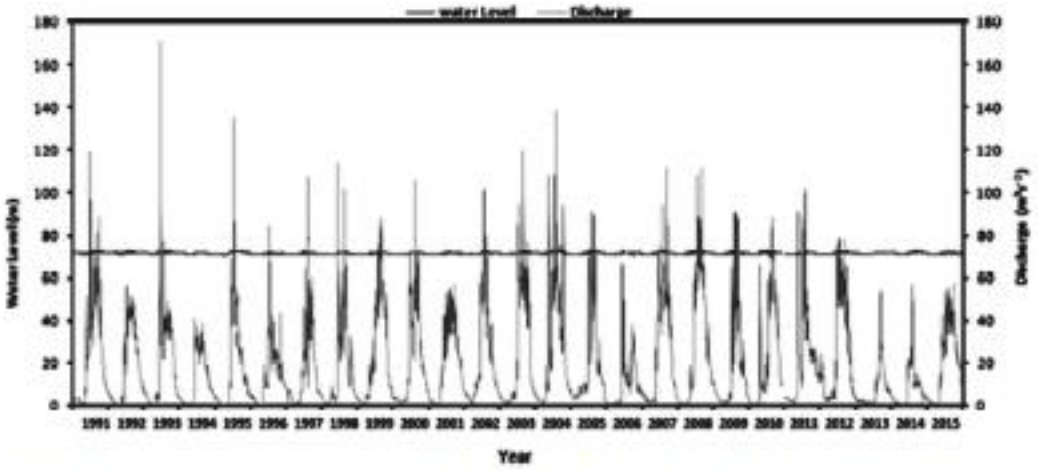

Fig. 2: Stage-discharge hydrograph of the Belsiri river from the year 1991 to 2015

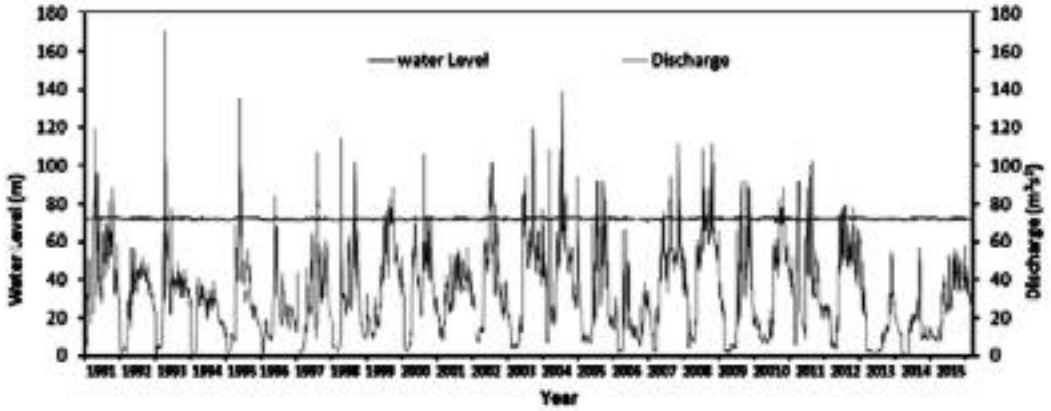

Fig. 3: Stage-discharge hydrograph of the Belsiri river of daily monsoon months from the year 1991 to 2015

Principal
Nowgong Girls' College
Nagaon :: Assam

Nowgong Girls' College ★ Nagaon :: Assam ★ ESTD: 1962

To understand flow characteristics further, probability curve for annual discharge is constructed and presented in figure 7. The probability curve for daily discharges estimates that during the 50% of the time (3781 days), the daily discharge was less than 48 m3s-l and during the 95% of the time (8132 days) the daily discharge does not exceed 108 m3s-l.

For any hydrological design and environmental management, it is necessary to know the probability of flood discharge. For this purpose, a maximum flow probability curve for the period 1991-2011 is constructed following the procedure suggested by British Avon River Authority and using the data presented in table 1. The maximum flow probability curve is presented in figure 8. In this graph the probability of highest flow of 171 m3s-l is recorded on 20 June 1993 is 4.54 %.. Similarly, the probability associated with the lowest flow of 39.15 m3s-l recorded on 24 august 1994 is 95.45 %.

Figures 6 and 8 bear significant finding if the probability percent is converted back to number of days. Probability of highest flow of 171 m3s-l is 4.54 %. This means highest flow of 171 m3s-l has the chance of occurring 4.54% of time, i.e. about 40 days in 20 years means 2 days in a year. Flood, if it continues for two days in the intensively settled and cropped areas can cause huge damage in terms of siltation/sedimentation, bank erosion, crop and livestocks. This can also damage transport network system to a great extent. Recurring siltation in the

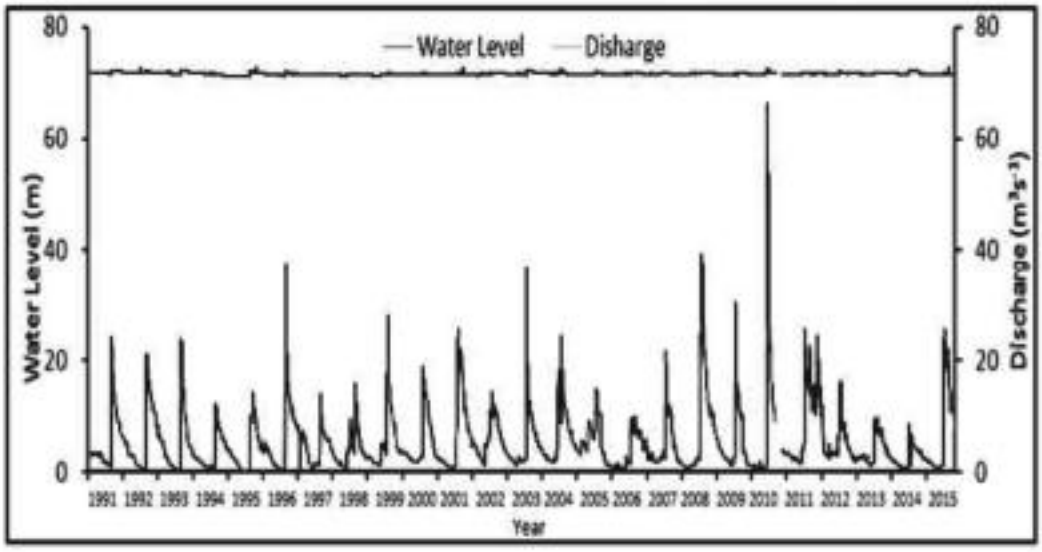

Fig. 4: Stage-discharge hydrograph of daily non-monsoon months of the Belsiri River, 1991-2015

Principal
Nowgong Girls' College
Nagaon :: Assam

Nowgong Girls' College
ESTD: 1962
Nagaon :: Assam

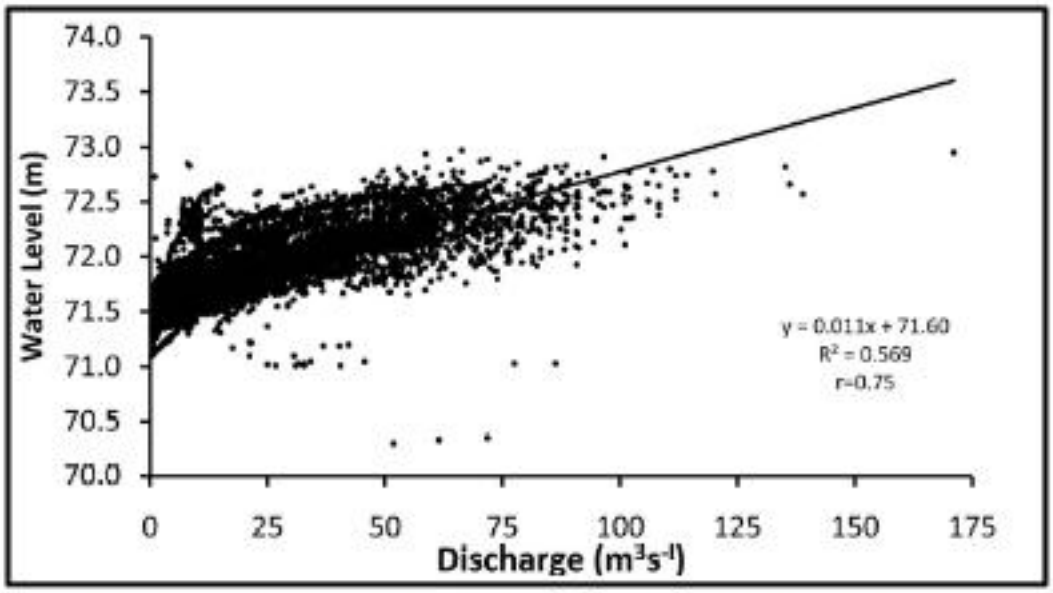

Fig. 5: Daily stage-discharge rating curve of the Belsiri River, 1991-2015

immediate bank of the channel leads to development of natural levee and back swamp in the floodplain beyond.

To examine the characteristics of sediment transport in the Belsiri River three rating curves representing entire period under study, monsoon season and non-monsoon season are constructed and presented in figure9, figure10 and figure11 respectively. It is observed in figure 9 that most of the points in the graph concentrates between sediment flow of 0.00001 hm to 0.1 hm and discharge of 1 m3s-1 to 180 m3s-1. Most of the sediments are evident to be transported in the high discharge period. This phenomenon is evident from the sediment rating curve presented in figure 10 i.e. rating curve constructed for the monsoon season. In this graph, most of the points concentrate between sediment flow of 0.01 hm to 0.1 hm and discharge of 50 m3s-1 to 180 m3s-1 , i.e. high discharges. Sediment transport is found to be low during non-monsoon period which conforms the low rainfall regime

The rating curve of the Belsiri river constructed taking discharge and sediment transport rates for the period 1997-1983 using logarithmic power function equation indicates strong positive correlation (+0.77). The correlation coefficients for the monsoon and non-monsoon periods are +0.68 and +0.53 respectively. Examination based on the limited available sediment transport data reveals that the river transported 26.71 hm sediment during 1977-1983 at N.T. Road crossing site. It is observed in the field work that several river islands and bars develop particularly in the downstream part of the

Principal
Nowgong Girls' College
Nagaon :: Assam

Nowgong Girls' College ★ Nagaon :: Assam ★ ESTD: 1962

Table 1: Annual maximum daily flow of the Belsiri River, 1991-2011

Year	Discharge (m3s-1)	Rank(M)	M/(n+1)	Plotting position % (Probability per cent of each flow occurring)
1991	120	5	0.2272	22.72
1992	57	20	0.909	90.90
1993	171	1	0.0454	4.54
1994	39	21	0.9545	95.45
1995	135	3	0.1363	13.63
1996	84	17	0.7727	77.27
1997	1076	9	0.409	40.90
1998	114	6	0.2727	27.27
1999	88	15	0.6818	68.18
2000	106	10	0.4545	45.45
2001	57	19	0.8636	86.36
2002	101	12	0.5454	54.54
2003	121	4	0.1818	18.18
2004	139	2	0.0909	9.09
2005	91	13	0.5909	59.09
2006	66	18	0.8181	81.81
2007	108	8	0.3636	36.36
2008	112	7	0.3181	31.81
2009	91	14	0.6363	63.63
2010	88	15	0.6818	68.18
2011	103	11	0.5000	50.00

Principal
Nowgong Girls' College
Nagaon :: Assam

Nowgong Girls' College
ESTD: 1962
Nagaon :: Assam

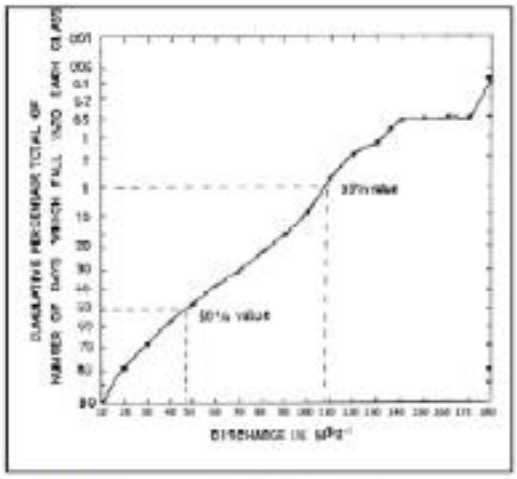

Fig. 7: Annual probability curve of Belsiri River

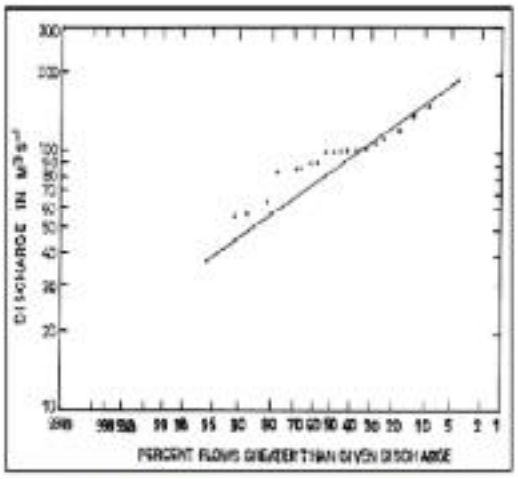

Fig. 8: Maximum annual flow probability of the Belsiri river (1991-2011)

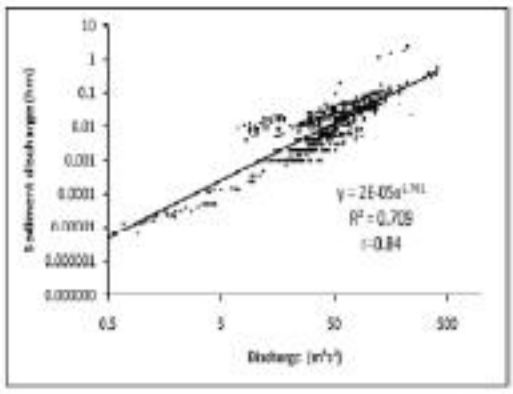

Fig. 10: Sediment rating curve of the Belsiri river, 1977-1983 (Monsoon months)

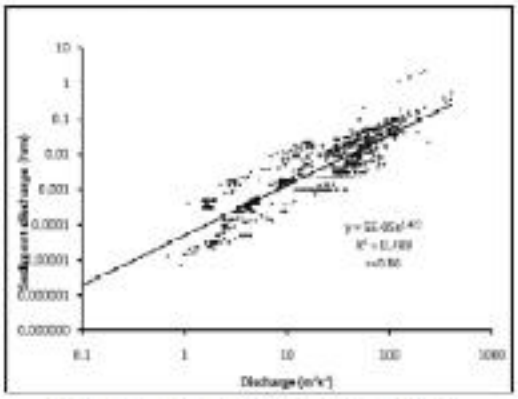

Fig. 9: Daily sediment rating curve of the Belsiri river, 1977-1983

N.T. Road crossing site. In this context, transportation of 26.71 hm of suspended sediment is considered to be significant. The facts mentioned above demonstrate that sediment transportation in the Belsiri river is quite significant in relation to flow magnitude.

Conclusion

The overall analysis of different flow aspects of the river Belsiri has revealed the variability pattern of the flow aspects of the river. High flow variability is seen during the monsoon periods compared to the non-

Principal
Nowgong Girls' College
Nagaon :: Assam

Nowgong Girls' College
ESTD: 1962
Nagaon :: Assam

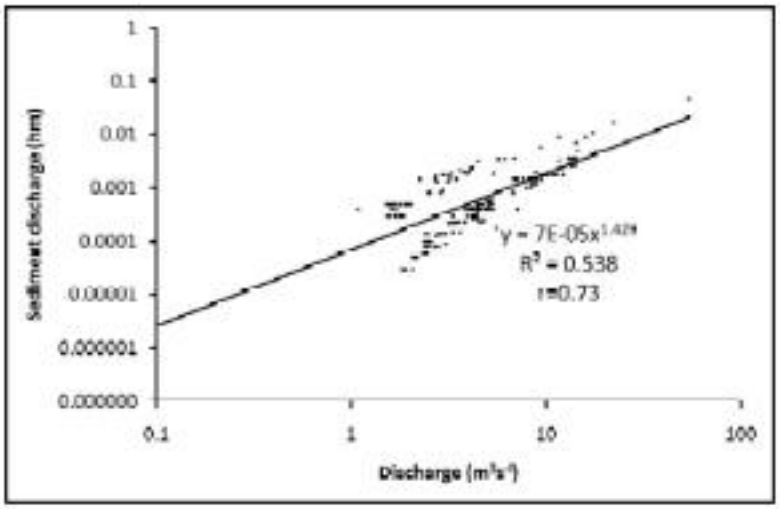

Fig. 11: Sediment rating curve of the Belsiri river, 1977-1983 (Non–monsoon months)

monsoon months. The hydrographs also show a strong relationship between rainfall amount and the discharge which suggests that higher the rainfall, higher is the flow peaks. The erosion of sediments from river banks is reflected in the volume of suspended sediment load and corresponding discharge. This study as a whole provides information about flow characteristics of the river, which are practically necessary for any effort towards water resource development in the basin.

References

Agarwal, C. S. and Mishra, A.K. (1987) Visual interpretation of F.C.C. satellite data for channel migration and water logging conditions along Ghaghra and Terhi rivers in part of districts Gonda and Baharaich, U.P., India, Photonirvachak, Jour. Of Ind. Soc.Of Remote Sensing, vol.15, No.1, pp. 19-28.

Bora, A.K. (2003) Flood dynamics and hazards in the Brahmaputra valley of India, Transactions, Japanese Geomorphological Union, 24-1, pp.65-85.

Bora, A.K. (1990) Jia Bharali river of Assam: A study in fluvial geomorphology, Unpublished Ph.D. thesis, GauhatiUniversity, pp.204-211.

Brice, J.C. (1964) Channel pattern and terraces of the Loup rivers in Nebraska, USGS Prof. Paper, pp.422-D.

Bristow, C.S. (1987) Brahmaputrariver: channel migration and deposition. *In*: Recent developments in Fluvial Sedimentology. F.G. Ethridge, R.M. Flores and M.D. Harvey (Eds.), Society of Economic Palaeontologists and Minerologists special publication No. 39, pp.63-73.

Coleman, J.M. (1969) Brahmaputra river: Channel processes and sedimentation, Sedimentary geology, vol.3, No.2/3, pp.129-239.

Principal
Nowgong Girls' College
Nagaon :: Assam

Nowgong Girls' College
ESTD: 1962
Nagaon :: Assam

Dietrich, W.E. and Smith, J.D. (1983) Influence of the point bar on flow through curved channels, Water Resource Research,vol.19, No.5, pp.1173-1192.

Duarah, B.P. (1999) Fluvio sedimentary environment of the Pagladia and Puthimari rivers: An investigation of their lower catchments in Assam, Unpublished Ph.D. thesis, pp.282-284.

Goswami, D.C. (1985a) Brahmaputra river, Assam, India: physiography, basin denudation and channel aggradation water Reso. Res., Amer. Geophys.Union, Vol.21, No.7, pp959-978.

Goswami, D.C. (1985b) Pattern of sediment yield from river basins of the Brahmaputra system, Northeast India, North Eastern Geographer, vol.17, No.1/2, pp.1-11.

Goswami, D.C. (1992) Satellite monitoring of bankline migration of the Brahmaputra river at Palasbari, Assam. Bulletin of NNRMS (B) – 15, pp.26-27.

Goswami, D.C. (1998) Fluvial regime and flood hydrology of the Brahmaputra river, Assam, Memoir Geol. Soc. of India, No.41, pp. 53-75.

Gottesfeld, A.S. and Gottesfeld, L.M.J. (1990) Floodplain dynamics of wandering river, dendrochronology of the Morice river, British Columbia, Canada, Geomorphology, 3(2), pp. 159-179.

Hazarika, U.M. (2003) Problems of flood, erosion and sedimentation in the Jiadhal river basin, Assam: A geo-environmental study, Unpublished Ph.D. thesis, GauhatiUniversity, pp.89-92, 91, 92-104.

Hill, A.R., (1973) Erosion of river banks composed of glacial till near Belfast, Northern Ireland, Geom., 17, pp.428-442.

Hooke, J.M. (1980) Magnitude and distribution of rates of river bank erosion, Earth surface, Processes and Landforms, 5, pp.143-157.

Kar, M. (1994) Flood hazard in Nagaon and Marigaon districts of Assam: A geographical perspective, Unpublished Ph.D. thesis Gauhati University.

Leopold L.B. and Wolman, M.G. (1957) River channel patterns: braided, meandering and straight, U.s. Geol. Survey, Prof. Paper, 282-B, pp.39-85.

Lewin, J., Hughes, D. and Blacknell, C. (1977) Incidence of river erosion, Area, 9, pp.177-180.

Lyons, J.K. and Beschta, R.(1983) Landuse, floods, and channel changes: Upper Middle Fork River, Oregon (1963-1980), Water Resource Research, vol.19, No.2, pp.463-471.

Mahanta, S.K. (1995) Some sedimentological and economic aspects of the recent sediments of the river Subansiri in and around Gerukamukh and Dirpaimukh, Assam, Unpublished Ph.D. thesis, GauhatiUniversity.

Mosley, M.P. (1975) channel changes on the river Bollin, Chesire, 1872-1973E, Mid. Geogr. 42, pp.185-199.

Mukhopadhyay, S.C. (1982) The Tista basin: A study in fluvial geomorphology, K.P.Bahchi & Co., Culcutta, pp.1-308.

Sarma, J.N. (1980) Drainage basin study of the Burhi Dihing river, Assam, Unpublished Ph.D. thesis, Dibrugarh University.

Sarmah, R and Goswami, D.C.(1998) ' Some aspects of flow behavior of the JiaDhansiri river (north), Assam, Indian Journal Of Geomorphology, vol. 3 number 2 (July-December) 1988, pp. 200-210.

Principal
Nowgong Girls' College
Nagaon :: Assam

Nowgong Girls' College
ESTD: 1962
Nagaon :: Assam

Sarmah, R. and Goswami D.C. (2000) Flood frequency analysis of the Jia Dhansiri river, Assam, Jour. Assam Science Society, Vol.41, No.3, pp.118-122.

Sarmah, R. (2001) Fluvial environment and mechanism of floodplain formation in the Jia Dhansiri river basin, Assam, Unpublished Ph.D. thesis, Gauhati University, pp.82, 118-119, 130-136.

Schmidt, J. C., and Graf, J. B., 1990, Aggradation and degradation of alluvial sand deposits, 1965-1986, Colorado River, Grand Canyon National Park, Arizona: U.S. Geological Survey professional Paper 1493, pp.74.

Schumm, S.A. (1960) The shape of alluvial channels in relation to sediment type, U.S. Geol. Survey Prof. paper 352-B, pp.17-30.

Schumm, S.A. (1969) River metamorphosis, Jour. of the hydraulics division proceedings of the Amer. Soc. of Civil Eng. 95, pp.255-273.

Slaa, B. T., Monar, F.C., and Laboyrie, H., (1994) Erosion control of the Meghna River, Bangladesh, in Integrated River Basin Development, edited by Kirby, C., and White, W.R. Chichester, Wiley and Sons, pp. 289-298.

Wolman, M.G. (1959) Factors influencing erosion of a cohesive river bank, Amer .Jour. of Sci., 257, pp.204-216.

Wolman, M.G. and Leopold L.B.(1970) River channels pattern, In: Dury, G.H. edited River and River Terraces, The Macmillan Press ltd., London. Pp.166-196.

World Bank, 1990, Flood control in Bangladesh: A plan for action. Technical Paper No. 119: The World Bank, Asia Region Technical Department, Washington, D.C.

Principal
Nowgong Girls' College
Nagaon :: Assam

Nowgong Girls' College
ESTD: 1962
Nagaon :: Assam

Papers published per teacher in the Journals notified on UGC website during the Academic Session: 2019-20

Submitted to the NAAC for 3rd Assessment Cycle of Assessment & Accreditation

NOWGONG GIRLS' COLLEGE

Re-accreditated at A Grade by the NAAC (2nd Cycle)

INTERNATIONAL JOURNAL OF PHARMACEUTICAL SCIENCES AND RESEARCH

Received on 13 December 2018; received in revised form, 13 July 2019; accepted, 20 August 2019; published 01 September 2019

PHYTOCHEMICAL ANALYSIS OF *DRYMARIA CORDATA* (L.) WILLD. EX SCHULT (WHOLE PLANT) USED BY TEA TRIBES OF ERSTWHILE NAGAON DISTRICT OF ASSAM INDIA

Rakhi Bhattacharyya *, Krishna Kanta Medhi and Sarat Borkataki

Department of Botany, Nowgong College, Nagaon - 782001, Assam, India.

Keywords:

Drymaria cordata, Bioactive compounds, Preliminary screening, FT-IR, GC–MS analysis

Correspondence to Author:
Rakhi Bhattacharyya
Research Scholar,
Department of Botany,
Nowgong College, Nagaon - 782001, Assam, India.

E-mail:rakhibhattacharyya86@gmail.com

ABSTRACT: Ethno-medicinal plants have a significant role in the field of natural product research and drug discovery since ancient times. *Drymaria cordata* (L.) Willd. Ex. Schult. belongs to the family Caryophyllaceae is an ethnomedicinal plant used as a home remedy in jaundice by the tea tribes of erstwhile Nagaon district of Assam. The present study deals with the evaluation of the phytoconstituents in *Drymaria cordata* using methanol extract. All the standard phytochemical procedures were followed for the detection of the phytoconstituents. The preliminary phytochemical screening revealed the occurrence of alkaloids, flavonoids, phenols, tannins and saponins. The presence of O-H stretch, C-O stretch, C-H stretch, C-H bend, N-H stretch and N-H bend were confirmed through FT-IR analysis. Several bioactive compounds like Cyclohexan-1,4,5-triol-3-one-1-carboxylic acid, Beta-D-glucopyranose-1,6-anhydro, L-gala-L-ido-octose, 3, 7, 11, 15-Tetramethyl-2-hexadecen-1-ol, n-Hexadecanoic acid, 9, 12 Octadecadienoic acids (Z,Z)-, 9,12-Octadecadienoic acid, methyl ester, Oleyl alcohol and 17-Octadecynoic acid were identified through GC–MS analysis. From the study, it can be concluded that *Drymaria cordata* possesses several medicinally important secondary metabolites. Further phytochemical and pharmacological investigations and isolation of the phyto-compounds is an urgent need which could be responsible for curing jaundice and several other ailments.

INTRODUCTION: Plants are used medicinally and are a rich source of several pharmacologically potent compounds. The therapeutic potentials of plant drugs are being used traditionally since pre-historic times. Plant products are the chief source of pharmaceutical agents used in the traditional remedy [1].

According to the World Health Organization (WHO), due to some economic and geographical constraints, 80% of the population in several Asian and African countries still depends on traditional therapies as their primary healthcare needs [2]. The curative properties of medicinal plants are chiefly due to the presence of various bioactive compounds present in the plants like alkaloids, flavonoids, phenols, saponins, tannins and terpenoids [3].

In recent years, evaluation of phytoconstituents is considered to be the most important and promising step in the medicinal plant research [4]. *Drymaria cordata* is an annual spreading herb native to tropical America and is now distributed widely

Principal
Nowgong Girls' College
Nagaon :: Assam

Nowgong Girls' College ESTD: 1962 Nagaon :: Assam

Changing Status of the Ahom Priestly Class

Dipankar Mohan

Abstract: ***Human society is the result of a continuous transformation process. In this transformation process religion plays a significant role. In every society customs, beliefs, behaviour, traditions are mostly connected with the religion. So in every society religion and religious traditions became the identity of a society. In case of Assam every tribes had their own priestly class to do priesthood. Similarly the Ahoms had their own priestly class to do priesthood. In this article an attempt has been made to assess the condition of the Ahom priestly class i.e. the Mohan, the Deodhai and the Bailungs.***

KEYWORDS: tradition, customs, priestly class, priesthood, religion.

I. INTRODUCTION

In every society, where there is a religion, a special place was reserved for those who deal with the religious functions, ideologies and customs. In traditional Hindu society where society was divided among the four classes i.e. the Brahmans, Kshatriyas, Vaishyas and Sudras; priesthood is generally ascribed to the Brahmanas. But from society to society it is different from each other. Generally Priestly class refers to the class of people who are associated with the priesthood or priestly activities. The tribes of Assam have their own priestly class to do the priesthood or the priestly activities. Among the Bodo community the *Deoris* are regarded as the priestly class who performs the priestly activities. In the same way the *mibu* or *deodhai* performs the priestly activities among the Mishings. The Dimasas called their priest as *Jontaizo* who belonged to the priestly class *Hojais* and all the religious rites were performed by him. Similarly the Karbi has *Ojha* or *Uche* as their priestly class.[i] But the social dignity and status of the caste Hindu priestly class i.e. the Brahmanas had far more higher position than the tribal priests. Like the same, the Tai Ahoms entered the Brahamputra valley, now called Assam valley early in the 13th century with a religion, culture and political system of their own.[ii] They brought with them a kind of heterogeneous beliefs and customs which was something new to the social life of early medieval Assam. The Ahoms also had the priestly class to do the priestly activities i.e. Mohan, Deodhai and Bailungs.

II. METHODOLOGY

The approach of this study is historical and exploratory in nature. To serve the purpose of the topic, both conventional and analytical methods of investigation are followed. Interviews are also taken for the purpose. However, the facts collected from edited books, journals are also taken.

III. REVIEW OF LITERATURE

Several works have been done by the researchers on the Ahom community. Some of these important works are:

'*Ahomxakolar Utsav Anusthan*' by Sukha Baruah draws upon the traditional festivals of the Ahoms in a descriptive way. She has discussed elaborately about the Ahom religious ceremonies such as *rikkhan*, *dam phi*, *jasingpha*, *phuralung puja*, *om pha puja*, etc. Moreover she has discussed elaborately about the influence of Hinduism on the Ahoms.

From Padmwshwar Gogoi's book '*Tai Ahom Religion and* Customs' we can have brief description of the traditional beliefs and customs of the Ahoms. His, another book, '*The Tai and the Tai Kingdoms*' deals the linkage of the Ahoms and other Tai races.

Dr. Birendra Kumar Gohain in his book '*The Ahoms and their Traditions*' has given a brief description on the Mohans, Deodhais and the Bailungs. Moreover, it has also given a brief description about traditional Ahom rites and rituals.

IV. DISCUSSION

Among the Tai-Ahoms, Mohung (Mohan), Changbun (deodhai) and Mo'plong (bailung) are the priestly classes who were entrusted with the duty of rites and rituals in the Ahom period. In the 'Pak Peyn Kaka' which is regarded as the holy text of the Ahoms the following lines were made about them-

"Mo'sham Mo'shai Mo'hung Mo'plong Changbun Kan Tun man.

Sham Mo Myung Wai Yin Kam Tun Man."

Meaning: Mohung Moplong Changbun, the three priestly clans of olden times also sprang up from Him, Phra Tyu Ching Phram Hum- the almighty God."

Revised Manuscript Received on July 22, 2019.

DIPANKAR MOHAN, Mphill Research Scholar, Department of History Dibrugarh University, Email: dipankarmohan44@gmail.com

Nowgong Girls' College ESTD: 1962 Nagaon :: Assam
Principal Nowgong Girls' College Nagaon :: Assam

The first Ahom king Sukapha who landed Assam in 1228 was accompanied by Mohan, Deodhai and the Bailungs along with other officials such as Buragohain, Borgohain and other some prominent officers. Mohan, Deodhai and Bailungs are mostly attached with their priestly activities and they were the repository of the vast knowledge of Ahom culture and traditions. From that time onwards, Mohan, Deodhai, Bailung through performing their religious activities helped the Ahom kings in administrative task. In some chronicles attached to the Ahom legend Mohan Deodhai and Bailungs are depicted as *ma-lik ma-li* which means scholarly people, *moru missing* which means honorary people and *sam ma mung* means three main people of country. In initial period of the Ahom rule, Ahom king paid great attention to the works of these people, fellow rulers also put emphasized to run the administration with the help of Mohan, Deodhai and the Bailungs. The Ahoms at the initial period followed their own religion but from the 16th century they started accepting Hinduism and the entire Ahom community became Hindus by the end of the 17th century. During the reign of Sudangpha or Bamuni konwer influence of Hinduism felt in Ahom court. Pratap Singha was the first when Brahmanical Hinduism slowly penetrated inside the Ahom court. Under the influence of Brahmin priests he took Hindu name, the Ahom origin was linked with Hindu god Indra. But Jayadhwaj Singha was the first Ahom king to formally accept Hinduism. Rudra Singha was the first who announced publicly of his inclination towards Hinduism and consequently he became a disciple of a Hindu priest and since then the condition of the three priestly classes got deteriorated. The Mohans, the Deodhais and the Bailungs remained steadfast to their traditional religion.

They are still maintaining the age old traditions, rituals and are still leading their lives professing and practicing the original religions, traditions and culture of the Tai Ahoms. They are still updating their genealogies.[iv] The Ahom priestly classes trace their descendant from the Mo'Laokhri, Pujakji and Po phi Su. However Mo'laokhri was the royal priest in the court of Lengdong, Pujakji was the king of Hitkhunban and Po phi su was the progenitor of the Bailung clan. Sukapha was accompanied by Thaomung Mo'sham of the Deodhai clan and Shengkaluk of the Mohung clan. In some *buranjis* it has been mentioned that the representative of the Bailung clan was already there in Assam.[v]

There are 7 phoids or clans of Mohans, 12 phoids or clans of the Deodhais, and 18 phoids of the Bailungs.[vi]

***Phoids* or clans of the Mohans:** Dihingia, Soraimoria, Khanamukhia, Matighoria, Sengelimoria, Rajghoria, Takouboria.

***Phoids* of Deodhais:** Kauriklau (goria), Ba ham ta, Sakoli, Che-pet-ta, Mo sa Ita, Kuk- cha, Dangdeng, Hatiborua, Dhuk la, Khanpia, Mo- ling.

***Phoids* of Bailungs:** Oka, Nora, Poka, Bahboria, Khumtai, Kolopia, Konsuria, Mothadongia, Safaguria, Dionia, Holguria, Lunpot, Simaluguria, Lefebara, Bantoria, Raidongia, Pirasachi, Dhak-Chowa, Pira-kotia.

Although the majority of the priestly class people inhabit Sivasagar district, some of them are residing in Jorhat district such as Mariaoni, Jhanji, Cheleng. In some parts of the Golaghat district, Dhemaji district, Lakhimpur district and in Guwahati city some of them are living. 'Mohan Deodhai Bailung Sanmilan, Assam' took a census of the priestly class people in 2012. However it was not completed but from the census it can be presumed that population of these people are more than 3. 50. lakhs.[vii]

A. ROLE OF THE AHOM PRIESTLY CLASS IN AHOM KINGDOM:

The Ahom Priestly Class i.e. the Mohan, Deodhai and the Bailungs had great role in Ahom kingdom and in the court. Performing religious ceremonies was the main task assigned to them. However, writing *buranjis* or keep recording political events as well as genealogies of the Ahom kings and other officials such as Buragohain, Borgohain etc. were their other task. They were the preserver of the Ahom tradition as well as the Tai Ahom language. These pundits or *molungs* had to teach the history, genealogies, culture and politics to the nobles and their sons and at the command of the king, they used to consult the books of astrology and divination, at the time of war or battle, when unnatural events took place when the king dies or whenever a good work was started.[viii]

Generally the Tai-Ahom Pundits or *molungs* were household pundits. They never had to give away their day to day family duties in maintaining their religious duties. The *molungs* or Tai Pundits had to pass several stages before he was given the status of '*molung*'. Generally all the important works related to priesthood or priestly activities were done in front of *puthi chang* and it was a more or less a custom that Tai Pundits should have a *puthi chang* in their home.[ix]

After attaining the knowledge of Tai language and other important knowledge from the elderly person of home or from other Tai pundits, they were given the responsibility of copying from original Tai manuscripts. Moreover they were taught about the making of ink, pen or any other important writing material. After this they were given the knowledge about the religious practices, astrology etc. After attaining maturity knowledge about the religious ceremonies they were appointed as helper to the chief *molung*. Those who attained maturity about this were inspired towards *seng hadhona* which was regarded as a higher spiritual attainment.[x]

The *molungs* used to advise the kings about the perfect time of going to a war, auspicious moment of starting a good work. In the coronation ceremony of a king, the *molungs* used to empower the royal throne by bringing *cheng* or divine power to the throne by performing a ritual. They used to study the manuscripts and fortune telling on the legs of a fowl.[xi]

The *molungs* were also given the opportunity to discuss important matters in the royal court. If there were important discussion on state

Nowgong Girls' College ESTD: 1962 Nagaon :: Assam
Principal Nowgong Girls' College Nagaon :: Assam

affairs or any personal discussion, king invited *molungs* personally. In all important matters their opinion were taken into considerations.[xii]

They used to take their livelihood from the cultivation. Moreover they took sword whenever there was in need of war or any other external aggression. The chief *molung* appointed in the royal palace was given *paiks* and other privileges. They were also appointed in other offices too. In this regard mention may be made of Mosai Sengkaluk who was entrusted in the charge of Tiru Pathar iron ore and in the charge of military department. This was mentioned in the Mohung Vamsavali.[xiii]

The *molungs* also knew about the use of medicinal plants and penned down the use of medicinal plants on several diseases in Tai scripts. They gave the knowledge of these from generation to generation.[xiv]

Till the acceptance of Hinduism by the Kings, the Priestly class i.e. the Mohan, Deodhai and the Bailungs played a vital role in administrative as well as spiritual well-being of the kingdom. With the inclination of the Ahom kings towards Hinduism, the Priestly class opposed the acceptance of Hinduism by the kings and resisted the king from doing this. Although the Ahom kings did not totally abandon their traditional customs, rites and rituals, from that time onwards the condition of the Priestly class people did not going well. They somehow become a lone fighter in preserving their traditional religion and customs. They were forced to live a secluded life. After the fall of the Ahom Kingdom and the arrival of the British to Assam, a new era can be noticed about the condition of the Ahoms.

B. CONDITION OF THE AHOM PRIESTLY CLASSS DURING THE BRITISH RULE:

The British came to power in Assam in 1826 and from that onwards the condition of the Tai-Ahoms became degraded. Although the Ahoms have made several attempts to recapture the power but all their attempts came into vain. In this situation the British made pre planned effort to subjugate the rebellious mind of the Ahoms. After the end of the Ahom rule, the *satra* Institution became powerful. During the days of the Ahom rule, the *satras* were gifted thousands acres of lands by the Ahom kings. After the end of the Ahom rule the de facto rule was transferred to the British. With the influence of *satras* and the conspiracy of the British took a concrete shape when the Ahoms started to take *saranas* from the *satras* and thus the *satras* dominated the Ahoms indirectly. The Ahoms more or less fell prey to the motive of the *satras* by taking *sarans* and they inclined a lot towards neo-vaisnavism and gave away their traditional customs and beliefs. Those who accepted Hinduism and *saranas* had abandoned several traditional beliefs and customs. However in this juncture, the Ahom Priestly Class [illegible] Mohan, Deodhai and the Bailungs refused to take *saranas* from the *satras* and resisted the change by confining them so well that they preserve their own traditional religious customs to a great extent. However all was not gone well for the Mohan, Deodhais and the Bailungs. In this situation the Priestly class became a lone fighter to preserve their original religious customs. On the other hand their condition even deteriorated so badly that they were forced to live a secluded life. Even the Ahoms totally neglected the Mohan, Deodhai and the Bailung clans and the stopped marriage relationship or any other social functions with the priestly class people. They totally boycotted the priestly class people in every matter of social life. They started to neglect the priestly class people for their non acceptance of Hinduism and used derogatory term on them such as *aa-sarania*, *abhogia* etc. In this juncture, economic condition of the priestly class deteriorated to even worse.

Due to the deprival of the British and negligence the caste Hindus, the Ahoms began to organize themselves under a common roof and the result of this motive was the formation of Ahom Sabha in 1893. However Ahom Sabha gave more importance on the political aspirations of the Ahoms rather than the issue of Ahom language and religion. In the pre-independence period the Ahom revival movement was carried by the Ahom Sabha but gradually the leaders of the Ahom Sabha got attracted by the national politics of the congress and thus the Ahom movement also got influenced by it. In post-independence era, although several organizations were established but all of them were elite in character and lost its credibility among the masses. In true sense Ahom revivalism took place with the establishment of the Mohan Deodhai Bailung Sanmilan, Assam in 1962. It became the torchbearer of the Ahom revival movement as it took a formidable step to revive the culture of the Ahoms. All the important organizations such as All Assam Phuralung Sangha, Purbanchal Tai Sahitya Sabha etc. were established with the initiative of the Mohan Deodhai Bailung Sanmilan. The Ahom revival movement in the post-colonial period is fully based on the Mohan, Deodhai and the Bailungs as they preserved the Ahom traditional rites and rituals. They are still preserving their traditional rites and rituals to a great extent.

V. CONCLUSION

A conclusion section is not required. Although a conclusion may review the main points of the paper, do not replicate the abstract as the conclusion. A conclusion might elaborate on the importance of the work or suggest applications and extensions. Among the Ahoms, the Mohan, Deodhai and the Bailungs are the three clans who perform the traditional rites and rituals. The Ahom king with their arrival in Assam in 1228 performed the traditional Ahom rites and rituals with the help of these priestly class people. In the time being, they mixed with the local people and adopted their rituals under their own domain. However things began to be changed from the 15th century, with the adoption of Hinduism the kings inclined towards the Hinduism and neglected their own religious traditions. Although they performed some rituals of the Ahom pantheon, the general condition of the Ahom priestly class began to be deteriorated. With the negligence of the kings and the officials, the Ahom priestly class had to live a secluded life. Although the Ahom Priestly Class [illegible] Mohans, Deodhais and Bailungs are among the seven royal clans of the Ahom

Nowgong Girls' College ESTD:1962 Nagaon :: Assam
CTC
Principal
Nowgong Girls' College
Nagaon :: Assam

dynasty, they did not get much attention of the Kings due to their non-acceptance of the Hinduism. So, in a vast period of history they have to reside lonely. They are still preserving their traditions to a great extent. But when the revival movement among the Ahoms began, the Priestly Class people soon attracted the attention of the larger section of the Ahom community.

REFERENCES

[1]. H.K., Barpujari (ed.), The Comprehensive History of Assam, Vol-III, Publication Board of Assam, Guwahati, 2007, p.254.
[2]. P., Gogoi, Tai Ahom Religion and Customs, Publication Board of Assam, Guwahati, 1976, p.35.
[3]. B.K., Gohain, The Ahoms and Their Traditions, Vol-I, Omsons Publications, New Delhi, 2011, p.102
[4]. ibid.
[5]. ibid., p.103.
[6]. Interview with Gyanendra Phukan.
[7]. Interview with Manuranjan Phukn.
[8]. B.K., Gohain, The Ahoms and Their Traditions, Vol-I, Omsons Publications, New Delhi, 2011, p.104.
[9]. Interview with Tileshwar Mohan.
[10]. Lakshminandan, Bora (Ed.), Tai Pandit Tengai Mohung Aru Mohan Deodhai Bailunghokol, Bakata Parijat, 2015, p.30.
[11]. B.K Gohain, op.cit., p.104.
[12]. Lakshminandan, Bora (Ed.), op.cit., p.30.
[13]. Interview with Gyananedra Phukan.
[14]. Lakshminandan, Bora (ed.), op.cit., p.30.

Nowgong Girls' College ESTD: 1962 Nagaon :: Assam

C.T.C.
Principal
Nowgong Girls' College
Nagaon :: Assam

Retrieval Number: B11630982S1019/2019©BEIESP
DOI:10.35940/ijrte.B1163.0982S1019

Published By:
Blue Eyes Intelligence Engineering
& Sciences Publication

Research Paper | Education | E-ISSN No : 2454-9916 | Volume : 5 | Issue : 9 | Sep 2019

EMPOWERMENT OF SECONDARY SCHOOL GIRLS - A STUDY

Dr. Manuj Kumar Chutia

Nowgong Girls' College, PO- Haibargaon, Dist: Nagaon, Assam – 782002, India.

ABSTRACT

Women empowerment is one of the most important issues for all nations of the world. It is significant not only from personal point of view but from the national development perspective too. It means powering or giving authority to women for developing strength and confidence in the field of social, political, educational, economic and other fields of life and prevents them from all forms of discrimination and violence against them.

Adolescence is the grounding stage of adulthood which is very much crucial and vulnerable period of one's life. The prevailing gender discrimination in human society put our adolescent girls at risk for their secure and healthy transition from childhood to adulthood. Empowering adolescent girls through education, life skills training, social support and awareness can help a lot to build up self-assurance and strength among them. Therefore, it is necessary to make them more sensitive about their righteous activities and intrinsic power through empowerment. This paper attempts to highlight the empowerment status of women in general and adolescent girls in particular with special reference to Nagaon sub-division area.

KEY WORDS: Women Empowerment, Adolescent girls, Awareness.

INTRODUCTION:

The development of a nation largely depends on the development of its individuals. If men and women are equally treated and opportunities are given proportionately, the possibility of complete development of the society and the nation increases. Therefore, development in its real sense requires gender equality which is lacking almost all societies of the world in general and India in particular. Gender inequality in Indian context is more evident in economic, political and social variables. In the economic field women still lagging behind than men and they are more likely to live in poverty, less likely to participate for work in the formal sector and major household responsibilities. In the political zone women have been seen lower representation in electoral bodies of any level. Similarly in social sector too huge inequality has been observed in the form of sex ratio, decision making, literacy rate, spirit of mobility and enrolment in higher education. Women are more likely to be the victims of domestic violence and sexual assault in the society (Singh, 2015). In India women have been given the secondary status in the household and work place which significantly affect women's health, status, education and political involvement. Women are commonly married young, quickly become mothers and then burdened by stringent domestic and financial responsibilities. It has been rightly observed that male domination in different societies still continues and all activities done keeping the benefits in front favouring men. Moreover, almost in all Indian communities, discrimination prevails between boy child and girl child and birth of a baby boy is celebrated with pride which is hardly noticed in case of baby girl. In some societies, the birth of a baby girl is considered to be a curse as a result of which crime against female foeticide and infanticide committed (Agarwal, 2012). Such kind of incidents take place not only in uneducated and poor sections of the society but educated and well to do families too in a large scale. More over least care is taken to the girl child due to which they suffer varied forms of illness because of malnutrition. Though many efforts have been endevoured by the nations of the world to bring gender equality in all aspects, the result is still frustrating. The United Nations Organization (UNO) too has set some targets for all its member nations to achieve by the end of 2015 in the name of Millennium Development Goals (MDGs) among which gender equality and women empowerment is the most prominent one.

Women Empowerment: Concept and Importance:

Empowerment is a process of enabling people to do their activities independently in different areas of life. Simply it means powering or enforcing people. It refers individuals acquiring the power to think and act freely, exercise choice and fulfill their potential as full and equal members of society (Lakshmi & Iyer, 2015). It is a multilevel construct referring to individuals, organizations and community. It cannot be restricted to a particular aspect rather in many dimensions. So, empowerment is a multi dimensional process, which should enable individuals and groups to realize their full identity and powers in all spheres of life (Nath & Anupama, 2008). Empowerment cannot be restricted to the boundaries of a particular region rather it is an international and global issue. As an international it is involving mutual respect, critical reflection, caring and collective participation, through which people lacking an equal share of valued resources gain greater access to and control over these resources (Lakshmi & Iyer, 2015).

Women empowerment has become a global issue now. This concept was first introduced at the international conference held in 1985 at Nairobi. Women empowerment refers to upliftment of women status in the field of social, political, educational, economic and other fields of life. It can also be said as the redistribution of social power and control of resources in favour of women. It prevents them from all forms of discrimination or violence against them. Women empowerment involves the building up of a society, a political environment, wherein women can breathe without the fear of oppression, exploitation, apprehension, discrimination and the general feeling of persecution which goes with being a woman in a traditionally male dominated structure (Shettar, 2015).

The UNO has taken some initiatives to bring gender equality highlighting the issues of women. Accordingly the year 1975 and the decade 1976-85 have been observed as 'International year for women' and 'International decade for women' respectively. In the same way, 11th October is being observed as 'International day for girl child' each year. The main theme of this day in the year 2014 was 'Empowering Adolescent Girls: Ending the Cycle of Violence'.

Though equality is an issue of top priority, women still tends to be dependent on their male counterparts on any issues including the household activities. They are hardly going out without having permission from in laws and others. We have also seen a section of women in our society who are completely dependent on their husbands or else even in some purely own affairs. These incidents signify how much dependent our women on their male counterparts. These observations highly signify the importance the empowerment of women.

Empowerment of Adolescent Girls:

Adolescence is a very crucial period of life which represents a stage of intensive growth and change in almost all aspects of child's physical, mental, social, spiritual, aesthetic and emotional life. There is no universally accepted definition regarding the period included in adolescence. Ordinarily, the period from 12/13 years to 18/19 years is called adolescence stage. But the UNO has considered the period from 10 years to 19 years as adolescence period. The growth achieved, the experiences gained, responsibilities felt and the relationships developed at this stage destine the complete future of an individual (Nath & Anupama, 2008). Adolescent girls are our potential mothers and future homemakers. It comprises nearly half of the growing period of human life. According to WHO adolescence is a period of life where a series of varied, rapid and extensive change occurs. It is a crucial phase to catch up growth in the life cycle of girls after infancy.

The world population is almost homogeneous as half of this is women. In India women constitute 48.26% of the total population as per 2011 census report. Similarly 253.2 million people (19.6%) of India are adolescent of which more than 119 million are girls. Thus almost every 5th person in India is an adolescent. India has more adolescents than never before and more than in any other country. In spite of having huge potential workforce, the future of adolescent girls seems dismal with various problems i.e. underweight, child marriage, unsafe abortion, mortality etc. According to UNICEF more than half of adolescent girls (56%) are anaemic and 43% are married off before the age of 18. Malnourishment among India's adolescent population is found to be higher than even some of the least developed countries of the world. Therefore, it is urgently required to make them aware

Nowgong Girls College ESTD: 1962 Accredited by NAAC

Principal Nowgong Girls' College Nagaon :: Assam

© 2019, IERJ. This open access article is published under the terms of the Creative Commons Attribution-NonCommercial 4.0 International License which permits Share (copy and redistribute the material in any medium or format) and Adapt (remix, transform, and build upon the material) under the Attribution-NonCommercial terms.

about their problems and appropriate remedies. As future of the nation is hide in adolescent girls in a large extent so it is necessary to make them prepare for all responsibilities in and outside the household through education and empowerment. So the nation should plan and execute adequate policies to prepare this large young workforce for productive purposes from national development perspectives.

Rationale of the study:

Adolescence is the preparation of adulthood which is very crucial period of life. It is a period of rapid growth with new capacities and physical changes that create not only opportunity for their progress but also problems as well. So it is necessary to prepare them for variety of roles in all spheres of life. Empowerment can give them a chance to perform their assigned roles in different stages of life effectively. Therefore we need to make them prepare in such a way that they can be able to protect themselves against any form of violence and discrimination. As today's adolescent girls are tomorrow's women and potential mothers so we need to make them more empowered. Keeping this consideration in mind the present study was undertaken.

OBJECTIVES OF THE STUDY:

i) To study the awareness status of empowerment of adolescent girls.

ii) To study the empowerment status of tribal and Non-tribal adolescent girls.

iii) To study the decision making capability of tribal and Non-tribal adolescent girls.

METHODOLOGY OF THE STUDY:

Sample:

A sample of 217 adolescent girls from class XII was selected randomly from 50 different educational institutions of Nagaon sub-division area among which 98 tribal and remaining 119 were from non tribal community.

Research tool:

The tool used in this study was 'Adolescence Girls Empowerment Scale' prepared by Dr. Devendra Singh Sisodia and Dr. Alpana Singh. The questionnaire has 49 statements from seven different areas altogether with reliability coefficient of 0.71 (Test- Retest Method) and high content and construct validity.

Data collection:

Descriptive survey method was applied in this study to collect data. Sampled students were personally approached and asked them to fill the questionnaire as per the guidelines given therewith.

RESULT AND DISCUSSION:

The result of the present study is expressed as follows:

Table 1: Empowerment status of adolescent Girls

Category	N	Level of empowerment (%)		
		Low	Average	High
Overall	217	0	38.46	61.54
Tribal	98	0	37.50	62.50
Non-Tribal	119	0	65.22	34.78

From the above table it has been revealed that most of the adolescent girls have high awareness status on empowerment. Here 61.54% adolescent girls have found to be placed in high empowerment status where as 38.46% in average category. No records have been observed in the category of low awareness status on empowerment. In case of tribal adolescent girls, 62.50% have exposed high empowerment status where as 37.50% have average. On the other hand 34.78% non-tribal girls have shown high empowerment status comparing to 65.22% average status.

Table 2: Significance of difference on empowerment between tribal and Non-tribal adolescent girls

Category	N	M	SD	Z	Sig. (2 tailed)	Remark
Tribal	98	199.88	20.51	3.93	2.58	S
Non-Tribal	119	186.13	15.54			

Significant level at P>0.01

The 'Z' value while comparing the significance of difference of empowerment status between tribal and non-tribal adolescent girls is found 3.93 (Z = 3.93 > .01), which is greater than the standard value of 2.58 at 1% level of significance. So the calculated value is significant at 1% level of significance and therefore, rejects the null hypothesis. It indicates that there is significant difference on empowerment status between tribal and non-tribal adolescent girls. Therefore, it can be said that differences exist on empowerment status between tribal and non-tribal adolescent girls and hence it varies from community to community.

Table 3: Significance of difference on decision making capability between tribal and Non-tribal adolescent girls

Category	N	M	SD	Z	Sig. (2 tailed)	Remark
Tribal	98	28.06	3.77	0.30	1.96	NS
Non-Tribal	119	27.83	4.54			

Significant level is at P < 0.05

The 'Z' value while comparing the significance of difference on decision making capability between tribal and non-tribal adolescent girls is found 0.30 (Z = 0.30 < .05), which is lower than the standard value of 1.96 at 5% level of significance. So the calculated value is not significant at 5% level of significance and therefore, null hypothesis cannot be rejected. It indicates that there is no significant difference on decision making capability which is one of the most important ingredients of empowerment between tribal and non-tribal adolescent girls. Therefore, it can be said that no difference exist on decision making capability between tribal and non-tribal adolescent girls.

MAJOR FINDINGS:

- Most of the adolescent girls in general and tribal adolescent girls in particular have high empowerment status.
- Most of the Non-tribal adolescent girls have average empowerment status.
- Tribal adolescent girls have high empowerment status than non-tribal adolescent girls.
- The average mean score on empowerment of adolescent girls is 197.33.
- The Mean empowerment status of tribal adolescent girls is higher (199.88) than non-tribal (186.13) adolescent girls.
- Significant difference exists on empowerment status between tribal and non-tribal adolescent girls.
- No significant difference exists on decision making capability between tribal and non-tribal adolescent girls.

CONCLUSION:

Women empowerment is a much debatable topic of the present era around the world. This issue has been gradually raising its popularity day by day. It is not because of emerging feminism in the society, but for long standing exploitation and dominance on women over the years. As almost half of the world population is women, so it is necessary to make them aware, developed, educated and empowered. Adolescence is the most promising stage of one's life and today's adolescent girls are tomorrows potential women and mothers, so it is very important to make them empowered in all spheres of life from gender equality perspective as well enhancing the possibility of progressive development of the nation. To conclude Empowered girls empowered nation.

REFERENCES:

1. Agarwal, S. (2012). Emerging Issues and Education. Guwahati: Bookland.
2. Bandiera, et al. (October, 2012). Empowering Adolescent Girls: Evidence from a randomized Control Trial in Uganda. www.econ.ise.ac.uk/staff/rchvargess/wp/ELA/
3. Choudhury, S. (March-April, 2016). A study of self concept and empowerment of adolescent girls. Scholarly Research Journal for Interdisciplinary studies, 3(23), 1791-1796.
4. Kumar, P. & Paul, T. (2007). Empowerment of women: Concept, Policy approach and Implications. www.isical.ac.in
5. Lakshmi, K. J. & Iyer, S. R. (April, 2015). Empowerment of women through education. Edutracks. 14(8), 8-12
6. Lamb, S. & Peterson, Z. D. (May, 2011). Adolescent Girls' Sexual Empowerment: Two Feminists Explore the Concept. Springer Science + Business Media, p.703-712.
7. Majumdar, R. & Ganguli, S. K. (2000). A study on adolescent girls in Rural. Health and Population –Perspectives and Issues, 23(2), 95-104.
8. Nath. B. K. & Anupama, P.(2007-08). Empowerment of adolescent girls in India- Policy perspective. M. Ed Dissertation, University of Calicut. www.academia.edu
9. Osumeri, N. M. & Anna, R. (March, 2015). Influence of Kudumbashree on women empowerment. Excellence International Journal of Education and Research, 1(8), 11-22.
10. Selvi, B. T. & Thangarajathi, S. (March, 2015). Women empowerment through Yoga. Edutracks, 14(7), 8-11.
11. Shettar, R. M. (April, 2015). A study on issues and challenges of women empowerment in India. IOSR Journal of Business and Management, 17(4), 13-19.
12. Singh, K. (March, 2015). Gender Inequality and concept of women empowerment. International Journal of Education and Research, 1(8), 55-66.
13. Sinha, S. L. (May-June, 2016). A study of the empowerment level of adolescent girls at senior secondary level with reference to Decision making & participation capability. Scholarly Research Journal for Interdisciplinary Studies, 3(24), 2126-2132.

Nowgong Girls College ESTD: 1962 Nagaon :: Assam
C.T.C.
Principal
Nowgong Girls College
Nagaon :: Assam

14. Sinha, S. L. (2016). A Comparative Study of women empowerment awareness level of Adolescent Girls in Private and Government Schools of Delhi. International Journal of Education and Information Studies, 6(1), 7-10.

Nowgong Girls' College ESTD: 1962 Nagaon :: Assam

Principal
Nowgong Girls' College
Nagaon :: Assam

Return to call 00:33

International Journal of Hindi Research

VOL. 5, ISSUE 6 (2019)

S. No.	Title and Authors Name
1	वर्तमान परिप्रेक्ष्य में अनुवाद की भूमिका युगल किशोर यादव Abstract | Download Pages: 01-03 | 1064 Views 259 Downloads
2	प्रेमचंद के उपन्यास में स्त्री जीवन का यथार्थ (कर्मभूमि के विशेष सन्दर्भ में) बेबी विश्वकर्मा | Download Pages: 04-05 | 175 Views 173 Downloads
3	छायावादी काव्य: भाषा और 'पल्लव' भारती | Download Pages: 06-08 | 808 Views 805 Downloads
4	संत कवयित्री मीराबाई की भक्ति और सामाजिक परिप्रेक्ष्य कंचन लता देवी, प्रेम सुमन शर्मा | Download Pages: 09-11 | 155 Views 153 Downloads
5	महाकवि गोस्वामी तुलसीदास विरचित रामचरितमानस में अरण्यकांड का अध्ययन कुमार० सतिश तिनाराक, धारता.डकर Pages: 12-14 | 1 Views 1 Downloads

Nowgong Girls' College ESTD: 1962 Nagaon :: Assam

lescent girls are our potential mothers and future homemakers. It comprises nearly one-fifth of the population in human life. According to WHO adolescence is a period of life where a series of varied, rapid and extensive change occurs. It is a crucial phase to catch up growth in the life cycle of girls after infancy.

The world population is almost homogeneous as half of this is women. In India women constitute 48.26% of the total population as per 2011 census report. Similarly 253.2 million people (19.6%) of India are adolescent of which more than 119 million are girls. Thus almost every 5th person in India is an adolescent. India has more adolescents than never before and more than in any other country. In spite of having huge potential workforce, the future of adolescent girls seems dismal with various problems i.e. underweight, child marriage, maternal mortal-

Principal
Nowgong Girls' College
Nagaon :: Assam

International Journal of Hindi Research
ISSN: 2455-2232; Impact Factor: RJIF 5.22
Received: 02-08-2019; Accepted: 04-09-2019
www.hindijournal.com
Volume 5; Issue 6; November 2019; Page No. 04-05

प्रेमचंद के उपन्यास में स्त्री जीवन का यथार्थ (कर्मभूमि के विशेष सन्दर्भ में)

केवी त्रिपाठकर्मा
शोधार्थी, राजीव गाँधी विश्वविद्यालय, अरुणाचल प्रदेश, दोइमुख, भारत

सारांश

प्रेमचंद का युग नवीन दृष्टिकोण और प्राचीन मान्यताओं के बीच का संक्रम काल था. एक वर्ग ऐसा था जो बचपन से सीधे मध्यकालीन मानदंडो के आधार पर जीवन को देख रहा था तो दूसरा वर्ग वह था जो आधुनिक जीवनशैली को अपना रहा था। प्रेमचंद की स्त्री विषयक दृष्टिकोण समन्वयकारी है जहाँ परंपरा और आधुनिकता का सम्मिश्रण है. प्रेमचंद के समय में नारी की स्थिति अच्छा न था। वे हर तरफ से दमित व पीड़ित थी। एक तरफ तो पारिवारिक संपत्ति में उनका कोई हक नहीं था तो दूसरी और आर्थिक रूप से भी वह पुरुष पर आश्रित थी। सामाजिक स्तर पर वह या तो केवल घर संभालने वाली सामान्य स्त्री थी या तो वेश्या थी। विवाह ही लड़कियों के जीवन का परम उद्देश्य माना जाता था। प्रेमचंद नारी के पीड़ा से अभिभूत थे। उनकी पहली हिन्दी उपन्यास सेवासदन नारी केन्द्रित है। प्रेमचंद पुरोन समाज में वेश्याओं को नीच समझा जाता था। उनको समाज का अनिष्टकारी अंग माना जाता था। ऐसे काल में प्रेमचंद सेवासदन लिखकर वेश्या और नारी जीवन के व्यथा के प्रति सहानुभूति जताते हैं। प्रेमचंद यह दिखाते हैं कि किस प्रकार नारी को आर्थिक,सामाजिक शोषण के दोहरे दंश झेलना पड़ता है। किस प्रकार उसकी आत्मसम्मान की रोज हत्या की जाती है। जिस समय में नारी को पुरुषों से हेय समझा जाता था उस समय प्रेमचंद सशक्त नारी चरित्रों का निर्माण कर नारी के पक्ष में खड़े थे। नारी शिक्षा, अनमेल विवाह, वेश्या समस्या, सम अधिकार आदि अनेक विषयों को लेकर प्रेमचंद नारी संबन्धित रचनाएँ लिख रहे थे। उनके नारी पात्र सशक्त हैं,जीवंत हैं। चाहे वह सेवासदन की सुमन हो या गबन की जालपा अथवा गोदान की धनिया अथवा सिलिया।

कर्मभूमि प्रेमचंद की प्रसिद्ध उपन्यास है। इसका मूल स्वर राष्ट्रवादी है। परंतु यहाँ भी नारी जीवन के अनेक पहलुओं को प्रेमचंद ने दिखाया है। उन्होंने कर्मभूमि उपन्यास के नारी चरित्रों का निर्माण अत्यंत बखूबी से किया है। प्रत्येक स्त्री पात्र एक दूसरे से भिन्न है तथा समाज के किसी न किसी पक्ष की प्रतिनिधि बनकर सामने आयी है। उपन्यास की प्रमुख पात्र सुखदा प्रेमचंद की ही विचारों की प्रतिनिधित्व करती है,ऐसा कहा जा सकता है। उसमें पारंपरिक मूल्य भी है साथ ही वह आधुनिक भी है। सुखदा के जरिये प्रेमचंद ने आधुनिक बनते समाज के उस स्त्री वर्ग को दिखाया है जो किताबें पढ़ती है, सिनेमा देखती है, खुली विचारों की है, स्वतंत्र है। सुखदा के जरिये प्रेमचंद मध्यकालीन संस्कारों से मुक्ति का प्रयत्न करते हैं। समाज और परिवार द्वारा बहिष्कृत बलात्कृत स्त्री को सुखदा अपने घर में जगह देना चाहती है और जब अमरकांत उससे पूछता है की क्या उसे घृणा न होगी? तो सुखदा कहती है- "अगर मैं कहूँ न होगी तो असत्य होगा...पर संस्कारों को मिटाना होगा। उसने कोई अपराध नहीं किया, फिर सजा क्यों दी जाए?"[1] इन बातों में कितनी सच्चाई है। वह अपनी खामी जानती है और उसे दूर करना भी चाहती है। सुखदा मध्यकालीन मान्यताओं से पीड़ित समाज में पली बढ़ी है। इसकारण उसके हृदय में उन मान्यताओं का होना स्वाभाविक है। परंतु प्रशंसनीय यह है की वह उन संस्कारों से उभरना चाहती है। वही देहाती लड़की जब दोषी सिपाहियों की हत्या कर डालती है तो उसके हित में सबसे पहले सुखदा ही खड़ी होती है। समाज के तथाकथित नेता तो केवल अपने भाषण देकर कर्तव्य की समाप्ती मान लेते हैं. सुखदा का मानना है की उस लड़की ने कोई अपराध नहीं किया है। जब उसका साथ देनेवाला कोई नहीं था तो उसने खुद ही न्याय किया, वह अपराधी नहीं है। उसे किसी भी प्रकार से सजा नहीं होनी चाहिए। सुखदा एक सशक्त नारी पात्र के रूप में उभरती है जो न्याय के पक्ष में लड़ती है चाहे वह बलात्कृत स्त्री के हक के लिए हो, हरिजनों के मंदिर प्रवेश का प्रसंग हो या फिर गरीबों की उत्थान के लिए हो. समाज के अन्यायपूर्ण मान्यताओं पर वह प्रश्न उठाती है। सुखदा कहती है की पुरुष को समाज में कुछ भी करने की स्वतंत्रता क्यों प्राप्त है। ऐसा क्यों है की जो मनचाहे वह कर ले और स्त्री को ही पतिव्रता बनकर रहना पड़ता है। सुखदा नारी के उस वर्ग का प्रतिनिधित्व करती है जो वर्ग अपने अधिकारों को पहचान रही थी। किसी से दमित होकर जीना इन्हे मंजूर नहीं। उनमे विद्रोह की भावना है। इसीकारण जब अमरकांत उसके साथ धोखा करता है तो वह उसे माफ नहीं करती, उसे मनाने भी नहीं जाती। वह प्रगतिशील विचारों की नारी है। हजारों गलती करने पर भी पति को परमेश्वर माने, ऐसी वह नहीं। उसमे आत्मसम्मान है, स्वाभिमान है। वह यह जानती है की ऐसा अभिचारी कार्य वह करती तो अमरकांत उसे कतई माफ नहीं करता। इसके विपरीत उसे मारने के लिए ही चला जाता। इसकारण अमरकांत के घर छोड़ने पर न ही वह उसके पास उसे मनाने के लिए जाती है और न ही पति वियोग में रोती कराहती रहती है। यह घटना सुखदा की जीवन को नया मोड़ देती है। दांपत्य जीवन के पराजय से वह टूट नहीं जाती। बल्कि उसका मनोबल और आत्मसम्मान बढ़ ही जाती है। वह समाज को यह दिखा देती है की जीवन में कुछ कर दिखाने के लिए किसी के सहारे की जरूरत नहीं है। स्त्री किसी की आश्रित नहीं है। उसका अपना मनोबल ही उसे जीवन में आगे ले जाने के लिए काफी है।

हमारे समाज में आज भी जिसके साथ बलात्कार होता है उसे ही हीन दृष्टि से देखा जाता है। प्रेमचंद ने सुखी के जरिये समाज की उस संवेदनहीनता को दिखाया हैं जहां बलात्कार होने पर उसकी सजा अपराधी को नहीं बल्कि पीड़ीत को भुगतना पड़ता है। सारा समाज उसे पतित समझकर उसे घृणा की दृष्टि से देखता है, उसका बहिष्कार करता है। अपराध किसी और का होता है और दंड किसी और को मिलती है. सुखी अपने परिवार से अत्यंत प्रेम करती है इसीकारण पति के अनेक मिन्नतों के बावजूद वह लौटने को तैयार नहीं होती। क्योंकि उसके मन में समाज का डर बसा था। भारतीय समाज में एक

बचपन से ही पीन सुचिता का पाठ पढ़ाया जाता है. इसी पीन मानसिकता का शिकार होने के कारण सुखी के मन में ही घृणा भर जाता है। बलात्कार से सम्बंधित मूल्य जुड़ी सोच्छल सिलसा है जो स्त्री की मानसिक असंतुलन बलात्कार बनता है. सुखी का चरित्र सभी पीड़ित स्त्रियों के लिए घृणा, अपना सर्वस्व खोने के बाद भी वह हार नहीं मानती और नैनीताल के गाँव में जाकर जिंदगी की एक नयी शुरुआत करती है। सारे दुःखों को वह अपना बना लेती है। वह सभी को माफ़ कर देती है, पुनः जीवन जीना सिखाती है, प्रेम करना सिखाती है. सुखी अपने जीवन

अतिवादी विचारधारा का परिणाम है. एक स्त्री पूर्णतः मानवी है, एक मानव के हैसियत से ही वह सम्मान की हकदार है तथा संपूर्ण मानवीय दुर्बी-अवगुणों के साथ वह स्वीकार्य है. उस पर देवीत्व के गुणों को आरोपित करना समीचीन नहीं है. प्रेमचंद की स्त्री दृष्टि की खासियत यह है कि उन्होंने पहली बार स्त्री को एक स्वतंत्र व्यक्तित्व के रूप में,'व्यक्ति'के रूप में प्रस्तुत किया. स्त्री सम्बन्धी कई घातक विचारों को तोड़ते हुए उन्होंने घर की देहलीज को लांघ कर आत्मनिर्भरशील बनती स्त्री छवि को केंद्र में लाया. चूंकि प्रेमचंद यथार्थोन्मुख आदर्शवादी रचनाकार थे, वे आदर्श के मोह से मुक्त नहीं हो पाए, जिसकारण वे स्त्री चरित्रों में क्रांतिकारी परिवर्तन

Nowgong Girls' College ★ ESTD: 1962 ★ Nagaon :: Assam
Principal
Nowgong Girls' College
Nagaon :: Assam

Journal of Food Measurement and Characterization
https://doi.org/10.1007/s11694-020-00440-1

ORIGINAL PAPER

Fuzzy logic approach for optimization of blended beverage of cold plasma treated TCW and orange juice

Hemanta Chutia[1] · Charu Lata Mahanta[1] · Namita Ojah[2] · Arup Jyoti Choudhury[2]

Received: 2 November 2019 / Accepted: 3 March 2020
© Springer Science+Business Media, LLC, part of Springer Nature 2020

Abstract

The process conditions of dielectric barrier discharge cold plasma using nonlinear regression analysis for enhanced shelf life of tender coconut water (TCW) were optimized. Face centre composite design was used to optimise process condition of cold plasma treatment and desirability of treated TCW was determined on the basis of microbial load, DPPH scavenging activity, free fatty acid content and transmittance. Microbial load, DPPH scavenging activity and transmittance decreased with plasma treatment time and voltage whereas fatty acid content increased. However, TCW developed 'chemical' odour at the optimized cold plasma treatment condition of 18.00 kV voltage and 1.75 min treatment time. Pasteurized orange juice (1–4%) was added to the cold plasma treated coconut water to counter the off flavour and the developed blended beverage was subjected to sensory optimization using fuzzy logic. From the application of fuzzy logic, it was determined that cold plasma treated TCW with 1% orange juice has acceptable sensory properties. The study revealed that cold plasma was helpful in reducing microbial load of TCW and its blending with 1% orange juice gave beverage that was acceptable for sensory attributes besides being able to mask the 'chemical' odour. Cold plasma can therefore be used in place of thermal treatment for processing of TCW.

Keywords TCW · Cold plasma · Beverage · Optimization · Fuzzy logic

Introduction

Coconut (*Cocos nucifera* L.) water has physiological health benefits and is helpful for anti-inflammatory property, restoration of electrolytes, oral rehydration, homeostasis, and treatment of conditions like childhood diarrhoea, gastroenteritis and cholera. It also has demand in the sport drinks market for its balanced electrolytes, taste, flavour, available nutrients and functional characteristics. TCW is a refreshing drink in tropical coastal areas but degrades in quality very rapidly. On exposure to air, it's sensory, nutritional and flavour characteristics are easily lost [1, 2]. Thermal treatment as followed in industrial processing helps to prolong the shelf life but the process causes loss in nutrients and its delicate flavour [1], which adversely affects its acceptability.

Several studies have reported an increase in the shelf life of coconut water on processing while retaining its quality. Campos et al. [3] and Costa et al. [4] used chemical preservative. Studies on the use of two-stage microfiltration technique in sterile atmosphere for preserving the water have been reported [5, 6], but microfiltration in a sterile atmosphere is a tedious and costly technique.

Cold plasma is one of the novel nonthermal techniques being widely studied for microbial decontamination of foods, inactivation of polyphenol peroxidase in fruit juices, enhancement of antioxidant activity and rate of germination of seeds among various other applications [7–10]. Cold plasma is generated in any neutral gas on the application of high energy. As the energy input is increased beyond a certain level in the gaseous state, the gas molecules are ionised and yields the plasma state [11]. The ionised gas comprises of electrons, ions, radicals and atoms which are both in ground and excited states [12]. The reactive oxygen species and reactive nitrogen species formed in the gas interact with food components and modify them [13]. The synergistic effect of the multiple constituents generated in the plasma have been found to

Charu Lata Mahanta
charu@iezu.rnet.in
Department of Food Engineering & Technology, Tezpur University, Tezpur, Assam, India
Department of Physics, Tezpur University, Tezpur University, Tezpur, Assam, India

Published online: 10 March 2020

Nowgong Girls' College ESTD 1962 Nagaon :: Assam
CTC
Principal
Nowgong Girls' College
Nagaon :: Assam

effectively kill or inactivate microorganisms on food surface while maintaining food nutrition [14]. Cold plasma is effective against both pathogenic and spoilage microorganisms [15]. The effect of cold plasma on different foods including dairy products [16], meat [17], bakery products [18], whole fruits like Strawberries [19] and kiwi fruit [20], juices of apple [21] and pomegranate [22] have been reported. The voltage applied for the generation of plasma and the treatment time are important process parameters. Voltage level of 90 kV for 30–120 s was used for orange juice [23], 70 kV for 15–60 s for cashew apple juice [24] and 80 kV for 1–4 min for white grape juice [25].

Blending of juices has been followed to develop refreshing beverage. Chauhan et al. [26] blended lemon with mature coconut water to develop a refreshing beverage with 13.5°Brix and reported that packaged beverage with 2% lemon juice gave shelf stability of 6 months when stored at 5 °C, 25 ± 2 °C and high 37 °C temperatures. A blended beverage using coconut water and clarified cashew apple juice ("cajuina") was observed to store well for 6 months [27]. Sindumathi and Amutha [28] developed a spice based ready to serve beverage of TCW and had shelf stability of 12 months duration at refrigerated temperature and 10 months duration at room temperature. Effect of cold plasma on the sensory attributes of TCW and development of a blended beverage with orange juice has not been reported.

Sensory evaluation is a scientific tool that measures, analyzes, and interprets sensory attributes perceived by human sensory organs [29]. Without appropriate sensory evaluation, there is a great chance of market failure [30] because it is the primary criteria for acceptability of food [31, 32]. Human perception is always fuzzy and assessors give their opinion in the linguistic form [33]. For analysis of human perception of sensory attributes Fuzzy sets can be used, which give better result as compared to average scores of the attributes [34]. Fuzzy logic is a computing based approach which helps to interpret imprecise and objective interpretations and conclusion are drawn on the acceptability, non acceptability of the product. The developed product can also be ranked on the basis of strong and weak attributes [30]. A comprehensive fuzzy model for ranking of product attributes developed by Zhang and Litchfield [35] has been successfully applied for evaluation of dahi powder [36], gluten-free pasta [37], and mango drinks [38].

In the present investigation, the process condition of cold plasma treatment of TCW was optimized and a blended beverage using cold plasma treated TCW and pasteurized orange juice was developed. Sensory attributes were evaluated by fuzzy logic.

Material and methods

Material

Green tender coconuts between 4 and 7 months of maturation were harvested from coconut trees grown nearby the campus of Tezpur University, Tezpur, Assam during end of August, 2017. Ten plants were selected for harvesting. Harvested nuts were immediately brought to the laboratory. Bruised fruits were discarded. Coconuts were processed on the same day of harvest.

Methods

Preparation and treatment of coconut water

Tender coconuts were washed and sanitized according to Mahnot et al. [6]. Just before processing coconuts were surface dried and cut open at the top. Coconuts were placed on a clean chopping board. A sharp chopper knife was used to cut open the nut at the broader end and the water was collected in a sterilized Borosil glass container in a laminar flow. Any contamination of TCW collected in this manner was unavoidable while obtaining water from the tender coconut for consumption. The collected coconut water was filtered through Whatman paper no 1 in a laminar flow and thereafter kept in freezer at − 20 °C in heavy duty vacuum bottles.

The set up and experimental conditions used for dielectric barrier discharge (DBD) plasma treatment extracted TCW is reported by Chutia et al. [39]. TCW was poured into a Petri plate inside a laminar flow which was then sealed and placed between the two dielectric plates keeping a gap of 15 mm. During DBD plasma treatment voltage, (X1) varied according to the experimental design from 18 to 28 kV and treatment time (X2) varied from 1 to 3 min.

Determination of DPPH (2,2-diphenyl-1-picrylhydrazyl) radical scavenging activity

A modified method of Fonseca et al. [40] was followed. In brief, 0.4 ml of TCW sample was added to a methanolic solution of DPPH (5.6 ml, 0.8 nM) and the solution was mixed vigorously and left undisturbed for 30 min in a dark chamber. TCW sample was replaced with 0.4 ml methanol for use as control and the mixture with no DPPH was used as blank. The developed colour was measured for absorbance at 517 nm in a UV–Vis spectrophotometer (CECIL 7400, 700 series, Aquarius). The inhibitory effects of DPPH radical or antioxidant activity was calculated.

Nowgong Girls' College ESTD: 1962 Nagaon :: Assam
C.T.C.
Principal
Nowgong Girls' College
Nagaon :: Assam

$$\text{Antioxidant activity}\,(\%) = \left(1 - \frac{A_{Sample(517nm)}}{A_{Control(517nm)}}\right) \times 100$$

Free fatty acid determination (FFA)

The titration method of Sadasivam and Manickam [41] was followed. Briefly, 5–10 ml of sample was taken in a conical flask to which 50 ml of neutral solvent added, followed by addition of a few drops phenolphthalein. The solution was titrated against 0.1 N KOH while constantly stirring till the development of mild pink colour that persisted for 15 s.

$$\text{Acid value (mg KOH/gm)} = \frac{Titrate\ value \times Normality\ of\ \text{KOH} \times 56.1}{Amount\ of\ sample}$$

Microbial load analysis

Microorganisms in TCW were determined using Nutrient Agar for aerobic microbial count and HiVeg Coliform Agar for fecal coliform count [5, 6]. Briefly, 100 µL of the samples under study was taken and spread on the plates containing nutrient agar media. The plates were then incubated at 30 °C for 48 h in an incubator for colony enumeration. Total counts were recorded and averaged [5].

Transmittance

The method of Jackson et al. [42] was followed to determine clarity of the sample against distilled water spectrophotometrically (CECIL 7400, 7000 Series, Aquarius) by measuring the transmittance at 610 nm. Hazy sediments in the coconut water were re-suspended by gently rocking the sample holder immediately before measurements were taken.

Experimental design

Response surface methodology (RSM) and face centred central composite design (FCCD) was used to optimize process conditions. Leiviska [43] mentioned that in FCCD only three levels of independent parameters are used ($\alpha = \pm 1$) which require less number of experiments and also it provides relatively high quality predictions over the entire design range. FCCD for two independent variables (input parameters of the plasma treatment) was used to fit a second-order polynomial model. Design-Expert Version 7.1.2 (Stat-Ease, Inc. MN) was used to design the experiment and in all, 13 runs were carried out as per the FCCD. Table 1 gives the real and coded values of the variables used.

Optimization

The variables were optimized on the basis of higher desirability value. Optimization was done by fixing the desired goal of dependent parameters viz maximize, minimize, target, within range, none and putting the exact value of dependent parameters of the possible goal. Then all the dependents parameters were combined into a response called "desirability function" wherein a value can lie between 0 and 1 (0 indicates one or more products are unacceptable and 1 indicates that all products are on target).

A second order polynomial equation, shown in Eq. (1) was used to predict the responses. The dependent parameters (Y_i) is the function of linear components, quadratic components and interaction components [44].

$$Y = \beta_o + \sum_{i=1}^{k} \beta_i X_i + \sum_{i<j}^{k} \beta_i X_{ij} + \sum_{i=1}^{k} \beta_{ii} X_i^2 + \ldots \quad (1)$$

where Y represents the dependent parameters, βo represents intercept of the graph, βi represents regression coefficients, X_i^2 is the nonlinear (quadratic) effect of the independent variables and X_{ij} represents the interactive effect of two independent variables. Xi represents the independent variables.

After regression analysis, each dependent parameter (yi) was transformed into an individual desirability function $d_i(y_i)$, a value that lies in the range $0 \le d_i(y_i) \le 1$ and increases with an increase in the desirability of the corresponding output. As FFA and microbial load are not desirable characteristics in TCW, desirability of the dependent parameters of FFA and microbial load was minimized and transmittance and DPPH activity was maximized. Then using geometric mean and combining the individual desirability of all the dependents parameters, overall desirability (D) (Eq. 2) was determined and the process was considered to be optimized [37].

$$D = \left(d_1 y_1 \times d_2 y_2 \times \ldots \times d_m y_m\right)^{\frac{1}{m}} \quad (2)$$

where y_1, y_2 and y_m are the dependent parameters and $_m$ denotes the number of dependent parameters.

Table 1 Real and coded values of the variables

Experimental Variables	Code	Coded levels				
		− 1.41	− 1	0	+1	+1.41
Voltage (kV)	X_1	15.93	18	23	28	30.07
Treatment Time (Min)	X_2	0.59	1	2	3	3.41

Nowgong Girls' College ESTD: 1962 Nagaon :: Assam
Principal Nowgong Girls' College Nagaon :: Assam

Blending of tender coconut water and orange juice

The optimized conditions for cold plasma treatment of TCW were followed to process coconut water. Orange juice was extracted using a household juicer (Philips juicer). The juice was strained through a muslin cloth and pasteurised at 90 °C for 60 s [45]. The time required to reach 90 °C at the centre was determined and the orange juice was held thereafter at 90 °C for 60 s. The processed water was blended with 0, 1, 2, 3, and 4% of pasteurized orange juice to develop the blended beverage inside a laminar flow, filled in sterilised bottle and tightly capped.

The five beverage samples were coded as S1 (Treated coconut water), S2 (Treated coconut water + 1% orange juice), S3 (Treated coconut water + 2% orange juice), S4 (Treated coconut water + 3% orange juice) and S5 (Treated coconut water + 4% orange juice).

Sensory evaluation

Sensory properties of the blended beverages were evaluated by 27 semi trained panel judges who were trained about the importance of impartial assessment of sensory attributes, definition of quality attributes to be evaluated, the content of the score sheet and the procedure for scoring. The judges rinsed their mouth with normal drinking water before tasting of each sample. Judges were advised to evaluate the quality attributes of the sample and assign a value in the fuzzy scale for each sensory attribute. The judges were told to categorize samples subjectively from 'Not satisfactory', 'Fair', 'Medium', 'Good' and 'Excellent' [36, 37]. Fuzzy logic was used to analyse all the sets of data noted by the judges.

Application of fuzzy logic on sensory data

Fuzzy logic uses imprecise and user-dependent data to obtain an output conclusion that helps to determine whether the quality attributes of the food are strong or weak and acceptable or not. It helps to rank foods according to the strength of the attributes. As followed by Jaya and Das [38], Das [31], and Sakre et al. [37], the developed blended beverage samples were ranked using triangular fuzzy membership distribution function. Fuzzy logic modelling follows the following steps for ranking of foods on the basis of sensory data [37, 38]:- (1) Formation of triplets from calculated overall sensory data of blended beverages; (2) Fuzzy membership function sensory scores of blended beverages; (3) Normalized fuzzy membership function; (4) Normalized fuzzy membership function matrix on standard fuzzy scale (5) Judgment membership function matrix; (6) Judgment subset; (7) Quality- ranking of blended beverage samples; and (8) Ranking of the blended beverages. Triplets were formed from the obtained sensory scores and similarity values were calculated and on the basis of this, ranking of developed beverage samples was done. Matlab (MATLAB R2012b, The MathWorks) was used to develop a programme for calculating the fuzzy logic steps. A set of three numbers set termed as 'triplets' were developed to get the triangular membership distribution pattern of the fuzzy set and 5-point sensory scales comprising of Not satisfactory/ Not at all important (0, 0, 25), Fair/Somewhat important (25, 25, 25), Medium/Important (50, 25, 25), Good/Highly important (75, 25, 25) and Excellent/Extremely important (100, 25, 0) were taken [37], as per Fig. 1. The first number of the triplet denotes the value of the abscissa, where the value of membership function was 1. The second and third numbers of the triplet indicate the distance to left and right, respectively, of the first number, where the membership function is 0 [31, 37].

Standard fuzzy scale also termed as the distribution pattern of triangular membership function of 6-point sensory scale is given in Fig. 2, where the sensory scales are represented as F1, F2, F3, F4, F5, and F6. Linguistically, the fuzzy scale for sensory analysis was categorised on a 5 point set as Not satisfactory/Not at all necessary, Fair/Somewhat necessary, Satisfactory/Necessary, Good/ Important, Very good/Highly important and Excellent/ Extremely important, according to Sakre et al. [37]. Each membership function of sensory fuzzy scale follows the triangular distribution structure where 1 is the maximum membership value.

Figure 3. shows the graphical representation of the overall membership function of sensory score as triplet (a, b, c). The figure represents that when the value of abscissa is a, the value of membership function is 1 while the value is zero when the abscissa is more than (a + c) or less than (a − b) [31, 36].

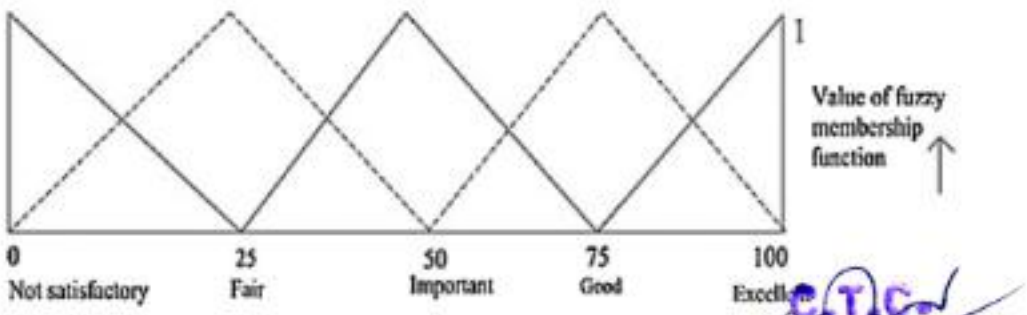

Fig. 1 Representation of triangular membership function distribution pattern of the sensory scale [26]

Nowgong Girls' College
ESTD: 1962
Nagaon :: Assam
Principal
Nowgong Girls' College
Nagaon :: Assam

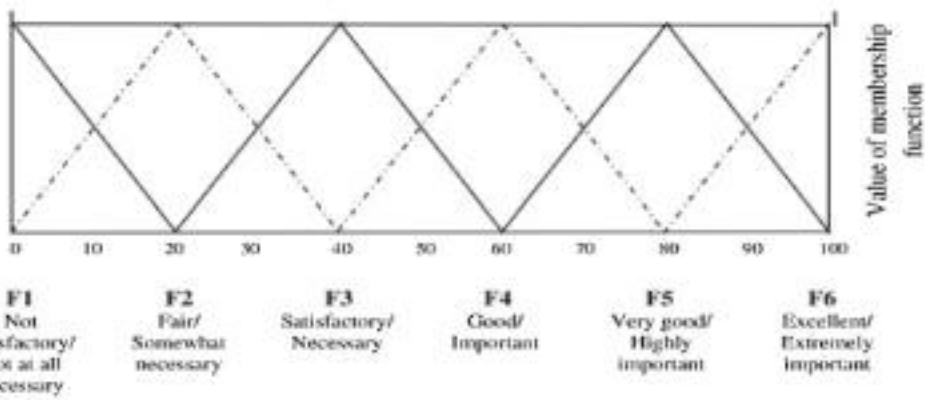

Fig. 2 Standard fuzzy scale used for ranking of the blended beverage samples [20]

Results and discussion

Effect of cold plasma on DPPH scavenging activity

The untreated TCW recorded 28.41 ± 9.43% DPPH scavenging activity. As shown in Fig. 4a, after cold plasma treatment, DPPH scavenging activity decreased with increase in voltage and time. Pankaj et al. [25] also reported that both DPPH free radical scavenging activity and total phenolic content of grape juice reduced after high voltage (80 kV) atmospheric cold plasma treatment. This may be attributed to the oxidation of ascorbic acid and phenolic compounds that are the major components of fruit juices by the plasma species [25, 46]. The antioxidant capacity was as such very low in untreated water and was further reduced as the antioxidants reacted with the free radicals generated by the plasma.

Effect of cold plasma on free fatty acid content

Free fatty acid content in untreated coconut water was 5.5 ± 0.54 mg KOH/100 ml. As shown in the Fig. 4b, the content of free fatty acids increased with an increase in the treatment time and voltage applied during cold plasma treatment. This was in agreement with the result reported by Yepez and Keener [47]. Total fat content in TCW varies from 0.01 to 0.2% [48, 49]. Meethawon et al. [50] reported lipase activity of 16 mmol/min/ml in TCW. The increase in free fatty acid can be attributed to increase in the activity of lipase on plasma treatment [51, 52] at the time and voltage combinations used in the present study that hydrolysed the triglycerides in the sample and released free fatty acids. Lipase activity was found to significantly increase with treatment time of helium radio frequency atmospheric pressure glow discharge plasma jet [51]. According to Tolouie et al. [52] time and voltage of plasma treatment are significant factors for lipase inactivation, even though there is no complete inactivation. The authors also observed recovery of lipase activity after plasma treatment of wheat germ.

Effect of cold plasma on microbial load analysis

There was no coliform in the plasma treated coconut water. The aerobic microbial load in TCW before plasma treatment was 150–175 cfu/ml. As shown in the Fig. 4c, with increase in the voltage and time the microbial inactivation was more rapid. Xu et al. [23] reported that the activity on microorganisms continues up to certain period of time after the treatment if the treated sample was held for some time without any processing. 5-log reduction of *S. enterica* was achieved after 30 s of HVACP treatment of 25-ml orange juice with air and

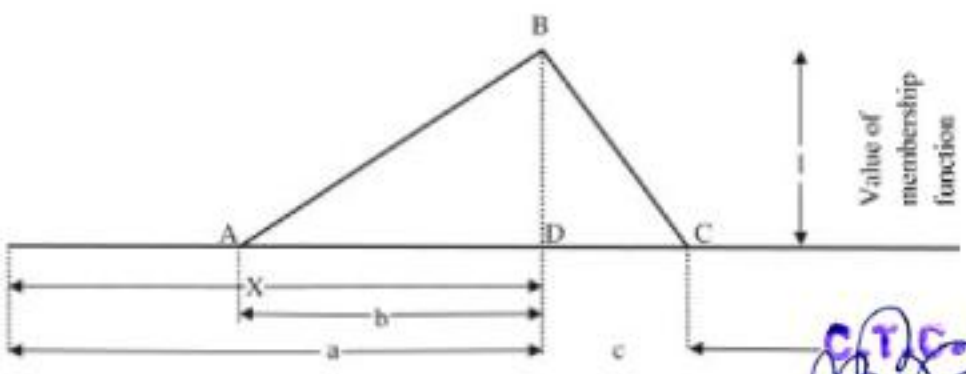

Fig. 3 Graphical view of overall sensory score as triangle ABC and triplet ABC [20]

Nowgong Girls' College
ESTD: 1962
Nagaon :: Assam
Principal
Nowgong Girls' College
Nagaon :: Assam

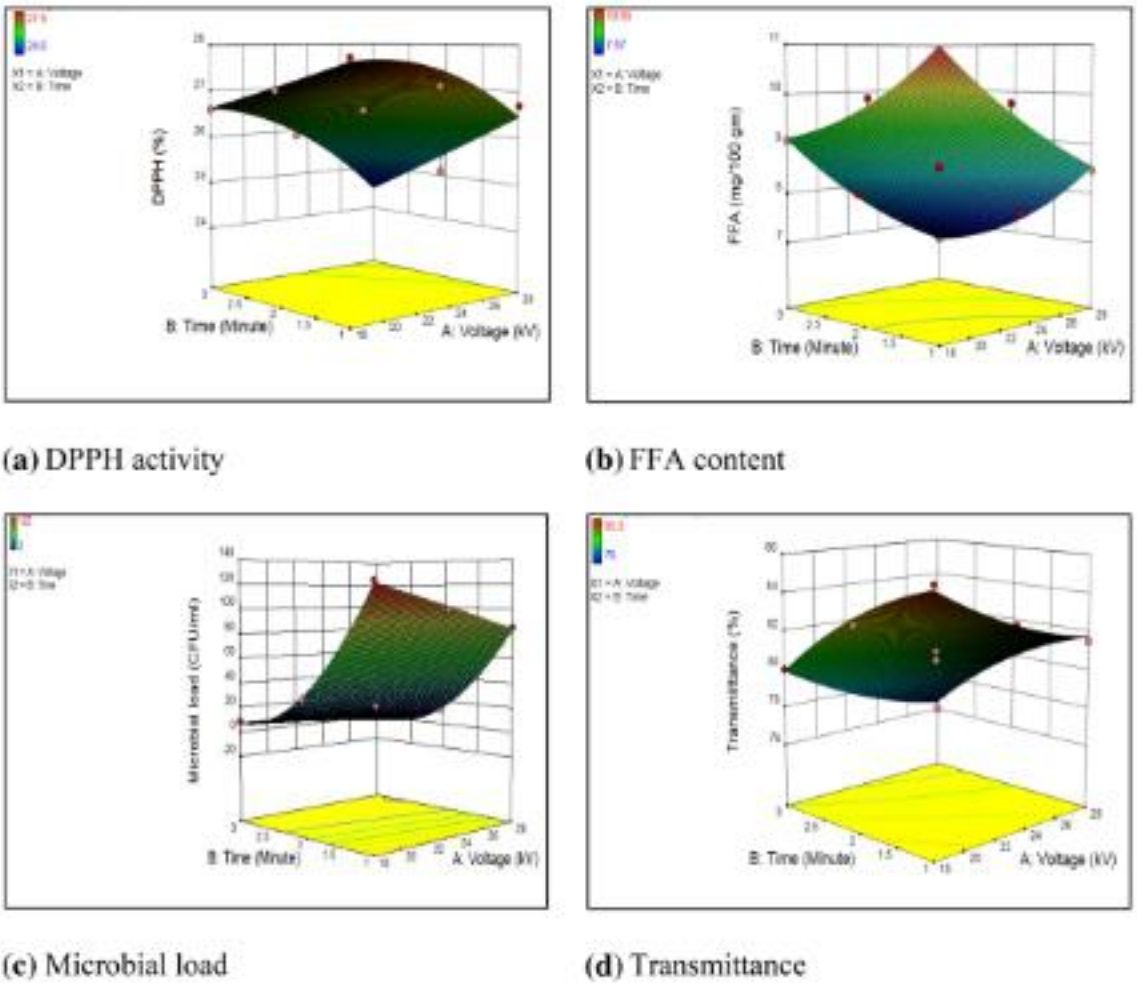

(a) DPPH activity

(b) FFA content

(c) Microbial load

(d) Transmittance

Fig. 4 Response surface graphs showing the effect of time and voltage of cold plasma on quality parameters of tcw **a** DPPH activity, **b** FFA content, **c** microbial load, and **d** transmittance

MA65 gas [23]. A sharp increase in membrane permeability of *Z. rouxii* cells and release of intracellular components observed after cold plasma treatment was attributed to the plasma-induced formation of permeability pores on *Z rouxii* cell membrane [53]. The authors suggested cytoplasmic membrane to be the key target for plasma induced inactivation of microorganisms. The short lived reactive species generated in the plasma gas inactivates microbial cells in aqueous environment [54, 55] with ·OH radical being the most potent. Plasma can cause oxidative stress in microbial cells, resulting in damage to DNA, proteins and lipids [56, 57].

Effect of cold plasma on transmittance

As shown in Fig. 4d, transmittance decreased with increasing treatment time and voltage. Sarangapan,et al. [58], and Lacombe, et al. [59] also reported similar results. Denaturation of protein, oxidation of chemical components and chemical reaction by reactive species [60] may have caused the decrease.

Modeling and validation

All the experimental data obtained from FCCD design were statistically analyzed (Design-Expert 7.0 software, Stat-Ease, Inc.) and fitted to the quadratic model equations. R^2 (high regression coefficient) values obtained were 0.95, 0.98, 0.99 and 0.97 for DPPH scavenging activity (Y_1), FFA content (Y_2), microbial load (Y_3) and transmittance (Y_4) of cold plasma treated coconut water, respectively (Table 2). The linear, quadratic and interaction terms were explained by quadratic model equations.

$$Y_1 = 26.74 - 0.85X_1 - 0.77X_2 - 0.23X_1X_2 - 0.43X_1^2 + 0.017X_2^2$$

$$Y_2 = 8.48 + 0.71X_1 + 0.99X_2 + 0.23X_1X_2 + [illegible]X_2^2$$

$$Y_3 = 24.52 - 10.50X_1 - 48.67X_2 + 7.7[illegible]$$

$$Y_4 = 81.07 - 1.75X_1 - 2.67X_2 + 0.5[illegible]X_2^2$$

Nowgong Girls' College ESTD: 1962 Nagaon :: Assam

Principal
Nowgong Girls' College
Nagaon :: Assam

Table 2 Analysis of variance for different models

Response	Sources	Sum of squares	df	Mean square	F	R^2	AdjR-Square	P Value
Y_1	Model	8.65	5	1.73	27.50	0.95	0.92	0.0002
	Lack of fit	0.35	3	0.12	5.34			0.069
	Residual	0.44	7	0.063				
	Pure error	0.088	4	0.022				
	Cor total	9.09	12					
Y_2	Model	9.98	5	2.00	89.26	0.98	0.97	< 0.0001
	Lack of fit	0.12	3	0.039	4.06			0.105
	Residual	0.16	7	0.022				
	Pure error	0.039	4	9.68×10^{-3}				
	Cor total	10.14	12					
Y_3	Model	17,903.16	5	3580.63	400.83	0.99	0.99	< 0.0001
	Lack of fit	21.73	3	7.24	0.71			0.594
	Residual	62.53	7	8.93				
	Pure error	40.80	4	10.20				
	Cor total	17,965.69	12					
Y_4	Model	62.73	5	12.55	58.32	0.97	0.95	< 0.0001
	Lack of fit	1.01	3	0.34	2.68			0.182
	Residual	1.51	7	0.22				
	Pure error	0.50	4	0.13				
	Cor total	64.23	12					

df degrees of freedom

As seen from Table 3, the lack-of fit for four responses studied were non significant which indicated the validation of models. Analyses of variance (ANOVA) for the models were significant (0.0002, < 0.0001, < 0.0001 and < 0.0001). This implied that the models had strongly fitted with the experimental data. Further, the quadratic model showed a good correlation between dependent and independent variables.

Optimization of responses

The optimum conditions of cold plasma treated TCW were predicted on the basis of maximum desirability [31, 37]. The multiple regression equations were obtained for maximum transmittance, maximum DPPH activity, minimum FFA and targeted microbial load (2 log cycle reduction of the acceptable level of 5000 CFU/ml) as stated by FAO. As seen from Table 3, there are three combinations of the independent variables with desirability ranging from 0.892–0.92. All values of independent parameters were found to be within the experimental range, indicating that the range of variables selected was valid. Thus the optimum cold plasma treatment conditions gave the maximum desirability of 0.920.

Sensory evaluation

The shelf life of TCW was enhanced on cold plasma treatment under optimized conditions by 7 to 10 times as compared to sample without treatment, but there was a negative effect on sensory quality. TCW exhibited 'chemical' type odour that was also reported for cold plasma treated apple slices [61]. Sample S1 (cold plasma treated TCW) in Table 4 got higher score for aroma being not satisfactory. So to overcome the undesirable odour, treated coconut water using optimized conditions was blended with pasteurized orange juice at 1–4% levels.

Table 4 presents the sensory scores given by the panel judges for blended beverage of TCW and orange juice. As seen from the Table, more number of panellists found

Table 3 Values of independent parameters following optimised conditions

Voltage (kV)	Time (min)	Transmittance (%)	FFA (mg/100 mg)	Microbial load (CFU/ml)	DPPH (%)	Desirability
18.00	1.752	83.943	7.942	50	27.29	0.920
18.00	1.745	83.960	7.937	50.5	27.294	0.919
18.00	1.502	84.470	7.792	70	27.430	0.892

Nowgong Girls' College ESTD: 1962 Nagaon :: Assam

Principal
Nowgong Girls' College
Nagaon :: Assam

Table 4 Sum of sensory scores for the quality attributes of blended beverage samples

Sensory quality parameters	Factors of sensory scale				
	Not Satisfactory	Fair	Medium	Good	Excellent
Colour					
S1	0	0	9	15	3
S2	0	0	10	14	3
S3	0	0	16	8	3
S4	0	3	18	3	3
S5	0	6	15	3	3
Aroma					
S1	9	0	12	5	0
S2	0	9	7	11	0
S3	3	6	5	9	0
S4	6	3	14	8	0
S5	3	6	14	3	0
Taste					
S1	3	9	12	3	0
S2	1	8	7	11	0
S3	6	9	5	7	0
S4	6	7	14	0	0
S5	3	10	14	0	0
Overall acceptability					
S1	1	8	12	6	0
S2	0	3	10	14	0
S3	0	6	16	5	0
S4	6	4	14	3	0
S5	3	13	11	0	0

sample S2 (blending with 1% orange juice) to be good for aroma, taste and overall acceptability indicating that addition of orange juice could successfully mask the 'chemical' flavour of plasma treated TCW. Beverage with 2–4% orange juice had distinct orange favour and was not liked by panellists. Fuzzy logic optimization for sensory attributes was performed to rank the beverage samples on the basis of sensory attributes. The results of fuzzy logic analysis of sensory attributes of blended TCW beverage that was done according to Sakre et al. [37] and Jaya and Das [38] are discussed in the coming sections.

Triplets for sensory quality of blended beverage samples

Triangular membership function distribution which is a set of three numbers was distributed from 0 to 100 of the sensory scale as described by Sakre et al. [37]. Triplets values were assigned to each of the sensory attribute evaluated by the sensory panellists to evaluate the numerical position of the quality attributes on the sensory scale. Sensory quality in triplets of the five samples were determined after taking into consideration (1) sensory scores given by judges added up (Table 4); (2) triplets associated with sensory scales; and (3) total number of panel judges (i.e., 27). The triplet numbers for sensory quality attribute of colour of the blended beverage sample S1 were calculated and the triplets value for colour (S1C) was determined as below.

$$\mathrm{S1C} = \frac{0(0,0,25)+0(25,25,25)+9(50,25,25)+15(75,25,25)+3(100,25,0)}{0+0+9+15+3}$$

$$\mathrm{S1C} = (69.444425\ 000022\ 2222)$$

where 0, 0, 9, 15, 3 at the numerator and denominator represent the number of sensory panellists. The triple values in the matrix denote the distribution function of sensory panellist preference on the sensory scale [37]. Similarly, triplets value for S1 sample quality attributes for taste (S1T), aroma (S1A) and overall acceptability (S1OAA) were obtained as follows:

$$\begin{aligned}
\mathrm{S1T} &= (\ 38.8889\ \ 22.2222\ \ 25.0000\ ) \\
\mathrm{S1T} &= (\ 37.5000\ \ 16.3462\ \ 25.0000\ ) \\
\mathrm{S1OAA} &= (\ 46.2963\ \ 24.0741\ \ 25.0000\ )
\end{aligned} \tag{4}$$

Similarly, triplets for colour, taste, aroma and overall acceptability were estimated for S2, S3, S4 and S5, as given below:

$$\begin{aligned}
\mathrm{S2C} &= (\ 68.5185\ \ 25.0000\ \ 22.2222\ ) \\
\mathrm{S2T} &= (\ 50.9259\ \ 24.0741\ \ 25.0000\ ) \\
\mathrm{S2A} &= (\ 51.8518\ \ 25.0000\ \ 25.0000\ ) \\
\mathrm{S2OAA} &= (\ 60.1852\ \ 25.0000\ \ 25.0000\ ) \\
\mathrm{S3C} &= (\ 62.9630\ \ 25.0000\ \ 22.2222\ ) \\
\mathrm{S3T} &= (\ 37.0370\ \ 19.4444\ \ 25.0000\ ) \\
\mathrm{S3A} &= (\ 46.7391\ \ 21.7391\ \ 25.0000\ ) \\
\mathrm{S3OAA} &= (\ 49.0741\ \ 25.0000\ \ 25.0000\ ) \\
\mathrm{S4C} &= (\ 55.5556\ \ 25.0000\ \ 22.2222\ ) \\
\mathrm{S4T} &= (\ 32.4074\ \ 19.4444\ \ 25.0000\ ) \\
\mathrm{S4A} &= (\ 44.3548\ \ 20.1613\ \ 25.0000\ ) \\
\mathrm{S4OAA} &= (\ 37.9630\ \ 19.4444\ \ 25.0000\ ) \\
\mathrm{S5C} &= (\ 52.7778\ \ 25.0000\ \ 22.2222\ ) \\
\mathrm{S5T} &= (\ 35.1852\ \ 22.2222\ \ 25.0000\ ) \\
\mathrm{S5A} &= (\ 41.3461\ \ 22.1153\ \ 25.0000\ ) \\
\mathrm{S5OAA} &= (\ 32.4074\ \ 22.2222\ \ 25.0000\ )
\end{aligned} \tag{5}$$

Nowgong Girls' College ESTD: 1962 Nagaon :: Assam
Springer
C.T.C.
Principal
Nowgong Girls' College
Nagaon :: Assam

Determination of important quality attributes based on triplet values

The quality attribute of the blended beverage samples that was perceived by panellists to be the most important on the basis of the sensory scores was identified. Colour, taste, aroma and overall acceptability of the blended beverage samples were the quality attributes judged by the panellists (Table 5). The importance that the judges gave to the quality attributes was determined by (1) sensory scores given by judges added up (Table 4); (2) triplets associated with sensory scales; and (3) total number of panel judges (i.e., 27), according to Sakre et al., [37] and Das [31] and Routran [36];. The importance of quality attribute of colour (QC) was determined as described below.

$$QC = \frac{0(0,0,25) + 0(25,25,25) + 3(50,25,25) + 15(75,25,25) + 9(100,25,0)}{0+0+3+15+9}$$

where 0, 0, 3, 15, 9 at the numerator and denominator represent the number of sensory panellists. Similarly, triplets for sensory panellist's preference for the importance of taste (QT), aroma (QA) and overall acceptability (QOOA) were obtained as below.

$$\begin{aligned} QC &= (\,80.5556\ \ 25.0000\ \ 16.6667\,) \\ QT &= (\,74.0741\ \ 22.2222\ \ 14.8148\,) \\ QA &= (\,82.4074\ \ 25.0000\ \ 14.8148\,) \\ QOAA &= (\,84.2593\ \ 25.0000\ \ 14.8148\,) \end{aligned} \tag{6}$$

Triplets for overall sensory scores of the blended beverage samples

In the next step, the overall sensory scores of the blended beverage samples were determined by multiplying the triplets for the sensory quality values with the triplets for important quality parameters as judged by sensory panellists for each sample. The multiplication of triplets (a, b, c) and (p,q,r) was done by the following method

$$(a, b, c) \times (p, q, r) = (a \times pa \times q + p \times ba \times r + p \times c) \tag{7}$$

In the above equation, if a and p value are between 0 and 100, multiplication product value a and p (a × p) will be between 0 and 1,000. The first digit value of the overall sensory score will be between 0 and 40,000. So, it is important to bring the first digit value of the overall sensory score between 0 and 100. In order to obtain this, as per Sakre et al. [37], Eq. (6) values were multiplied by the factor $1/Q_{sum}$, where Q_{sum} is the summation of the first digit value of the triplets. 'Relative weightage of the quality attribute' was expressed for colour as: $QC_{rel} = QC/Q_{sum}$, taste: $QT_{rel} = QT/Q_{sum}$, aroma: $_{rel}QA_{rel} = QA/Q_{sum}$ and for OAA: $=QOAA_{rel}QOAA/Q_{sum}$

From the Eq. (6),

$$Q_{Sum} = (80.5556 + 74.0741 + 82.4074 + 84.2593) = 321.2964$$

In the next step, the relative weightage value for each quality attribute was determined in the form of triplets. The calculation for determining the triplets for relative weightage value for colour is given below.

For colour relative weightage of triplet (QC_{rel}) was

$$QC_{rel} = \frac{QC}{Q_{Sum}} = (\,80.5556/321.2964\ \ 25/321.2964\ \ 16.6667/321.2964\,)$$

Similarly, for the other quality attributes, relative weightage of triplets were determined to be:

$$\begin{aligned} QC_{rel} &= (\,0.2507\ \ 0.0778\ \ 0.0519\,) \\ QT_{rel} &= (\,0.2305\ \ 0.0692\ \ 0.0461\,) \\ QA_{rel} &= (\,0.2565\ \ 0.0778\ \ 0.0461\,) \\ QOAA_{rel} &= (\,0.2622\ \ 0.0778\ \ 0.0461\,) \end{aligned} \tag{8}$$

Overall sensory score (SO1) for S1 was calculated by using the triplet multiplication method (Eq. 8), as obtained below.

$$\begin{aligned} SO1 &= S1C \times QC_{rel} + S1T \times QT_{rel} + S1A \times QA_{rel} + S1OAA \times QOAA_{rel} \\ SO1 &= (\,48.1361\ \ 36.5105\ \ 33.5628\,) \end{aligned} \tag{9}$$

Table 5 Preferences to the importance of quality attributes of blended beverage

Sensory quality parameters	Factors of sensory scale				
	Not at all important	Somewhat important	Important	Highly important	Extremely important
Colour	0	0	3	15	9
Aroma	0	0	3	13	11
Taste	3	0	3	10	11
Overall acceptability	0	0	1	15	

Nowgong Girls' College ESTD: 1962 Nagaon :: Assam

Springer

Principal Nowgong Girls' College Nagaon :: Assam

Similarly for others, the overall sensory scores were calculated

$$\begin{aligned} SO2 &= (\,58.0025\ \ 42.3578\ \ 35.3720\,) \\ SO3 &= (\,49.1823\ \ 37.7988\ \ 33.6953\,) \\ SO4 &= (\,42.7324\ \ 33.9905\ \ 32.4753\,) \\ SO5 &= (\,32.2962\ \ 27.04254\ \ 23.9819\,) \end{aligned} \tag{10}$$

Ranking of blended beverage on sensory fuzzy scale

Standard sensory fuzzy scale has been described by Routay and Mishra [36], Sakre et al. [37]. The standard sensory fuzzy scale was categorised on a 6 point set as Not satisfactory/Not at all necessary, Fair/Somewhat necessary, Satisfactory/Necessary, Good/Important, Very good/Highly important and Excellent/Extremely important (Fig. 2), according to Sakre et al. [37]. Each membership function of sensory fuzzy scale follows the triangular distribution structure where 1 is the maximum membership value [31]. In this step, the overall quality score of the blended beverage samples was matched with the standard fuzzy scale. For that, on the basis of overall sensory scores of the blended beverage samples, the overall quality of the samples was measured. The triplet (a, b, c) for overall quality of the blended beverage samples, was expressed by a triangle ABC, as per Fig. 3. The location of the centroid of the triangle ABC, as depicted by the triplet (a, b, c), was used to rank blended beverage samples [36, 37]. It was observed that ABD and BDC are right-angled triangles, so the area covered by ABC, ABD and BDC triangles will be 0.5(b + c), 0.5b and 0.5c, respectively. Thus, if X is the distance of the centroid of triangle ABC, its value is calculated as

$$X = \frac{a - (b - c)}{3} \tag{11}$$

$$\begin{aligned} X_{s1} &= 15.0628 \\ X_{s2} &= 17.0056 \\ X_{s3} &= 15.0263 \\ X_{s4} &= 13.7391 \\ X_{s5} &= 9.7452 \end{aligned} \tag{12}$$

From the above X value (Eq. 12), the ranking of overall quality of the developed blended beverage was in the following order:

S2 > S1 > S3 > S4 > S5

Ranking of blended beverage on the basis of quality attributes

In this step the developed blended beverage samples were graded on the basis of quality attributes. Here, the triplets values obtained for importance of quality as per the preference given by the sensory panellists were put into Eq. (11). Accordingly, the relative importance of colour, taste, aroma and overall acceptability, X_{QC}, X_{QT}, X_{QA} and X_{QOAA}, of the blended beverage were

$$\begin{aligned} X_{QC} &= 24.0741 \\ X_{QT} &= 22.2222 \\ X_{QA} &= 24.0741 \\ X_{QOAA} &= 24.6914 \end{aligned} \tag{13}$$

From the above values of X_{QC}, X_{QT}, X_{QA} and X_{QOAA}, blended beverage were graded on the basis of quality attributes in this order: Overall acceptability > Color = Aroma > taste .

Similarity analysis for blended beverage samples on standard fuzzy scale

Distribution pattern of overall sensory score of samples can be represented by similarity analysis in the form of six sensory scales of standard fuzzy scale. It helped to rank and classify sample attributes according to sensory scores in linguistic form. Membership function F1–F6 value of sensory scale expressed by set of 10 numbers [31, 37, 38] was between 0 and 10; between 10 and 20; between 20 and 30; between 30 and 40; between 40 and 50; between 50 and 60; between 60 and 70; between 70 and 80; between 80 and 90; and between 90 and 100.

Following Fig. 2, the membership functions values F1, F2, F3, F4, F5 and F6 can be expressed as [37]:

$$\begin{aligned} \text{Not satisfactory}: \ F1 &= [1, 0.5, 0, 0, 0, 0, 0, 0, 0, 0] \\ \text{Fair}: \ F2 &= [0.5, 1, 1, 0.5, 0, 0, 0, 0, 0, 0] \\ \text{Satisfactory}: \ F3 &= [0, 0, 0.5, 1, 1, 0.5, 0, 0, 0, 0] \\ \text{Good}: \ F4 &= [0, 0, 0, 0, 0.5, 1, 1, 0.5, 0, 0] \\ \text{Very good}: \ F5 &= [0, 0, 0, 0, 0, 0, 0.5, 1, 1, 0.5] \\ \text{Excellent}: \ F6 &= [0, 0, 0, 0, 0, 0, 0, 0, 0.5, 1] \end{aligned} \tag{14}$$

Membership function of overall sensory scores on standard fuzzy scale

In this step, by using the standard fuzzy scales (values of F1–F6) membership function value of the overall scores for the blended beverage samples were determined. The sensory scores were represented as triplets in Eq. (11). From Fig. 3,

Nowgong Girls' College ESTD: 1962 Nagaon :: Assam

Principal
Nowgong Girls' College
Nagaon :: Assam

for a given abscissa value " x", membership function value B_X can be calculated as

$$\begin{aligned} B_X &= \frac{X-(a-b)}{b} \quad \text{for } (a-b) < X < a \\ &= \frac{(a+c)-X}{c} \quad \text{for } a < X < (a+c) \\ &= 0 \quad \text{for all other values of X.} \end{aligned} \tag{15}$$

Thus, the membership function values of B_X for blended beverage samples at X equal to 0, 10, 20, 30, 40, 50, 60, 70, 80, 90 and 100 were calculated by using Eq. (15), according to Sakre et al. [37] and Das [31]. The membership function value of overall sensory scores of each developed blended sample on standard fuzzy scale was identified by a set of 10 numbers, where the maximum values of B_X in the 10 intervals from 0 to 100 is in the mentioned range of X. The output products are presented below (Eq. 16):

$$\begin{aligned} B1 &= (0, 0.2294, 0.5033, 0.7772, 1, 0.9445, 0.6465, 0.3486, 0.0506, 0) \\ B2 &= (0, 0.1028, 0.3389, 0.4199, 0.575, 1, 0.9435, 0.6608, 0.3781, 0.0954) \\ B3 &= (0, 0.228, 0.4925, 0.7571, 1, 0.9757, 0.6790, 0.3822, 0.0854, 0) \\ B4 &= (0.0370, 0.6254, 0.6254, 0.9196, 1, 0.7762, 0.4683, 0.1604, 0, 0) \\ B5 &= (0.1755, 0.5453, 0.9151, 1, 0.6788, 0.2618, 0, 0, 0, 0) \end{aligned} \tag{16}$$

where B1, B2, B3, B4 and B5 represents the overall sensory scores distribution pattern of S1, S2, S3, S4 and S5 on the standard fuzzy scale.

Similarity values for blended beverage samples

The membership function (B1, B2, B3, B4, B5) for each of the developed samples S1, S2, S3, S4 and S5 were expressed in Eq. (14). These values were compared with the corresponding membership function value of standard fuzzy scale (F1–F6) from Eq. (14). Similarity value (S_m) for the samples were calculated as

$$S_m = \frac{F \times B^T}{maximum\ of\ (F1 \times F1 and B1 \times B1^T)} \tag{17}$$

The calculated similarity values for blended beverages samples are shown in Table 6. The samples were judged by the maximum similarity value. As seen from Table 6, the similarity value and their categories for S1, S2, S3, S4 and S5 were 0.7479 (Satisfactory), 0.8233 (Good), 0.7254 (Satisfactory), 0.7537 (Satisfactory), and 0.8414 (Satisfactory), respectively. Similarity values were used to rank the blended beverages as: S2 (Good) > S5 (Satisfactory) > S4 (Satisfactory) > S1 (Satisfactory) > S3 (Satisfactory). According to fuzzy analysis S2 showed the highest acceptability among these five samples due to its highest similarity value. S2 was a blended beverage of cold plasma treated TCW with 1% orange juice. Fuzzy logic interpretation of sensory data has helped to arrive at a conclusion on the basis of ranking of the blended beverage for its strong attributes.

Table 6 Similarity values for blended beverage samples

Scale factor	S1	S2	S3	S4	S5
Not satisfactory	0.0343	0.0165	0.0332	0.1006	0.1663
Fair	0.3353	0.2095	0.3200	0.4973	0.7601
Satisfactory	0.7479	0.5349	0.7254	0.7537	0.8414
Good	0.6774	0.8233	0.6830	0.5248	0.2230
Very Good	0.2160	0.5009	0.2350	0.1134	0
Excellent	0.0075	0.0914	0.0124	0	0

Conclusion

Desirability approach was followed to optimize process parameters of DBD cold plasma treatment of TCW. The processing parameters of DBD cold plasma were optimized on the basis of DPPH activity, FFA content, microbial load and transmittance. Increase in cold plasma treatment time and voltage reduced antioxidant activity, microbial load and transmittance and increased free fatty acids. Cold plasma treated TCW developed 'chemical taste' that reduced its acceptability. TCW treated with the optimized conditions was blended with pasteurized orange juice at different levels (1 to 4%) to mask the 'chemical taste'. Fuzzy logic was used for evaluating sensory attributes of the blended beverage. Through fuzzy logic, it was found that the sensory panellists judged the sample treated with cold plasma at 18.00 kV voltage for 1.75 min and blended with 1% orange to be more acceptable than the samples with higher concentrations of orange juice. This implied that cold plasma treatment enhances the shelf stability of TCW by reducing microbial load but the disadvantage related to unacceptable sensory attributes can be overcome on adding with 1% orange juice.

Acknowledgements [illegible] are grateful to [illegible] University, Assam, India, for facilities and [illegible]CTE for GATE Fellowship (Student ID: 1-3139726178) to [illegible] first author.

CTC
Principal
Nowgong Girls' College
Nagaon :: Assam

Nowgong Girls' College
ESTD: 1962
Nagaon :: Assam

Compliance with ethical standards

Conflict of interest The authors declare that there is no conflict of interest.

References

1. S. Damar, Unpublished Doctoral thesis, University of Florida, (2006)
2. M. Das Purkayastha, Unpublished M.Sc thesis, Tezpur University, (2010)
3. C.F. Campos, P.E. Souza, J.V. Coelho, M.B. Glória, Chemical composition, enzyme activity and effect of enzyme inactivation on flavor quality of green coconut water. J. Food Process. Preserv. **20**, 487 (1996)
4. L.M. Costa, G.A. Maia, J.M. Costa, R.W. Figueiredo, M. Rodrigues, P.H.M. Sousa, A.M. Pinheiro, Qualidade e vida de prateleira da agua de coco obtida pelo processo de enchimento a quente. Rev. Bras. Armaz. **31**, 95–102 (2006)
5. M. Das Purkayastha, D. Kalita, N.K. Mahnot, C.L. Mahanta, M. Mandal, M.K. Chaudhuri, Effect of l-ascorbic acid addition on the quality attributes of micro-filtered coconut water stored at 4 C, Innov. Food Sci. Emerg. Technol. 16:69–79 (2012)
6. N.K. Mahnot, D. Kalita, C.L. Mahanta, M.K. Chaudhuri, Effect of additives on the quality of TCW processed by nonthermal two stage microfiltration technique. LWT-Food Sci. Technol. **59**(2), 1191–1195 (2014)
7. N.N. Misra, K.M. Keener, P. Bourke, J.P. Mosnier, P.J. Cullen, In-package atmospheric pressure cold plasma treatment of cherry tomatoes. J. Biosci. Bioeng. **118**(2), 177–182 (2014)
8. M. Stoica, P. Alexe, L. Mihalcea, Atmospheric cold plasma as new strategy for foods processing-an overview. Innov. Roman. Food Biotechnol. **1**, 15 (2014)
9. S. Tappi, G. Giorgia, L. Vannini, A. Berardinelli, S. Romani, L. Ragni, P. Rocculi, Cold plasma treatment for fresh-cut melon stabilization. Innov. Food Sci. Emerg. Technol. **33**, 225–233 (2016)
10. S. Pankaj, Z. Wan, K. Keener, Effects of cold plasma on food quality. A review. Foods **7**(1), 4 (2018)
11. Q.Z. Luo, N. D'angelo, R.L. Merlino, Shock formation in a negative ion plasma. Phys. Plasmas **5**(8), 2868–2870 (1998)
12. S. Tappi, A. Berardinelli, L. Ragni, M. Dalla Rosa, A. Guarnieri, P. Rocculi, Atmospheric gas plasma treatment of fresh-cut apples. Innov. Food Sci. Emerg. Technol. **21**, 114–122 (2014)
13. I. Ramazzina, S. Tappi, P. Rocculi, G. Sacchetti, A. Berardinelli, A. Marseglia, F. Rizzi, Effect of cold plasma treatment on the functional properties of fresh-cut apples. J. Agric. Food Chem. **64**(42), 8010–8018 (2016)
14. X. Li, M. Li, N. Ji, P. Jin, J. Zhang, Y. Zheng et al., Cold plasma treatment induces phenolic accumulation and enhances antioxidant activity in fresh-cut pitaya (Hylocereus undatus) fruit. LWT **115**, 108447 (2019)
15. M.J. Rothrock, H. Zhuang, K.C. Lawrence, B.C. Bowker, G.R. Gamble, K.L. Hiett, In-package inactivation of pathogenic and spoilage bacteria associated with poultry using dielectric barrier discharge-cold plasma treatments. Curr. Microbiol. **74**(2), 149–158 (2017)
16. N.M. Coutinho, M.R. Silveira, T.C. Pimentel, M.Q. Freitas, J. Moraes, L.M. Fernandes et al., Chocolate milk drink processed by cold plasma technology: Physical characteristics, thermal behavior and microstructure. LWT **102**, 324–329 (2019)
17. J. Lee, K. Jo, Y. Lim, H.J. Jeon, J.H. Choe, C. Jo, S. Jung, The use of atmospheric pressure plasma as a curing process for canned ground ham. Food Chem. **240**, 430–436 (2018)
18. N. Bahrami, D. Bayliss, G. Chope, S. Penson, T. Perehinec, I.D. Fisk, Cold plasma: a new technology to modify wheat flour functionality. Food Chem. **202**, 247–253 (2016)
19. R. Ma, G. Wang, Y. Tian, K. Wang, J. Zhang, J. Fang, Non-thermal plasma-activated water inactivation of food-borne pathogen on fresh produce. J. Hazard. Mater. **300**, 643–651 (2015)
20. I. Ramazzina, A. Berardinelli, F. Rizzi, S. Tappi, L. Ragni, G. Sacchetti, P. Rocculi, Effect of cold plasma treatment on physico-chemical parameters and antioxidant activity of minimally processed kiwifruit. Postharvest Biol. Technol. **107**, 55–65 (2015)
21. X. Liao, J. Li, A.I. Muhammad, Y. Suo, S. Chen, X. Ye et al., Application of a dielectric barrier discharge atmospheric cold plasma (Dbd-Acp) for *Eshcerichia Coli* inactivation in apple juice. J. Food Sci. **83**(2), 401–408 (2018)
22. P. Putnik, Z. Kresoja, T. Bosiljkov, A.R. Jambrak, F.J. Barba, J.M. Lorenzo et al., Comparing the effects of thermal and non-thermal technologies on pomegranate juice quality: a review. Food Chem. **279**, 150–161 (2019)
23. L. Xu, A.L. Garner, B. Tao, K.M. Keener, Microbial inactivation and quality changes in orange juice treated by high voltage atmospheric cold plasma. Food Bioprocess Technol. **10**(10), 1778–1791 (2017)
24. O. Rodríguez, W.F. Gomes, S. Rodrigues, F.A. Fernandes, Effect of indirect cold plasma treatment on cashew apple juice (*Anacardium occidentale* L.). LWT **84**, 457–463 (2017)
25. S.K. Pankaj, Z. Wan, W. Colonna, K.M. Keener, Effect of high voltage atmospheric cold plasma on white grape juice quality. J. Sci. Food Agric. **97**(12), 4016–4021 (2017)
26. O.P. Chauhan, B.S. Archana, A. Singh, P.S. Raju, A.S. Bawa, A refreshing beverage from mature coconut water blended with lemon juice. J. Food Sci. Technol. **51**(11), 3355–3361 (2014)
27. J.M. De Carvalho, G.A. Maia, R.W. De Figueiredo, E.S. De Brito, S. Rodrigues, Development of a blended nonalcoholic beverage composed of coconut water and cashew apple juice containing caffeine. J. Food Qual. **30**(5), 664–681 (2007 Oct)
28. G. Sindumathi, and S. Amutha, Development of Spiced TCW Ready to Serve Beverage, Int. J. Sci. Res. 2319–7064 (2013)
29. H. Stone, J.L. Sidel, *Discrimination Testing, Sensory Evaluation Practices*, 3rd edn. (Elsevier, London, 2004), p. 177
30. K.P. Singh, A. Mishra, H.N. Mishra, Fuzzy analysis of sensory attributes of bread prepared from millet-based composite flours. LWT Food Sci. Technol. **48**(2), 276–282 (2012)
31. H. Das, *Food Processing Operations Analysis* (Asian Books Private Limited, New Delhi, 2005)
32. B.Y. Imm, J.H. Lee, S.H. Lee, Sensory quality index (SQI) for commercial food products. Food Qual. Pref. **22**(8), 748–752 (2011)
33. C. Debjani, S. Das, H. Das, Aggregation of sensory data using fuzzy logic for sensory quality evaluation of food. J. Food Sci. Technol. **50**(6), 1088–1096 (2013)
34. H.L. Westenberg, S. Jong, D.A. Meel, J.F. Quadt, E. Backer, R.P. Duin, Fuzzy set theory applied to product classification by a sensory panel. J. Sens. Stud. **4**(1), 55–72 (1989)
35. Q. Zhang, J.B. Litchfield, An optimization of intermittent corn drying in a laboratory scale thin layer dryer. Drying Technol. **9**(2), 383–395 (1991)
36. W. Routray, H.N. Mishra, Sensory evaluation of different drinks formulated from dahi (indian yogurt) powder using fuzzy logic. J. Food Process. Preserv. **36**(1), 1 (2012)
37. N. Sakre, A.B. Das, P.P. Srivastav, Fuzzy Logic Approach for Process Optimization of Gluten-Free Pasta. J. Food Process. Preserv. [illegible] 840–849 (2016)

Nowgong Girls' College ESTD: 1962 Nagaon

C.T.C.

Principal
Nowgong Girls' College
Nagaon :: Assam

38. S. Jaya, H. Das, Sensory evaluation of mango drinks using fuzzy logic. J. Sens. Stud. **18**(2), 163–176 (2003)
39. H. Chutia, D. Kalita, C.L. Mahanta, N. Ojah, A.J. Choudhury, Kinetics of inactivation of peroxidase and polyphenol oxidase in TCW by dielectric barrier discharge plasma. LWT Food Sci. Technol. **1**(101), 625–629 (2019)
40. A.M. Fonseca, A. Bizerra, J.S. Souza, F.J. Monte, M.D. Oliveira, M.C. Mattos, G.A. Cordell, R. Braz-Filho, T.L. Lemos, Constituents and antioxidant activity of two varieties of coconut water (*Cocos nucifera* L.). Rev. Bras. Farm. **19**(1B), 193–198 (2009)
41. S. Sadasivam, A. Manickam, *Biochemical methods* (New age international (P) Limited, New Delhi., 2008)
42. J.C. Jackson, A. Gordon, G. Wizzard, K. McCook, R. Rolle, Changes in chemical composition of coconut (Cocos nucifera) water during maturation of the fruit. J. Sci. Food Agric. **84**(9), 1049–1052 (2004 Jul)
43. K. Leiviskä, Introduction to experiment design. University of Oulu, Control Engineering Laboratory. 5 (2013)
44. S. Şahin, R. Şamlı, Optimization of olive leaf extract obtained by ultrasound-assisted extraction with response surface methodology. Ultrason. Sonochem. **20**(1), 595–602 (2013)
45. J. Sadecka, M. Polovka, E. Kolek, E. Belajova, B. Tobolkova, L. Duško, J.A.N. Durec, Orange juice with pulp: impact of pasteurization and storage on flavour, polyphenols, ascorbic acid and antioxidant activity. J. Food Nutr. Res. **53**(4), 371–388 (2014)
46. F.D. Almeida, R.S. Cavalcante, P.J. Cullen, J.M. Frias, P. Bourke, F.A. Fernandes, S. Rodrigues, Effects of atmospheric cold plasma and ozone on prebiotic orange juice. Innov. Food Sci. Emerg. Technol. **1**(32), 127–135 (2015 Dec)
47. X.V. Yepez, K.M. Keener, High-voltage atmospheric cold plasma (HVACP) hydrogenation of soybean oil without trans-fatty acids. Innov. Food Sci. Emerg. Technol. **1**(38), 169–174 (2016 Dec)
48. U. Santoso, K. Kubo, T. Ota, T. Tadokoro, A. Maekawa, Nutrient composition of kopyor coconuts (*Cocos nucifera* L.). Food Chem. **57**(2), 299–304 (1996)
49. M.N. Shubhashree, G. Venkateshwarlu, S.H. Doddamani, Therapeutic and nutritional values of Narikelodaka (TCW) – a review. Res. J. Pharm. Phytochem. **6**(4), 195–201 (2014 Oct)
50. Meethaworn K, Siriphanich J (2014) Volatiles and enzymes involved in off-flavor development in trimmed young coconut water during low temperature storage. In XXIX International Horticultural Congress on Horticulture: Sustaining Lives, Livelihoods and Landscapes (IHC2014): 1178 (pp. 105–110)
51. H.P. Li, L.Y. Wang, G. Li, L.H. Jin, P.S. Le, H.X. Zhao et al., Manipulation of lipase activity by the helium radio-frequency, atmospheric-pressure glow discharge plasma jet. Plasma Proc. Polym. **8**(3), 224–229 (2011)
52. H. Tolouie, M.A. Mohammadifar, H. Ghomi, A.S. Yaghoubi, M. Hashemi, The impact of atmospheric cold plasma treatment on inactivation of lipase and lipoxygenase of wheat germs. Innov. Food Sci. Emerg. Technol. **47**, 346–352 (2018)
53. Q. Xiang, X. Liu, J. Li, S. Liu, H. Zhang, Y. Bai, Effects of dielectric barrier discharge plasma on the inactivation of Zygosaccharomyces rouxii and quality of apple juice. Food Chem. **254**, 201–207 (2018)
54. Y. Gorbanev, A. Privat-Maldonado, A. Bogaerts, Analysis of short-lived reactive species in plasma–air–water systems: the dos and the do nots. Anal. Chem. **90**, 13151–13158 (2018)
55. H.A. Aboubakr, U. Gangal, M.M. Youssef, S.M. Goyal, P.J. Bruggeman, Inactivation of virus in solution by cold atmospheric pressure plasma: identification of chemical inactivation pathways. J. Phys. D **49**(20), 204001 (2016)
56. L. Han, S. Patil, D. Boehm, V. Milosavljević, P.J. Cullen, P. Bourke, Mechanisms of inactivation by high-voltage atmospheric cold plasma differ for *Escherichia coli* and Staphylococcus aureus. Appl. Environ. Microbiol. **82**(2), 450–458 (2015)
57. O. Lunov, V. Zablotskii, O. Churpita, A. Jäger, L. Polívka, L. Syková et al., The interplay between biological and physical scenarios of bacterial death induced by non-thermal plasma. Biomaterials **82**, 71–83 (2016)
58. C. Sarangapani, G. O'Toole, P.J. Cullen, P. Bourke, Atmospheric cold plasma dissipation efficiency of agrochemicals on blueberries. Innov. Food Sci. Emerg. Technol. **1**(44), 235–241 (2017)
59. A. Lacombe, B.A. Niemira, J.B. Gurtler, X. Fan, J. Sites, G. Boyd, H. Chen, Atmospheric cold plasma inactivation of aerobic microorganisms on blueberries and effects on quality attributes. Food Microbiol. **1**(46), 479–484 (2015)
60. D. Bermúdez-Aguirre, E. Wemlinger, P. Pedrow, G. Barbosa-Cánovas, M. Garcia-Perez, Effect of atmospheric pressure cold plasma (APCP) on the inactivation of Escherichia coli in fresh produce. Food Control **34**(1), 149–157 (2013)
61. U. Schnabel, R. Niquet, O. Schlüter, H. Gniffke, J. Ehlbeck, Decontamination and sensory properties of microbiologically contaminated fresh fruits and vegetables by microwave plasma processed air (PPA). J. Food Process. Preserv. **39**(6), 653–662 (2015)

Publisher's Note Springer Nature remains neutral with regard to jurisdictional claims in published maps and institutional affiliations.

Nowgong Girls' College ESTD: 1962 Nagaon :: Assam

Principal
Nowgong Girls' College
Nagaon :: Assam

Bio-Inspired Localized Surface Plasmon Resonance Enhanced Sensing of Mercury Through Green Synthesized Silver Nanoparticle

Bijoy Sankar Boruah, Namita Ojah, and Rajib Biswas

***Abstract*—We report sensing of mercury ion through localized surface plasmon resonance based intensity modulation. A U-shaped probe is utilized for this purpose that is functionalized with Chitosan mediated silver nanoparticles. The nanoparticles have been synthesized through a green route. The as-synthesized silver nanoparticles are found to be ~44 nm, as affirmed by absorption curves and DLS experiment. Subject to the dipping of as- fabricated probe in various heavy metal ion solutions, we attain excellent selectivity towards mercury. The sensing offers a limit of detection of 1.5 ppb with an excellent linearity ~0.97. The eco-friendly as well as cost-effective with simplistic design approach has enough potential for the application in real time monitoring of heavy metal contaminants in aqueous solutions.**

***Index Terms*—Chitosan, green synthesis, mercury, silver nanoparticles, U-shaped probe.**

I. Introduction

WATER pollution has become an acute problem for the world, especially for developing countries. The alarming rise of water pollution has substantially jeopardized sustainability issues. In general, water pollution occurs in two ways; either caused by man-made or by natural means [1]. Irrespective of the causes, heavy metal ions such as mercury, iron, cadmium etc. are regarded as major pollutants. Among them, mercury is widely known for its toxicity. For instance, intake of mercury-polluted water can lead to several ailments like brain damage, neurotoxic effect [2]. WHO recommends 2 ppb as the permissible level of concentration of mercury in water [3]. The significant demand of mercury compounds fuels their excessive use in industrial applications. This eventually leads to the release of non-degradable mercury ions into the aqueous system. Over the years, the exponential rise in these waste materials has put the flora and fauna at high risk. It is indeed essential to explore qualitative and quantitative assays towards monitoring heavy metal ions, which can help in restricting concentration within the WHO limit.

Towards the detection of metal ions, there are several analytical methods such as atomic absorption spectrometry [4], inductively coupled mass plasma spectrometry [5] etc. These methods are robust and have selectivity as well as sensitivity towards metal ions. However, they lack in several aspects such as being more expensive, time consuming along with requirements of fully furnished laboratory and trained personnel [6]. In this regard, electrochemical and colorimetric methods can be cited. They enable detection of lead [7], [8], mercury [9], [10] and arsenic [11], [12]. Although they are prudent, however sensitivity analysis is to be executed in sophisticated instruments. Interestingly, nanoparticle coated optical fiber-based sensor systems are superior to many analytical methods. To improve the sensitivity of the optical fiber based sensors, there are diverse implementations such as tapered [13], D-shaped [14], S- shaped [15] and U-shaped [16]. Based on these probes, many research works have been reported in the field of gas sensing [17], [18], bio sensing [19], [20], temperature sensing [21], [22] and metal ions detection [23], [24]. It is found that U-shaped optical probe owns higher sensitivity than others [25], [26]. This is due to multiple reflections of light in the U-shaped region, causing a deeper penetration of the evanescent field. Although, there are several reports of implementation of U-shaped fiber for sensing analytes with immobilization of nanoparticles; however, there are few reports entailing detection of heavy metal ions through a greener approach. This motivates us to take up this endeavor of systematic adoption of U-shaped fiber towards the detection heavy metal ions.

In this work, we have reported a facile and low-cost technique for the detection of mercury ions in an aqueous medium based on an optical fiber probe. Nanoparticles are synthesized by a green route to reduce its toxicity towards the environment. In general, they are synthesized through chemical reduction method that might yield toxic sludge. However, we synthesize our functionalized silver nanoparticles through incorporation of chitosan and polyethylene glycol. The biodegradable and biopolymer chitosan facilitates selective detection of metal ions. As evidenced in several literatures, chitosan and PVA are widely used as biomaterial in synthesis as well as in diverse biomedical applications [27]–[34]. As the synthesis of nanoparticles as well as functionalization, is done with eco-friendly materials, so we term the unit as a green [illegible] that is a

Manuscript received October 5, 2019; revised December 5, 2019; accepted January 4, 2020. Date of publication February 3, 2020; date of current version April 1, 2020. *(Corresponding author: Rajib Biswas.)*

B. S. Boruah and R. Biswas are with the Applied Optics and Photonic Research Laboratory, Department of Physics, Tezpur University, Napaam 784028, Assam, India (e-mail: [illegible]; rajib@tezu.ernet.in).

N. Ojah is with the Laboratory of Plasma Processing of Materials, Department of Physics, Tezpur University, Napaam 784028, Assam, India (e-mail: [illegible]).

Color versions of one or more of the figures in this article are available online at https://ieeexplore.ieee.org.

Digital Object Identifier 10.1109/JLT.2020.2971252

0733-8724 © 2020 IEEE. Personal use is permitted, but republication/redistribution requires IEEE permission.
See https://www.ieee.org/publications/rights/index.html for more information.

Nowgong Girls' College ESTD 1962 Nagaon :: Assam

Principal
Nowgong Girls' College
Nagaon :: Assam

Authorized licensed use limited to: Auckland University of Technology. Downloaded on May 28,2020 at 07:39:44 UTC from IEEE Xplore. Restrictions apply.

unique amalgamation of silver nanoparticles and chitosan. The U-shaped probe is coated with the green receptor and hence used for detection of metal ions. To measure the output of the sensing probe, we have used an optical detector instead of a spectrometer, which will further reduce the cost, as well as make the whole set up compact.

II. Experimental Section

A. Materials and Chemicals

Silver nitrate, polyethylene glycol (Mw = 200) and chitosan were purchased from Sigma Aldrich (U.S.A). Mercury chloride, cadmium chloride, sodium arsenite, nickel chloride and lead nitrate were bought from Merck (U.S.A). A plastic optical fiber of core radius 600 μm was bought from Thorlabs (U.S.A). Double distilled water is used to prepare all necessary solutions. All glassware were washed using aqua-regia solution and dried at 60 °C before synthesis of nanoparticles.

B. Synthesis of Silver Nanoparticles

Green procedure is followed to synthesize the silver nanoparticles (AgNPs). Initially, 10 ml of 0.017 gm silver nitrate solution is prepared. Polyethylene glycol of molecular weight 200 is used as reducing agent, which is a water-soluble biocompatible polymer and acts as a green reducing reagent. Sodium hydroxide (NaOH) of 1% is used to accelerate the process of synthesis. In 90 ml water, 1 ml polyethylene glycol and 0.5 ml NaOH were added and put on a magnetic stirrer at 50 °C. When the solution started to boil, we added the silver nitrate solution to this solution. Few minutes later, it is found that the solution turned into light yellow color, indicating the formation of AgNPs [31], [32]. Afterwards, it is cooled at room temperature. Then, we have functionalized the as-synthesized AgNPs with chitosan. For this purpose, 10 ml AgNPs are taken in a centrifuge tube. Chitosan solution is prepared in 0.2 M acetic acid. 5ml chitosan solution was added to the centrifuge tube containing AgNPs and it was kept for 1 hour [33]–[35]. UV-visible spectroscopy was done to measure the optical properties of functionalized AgNPs.

C. Instrumentation

Optical properties of the as-synthesized silver nanoparticles were recorded using UV-vis spectrometer (UV2450, Shimadzu). pH of all solutions is determined by a pH meter (Eco tester pH1, Eutech Instruments). White LED as a light source is used (Thorlabs, U.S.A). Transmittance was sensed through using an optical detector (Coherent Optics, U.S.A).

D. U-Shaped Probe Preparation and Optical Set-Up

There are different types of optical fiber probes like U-shaped, D-shaped, tapered, S-shaped etc. that are mostly used in sensing applications. In our work, we have chosen U-shaped probe for making the sensor. The hitherto choice is described to higher sensitivity owing to greater penetration depth of the evanescent wave, which is maximum in this region. For making the probe, 10 cm long optical fiber having a diameter of 600 μm was taken. From the middle portion, a 2 cm length of cladding is removed using a surgical blade and cleaned with double distilled water. This portion is heated with a wax candle and slowly bent to U-shape [16], [19]. Then, we clean it by aqua-regia solution and finally with double distilled water. Afterwards, it is kept in a desiccator for experimental purpose. Schematic of U-bent probe and optical set-up are shown in Figs. 1(a), (b) and (c), respectively. In the optical set-up, there is a white LED as light source, U-shaped optical fiber as sensing probe and a coherent field max detector to measure the light intensity.

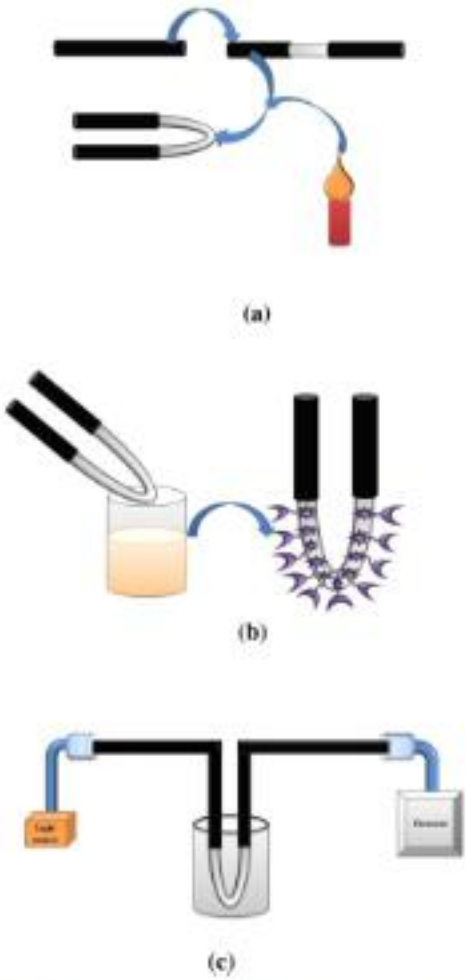

Fig. 1. Graphical description of (a) U-shaped probe preparation (b) coating of functionalized nanoparticles, and (c) optical set-up for metal ions detection.

Before performing detection, the U-shaped probe was dip-coated in green receptor solutions (AgNPs-chitosan), followed by drying at room temperature. After this process, the U-shaped probe is made ready for sensing application as shown in Fig. 1(c).

E. Working Principle of the Sensor Probe

In our work, we have reported U-shaped optical fiber coated with green receptor in the form of AgNPs-Chitosan for the sensitive detection of mercury. In an optical fiber, light travels through it by total internal reflection, which is a function of refractive index. During propagation, a small portion of light,

Nowgong Girls' College Nagaon :: Assam
Principal
Nowgong Girls' College
Nagaon :: Assam
Authorized licensed use limited to: Auckland University of Technology. Downloaded on May 28,2020 at 07:39:44 UTC from IEEE Xplore. Restrictions apply.

from the core of the fiber, penetrates to the cladding region and this field is known as evanescent wave. Evanescent wave decreases exponentially with increase in the distance [16], [47]. If we remove a small portion of cladding of the fiber, then the evanescent wave field is on the core of the fiber and meets the surrounding. Any change in surrounding has changed the local refractive index of the medium and hence it affects the evanescent wave [45]. It means that the intensity of light propagation through the fiber has changed owing to the interaction of evanescent wave with surrounding medium. This is the principle of optical fiber-based sensors.

Chitosan is a non-toxic and biodegradable biopolymer. Its structure is similar to glucose. The non-toxicity, biocompatibility and biodegradable nature make this polymer for wide application in biomedical, food chemistry and sensing fields [35]. Chitosan has hydroxyl (–OH) and amino ($-NH_2$) groups. These two groups bind with various biomolecules for which its applications in sensing field rapidly increase in recent years [37], [49]. Here, we have used chitosan as a receptor for metal ions along with AgNPs and coated in U-shaped region of the fiber. When the metal ions bind with –OH or $-NH_2$ groups of chitosan, then refractive index as well as local environment surrounding the sensing probes has changed. Due to this binding and change in local environment, light intensity gets modulated. This means that transmitted light intensity of the bare coated probe differs from the attained intensity after the coated probe is dipped into to the heavy metal ions solutions. Therefore, the difference between these two values is a direct measure of concentrations of metal ions solutions [50], [59].

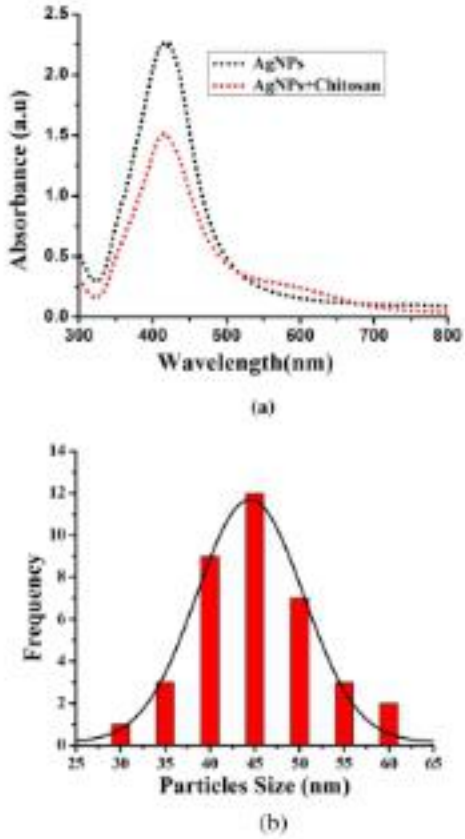

Fig. 2. Characterization of AgNPs (a) optical absorption and (b) Particles size determination

III. Results and Discussion

A. Characterization of AgNPs

Optical absorption properties of green synthesized and chitosan functionalized silver nanoparticles are characterized through a UV-vis spectrometer. Nanoparticles sizes are determined through dynamic light scattering (DLS).

Fig. 2(a) shows the absorption properties of nanoparticles. As evident, the characteristic surface plasmon peak could be seen at 415 nm. This indicates that nanoparticles are almost spherical in shape. Further, the sizes of the nanoparticles are found to be of size ~44 nm as shown in Fig. 2(b).

B. Selectivity Test and Interaction Mechanism

U-shaped optical fiber probe coated with a green receptor is tested with diverse metal ions such as mercury, cadmium, nickel, arsenic and lead to know the detection capability of these ions. Aqueous solutions of these ions except mercury are taken at concentrations of 10 ppb. Concentration of mercury was kept intentionally at 4 ppb. U-shaped probe is inserted in these solutions and output is measured in terms of intensity. It is observed that the output response corresponding to mercury is easily distinguishable from others as shown in Fig. 3 even though the concentration of mercury ion was two or more times less than other ions. This implies that this sensing unit coated with the green receptor is capable of selective detection of mercury in aqueous medium [36]. Inset in Fig. 3 has shown the histogram representation of intensity of different metal ions.

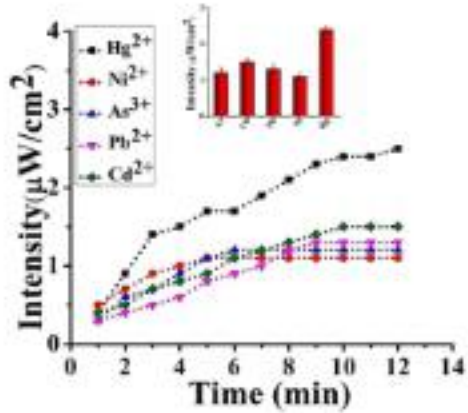

Fig. 3. Selectivity test for different metal ions and histogram presentation of relative intensity of various metal ions solutions.

Selectivity of mercury, among other ions is mainly due to the binding interaction with a green receptor. The green receptor consists of silver nanoparticles functionalized with chitosan. It has the hydroxyl and the amino groups for which it is widely used in biomedical as well as sensing applications [37]–[39]. Here, we have used chitosan as receptor and silver nanoparticles to induce localized surface plasmon resonance (LSPR). It is well known

Nowgong Girls' College ESTD 1962 Nagaon :: Assam
Principal Nowgong Girls' College Nagaon :: Assam
Authorized licensed use limited to: Auckland University of Technology. Downloaded on May 28,2020 at 07:39:44 UTC from IEEE Xplore. Restrictions apply.

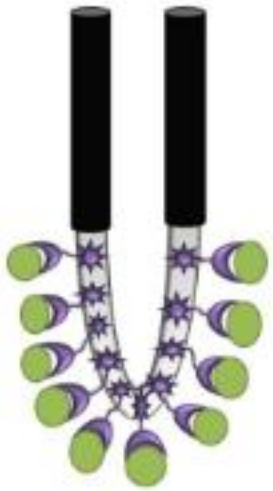

Fig. 4. Interaction mechanism of mercury with sensing probe.

that AgNPs are highly sensitive and they possess high optical extinction coefficient. In the visible region of electromagnetic waves, these nanoparticles have their unique localized surface plasmon resonance properties. Localized surface plasmon resonance (LSPR) refers to the collective oscillation of conduction electrons surrounding the surface of the nanoparticle. This LSPR property of the nanoparticles depends on the shape, size and surrounding environment of the nanoparticles. Since in our experiment, the shape and size of the nanoparticles are almost fixed; hence, only surrounding environment plays important role in this work.

As the sensor probe is introduced with mercury ions, amino and hydroxyl group of the sensor probe bind with mercury ions [39]. This implies that the surrounding environment of the sensor probe has changed. As the surrounding environment of sensor probe changes, localized surface plasmon resonance property of nanoparticles are also changed. As the concentration of mercury ions increased, we get the increasing output response of the sensor probe [40]– [42], [55]–[58] as shown in Fig. 4. This is because as the concentration increases, more and more mercury ions bind with the sensor probe for which absorption of light also increases. This absorption of light increases the resonance of the nanoparticles that gives rise to a modulated intensity [43]. However, after achieving a certain concentration, saturation has occurred in the sensor probe and it can no longer bind with mercury ions. Due to this saturation, the surrounding environment of the sensor probe does not change further.

C. Sensitivity Analysis of the Sensor Probe

From the selection test, it is observed that this sensing probe is highly selective towards mercury ions. Therefore, this probe has potential application in mercury ions detection in an aqueous medium. To study the sensitivity of this probe, mercury ion solutions of different concentrations are made from mercury chloride by series dilution. The green receptor coated U-shaped optical probe has been dipped in these solutions one by one and thereby we recorded the output intensity concerning time.

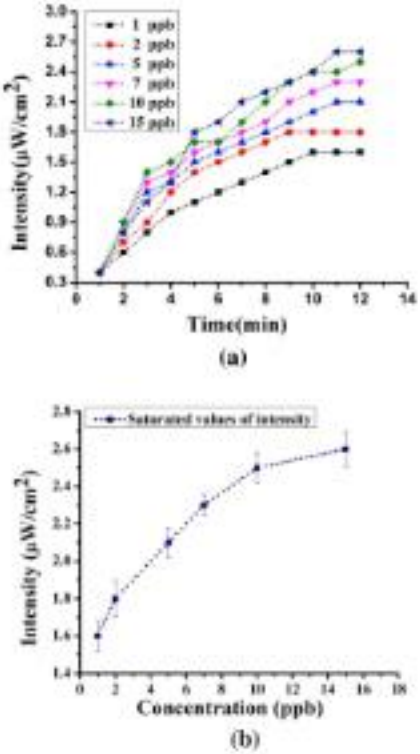

Fig. 5. Output of the sensor probe (a) intensity vs. time at various concentrations of mercury ions solutions and (b) saturated values of the output vs. concentration.

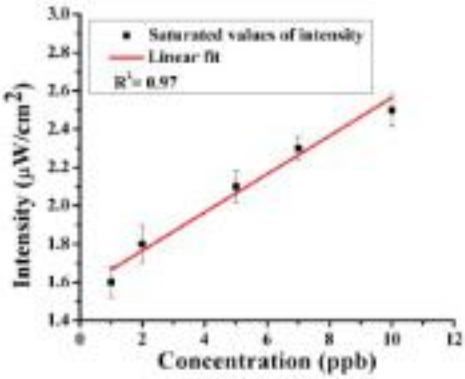

Fig. 6. Linear range of the sensor probe for various concentrations of mercury ions solutions.

Figure 5(a) depicts the response of the U-shaped probe for various concentrations of mercury ions solutions. It is evident that the output responses of the sensing probe are linear to a certain time and after that, they become saturated. The saturated values of the sensor probe for various concentrations of mercury ions solutions are shown in Fig. 5(b). The reason of saturation of the sensor output values is due to the saturation of binding interaction of mercury ions with the green receptor after certain time interval [17], [44], [45]. From Fig. 5(b), we have noticed that the saturated values provide a linear range within the concentration range of 1 ppb to 10 ppb of mercury ions. This linear range is shown in Fig. 6.

Nowgong Girls' College ★ Est. 1962 ★ Nagaon :: Assam
Principal
Nowgong Girls' College
Nagaon :: Assam

Authorized licensed use limited to: Auckland University of Technology. Downloaded on May 28,2020 at 07:39:44 UTC from IEEE Xplore. Restrictions apply.

TABLE I
COMPARISON OF LIMIT OF DETECTION OF THIS PROBE WITH PREVIOUSLY REPORTED WORKS

Methods	LOD (ppb)	References
Colorimetric	40	[51]
Colorimetric	10	[52]
Electrochemical	28.2	[53]
Electrochemical	195	[10]
Optical fiber	200	[54]
U-shaped probe	2	[59]
U-shaped optical probe	1.5	Present work

When we do the linear fitting of experimental data, a good regression value of $R^2 \sim 0.97$ is attained. From this linear fit, the limit of detection of the sensor probe has been calculated using the formula $3\,\sigma/m$; as done in previously reported works [46], [60]. Here σ and m are the standard deviation and slope of the linear curve, respectively. Limit of detection of the sensor probe is found to be 1.5 ppb that is below the WHO permissible limit 2 ppb. Apart from this, the sensitivity of the sensor probe is 0.09815 μW/ppb and the resolution is 5.2 μW/ppb.

D. Comparison with Other Reported Works

To validate the performance of this sensor probe, we have made a comparison with already reported works. Table I shows the comparison of this sensing probe with other reported works in terms of limit of detection. From the table, it is observed that this sensing probe has limit of detection 1.5 ppb that is lower than other reported works. Eco friendly properties of the green receptor have made the sensing probe more useful that can be used to detect mercury ions below WHO limit.

IV. CONCLUSION

In summary, U-shaped optical fiber probe coated with chitosan functionalized silver nanoparticles have been fabricated and implemented for selective detection of mercury ions in an aqueous medium. Owing to AgNPs synthesized through a green route as well as use of a biodegradable polymer, this sensor unit emerges to be non-toxic and hence environment friendly. This sensing unit has exhibited excellent selectivity towards mercury among other metal ions and possesses the limit of detection of 1.5 ppb. The use of optical fiber and an optical detector has made this sensing unit low cost, facile as well as environment friendly and can be used for real-time monitoring of mercury ions.

ACKNOWLEDGMENT

Author BSB acknowledges Tezpur University for providing instrumental facilities during this work. BSB is also grateful to Tezpur University for the Research and Innovation Grant. Author BSB also likes to thank Dr. P. Nath and Dr. A. J. Bhattacharyya, Department of Physics, Tezpur University, for allowing their laboratory facilities to carry out this work. The editors as well as anonymous reviewers are sincerely acknowledged for their constructive suggestions that help us to revise the manuscript to the best possible extent.

REFERENCES

[1] Z. Q. Zhou *et al.*, "Highly selective and sensitive detection of Hg2+ based on fluorescence enhancement of Mn-doped ZnSe QDs by Hg2+-Mn2+ replacement," *Sensors Actuators B: Chem.*, vol. 254, pp. 8–15, 2018.
[2] N. Zohora, D. Kumar, M. Yazdani, V. M. Rotello, R. Ramanathan, and V. Bansal, "Rapid colorimetric detection of mercury using biosynthesized gold nanoparticles," *Colloids Surf. A: Physicochemical Eng. Aspects*, vol. 532, pp. 451–457, 2017.
[3] M. Rana, M. Balcioglu, N. M. Robertson, M. S. Hizir, S. Yumak, and M. V. Yigit, "Low picomolar, instrument-free visual detection of mercury and silver ions using low-cost programmable nanoprobes," *Chem. Sci.*, vol. 8, no. 2, pp. 1200–1208.
[4] E. Kopysc, K. Pyrzynska, S. Garbos, and E. Bulska, "Determination of mercury by cold-vapor atomic absorption spectrometry with preconcentration on a gold-trap," *Anal. Sci.*, vol. 16, no. 12, pp. 1309–1312, 2000.
[5] D. Karunasagar, J. Arunachalam, and S. Gangadharan, "Development of a 'collect and punch'cold vapour inductively coupled plasma mass spectrometric method for the direct determination of mercury at nanograms per litre levels," *J. Anal. Atomic Spectrometry*, vol. 13, no. 7, pp. 679–682. 1998.
[6] L. Chen, J. Li, and L. Chen, "Colorimetric detection of mercury species based on functionalized gold nanoparticles," *ACS Appl. Mater. Interfaces*, vol. 6, no. 18, pp. 15897–15904, 2014.
[7] S. Thatai, P. Khurana, S. Prasad, S. K. Soni, and D. Kumar, "Trace colorimetric detection of Pb2+ using plasmonic gold nanoparticles and silica–gold nanocomposites," *Microchem. J.*, vol. 124, pp. 104–110, 2016.
[8] F. E. Salih, A. Ouarzane, and M. El Rhazi, "Electrochemical detection of lead (II) at bismuth/poly (1, 8-diaminonaphthalene) modified carbon paste electrode," *Arabian J. Chem.*, vol. 10, no. 5, pp. 596–603, 2017.
[9] F. Long *et al.*, "Reusable evanescent wave DNA biosensor for rapid, highly sensitive, and selective detection of mercury ions," *Biosensors Bioelectron.*, vol. 26, no. 10, pp. 4018–4023, 2011.
[10] D. S. Rajawat, S. Srivastava, and S. P. Satsangee, "Electrochemical determination of mercury at trace levels using eichhornia crassipes modified carbon paste electrode," *Int. J. Electrochem. Sci.*, vol. 7, no. 11, pp. 11456–11469, 2012.
[11] B. S. Boruah and R. Biswas, "Selective detection of arsenic (III) based on colorimetric approach in aqueous medium using functionalized gold nanoparticles unit," *Mater. Res. Express.*, vol. 5, no. 1, 2018.
[12] M. Rajkumar, S. Thiagarajan, and S. M. Chen, "Electrochemical detection of arsenic in various water samples," *Int. J. Electrochem. Sci.*, vol. 6, pp. 3164–3177, 2011.
[13] S. Kumar, G. Sharma, and V. Singh, "Sensitivity of tapered optical fiber surface plasmon resonance sensors," *Opt. Fiber Technol.*, vol. 20, no. 4, pp. 333–335, 2014.
[14] R. Zakaria, W. Kam, Y. S. Ong, S. F. A. Z. Yusoff, H. Ahmad, and W. S. Mohammed, "Fabrication and simulation studies on D-shaped optical fiber sensor via surface plasmon resonance," *J. Modern Opt.*, vol. 64, no. 14, pp. 1443–1449, 2017.
[15] S. Chauhan, N. Punjabi, D. Sharma, and S. Mukherji, "Evanescent wave absorption based S-shaped fiber-optic biosensor for immunosensing applications," *Procedia Eng.*, vol. 168, pp. 117–120, 2016.
[16] S. Jiang *et al.*, "A novel U-bent plastic optical fibre local surface plasmon resonance sensor based on a graphene and silver nanoparticle hybrid structure," *J. Phys. D: Appl. Phys.*, vol. 50, no. 16, 2017, Art. no. 165105.
[17] D. Paul, S. Dutta, D. Saha, and R. Biswas, "LSPR based Ultra-sensitive low cost U-bent optical fiber for volatile liquid sensing," *Sensors Actuators B: Chem.*, vol. 250, pp. 198–207, 2017.
[18] D. Paul, S. Dutta, and R. Biswas, "LSPR enhanced gasoline sensing with a U-bent optical fiber," *J. Phys. D: Appl. Phys.*, vol. 49, no. 30, 2016, Art. no. 305104.
[19] V. V. R. Sai, T. Kundu, and S. Mukherji, "Novel U-bent fiber optic probe for localized surface plasmon resonance based biosensor," *Biosensors Bioelectron.*, vol. 24, no. 9, pp. 2804–2809, 2009.
[20] S. K. Srivastava, V. Arora, S. Sapra, and B. D. Gupta, "Localized surface plasmon resonance-based fiber optic U-shaped biosensor for the detection of blood glucose," *Plasmonics*, vol. 7, no. 2, pp. 261–268, 2012.
[21] X. Peng, Y. Cha, H. Zhang, Y. Li, and J. Ye, "Light intensity modulation temperature sensor based on U-shaped [illegible] single-mode fiber," *Optik-Int. J. Light Electron Opt.*, vol. 130, pp. [illegible] 2017.
[22] H. Yan, P. Li, H. Zhang, X. Shen, [illegible] Y. Peng, "A micro S-shaped optical fiber temperature sensor based on dislocation fiber splice," *Photonic Sensors*, vol. 7, no. 4, pp. 372–[illegible] 2017.

Nowgong Girls' College ESTD 1962 Nagaon Assam
CTC Principal Nowgong Girls' College Nagaon :: Assam

Authorized licensed use limited to: Auckland University of Technology. Downloaded on May 28,2020 at 07:39:44 UTC from IEEE Xplore. Restrictions apply.

[23] C. K. Tagad, A. Kulkarni, R. C. Aiyer, D. Patil, and S. G. Sabharwal, "A miniaturized optical biosensor for the detection of Hg2+ based on acid phosphatase inhibition," *Optik-Int. J. Light Electron Opt.*, vol. 127, no. 20, pp. 8807–8811, 2016.
[24] S. J. Lee, J. E. Lee, J. Seo, I. Y. Jeong, S. S. Lee, and J. H. Jung, "Optical sensor based on nanomaterial for the selective detection of toxic metal ions," *Adv. Functional Mater.*, vol. 17, no. 17, pp. 3441–3446, 2007.
[25] J. Satija, N. S. Punjabi, V. V. R. Sai, and S. Mukherji, "Optimal design for U-bent fiber-optic LSPR sensor probes," *Plasmonics*, vol. 9, no. 2, pp. 251–260, 2014.
[26] C. Zhang *et al.*, "U-bent fiber optic SPR sensor based on graphene/AgNPs," *Sensors Actuators B: Chem.*, vol. 251, pp. 127–133, 2017.
[27] W. Paul and C. P. Sharma, "Chitosan, a drug carrier for the 21st century: A review," *STP Pharma Sciences*, vol. 10, no. 1, pp. 5–22, 2000.
[28] A. K. S. Chandel, C. U. Kumar, and S. K. Jewrajka, "Effect of polyethylene glycol on properties and drug encapsulation–release performance of biodegradable/cytocompatible agarose–polyethylene glycol–polycaprolactone amphiphilic co-network gels," *ACS Appl. Mater. Interfaces*, vol. 8, no. 5, pp. 3182–3192, 2016.
[29] S. Pirtarighat, M. Ghannadnia, and S. Baghshahi, "Green synthesis of silver nanoparticles using the plant extract of Salvia spinosa grown in vitro and their antibacterial activity assessment," *J. Nanostructure Chem.*, vol. 9, no. 1, pp. 1–9, 2019.
[30] A. Roy, O. Bulut, S. Some, A. K. Mandal, and M. D. Yilmaz, "Green synthesis of silver nanoparticles: biomolecule-nanoparticle organizations targeting antimicrobial activity," *RSC Adv.*, vol. 9, no. 5, pp. 2673–2702, 2019.
[31] K. Shameli *et al.*, "Synthesis and characterization of polyethylene glycol mediated silver nanoparticles by the green method," *Int. J. Mol. Sciences*, vol. 13, no. 6, pp. 6639–6650, 2012.
[32] M. B. Ahmad, M. Y. Tay, K. Shameli, M. Z. Hussein, and J. J. Lim, "Green synthesis and characterization of silver/chitosan/polyethylene glycol nanocomposites without any reducing agent," *Int. J. mol. Sci.*, vol. 12, no. 8, pp. 4872–4884, 2011.
[33] N. Ratnarathorn, O. Chailapakul, and W. Dungchai, "Highly sensitive colorimetric detection of lead using maleic acid functionalized gold nanoparticles," *Talanta*, vol. 132, pp. 613–618, 2015.
[34] D. Zhu, X. Li, X. Liu, J. Wang, and Z. Wang, "Designing bifunctionalized gold nanoparticle for colorimetric detection of Pb2+ under physiological condition," *Biosensors Bioelectron.*, vol. 31, no. 1, pp. 505–509, 2012.
[35] C. K. S. Pillai, W. Paul, and C. P Sharma, "Chitin and chitosan polymers: Chemistry, solubility and fiber formation," *Prog. Polym. Sci.*, vol. 34, no. 7, pp. 641–678, 2009.
[36] T. J. Lin and M. F. Chung, "Detection of cadmium by a fiber-optic biosensor based on localized surface plasmon resonance," *Biosensors Bioelectron.*, vol. 24, no. 5, pp. 1213–1218, 2009.
[37] W. W. Ngah, L. C. Teong, and M. A. K. M. Hanafiah, "Adsorption of dyes and heavy metal ions by chitosan composites: A review," *Carbohydrate Polymers*, vol. 83, no. 4, pp. 1446–1456, 2011.
[38] M. Ahmad, S. Ahmed, B. L. Swami, and S. Ikram, "Adsorption of heavy metal ions: Role of chitosan and cellulose for water treatment," *Langmuir*, vol. 79, pp. 109–155, 2015.
[39] Z. Chen, Z. Wang, X. Chen, H. Xu, and J. Liu, "Chitosan-capped gold nanoparticles for selective and colorimetric sensing of heparin," *J. Nanoparticle Res.*, vol. 15, no. 9, 2013, Art. no. 1930.
[40] T. R. Sobahi, M. Y. Abdelaal, and M. S. Makki, "Chemical modification of chitosan for metal ion removal," *Arabian J. Chem.*, vol. 7, no. 5, pp. 741–746, 2014.
[41] Z. Chen *et al.*, "Chitosan-functionalized gold nanoparticles for colorimetric detection of mercury ions based on chelation-induced aggregation," *Microchimica Acta*, vol. 182, no. 3–4, pp. 611–616, 2015.
[42] F. L. Mi, S. J. Wu, W. Q. Zhong, and C. Y. Huang, "Preparation of a silver nanoparticle-based dual-functional sensor using a complexation–redu[illegible]," *Physical Chemi. Chem. Phys.*, vol. 17, no. 33, [illegible]
[43] S. Unser, I. Bruzas, J. He, and L. Sagle, "Localized surface plasmon resonance biosensing: Current challenges and approaches," *Sensors*, vol. 15, no. 7, pp. 15684–15716, 2015.
[44] R. Verma and B. D. Gupta, "Detection of heavy metal ions in contaminated water by surface plasmon resonance based optical fibre sensor using conducting polymer and chitosan," *Food Chem.*, vol. 166, pp. 568–575, 2015.
[45] H. Filik and Z. Yanaz, "A sensitive method for determining total vanadium in water samples using colorimetric-solid-phase extraction-fiber optic reflectance spectroscopy," *J. Hazardous Mater.*, vol. 172, no. 2–3, pp. 1297–1302, 2009.
[46] C. H. Chen *et al.*, "Novel U-shape gold nanoparticles-modified optical fiber for localized plasmon resonance chemical sensing," *Microsystem Technol.*, vol. 16, no. 7, pp. 1207–1214, 2010.
[47] B. D. Gupta and R. K. Verma, "Surface plasmon resonance based fiber optic sensors: Principle, Probe Designs, and Some Applications," *J. Sens.*, vol. 2009, no. 2, Jul. 2009, Art. no. 979761.
[48] A. Urrutia, J. Goicoechea, and F. J. Arregui, "Optical fiber sensors based on nanoparticle-embedded coatings," *J. Sensors*, vol. 2015, 2015, Art. no. 805053.
[49] L. Zhang, Y. Zeng, and Z. Cheng, "Removal of heavy metal ions using chitosan and modified chitosan: A review," *J. Mol. Liquids*, vol. 214, pp. 175–191, 2016.
[50] B. D. Gupta and C. D. Singh, "Fiber-optic evanescent field absorption sensor: A theoretical evaluation," *Fiber Integr. Opt.*, vol. 13, no. 4, pp. 433–443, 1994.
[51] D. Maity, A. Kumar, R. Gunupuru, and P. Paul, "Colorimetric detection of mercury (II) in aqueous media with high selectivity using calixarene functionalized gold nanoparticles," *Colloids Surf. A: Physicochem. Eng. Aspects*, vol. 455, pp. 122–128, 2014.
[52] J. S. Lee, M. S. Han, and C. A. Mirkin, "Colorimetric detection of mercuric ion (Hg2+) in aqueous media using DNA-functionalized gold nanoparticles," *Angewandte Chemie*, vol. 119, no. 22, pp. 4171–4174, 2007.
[53] P. Kanchana, N. Sudhan, S. Anandhakumar, J. Mathiyarasu, P. Manisankar, and C. Sekar, "Electrochemical detection of mercury using biosynthesized hydroxyapatite nanoparticles modified glassy carbon electrodes without preconcentration," *RSC Adv.*, vol. 5, no. 84, pp. 68587–68594, 2015.
[54] D. R. Raj, S. Prasanth, T. V. Vineeshkumar, and C. Sudarsanakumar, "Surface Plasmon Resonance based fiber optic sensor for mercury detection using gold nanoparticles PVA hybrid," *Opt. Commun.*, vol. 367, pp. 102–107, 2016.
[55] B. S. Boruah and R. Biswas, "Probing lead ion contamination in aqueous solution through bio-inspired surface modification of gold nanoparticles on D-shaped fiber," *IEEE Trans. Nanotechnol.*, vol. 18, pp. 770–775, 2019. doi: 10.1109/TNANO.2019.2929058.
[56] Y. J. He, "Novel and high-performance LSPR biochemical fiber sensor," *Sensors Actuators B: Chem.*, vol. 206, pp. 212–219, 2015.
[57] S. S. Gao *et al.*, "Absorbance response of a graphene oxide coated U-bent optical fiber sensor for aqueous ethanol detection," *RSC Adv.*, vol. 6, no. 19, pp. 15808–15815, 2016.
[58] R. Bharadwaj and S. Mukherji, "Gold nanoparticle coated U-bend fibre optic probe for localized surface plasmon resonance based detection of explosive vapours," *Sensors Actuators B: Chem.*, vol. 192, pp. 804–811, 2014.
[59] G. M. Shukla, N. Punjabi, T. Kundu, and S. Mukherji, "Optimization of Plasmonic U-shaped optical fiber sensor for mercury ions detection using glucose capped silver nanoparticles," *IEEE Sensors J.*, vol. 19, no. 9, pp. 3224–3231, May. 2019.
[60] B. S. Boruah, D. Gogoi, and R. Biswas, "Bio-inspired finger like Cu-electrodes as an effective sensing tool for heavy metal ion in aqueous solution," *J. Electrochem. Soc.*, vol. 167, no. 2, 2020, Art. no. 027526. doi: 10.1149/1945-7111/ab6a86.

Nowgong Girls' College ESTD: 1962 Nagaon :: Assam

Principal
Nowgong Girls' College
Nagaon :: Assam

Authorized licensed use limited to: Auckland University of Technology. Downloaded on May 28,2020 at 07:39:44 UTC from IEEE Xplore. Restrictions apply.

JOURNAL OF NATURAL REMEDIES
DOI: 10.18311/jnr/2020/23879

REVIEW ARTICLE

An Ethnobotanical Study of Medicinal Plants used against Jaundice by Tea Tribes of Morigaon District, Assam (India)

Rakhi Bhattacharyya[1*], Krishna Kanta Medhi[1], Sashin Kumar Borthakur[2] and Sarat Borkataki[1]

[1]Department of Botany, Nowgong College, Nagaon - 782001, Assam, India; rakhibhattacharyya06@gmail.com

[2]Department of Botany, Gauhati University, Guwahati - 781014, Assam, India

Abstract

The present study was conducted to document the ethnomedicinal plants used against jaundice by the tea tribes of Morigaon district of Assam, India. An ethnomedicinal field study was carried out from June 2016 - July 2017. Information was gathered by using a semi-structured questionnaire about the traditional knowledge of medicinal plants used against jaundice by the tea tribes of Morigaon district of Assam. Documented data was evaluated using the quantitative ethno-botanical indices of fidelity level (FL), Use Value (UV) and Family Use Value (FUV). From the ethno-botanical investigation, a total of 39 species of plants covering 36 genera and 27 families respectively have been enumerated. A total of 53 informants aged from 20-75 years were interviewed to record the ethnomedicinal data. Lamiaceae was the dominant family. Among the plant portions, leaves were most frequently used. Among the 39 medicinal plant species recognized mostly were herbs. The plants species having the highest use value were *Drymaria cordata* trailed by *Xyloxma longifolia* and *Achyranthes aspera*, *Aegle marmelos*, *Alstonia scholaris* and *Justicia gendarussa*. The fidelity level was 100% for *Achyranthes aspera*, *Cheilocostus speciosus*, *Clerodendrum infortunatum*, *Justicia gendarussa*, *Lawsonia inermis*, *Coffea benghalensis* and *Saccharum officinarum*. The tea tribes of Morigaon district still relies on herbal therapies for curing jaundice. *Coffea benghalensis* has not been previously reported as a remedy of jaundice from Northeast India. Further research is needed to investigate the phytochemistry and pharmacological effectiveness of the plant species that could be the basis for the isolation and development of some novel phyto-therapeutic active compounds in the future.

Keywords: Ethnobotanical Study, Jaundice, Medicinal Plants, Morigaon District, Tea Tribes

Abbreviations Used

WHO: World Health Organization; FL: Fidelity Level; UV: Use Value; FUV: Family Use Value; Ass: Assamese name; TT: Tea Tribal name

1. Introduction

Ethno-medicine has evolved and developed since the prehistoric period. Traditional medicine is still the main source for treating health related problems around the planet[1]. Despite globalization and modernization, about 60-85% of the world's population in the developing countries relies on natural and traditional medicine[2]. According to WHO, around 21,000 plant species have been estimated which can be potentially used for medicinal purpose[3-5]. Ethnic groups store an immense knowledge on traditional herbal medicine and this need to be properly documented[5]. Ethnobotanical studies are the key sources for the discovery of novel drugs from

*Author for correspondence

Article Received on: 04.07.2019 Revised on: 18.10.2019 Accepted on: 23.01.2020

Nowgong Girls' College ESTD: 1962 Nagaon :: Assam

Principal
Nowgong Girls' College
Nagaon :: Assam

INTERNATIONAL JOURNAL OF PHARMACEUTICAL SCIENCES AND RESEARCH

Received on 03 July 2019; received in revised form, 22 October 2019; accepted, 08 February 2020; published 01 May 2020

PHYTOCHEMICAL ANALYSIS OF LEAVES OF *XYLOSMA LONGIFOLIA* CLOS.: A PLANT OF ETHNOMEDICINAL IMPORTANCE

Rakhi Bhattacharyya [1], Jayanta Sarmah Boruah [2], Krishna Kanta Medhi [*1] and Sarat Borkataki [1]

Department of Botany [1], Nowgong College, Nagaon - 782001, Assam, India.
Material Nanochemistry Laboratory [2], Physical Sciences Division, Institute of Advanced Study in Science and Technology, Paschim Boragaon, Guwahati - 781035, Assam, India.

Keywords:

Xylosma longifolia Clos., Preliminary screening, Quantitative determination, FT-IR, GC-MS analysis

Correspondence to Author:
Dr. Krishna Kanta Medhi

Associate Professor,
Department of Botany,
Nowgong College, Nagaon - 782001, Assam, India.

E-mail: medhikrishna@gmail.com

ABSTRACT: The present study deals with the phytochemical study of leaves of *Xylosma longifolia* Clos. It belongs to the family Flacourtiaceae and is commonly known as 'Long leaved xylosma', whereas the plant is locally known as '*Kathgoromol*' in Assam. *Xylosma longifolia* is an important ethnomedicinal plant used in the North-eastern region of India. The aim of the study is to investigate the bioactive components present and to evaluate the significance of the therapeutic and pharmacological uses of the phytoconstituents. All the standard phytochemical and spectroscopic procedures were followed for the detection and estimation of the phytoconstituents. The leaves of *Xylosma longifolia* were collected for the preparation of 95% methanol extract. Preliminary phytochemical screening of the methanol extract of *Xylosma longifolia* reveals the occurrence of several secondary metabolites like alkaloids, flavonoids, phenols, tannins, terpenoids and saponins. The quantitative phytochemical analysis exhibited the presence of alkaloids, flavonoids and phenols in considerable quantity. The presence of O-H stretch, C-O stretch, C-H stretch, C-H bend, C=C stretch, N-H stretch and C=O stretch were confirmed through FT-IR analysis. Several major and minor bioactive components were identified through GC-MS analysis. From this study, it can be concluded that the ethnomedicinal plant *Xylosma longifolia* contains various bioactive components. Further phytochemical and pharmacological studies are an urgent need for the isolation and discovery of some novel drugs to cure several disorders.

INTRODUCTION: Medicinal plants are the mainstay of every traditional or folk medicine. From the beginning of human history, people are exploring plant species in search of therapeutic properties and management of a wide range of infectious and ailments [1, 2]. About 350,000 higher plants are estimated to exist, among which very less number of medicinal plants has been studied scientifically [3, 4].

QUICK RESPONSE CODE

DOI:
10.13040/IJPSR.0975-8232.11(5).2065-74

This article can be accessed online on www.ijpsr.com

DOI link: http://dx.doi.org/10.13040/IJPSR.0975-8232.11(5).2065-74

The various parts of medicinal plants like bark, leaves, flowers, fruits, stem, roots, and even the whole plant are used in the treatment of an illness are a rich source of several biologically active components such as alkaloids, flavonoids, phenols, saponins, steroids, tannins and terpenoids [5, 6]. The study of phytochemicals is very important for finding out new sources of ingredients and also for the discovery of some new potential compounds [7].

Xylosma longifolia is a small-sized tree belongs to the family Flacourtiaceae and is distributed throughout in China, North-east India, Pakistan, sub-tropical Himalaya and Vietnam [8-11]. The leaf and stem bark of the plant is known to have important therapeutic uses and are extensively used

Nowgong Girls' College ESTD: 1962 Nagaon :: Assam

Principal
Nowgong Girls' College
Nagaon :: Assam

Biologia
https://doi.org/10.2478/s11756-020-00443-9

ORIGINAL ARTICLE

Genetic diversity based on osmotic stress tolerance-related morpho-physiological traits and molecular markers in traditional rice cultivars

Shamsun Nahar[1] · Lipika Lahkar[1] · Md Aminul Islam[2] · Debanjali Saikia[1] · Zina Moni Shandilya[1] · Lakshminarayana R. Vemireddy[3] · Lingaraj Sahoo[4] · Bhaben Tanti[1]

Received: 2 September 2019 / Accepted: 31 January 2020
© Plant Science and Biodiversity Centre, Slovak Academy of Sciences 2020

Abstract

Osmotic stress is one of the major global constraints for the rice cultivation, especially in the rainfed cropping system practiced in Assam, India. Hence, exploration of the discrepancy in functional along with germplasm structure among the traditional rice cultivars is needed. Morpho-physiological traits induced by osmotic and inter simple sequence repeat (ISSR) markers were considered to survey genetic array in growth chamber trials. Twenty one traditional rice cultivars from different agro-climatic regions of Assam, previously used in our laboratory were used in this study along with *Sahbhagi* and *IR64* as control that revealed a high differentiation in phenotypic performance under osmotic stress. On the basis of standardized osmotic tolerant related morpho-physiological parameters, all the rice cultivars could be assembled into five clusters. The cultivars included in a single group revealed almost identical osmotic tolerance levels. The rice cultivars from different agroclimatic zone viz., upper Brahmaputra valley, lower Brahmaputra valley and hill Zones revealed highest genetic diversity as judged by Jaccard coefficient matrix with polymorphism information content (PIC) 0.30. Furthermore, rice cultivars were observed to be constituted into five major clusters depending on ISSR markers that were relatively congruous to the agro climatic regions and specific traditional cultivation practices. The mantel test of the rice varieties between morpho-physiological and ISSR markers exhibited low

Nowgong Girls' College ESTD: 1962 Nagaon :: Assam

Principal
Nowgong Girls' College
Nagaon :: Assam

Vegetos
https://doi.org/10.1007/s42535-019-00092-7

RESEARCH ARTICLES

Comparative biochemical, histochemical and expression analysis of SOD gene in a few traditional rice varieties under aluminium toxicity and phosphorous deficiency in Assam, India

Zina Moni Shandilya[1] · Bhaben Tanti[1]

Received: 21 October 2019 / Revised: 4 December 2019 / Accepted: 24 December 2019
© Society for Plant Research 2020

Abstract
Assam soil is mostly acidic where rice is extensively cultivated that causes serious problems of aluminium (Al) toxicity and phosphorus (P) deficiency. Al is one of the major constraints that limit nutrient uptake and consequently growth and yield in rice. Identifying promising rice varieties having genetic ability that can cope up with Al toxicity and P deficiency is essential. In this study, five rice varieties with contrasting characters viz., *Holpuna* (tolerant), *Soria sali*, *Beto* (moderately tolerant), *Baismathi* and *Moti* (susceptible) were selected to evaluate a comparative antioxidant protection mechanism under Al toxicity and P deficiency through standard biochemical, enzymatic and non-enzymatic analyses. *Holpuna* was seen to have enhanced capabilities of antioxidant protection in all the enzymatic and non-enzymatic analyses. Moreover, increasing tendency in malone dialdehyde (MDA), superoxide dismutase (SOD), ascorbate peroxidase (APX) and hydrogen peroxide on exposure to stress suggests the activation of internal detoxification of plant to cope with the surrounding stress. Histochemical assay also elucidate the level of reactive oxygen species (ROS) accumulation in the seedlings, showing higher accumulation of singlet oxygen in the susceptible varieties that forms dark complexes with the stain. Gene expression patterns further strengthen the expression of superoxide radicals in the tolerant and susceptible varieties. The susceptible varieties on exposure to 100 µM concentration of stress showed relatively higher fold change and vice versa in case of *Holpuna*. Findings of the work would be useful to identify potential rice variety for further recommendation for rice breeding programme.

Nowgong Girls' College ESTD: 1962 Nagaon :: Assam

Principal
Nowgong Girls' College
Nagaon :: Assam

7:31 PM 0.0KB/s
March 2020 (Ank)...

समयांतर

स्थापना वर्ष : 1970
पुनर्प्रकाशन: अक्टूबर, 1998 से निरंतर

ISSN 2249-0469

संपादक : पंकज बिष्ट

व्यवस्था : ठाकुर प्रसाद चौबे
व्यवस्था सहयोग : सुशील शर्मा
टाइपसेट : राधा

चंदे की दरें
सामान्य : एक वर्ष : रु. 350;
दो वर्ष : रु. 600
तीन वर्ष : रु. 850;
पांच वर्ष : रु. 1350
मित्र : एक वर्ष : रु. 500; दो वर्ष : रु. 800
तीन वर्ष : रु. 1000; पांच वर्ष : रु. 1500

छात्रों के लिए :
एक वर्ष : रु. 250; दो वर्ष : रु. 350
(अपना पत्र अंकित करें या)

संस्थाओं के लिए : एक वर्ष : रु. 500.00
(रजिस्टर्ड डाक से मंगवाने के लिए एक वर्ष के कृपया रु. 250 अतिरिक्त भेजें)

विशेष सहयोग
आजीवन : **दस हजार रुपए**
दस वर्ष : **पांच हजार रुपए**

विदेशों में (हवाई डाक से)
एक वर्ष : **25 अमेरिकी डालर**
कृपया चंदा मनीऑर्डर अथवा डिमांड ड्राफ्ट से ही **समयांतर** के नाम भेजें। स्थानीय व बहुराष्ट्रीय चेक स्वीकार्य हैं।

बैंक के माध्यम से शुल्क भेजने के लिए
Samayantar Current a/c
No. 27520200000094
IFSC code: BARB0MAYVIH
Bank of Baroda, Mayur Vihar Ph.-I,
Delhi-110091
कृपया रेमिटेंस की सूचना तत्काल ईमेल अथवा एसएमएस से दें।

समयांतर, 79-ए, दिलशाद गार्डन, दिल्ली-110095
फोन : 09868302298 (संपादकीय)
09871403943 (व्यवस्था)

email: samayantar.monthly@gmail.com
samayantar@yahoo.com

...संबंधित सभी विवाद्यस्पद ...दिल्ली न्यायालय के अधीन होंगे।

इस अंक में

मार्च 2020, वर्ष : 51, अंक : 6

संपादकीय

5. **हिंसा की गलियों और दिल्ली के दंगे**

पत्र

7. **क्यूबा में हेमिंग्वे** — भारत भारद्वाज

विचार

8. **आरक्षण और न्यायपालिका** — अनंत सिंजन
11. **दिल्ली में तांडव : बर्बरता और अराजकता की ओर बढ़ता देश** — सिद्धार्थ
13. **आप की जीत और उम्मीदों का भ्रम** — जावेद अनीस
14. **दिल्ली हिंसा का सबक** — अजय सिंह
15. **अपने ही जन के खिलाफ युद्धरत एक राज्य** — शैलेश
19. **बनारस शहर और बीएचयू का जातिवाद** — प्रमोद कुमार अग्रवाल
24. **मुक्ता साल्वे और ऐन फ्रिक** — मोहन आर्या

साक्षात्कार

27. **'राजतंत्र को अंदर ही अंदर कब्जा लिया गया है'**
— एजाज अहमद से जिमसन जॉन और जितीश पी. एम. की बातचीत

सुबह की सैर

38. **प्राइम टाइम का शोर और चीयर-लीडर बनते लोग** — राजेश कुमार

साहित्य और संस्कृति

40. **फिल्म और परिवार** — विद्यार्थी चटर्जी
42. **साहित्य में एक संत** — पंकज बिष्ट
45. **टेलीविजन धारावाहिकों की स्त्रियां** — बेबी विश्वकर्मा
49. **साहित्य और नैतिकता के सवाल** — धीरेश सैनी

समीक्षा

47. **देश गंवाने के अचूक नुस्खे** — महेश मिश्र

आवरण : फ्रांसीसी चित्रकार **जेरार्द गरूस्से** की एक कृति। गलसे अपने चित्रों की भारीकीयता के लिए जाने जाते हैं। उनके चित्रों की प्रदर्शनी दिल्ली के आधुनिक कला संग्रहालय में 29 मार्च तक देखी जा सकती है।

Nowgong Girls' College ESTD: 1962 Nagaon :: Assam
Principal
Nowgong Girls' College
Nagaon :: Assam

का आधिकारिक घोषणा हुई तो कद जा का नाम गायब था। यह कैसे हुआ? इसका उत्तर तत्कालीन पुरस्कारों और अकादमियों की राजनीति को समझे बगैर नहीं दिया जा सकता।

हुआ यह कि पुरस्कारों पर नियंत्रण करने वाले वामपंथी गुट की करीबी एक महिला

द्वारा *वह आए थ।*

चाट क संग्रह: *भूख आग है, हमारी बुढ़िया, सवाल और प्रश्न।*

डायरी: *अब क्या सोच है, हवा क्या है*

सैम्युएल बेकेट के प्रसिद्ध नाटक *वेटिंग फॉर गोदो* के अलावा और भी कई लेखकों का उन्होंने अनुवाद किया है। ■

व्यवस्थापक

79-ए दिलशाद गार्डन

दिल्ली - 110095

वर्ष 2019 के गोदावरी देवी पुरस्कार से सम्मानित रचना

टेलीविजन धारावाहिकों की स्त्रियां

बेबी विश्वकर्मा

धारावाहिकों में स्त्री चरित्र का कोरा विभाजन पूर्णत: प्रतिगामी है जो स्त्री के शोषण में तथा स्त्री को पुरुष अधीनस्थ बनाए रखने की साजिश में सहभागी बनता है। वर्तमान स्त्री के समक्ष जीवन जीने की अनेक संभावनाएं खुल गई हैं। वह पुरुष आश्रित नहीं बल्कि आत्मनिर्भर बनने का विकल्प चुन सकती है, उसकी आशा, आकांक्षाएं बदल रही हैं लेकिन बदलते परिप्रेक्ष्य में बदल रही स्त्री जीवन के विविधरंगी पक्षों का जिक्र धारावाहिकों में बहुत कम है।

हिंदी के टेलीविजन धारावाहिक अक्सर 'आदर्श स्त्री चरित्र' के मिथ को चरितार्थ करते नजर आते हैं। प्राय: सभी धारावाहिकों में एक ही कहानी भिन्न-भिन्न पैकेजिंग के साथ चलती है जहां पितृसत्ता का बोझ ढोती 'आदर्श भारतीय स्त्रियां' सजी-संजाई गुलदस्ते के रूप में दर्शक के सामने पेश की जाती हैं। स्त्री की चारंपरिक छवि का प्रचार-प्रसार इन धारावाहिकों द्वारा हो रहा है जहां नायिकाएं पुरुष स्वीकृत व्यवहार एवं पुरुषनिर्मित नियमों का नतमस्तक होकर पालन करती हैं। पुरुषवर्चस्ववादी समाज व्यवस्था में रूढ़ हो चुकी स्त्री छवि को अधिक दृढ़ करते हुए इन धारावाहिकों में स्त्री चरित्र का मुख्यत: दो ही पक्षों का चित्रण मिलता है - या तो स्त्री लज्जाशील, पारंपरिक, आज्ञाकारी, पतिव्रता, दया, त्याग, श्रद्धा, सहनशीलता की प्रतिमूर्ति 'आदर्श भारतीय नारी' है, नहीं तो अधम विचारों वाली कुटनी, पतिता है जो अपनी सारी ऊर्जा एवं जीवन के अमूल्य क्षण उस 'आदर्श नायिका' के विरुद्ध षड्यंत्र रचने में व्यतीत करती है।

स्त्री चरित्र का यह कोरा विभाजन पूर्णत: प्रतिगामी है जो स्त्री के शोषण में तथा स्त्री को पुरुष अधीनस्थ बनाए रखने के साजिश में सहभागी बनता है। वर्तमान स्त्री के समक्ष जीवन जीने की अनेक संभावनाएं खुल गई [illegible] पुरुष आश्रित नहीं बल्कि आत्मनिर्भर बनने का विकल्प चुन सकती है, उसकी आशा, आकांक्षाएं बदल रही हैं लेकिन बदलते परिप्रेक्ष्य में बदल रही स्त्री जीवन के विविधरंगी पक्षों का जिक्र धारावाहिकों में बहुत कम है। एक ओर समाज में महिलाएं मुक्ति की, सम अधिकार की लड़ाइयां लड़ रही है, बंद दीवारों को तोड़कर बाहरी दुनिया में प्रवेश करने के लिए संघर्षरत हैं तो दूसरी ओर प्रचलित धारावाहिकों की स्त्री पात्र घर की चारदीवार के संकुचित दायरे में चौका-बर्तन के खल सिमटकर रह गई है। दूरदर्शन द्वारा प्रसारित 'उड़ान', 'शांति' जैसे धारावाहिकों में आधुनिक महिला की परिवर्तित होती छवि उभरकर आई जो महत्वाकांक्षी थी, सशक्त थी, अपनी पहचान बनाने के लिए व्यवस्था को चुनौती दे रही थी। छोटे पर्दे पर एकता कपूर का पदार्पण हिंदी धारावाहिकों के इतिहास का दूसरा पड़ाव था जहां स्त्री चरित्र प्रगतिशीलता को त्याग पुन: रूढ़िवादिता की ओर लौटे। यथार्थ से दूर हटता इन धारावाहिकों में प्राय: एक दरिद्र या मध्यवर्गीय स्त्री का विवाह अमीर घराने में होता है और उसकी कहानी उसी घर से शुरू होकर उसी घर के अंदर खत्म हो जाती है। 'औरत ही औरत की दुश्मन है'- पितृसत्ता द्वारा फैलाए गए इस भ्रम को सच्चाई में तब्दील करती इन 'क' धारावाहिकों की कहानी सास-बहू, ननद-भाई, बहन-बहन के बीच की अतिरंजित हिंसा, द्वेष, ईर्ष्या के इर्द-गिर्द घूमती रहती है। एकता कपूर का धारावाहिक 'क्योंकि सास भी कभी बहू थी' अब तक का सर्वाधिक जनप्रिय एवं आठ साल की सर्वाधिक लंबी अवधि तक चलने वाला धारावाहिक रहा है। इन धारावाहिकों का ऐसा गहरा असर भारतीय दर्शकों के मानस पर पड़ा कि इतने दशक गुजरने के बाद आज भी ऐसी ही एकरसता में डूबी कहानियों को देखने की भूख मची रहती है।

कई धारावाहिक आए जिनकी शुरुआत तो आशाजनक लगी परंतु अंतत: वे भी 'सास-बहू' की साजिशों में उलझकर रह गए। कलर्स द्वारा प्रसारित 'उड़ान' एवं स्टार प्लस द्वारा प्रसारित 'दीया और बाती हम' की परिकल्पना तो अनोखी थी लेकिन जैसे ही 'उड़ान' को चकोर जवान हुई तो उसकी भूमिका भी क्रांतिकारी से 'बहू' तक सीमित होकर रह गई। दूसरी ओर आईपीएस अफसर बनने की महत्वाकांक्षा रखने वाली 'दीया और बाती हम' की संध्या घूंघट ओढ़े पति और ससुराल वालों को खुश करने में व्यस्त हो गई। महत्वाकांक्षी महिलाओं की सकारात्मक छवि, कामकाजी महिलाओं की जीवन से जुड़ी समस्याएं हिंदी धारावाहिकों में बहुत कम उभरी हैं। एक लोकप्रिय धारावाहिक 'ससुराल सिमर का' में सिमर की नौकरी करने या न करने का फैसला एक साधारण लड्डू के स्वाद के ऊपर निर्भर करता है। क्योंकि एक आदर्श भारतीय स्त्री के जीवन में पति और परिवार ही सर्वोपरि हैं जिनकी सेवा करना, जिनके द्वारा स्वीकृति प्राप्त करना ही स्त्रीत्व का लक्ष्य है। उनके कहने पर स्त्री अपना करियर तो क्या अपनी सारी आशा-आकांक्षाएं, कष्ट अर्जित दक्षता त्याग सकती है क्योंकि परम आज्ञाकारी बनना ही उसका धर्म है। इसीलिए करियर उन्मुख महिला की कहानी उपकथा हो सकती है, मूलकथा नहीं।

हिंदी टीवी धारावाहिकों की विडंबना यह है कि इनकी कहानियां स्त्री केंद्रित होने के बावजूद स्त्री का सफल प्रतिनिधित्व करने में असमर्थ हैं। स्त्री के प्रति इनका दृष्टिकोण एक आयामी रहा है। स्त्री की 'बहू' या 'बेटी' छवि ही सर्वत्र दिखता है जिनका जीवन घर के भीतर ही गृहकलह और रोने-धोने में बीतता है। चारंपरिक लिंगगत भूमिकाओं को दृढ़ कर रही इन धारावाहिकों में स्त्रियां पुरुष आश्रित हैं, घर के मर्द ही आर्थिक जिम्मेदारी निभाते हैं और पारिवारिक जिम्मेदारी का भार स्त्री पर होता है। इसके अतिरिक्त अन्य भूमिकाओं में स्त्री चरित्रों का चित्रण बहुत कम है। इन धारावाहिकों में प्रेम और रोमांस के नाम पर कतिपय आपत्तिजनक विचारों को बढ़ावा मिल रहा है जो स्त्री के शोषण एवं उत्पीड़न का कारण बनती हैं। बहुपत्नीत्व, जबरन विवाह हिंदी धारावाहिकों का प्रिय विषय है।

Nowgong Girls' College ESTD: 1962 Nagaon :: Assam

C.T.C.

Principal
Nowgong Girls' College
Nagaon :: Assam

Papers published per teacher in the Journals notified on UGC website during the Academic Session: 2020-21

Submitted to the NAAC for 3rd Assessment Cycle of Assessment & Accreditation

NOWGONG GIRLS' COLLEGE

Re-accreditated at A Grade by the NAAC (2nd Cycle)

ISSN : 2347-7180

Dogo Rangsang Research Journal
(A Bilingual Research Journal indexed in UGC-CARE List)

Research Journal

DOGO RANGSANG

Vol.: VII • Issue: XII • July, 2020

দগো ৰাংছাং

গৱেষণা পত্রিকা

Chief Editor (Hon.) : Dr. Upen Rabha Hakacham
Editors (Hon.) : Dr. Lalit Chandra Rabha
: Dr. Neeva Rani Phukan

মুখ্য সম্পাদক (অবৈতনিক) : ড° উপেন ৰাভা হাকাচাম
সম্পাদকদ্বয় (অবৈতনিক) : ড° ললিত চন্দ্র ৰাভা
: ড° নিভা ৰাণী ফুকন

C.T.C.
Principal
Nowgong Girls' College
Nagaon :: Assam

Nowgong Girls' College
ESTD: 1962
Nagaon :: Assam

A Peer Reviewed Bilingual Research Journal
(Indexed in UGC-CARE List)

ISSN 2347-7180

DOGO RANGSANG RESEARCH JOURNAL
দগো ৰাংছাং গৱেষণা পত্রিকা

Vol. VII, Issue. XII
সপ্তম বছৰ, দ্বাদশ সংখ্যা
July, 2020
জুলাই, ২০২০

Chief Editor (Hon.) : Dr. Upen Rabha Hakacham
Editors (Hon.) : Dr. Lalit Chandra Rabha
Dr. Neeva Rani Phukan

মুখ্য সম্পাদক (অবৈতনিক) : ড° উপেন ৰাভা হাকাচাম
সম্পাদকদ্বয় (অবৈতনিক) : ড° ললিত চন্দ্র ৰাভা
ড° নিভা ৰাণী ফুকন

Dogo Rangsang Research Society
Reg. No. KAM-M/263/L/ 595 of 2015-16
Gauhati University Campus
Guwahati - 781014

Principal
Nowgong Girls' College
Nagaon :: Assam

Nowgong Girls' College
ESTD: 1962
Nagaon :: Assam

(১৮) অসমীয়া আৰু বাংলা ভাষাৰ শব্দ সাধন প্ৰক্ৰিয়া :
পাৰস্পৰিক সাদৃশ্য আৰু প্ৰভাব
❑ ড° অৰ্চিতা ভট্টাচাৰ্য/১৫৬
(১৯) আধুনিক অসমীয়া অভিধানৰ প্ৰকৃতি বিচাৰ
❑ বৰ্ণালী শইকীয়া/১৬৩
(২০) বীৰেন্দ্ৰ কুমাৰ ভট্টাচাৰ্যৰ 'মৃত্যুঞ্জয়' উপন্যাসত প্ৰতিফলিত সমাজ জীৱন : এটি আলোচনা
❑ ব্ৰজেন বৈশ্য/১৬৯
(২১) কৈৱৰ্ত সমাজ আৰু হোমেন বৰগোহাঞিৰ মৎস্যগন্ধা উপন্যাস :
এক বিশ্লেষণাত্মক অধ্যয়ন
❑ লক্ষ্মী জ্যোতি দাস /১৭৫
(২২) অসমীয়া সংস্কৃতিত বাঁহ : এক অধ্যয়ন
❑ কুঁহি সপোন বৰগোহাঁই/১৮১
(২৩) পশ্চিম অসমৰ মাগন গীত : এউৰী
❑ মনোজ কুমাৰ শৰ্মা/১৮৭
(২৪) বাউল আৰু দেহবিচাৰ গীত : এক তুলনামূলক অধ্যয়ন
❑ ড° সংগীতা শইকীয়া/১৯৫

English Section :

(25) **Saurabh Kumar Chaliha's Science Fiction : Plots, Presentations, Social Imprints and Scientific Views**
❑ Nabajyoti Dutta /**211**
(26) **Beliefs and Practices Centering Round Silk Rearing and Weaving in Assam**
❑ Dr. Mridutpal Goswami /**218**
(27) **Snapshots in British India: Sahityarathi Lakshminath Bezbaroa discovered Sambalpur for Assam**
❑ Dr. Maheswar Kalita /**224**
(28) **Unfolding relationship of Word discourse & Time Factor through 'Word Knowledge Acquisition'**
❑ Dr. Rudranarayan Mohapatra &
❑ Dr. Ambeswar Gogoi /**233**
(29) **Symbolic Representation of Identity: A Fight for Freedom, Choice and Existence in Santhal Folktales and Contemporary Writings**
❑ Dr. Rabindranath Sarma &
❑ Ms. Ria Mukherjee /**242**
(30) **Dravidian Elements in Assamese Language**
❑ Biswajit Das /**253**
(31) **An Appraisal of the Religious Thinking of Sankaracharya and Vivekananda on the Concept of 'Moksha' in the Advaita Vedanta Philosophy**
❑ Dr. Naba Kumar Kalita /**261**

Principal
Nowgong Girls' College
Nagaon :: Assam

Nowgong Girls' College
ESTD: 1962
Nagaon :: Assam

Dogo Rangsang Research Journal
(A Bilingual Research Journal
Indexed in UGC-CARE List)

ISSN : 2347-7180
Vol. VII, Issue XII, July, 2020

Dravidian Elements in Assamese Language

❑ **Biswajit Das**
Associate Professor, Department of Assamese, Nowgong Girls' College, Nagaon,
Mobile : 9435162097
Email : drbiswajitdas555@gmail.com

Abstract : Assamese is an Indo-Aryan language derived from MagadhiPrakrit and one of the major languages of India mainly used in Northeastern region. Assam is the heterogeneous state in terms of language and community. Anthropologists claim that the pre-Aryan Australoids and Dravidians were the first who inhabited the region. But Dravidians have lost their physical identity with the assimilation of other local communities. The Australoid, Mongoloid characters are still distinct among the people of Assam and Northeast despite their assimilations. The people those who engaged in fishing and plying boat are called Koiborta. Many anthropologists claim that these Koibatra people of Assam are originally Dravidian or Mediterean. (B.M Das)

The Dravidians are the oldest (with Australoid) inhabitant of Assam. Simultaneously many linguists also claim that Assamese has some elements of Dravidian languages. Some of them are root morphemes. Some morphs relating to place names and river names of this region are very similar to Dravidian languages. Of course, there have been different opinions about the origin of the words among the linguists. I mentioned here two examples which are the oldest name of Assam. The first one is Prâgjyotishpura and the second one is Kâmrupa. Prâgjytishpura is older than Kâmpura. From, 4th to 12th century, both Prâgjyotishpura and kâmrupa both are used simultaneously in different inscriptions in India. DrBanikantakakati, an eminent linguist and scholar of Assam opines that the origin of Prâgjyotishpura and Kâmrupa both are sanskritize forms of the Austric word (AFD, 1941) discarding the Hindu

C.T.C.
Principal
Nowgong Girls' College
Nagaon :: Assam

Nowgong Girls' College
ESTD: 1962
Nagaon :: Assam

mythology interpretation. In different Puranas, prâgjyotishpura seems to be connected with topographical features of the land. He opines that Prâgjyotishpura is an Austric formation like pâuger, hill (pâu, hill, ger, hill) jo or juh, high, tic or ti , long; that is, (a region of) extensive or long (tic or ti) high (jo or juh) hills (pau, or ger or pauger). Both are sanskritize form of Pre-Aryan derivation but the source is not beyond doubts. There is another Dravidian group of words which is very similar to Pragjyotishpura. Dravidian words pâr-go (ko) tuti is which designate the inhabiting place ('is', suffix for Dravidian place-names (vide DOW p-138) on the top (tuti/duti) of extensive (pâr) mountains (go, go).

The other name Kâmrupa, I would like to mention here a noteworthy opinion of DrLahovary: "South Dravidian ka, kampaGa, a district of kampalai, titled field, fertile country; Ma, câmpu, length, stretch; .... are all a pre-Indo-Aryan heritage." Therefore, Dr Moral opines that: 'Kamrupa is therefore, Aryanaised form of the Dravidian words where kâm or kamia a plain on the top of hills or a fertile valley or country and ru is suffix denoting the place name.' (Assamese its origin and Substratum, 2009)

There are other some Dravidian affixes which are an important component of denoting to place and river names of Assam. In my paper, I am going to explore how these morphs are related with Dravidian languages.

The relation between the people of both regions are pre-Aryan and some interlinks are still exists. I will take help from printed articles, books of scholars of anthropology and linguistics fields to establish my point.

Key Words: Koibatra, place names, river names, root morphemes.

Assam is known for its heterogeneous cultures and languages. The languages belong to this area are Sino-Tibetan, Indo-Aryan, Austric and Tai-Kradai. Tibeto-Burman represents Boro, Mishing, Tiwa, Deuri, Rabha etc. and Tai-Kradai represents Tai-Ahom, Tai-Khamti, Tai-Turung, Tai-Phake, Tai-Khamyang, and Tai-Aiton. The Khasi and Syntang Languages represent Mon-Khmer group of Austro-Asiatic family. The rest are the Assamese, Bengali and Bishnupriya Manipuri which belong to an Indo-Aryan group of Languages. Interestingly, we have not found a single Dravidian language in this region. Many scholars opine that the Assamese language has some Dravidian elements (Kakati 1987, Moral 2009 et al). How these elements come to the Assamese language is questionable. Many linguist and anthropologist (Das, 2003) claims that it was a result of pre Vedic contacts.

Assamese is an Aryan language. But the Aryans were late comers. Anthropologists claim that the Austro-Asiatic was the first inhabitants of Assam. Although it is a matter of debate, it is noteworthy to mention that some other anthropologists opine that Dravidian were the first

Nowgong Girls' College ESTD: 1962 Nagaon :: Assam

C.T.C.

Principal
Nowgong Girls' College
Nagaon :: Assam

inhabitants of Assam. Even though they had tried to establish the genealogical evidence (Das, 1970). But cultural anthropology helps to find out some significant similarities between the people of Northeast India and South India are crucial for this discussion. The Aryans have entered Assam from the west. It would be relevant to what Suniti Kumar Chatterji stated in ODBL:

> 'The people of Bengal, in the middle of 1st millennium B.C. do not seem to have been Aryan speakers,' (Chatterji, 2011:70)

Kakati has mentioned that there are a lot of elements of languages like Kol, Munda, Khasi and Bodo in Assamese. Scholars have unanimously agreed that these are pre-Aryan languages of Assam and all of them were somehow contacted with Dravidians. Anthropologists also assumed that the *kaibatras* of Assam are Dravidian on the basis of physical anthropology (Das, 2003). 'These early tribes of Bengal, Dravidian speakers mainly, were all organized, and they seem to have possessed a culture their own. The early history of Burma and Siam tells us that at a time when the Tibetan-Chinese tribes (Burmese, and Tai) had not yet arrival on the scene, and these countries were inhabited only by Mon-Khmer peoples, Dravidians from Bengal and Kalinga were emigrating these lands, and becoming the ruling race there. Later, when these non-Aryans from India assimilated Brahmanic culture, their princess claimed connection with the ancient royal houses of Aryan Upper India...' (Chatterji, 2011: 69). The process of Aryanisation started thereafter and still being continued.

Assam was once known as *Pragjyotishpura* and then as *Kamrupa*. The present name *Assam* is popularized in the nineteenth century after the colonization of British. Etymological analysis of these words had been done by scholars of Assam and all of them are at least consensus that these are Sanskritisation or Aryanisation of non-Aryan words. The Assamese language plays the role of lingua franca among the different ethnic communities of Assam from the beginning of its journey. This is Because of its speakers, who belongs to the different Sino-Tibetan and Austro-Asiatic languages used Assamese for inter-community interactions. The pluro-lingual contact changed Assamese in many ways. Moral has stated about this linguistic situation, as

> 'Language diffusion of linguistic innovations has been taking place between Asamiya, the Sino-Tibetan languages, and Khasi in this area for a long time, which has resulted in many common linguistic features binding all these languages in a common thread even though they are not related genetically. This is a direct result of linguistic innovations originating in one language spreading to neighboring varieties through the medium of bilingual speakers.'(1997: 44).

Place names of Assam:

The place name study would not be possible without the help of Dravidian linguistic analysis. In Bengali, Chatterji stated : 'An investigation of place names in Bengal, as in other parts of

C.T.C.
Principal
Nowgong Girls' College
Nagaon :: Assam
Nowgong Girls' College ★ ESTD: 1962 ★ Nagaon :: Assam

Aryan India, is sure to reveal the presence of non-Aryan speakers, mostly Dravidians, all over the land before the establishment of the Aryan tongue' (ODBL). This is not only true for Bengal; the same is applicable for Assam too.

I would like to mention here some place names which are comparable:

Prâgjyotishpura and Kâmrupa, both are sanskritized forms of the Austric word (AFD, 1941) discarding the Hindu mythology interpretation. In different Puranas, Prâgjyotishpura seems to be connected with topographical features of the land. He opines that Prâgjyotishpura is an Austric formation like *pâuger*, hill (pâu, hill, ger, hill) *jo* or *juh*, high, *tic* or *ti*, long; that is, (a region of) extensive or long (*tic* or *ti*) high (*jo* or *juh*) hills (*pau*, or *ger* or *pauger*). Both are sanskritized form of Pre-Aryan derivation but the source is not beyond doubts. There is another Dravidian group of words which is very similar to *Pragjyotishpura*. Dravidian words *pâr-go* (*ko*) *tuti* is which designate the inhabiting place ('*is*', suffix for Dravidian place-names (vide DOW p-138) on the top (*tuti/dutī*) of extensive (*pâr*) mountains (*go, go*).

Kâmrupa: According to Lahovary: "South Dravidian *ka, kampaGa*, a district of *kampalai*, titled field, fertile country; Ma. *câmpu*, length, stretch; .... are all a pre-Indo-Aryan heritage." Therefore, Moral opines that: 'Kamrupa is therefore, Aryanaised form of the Dravidian words where *kâm* or *kam* is a plain on the top of hills or a fertile valley or country and *-ru* is suffix denoting the place name.' (Cited from Moral, 2009). But, Kakati's view is differing from Lahovary. But, Kakati opines: 'Perhaps popularly the country was known as kâmaru or kâmrut(d) (cf. Santali kâmbru, kâmru, name of a lesser divinity worshipped by Santals)-t being a suffix of place names' (AFD, 54). A Hindu mythical form was added with the name of Kamrupa. The Kamrupa form is constituted with two parts: *Kâm*, desire+ rupa, form. In Puranas, Kamrupa was the place where Kamadeva, the God of love regained his form (rupa) after having been burnt by the Shiva. There are some others who have been provided some interesting views: 'The topographical feature of the land indicate the probable of the name Kâmaru and it is connected with the pre-Aryan tongue. The pre-Aryan i.e. Dravidian words like Kâma, Kâm (a plain on the top of a hill or fertile valley, N.Lahovary, Dow 1963, PP.240, 334, 338) and ru a pre-Aryan suffix for place names may be connected with the formation of this name (Moral, 2009:146).

Chatterji has mentioned some affixes which are added with the place names found in early inscriptions in Bengal are given below:

-Jôla, -jôma, jôli, -jôtikâ,...bhImâ, -haG
a, -vadâ; -kuGda,.cavamI, cavâ
a etc. (ODBL, 2011:65-66)

These affixes are not only used in place names of Bengal but also used in Assam. Some of them are:

-jôla, -jôma, jôli :<juli e.g. Dhekiajuli (A small town in Sonitpur District)

C.T.C.
Principal
Nowgong Girls' College
Nagaon :: Assam
Nowgong Girls' College ESTD: 1962 Nagaon :: Assam

Hugrajuli (A small town)
Majuli(A river Island of Assam)

Rongjuli, Sonajuli, Rupajuli are some other names constituted with the suffix –juli. The *–jola* suffix had also mentioned in a Plate of 12th century AD by king Dharmapala Deva. The river *Diyambarjola* formed the northern boundary of the land granted to Kamdeva son of Basudeva of Bharadvajagotra by Ratnapala (Phukan, 2012: 292). *-Jola* is also mentioned jolaka (ibid).

-gui: <guri (ASM)
Te. gadda, Ka. gaddi = lump, mass, clot, bank, brink
There are thousands of place names in Assam with the suffix –guri.
e. g. Amguri, Ximaluguri, Ganeshguri etc.

bhimâ: < bhimhâ, e.g. pitribhithâ (the land own by his/her father)

-kunda: <Te. *kuGda* (rock, hill)
Bhairabkunda (A place where *Bhairobi* Temple situated)
Paraxuramkunda (A mythological place in Arunachal Pradesh)

-râ: < *vadâ* < *[â* (BNG), *râ* (ASM)
Bagura, Bogra (a place mentioned in *Koch BiharerItihas*)

These are the affixes of Dravidian origin:

-Kosa/-kusi: Ta. *ku[icci* (village in the hilly tract; village); Ka. *ku[ika* (village), To. *koca* (small valley, a room)
xualkusi (A famous village for weaving of silk in Kamrup)
'*-Patti*': means small village or town, a locality < Ta. pammi (Village, dwelling)
Compare to Sanskrit. *Patti>pammi, tt>mm*) *BangiyaSabdakosh*Vol.II

In Assamese, the meaning of *-patti* is same as Dravidian Languages. e.g. *Kamarpatti, Islampatti, Dhakaipatti* etc.

-bar/-bari: ASM Meaning: a compound, a flower or fruit garden, e.g. *Titabar, Kaliabar*. In Dravidian Languages the term *-bar/-bari means*

Ta.*-pari* (town, city, temple)
Ka. *bara* (limit); *bari* (road) *på*
Te. *bore* (hill, hight)

In Assamese, the suffix *-bâri* used to indicate the compound of certain fruits field or gaden. e.g. *Tamolbari* (betel-nuts garden), *kuhinyarbari* (sugarcanes garden). Even Some place names are also in Assam with the suffix *Ambari* (a place in Guwahati), *Xarthebari*(a small town in lower Assam).

-pur/-puri: The suffix *–pur/-puri* (means town or city) is very common in place names in every part of India. It has been said that some other equivalent words are used simultaneously in different parts of India i.e. *Pur= pura= kûra=ûra=ûri= ko*

C.T.C.
Principal
Nowgong Girls' College
Nagaon :: Assam
Nowgong Girls' College ESTD: 1962 Nagaon :: Assam

i etc. town or city (Moral, 2009: 160). Scholars have unanimously agreed that this affix (*pur*) is Dravidian. The Suffix might have come later period through the Aryan. There are lots of villages or towns where ending *-pur* are found:

-pur: *Tezpur, Gohpur, Narayanpur, Dhalpur, Lakhimpur, Dispur.*

-puri: *Abhayapuri*

River names:

juri: <*Jôli*

Ko. *jor- (jo ry)* (tears and snot) run in streams.

Kartowâ and *Tristâ*, both are now in North Bengal. Once, the *Kartowâ*was traced as the western boundary of ancient Kamrupa. The affixes *–tiu, tu, diu, lao* particles are used to means water or river in Austric (AFD: 1941). It may be mentioned here that the Dravidian particles in comparison to Austric words.

There is another etymological analysis stated by Moral (2009:173) in the following way:

Kartowâ:Te. *kar* (black); ka., Tu. K*âru/ kari*(black)

Ta. karai (bank);

Ma. kara (shore, riverside, land (opp. to sea)), *karal* (border, margin, edge).

Tu. karè (bank of a river, border)

Br. karrak (bank, shore, brim, border, edging, near).

Then, suffix pre-Aryan *–toya* (water).

Tista (the river of sour water): Kur.*Tissa* (sour) and Austric *ti, toya* (water)

Digaru:<ik-/ig-+ *-âru*, ik-/ig- igul-/igl- (to descend) + *-âru: **Ta**. aruvi* (river's mouth); *Tu. aruve* (mouth of a river)/ Tu. i7ijârù a slope, slipperiness.

Dikkura:< *(Di-+-ikkara*), Di, water (Austric) + *Ka.* i aku to pinch, tweak; ikkur, ikkura, ikkara, ikra pair of tongs.

Dikkura is a river referred in the Ulubari Plate of King Balavarmana-III, AD 9th century. The river was situated in old Kamrupa.

Kolong: Ta. *Kal/ kali* (sour rice-gruel)

Te. *Kali* (the water in which rice has been washed, kept until ferments)

There are some other significant affixes or morphemes which are related to the river names of Assam. These are:

- *âru: **Ta**. aruvi* (river's mouth); *Tu. aruve* (mouth of a river)

Ta. aruvu (aruvi-) to spring out and gently flow down; *aruvi* waterfall, spring at the foot of a hill. *Ma. aruvuka* (to spring out and flow down gently); *aruvi/arivi* (waterfall)

e.g. Digaru (a river in Kamrupa) compare to Ta. *kilâi*(dig up), *ki7âru*(dig up); Ma. *ki7â*(digging).

- *âl/ âli :* Ta. Water, flood; Ma. *âl* water;

C.T.C.
Principal
Nowgong Girls' College
Nagaon :: Assam

Nowgong Girls' College
ESTD: 1962
Nagaon :: Assam

Ta. âli raindrops, opening shower of the rainy season; wind.

e.g. Bharali, Bharali (Assamese)

sira/siri: <*Ma. ci_i, ci_a, ciri* (lip); *ki_i* (corner of the mouth):

Slang words:

Kelâ: means penis. This word is very similar to

Te.:culla, culli (penis), Ta.: Cûttu, cûru (anus), Ma: cûttu, kuGGa, kumpi, cuGGi (penis)

Dudu: Breast's nipple

Ma. Ka. Tu.: tommu (nipple); Kati: means anus or female organ

Ta. Cuttu. curu (anus); Te: kutte (anus)

Pokar: means anus.

Ka: *pukku, pukuli, pukali; Tulu: pukuli* (anus);

Ma: *pokkara* (low people)

Some fundamental words used in Assamese are very similar to Dravidian Languages, e.g.

âpâ/*âpi*: used mainly in Lower Assam, meaning- boy/girl.

Ta: appi- mistress of house; *appâttai*- elder sister, elder sister

Ma. appan father; *appu* affectionate appellation of boys.

Ka. appa father; frequently added to the proper names of men as a term of common respect; used endearingly to children by their elders; *apa* father;

Kinship words:

Some affixes used in kinship terms of Dravidian languages are very common in Assamese. These are:

-âri: ASM e.g. (jiyari-daughter, bowari- son in law)

In Dravidian Languages *âri* means daughter.

-âbu: ASM. Grand mother

Ta: *avvai* - mother, old woman, woman ascetic;

Ka. avve, avva mother (used as a title of respect and love), grandmother, any elderly woman.

Te. avva (mother, grandmother, an old woman)

-kurâ: Ta. *Kufai* (be over boiled, cause to melt)

In Assamese -kurâ is used as a determinate with the term fire. *e.g. zuikurâ*

tâwoi: Father's equal, father's friend

Ta. tantai (father);

Other words:

There are some words in Assamese which are very similar to Dravidian Languages. Some of them are:

C.T.C.
Principal
Nowgong Girls' College
Nagaon :: Assam

Nowgong Girls' College
ESTD: 1962
Nagaon :: Assam

bis: to fan, to blow

Ta: *vIcu-* cast (i.e. put bamboo rafters on a sloping roof), fan, blow as the wind,

bisani: (A fan made by bamboo)

Ta: *bisaGige, bisaGike* (fan)

tiyâ/ titâ : to become wet

Ta.- *tuvai* (-pp-,-tt-) to dip in, soak), (-v-, nt-) (to be dipped (as cloth in dye), be moistened with starch)

Ma. tuvekka to steep, soak in water.

donâ: *Ta. tOlai* (cup made of plantain or other leaf.)

Ma. donna (cup made out of a leaf, for Brahmans to drink pepper-water, etc.)

Ka. donne, jonne (leaf-cup). *Tu. donne* (cup made of plantain) leaves, etc. *Te. donne* (cup made of leaves).

Conclusion:

The place names and river names of Assam mentioned in this paper are somehow similar to Dravidian linguistics. These similarities might have come from the result of contact situations among the groups of the people of the both regions. The cultural anthropology of the people of both areas could have helped us to find out the connection. The place names and river names of Assam stated in the inscriptions and plates needs further etymological study. In my paper, I am drawing out the similarities between the Assamese and the Dravidian linguistic. This discussion required more attention from the scholars of both regions. ❑❑

Abbreviation used in the paper.

ASM= Assamese, BEN= Bengali, Ta= Tamil, Te= Telegu, Ma= Malayalm, Ka= Kanada, Tu= Tulu, AFD= Assamese, Its Formation and Development

ODBL= Original and Development of Bengali Language

Diacritical Marks:

< means changed to

> means derived from

Reference:

Burrow, T., and M. B. Emeneau. 1984. *A Dravidian etymological dictionary* 2nd ed. Oxford [Oxford shire] : Clarendon Press.

Chatterji, S.k.2009. *Originaland Development of Bengali Language*, Rupa Publications India Pvt. Ltd., New Delhi

Das, B.M.2003. *The People of Assam Origin and Composition*, Gyan Publishing House, New Delhi

Kakati, Banikanta. 1987.*Assamese, Its Formation and Development*, Fourth Edition, Lawyers Book Stall, Guwahati

Krishnamurti, Bhadriraju.2006. *The Dravidian Languages*, Cambridge University Press

Medhi, Kaliram.1988.*Assamese Grammar and the Origin of the Assamese Language*, Publication Board, Assam,

Moral, Bhagaban.2009. *Assamese Its Origin and Substratum*, Panchjyjyoti Prakash, Guwahati.

Moral, Dipankar. 1997. *North-east India as a Linguistic Area*, Mon-Khmer Studies Journal, MKS 27:43-51

C.T.C.
Principal
Nowgong Girls' College
Nagaon :: Assam

Nowgong Girls' College
ESTD: 1962
Nagaon :: Assam

JOURNAL OF NATURAL REMEDIES
DOI: 10.18311/jnr/2020/23879

REVIEW ARTICLE

An Ethnobotanical Study of Medicinal Plants used against Jaundice by Tea Tribes of Morigaon District, Assam (India)

Rakhi Bhattacharyya[1*], Krishna Kanta Medhi[1], Sashin Kumar Borthakur[2] and Sarat Borkataki[1]

[1]Department of Botany, Nowgong College, Nagaon - 782001, Assam, India; rakhibhattacharyya06@gmail.com
[2]Department of Botany, Gauhati University, Guwahati - 781014, Assam, India

Abstract

The present study was conducted to document the ethnomedicinal plants used against jaundice by the tea tribes of Morigaon district of Assam, India. An ethnomedicinal field study was carried out from June 2016 - July 2017. Information was gathered by using a semi-structured questionnaire about the traditional knowledge of medicinal plants used against jaundice by the tea tribes of Morigaon district of Assam. Documented data was evaluated using the quantitative ethno-botanical indices of fidelity level (FL), Use Value (UV) and Family Use Value (FUV). From the ethno-botanical investigation, a total of 39 species of plants covering 36 genera and 27 families respectively have been enumerated. A total of 53 informants aged from 20-75 years were interviewed to record the ethnomedicinal data. Lamiaceae was the dominant family. Among the plant portions, leaves were most frequently used. Among the 39 medicinal plant species recognized mostly were herbs. The plants species having the highest use value were *Drymaria cordata* trailed by *Xylosma longifolia* and *Achyranthes aspera, Aegle marmelos, Alstonia scholaris* and *Justicia gendarussa*. The fidelity level was 100% for *Achyranthes aspera, Cheilocostus speciosus, Clerodendrum infortunatum, Justicia gendarussa, Lawsonia inermis, Coffea benghalensis* and *Saccharum officinarum*. The tea tribes of Morigaon district still relies on herbal therapies for curing jaundice. *Coffea benghalensis* has not been previously reported as a remedy of jaundice from Northeast India. Further research is needed to investigate the phytochemistry and pharmacological effectiveness of the plant species that could be the basis for the isolation and development of some novel phyto-therapeutic active compounds in the future.

Keywords: Ethnobotanical Study, Jaundice, Medicinal Plants, Morigaon District, Tea Tribes

Abbreviations Used

WHO: World Health Organization; FL: Fidelity Level; UV: Use Value; FUV: Family Use Value; Ass: Assamese name; TT: Tea Tribal name

1. Introduction

Ethnomedicine has evolved and developed since the prehistoric period. Traditional medicine is still the main source for treating health related problems around the planet[1]. Despite globalization and modernization, about 60-85% of the world's population in the developing countries relies on natural and traditional medicine[2]. According to WHO, around 21,000 plant species have been estimated which can be potentially used for medicinal purpose[3,4]. Ethnic groups store an immense knowledge on traditional herbal medicine and this need to be properly documented[5]. Ethnobotanical studies are the key sources for the discovery of novel drugs from

*Author for correspondence

Article Received on: 04.07.2019 Revised on: 18.10.2019 Accepted on: 23.01.2020

C.T.C.
Principal
Nowgong Girls' College
Nagaon :: Assam
Nowgong Girls' College ESTD: 1962 Nagaon :: Assam

the plant species[6]. India is considered as the leading producer of medicinal plants and represents one of the greatest reservoirs of ethno-botanical wealth[7,8]. Nearly, 65% of the Indian population depends on traditional therapies[9]. North-east India including Assam is considered as the paradise for anthropologists and ethno-botanists as it has a rich vegetation wealth due to topographic and climatic specificity and is among the most diverse regions in the world with more than 150 tribes existing and the tea tribes are one among them[10,11].

Jaundice is a complex ailment caused due to the malfunctioning of the liver, which results in the excessive level of yellow-orange bile pigment i.e. bilirubin, which gets deposited in the tissues of skin, mucous membranes and the sclera[12]. The word jaundice is a derivative of French word 'Jaune' that means 'yellow'. The causes of jaundice are either acquired or congenital[13]. Jaundice is a symptom rather than a disease. There are several possible causes of jaundice viz., hepatitis (A, B, C, D and E), obstruction of bile ducts, liver cirrhosis, gall-bladder stones, inflammation of the liver, pancreatic cancer, alcoholic liver disease, tuberculosis, typhoid, malaria, haemolytic anaemia, yellow fever, certain medication, neonatal jaundice and pregnancy. A large number of plant species claim to possess the liver protecting activity[14]. Almost 160 phyto-compounds from 101 plants claim to possess the hepatoprotective activity[15]. The tea garden community of Assam uses a number of self-remedial medications and herbal therapies for the treatment of jaundice. This acquired knowledge about the traditional medicinal plants may be helpful for developing new medicines for Jaundice by identifying novel bioactive compounds[16]. The chief objective of the study was to measure and document the richness of indigenous knowledge on medicinal plants against jaundice used by the tea tribes of Morigaon district of Assam, so that the documented plant species can be used for phytochemical and pharmacological discoveries in the future.

2. Materials and Method

2.1 Study Area and the People

An exploratory investigation was undertaken in the tea gardens of Morigaon district of Assam, which is located in the central region of Assam. The district lies between 26° 45' North Latitudes and 93° 50' East Longitude, covering a geographical area of 1,704 square kilometers (658 square miles). The Morigaon district is bordered by river Brahmaputra in the North, West Karbi-Anglong district in the south, Nagaon district in the east, and the Kamrup district in the west, where it also shares a small border with Meghalaya. The climate is of general monsoon type with an average rainfall of about 1,753 mm. The tea tribes of Morigaon district were originally from Andhra Pradesh, Bihar, Jharkhand, Orissa, Tamilnadu and West Bengal including *Bhumij, Bhil, Bhuyan, Kohar, Kurmi, Khariya, Garh, Munda, Mahanty, Tanti, Telenga, Lohar, Orang, Oriya, Sundi, Ghatwal, Goala, Kalindi, Kaul, Santhal,* and *Gonju* tribes[17,18]. The main languages spoken by the tea tribes are *Assamese, Baganiya bhasa* / Tea tribal language (amalgamation of *Bengali, Oriya* and *Shadri* languages). The major sources of livelihood for the tea tribes are working as laborers in the tea gardens and also as traditional herbal practitioners (*bej*). The present communication provides results of indigenous uses of phyto-medicines against jaundice used by the tea tribes of the Morigaon district.

2.2 Documentation and Collection of Ethnomedicinal Data

Extensive field surveys conducted in the tea gardens of Morigaon district during June 2016 -September 2017 and maximum information provided by the tea tribes were collected (Figure 1). In total 53 informants were interviewed within the age group of 20-75 years. The

Figure 1. Geographical location of Morigaon district.

Nowgong Girls' College ESTD: 1962 Nagaon :: Assam
C.T.C.
Principal
Nowgong Girls' College
Nagaon :: Assam

information was obtained through semi-structured questionnaires, interviews, consultations and group discussions on the medicinal use of the plants against jaundice and detailed information about mode of preparation (i.e., decoction, infusion, juice or extract, paste, powder and external use) was documented[19,20]. Prior permission was sought from the concerned authorities of the tea gardens for the collection of the ethnomedicinal data along with the plants and also the related plant parts required from the study area. Before proceeding with the interview, consent of the respondents was also obtained to carry out the study. The collected specimens were processed and mounted in a herbarium using convenient techniques and were cross-checked and identified with the help of relevant floras and were matched at the Gauhati University Herbarium and Nowgong College Herbarium and then their identity was confirmed[21,22]. Nomenclatures of plants were updated using The Plant List and the specimens are deposited at Department of Botany, Nowgong College (Nagaon) for future references [23]. All the recorded plant species are presented in tabular format, alongside the family, common names and the ethnomedicinal usage information.

2.3 Quantitative Analysis of Ethnomedicinal Data

An illustrative method of using the frequencies and percentages was used to evaluate the socio-demographic data of the informants. The ethnomedicinal usage of plants was quantitatively accessed using the Fidelity Level (FL), Use Value (UV) and Family Use Value (FUV).

2.3.1 Fidelity Level (FL)

The Fidelity Level (FL) was calculated to determine the percentage of informants who mentioned the uses of certain plant species to treat a particular ailment in the study area.

$$FL\ (\%) = \left(\frac{Ip}{Iu}\right) \times 100$$

Where, Ip is the number of informants who independently claimed the utilization of a plant species for the same major ailment and Iu is the number of informants who mentioned the plant for any major ailment[24,25].

2.3.2 Use Value (UV)

The Use Value (UV) determines the relative importance of plants known in locally. It was calculated using the following formula[26].

$$UV = \frac{\sum Ui}{N}$$

Where, U_i is the number of uses mentioned by each informant for a given species and N is the total number of informants.

2.3.3 Family Use Value (FUV)

The significance of the plant families were identified by calculating the Family Use Value (FUV) using the following formula[27].

$$FUV = \frac{UVs}{Ns}$$

Where, UVs is the use value of the species and Ns is the total number of species within each family.

3. Results and Discussion

3.1 Socio-Demographic Data of the Study

A total of 53 informants have participated in the present study. The age groups of the informants were confined between 20 and 75 years are represented in Table 1.

A total of 53 informants were interviewed and all were indigenous people with ages ranging from 20 years to 75 years (Table 1). They comprised of 73.58% men 26.41% women. A large number of people were in the age of 50-60 years (33.96%) and 40-50 years (24.52%). Most of the people in the study area were laborers (79.24%) and traditional health practitioners (13.2%). Regarding the level of education, 67.92 % were illiterate and 32.07 % were literate.

3.2 Plant Species, Botanical Families, Mode of Remedy Preparation and Quantitative Value

The plant species recorded in the present study are arranged in an alphabetical order and are enumerated

C.T.C.
Principal
Nowgong Girls' College
Nagaon :: Assam
Nowgong Girls' College ESTD: 1962 Nagaon :: Assam

Table 1. Socio-demographic data of the tea tribe informants of Morigaon district, Assam (N=53)

Sl. No.	Variable	Categories	No. of informants	Frequency (%)
1.	Gender	Male	39	73.58 %
		Female	14	26.41 %
2.	Age	20 - 30 years	6	11.32 %
		30 - 40 years	9	16.98 %
		40 - 50 years	13	24.52 %
		50 - 60 years	18	33.96 %
		60 - 75 years	7	13.20 %
3.	Category of the informants	Indigenous people	53	100 %
		Traditional health practitioners	17	13.20 %
		Laborer	32	79.24 %
		Service man	4	7.54 %
4.	Experience of the Traditional Health Practitioner	≤ 1 year	1	1.89 %
		1 - 10 years	4	7.54 %
		10 - 20 years	7	13.20 %
		20 - 30 years	3	5.66 %
		≥ 30 years	2	3.77 %
5.	Literacy rate	Literate	17	32.07 %
		Illiterate	36	67.92 %

along with their correct botanical names, family, parts used, mode of preparation, and route of administration, UV and FL are summarized in Table 2. A total of 39 medicinal plants belonging to 36 genera and 27 families recorded to be used by the tea tribes as a remedy for jaundice in the study area.

The medicinal plant species documented from the study were distributed amongst 27 families and 36 genera. The highest numbers of plants were documented in the family Lamiaceae (5) followed by Leguminosae (3) and Acanthaceae (2), Oxalidaceae (2), Phyllanthaceae (2), Piperaceae (2), Poaceae (2) and Rutaceae (2) shown in Figure 2. Plant parts used by the tea tribes to treat jaundice were mainly aerial part, leaf, stem, bark of stem, fruit, rhizome, root, bark of root and whole plant. The most frequently used plant portion for the traditional preparation was the leaf (35.89%) trailed by fruit (17.94%), stem bark, whole plant (12.82%), aerial part of plant, rhizome, root (5.12%), calyx, flower, seed, stem bark and root bark (2.56%) (Figure 3). There is no specific time to collect the plant materials used for herbal therapy as reported by the informants of the study area. Amongst the 39 medicinal plant species recognized, 33.33 % are herbs followed by shrubs and trees (25.64%) and lastly climbers and under-shrubs (7.69%) (Figure 4).

Several forms of remedial preparation are used by the tea tribes in the study area and the most frequently used preparation was juice or extract with 43.58 % trailed by infusions (20.51 %), paste (15.38%), decoction and powder (7.69%), concoction and garland (5.12%) (Figure 5). The commonly used route of administration was oral (94.87%) followed by external or topical use (2.56 %) and both oral and external use (2.56%).

Most of the plants documented during the field study are wild in nature and are also available in the estates, residences, roadside, river-side and in hills and forest. *Aloe vera, Averrhoa carambola, Cajanas cajan, Curcuma longa, Hibiscus rosa-sinensis, Lawsonia inermis, Mentha arvensis, Ocimum tenuiflorum, Piper nigrum, Saccharum officinarum* are mainly cultivated

Principal
Nowgong Girls' College
Nagaon :: Assam

Nowgong Girls' College ESTD: 1962 Nagaon :: Assam

Table 2. Ethno-medicines used against jaundice by tea tribes of Morigaon district, Assam

Sl. No.	Name of Plant and Collection Number	Family	Local name(s)	Habit	Part(s) used	Mode of prepa-ration(s)	Route of admint-ration	Use Value (UV)	Fidelity Level % (FL)
1.	*Achyranthes aspera* L. RBNG-03	Amaranthaceae	*Ubhotakata* (Ass); *Apamargo* (Ass and TT)	Under-shrub	Stem	Worn as garland (chest length long).	External	0.15	100
2.	*Aegle marmelos* (L.) Correa RBNG-02	Rutaceae	*Bel* (Ass and TT)	Tree	Leaf	Infusion	Oral	0.15	87.5
3.	*Aloe vera* (L.) Burm.f. RBNG-01	Xanthorrhoeceae	*Salkuwori* (Ass); *Ghritokumari* (Ass and TT); *Dahidahiya* (TT)	Herb	Leaf	Juice/ Ex-tract	Oral	0.09	60
4.	*Alstonia scholaris* (L.) R.Br. RBNG-05	Apocynaceae	*Satiana* (Ass and TT); *Rani Gamari* (TT)	Tree	Stem	Powder	Oral	0.15	75
5.	*Argemone mexicana* L. RBNG-25	Papaveraceae	*Siyalkata* (Ass and TT); *Udishmari* (TT)	Herb	Leaf	Juice/ Ex-tract	Oral	0.05	33.3
6.	*Averrhoa carambola* L.RBNG-52	Oxalidaceae	*Kordoi* (Ass and TT)	Tree	Fruit	Juice/Ex-tract	Oral	0.09	57.1
7.	*Azadirachta indica* A. Juss RBNG-20	Meliaceae	*Mohaneem* (Ass); *Neem* (TT)	Tree	Leaf	Paste	Oral	0.11	71.4
8.	*Cajanus cajan* (L.) Millsp. RBNG-09	Leguminosae	*Rahar* (Ass); *Arhar* (TT)	Shrub	Leaf	Juice/Ex-tract	Oral	0.05	66.6
9.	*Cassia fistula* L.RBNG-06	Leguminosae	*Sonaru* (Ass); *Sonari gocho* (TT)	Tree	Seed	Decoction	Oral	0.05	66.6
10.	*Cheilocostus speciosus* (J.Konig) C. Specht RBNG-08	Costaceae	*Jamlakhuti* (Ass); *God* (TT)	Under-shrub	Rhi-zome	Decoction	Oral	0.07	100
11.	*Clerodendrum indicum* (L.) Kuntze RBNG-18	Lamiaceae	*Akal bih* (Ass); *Nagrikhari* (TT)	Shrub	Leaf, Stem	1.Juice/ Extract (leaf) 2. Worn as garland (stem)	Oral and external	0.07	28.5
12.	*Clerodendrum infortunatum* L. RBNG-[illegible]	Lamiaceae	*Bhet-tita* (Ass); *Kumotia* (TT)	Under-shrub	Leaf	Paste	Oral	0.09	100
13.	*Coffea benghalensis* B. Heyne ex schult. RBNG-47	Rubiaceae	*Sagoliphul* (Ass and TT)	Shrub	Root	Powder	Oral	[illegible]	100

C.T.C.
Principal
Nowgong Girls' College
Nagaon :: Assam
Nowgong Girls' College ESTD: 1962 Nagaon :: Assam

14.	*Curcuma longa* L. RBNG-13	Zingiberaceae	*Halodhi* (Ass); *Haldhi* (TT)	Herb	Rhi-zome	Paste or Powder	Oral	0.09	80
15.	*Cynodon dactylon*(L.) Pers. RBNG-21	Poaceae	*Dubori bon* (Ass and TT); *Dub bon* (TT)	Herb	Whole plant	Paste	Oral	0.11	42.8
16.	*Drymaria cordata* (L.) Willd. ex Schult. RBNG-23	Caryo-phyllaceae	*Laijabori* (Ass and TT)	Herb	Whole plant	Infusion	Oral	0.22	90.9
17.	*Ficus racemosa* L. RBNG-19	Moraceae	*Dimoru* (Ass and TT); *Dimri* (TT)	Tree	Fruit	Decoction	Oral	0.05	66.6
18.	*Glycosmis pentaphylla* (Retz.) DC. RBNG-16	Rutaceae	*Chaul-dhowa, Bon nemu* (Ass); *Bon nimbu, Ashhoura* (TT)	Shrub	Leaf	Juice/ Extract	Oral	0.07	75
19.	*Hibiscus sabdariffa* L. RBNG-26	Malvaceae	*Khaseng-tenga, Mesta-tenga* (Ass); *Tengamora* (Ass and TT)	Shrub	Calyx and Fruit	Juice/ Ex-tract	Oral	0.07	75
20.	*Houttuyunia cordata* Thunb. RBNG-29	Saururaceae	*Masundori* (Ass and TT)	Herb	Leaf	Infusion	Oral	0.07	60
21.	*Hydrocotyle sibthorpioides* Lam. RBNG-30	Araliaceae	*Sarumani-muni* (Ass); *Chhoto-manimuni* (TT)	Herb	Whole plant	Juice/Ex-tract	Oral	0.09	55.5
22.	*Justicia adhatoda* L. RBNG-04	Acanthaceae	*Vahak* (Ass); *Vasak, Basanti, Hej* (TT)	Shrub	Leaf	Juice/Ex-tract		0.07	44.4
23.	*Justicia gendarussa* Burm. f. RBNG-32	Acanthaceae	*Jatrasiddhi* (Ass); *Kaliadama, Brindaban* (TT)	Shrub	Leaf	Paste	Oral	0.15	100
24.	*Lawsonia inermis* L. RBNG-34	Lythraceae	*Jetuka* (Ass); *Mehndi* (TT)	Shrub	Root	Con-coction	Oral	0.07	100
25.	*Leucas aspera* (Willd.) RBNG-31	Lamiaceae	*Durun* (Ass and TT)	Herb	Leaf	Juice/ Extract	Oral	0.05	60
26.	*Mangifera indica* L. RBNG-33	Anacardiaceae	*Aam* (Ass and TT)	Tree	Bark of Stem	Paste	Oral	0.07	30.7
27.	*Mentha arvensis* L. RBNG-40	Lamiaceae	*Podina* (Ass); *Pudina* (TT)	Herb	Aerial part	Juice/Ex-tract	Oral	0.05	50
28.	*Ocimum tenuiflorum* L. RBNG-35	Lamiaceae	*Koliyatulosi* (Ass); *Tulsi* (TT)	Shrub	Leaf	Infusion of crushed leaves	Oral	0.13	58.3
29.	*Oxalis corniculata* L.RBNG-43	Oxalidaceae	*Tengesi tenga* (Ass); *Jhunjhuni* (TT)	Herb	Whole Plant	Juice/ Extract	Oral	0.07	44.4
30.	*Passiflora edulis* Sims RBNG-41	Passifloraceae	*Lota-bel* (Ass); *Kointho* (TT)	Climber	Flower and Fruit	Juice/ Extract	Oral	0.09	66.3
31.	*Peperomia pellucida* (L.) Kunth RBNG-36	Piperaceae	*Pananua* (Ass and TT)	Herb	Aerial part	Juice/Ex-tract	Oral	0.02	33.3
32.	*Phyllanthus emblica* L. RBNG-42	Phyllanthaceae	*Amlokhi* (Ass and TT); *Amlokhu* (TT)	Tree	Fruit	Juice/Ex-tract	Oral	0.09	62.4

Principal
Nowgong Girls' College
Nagaon :: Assam

Nowgong Girls' College ESTD 1962 Nagaon :: Assam

33.	*Phyllanthus fraternus* G.L. Webster RBNG-39	Phyllanthaceae	*Mati-amlokhi* (Ass); *Bhui-aaola* (TT)	Herb	Whole Plant	Infusion	Oral	0.11	85.7
34.	*Piper nigrum* L. RBNG-43	Piperaceae	*Jaluk* (Ass); *Gul-morich* (TT)	Climber	Fruit	Concoction	Oral	0.07	44.4
35.	*Plumbago zeylanica* L. RBNG-46	Plumbaginaceae	*Agyasit* (Ass); *Agniboth, Chitamool, Raiputi* (TT)	Shrub	Bark of root	Infusion	Oral	0.07	57.1
36.	*Saccharum officinarum* L. RBNG-48	Poaceae	*Kuhiyar* (Ass and TT)	Herb	Stem	Juice/ Ex-tract	Oral	0.09	100
37.	*Tamarindus indica* L. RBNG-49	Leguminosae	*Teteli* (Ass); *Tetul* (TT)	Tree	Fruit	Infusion	Oral	0.04	66.6
38.	*Tinospora sinensis* (Lour.) Merr. RBNG-24	Menispermaceae	*Amar-lota* (Ass); *Guduchi, Choidoguni, Amar-lot, Gulchhi* (TT)	Clim-ber	Stem	Infusion	Oral	0.13	77.7
39.	*Xylosma longifolia* Clos. RBNG-51	Salicaceae	*Mota-koli* (Ass); *Kataponial* (Ass and TT)	Tree	Leaf	Juice/ Ex-tract	Oral	0.17	69.2

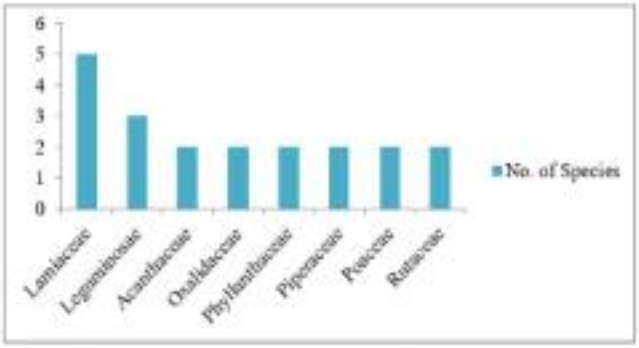

Figure 2. Dominant of the distributed medicinal plants.

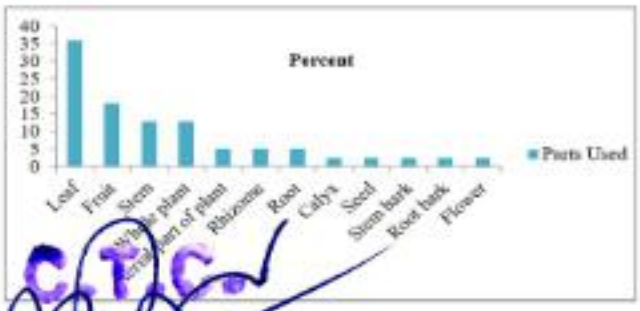

Figure 3. Plant parts used in the study area against jaundice.

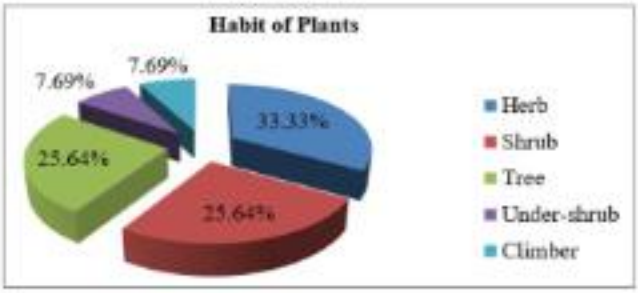

Figure 4. Habit of the plant species recorded in thestudy area.

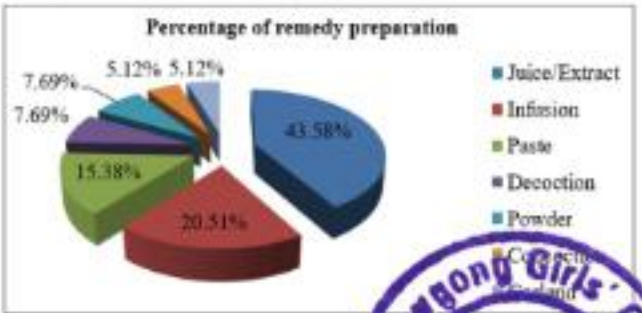

Figure 5. Mode of remedy preparation.

Principal
Nowgong Girls' College
Nagaon :: Assam

Nowgong Girls' College
ESTD: 1962
Nagaon :: Assam

in the study area. During the field study, systematic and proper care was taken in the collection methods.

This is the first quantitative ethnobotanical study conducted in this study area The highest UV ranked the *Drymaria cordata (0.22)* first, followed by *Xylosma longifolia (0.17), Achyranthes aspera, Aegle marmelos, Alstonia scholaris and Justicia gendarussa* (0.15) as second and third respectively. The Family Use Value (FUV) ranged between the lowest values (0.05) and the highest value (0.30). Lamiaceae family (0.30) was the highest FUV trailed by Caryophyllaceae (0.22) and Rutaceae (0.18) shown in Table 3. The high values of UV and FUV can be explained by the fact that these plants are highly used and acknowledged by the majority of the informants in the study area. The Fidelity Level (FL) of the recorded plants have been calculated which showed the highest percentage of 100% for *Achyranthes aspera, Cheilocostus speciosus, Clerodendrum infortunatum, Justicia gendarussa, Lawsonia inermis, Coffea benghalensis* and *Saccharum officinarum* followed by *Drymaria cordata* (90.9%) and *Aegle marmelos* (87.5%).

Table 3. FUV of the plant families calculated from the actual and estimated UV of the plant species

Family	FUV
Acanthaceae	0.15
Amaranthaceae	0.15
Anacardiaceae	0.07
Apocynaceae	0.15
Araliaceae	0.09
Caryophyllaceae	0.22
Costaceae	0.07
Lamiaceae	0.30
Leguminosae	0.12
Lythraceae	0.07
Malvaceae	0.07
Meliaceae	0.11
Menispermaceae	0.13
Moraceae	0.05
Oxalidaceae	0.13
Papaveraceae	0.05
Passifloraceae	0.09
Phyllanthaceae	0.15
Piperaceae	0.05
Plumbaginaceae	0.07
Poaceae	0.16
Rubiaceae	0.05
Rutaceae	0.18
Sa[illegible]ceae	0.16
Sa[illegible]ceae	0.07
Xanthoxylaceae	0.09
Zingiberaceae	0.09

In Morigaon district, jaundice is a common problem among the tea tribes due to their poor food habits, preventive care, and hygiene. They have gained the traditional knowledge on medicinal plants from the elders of their family and the village chiefs by word of mouth. However, there is a threat to the indigenous knowledge due to modernization; the knowledge may eventually be lost following the decease of the elderly and knowledgeable inhabitants of the study area. The documentation of this traditional knowledge is valuable for the indigenous people and their future generations for the wider use of the plants against jaundice. The majority of the informants were males (73.58%) and females (26.41%). Most of the ethno-pharmacological studies confirm that leaves are the major parts used for treating jaundice and resembles the present study[14,28,29]. Most informants preferred to use fresh juice or extract of the plants to treat jaundice. The plants used by the informants are mostly wild in nature (71.8%) while the cultivated plants represent only (28.2%).

3.3 A Brief Review on the Hepato-protective Activity of the Documented Plants of the Study

In-vivo and in-vitro hepatoprotective activity of crude extracts of 29 of the 39 plant species identified in this study have been reported in the literature namely *Achyranthes aspera, Aegle marmelos, Aloe vera, Alstonia scholaris, Argemone mexicana, Averrhoa carambola, Cajanus cajan, Cassia fistula, Cheilocostus speciosus, Clerodendrum infortunatum, Curcuma longa, Cynodon dactylon, Ficus racemosa, Glycosmis pentaphylla, Justicia adhatoda, Justicia gendarussa, Lawsonia inermis, Mentha arvensis, Passiflora edulis, Ocimun tenuiflorum, Oxalis corniculata, Phyllanthus emblica, Phyllanthus fraternus, Piper nigrum, Tinospora*

C.T.C.
Principal
Nowgong Girls' College
Nagaon :: Assam
Nowgong Girls' College ESTD. 1962 Nagaon :: Assam

Table 4. Literature review of hepatoprotective effects of the documented plants of the study area

Name of the species	Hepatoprotective activity
Achyranthes aspera L.	Effect of methanolic extract on rifampicin-induced hepatotoxicity and bi-herbal ethanolic extract against paracetamol induced hepatic damage in albino rats[30, 31]
Aegle marmelos (L.) Correa	Effect of the methanolic extract of leaves in paracetamol intoxicated albino rats[32]
Aloe vera (L.) Burm.f.	Hepatoprotective activity of the gel against paracetamol induced hepatotoxicity in albino rats[33]
Alstonia scholaris (L.) R.Br.	Effect of methanolic extract of stem bark [34]
Argemone mexicana L.	In vivo activity of aerial part extract on CCl_4 induced liver damage in wister rats [35]
Averrhoa carambola L.	Effect against CCl_4 and paracetamol induced liver toxicity[36, 37]
Azadirachta indica A. Juss	Protective effect of leaf extract in rats against paracetamol induced hepatic damages[38]
Cajanas cajan (L.) Huth	Effects on tissue defense system in D-galactosamine induced hepatitis in rats[39, 40]
Cassia fistula L.	Effect of aqueous extract of leaf and stem against CCl_4 induced liver damage in rats[41-43]
Cheilocostus speciosus (J.Konig) C. Specht	Hepatoprotective effect on paracetamol induced liver injury[44]
Clerodendrum indicum (L.) Kuntze	No reference
Clerodendrum infortunatum L.	Potentiality of methanol extract against CCl_4 induced hepatotoxicity in rats[45]
Coffea benghalensis (Roxb. ex. Schult.) J.-F.Leroy	No reference
Curcuma longa L.	Protective effects on $CuSO_4$ induced hepatotoxicity and nephrotoxicity. Immunomodulatory and hepatoprotective properties of aqueous extract against CCl_4 intoxicity in swiss albino mice[46, 47]
Cynodon dactylon (L.) Pers.	Protective effects of aerial plants against CCl_4 induced hepatotoxicity in rats[48]
Drymaria cordata (L.)Willd.ex Schult.	No reference
Ficus racemosa L.	Activity of leaf extract on liver damage in rats caused by CCl_4. And hepatoprotective effects of stem bark in albino rats against CCl_4 hepatic damages[49, 50]
Glycosmis pentaphylla (Retz.) DC.	Activity against paracetamol induced hepatotoxity in swiss albino rats[51]
Hibiscus sabdariffa L.	No reference
Houttuyunia cordata Thunb.	No reference
Hydrocotyle sibthorpioides Lam.	No reference
Justicia adhatoda L.	Hepatotoprotective activity of aqueous, ethanol and methanol extracts against liver injury in albino mice caused by CCl_4[52]
Justicia gendarussa Burm. f.	In vitro hepatoprotective effects of stem against hepatotoxicity induced by CCl_4 in rats[53]
Lawsonia inermis L.	Effect of warm aqueous extract in wister rats in CCl_4 and 2-acetylaminoflourene induced hepatic injury[54, 55]
Leucas aspera (Willd.)	No reference
Mangifera indica L.	No reference
Mentha arvensis L.	Protective effect of leaves against CCl_4 induced liver damages in rat[56]
Momordica charantia L.	Alcoholic effect of leaf extract against paracetamol induced liver damage in rats[57]
Oxalis corniculata L.	Activity of ethanolic extract against paracetamol induced hepatotoxicity in wister rats[58]
Passiflora edulis Sims	Hepatoprotective effect of peel extract of the Passion fruit in albino [illegible]
Phyllanthus amarus Schum. & Thonn.	No reference
Phyllanthus emblica L.	Hepatoprotective effects of ethanol extract[60]

CTTC
Principal
Nowgong Girls' College
Nagaon :: Assam
Nowgong Girls' College ESTD: 1962 Nagaon :: Assam

Phyllanthus fraternus G.L. Webster	Effect of whole plant extracts on liver of *Staphylococcus aureus* intoxicated albino rats [61]
Piper nigrum L.	Effect of methanolic extract against ethanol-CCl_4 hepatotoxicity in wister rats[62]
Plumbago zeylanica L.	Effect on paracetamol induced liver toxicity in rats[63]
Saccharum officinarum L.	Effect of juice in isoniazed induced hepatotoxicity in male albino rats[64]
Tamarindus indica L.	Ameliorating, anti-oxidant and hepatoprotective activity[65,66]
Tinospora sinensis (Lour.) Merr.	Aqueous extract hepatoprotective activity[67]
Xylosma longifolia Clos.	No reference

zeylanica, *Saccharum officinarum*, *Tamarindus indica* and *Tinospora sinensis* (Table 4).

Plant species like *Clerodendrum indicum*, *Drymaria cordata*, *Hibiscus sabdariffa*, *Houttuyunia cordata*, *Hydrocotyle sibthorpioides*, *Leucas aspera*, *Mangifera indica*, *Peperomia pellucida*, *Coffea benghalensis* and *Xylosma longifolia* are needed to analyze their hepatoprotective and other biological properties for development of some novel phyto-therapeutic active compounds.

4. Conclusion

The field studies carried out in the tea gardens of Morigaon district have led to the documentation of ethnomedicinal uses for 39 plant species. The reports provided by the tea tribal people of the study area, certainly increases the validity of the said purpose. From the above results and discussions, the tea tribes of the Morigaon district are still dependent on wild plants to cure jaundice. From the best of our knowledge *Coffea benghalensis* has not been reported earlier as a remedy for jaundice from Northeast India. The most widely used plants against jaundice recorded in this study such as *Drymaria cordata*, *Xylosma longifolia*, *Achyranthes aspera*, *Cheilocostus speciosus*, *Clerodendrum infortunatum*, *Justicia gendarussa*, *Lawsonia inermis*, *Coffea benghalensis*, *Saccharum officinarum* and *Aegle marmelos* and some plant species that have not yet been analyzed for the hepatoprotective properties should be prioritized for further phytochemical and pharmacological studies to identify the unknown compounds and their functional groups. Isolation of the bioactive compounds and elucidation of their chemical structures will help to develop new medicines for the treatment of jaundice in the future.

5. Acknowledgements

We are highly indebted to the tea tribe people of the selected study area for sharing their valuable indigenous knowledge. Prof. D. Borthakur from Department of Molecular Biosciences and Bioengineering, University of Hawai'i at Manoa is highly acknowledged for his invaluable support in the present work. We thank Dr. Smarajit Ojah from the Department of Geography of Nowgong Girls' College (Nagaon) for drawing the Morigaon district geographical map.

6. Conflict of Interests

No conflict of interest.

7. References

1. Grønhaug TE, Glæserud S, Skogsrud M, Ballo N, Bah S, Diallo D, Paulsen BS. Ethnopharmacological survey of six medicinal plants from Mali, West-Africa. Journal of Ethnobiology and Ethnomedicine. 2008; 4:26. https://doi.org/10.1186/1746-4269-4-26. PMid:19111068, PMCid:PMC2633328.
2. Sofowora A. Medicinal Plants and Traditional Medicine in Africa, John Wiley and Sons, New York, USA; 1982.
3. Lucy H, Edgar JD. Medicinal plants: A re-emerging health aid, division of life sciences UNESCO; 1999.
4. Tefera BN, Kim YD. Ethnobotanical study of medicinal plants in the Hawassa Zuria district, Sidama zone, Southern Ethiopia. Journal of Ethnobiology and Ethnomedicine. 2019; 15:25. https://doi.org/10.1186/s13002-019-0302-7. PMid:30926126296, PMCid:PMC6534827.

Principal
Nowgong Girls' College
Nagaon :: Assam
Nowgong Girls' College ESTD: 1962 Nagaon :: Assam

5. Karunamoorthi K, Tsehaye E. Ethnomedicinal knowledge, belief and self-reported practice of local inhabitants on traditional antimalarial plants and phytotherapy. J. Ethnopharmacol. 2012; 141(1):143-150. https://doi.org/10.1016/j.jep.2012.02.012, https://doi.org/10.1016/j.jep.2012.02.022.
6. Balunas MJ, Kinghorn AD. Drug discovery from medicinal plants. Life Sci. 2005; 78:431-441. https://doi.org/10.1016/j.lfs.2005.09.012. PMid:16198377.
7. Maikhuri RK, Gangwar AK. Ethnobiological notes on the Khasi and Garo tribes of Meghalaya, Northeast India. Econ. Bot. 1993; 47:345. https://doi.org/10.1007/BF02907348.
8. Prakash JW, Anpin Raja RD, Asbin Anderson N, Williams C, Regini GS, Bensar K, Rajeev R, Kiruba S, Jeeva S, Das SSM. Ethnomedicinal plants used by Kani tribes of Agasthiyarmalai biosphere reserve, southern Western Ghats. Indian J. Traditional Knowledge. 2008; 7(3):410-413.
9. Timmermans K. Intellectual property right and traditional medicine: policy dilemmas at the interface. Soc. Sci. Med. 2003; 57(4):745-756. https://doi.org/10.1016/S0277-9536(02)00425-2.
10. Dutta BK, Dutta PK. Potential of ethnobotanical studies in North East India: An overview. Indian J. Traditional Knowledge. 2005; 4(1):7-14.
11. Mao AA, Roy DK. Ethnobotanical studies in Northeast India: A review. In: Jain AK ed. Indian Ethnobotany: Emerging trends. Scientific publisher, India; 2016. p. 99-112.
12. Roche SP, Kobos R. Jaundice in the adult patient. Am. Fam. Physician. 2004; 69(2):299-304.
13. Abbas MW, Shamshad T, Ashraf MA, Javaid R. Jaundice: a basic review. Int. J. Res. Med. Sci. 2016; 4:1313-1319. https://doi.org/10.18203/2320-6012.ijrms20161196.
14. Sharma J, Gairola S, Gaur RD, Painuli RM. The treatment of jaundice with medicinal plants in indigenous communities of the Sub-Himalayan region of Uttarakhand, India. J. Ethnopharmacol. 2012; 143:262-291. https://doi.org/10.1016/j.jep.2012.06.034. PMid:22759701.
15. Handa SS, Sharma A, Chakraborty K. Natural products as liver protecting drugs. Fitoterapia.1986; 57:307-351.
16. Narzary H, Brahma S, Basumatary S. Wild edible vegetables consumed by Bodo Tribe of Kokrajhar district (Assam), North-East India. Arch. Appl. Sci. Res. 2013; 5:182-190.
17. Das RK. Plantation Labour in India. Prabashi Press, India; 1931.
18. Griffiths P. The history of Indian tea industry. Weidenfield and Nicolson, London; 1967.
19. Martin GJ. Ethnobotany. A "people and plants" conservation manual. World Wide Fund for Nature, Chapman and Hall, London; 1995.
20. [illegible] K. Methods and approaches in ethnobotany. Deep Publication, New Delhi; 1989.
21. Kanjilal UC, Das A, Kanjilal PC, De RN. Flora of Assam, Vol 1-5. Government of Assam, Shillong; 1934-1940.
22. Jain SK, Rao RR. A handbook of field and herbarium technique. Today and Tomorrow Publication, New Delhi; 1977.
23. The Plant List (The Plant List Version 1.1, 2013) Accessed in 1st April 2018. www.theplantlist.org.
24. Friedman J, Yaniv Z, Dafni A, Palewitch D. A preliminary classification of the healing potential of medicinal plants, based on the rational analysis of ethnopharmacological field survey among Bedouins in Negev Desert, Israel. J. Ethnopharmacol.1986; 16:275-287. https://doi.org/10.1016/0378-8741(86)90094-2.
25. Alexiades MN, Sheldon JW. Selected guidelines for ethnobotanical research: A field manual. The New York Botanical garden, Boranx, New York. 1996; p. 99-133.
26. Tardio J, Pardo-de-Santayana M. Cultural importance indices: a comparative analysis bases on the useful wild plants of southern Cantabria (Northern Spain). Econ. Bot. 2008; 62:24-39. https://doi.org/10.1007/s12231-007-9004-5.
27. Zougagh S, Belghiti A, Rochd T et al. Medicinal and aromatic plants used in traditional treatment of the oral pathology: The ethnobotanical survey in the economic capital Casablance, Morocco (North Africa). Natural Products and Bioprospecting. 2019; 9:35. https://doi.org/10.1007/s13659-018-0194-6. PMid:30484065, PMCid:PMC6328421.
28. Bhattacharyya R, Medhi KK, Borkataki S. Ethnomedicinal plants used against jaundice by the tea tribes of Nagaon district, Assam. Ethnobotany. 2016; 27:36-42.
29. Maruthupandian A, Mohan VR, Kottaimuthu R. Ethnomedicinal plants used for the treatment of diabetes and Jaundice by Palliyar tribals in Sirumalai hills, Western Ghats, Tamilnadu, India. Indian Journal of Natural Products and Resources. 2011; 2(4):493-497.
30. Bafna A, Mishra SH. Effect of methanol of *Achyranthes aspera* Linn. on rifampicin-induced hepatotoxicity in rats. Ars. Pharmaceutica. 2004; 45(4): 343-351 (2004).
31. Krishna Chaitanya DA, Reddy Challa S, Reddy AM. Hepatoprotective effect of biherbalethanolic extract against paracetamol induced hepatic damage in albino rats. J. Ayurveda Integr. Med. 2012; 3(4):198-203. https://doi.org/10.4103/0975-9476.104436. PMid:23326091, PMCid:PMC3545240.
32. Ramamurthy V, Raveendran S, Kumar HVA, Hepatoprotective activity of the methanolic extract of Aegle marmelos leaves in paracetamol intoxicated albino rats. Int. J. Universal Pharmacy and Bio. Sci. 2014; 3(2):1-10.
33. Nayak V, Gincy TB, Prakash M, Joshi C, Rao S, Somayaji SN. Hepatoprotective activity of Aloe vera gel against paracetamol induced hepatotoxicity in [illegible]. Asian J. Phar. Biol. Res. 2011; 1(2):94-98.
34. Kumar A, Khan MA, Saxena [illegible] Singh RB. Hepatoprotective activity of methanolic extract of stem of Alstonia scholaris (L.)R. Br. Am. J. Pharma. Tech. Res. 2012; 2:2.

CTC
Principal
Nowgong Girls' College
Nagaon :: Assam
Nowgong Girls' College ESTD: 1962 Nagaon :: Assam

35. Adam SIY, Idris IA, Abdelgadir EH, Ahmed RH, Kamal EE. Evaluation of hepatoprotective activity of Argemone mexicana aerial part extract on CCl4 induced liver damage in wister rats. British Journal of Pharmacology and Toxicology.2011; 2(5):251-256.
36. Ajeem AK, Mathew M, Nair C and Dilip C. Hepatoprotective effect of *Averrhoa carambola* fruit extract on carbon tetrachloride induced hepatotoxicity in mice. Asian Pacific Journal of Tropical Medicine. 2012; 3(8):610-613. https://doi.org/10.1016/S1995-7645(10)60148-4.
37. Kumar GR, Prema P, Gupta P. Hepatoprotective activity of *Averrhoa carambola* against paracetamol induced liver toxicity in mice. International Journal of Botany Studies. 2016; 1(7):4-6.
38. Chattopadhyay R, Bandyopadhyay M. Possible mechanism of hepatoprotective activity of Azadirachta indica leaf extract against paracetamol induced hepatic damage in rats: Part III. Indian J. Pharmacol. 2005; 37:184-185. https://doi.org/10.4103/0253-7613.16218.
39. Akinloye OA, Olaniyi MO. Hepato-protective effect of Cajanus cajan on tissue defense system in D-galactosamine-induced hepatitis in rats. Turk J. Biochem. 2011; 36:237-241.
40. Gogoi JC, Mohanta D, Borah PK. Hepatoprotective Activity of *Averrhoa carambola*, *Cajanus cajan* and *Paederia foetida* against Acetaminophen and D-Galactosamine induced hepatotoxicity in rats. Journal of Pharmaceutical Research. 2010; 9(2):76-80. https://doi.org/10.18579/jpcrkc/2010/9/2/79491.
41. Hui Mei L, Hsien Chun T, Chau Jong W, Jin-Jin L, Chia Wen L, Fen-Pi C. Hepatoprotective effects of *Cassia fistula* Linn extract against CCl4 induced oxidative damage in rats. Chem. Biol. Interact. 2008; 171:283-293. https://doi.org/10.1016/j.cbi.2007.08.008. PMid:18045581.
42. Wasu SJ, Muley BP. Hepatotective effect of *Cassia fistula*. Ethnobotanical Leaflets. 2009; 13:910-916.
43. Chaudhari NB, Chittam KP, Patil VR. Hepatoprotective activity of *Cassia fistula* seeds against paracetamol-induced hepatic injury in rats. Arch. Pharm. Sci. Res. 2009; 1:218-221.
44. AlSaadi BH, AlHarbi SH, Ibrahim SRM, El-Kholy AA, El-Agamy DS, Mohamed GA. Hepatoprotective activity of Costusspeciosus (koen. Ex. Retz.) against paracetamol-induced liver injury in mice. Afr. J. Tradit. Complement Altern. Med. 2018; 15(2):35-41. https://doi.org/10.21010/ajtcamv15i2.5, https://doi.org/10.21010/ajtcam.v15i2.5.
45. Sannigrahi S, Mazumder UK, Pal D, Mishra SL. Hepatoprotective potential of methanol extract of *Clerodendrum infortunatum* Linn. against CCl4 induced hepatotoxicity in rats. Phcog. Mag. 2008; 5(20):390-395.
46. Sengupta A, Ghosh M, Chakraborty B. Hepatoprotective and immunomodulatory properties of aqueous extract of *Curculigo orchioides* in carbon tetrachloride intoxicated swiss albino mice. Asian Pac. J. Trop. Biomed. 2011; 1(3):193-199. https://doi.org/10.1016/S2221-1691(11)60026-9.
47. Hashish EA, Elgami SA. Hepatoprotective and nephroprotective effect of Curcumin against copper toxicity in rats. Indian J. Chin. Biochem. 2016; 31(3):270-277. https://doi.org/10.1007/s12291-015-0527-8. PMid:27382197, PMCid:PMC4910845.
48. Surendra V, Prakash T, Sharma UR, Goli D, Dayalal S, Kotresha F. Hepatoprotective activity of aerial plants of *Cynodon dactylon* against CC14-induced hepatotoxicity in rats. J. Pharmacogn. Mag. 2008; 4:195-201.
49. Mandal SC, Maity TK, Das J, Pal M, Saha BP. Hepatoprotective activity of *Ficus racemosa* leaf extract on liver damage caused by carbon tetrachloride in rats. Phytother. Res. 1999; 13(5):430-432. https://doi.org/10.1002/(SICI)1099-1573(199908/09)13:5<430::AID-PTR456>3.0.CO;2-G.
50. Ahmed F, Urooj A. Hepatoprotective effects of *Ficus racemosa* stem bark against carbon tetrachloride induced hepatic damage in albino rats. Pharmaceutical Biology. 2010; 48(2):210-216. https://doi.org/10.3109/13880200903081788. PMid: 20645843.
51. Nayak SS, Jain R, Sahoo AK, Hepatoprotective activity of *Glycosmis pentaphylla* against paracetamol-induced hepatotoxicity in swiss albino mice. Pharma Biol. 2011; 49(2):111-117. https://doi.org/10.3109/13880209.2010.501084. PMid:20942640.
52. Afjal U, Gulfraz M, Hussain SS, Malix F. Hepatoprotective effects of *Justicia adahtoda* L. induced liver injury in Swiss albino mice. African Journal of Pharmacy and Pharmacology. 2013; 7:8-14. https://doi.org/10.5897/AJPP12.501.
53. Krishna KL, Mehta TA, Patel JA. In vitro hepatoprotective activity of Justicia gendarussa stem on isolated rat hepatocytes. Pharmacology Online. 2010; 2:9-13.
54. Hossain MC, Himangshu S, Maji, Chakraborty P. Hepatoprotective activity of *Lawsonia inermis* Linn. of warm aqueous extract in carbon tetrachloride induced hepatic injury in wister rats. Asian Journal of Pharmaceutical and Clinical Research.2011; 4:3.
55. Kumar M, Kaur P, Chandel M, Singh AP, Jain A, Kaur S. Antioxidant and hepatoprotective potential of *Lawsonia inermis* L. leaves against 2-acetylaminoflourene induced hepatic damage in male wister rats. BMC Complement Altern. Med. 2017; 17:56. https://doi.org/10.1186/s12906-017-1567-9. PMid:28100199, PMCid:PMC5242058.
56. Patil K, Mall A. Hepatoprotective activity of *Mentha arvensis* Linn. leaves against CCl4 induced liver damage in rats. Asian Pacific Journal of Tropical Disease. 2012; 2(1):223-226. https://doi.org/10.1016/S2222-1808(12)60156-X.
57. Sahu K, Das S.Hepatoprotective activity of Ocimum sanctum alcoholic leaf extract against paracetamol-induced liver damage in albino rats. Pharmacognosy Res. 2011; 3:13-18. https://doi.org/10.4103/0974-8490.79110. PMid:21731390, PMCid:PMC3119265.

GTC
Principal
Nowgong Girls' College
Nagaon :: Assam
Nowgong Girls College ESTD: 1962 Nagaon :: Assam

58. Sreejith G, Jayshree M, Latha PG, Suja SR, Shymal S, Shine VJ, Anuja G, Sini S, Shikha P, Krishnakumar NM, Vilash V, Shoumya S, Rajasekharan S. Hepatoprotective activity of *Oxalis corniculata* L. ethanolic extract against paracetamol induced hepatocity in wister rats and invite antioxidant effects. Indian J. Exp. Biol. 2014; 52(2):147-152.
59. Nerdy N, Ritarwan K. Hepatoprotective activity and Nephroprotective activity of peel extract from three varieties of the passion fruit (Passiflora sp.) in the albino rat. Open Access Maced. J. Med. Sci. 2019; 7(4):536-542. https://doi.org/10.3889/oamjms.2019.153. PMid:30894908, PMCid:PMC6420947.
60. Pramyothin P, Samosorn P, Poungshompoo S, Chaichantipyuth C. The protective effects of *Phyllanthus emblica* Linn. extract on ethanol induced rat hepatic injury. J. Ethnopharmacol. 2006; 107:361-364. https://doi.org/10.1016/j.jep.2006.03.035. PMid:16750340.
61. Ramamurthy V, Abarna T. Hepatoprotective Activity of *Phyllanthus niruri* whole plant extracts against *Staphylococcus aureus* intoxicated Albino Rats. Global J. *Biol Agricul.* Health Sci. 2014; 3(3):256-260.
62. Nirwane AM, Bapat AR. Effect of methanolic extract of *Piper nigrum* fruits in ethanol-CCl4 induced hepatotoxicity in wistar rats. Der. Pharmacia Lettre. 2012; 4:795-802.
63. Kanchana N, Sadiq AM. Hepatoprotective effect of *Plumbago zeylanica* on paracetamol induced liver toxicity in rats. Int. J. Pharm Sci. 2011; 3:32-39.
64. Khan SW, Tahir M, Lone KP, Munir B, Latif W. Protective effect of *Saccharum officinarum* L. (sugarcane) juice on isonised induced hepatotoxicity in male albino mice. J. Ayub. Med. Coll. Abbottabad. 2015; 27(2):346-350.
65. Amir M, Khan MA, Ahmed S, Akhter M, Mujeeb M, Ahmed A. Ameliorating effects of *Tamarindus indica* fruits extract on anti-tubercular drugs induced liver toxicity in rats. Nat. Prod. Res. 2015; 30(6):715-719. https://doi.org/10.1080/14786419.2015.1039001. PMid: 25978515.
66. Rodriguez Amado JR, Lafourcade-Prada A, Escalona-Arranz JC, Peraz-Roses R, Morris-Quevedo H, Keita H. Antioxidant and hepatoprotective activity of a new tablet formulation from *Tamarindus indica* L. Evid. Based Complement Alternat. Med. 2016; 7. https://doi.org/10.1155/2016/3918219. PMid:27143986, PMCid:PMC4838804.
67. Kumar V, Modi VK, Saxena KK. Exploration of hepatoprotective activity of aqueous extract of *Tinospora cordifolia*- an experimental study. Asian J. Pharm. Clin. Res. 2013; 6(1):87-91.

C.T.C.
Principal
Nowgong Girls' College
Nagaon :: Assam

Nowgong Girls' College ESTD: 1962 Nagaon :: Assam

IJPSR (2020), Volume 11, Issue 5 (Research Article)

INTERNATIONAL JOURNAL OF PHARMACEUTICAL SCIENCES AND RESEARCH

Received on 03 July 2019; received in revised form, 22 October 2019; accepted, 08 February 2020; published 01 May 2020

PHYTOCHEMICAL ANALYSIS OF LEAVES OF *XYLOSMA LONGIFOLIA* CLOS.: A PLANT OF ETHNOMEDICINAL IMPORTANCE

Rakhi Bhattacharyya [1], Jayanta Sarmah Boruah [2], Krishna Kanta Medhi [*1] and Sarat Borkataki [1]

Department of Botany [1], Nowgong College, Nagaon - 782001, Assam, India.
Material Nanochemistry Laboratory [2], Physical Sciences Division, Institute of Advanced Study in Science and Technology, Paschim Boragaon, Guwahati - 781035, Assam, India.

Keywords:

Xylosma longifolia Clos., Preliminary screening, Quantitative determination, FT-IR, GC-MS analysis

Correspondence to Author:
Dr. Krishna Kanta Medhi

Associate Professor,
Department of Botany,
Nowgong College, Nagaon - 782001, Assam, India.

E-mail: medhikrishnc@gmail.com

ABSTRACT: The present study deals with the phytochemical study of leaves of *Xylosma longifolia* Clos. It belongs to the family Flacourtiaceae and is commonly known as 'Long leaved xylosma', whereas the plant is locally known as '*Kataponial*' in Assam. *Xylosma longifolia* is an important ethnomedicinal plant used in the North-eastern region of India. The aim of the study is to investigate the bioactive compounds present and to evaluate the significance of the therapeutic and pharmacological uses of the phytoconstituents. All the standard phytochemical and spectroscopic procedures were followed for the detection and estimation of the phytoconstituents. The leaves of *Xylosma longifolia* were collected for the preparation of 95% methanol extract. Preliminary phytochemical screening of the methanol extract of *Xylosma longifolia* reveals the occurrence of several secondary metabolites like alkaloids, flavonoids, phenols, tannins, terpenoids and saponins. The quantitative phytochemical analysis exhibited the presence of alkaloids, flavonoids and phenols in considerable quantity. The presence of O-H stretch, C-O stretch, C-H stretch, C-H bend, C=C stretch, N-H stretch and C=O stretch were confirmed through FT-IR analysis. Several major and minor bioactive compounds were identified through GC-MS analysis. From this study, it can be concluded that the ethnomedicinal plant *Xylosma longifolia* contains various bioactive compounds. Further phytochemical and pharmacological studies are an urgent need for the isolation and discovery of some novel drugs to cure several disorders.

INTRODUCTION: Medicinal plants are the mainstay of every traditional or folk medicine. From the beginning of human history, people are exploring plant species in search of therapeutic properties and management of a wide range of infections and ailments [1, 2]. About 350,000 higher plants are estimated to exist, among which very less number of medicinal plants has been studied scientifically [3, 4].

The various parts of medicinal plants like bark, leaves, flowers, fruits, stem, roots, and even the whole plant are used in the treatment of an illness are a rich source of several biologically active components such as alkaloids, flavonoids, phenols, saponins, steroids, tannins and terpenoids [5, 6]. The study of phytochemicals is very important for finding out new sources of ingredients and also for the discovery of some new potential compounds [7].

Xylosma longifolia is a small sized tree belongs to the family Flacourtiaceae and is distributed throughout in China, Northeast India, Pakistan, sub-tropical Himalaya and Vietnam [8-11]. The leaf and stem bark of the plant is known to have important therapeutic uses and are extensively used

QUICK RESPONSE CODE

DOI: 10.13040/IJPSR.0975-8232.11(5).2065-74

This article can be accessed online on www.ijpsr.com

DOI link: http://dx.doi.org/10.13040/IJPSR.0975-8232.11(5).2065-74

Nowgong Girls' College Principal
Nowgong Girls' College Nagaon :: Assam
Nowgong Girls' College ESTD. 1960 Nagaon :: Assam

for several purposes in the indigenous medicinal system. The plant is highly prescribed for several disorders in the indigenous medicinal system in Assam and Manipur. The plant has been reported for intoxication, liver ailments, ringworm, piles, stomach pain, scabies, acne, gastritis, dysentery, killing lice, dizziness, hoarseness, regulation of blood circulation, insomnia, restlessness, cough, kidney stone, physical injuries, anxiety and also exhibit antispasmodic, anti-oxidant, antifungal or anti-dermatophytic and anti-tubercular properties [9,10, 12-23].

The aim of the study is to investigate the bioactive compounds present in *Xylosma longifolia* and to evaluate the significance of the therapeutic and pharmacological uses of the phytoconstituents present in the plant.

MATERIALS AND METHODS:

Collection of Plant Material: The leaves of *Xylosma longifolia* were collected from different parts of Nagaon district of Assam. The collected plant material of *Xylosma longifolia* was authenticated by the Department of Botany, Nowgong College, Nagaon. The voucher specimen (RBNG-51) in the form of herbarium is maintained (using standard method) in the Botany Department of Nowgong College for future references [24].

Chemicals: In the present study, all the chemicals including the solvents were of analytical grade and are purchased from Sigma Chemical Co. (USA) and Merck Chemical Supplier (India).

Preparation of the Extract: The collected leaves of the plant were washed properly. The materials are chopped and dried under shade at room temperature until it is dried completely. The dried samples were powdered using a clean and sterile electric grinder 500 gm of powdered plant material was placed in a conical glass percolator. A sufficient quantity of 95% methanol is added into the percolator so as to allow the powdered plant sample to become thoroughly soaked. After 24 h the percolate was filtered using Whatman's filter paper and the extraction procedure is repeated three times. The combined methanol filtrates were concentrated in the rotary evaporator and the extract was calculated for the extractive value. The concentrated plant samples were transferred into an airtight glass container and stored at the Department of Botany, Nowgong College, Nagaon, Assam, for further analysis [25].

Preliminary Phytochemical Screening: The methanol extract of *Xylosma longifolia* was subjected to phytochemical analysis to identify the occurrence of alkaloids, flavonoids, phenols, tannins, saponins, steroids, and terpenoids. The existence of the bioactive compounds was determined using standard methods [26-28].

Test for Alkaloids: Mayer's Test: To 1.0 ml of the extract few drops of Mayer's reagent were added and the formation of a white creamy precipitate indicates the occurrence of alkaloids.

Dragendorff's Test: About 1.0 ml of the filtrate was treated with Dragendorff's reagent and the formation of an orange-reddish precipitate indicates the presence of alkaloids.

Test for Flavonoids:

Zinc-Hydrochloride Reduction Test: The filtrate was treated with a mixture of zinc dust followed by concentrated hydrochloric acid. The appearance of a red color indicates the presence of flavonoids.

Shinoda Test: The extract solution was treated with small pieces of magnesium ribbon followed by pouring concentrated hydrochloric acid dropwise and the formation of pink, crimson red or green color indicates the occurrence of flavonoids.

Test for Phenols:

Ferric-Chloride ($FeCl_3$) Test: The extract solution gives blue-green color with the addition of $FeCl_3$ droplets indicates the presence of phenols.

Shinoda Test: To 1.0 ml of the extract solution few fragments of Magnesium ribbons were added and followed by drops of concentrated hydrochloric acid. The appearance of yellowish color indicates the presence of phenols.

Test for Saponins: Foam Test: To 5.0 ml of the extract solution a little quantity of distilled water was added and shaken vigorously. Development of foam indicates the presence of saponins.

Test for Tannins:

Ferric-Chloride ($FeCl_3$) Test: The filtrate was treated with $FeCl_3$ and the formation of dark green color precipitate indicates the presence of tannins.

CTC
Principal
Nowgong Girls' College
Nagaon :: Assam
Nowgong Girls' College
ESTD: 1962
Nagaon :: Assam

Gelatin Test: The extract was dissolved in distilled water and 1% solution of gelatin containing 10% sodium chloride was added to it. The appearance of white precipitates indicates the occurrence of phenols.

Test for Steroids and Terpenoids:
Salkowski's Test: To the extract solutions few drops of chloroform and concentrated sulphuric acid were added. Appearance of red color in lower layer indicates the occurrence of steroids whereas yellow color indicates the presence of terpenoids.

Quantitative Analysis:
Estimation of Alkaloid Content: 1.0 mg of the plant extract was dissolved in dimethyl sulphoxide. Followed by the addition of 1.0 ml of 2N hydrochloric acid and then filtered. The reaction mixture was transferred into a separating funnel where 5.0 ml of bromocresol-green solution and 5.0 ml phosphate buffer were added and followed by the addition of chloroform and was shaken vigorously and was collected in a volumetric flask and diluted to the volume with chloroform.

The absorbance of the resulting test and standard solutions were determined at 470 nm against the reagent blank using a UV/Visible spectrophotometer. The total alkaloid content was expressed as mg of atropine equivalents (AE) of the extract [29].

Estimation of Flavonoid Content: The total flavonoid content was measured by the $AlCl_3$ colorimetric assay. To 1.0 ml of the extract 4 ml distilled water was added. To the reaction mixture, 0.30 ml of 5% sodium nitrite was added. And after 5 minutes, it was followed by the addition of 0.30 ml 10% aluminum chloride and after 5 min 2.0 ml of sodium hydroxide (1M) was treated. The reaction mixture was diluted to 10 ml with distilled water. The absorbance of the resulting test solution was determined at 510 nm against the reagent blank using a UV/Visible spectrophotometer. The total flavonoid content was expressed as mg of quercetin equivalents (QE) of the extract [30].

Estimation of Phenol Content: The total phenolic content was measured by the Folin-Ciocalteu assay method. 1.0 ml of the plant extract was mixed with 9.0 ml of distilled water and was followed by treating of 1.0 ml of Folin-Ciocalteu phenol reagent and was shaken properly. After 3 min, 2.0 ml of 20% sodium carbonate solution was added thoroughly. The absorbance of the resulting test solution was determined at 650 nm against the reagent blank using a UV/Visible spectrophotometer after 90 min. The total phenolic content was expressed as mg of catechol equivalents (CE) of the extract [31, 32].

Analysis by Fourier-Transform Infrared Spectroscopy (FT-IR): FT-IR is used to detect the functional group of the phyto-components present in *Xylosma longifolia*. The absorption spectra of methanol extracts were measured between 4000 and 500 cm^{-1} on Alpha FT-IR instrument from Bruker Optics (OPUS 7.5 software) at Department of Chemistry, Nowgong College, Nagaon, Assam.

Analysis by Gas Chromatography-Mass Spectroscopy (GC-MS): The methanol extract of *Xylosma longifolia* was analyzed through GC-MS, performed at Biotech-Park, IIT Campus, Guwahati in Clarus 680 GC & Clarus 600C MS PerkinElmer, USA; with Liquid Autosampler (Turbo mass software). The stationary phase used in a capillary column of 60 metre in length, 0.25 mm diameter and 0.25 µm film thickness having a phase of 5% diphenyl 95% dimethyl polysiloxane (low bleed). Helium gas (99.99%) was used as carrier gas (*i.e.* mobile phase) at a flow rate of 1.0 ml/min. 2.0 µl of the sample was injected in the GCMS through auto-sampler in split mode (split ratio 10:1). Injector temperature was 280 °C and the ion-source temperature was 180 °C. The oven temperature was programmed at 60 °C (for 3 min), with an increase at the rate 5 °C/min to 200 °C (hold for 3 min) and finally an increase at the rate 6 °C/min to 300 °C (hold for 10 min).

The total run time is 51.83 min. Mass Spectra was taken in Electron Impact positive (EI+) mode at 70 eV. A solvent delay of 8 min was there for MS scan. Mass range i.e. m/z range is 40-600 amu.

Identification of the Compounds: Mass spectra were developed with the help of NIST National Institute of Standards and Technology) library 2008. Spectrum of the unknown was compared with the patterns of the mass spectra and retention indices of the known patterns in the databases of NIST library 2008.

Principal
Nowgong Girls' College
Nagaon :: Assam

Statistical Analysis: The experiments were performed three times and the data were reported as the mean ± SD (Standard deviation) of three measurements.

RESULTS AND DISCUSSION: In the following sub-sections, the results obtained from extraction, preliminary phytochemical screening, quantitative determination, FT-IR and GC-MS analysis are presented.

Extractive Value: The color and extractive value of the methanol extract of *Xylosma longifolia* is given in **Table 1**.

TABLE 1: PERCENTAGE YIELD OF METHANOL EXTRACT OF LEAVES OF *XYLOSMA LONGIFOLIA*

Solvent	Part	Color of extract	Yield (% w/w)
Methanol	Leaf	Blackish	3.8

Preliminary Phytochemical Analysis: The preliminary phytochemical analysis of the methanolic extract of leaves of *Xylosma longifolia* showed the presence of secondary metabolites like alkaloids, flavonoids, phenols, tannins, saponins, and terpenoids, whereas, steroids are found to absent **Table 2**.

TABLE 2: PRELIMINARY PHYTOCHEMICAL ANALYSIS OF METHANOL EXTRACT OF LEAVES OF *XYLOSMA LONGIFOLIA*

S. no.	Phytochemicals	Test	Occurrence
1	Alkaloids	Mayer' Test	+
		Dragendorff's Test	+
2	Flavonoids	Zinc-Chloride Test	+
		Shinoda Test	+
3	Phenols	Ferric-Chloride Test	+
		Shinoda Test	-
4	Tannins	Ferric-Chloride Test	-
		Gelatin Test	+
5	Saponins	Foam Test	+
6	Terpenoids	Salkowski's Test	+
7	Steroids	Salkowski's Test	-

+ = Presence of phytoconstituents; − = Absence of phytoconstituents

Quantitative Analysis: From the quantitative analysis of methanol extract of *Xylosma longifolia* the total alkaloid content (44.2 ± 0.8 mg AE/g) was the highest followed by the total phenol content (42.9 ± 2.43 mg CE/g) and total flavonoid content (32.8 ± 0.2 mg QE/g) **Table 3**.

TABLE 3: QUANTITATIVE ESTIMATION OF ALKALOID, FLAVONOID AND PHENOL OF LEAVES OF *XYLOSMA LONGIFOLIA*

Plant name	Total alkaloid content	Total flavonoid content	Total phenol content
Xylosma longifolia	44.2 ± 0.8 mg AE/g	32.8 ± 0.2 mg QE/g	42.9 ± 2.43 mg CE/g

FT-IR Analysis: The IR spectroscopy of *Xylosma longifolia* indicated the occurrence of alcohols, alkanes, alkenes, amines, amides, carbohydrates, carboxylic acid, esters, ethers, and phenols. A broad strong peak at around 3315 cm^{-1} indicates the presence of O-H stretching vibration. N-H stretching vibration may also be present in the system which may be overlapped with the O-H stretching band. Two strong peaks around 2920 cm^{-1} and 2810 cm^{-1} may be assigned to the C-H asymmetric and symmetric stretching vibration respectively. The strong peak near 1665 cm^{-1} indicates the occurrence of C=O stretching vibration.

However, the wavenumber at 1440 cm^{-1} indicated the existence of a C-H bend. The peak obtained at around 1410 cm^{-1} indicates C=C stretching vibration. The strong peak obtained at 1020 cm^{-1} with a shoulder peak near 1120 cm^{-1} indicated the presence of the C-O stretching vibration. The FTIR spectrum of methanol extract of *Xylosma longifolia* is presented in **Table 4** and **Fig. 1**.

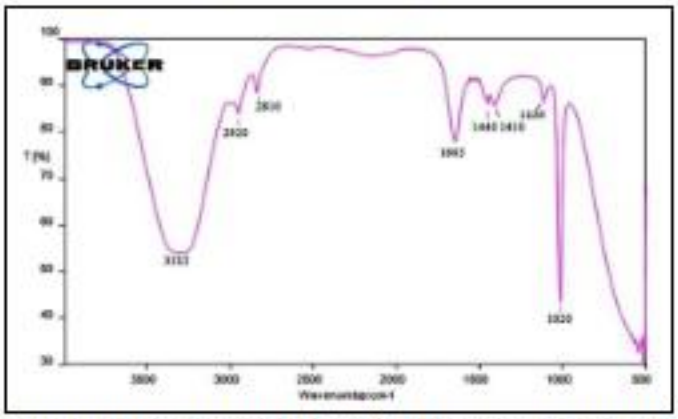

FIG. 1: FTIR SPECTRUM OF METHANOL EXTRACT OF LEAVES OF *XYLOSMA LONGIFOLIA*

The IR spectrum of *Xylosma longifolia* found to have broadband at 3315 cm^{-1} was indicative of O-H stretch which revealed the presence of flavonoids and phenols. The occurrence of phenols is also due to the C-O stretch at 1120 cm^{-1} and 1020 cm^{-1}.

Principal
Nowgong Girls' College
Nagaon :: Assam
Nowgong Girls' College ESTD. 1962 Nagaon :: Assam

The ester peak for C=O at 1665 cm^{-1} and C-O stretch at 1120 cm^{-1} and 1020 cm^{-1} were due to the presence of terpenoids and steroids. The N-H stretch at 3315 cm^{-1} revealed the occurrence of alkaloids. The terpenes were present with C-H stretch at 2920 cm^{-1} and 2810 cm^{-1}, C-H bend at 1440 cm^{-1} and C=C stretch at 1410 cm^{-1}. The presence of carbohydrates is considered due to the O-H stretch at 3315 cm^{-1} [2, 33].

TABLE 4: FTIR SPECTRAL WAVE-NUMBER VALUES AND FUNCTIONAL GROUPS OBTAINED FROM THE LEAVES OF *XYLOSMA LONGIFOLIA*

S. no.	Functional groups	Vibrations	Peaks (cm^{-1})
1	Alcohols	O-H stretch	3315
		C-O stretch	1120, 1020
2	Alkanes	C-H stretch	2920, 2810
		C-H bend	1440
3	Alkenes	C=C stretch	1410
4	Amines	N-H stretch	3315
5	Amides	N-H stretch	3315
		C=O stretch	1665
6	Carbohydrates	O-H stretch	3315
7	Carboxylic acid	O-H stretch	3315
		C=O stretch	1665
8	Esters	C=O stretch	1665
9	Ethers	C-O stretch	1120, 1020
10	Phenols	O-H stretch	3315

GC-MS Analysis: Phyto-constituents of *Xylosma longifolia* were analyzed through GC-MS also. The GC-MS analysis of methanol extract of leaves of *Xylosma longifolia* has led to the identification of 12 bioactive compounds having various pharmacological properties. The major compounds identified were L-(+)-Ascorbic acid 2, 6- dihexa-decanoate (16.14%) and N, N-dimethylglycine (13.25 %). The minor compounds with the lowest peak value obtained are 17-Octadecynoic acid (9.0%), n-Hexadecanoic acid (7.53%), 3,7,11,15-Tetramethyl-2-hexadecen-1-ol (6.43%), Phytol (5.70%), Sucrose (4.50%), 9, 12-Octadecadienoic acid (Z,Z)- (4.20%), 3-Heptadecen-5-yne, (Z)- (3.21%), Trichloroacetic acid, tridec-2-ynyl ester (1.99%), Cis-13, 16-docadienoic acid (1.30%) and Cyclododecanol (0.33%). The results are tabulated in **Table 5** and **Fig. 2**.

The mass spectra and molecular structures of the phytoconstituents identified from GC-MS analysis were given in **Fig. 3 - Fig. 14**.

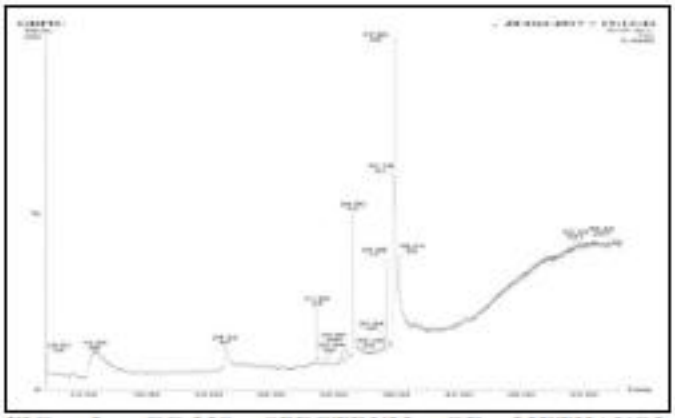

FIG. 2: GC-MS SPECTRUM OF METHANOL EXTRACT OF LEAVES OF *XYLOSMA LONGIFOLIA*

TABLE 5: COMPOUNDS REPORTED IN THE METHANOLIC EXTRACT OF *XYLOSMA LONGIFOLIA* THROUGH GC-MS

S. no.	Retention Time	Name of the compound	Peak area %	Molecular weight	Molecular formula
1	13.86	N,N-dimethylglycine	13.25	103	$C_4H_9O_2N$
2	24.32	Sucrose	4.50	342	$C_{12}H_{22}O_{11}$
3	31.68	3,7,11,15-Tetramethyl-2-hexadecen-1-ol	6.43	296	$C_{20}H_{40}O$
4	32.64	Cyclododecanol	0.33	184	$C_{12}H_{24}O$
5	33.99	3-Heptadecen-5-yne, (Z)-c	3.21	234	$C_{17}H_{30}$
6	34.50	n-Hexadecanoic acid	7.53	256	$C_{16}H_{32}O_2$
7	36.39	Cis-13,16-docasadienoic acid	1.30	336	$C_{22}H_{40}O_2$
8	37.04	Trichloroacetic acid, tridec-2-ynyl ester	1.99	340	$C_{15}H_{23}Cl_3O_2$
9	37.26	Phytol	5.70	296	$C_{20}H_{40}O$
10	37.79	9,12-Octadecadienoic acid (Z,Z)-	4.20	280	$C_{18}H_{32}O_2$
11	37.90	L-(+)- Ascorbic acid 2,6-dihexadecanoate	16.14	652	$C_{38}H_{68}O_8$
12	38.23	17-Octadecynoic acid	9.00	280	$C_{18}H_{32}O_2$

Principal
Nowgong Girls' College
Nagaon :: Assam
Nowgong Girls College ESTD: 1962 Nagaon :: Assam

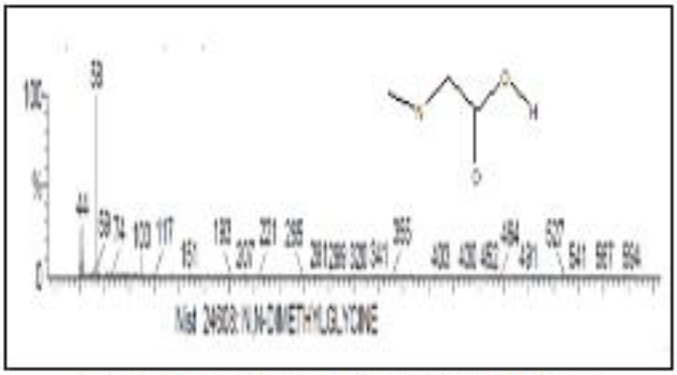

FIG. 3: MASS SPECTRUM AND MOLECULAR STRUCTURE OF N, N-DIMETHYLGLYCINE WITH RETENTION TIME (RT) = 13.86

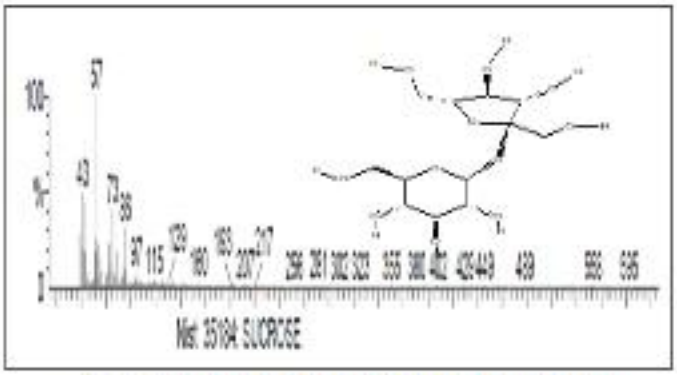

FIG. 4: MASS SPECTRUM AND MOLECULAR STRUCTURE OF SUCROSE WITH RETENTION TIME (RT) = 24.32

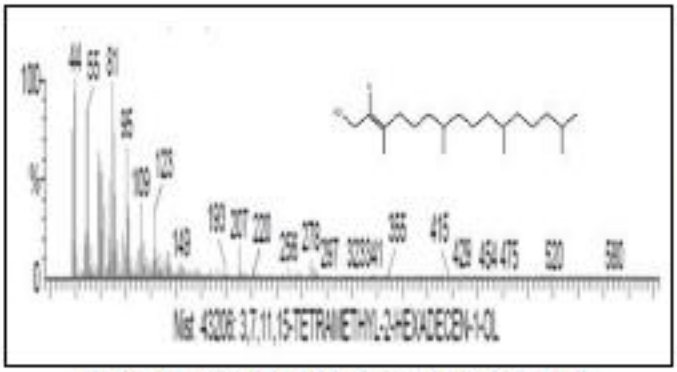

FIG. 5: MASS SPECTRUM AND MOLECULAR STRUCTURE OF 3, 7, 11, 15-TETRAMETHYL-2-HEXADECEN-1-OL WITH RETENTION TIME (RT) = 31.68

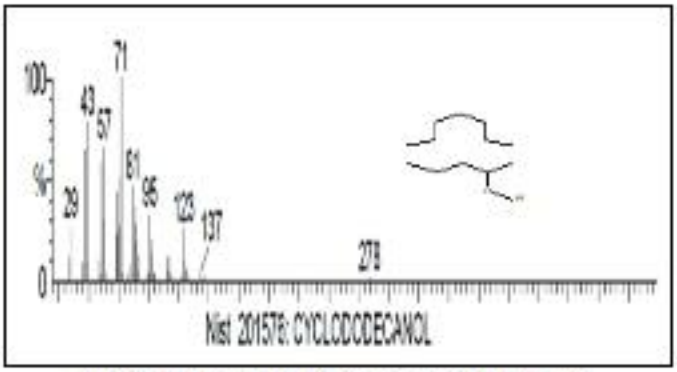

FIG. 6: MASS SPECTRUM AND MOLECULAR STRUCTURE OF CYCLODODECANOL WITH RETENTION TIME (RT) = 32.64

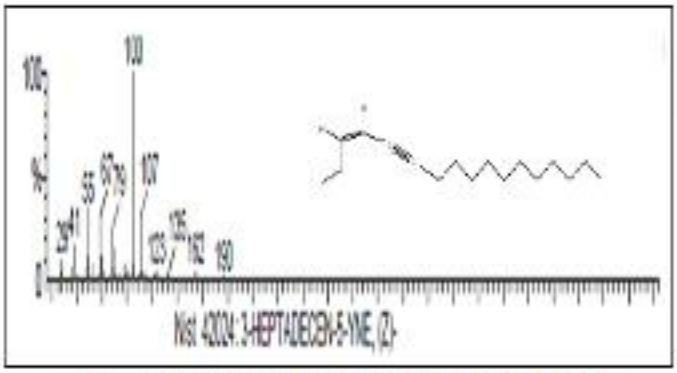

FIG. 7: MASS SPECTRUM AND MOLECULAR STRUCTURE OF 3-HEPTADECEN-5-YNE, (Z)- WITH RETENTION TIME (RT) = 33.99

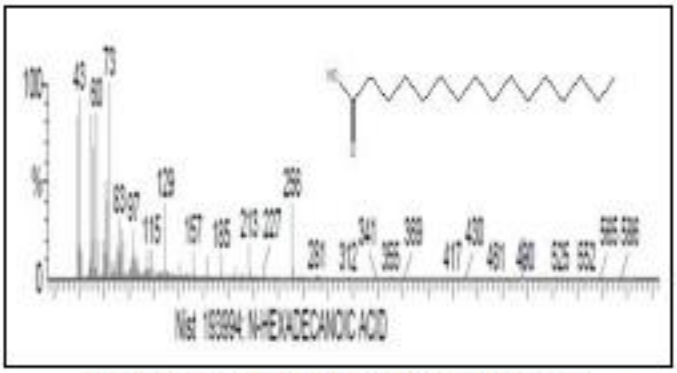

FIG. 8: MASS SPECTRUM AND MOLECULAR STRUCTURE OF N-HEXADECANOIC ACID WITH RETENTION TIME (RT) = 34.50

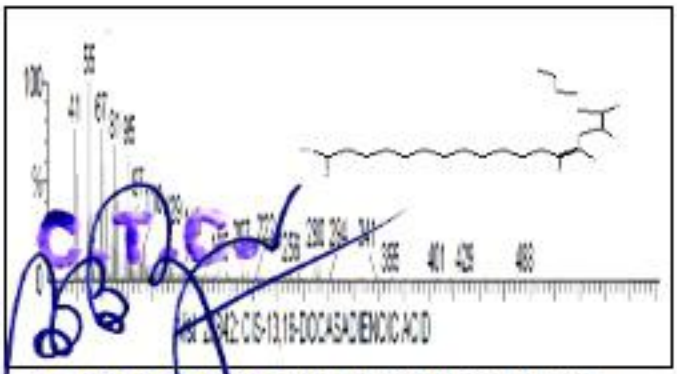

FIG. 9: MASS SPECTRUM AND MOLECULAR STRUCTURE OF CIS-13, 16-DOCASADIENOIC ACID WITH RETENTION TIME (RT) = 36.39

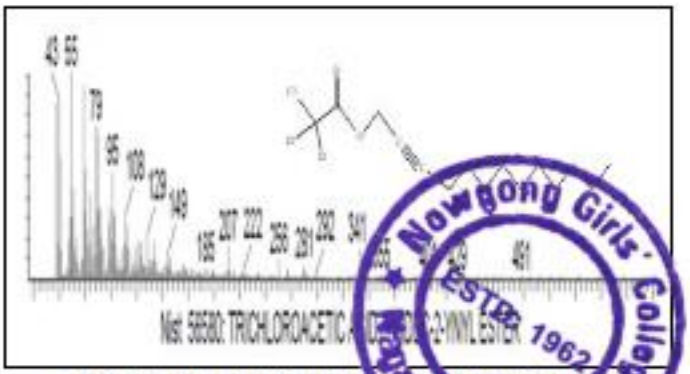

FIG. 10: MASS SPECTRUM AND MOLECULAR STRUCTURE OF TRICHLOROACETIC ACID, TRIDEC-2-YNYL ESTER WITH RETENTION TIME (RT) = 37.69

Principal
Nowgong Girls' College
Nagaon :: Assam

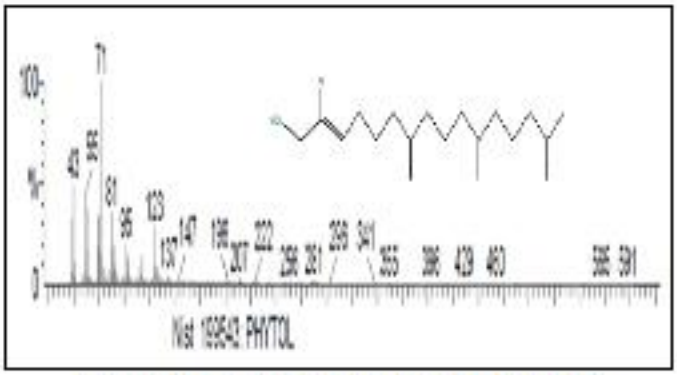

FIG. 11: MASS SPECTRUM AND MOLECULAR STRUCTURE OF PHYTOL WITH RETENTION TIME (RT) = 37.26

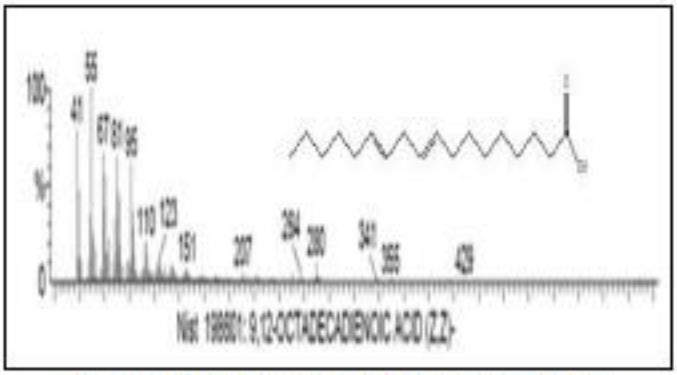

FIG. 12: MASS SPECTRUM AND MOLECULAR STRUCTURE OF 9, 12-OCTADECADIENOIC ACID (Z,Z)- WITH RETENTION TIME (RT) = 37.79

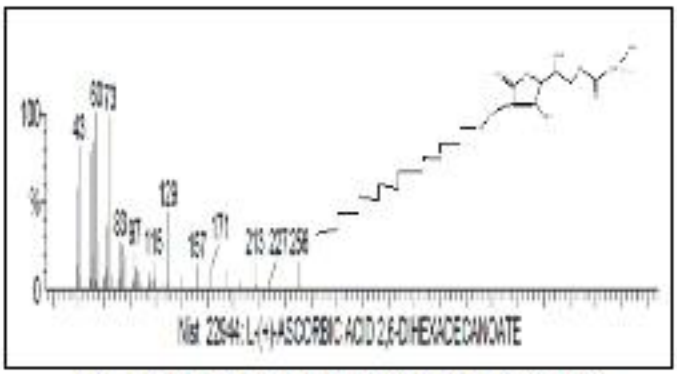

FIG. 13: MASS SPECTRUM AND MOLECULAR STRUCTURE OF L-(+)- ASCORBIC ACID 2,6-DIHEXADECANOATE WITH RETENTION TIME (RT) = 37.90

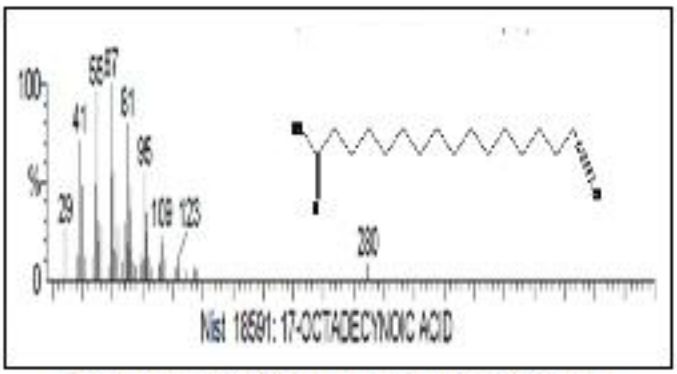

FIG. 14: MASS SPECTRUM AND MOLECULAR STRUCTURE OF 17-OCTADECYNOIC ACID WITH RETENTION TIME (RT) = 38.23

Xylosma longifolia is an important ethnomedicinal plant and have various ethnopharmacological properties used by several tribal communities in the North-eastern and Himalayan region of India. The preliminary phytochemical analysis of the methanolic extract of leaves of *Xylosma longifolia* has shown the occurrence of secondary metabolites like alkaloids, flavonoids, phenols, tannins, saponins and terpenoids, whereas, steroids are found to absent. The IR spectrum of methanol extract of *Xylosma longifolia* has revealed the occurrence of several secondary metabolites like flavonoids, phenols, alkaloids, terpenoids, steroids, terpenes and primary metabolite carbohydrates. A considerable amount of alkaloids, flavonoids and phenols have been estimated by using UV-spectrophotometer. The secondary metabolites are reported to have many pharmacological properties [34-36].

Different classes of alkaloids reported to exhibit several pharmacological activities like antibacterial, cytotoxicity effect, antifungal, antiviral, mutagenic or carcinogenic activity, insecticidal, analgesics, antiseptics, bradycardia, hypotensive, antioxidant, sedative properties, electrolyte transport inhibition, anti-malarial, anti-tumor, anti-inflammatory, Cerebro-protective, mutagenic, anti-cough remedy, hepatoprotective, vaso-relaxing, anxiolytic, immune-regulative, anti-diarrhetic and anti-ulcer effect [37]. Hepatoprotective activity of alkaloid fractions from the ethanol extract of the leaves of *Murraya koenigii* has been evaluated [38]. Antihepatotoxic and hepatoprotective effects of the total alkaloid fraction of leaves of *Hygrophila auriculata* and *Solanum pseudocapsicum* were evaluated and were able to normalize the biochemical levels which were altered due to carbon tetrachloride (CCl_4) intoxication [39,40].

Alkaloids like 6- hydroxyhaemanthamine, heamanthin, lycorine, galanthamine and tazettine have potent antimalarial activity extracted from Amaryllidaceae plants (*Pancratium maritimum*, *Leucojum aestivum*, and *Narcissus tazetta* ssp. *tazetta*) [41]. Alkaloids isolated from *Stephania rotunda* possess antimalarial activity [42].

Flavonoids possess pharmacological properties like anti-oxidant, anti-inflammatory, anti-thrombogenic

CTC
Principal
Nowgong Girls' College
Nagaon :: Assam
Nowgong Girls College ESTD: 1962 Nagaon Assam

activity, anti-tumor, anti-malarial, antiosteoporotic effects, antiviral, antibacterial, antifungal, anticancer, hepatoprotective, free-radical scavenging capacity and coronary heart disease prevention [43, 44]. In-vitro antiplasmodial activity of flavonoids like dehydrosilybinand 8-(1, 1)-DMA-kaempferida has been evaluated against *P. falciparum* strains [45]. Phenolic acids, ellagitannins and tannin-rich fractions of *Punica granatum* L. shows anti-oxidant, anti-malarial and anti-microbial activities [46]. The biological and pharmacological activities of saponins are anti-cancer, antiphlogistic, anti-allergic, immunomodulatory, antihepatotoxic, antiviral, antifungal, anti-inflammatory, hypoglycemic and molluscicidal activities [47].

Several major and minor compounds are identified in the present study through GC-MS possessing many pharmacological properties. N, N-dimethylglycine is also known as dimethylglycine is the athletic performance enhancer, decrease oxidative stress, dietary supplements for patients with Autism, anti-convulsant, anti-depressant, protects the liver, improves immune response and epilepsy [48-50]. The disaccharide sucrose possesses antinociceptive and anti-oxidant properties [51]. Phytol is diterpene alcohol possesses anti-cancer, anti-inflammatory, antimicrobial, antioxidant, diuretic and antinociceptive properties [52, 53]. L-(+)-Ascorbic acid 2,6-dihexadecanoate exhibit antinociceptive, anti-inflammatory and anti-oxidant properties [54, 55]. 3, 7, 11, 15-Tetramethyl-2-hexadecen-1-ol have several biological activities like anti-inflammatory and antimicrobial [56]. N-hexadecanoic acid also known as Palmitic acid possesses 5-alpha reductase inhibitor activities anti-androgenic, antioxidant, hypocholesterolemic, lubricant, hemolytic, flavor, nematicide, pesticide and mosquito larvicide [55, 56].

The 9,12-Octadecadienoic acid (Z,Z)- (Linoleic acid) obtained from the methanol extract exhibit more biological activities like anti-acne, anti-androgenic, anti-arthritic, anti-coronary, anti-eczemic, antihistamine, anti-inflammatory, cancer preventive, hepatoprotective, hypercholesterolemic, insectifuge, nematicide, and 5-alpha reductase inhibitor [56]. The bioactive compounds present in *Xylosma longifolia* have various pharmacological and therapeutic activities. Further *in-vitro* and *in-vivo* pharmacological investigations on animal models of the phytochemicals isolated from the plant should be prioritized and could lead to the development and discovery of the new potent drug.

CONCLUSION: The preliminary phytochemical screening, quantitative estimation and FT-IR results reveal that the methanolic extract of the leaves of *Xylosma longifolia* consists of various bioactive compounds like alkaloids, flavonoids, phenols, tannins, terpenoids, saponins and carbohydrates. Several major and minor constituents have been analyzed through GC-MS having various pharmacological properties. The result validates the importance and remedial uses of the ethnomedicinal plant *Xylosma longifolia*. Further phytochemical and pharmacological studies are an urgent requirement of *Xylosma longifolia* for identification, isolation and elucidation of the biologically active compounds and for the development of novel potent drugs for curing various disorders.

ACKNOWLEDGEMENT: The first author is greatly thankful to the Head of Chemistry Department, Nowgong College and Coordinator of Institutional Biotech Hub of Gauhati University for providing the laboratory facilities and equipment to conduct the research works. Dr. M.G. Barthakur, Senior Scientist, Biotech Park, IIT Campus (Guwahati) and Dr. Mukul Kalita, Department of Chemistry, Jorhat Engineering College (Jorhat) are gratefully acknowledged for their invaluable support provided in the present research.

CONFLICTS OF INTEREST: The authors declare no conflicts of interest.

REFERENCES:

1. Farnsworth N: The role of ethnopharmacology in drug development. Bioactive compounds from plants. John Wiley and Sons 2008.
2. Maobe AGM and Nyarango MR: Fourier Transformer Infra-Red Spectrophotometer analysis of *Warburgia ugandensis* medicinal herb used in the treatment of diabetes, malaria and ... in Kisii region, Southwest Kenya. Global ... Pharmacology 2013; 7(1): 61-68.
3. Heywood V: ... pharmacology, food production, nutrition and ... biodiversity conservation: towardsa sustainable future ... indigenous peoples. Journal of Ethnopharmacology ... 137(1): 1-13.
4. Shikov AN, Pozharitskaya ON, Makarov ... Wagner H, Verpoorte, R and Hei... M: Medicinal plants of Russian

Nowgong Girls' College ESTD: 1962 Nagaon :: Assam
Principal
Nowgong Girls' College
Nagaon :: Assam

Pharmacopoeia; their history and applications. Journal of Ethnopharmacology 2014; 154(3): 481-36.
5. Falodun A: Herbal medicine in Africa- distribution, standardization and prospects. Research Journal of Phytochemistry 2010; 4: 154-61.
6. Murugesh S and Vino P: Phytochemical constituents, antioxidant activity and FT-IR analysis of *Pisonia grandis* leaf extracts. International Journal of Pharmacognosy and Phytochemical Research 2017; 9(7): 933-38.
7. Fransworth NR: Biological and phytochemical screening of plants. J of Pharmaceutical Sci 1966; 55(3): 225-76.
8. Vo VC: Dictionary of Vientnamese medicinal plants. Medicine Publishing, Hanoi 1999; 1085.
9. Truong BN, Pham VC, Mai HDT, Nguyen VH, Nguyen MC, Nguyen TH, Zhang H, Fong HHS, Franzblau SG, Soejarto DD and Chau VM: Chemical constituents from Xylosma longifolia and their anti-tubercular activity. Phytochemistry Letters 2011; 4(3): 250-53.
10. Devi WR, Singh SB and Singh CB: Anti-dermatophytic properties leaf and stem bark of *Xylosma longifolium* Clos. BMC Complementary and Alternative Medicine 2013; 13: 155.
11. Sultana S, Ali M and Jameel M: Aliphatic constituents from the leaves of *Dillenia indica* L., *Halothamus bottae* Jaub. and *Xylosma longifolium* Clos. Chemistry Research Journal 2018; 3(3): 109-17.
12. Sinha SC: Medicinal plants of Manipur. Manipur Cultural Integration Conference Publishers 1996.
13. Chadha HR: The wealth of India raw materials. CSIR, New Delhi 2003.
14. Devi AK, Khan MI and Tripathi RS: Ethnomedicinal plants in the sacred groves of Manipur. Indian Journal of Traditional Knowledge 2005; 4(1): 21-32.
15. Khare CP: Indian medicinal plants: an illustrated dictionary. Springer-Verlag, Berlin Heidelberg, New York 2007; 725.
16. Adhikari BS, Babu MM and Saklani PL: Medicinal plants and their conservation status in wildlife institute of India (WII) Campus, Dehradun. Ethnobotanical leaflets 2010; 14: 46-83.
17. Bajpai O, Pandey J and Chaudhary LB: Ethnomedicinal uses of tree species by Tharu tribes in the Himalayan Terai region of India. Research Journal of Medicinal Plant 2016; 10(1): 19-41.
18. Yuhlung CC and Bhattacharyya M: Indigenous medicinal plants used by the Maring tribe of Manipur, Northeast India. J of Ayurvedic and Herbal Med 2016; 2(4): 146-53.
19. Devi WR: Traditional medicinal plants used for various skin diseases and cosmoceuticals in Manipur, North-east India. In Ed Kshetrimayum B. Medicinal plants and its therapeutic uses. OMICS Groups eBook, USA 2017; 21-36.
20. Kom LE, Tilotama K, Singh TD, Rawat AKS and Thokchom DS: Ethnomedicinal plants used by the Kom community of Thayong village, Manipur. Journal of Ayurvedic and Herbal Medicine 2018; 4(4): 171-79.
21. Teron R: Cross-cultural ethnobotanical exploration of diversity and utilization of medicinal plants in Karbi-Anglong district, Assam, Noetheast India. NeBio 2019; 10(1): 1-20.
22. Singh TT, Devi AR and Sharma HM: Ethnopharmacological survey of medicinal plants in Andro village in Manipur (India). Res J of Life Sciences, Bioinformatics, Pharmaceutical and Chemical Sci 2018; 4(5): 606-26.
23. Medicinal plants of Bangladesh and West Bengal: Botany, natural products and ethnopharmacology. Phytochemistry Group 2019; 103.
24. Jain SK and Rao RR: A handbook of field and herbarium technique. Today and Tomorrow Publication, New Delhi 1977.
25. Handa SS, Khanuja SPS, Longo G and Rakesh DD: Extraction technologies of medicinal and aromatic plants. Trieste: ICS UNIDO 2008.
26. Harborne JB: Phytochemical methods: a guide to modern techniques of plant analysis. Chapman and Hall, London 1984.
27. Trease GE and Evans WC: Pharmacognosy. Balliere Tindall, London, 13th Edition 1989.
28. Sofowara A: Medicinal plants and traditional medicine in Africa. Spectrum Books Ltd, Ibadan, Nigeria 1993.
29. Shamsa F, Monsef H, Ghamooshi R and Verdian-rizi M: Spectrophotometric determination of total alkaloids is some Iranian medicinal plants. Thai Journal of Pharmaceutical Sciences 2008; 32: 17-20.
30. Lobo R, Sodde V and Dashora N: Quantification of flavonoid and phenol content from *Macrosolen parasiticus* (L.) Danser. Journal of Natural Product and Plant Resources 2011; 1(4): 96-99.
31. Singleton VL and Rossi JA: Colorimetry of total phenolics with phosphomolybdic-phosphotungstic acid reagents. American Journal of Enology and Viticulture 1965; 16: 144-58.
32. Malick EP and Singh MB: Plant enzymology and Hittoenzymology. Kalyani Publishers, New Delhi 1980.
33. Ragavendran P, Sophia D, Raj CA and Gpalakrishnan VK: Functional group analysis by FTIR spectrum. Pharmacology Online 2011; 1: 358-64.
34. Vishnu R, Nisha R, Jamuna S and Paulsamy S: Quantification of total phenolics and flavonoids and evaluation of *in-vitro* antioxidant properties of methanolic leaf extract of Tarenna asiatica- an endemic medicinal plant species of Maruthamali hills, Western Ghats, Tamilnadu. Journal of Research in Plant Sciences 2013; 2(2): 196-04.
35. Benedec D, Vlase L, Oniga I, Mot AC, Damian G and Hanganu D: Polyphenolic composition, antioxidant and antibacterial activities for two Romanian subspecies of *Achillea distans* Waldst. et Kit. Ex Wild. Molecules 2013; 18: 8725-39.
36. Senguttuvan J, Paulsamy S and Karthika K: Phytochemical analysis and evaluation of leaf and root parts of the medicinal herb, *Hypochaeris radica* L. for *in-vitro* antioxidant activities. Asian Pacific Journal of Tropical Biomedicine. 2014; 4(S1): S359-S367.
37. Bribi N: Pharmacological activity of alkaloids: A review. Asian Journal of Botany 2018; 1: 1-6.
38. Sangale P and Patil R: Hepatoprotective activity of alkaloid fractions from ethanol extract of *Murraya koienigii* leaves in experimental animals. Journal of Pharmaceutical Sciences and Pharmacology 2010; 3(1): 28-33.
39. Vasanth PR, Raghu HC, Vijayan P, Dhanaraj SA, Mallikarjuna CR, Venkata JR and Nitesh K: *In-vitro* and *in-vivo* hepatoprotective effects of the total alkaloid fraction of *Hygrophila auriculata* leaves. Indian Journal of Pharmacology 2010; 42(2): 79-83.
40. Vijayan P, Prashanth [illegible] Vijayraj P, Dhanaraj SA, Badami S and Suresh B: Hepatoprotective effects of the alkaloid fraction of *Solanum pseudocapsicum* leaves. Pharmaceutical Biology 2004; 41(6): 443-48.
41. Sener B, Orhan L and Satayavivad J: Antimalarial activity screening of some alkaloids and the plant extracts from Amaryllidaceae. Phytotherapy Research 2003; 17(10): 1220-1223.

Principal
Nowgong Girls' College
Nagaon :: Assam
Nowgong Girls College ESTD: 1962 Nagaon :: Assam

42. Chea A, Hout S, Bun SS, Tabatadze N, Gasquet M, Azas N, Elias R and Balansard G: Anti-malarial activity of alkaloids isolated from *Stephania rotunda*. Journal of Ethnopharmacology 2007; 112(1): 132-37.
43. Agarwal AD: Pharmacological activities of flavonoids: A review. International Journal of Pharamceutical Scienecs and Nanotechnology 2011; 4(2): 1394-98.
44. Kumar S and Pandey SK: Chemistry and Biological activities of flavonoids: An overview. The Scientific World Journal 2013; 162750.
45. de Monbrison F, Maitrejean M, Latour C, Bugnazet, F, Peyron F, Barron D and Picot S: *In-vitro* antimalarial activity of flavonoid derievatives dehydrosilybin and 8-(1:1)- DMA-Kaempferida. Acta Tropi 2006; 97(1): 102-07
46. Reddy MK, Gupta SK, Jacob MR, Khan SI and Ferreira D: Anti-oxidant, antimalarial and antimicrobial activities of tannin rich- fractions, ellagitannins and phenolic acid from *Punica granatum* L. Planta Medica 2007; 73(5): 461-67.
47. Lacaille-Dubois MA and Wagner H: A review of the biological and pharmacological activities of saponins. Phytomedicine 1996; 2(4): 363-86.
48. Roach E and Carlin L: N,N-Dimethylglycine for epilepsy. New England Journal of Medicine 1982; 307: 1081.
49. Rimland B: Dimethylglycine, a nontoxic metabolite, and autism. Research Review International 1990; 4(3).
50. Bolman WM and Richmond JA: A double-blind, placebo-controlled, cross over pilot trial of low dose dimethyl-glycine in patients with autistic disorder. Journal of Autism and Developmental Disorders 1999; 29(3): 191-94.
51. Gibbins S and Stevens B: Mechanisms of sucrose and non-nutritive sucking in procedural pain management in infants. Pain Research and Management 2001; 6(1): 21-28.
52. Krishnamoorthy K and Subramaniam P: Phytochemical profiling of leaf, stem and tuber parts of *Solena amplexicaulis* (Lam.) Gandhi using GC-MS. International Scholarly Research 2014; 567409.
53. Santos CCMP, Salvadori MS, Mota VG, Costa LM, de Almeida AAC, de Oliveira GAL, Costa JP, de Sousa DP, de Freitas RM and de Almeida RN: Antinociceptive and antioxidant activities of phytol *in-vivo* and *in-vitro* models. Neuroscience Journal 2013; 949452.
54. Bruneton J: Pharmacognosy, Phytochemistry, Medicinal Plants. Lavoisier technique and documentation, Paris 1999.
55. Kumar M, Gayatri N, Sivasudha T and Ruckmani K: Profiling of bioactive components present in *Ziziphus mauritiana* lam for *in-vitro* antioxidant and *in-vivo* anti-inflammatory activities. International Research Journal of Pharmacy 2017; 8(9).
56. Rajalakshmi K and Mohan VR: GC-MS analysis of bioactive components of *Myxopyrum serratum* A.W. Hill (Oleaceae). International Journal of Pharmaceutical Sciences Review and Research 2016; 38(1): 30-35.

How to cite this article:
Bhattacharyya R, Boruah JS, Medhi KK and Borkataki S: Phytochemical analysis of leaves of *Xylosma longifolia* Clos.: a plant of ethnomedicinal importance. Int J Pharm Sci & Res 2020; 11(5): 2065-74. doi: 10.13040/IJPSR.0975-8232.11(5).2065-74.

All © 2013 are reserved by the International Journal of Pharmaceutical Sciences and Research. This Journal licensed under a Creative Commons Attribution-NonCommercial-ShareAlike 3.0 Unported License.

This article can be downloaded to **Android OS** based mobile. Scan QR Code using Code/Bar Scanner from your mobile. (Scanners are available on Google Playstore)

C.T.C.
Principal
Nowgong Girls' College
Nagaon :: Assam

Nowgong Girls' College
ESTD: 1962
Nagaon :: Assam

Progress In Biomaterials (2020) 9:219–237
https://doi.org/10.1007/s40204-020-00144-1

ORIGINAL RESEARCH

Surface modification of electrospun silk/AMOX/PVA nanofibers by dielectric barrier discharge plasma: physiochemical properties, drug delivery and in-vitro biocompatibility

Namita Ojah[1] · Rajiv Borah[2] · Gazi Ameen Ahmed[1] · Manabendra Mandal[3] · Arup Jyoti Choudhury[1]

Received: 27 June 2020 / Accepted: 27 October 2020 / Published online: 18 November 2020
© Islamic Azad University 2020

Abstract

The naturally obtained protein *Bombyxmori* silk is a biocompatible polymer with excellent mechanical properties and have the potential in controlled drug delivery applications. In this work, we have demonstrated dielectric barrier discharge (DBD) oxygen (O_2) plasma surface modified electrospun *Bombyxmori* silk/Amoxicillin hydrochloride trihydrate (AMOX)/polyvinyl alcohol (PVA) nanofibers for drug release applications with controlled plasma treatment duration (1–10 min). The findings indicate that plasma treated electrospun nanofibers for 1–3 min exhibited significant enhancement in tensile strength, Young's modulus, wettability and surface energy. The plasma treated electrospun nanofibers for 1–5 min showed remarkable increase in AMOX released rate, whereas the electrospun nanofibers treated with plasma irradiation beyond 5 min showed only marginal increase. Moreover, the plasma treated nanofibers also exhibited good antibacterial activity against both *E. coli* (gram negative) and *S. aureus* (gram positive) bacteria. The untreated and the plasma treated silk/AMOX/PVA electrospun nanofibers for 1–3 min showed enhanced viability of primary adipose derived mesenchymal stem cells (ADMSCs) growth on them and much less hemolysis activity (< 5%). The in vitro biocompatibility of various electrospun nanofibers were further corroborated by live/dead imaging and cytoskeletal architecture assessment demonstrating enhanced cell adhesion and spreading on the plasma treated nanofibers for 1–3 min. The findings of the present study suggest that the silk/AMOX/PVA electrospun nanofibers with plasma treatment (1–3 min) due to their enhanced drug release ability and biocompatibility can be used as potential wound dressing applications.

Electronic supplementary material The online version of this article (https://doi.org/10.1007/s40204-020-00144-1) contains supplementary material, which is available to authorized users.

✉ Arup Jyoti Choudhury
choudharyajc@gmail.com

[1] Laboratory for Plasma Processing of Materials, Department of Physics, Tezpur University, Tezpur, Assam 784028, India

[2] Beneficiary Division, Institute of Advanced Study in Science and Technology, Guwahati, Assam 781035, India

[3] Department of Molecular Biology and Biotechnology, Tezpur University, Tezpur, Assam 784028, India

Principal
Nowgong Girls' College
Nagaon :: Assam

Nowgong Girls' College
ESTD: 1962
Nagaon :: Assam

Graphic abstract

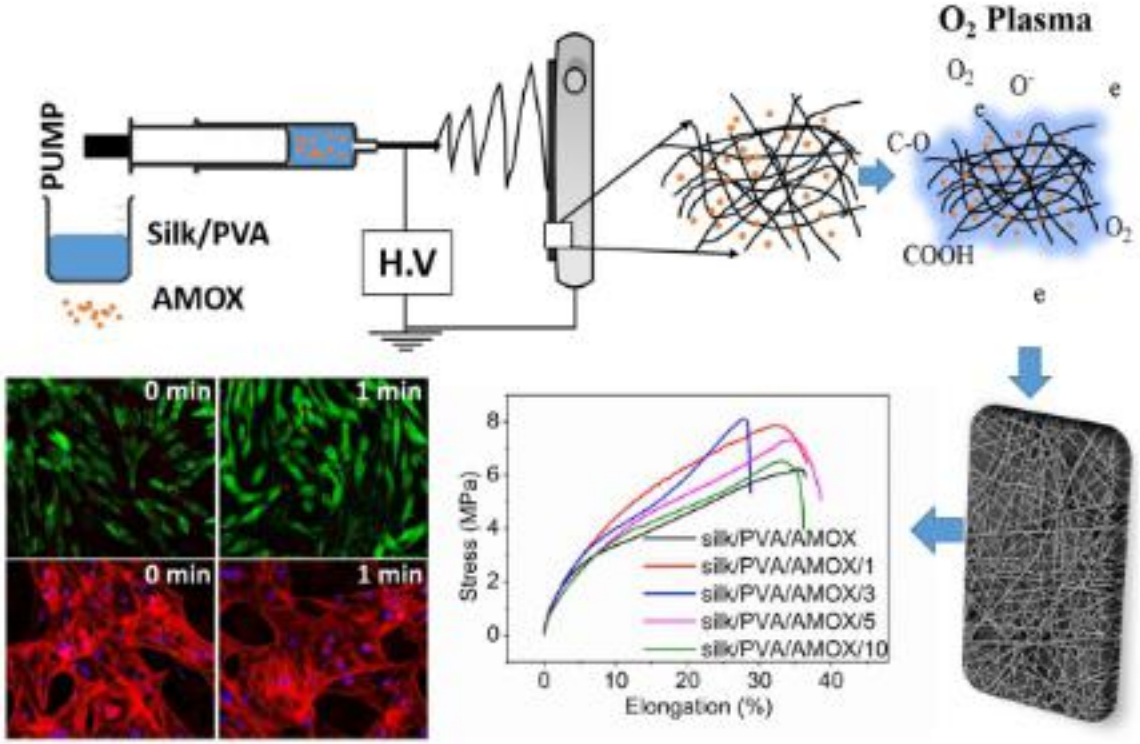

Article Highlights

- **Effect of O_2 DBD plasma treatment time on the surface properties of silk/AMOX/PVA nanofibers.**
- **Plasma treatment time of 1 min shows the highest rate of surface modifications in terms of chemical, mechanical, wettability and surface energy improvement.**
- **Increase in plasma treatment time up to 5 min results in continuous increasing drug release rate.**
- **The plasma treatment time does not cause any hemolytic effect, also improved cell viability and cell attachment with cell spreading is observed after 1–3 min of plasma treatment time.**

Keywords Silk · Dielectric barrier discharge · Surface modification · Hydrophilicity · Drug delivery · Biocompatibility

Introduction

Polymeric electrospun nanofiber-based drug delivery systems have been extensively widely due to their unique porous structure and high surface to volume ratio (Shababdoust; et al. 2018; Sacco et al. 2017). The nanoscale electrospun fibers were used in therapeutic targeted drug delivery with a wide range of drug release kinetics (Ojah et al. 2019a; Kajdic et al. 2019). However, the surface properties of any material have an important role to play in specific biological applications as the surface of the material encounters the target (Nedela et al. 2017; Hetemi and Pinson 2017). It is not always likely to have all the desired properties in a single material. A few desired surface properties such as surface roughness, wettability, tensile strength etc., can be externally aided to a material using appropriate surface modification techniques (Molavi et al. 2020; Krishnakumar et al. 2019; Yoshida et al. 2013). Regarding this, the low temperature plasma surface modification of polymers have gained considerable research interest due to its energy efficient and green approach (Das et al. 2018; Ojah et al. 2019a, b). The non-uniform and highly complex plasma species (electrons, ions, neutral atoms, reactive species, metastable states etc.) transfer energy to the polymer surface through direct collision with the surface, thereby introducing new and enhanced surface properties such as surface roughness, incorporation of polar functional groups, wettability, surface energy, higher mechanical strength etc. (Das et al. 2015; Ojah et al. 2019a).

Low temperature plasma irradiation technique has been shown in the past in surface modification of polymeric

Principal
Nowgong Girls' College
Nagaon :: Assam
Nowgong Girls' College ESTD: 1962 Nagaon :: Assam

materials (Meghdadi et al. 2019; Ojah et al. 2019a, b; Theapsak et al. 2010; Chutia et al. 2019). Recently, low temperature atmospheric pressure dielectric barrier discharge (DBD) plasma has been utilized widely in various fields of material processing such as etching, surface cleaning, polymerization, surface modification, ozone generation, medical treatments and in semiconductor devices etc. (Rezaei et al. 2016; Simor et al. 2010). The plasma generation in DBD is due to the application of a very high voltage in the order of kV (Foruzan et al. 2018; Balcon et al. 2007). The DBD plasma irradiation has gained increasing popularity in materials surface engineering due to its low cost as it does not require any expensive and complicated vacuum arrangements and its simple structure (Ozkan et al. 2016; Xiaoping et al. 2012).

Plasma irradiation technique with a constant processing parameter was employed previously in surface modification of silk based biomaterials (Zhang et al. 2019; Choudhury et al. 2016; Ojah et al. 2019a, b). The versatile biopolymer silk has inspired increasing interest in the field of biomedical, pharmaceutical, optic and optoelectronic devices due to its favourable and attractive properties (Tomeh et al. 2019; Kundu et al. 2014). Silk exhibits high biocompatibility, slow degradability with mild processing conditions which makes it suitable for developing into various forms such as films, hydrogels, nanofibers and scaffolds (Kundu et al. 2014). The primary structure of silk consists of three major amino acids, namely glycine (Gly), alanine (Ala) and serine (Ser) in a ratio of 3:2:1 (Dyakonov et al. 2012). The secondary structure of silk is characterized by amorphous random coil and anti-parallel hydrogen bonded β-sheet structure (crystallizable and hydrophobic) which eventually provides good stretchability excellent mechanical strength and biocompatibility with high thermal stability (~250 °C) (Pollini and Paladini 2020; Yucel et al. 2014). Moreover, the presence of amino and carboxylic groups in silk fibroin aids in bio-functionalization of ligands and biomolecules for targeted drug delivery (Tomeh et al. 2019). It is also reported that silk-based drug delivery systems has the ability to enhance the stability of loaded drugs and proteins (Tomeh et al. 2019). The silk-based biomaterials undergo gel formation upon contact with aqueous media, thus diffusion of liquid into the silk matrix is followed by antibiotic particles released from the biomaterials (Dyakonov et al. 2012; Subia and Kundu 2012). Moreover, the silk fibroin has been recognized as good wound dressing biomaterial due to its ability of maintaining a moist environment at the wound site, proper air permeability and minimal inflammatory reaction. Besides, it can provide improved cell attachment and proliferation at various stages of complete wound healing process (Choulon and Mandal 2020; Pollini and Paladini 2020; Dyakonov et al. 2012). It has also been reported that with addition of suitable antimicrobial agents, silk-based drug delivery systems have further advantages of overall improvement in mechanical properties, modification of drug release kinetics and enhanced cell adhesion with improved biocompatibility which can provide necessary supports for complete wound healing (Tomeh et al. 2019; Pollini and Paladini 2020). In the context of surface modification, it was reported that low temperature plasma can tailor the surface properties of silk-based biomaterials which eventually helps in better wettability, improved bioadhesion and higher drug loading efficiency (Ojah et al. 2019b; Ribeiro et al. 2016; Jeong et al. 2009). In addition to that, low temperature plasma has been found efficient in modulating the cell proliferation and adhesion of silk-based nanofibrous membranes (Lee et al. 2014). Moreover, plasma surface modification has also proven to be effective in improving drug release kinetics of non-degradable polymers where, plasma treatment can influence the water penetration rate of polymeric scaffolds and thereby controlling the drug release kinetics (Yoshida et al. 2013). The higher wettability of biomaterials by plasma treatment can also accelerate the degradation rate, which in turn can modify the drug release (Petlin et al. 2017). Moreover, plasma treatment is utilized to fabricate hydrophobic coatings on the material surface to delay its degradation and hence the slow drug release (Yoshida et al. 2013; Petlin et al. 2017). However, it is well established that the effect of plasma treatment on material surface depends on the processing parameters of the plasma itself and any small change in such parameters can lead to a vivid change in the surface chemistry of a material (Foruzan et al. 2018). In that regard, it is important to study the impact of varying plasma processing parameters on the material surface.

Herein, we have investigated the effect of plasma treatment by varying irradiation time on various surface properties of the electrospun *Bombyxmori* silk/Amoxicillin hydrochloride trihydrate/polyvinyl alcohol (silk/AMOX/PVA) nanofibers and showed an optimized irradiation approach to improve the drug release rate and biocompatibility of the electrospun nanofibers for potential applications in wound healing. AMOX is a well-known antibiotic effective against both gram positive and gram negative bacteria and this could be helpful in preventing bacterial growth in the wound site (Ojah et al. 2019b). To fulfill the aim, all the other operating parameters of the DBD plasma setup were kept fixed such as: the electrode gap, applying voltage and gas flow rate except the treatment time. The electrospun nanofibers were irradiated with DBD O_2 plasma by varying irradiation time for 1, 3, 5 and 10 min, while other operating parameters such as the electrode gap, applied voltage and gas flow rate of the DBD plasma setup were kept fixed. The physicochemical properties of the untreated and plasma treated electrospun nanofibers were assessed by FESEM, ATR-FTIR, tensile analyzer, and contact angle measurement analysis. Drug release behavior of different electrospun nanofibers were also studied to explore the potential in wound

Principal
Nowgong Girls' College
Nagaon :: Assam

Nowgong Girls' College
Estd. 1962
Nagaon :: Assam

Springer

healing applications. Subsequently, in-vitro biological studies were assessed with the help of hemolytic activity assay, MTS assay, live/dead and rhodamine-phalloidin staining. To evaluate the biocompatibility of various silk/AMOX/PVA electrospun nanofibers, porcine adipose derived mesenchymal stem cells (ADMSCs) were used. ADMSCs are pluripotent stem cells which can differentiate into different lineages and secrete paracrine factors for inducing tissue regeneration (Hassan et al. 2014). In fact, ADMSCs play a major role in three main phases of a wound healing process, which are inflammatory, proliferative, and remodeling phase through paracrine signalling (Demirci et al. 2018). Thus, the advances in understanding the immunosuppression and secretion of pro-angiogenic factors by ADMSCs, have inspired the scientists and researchers across the world to explore the potential of ADMSCs alone or in combination with matrix scaffold for both acute and chronic wound repairs. The goal of the present study is to fabricate and optimize a wound dressing in nanofibrous matrix form using biodegradable and biocompatible FDA approved *Bombyxmori* silk fibroin and PVA with incorporation of antibiotic AMOX, wherein dielectric barrier discharge (DBD) oxygen (O_2) plasma treatment has been employed to optimize the antibiotic release profile for infection resistance. However, we envisage that the proposed wound dressing is not limited to infection resistance but may have the potential to promote wound healing when combined with ADMSCs. Hence, the current work is also focused on preliminary evaluation of biocompatibility and cell behavior on these nanofibrous mats.

Experimental

Materials

Bombyxmori silk cocoons were collected from Central silk board, Morigaon, Assam, India. The polyvinyl alcohol (PVA) (fully hydrolyzed, M_w 145 kDa) was purchased from Merck, India. Sodium bicarbonate ($NaHCO_3$, ≥ 99%) and acetic acid (glacial, ≥ 99%) were supplied by Sigma Aldrich, India. Diiodemethane and phosphate buffer saline (PBS) were acquired from Sigma Aldrich, USA. The dialysis membrane (12 kDa molecular cut off) was supplied by Himedia, India. The antibiotic amoxicillin hydrochloride trihydrate (AMOX) and lithium bromide (LiBr) were purchased from BR Biochem Life Sciences, India and Tokyo Chemical Industries, Japan respectively. The chemicals were directly used without any further purification.

Preparation of precursor solutions and electrospinning

The *Bombyxmori* silk solution was prepared by the method already described in previous work (Ojah et al. 2019a). The final concentration of the silk solution was obtained as 6.8% (*w/v*). The PVA solution was prepared with a concentration of 8% (*w/v*) with rigorous stirring and constant heating at 80 °C for 3 h (Das et al. 2018; Ojah et al. 2019a). The PVA and silk solutions were mixed in a ratio of 2:1 (silk: PVA) by mild stirring for 15 min. The antibiotic AMOX was added to the silk/PVA solution with concentration 1500 µg/mL with mild stirring for 15 min. The final silk/AMOX/PVA solution was then allowed to settle down prior to electrospinning. The schematic diagram and procedure of electrospinning was elaborated earlier (Das et al. 2018). Briefly, the solution was loaded into a syringe with 20 G needle and electrospun at a high voltage of 18 kV with flow rate 0.5 mL/h. The nanofibers were collected in an aluminum foil attached to a grounded static collector plate (150 mm × 150 mm). After electrospinning, the aluminum foil was collected and kept in a vacuum desiccator for future use (temperature 27 °C, humidity 50%).

DBD plasma treatment

The experimental setup of DBD plasma treatment is reported elsewhere (Ojah et al. 2019a, b). Briefly, the setup consists of one high voltage electrode and one ground electrode (250 mm × 250 mm). Both electrodes were covered with two glass plates of thickness 3 mm. The nanofibers were peeled off from the aluminum foil prior to plasma treatment and cut into pieces of certain dimensions according to the requirement and placed at the bottom electrode of the DBD setup. The nanofibers were plasma treated at a constant applied voltage of 15 kV with an electrode gap of 6 mm. The nanofibers were plasma treated for different time periods such as 1, 3, 5 and 10 min respectively. During the experiment, continuous O_2 gas flow into the chamber with a flow rate of 2 SLPM was controlled by a mass flow controller (Alicat Scientific, India). The discharge characteristics of the DBD plasma setup was analyzed using a high voltage probe (Tetronix, P6015A, 1000:1 and a digital oscilloscope (Tetronix, TPS2024B, 200 MHz) (Ojah et al. 2019b). The discharge was found uniform throughout the whole experiment and the respective discharge current–voltage waveforms for these particular parameters are reported [illegible]. The effective electric energy (W) associated with a discharge cycle was also calculated in this work by plotting the transported charge along Y-axis and the applied voltage along X-axis which eventually gives the Lissajous figure (Fig. 1) (Ojah

C.T.C.
Principal
Nowgong Girls' College
Nagaon :: Assam
Nowgong Girls College Estd. 1962 Nagaon :: Assam

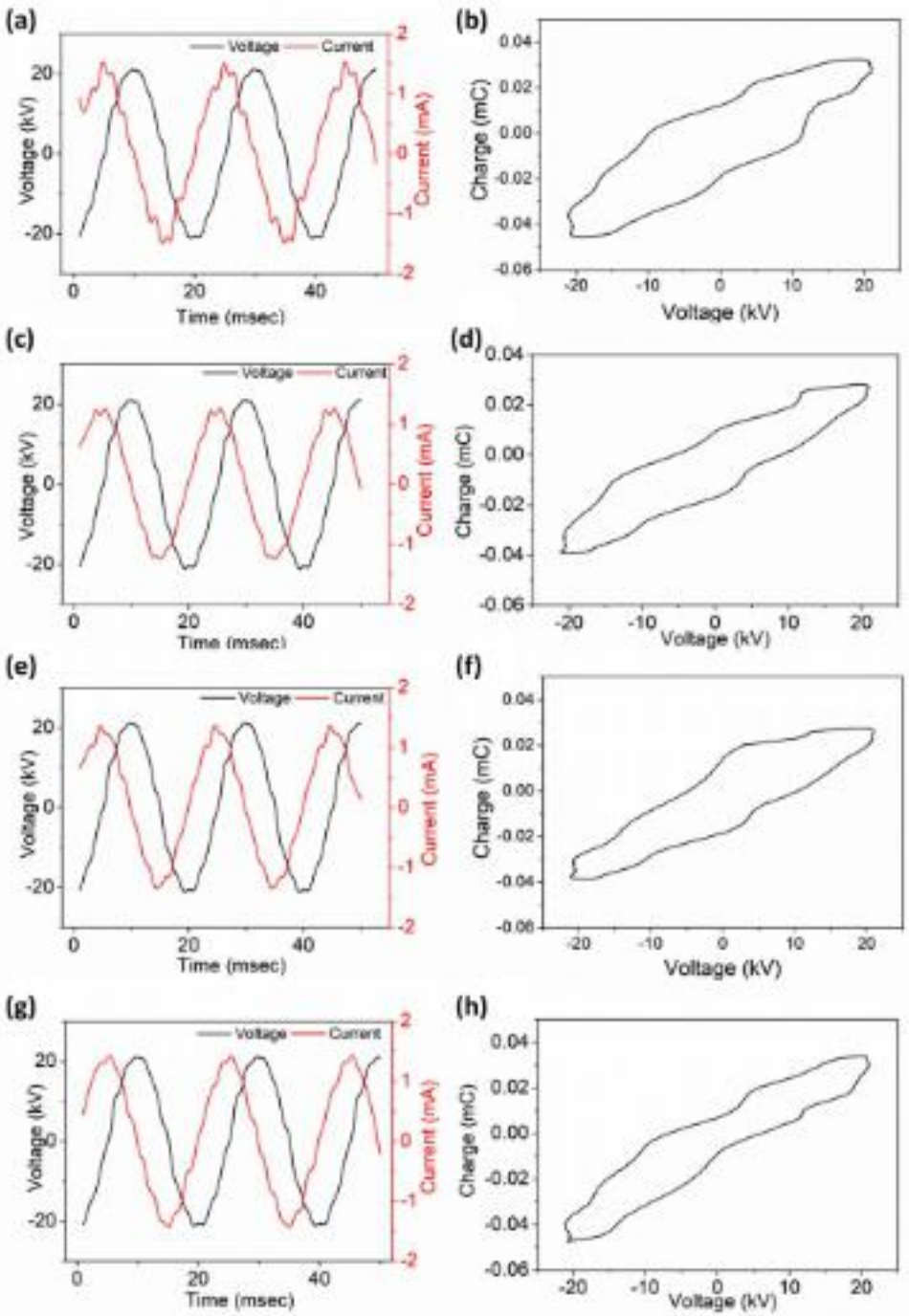

Fig. 1 Discharge characteristics of the DBD plasma at constant operating voltage of 15 kV for different treatment time. Where **a**, **b** are for 1 min; **c**, **d** are for 3 min; **e**, **f** are for 5 min and **g**, **h** are for 10 min plasma treatment time

Table 1 Discharge energy and power of the DBD plasma setup at operating voltage 15 kV, $d = 6$ mm, $f = 50$ Hz

Treatment time (min)	Discharge energy (J)	Discharge power (W)
1	0.89 ± 0.20	44.50 ± 3.28
3	0.81 ± 0.31	40.50 ± 5.32
5	0.83 ± 0.12	41.50 ± 2.95
10	0.80 ± 0.21	40.00 ± 3.14

et al. 2016; Kostov et al. 2009; Wang et al. 2012). The area enclosed by the lissajous figure automatically gives the electric energy (W) dissipated in one discharge cycle of the DBD plasma (Wang et al. 2012). However, similarly the power dissipated in one discharge was also calculated in this work using the following formula and is shown in Table 1 (Ray et al. 2016; Wang et al. 2012):

$$P = f.W,$$

Principal
Nowgong Girls' College
Nagaon :: Assam
Nowgong Girls' College ESTD: 1962 Nagaon :: Assam

where f is the frequency of the applied voltage and W is the electric energy dissipated in one discharge cycle.

Characterization techniques

The surface morphology of the prepared silk/AMOX/PVA nanofibers were evaluated using field emission scanning electron microscope (FESEM, Zeiss, Sigma, Germany). For better comparison, the FESEM images of O_2 plasma treated nanofibers were assessed at different time intervals. For the measurement, the nanofibers along with the aluminum foil were cut into pieces of 5 mm × 5 mm and coated with gold (SC7620, Emitech) at low vacuum. The average nanofiber diameter was calculated using imageJ software.

The chemical composition analysis of the nanofibers with/without O_2 plasma treatment were evaluated by attenuated total reflectance Fourier transform infrared spectroscopy (ATR-FTIR, IMPACT 410, NICOLET, USA). The spectra were taken in transmittance mode with a spectral region of 400–4000 cm^{-1} and resolution 4 cm^{-1}.

The mechanical performances of the electrospun silk/AMOX/PVA and silk/AMOX/PVA/O_2 nanofibers were evaluated using Universal testing machine (UTM, INSTRON 4204) at a constant speed of 10 mm min^{-1} with a 10 kN load (temperature: 27 °C and humidity: 50%). The nanofibers were cut into dimensions of 10 mm × 50 mm (thickness = 0.3 mm) and a total of five measurements were made for each sample. From the stress–strain curve the tensile strength, Young's modulus and elongation-at-break (%) are calculated and reported as mean ± SD.

The wettability of the nanofibers were evaluated using water contact angle measurement employing sessile drop method (Data Physics OCA 20, Germany) (Das et al. 2018). For calculation of surface energy (γ_s) OWRK method was used, where the double distilled water and non-polar liquid diiodemethane were both dropped on the nanofiber surface and the image as well as the contact angle was recorded instantly (Das et al. 2018; Ojah et al. 2019a). The total surface energy of the silk/AMOX/PVA and silk/AMOX/PVA/O_2 nanofibers were calculated using the following relation (Das et al. 2018; Ojah et al. 2019a)

$$\gamma_s = \gamma_s^p + \gamma_s^d, \tag{2}$$

where γ_s^p and γ_s^d are polar and dispersive components of surface energy (γ_s) respectively.

To determine the surface energy (γ_s), the polar and dispersive components were calculated using the following equations using two liquids, water and diiodomethane.

$$\begin{aligned}(\gamma_s^d)^{0.5} + 1.53(\gamma_s^p)^{0.5} &= 7.80(1 + \cos\theta_W)\\ (\gamma_s^d)^{0.5} + 0.22(\gamma_s^p)^{0.5} &= 3.6(1 + \cos\theta_D)\end{aligned} \tag{3}$$

where θ_W and θ_D are water and diiodemethane contact angles respectively. The data was recorded at different positions of a sample of dimension 10 mm × 10 mm area.

Drug release study

The rate of AMOX release from the silk/AMOX/PVA nanofibers were evaluated by taking absorbance of PBS at 273 nm using a UV visible spectrometer (Perkin Elmer model no: Lambda 365). The untreated and O_2 plasma treated nanofibers of specific amount with three parallel sets were put into centrifuge tubes containing 10 mL PBS (pH 7.4) and were incubated at 37 °C during the whole experiment period. At certain time interval, 1 mL of PBS was taken out from the centrifuge tubes and the UV absorbance value was recorded at 273 nm immediately. To retain the final volume of the nanofiber immersed solutions, simultaneously fresh PBS solution was added into the tubes each time.

Swelling and degradation Study

The swelling study of the plasma treated and untreated silk/PVA nanofibers was carried out by their immersion into PBS (pH 7.4) at 37 °C. The initial weight (W_0) of the untreated and plasma treated electrospun nanofibers were measured carefully before their immersion into PBS. At certain time intervals the nanofibers were taken out from PBS and the excess surface water was removed by a filter paper, followed by measuring the swollen weight (W_s) of the nanofibers again and then placed in the same PBS. The swelling ratio of the nanofibers were calculated by the following equation

$$\text{Swelling ratio} = \frac{W_s - W_0}{W_0}. \tag{4}$$

The degradation test of the nanofibers before and after plasma treatment was also carried out in similar procedure. The degradation was calculated using the following formula

$$\text{Degradation}(\%) = \frac{W_0 - W_d}{W_0} \times 100, \tag{5}$$

where W_0 is the initial weight of the nanofibers before immersion into PBS and W_d is the dry weight of the nanofibers after immersion into PBS.

Water vapor transmission rate (WVTR)

The water vapor transmission rate (WVTR) was measured according to American Society for Testing and Materials (ASTM) standard (Xu et al. 2016). Briefly, the experiment was performed in a desiccator incubated at 37 °C and

Nowgong Girls' College ESTD: 1962 Nagaon :: Assam
Principal
Nowgong Girls' College
Nagaon :: Assam

relative humidity of 50%. Permeability cups were filled with 1 g of dehydrated $CaCl_2$. The cups were immediately covered with the silk/AMOX/PVA and silk/AMOX/PVA/O_2 nanofibers treated at different plasma times and sealed properly by laboratory parafilm (USA, Neenah, WI 54,956) across the edges. The weight of the whole assembly after mounting the nanofibers was measured in a digital balance (Metler, accuracy 0.0001 gm) and placed in the desiccator. An open cup was considered as control. The WVTR has been measured by calculating the weight difference of the cups after 24 h and using the following formula

$$\mathrm{WVTR} = \frac{\Delta\, m}{A \times \mathrm{time}}, \tag{6}$$

where $\Delta\, m$ is the weight difference between the cups before and after incubation and A is the surface area of the film which was exposed to air. The experiments were performed in triplicates and data are presented with mean ± SD.

Antibacterial test

The antibacterial study for all the untreated and plasma treated silk/AMOX/PVA nanofibers were evaluated for both gram positive *S. aureus* and gram negative *E. coli* bacteria. The detailed procedure for the same was reported earlier (Ojah et al. 2019a, b). Briefly, specific amount of nanofibers were placed in agar plates where bacteria was already cultured and grown fully with the help of sterilized forceps and pressed gently. The plates were incubated at 37 °C; after 24 h the plates were taken out and the images were captured by a single lens-digital reflex camera (DSLR, Nikon D7200) and reported.

In-vitro biological studies

Hemolytic activity test

For hemolysis study, fresh venous blood was used which was collected from a healthy human donor in heparinized tubes. The plasma treated/untreated silk/AMOX/PVA nanofibers (50 mm × 50 mm) were incubated with 150 µL of human blood with 10% RBC suspension (prepared by dilution with 0.9% NaCl) and volume was adjusted to 2 mL with 0.9% NaCl followed by incubation for 1 h at 37 °C. Blood incubated with 0.9% NaCl was considered as negative control and with distilled water without test material as positive control for the test. After 1 h of incubation, the reaction mixture was centrifuged at 10,000 rpm for 10 min. The free hemoglobin present in the supernatant was measured using a UV–visible spectrophotometer at 540 nm wavelength. The percentage of hemolysis was calculated using the following relation,

$$\mathrm{Hemolysis}\,(\%) = \frac{\mathrm{Abs}_{\mathrm{sample}} - \mathrm{Abs}_{-\mathrm{vecontrol}}}{\mathrm{Abs}_{+\mathrm{vecontrol}} - \mathrm{Abs}_{-\mathrm{vecontrol}}} \times 100. \tag{7}$$

Cell isolation and sample preparation

To evaluate the biocompatibility of various silk/AMOX/PVA electrospun nanofibers, porcine adipose derived mesenchymal stem cells (ADSCs) were used. ADMSCs were isolated from the subcutaneous fat as per the previously reported protocol, which was harvested from the dorsal abdominal area of porcine at a local abattoir (Williams et al. 2011). Briefly, the harvested subcutaneous fat was obtained in cold PBS. The tissue was finely minced using sterilized scissors by separating the dermal and muscle part followed by washing with cold PBS containing penicillin 100 units/mL, 100 µg/mL streptomycin and amphotericin-B 2.5 µg/mL (Gibco, USA). Then, the tissue was digested in 0.1% (*w/v*) Type-IA collagenase solution in incomplete DMEM (($\geq$ 125 CDU/mg, Sigma, USA) under mild shaking for 2 h at 37 °C. The digested tissue was transferred into a fresh 50 mL centrifuge tube followed by vigorous shaking for 30–60 s to promote separation of the stromal vascular fraction and neutralized by adding equal volume of DMEM with 10% (*v/v*) FBS. The whole mixture was centrifuged twice at 300 g for 15 min to pellet down the stromal vascular fraction. After centrifugation, the floating adipocytes were aspirated, and the cell suspension was filtered through a dual filter system into a fresh 50 mL centrifuge tube and washed twice with DMEM media. Following filtration, the cell suspension was again centrifuged at 300 g for 5 min, the supernatant aspirated, and the pelleted stromal cells resuspended in 1 mL of high glucose DMEM supplemented with 10% (*v/v*) FBS and 1X antibiotic/antimycotic solution. Then, the cells were plated in 90 mm Petri-dishes at a density of 6×10^5 cells/dish and incubated at 37 °C under a 5% CO_2 in air humidified atmosphere. After 24 h of initial plating, expansion medium was replaced with fresh medium to remove non-adherent cells. Thereafter, the media was changed in every 3–4 days and cells were passaged at 70–90% confluence. Cells from passages 3–5 were in further experiments.

For biological assessment, the various electrospun nanofibrous mats were cut into dimensions of 5 mm × 5 mm and sterilized by autoclaving in hydrated conditions. Prior to cell seeding, the electrospun mats were conditioned in growth media overnight and subsequently used in in vitro biological studies.

MTS cell proliferation assay

The MTS proliferation assay was carried out to evaluate the cytotoxicity of the electrospun nanofibers following

Principal
Nowgong Girls' College
Nagaon :: Assam
Nowgong Girls College ESTD 1962 Nagaon :: Assam

incubation with ADMSCs. Briefly, ADMSCs were seeded on different substrates at a concentration of 5×10^3 cells/well in a 96 well plate for the MTS assay. Cell viability after incubation of 24 and 48 h on the materials was quantified using Cell Titer 96® AQueous One Solution containing 3-(4,5-dimethylthiazol-2-yl)-5-(3-carboxymethoxyphenyl)-2-(4-sulfophenyl)-2*H*-tetrazolium, inner salt) (MTS). The cultured materials were washed with sterile PBS twice, and MTS reagent diluted 1:5 in media was added directly to all the wells except the blank. The plates were incubated for 2 h at 37 °C and optical density (OD) was measured at 490 nm. All experiments were performed at $n = 3$.

Live/dead staining

The viable and dead cells seeded on different electrospun nanofibers were visualized using calcein-AM and ethidium homodimer (Sigma-Aldrich) staining after 48 h of culture. Briefly, the cell seeded nanofibers were washed with PBS once and incubated at 37 °C and 5% CO_2 with 40 nM calcein-AM (stain live cells) and 20 nM ethidium homodimer (stain dead cells) for 20 min. Then, the dye was removed and washed the nanofibers twice with PBS, subsequently visualized underhydrated conditions in fluorescent microscope (EVOS XL digital microscope, Thermo Fisher Scientific, USA) with viable cells appearing green and dead cells appearing red.

Rhodamine-Hoechst staining

To visualize the cytoskeletal architecture of the cells seeded on the electrospun nanofibers, the cell seeded nanofibers were fixed with neutral buffered formalin (NBF) (Sigma-Aldrich) after 72 h of culture. The fixed constructs were treated with 0.165 µM phalloidin conjugated to rhodamine (Life technologies, USA.) to stain the F-actin and counter stained with Hoechst-33342 (Sigma-Aldrich) for nucleus. The nanofibers were then visualized under fluorescence microscope (EVOS XL Digital microscope) and representative images are presented.

Statistical analysis

The results are expressed with mean ± SD. The significant difference between various experimental sets are evaluated using one-way analysis of variance (ANOVA) followed by Tukey test for several comparisons where p value < 0.05 is considered as significant.

Results and discussion

DBD plasma characteristics

The uniform discharge mode of the DBD plasma is very much important for even surface treatment. In this work, the DBD plasma showed uniform discharge mode throughout the whole experiment and the same was confirmed from the discharge characteristics of the plasma setup. The uniform discharge current curves for different treatment times, as shown in Fig. 1, confirming the uniform discharge mode of the DBD plasma setup at operating parameters of $V = 15$ kV and $d = 6$ mm) (Ojah et al. 2019b; Wang et al. 2012). Since, the operating parameters of the DBD plasma except the treatment time were constant; therefore, the similar intensity discharge current–voltage curves are expected in each set of experiments. The lissajous figures are also plotted in Fig. 1 and the electric energy dissipated in one discharge cycle was calculated for each set of treatment time. It is expected that due to fixed plasma parameters, the energy values and the shape of the lissajous figures should remain almost similar in each time. The calculated electric energy dissipated in one discharge cycle were found to be 0.89 J, 0.81 J, 0.83 J and 0.80 J for 1, 3, 5 and 10 min of treatment time, respectively. From the electric energy, the discharge power was calculated and is depicted in Table 1. It is clear that the discharge energy remains similar for all the set of treatments due to the fixed applied voltage, frequency (50 Hz) and discharge gap. Therefore, the overall average discharge power for operating voltage 15 kV with electrode gap 6 mm was calculated as 41.62 ± 2.01 W.

Surface morphology analysis

Figure 2 shows the FESEM images of untreated and plasma treated silk/AMOX/PVA nanofibers, confirming the formation of beads free and randomly oriented nanofibers with average fiber diameter of 140 ± 5.23 nm. However, the FESEM images do not reveal any noticeable changes in the surface morphology of the nanofibers after O_2 plasma treatment independent of the treatment time. The average diameter of the plasma treated nanofibers was also evaluated for better comparison and it was found as similar (140 ± 4.35 nm) to the untreated nanofibers independent of the treatment time. In earlier work, similar results were reported with constant plasma treatment time of 1 min (Das et al. 2018; Ojah et al. 2019a). However, no morphological changes in the nanofibers structure were observed with increasing plasma treatment time in the present work.

Nowgong Girls' College ESTD: 1962 Nagaon :: Assam

Principal
Nowgong Girls' College
Nagaon :: Assam

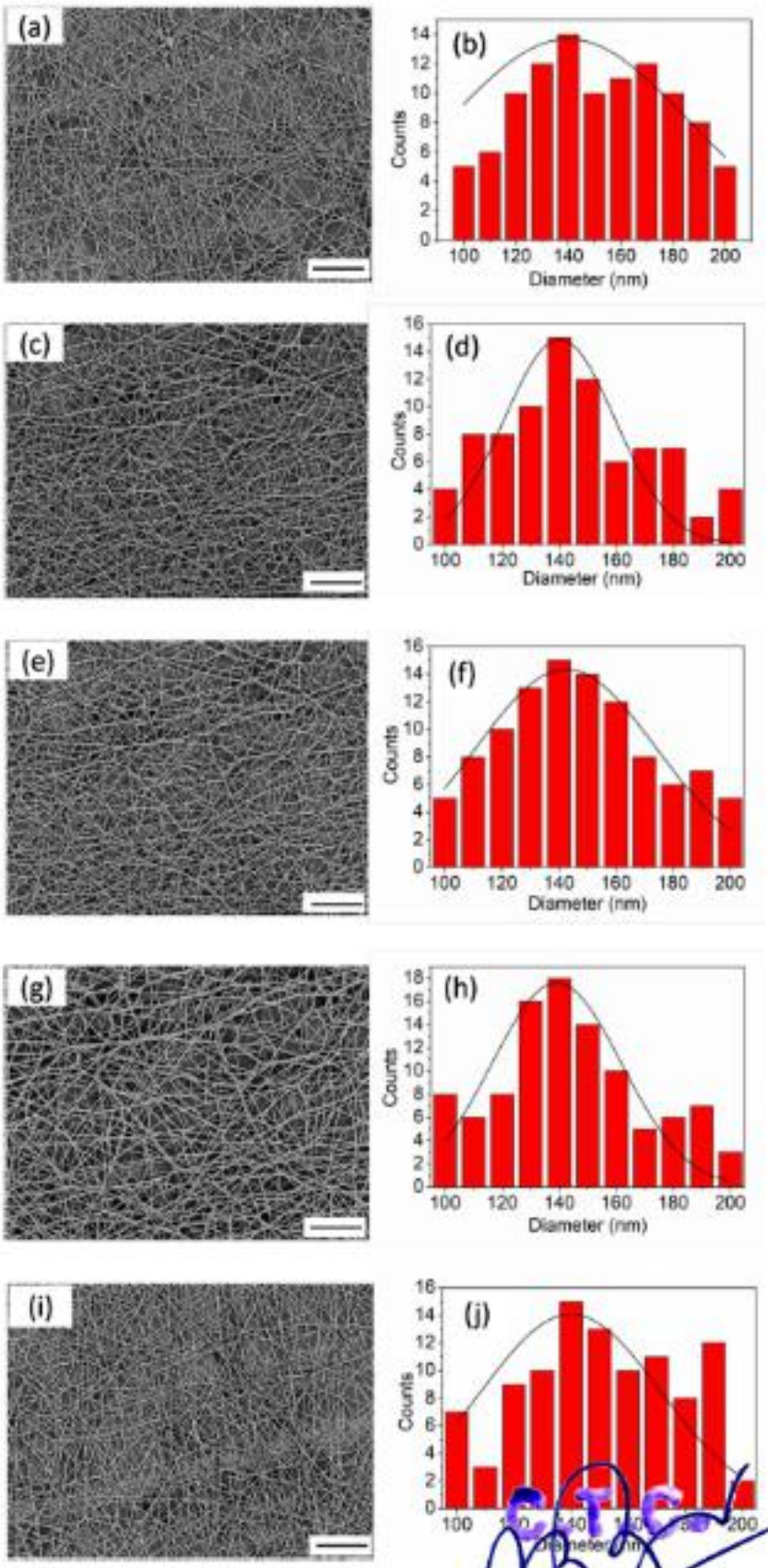

Fig. 2 FESEM images and diameter distribution of the untreated and plasma treated silk/AMOX/PVA nanofibers. Where **a**, **b** are untreated; **c**, **d** are 1 min plasma treated; **e**, **f** are 3 min plasma treated; **g**, **h** are 5 min plasma treated and **i**, **j** are 10 min plasma treated silk/AMOX/PVA nanofibers (FESEM image, scale:10 μm)

Nowgong Girls' College ESTD: 1962 Nagaon :: Assam
Principal
Nowgong Girls' College
Nagaon :: Assam

Table 2 Water contact angle and surface energy

Samples	Water contact angle (°)	Polar (mJm^{-2})	Dispersive (mJm^{-2})	Total S.E. (mJm^{-2})
Silk/AMOX/PVA	78.20 ± 2.16	2.54 ± 0.32	48.30 ± 2.35	50.84 ± 2.35
Silk/AMOX/PVA/1 min	31.50 ± 3.39	29.78 ± 1.32	37.22 ± 1.38	67.00 ± 1.90
Silk/AMOX/PVA/3 min	29.50 ± 1.80	35.45 ± 2.30	35.89 ± 1.58	71.34 ± 2.79
Silk/AMOX/PVA/5 min	27.91 ± 1.86	36.55 ± 1.20	35.65 ± 3.58	72.20 ± 3.77
Silk/AMOX/PVA/10 min	26.80 ± 3.74	36.98 ± 1.58	35.52 ± 2.85	72.50 ± 3.02

Wettability and surface energy measurements

The contact angle measurement is the simplest way to measure the wettability of any polymeric surface. Table 2 shows the water contact values for the untreated and O_2 plasma treated silk/AMOX/PVA nanofibers. The untreated nanofiber showed average water contact angle value of 78.20 ± 5.30° and the plasma treated nanofibers showed significantly lower contact angle value as compared to the untreated nanofiber. The contact angle dropped rapidly to 31.50 ± 3.39° and 27.50 ± 1.80° just after plasma treatment of 1 and 3 min, respectively, indicating improved wettability of the electrospun mats. However, with further increase in treatment time up to 5–10 min no such significant reduction of contact angle was observed.

The higher wettability generally results in higher surface energy of a polymer surface and O_2 plasma treatment improves wettability by incorporating oxygenated polar functional groups (O, O_2, O_2^-, COOH, C = Oetc.) to the surface (Das et al. 2018; Ojah et al. 2019a, b). These polar functional groups attached to the nanofibers surface strongly interacts with the water molecules resulting in lower water contact angle value (Das et al. 2018; Ojah et al. 2019a). The schematic representation of such interactions were reported elsewhere (Ojah et al. 2019a). Therefore, the respective surface energies along with their polar and dispersive components were determined to assess the surface polarity of the electrospun mats. Table 2 shows that after plasma treatment the polar components have been increased significantly as well as the surface energy also increased consequently. This improvement is a direct indication of incorporation of polar functional groups to the silk/AMOX/PVA nanofiber surface after plasma treatment (Das et al. 2018; Ojah et al. 2019a). However, after 5–10 min of plasma treatment, no further significant improvement is observed in surface energy and its polar component. It indicates that the surfaces were saturated beyond plasma treatment for 3 min.

Mechanical properties

The mechanical properties of the silk/AMOX/PVA nanofibers were evaluated in terms of its tensile strength, Young's modulus and elongation-at-break (%). For better understanding of the effect of O_2 plasma treatment, the mechanical properties of the plasma treated nanofibers for different times were also evaluated and are presented in Table 3. The untreated nanofibers exhibit tensile strength value of 6.22 ± 1.20 MPa with Young's modulus 61.29 ± 5.28 MPa. However, after O_2 plasma treatment, reasonable improvement in the tensile strength as well as in the Young's modulus values are observed. The electrospun nanofibers with plasma treated for 1 min shows improved tensile strength of 7.91 ± 1.31 MPa and Young's modulus of 67.60 ± 6.37 MPa. Similarly, the nanofibers plasma treated for 3 min shows further enhanced value of tensile strength (8.15 ± 1.26 MPa) and Young's modulus (68.22 ± 3.98 MPa). The reason behind such improvement can be explained by formation of hydrogen bonds on the nanofiber surface after O_2 plasma treatment (Das et al. 2018; Ojah et al. 2019a). As mentioned in earlier reported work, the oxygenated species formed during O_2 plasma treatment not only attaches to the nanofiber surface through hydrogen bonding but also they form hydrogen bonds among themselves (Das et al. 2018; Ojah et al. 2019a, b). This hydrogen bonded assembly leads to an extraordinarily complex structure at the nanofiber surface and eventually this contributes to the enhanced mechanical performance of the nanofibers (Das et al. 2018; Ojah et al. 2019a, b). Therefore, it is expected that number of

Table 3 Mechanical properties [illegible] Silk/AMOX/PVA [illegible] and without [illegible] treatment

Sample	Tensile strength (MPa)	Young's modulus (MPa)	Elongation (%)
Silk/AMOX/PVA	6.22 ± 1.20	61.29 ± 5.28	35.72 ± 4.6[illegible]
Silk/AMOX/PVA/1 min	7.91 ± 1.31	67.60 ± 6.37	[illegible]
Silk/AMOX/PVA/3 min	8.15 ± 1.26	68.22 ± 3.98	[illegible]
Silk/AMOX/PVA/5 min	7.33 ± 2.01	61.68 ± 6.9[illegible]	[illegible] ± 4.31
Silk/AMOX/PVA/10 min	6.53 ± 1.07	53.48 ± 6.8[illegible]	[illegible] ± 3.64

Nowgong Girls' College ESTD: 1962 Nagaon :: Assam
C.T.C.
Principal
Nowgong Girls' College
Nagaon :: Assam

hydrogen bonds with incorporation of oxygenated plasma species should be higher with higher treatment time and due to which the 3 min plasma treated nanofiber shows better mechanical properties than 1 min plasma treated nanofibers. However, this always cannot be true as there must be a saturation point for each type of surface modification. Eventually, it was reported that after longer exposure to plasma species a surface may experience dehydration and etching which results in loosing of inherent strength of the polymer chains due to which weak mechanical properties may result (Baltazar-y-Jimenez et al. 2008). In this work, similar results are observed after 5 and 10 min of plasma treatment, where the mechanical performance of the nanofibers in terms of tensile strength and Young's modulus decrease further. Therefore, 1–3 min of DBD plasma treatment time should be sufficient for improvement of mechanical properties of silk/AMOX/PVA nanofibers. However, the rate of improvement of tensile strength from untreated to 1 min plasma-treated silk/AMOX/PVA nanofiber has been found to be much higher (27.17%) than when compared to that of 1–3 min plasma-treated nanofibers (3.03%). Therefore, it is obvious that major part of the modifications was already facilitated by 1 min O_2 plasma treatment. However, with increase in tensile strength, the elongation-at-break is found to be decreased after O_2 plasma treatment. This indicates incorporation of rigidity or stiffness to the nanofiber surface through O_2 plasma treatment (Das et al. 2018; Ojah et al. 2019a, b).

Chemical analysis

The chemical properties of the nanofibers were studied with the help of ATR-FTIR analysis. Figure 3a shows the ATR-FTIR spectra of *Bombyx mori* silk, PVA, AMOX and silk/AMOX/PVA nanofiber. The *Bombyx mori* silk shows its characteristic peaks at 1619, 1511 and 1228 cm^{-1} which corresponds to amide-I (C=O stretching), amide-II (secondary NH bending), and amide-III (C–N and N–H functionalities) respectively (Ojah et al. 2019a). The wide-ranging band between 3000 and 3500 cm^{-1} corresponds to the overlapping of hydrogen bonded -OH stretching vibration and -NH stretching vibrations of the primary amine groups (Ojah et al. 2019a). PVA shows the -OH stretching vibration of intermolecular and intramolecular hydrogen bonding at 3276 cm^{-1}, the symmetric and asymmetric vibrations of CH groups are found at 2941 and 2910 cm^{-1}, respectively (Ojah et al. 2019a). The other characteristic peaks of PVA have been observed at 1650, 1542, 1416 and 1378 cm^{-1} which

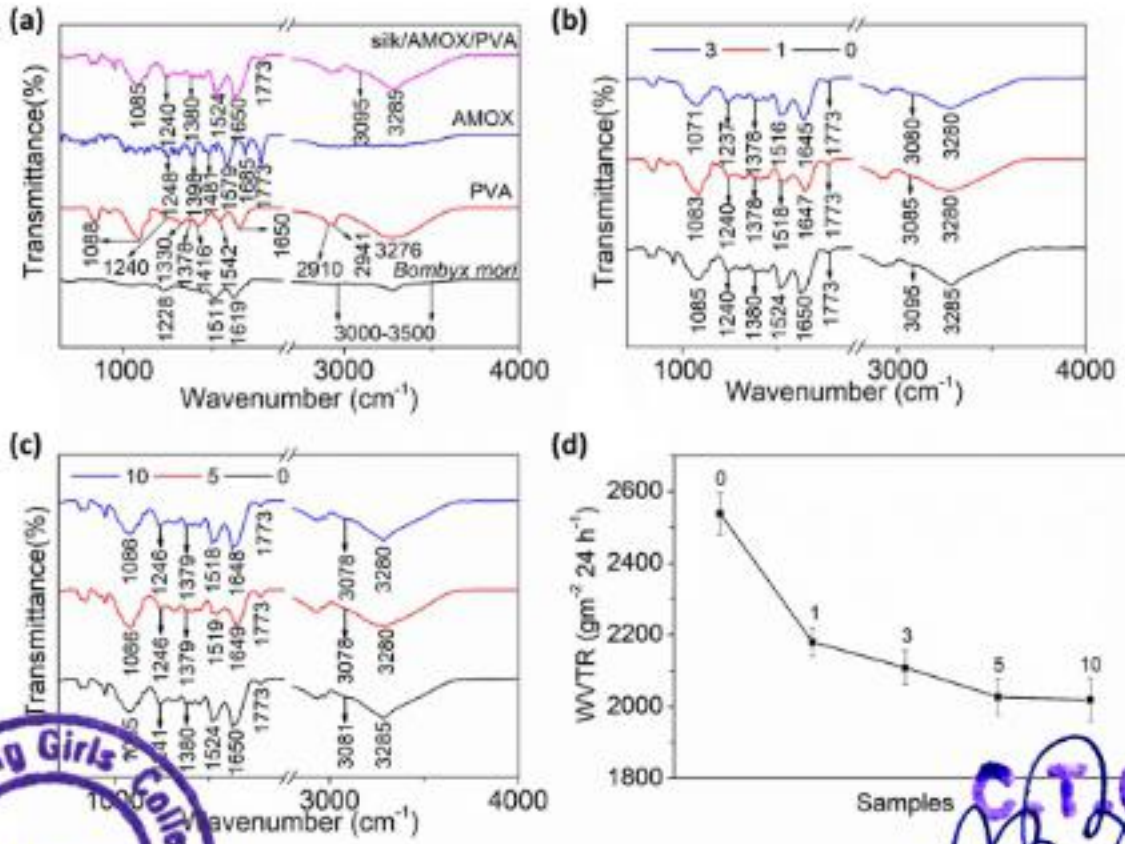

Fig. 3 a–c ATR-FTIR and d WVTR of the plasma treated and untreated silk/AMOX/PVA nanofibers. Where 0 indicates untreated silk/AMOX/PVA nanofibers and 1, 3, 5 and 10 indicates silk/AMOX/PVA nanofibers plasma treated for 1, 3, 5 and 10 min respectively

Nowgong Girls College ESTD: 1962 Nagaon :: Assam
Principal Nowgong Girls' College Nagaon :: Assam

correspond to the C–O stretching vibrations, C=C stretching vibrations, CH_2 bending vibrations and CH stretching vibrations respectively (Das et al. 2018; Ojah et al. 2019a). The peaks at 1330, 1240 and 1088 cm^{-1} are due to CH deformation, CH wagging and C–O stretching vibrations of acetyl groups (Ojah et al. 2019a). The ATR-FTIR spectra of AMOX was also evaluated for a better comparison. The characteristic peaks of AMOX are observed at 1773, 1685, 1481 and 1248 cm^{-1} which correspond to the β-lactam ring of AMOX, C=O stretching vibration (amide I), N–H bending of secondary amine/C–C stretching of aromatic ring and C–N stretching vibration of primary amine (Ojah et al. 2019a, b). The peaks at 1579 and 1398 cm^{-1} correspond to the asymmetric and symmetric vibrations of carboxylate COO^- group (Ojah et al. 2019a, b). The ATR-FTIR curve for the composite nanofiber silk/AMOX/PVA was also plotted for further understanding. The composite nanofiber shows both peaks of silk and PVA. Furthermore, the peaks of AMOX are also clearly observed in the nanofiber backbone.

To evaluate the possible effects of O_2 plasma treatment time on the nanofiber chemical structure, the ATR-FTIR spectra of the plasma treated nanofibers at different times were also plotted for clear understanding and evaluations. All the nanofibers, independent of the treatment time, show the silk, PVA and AMOX peaks clearly. However, few changes are observed in the ATR-FTIR spectra of the plasma-treated nanofibers in terms of their peak positions.

The ATR-FTIR spectra of O_2 plasma treated silk/AMOX/PVA nanofibers are plotted in Fig. 3b, c. A one minute plasma-treated silk/AMOX/PVA nanofibers show broadening and shifting of the OH-NH band (3285–3280 cm^{-1}) towards lower wavenumber. The shifting and broadening of this band is due to incorporation of polar functional groups on the silk/AMOX/PVA nanofibers surface which is also evidenced in water contact angle and surface energy calculations (Das et al. 2018; Ojah et al. 2019a). The change in surface chemistry of the nanofibers after plasma treatment is also evidenced by shifting of the peaks 3095, 1650, 1524, 1380 and 1085 cm^{-1} simultaneously towards lower wavenumbers such as 3085, 1647, 1518, 1378 and 1083 cm^{-1} respectively. These observations are clearly proof of hydrogen bond formation as well as incorporation of oxygen species such as O, O_2, O_2^- etc., on the silk/AMOX/PVA nanofibers surface (Das et al. 2018; Ojah et al. 2019a; Baltazar-y-Jimenez et al. 2008). Similar changes are observed after increasing the plasma treatment time up to 3 min. The peaks have also shifted slightly further towards lower wavenumbers region after 3 min plasma treatment. However, after further increasing the treatment time up to 5 and 10 min, no further shifting of the peak positions are observed. The results are in accordance with other characterizations performed in this work. The incorporation of polar functional groups and increase surface energy of the silk/AMOX/PVA nanofibers is observed to be saturated after 3 min of plasma treatment and hence similar pattern is also observed in the ATR-FTIR analysis in terms of the bands shifting after 3 min of plasma treatment time. Therefore, increasing treatment time beyond 3 min can have no further significant change in the surface chemistry of silk/AMOX/PVA nanofiber.

Water vapor transmission rate study

It was already reported that the cells in a desiccated wound may lose its vitality and functionality and as a result it can die easily (Xu et al. 2016). Furthermore, the dressing in a dehydrated wounded surface is expected to shrink easily and consequently the wound edge exposure might occur which can break the bacterial barrier (Ujang et al. 2014; Queen et al. 1987). Therefore, a good WVTR is important for specific wounds to preserve the hydration and lock moisture into the wounded skin to heal quicker (Xu et al. 2016; Queen et al. 1987). A typical of 2000–2500 gm^{-2} 24 h^{-1} has been considered as standard WVTR for convenient wound dressing, where WVTR values closer to the lower limit (~2000 gm^{-2} 24 h^{-1}) are found very suitable for practical applications (Queen et al. 1987). In this work, the WVTR for the silk/AMOX/PVA nanofibers was found to be 2538 ± 58 gm^{-2} 24 h^{-1} which is towards the higher side of the standard limit. Similarly, the WVTR calculated for the O_2 plasma treated nanofibers were found as 2180 ± 39 gm^{-2} 24 h^{-1}, 2109 ± 48 gm^{-2} 24 h^{-1}, 2027 ± 52 gm^{-2} 24 h^{-1} and 2019 ± 61 gm^{-2} 24 h^{-1} respectively for 1, 3, 5 and 10 min of plasma treatment, respectively. The data are plotted in Fig. 3d for the untreated and plasma-treated silk/AMOX/PVA nanofibers. It is observed that with increasing treatment time the WVTR decreases continuously up to 5 min and thereafter it becomes almost saturated. Therefore, it is observed that the plasma treatment gives a much stronger barrier for the water vapor to pass through the nanofiber area. Similar work was reported already, where low temperature plasma treatment was utilized to improve the barrier properties of polymeric films or scaffolds (Wang et al. 2011). However, in this work, the WVTR rates after plasma treatment are not only still under the standard limit but also it is much closer to the lower limit of the standard values which is to a certain extent much acceptable in case of a good wound healing scaffold (Queen et al. 1987).

Drug release study

The drug release rate of silk/AMOX/PVA nanofiber was studied until saturation was obtained in the release profile. The standardization graph and the release profiles of the untreated and O_2 plasma treated nanofibers are shown in Fig. 4. It is observed that all the nanofiber showed a faster

Nowgong Girls' College ESTD: 1962 Springer Nagaon :: Assam
Principal
Nowgong Girls' College
Nagaon :: Assam

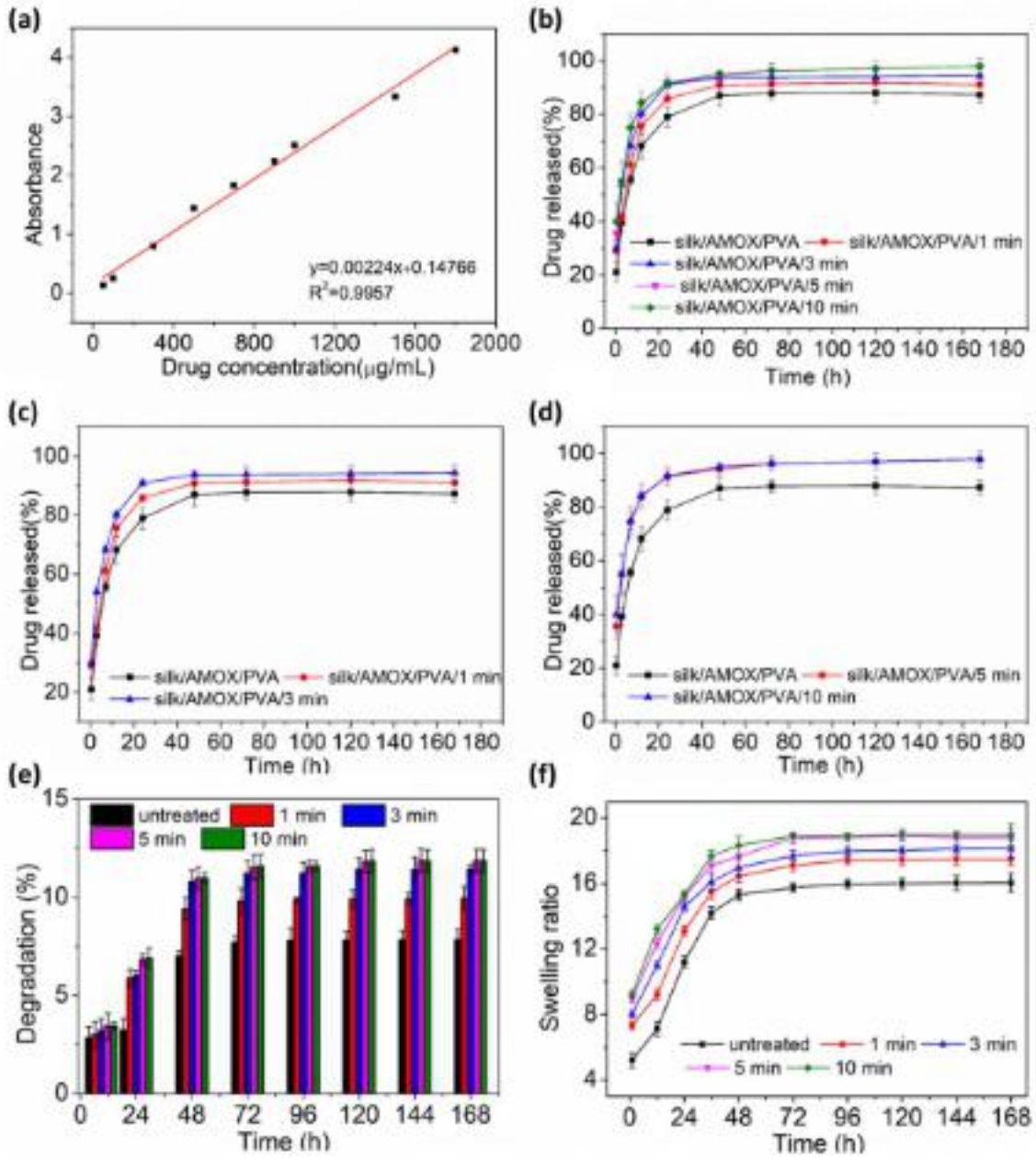

Fig. 4 **a** Standardization graph for AMOX released in PBS 7.4pH for different drug concentrations. **b–d** are drug release profiles of the plasma treated and untreated silk/AMOX/PVA nanofibers with different treatment time ranging from 1 to 10 min. **e** and **f** are degradation (%) and swelling ratio of the untreated and plasma treated silk/PVA nanofibers for 1, 3, 5, 10 min respectively

and continuous drug release rate up to 3 days and thereafter saturation was obtained. The untreated nanofiber showed a release of 78.94% after 24 h. At the same time the plasma treated nanofibers showed a release of 85.83%, 90.97%, 91.55% and 91.71% respectively after 1, 3, 5 and 10 min of plasma treatment. Therefore, most of the drug release was observed within just 24 h of incubation time. Moreover, a comparatively higher drug release rate was observed after plasma treatment. The drug release rate was found to be higher with increase in treatment time up to 5 min and thereafter no further increase in drug release rate was observed, even for increasing treatment time up to 10 min. The increase in drug release rate with plasma treatment is due to increase in wettability of the nanofibers after plasma treatment (Ojah et al. 2019a). As observed from the water contact angle measurement, the wettability was increased with increasing treatment time and it saturated after 5 min of treatment time. Therefore, it is expected that the nanofiber with higher wettability would tend to degrade faster (Ojah et al. 2019a). The degradation of the nanofibers is presented

Nowgong Girls' College
ESTD: 1962
Nagaon :: Assam
Principal
Nowgong Girls' College
Nagaon :: Assam

in Fig. 4e. From Fig. 4e, a low percentage of degradation was observed which is due to the PVA content of the nanofibers as the *bombyx mori* silk has a slow degradation rate in neutral PBS (Liu et al. 2015). The increase in percentage of degradation will result in release of more encapsulated AMOX particles from the nanofiber backbone (Ojah et al. 2019a) and, therefore, increase in drug release rate was recorded for plasma treated electrospun nanofibers. However, in the drug release process from the nanofibers, along with degradation the swelling also plays an important role (Ojah et al 2019b). The β-sheet structure of the silk fibroin gives rise to its characteristic hydrophobicity, crystallinity and insolubility in neutral aqueous medium (Tomeh et al. 2019; Kundu et al. 2014). The silk fibroin begins to swell and form gel-like consistency as soon as it encounters the aqueous medium (Dyakonov et al. 2012; Pollini and Paladini 2020). The gel transition causes hydration and relaxation of the silk polymer chains (Dyakonov et al. 2012; Subia and Kundu 2012). This would cause the drug molecules being lost from the nanofiber backbone and releasing of the drug into the aqueous medium is observed. Therefore, this could also be a reason behind the release of AMOX particles attached onto the nanofibers (Subia and Kundu 2012; Ojah et al 2019a, b). The swelling ratio of the nanofibers is reported in Fig. 4f. It is observed that the plasma treatment enhances the swelling ratio of the nanofibers, which increases with increasing treatment time and eventually saturates after 5 min of treatment time.

However, the drug release rate observed in this case is found much higher than earlier reported work (Ojah et al. 2019a). The silk/PVA nanofiber reported earlier showed a comparatively slower drug release rate for a longer period of time due to its core–shell structure (Ojah et al. 2019a). The drug was enclosed by PVA barrier, and therefore, it took longer to be released from the nanofiber structure (Ojah et al. 2019a). However, in case of silk/AMOX/PVA nanofiber, the antibiotic drug AMOX has been encapsulated at the surface as well as within the nanofibers porous structure. Therefore, it is obvious to observe faster drug release rates in this case. The drugs present at the surface will release as soon as it comes into contact with the aqueous media and the rest will eventually release with increase in incubation time through degradation and swelling as discussed above.

Antibacterial activity

Figure 5 shows the qualitative bacterial test results against *E. coli* (gram negative) and *S. aureus* (gram positive) bacteria for the untreated and plasma-treated silk/AMOX/PVA nanofibers after 24 h of incubation. All the nanofibers showed almost clear inhibition zone against both bacteria. The untreated silk/AMOX/PVA nanofibers showed minimal inhibition zone of 21.45 ± 4.36 mm and 31.87 ± 5.36 mm against *E. coli* and *S. aureus*. The respective zone of inhibition for all the nanofibers against both *E. coli* and *S. aureus* is represented in Fig. 5. The inhibition zone for the untreated nanofibers starts to decrease from the next day and finally vanishes after 72 h. However, plasma-treated nanofibers with variable time showed a slightly higher inhibition zone compared with untreated nanofibers. The plasma-treated nanofibers with longer treatment time showed increasingly higher inhibition zone. The higher drug release after plasma treatment is the reason behind such greater inhibition zone. All the other plasma-treated nanofibers (1, 3, 5 min) showed clear inhibition zone for 48 h, which later decreased gradually and finally vanished after 120 h.

Hemolytic activity analysis

To explore the potential application of the electrospun nanofibers as a wound dressing, hemocompatibility of all the nanofibers was assessed with the help of hemolysis activity assay. The hemolysis activity of various O_2 plasma-treated and untreated electrospun silk/AMOX/PVA nanofibers is shown in Fig. 6a. All the electrospun nanofibers show much less hemolysis activity below 0.4%, suggesting their hemocompatibility behavior, when compared to the positive control in 100% cell lysis. However, there is no statistical difference in the percentage of hemolysis activity among the O_2 plasma-treated and untreated nanofibers. The percentage of hemolysis activity of the untreated nanofibers and O_2 plasma-treated nanofibers for 1 and 3 min are almost similar, whereas nanofibers treated with O_2 plasma for 5 and 10 min are slightly higher (Fig. 6a). The slight variations in this observation have been discussed below.

The intrinsic hemocompatibility of silk fibroin and PVA is already demonstrated (Marilia et al. 2014; Nuno et al. 2014). O_2 gas plasma is very reactive etching agent due to higher electronegativity of oxygen. The successful incorporation of oxygen containing polar functional groups (viz. hydroxyl (-OH), aldehyde (-CHO), carboxyl (-COOH), etc.) after O_2 plasma treatment was demonstrated by ATR-FTIR results. It is likely possible that the increased surface hydrophilicity (as indicated by contact angle measurement and analysis) due to incorporation of the above polar functionaries, aid the covalent interaction between the nanofibers and the cell surface proteins leading to minimal hemolysis. Additionally, O_2 plasma treatment also creates intermediate free radicals on polymer surface as previously reported (Kumar and Borah 2016). Hence, the possible [illegible] of the free radicals created due to [illegible] plasma treatment (5 and 10 min) may evoke [illegible] static interaction

Principal
Nowgong Girls' College
Nagaon :: Assam
Nowgong Girls' College ESTD: 1962 Nagaon :: Assam

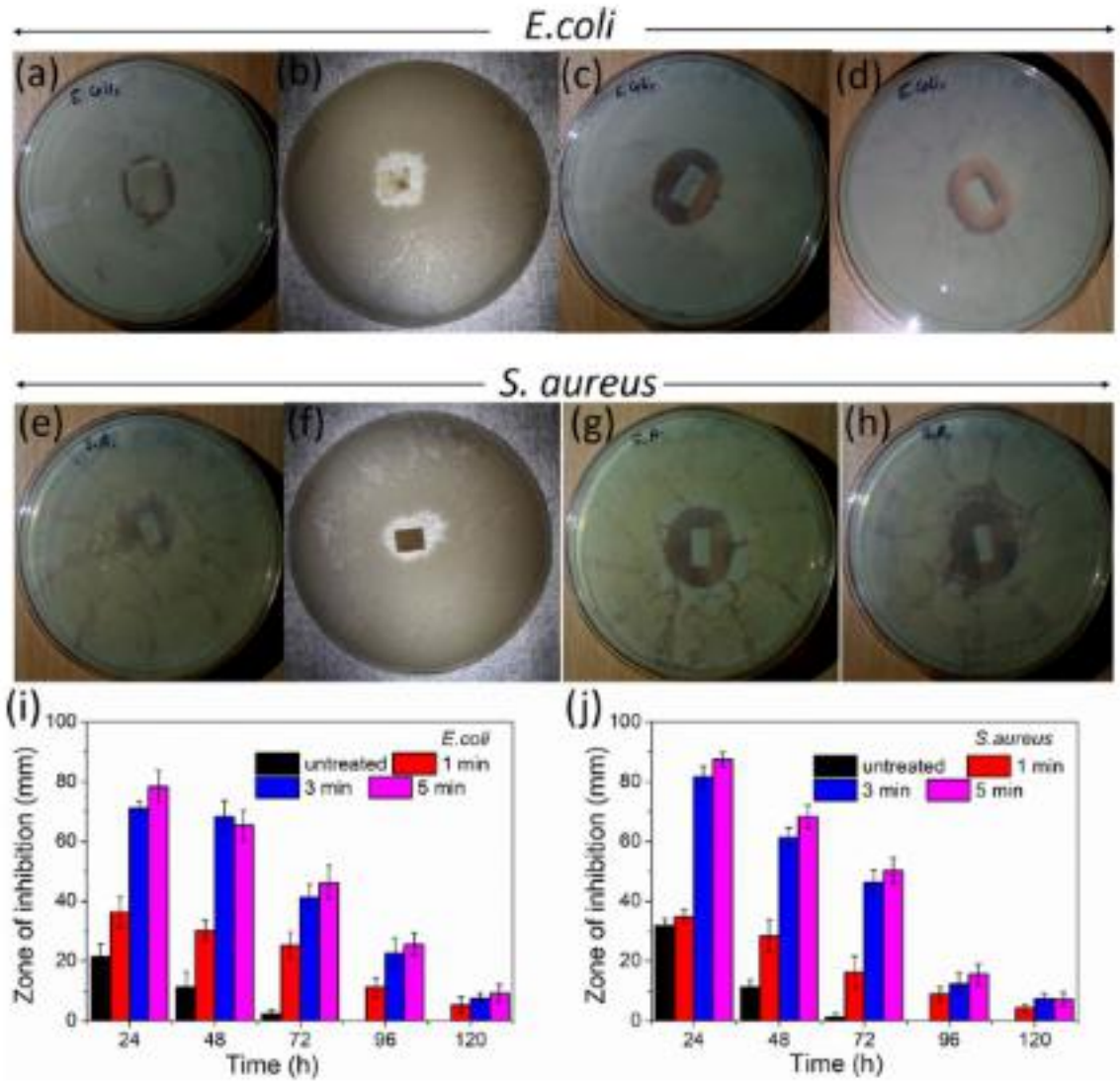

Fig. 5 Antibacterial activities of the untreated and plasma treated nanofibers against *S. aureus* and *E. coli* bacteria. Where, **a**, **e** are untreated; **b**, **f** are 1 min; **c**, **g** are 3 min; **d**, **h** are 5 min plasma treated nanofibers. **i** and **j** are zone of inhibition for the untreated and plasma treated silk/AMOX/PVA nanofibers for 1, 3, 5 min respectivelyagainst *E. coli* and *S. aureus* bacteria

between the nanofiber surface and cell surface, leading to slight increase in the hemolysis percentage.

Overall, the results suggest that there is no adverse effect of O_2 plasma treatment on the electrospun nanofibers, which causes very less hemolysis (below 0.4%) well within the acceptable limit of 5% hemolysis to qualify for biological applications.

Cell viability test

In vitro cell viability studies were carried out to investigate the cytocompatibility of the various electrospun nanofibers by MTS proliferation assay and live/dead staining of primary hUMSCs. The MTS results are presented in terms of percentage cell viability after 24 and 48 h of culture time on various electrospun nanofibers, as shown in Fig. 6b. The results reveal that all the nanofibers (both O_2 plasma-treated and untreated) supported cell growth viability of 70–80% at the initial 24 h except the nanofibers treated with O_2 plasma for 1 min revealing slightly higher 80% cell viability, which is an accepted value for biocompatible materials (Bae et al. 2012). However, after 48 h, all the electrospun nanofibers supported more than 80% cell viability, with O_2 plasma-treated nanofibers for 1 and 3 min showing more than 100% cell viability. Biocompatibility of the silk fibroin and PVA is well explored which supports the observed cytocompatibility of the untreated nanofibers (Wang et al. [illegible] et al. 2012). The MTS results are in well agreement with the

CTC
Principal
Nowgong Girls' College
Nagaon :: Assam
Nowgong Girls' College
ESTD: 1962
Nagaon :: Assam

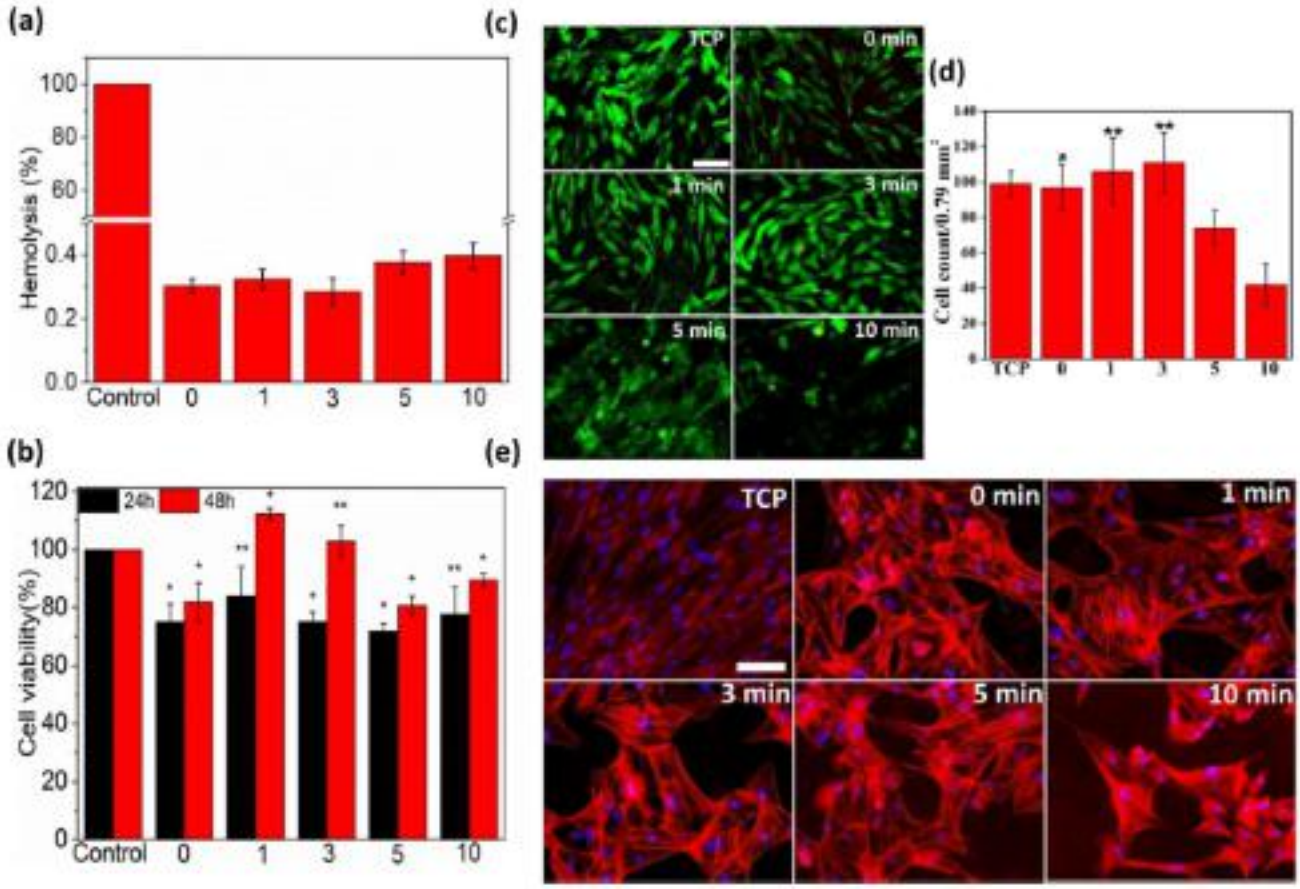

Fig. 6 In-vitro biological studies results. **a** Percentage of hemolysis (Mean ± S.D, $n = 3$) shown by untreated and O_2 plasma treated silk/AMOX/PVA nanofibers, where, 0 indicates untreated nanofibers and 1, 3, 5 and 10 indicates plasma treated nanofibers for 1, 3, 5 and 10 min, respectively, as compared to positive control (Triton X 100). **b** Percentage cell viability on different silk/AMOX/PVA nanofibers as compared to tissue culture plastic (TCP) as a negative control. **c** Representative fluorescent images of ADMSCs stained with calcein AM (green) and EthD-1 (red) during live/dead assay after 48 h of culture on control TCP and the different electrospun nanofibers as indicated. **d** Live cell count on untreated and plasma treated electrospun nanofibers. **e** Representative fluorescent images of ADMSCs stained with rhodamine phalloidin for the actin filaments (red) and nuclei counterstained with Hoechst (blue) after 72 h of culture on control TCP and different electrospun nanofibers as indicated. *and **indicate statistically significance at $p < 0.05$ and $p < 0.01$. [Microscope image, scale: 200 mm]

hemolysis activity results in the sense that the silk/AMOX/PVA electrospun nanofibers treated with O_2 plasma for 1 and 3 min demonstrated the higher cell growth and hemocompatibility, when compared to those of the untreated and the other plasma-treated nanofibers for longer period. In fact, all the O_2 plasma-treated silk/AMOX/PVA electrospun nanofibers supported significantly higher cell growth when compared to that of the untreated nanofibers. This can be attributed to the incorporation of oxygen-containing polar functionalities on the nanofiber's surface leading to favorable cell-biomaterial interaction for cell growth. This initial observation suggests no cytotoxic effect of the O_2 plasma treatment on cell growth. Yet the plasma-treated nanofibers for 1 and 3 min demonstrated highest viability of the primary mesenchymal stem cells even more that on the control tissue culture plastic (TCP), which are statistically significant.

To further confirm the MTS results, the live/dead assay was performed to visualize the viable ADMSCs cultured on different electrospun nanofibers by staining the cells with calcein AM (stained live cells in green) and EthD-1 (stained dead cells in red) after 48 h of culture. Representative fluorescent images of the ADMSCs seeded on the untreated and O_2 plasma- treated silk/AMOX/PVA nanofibers are shown in Fig. 6c. The green-fluorescent calcein AM can be visualized throughout almost all the cell bodies seeded on different electrospun nanofibers indicating the viable cells, except few dead cells (red). For further validation, live cell counting has been performed using calcein AM stained (green) cells and is presented in Fig. 6d. It has been observed that O_2 plasma treated electrospun nanofibers for 1 and 3 min showed significantly higher live cell density, i.e., 1[illegible] per image and

Principal
Nowgong Girls' College
Nagaon :: Assam
Springer
Nowgong Girls' College
ESTD: 1962
Nagaon :: Assam

111 ± 16/per image, respectively than that on the untreated (95 ± 13/per image) and other O_2 plasma-treated electrospun nanofibers for 5 min (74 ± 12/per image) and 10 min (42 ± 10/per image) ($p \leq 0.01$) and the untreated (95 ± 13/per image) nanofibers ($p \leq 0.05$). However, there are no statistical differences in live cell density exist between the control TCP and the 1 and 3 min plasma treated nanofibers. This indicates that 1 and 3 min plasma treated nanofibers exhibit similar live cell density to that on the control TCP indicating good cell viability and adhesion, while other plasma treated nanofibers for 5 and 10 min revealed significantly less live cell density indicating poor cell viability and adhesion. The ADMSCs seeded on the untreated and plasma-treated nanofibers for 1 and 3 min, appeared to be spindle shaped, elongated and healthier when compared to the poor and round- shaped cell morphology on the electrospun nanofibers treated with O_2 plasma for 5 and 10 min. Furthermore, the ADMSCs adopted randomized orientation owing to the randomly oriented nanofiber morphology. The enhanced cell adhesion and improved cell morphology on the O_2 plasma-treated electrospun nanofibers may be attributed to the presence of oxygen-containing polar functional groups on the surface of the nanofiber, which induces better interaction between the nanofibers and the cell surface integrin proteins. However, lower live cell density and poor cell morphology on the electrospun nanofibers treated with O_2 plasma for 5 and 10 min may be due to the free radicals present on the surface of the nanofibers, which induce unfavorable electrostatic interaction/oxidative stress causing cell death.

The live/dead staining results also demonstrate the cytocompatibility of the O_2 plasma- treated electrospun meshes matching the findings of the hemolysis and MTS results. It further reveals that O_2 plasma treatment for shorter period (1 and 3 min) aids favorable surface hydrophilicity towards cell adhesion and spreading when compared to those plasma-treated nanofibers for longer period (5 and 10 min).

Cytoskeletal architecture assessment

To further confirm the cell adhesion and cell morphology as observed during live/dead staining, the ADMSCs seeded on different electrospun nanofibers were stained using rhodamine conjugated to phalloidin after 72 h of culture, which again counter-stained with hochest for nucleus. Representative fluorescent images of ADMSCs seeded on different nanofibers are shown in Fig. 8e. The results confirm the ADMSCs attachment on various electrospun nanofibers. The cell number counted from hochest nucleus staining were found to be 29 ± 4 (untreated), 33 ± 5 (1 min), 28 ± 5 (3 min), 20 ± 3 (5 min), and 18 ± 13 (10 min), while for TCP it is 78 ± 15 per image. Although, these numbers are not statistically different, it postulated that there is no negative impact of O_2 plasma treatment for shorter period on the cell adhesion. It further validated our previous observation during hemolysis assay, MTS assay and live/dead staining that the plasma treatment for longer period (particularly, 5 and 10 min) do not hold biological efficiency in terms of hemocompatibility and cell growth. It is important to note that although TCP showed highest cell numbers attached to it, cell morphology is different from those on the electrospun nanofibers offering 3D paradigm for cell growth/spreading (polygonal shaped), while TCP is a flat surface (spindle shaped). Moreover, the cells grown on the untreated and O_2 plasma-treated electrospun nanofibers for 1, 3 and 5 min appeared to be bigger in size, when compared to that on the TCP. In fact, the ADMSCs grown on the TCP appeared to acquire a fibroblastic phenotype, characterized by wide spreading of cells (Ma et al. 2016). The randomized orientation of actin filaments of the ADMSCs grown on various electrospun nanofibers suggest cell spreading in random directions owing to the randomized nanofiber network.

Conclusion

In this study, the effect of treatment time of atmospheric pressure DBD O_2 plasma on the surface properties of silk/AMOX/PVA nanofibers is reported. The treatment time does not cause any morphological changes of the nanofibers which is confirmed by FESEM images. The plasma treatment time of 1–3 min facilitates incorporation of polar functional groups on the surface of the silk/AMOX/PVA nanofiber, which results in improved wettability and higher surface energy values. However, WVTR is observed to be reduced and comes within the suitable range for practical applications with increasing treatment time up to 1–3 min which further saturates with longer treatment time. Similarly, the plasma treatment for an appropriate time (1–3 min) also increases the tensile strength and Young's modulus of silk/AMOX/PVA nanofibers significantly. An increase in drug release rate is also observed with increase in treatment time which eventually helps in the antibacterial activity of the nanofibers for showing a good inhibition zone for a prolonged time. However, despite all the changes, the nanofibers do not show hemolytic effect independent of plasma treatment time. It is also evidenced that, silk/AMOX/PVA nanofibers plasma-treated for shorter period of time (1–3 min) not only shows improved cell viability (> 80%) but also promotes cell spreading with better cell adhesion. However, the rate of surface modification in every characterizations including wettability, surface energy, WVTR, tensile strength, Young's modulus, cell viability etc., are found highest for 1 min of O_2 plasma treatment. Therefore, all these findings can suggest that, DBD plasma treatment for shorter period

Principal
Nowgong Girls' College
Nagaon :: Assam
Nowgong Girls' College ESTD: 1962 Nagaon :: Assam

of time is sufficient for incorporating all the necessary surface modifications to the silk/AMOX/PVA nanofibers which embraces suitable wettability and WVTR, tensile strength and good cellular growth. Moreover, the mechanically stronger silk/AMOX/PVA/O_2 nanofibers can be used further for drug delivery applications where a faster release rate is required. The present study also provides the initial indication of future scope of using ADMSCs based approach in combination with the as-fabricated nanofibrous matrix with antibacterial properties in wound healing applications.

Acknowledgements This research work is supported by DST-SERB (Grant Nos. SR/FTP/PS-147/2012 and EMR/2016/006146) funded by the Department of Science and Technology (DST), India. Science and Technology (DST), Arup Jyoti Choudhury expresses his gratitude to the DST-INSPIRE Faculty Fellowship (Grant No. IFA14-PH-93) for the financial support to carry out this research work and Tezpur University, Assam, India for hosting the fellowship. Namita Ojah acknowledges the support provided by DST-INSPIRE and DST-SERB in the form of fellowship. The assistance of Kaushik Nath, Aftab Ansari, Dr. Dambarudhar Mohanta and Piyush Kumar Mishra, Department of Physics, Tezpur University, in carrying out the hemolysis test and UV measurement is acknowledged gratefully. The assistance of Dr. Saurav Haloi, Department of Molecular Biology and Biotechnology is acknowledged thankfully in carrying out the antibacterial tests.

Compliance with ethical standards

Conflict of Interest The authors declare no conflict of interest.

Ethical approval This article does not contain any studies with human participants or animals performed by any of the authors.

References

Bae SH, Che JH, Seo JM, Jeong J, Kim ET, Lee SW, Koo KI, Suaning GJ, Lovell NH, Cho DD, Kim SJ, Chung H (2012) In vitro biocompatibility of various polymer-based microelectrode arrays for retinal prosthesis. Invest Ophthal Vis Sci 53:2653–2657

Balcon N, Aanesland A, Boswell R (2007) Pulsed RF discharges, glow and filamentary mode at atmospheric pressure in argon. Plas Sour Sci Technol 16:217–225

Baltazar-y-Jimenez A, Bistritz M, Schulz E, Bismarck A (2008) Atmospheric air pressure plasma treatment of lignocellulosic fibres: impact on mechanical properties and adhesion to cellulose acetate butyrate. Compo Sci Tech 68:215–227

Cestari M, Muller V, Rodrigues JHDS, Nakamura CV, Rubira AF, Muniz EC (2014) Preparing silk fibroin nanofibers through electrospinning: further heparin immobilization toward hemocompatibility improvement. Biomacromol 15:1762–1767

Choudhury AJ, Gogoi D, Kandimalla R, Kalita S, Choudhary YB, Khan MR, Kotoky J, Chutia J (2016) Penicillin impregnation on oxygen plasma surface functionalized chitosan/Antheraea assama silk fibroin: studies of antibacterial activity and antithrombogenic property. Mater Sci Engg C 60:475–484

Chouhan D, Mandal BB (2020) Silk biomaterials in wound healing and skin regeneration therapeutics: from bench to bedside. Acta Biomater 103:24–51

Chutia H, Kalita D, Mahanta C, Ojah N, Choudhury AJ (2019) Kinetics of inactivation of peroxidase and polyphenol oxidase intender coconut water by dielectric barrier discharge plasma. LWT-Food Sci Tech 101:625–629

Das P, Ojah N, Kandimalla R, Mohan K, Gogoi D, Duloi SK, Choudhury AJ (2018) Surface modification of electrospun PVA/chitosan nanofibers by dielectric barrier discharge plasma at atmospheric pressure and studies of their mechanical properties and biocompatibility. Int J Biol Macromol 114:1026–1032

Demirci S, Doğan A, Sahin F (2018) Role of adipose-derived stem cells in wound healing: an update from isolation to transplantation. Wound healing: stem cells repair and restorations, basic and clinical aspects, pp 133–147

Dyakonov T, Yang CH, Bush D, Gosangari S, Majuru S, Fatmi S (2012) Design and characterization of a silk-fibroin-based drug delivery platform using Naproxen as a model drug. J Drug Delivery 2012:490514

Foruzan E, Akmal AAS, Niayesh K, Lin J, Sharma DD (2018) Comparative study on various dielectric barriers and their effect on breakdown voltage. High Volt 3:51–59

Gomide VS, Zonari A, Ocarino NM, Goes AM, Serakides R, Pereira MM (2012) In vitro and in vivo osteogenic potential of bioactive glass–PVA hybrid scaffolds colonized by mesenchymal stem cells. Biomed Mater 7:01500

Hassan WU, Greiser U, Wang W (2014) Role of adipose-derived stem cells in wound healing. Wound Repair Regener 22:313–325

Hetemi D, Pinson J (2017) Surface functionalisation of polymers. Chem Soc Rev 46:5701

Jeong S, Yeo IS, Kim HN, Yoon YI, Jung SY, Min BM, Park WH (2009) Plasma-treated silk fibroin nanofibers for skin regeneration. Int J Biol Macromol 44:222–228

Kajdic S, Planinsek O, Gasperlin M, Kocbek P (2019) Electrospun nanofibers for customized drug-delivery systems. J Drug Delivery Sci Technol 51:672–681

Krishnakumar GS, Sampath S, Muthusamy S, John MA (2019) Importance of crosslinking strategies in designing smart biomaterials for bone tissue engineering: a systematic review. Mater Sci Engg C96:941–954

Kumar A, Borah R (2016) Effect of plasma irradiation on biocompatibility and cell adhesion of polyaniline/chitosan nanocomposites towards Hep G2 and PBMC cells. Adv Mater Proc 1:146–155

Kundu B, Kurland NE, Yadavalli VK, Kundu SC (2014) Isolation and processing of silk proteins for biomedical applications. Int J Bio Macromol 70:70–77

Lee M, Ko YG, Lee JB, Park WH, Cho D, Kwon OH (2014) Hydrophobization of silk fibroin nanofibrous membranes by fluorocarbon plasma treatment to modulate cell adhesion and proliferation behavior. Macromol Res 22:746–752

Liu B, Song YW, Jin L, Wang ZJ, Pu DY, Lin SQ, Zhou C, You HJ, Ma Y, Li JM, Yang L, Sung KLP, Zhang YG (2015) Silk structure and degradation. Colloids Surf B 131:122–128

Ma S, Xie N, Li W, Yuan B, Shi Y, Wang Y (2014) Immunobiology of mesenchymal stem cells. Cell Death Differ 24:216–225

Meghdadi M, Atyabi SM, Pezeshki-Modaress M, Irani S, Noormohammadi Z, Zandi M (2019) Cold atmospheric plasma as a promising approach for gelatin immobilization on polyε-caprolactone electrospun scaffolds. Prog Biom[illegible]:65–[illegible]

Molavi AM, Sadeghi-Avalshahr A, [illegible], Nokhasteh S, Mohammadi-Samani S, Mohammadi H (2020) Enhanced biological properties of collagen/chitosan coated poly(ε-caprolactone) scaffolds by surface modification with GHK-Cu peptide and 58S bioglass. Prog Biomater 9:25–34

Nedela O, Slepicka P, Švorčík V (2017) Surface modification of polymer substrates for biomedical applications. Mater 10:1115

Nowgong Girls' College ESTD: 1962 Springer Nagaon :: Assam

GSTC

Principal
Nowgong Girls' College
Nagaon :: Assam

Nuno A, Ribeiro GA, Pereira T, Amorim I, Fragoso J, Lopes A, Fernandes J, Costa E, Santos Silva A, Rodrigues M, Santos JD, Mauricio AC, Luis AL (2014) Biocompatibility and hemocompatibility of polyvinyl alcohol hydrogel used for vascular grafting—In vitro and in vivo studies. J Biomed Mater Res Part A 102:4262–4275

Ojah N, Saikia D, Gogoi D, Baishya P, Ahmed GA, Ramteke A, Choudhury AJ (2019) Surface modification of core-shell silk/PVA nanofibers by oxygen dielectric barrier discharge plasma: studies of physico-chemical properties and drug release behavior. App Surf Sci 475:219–229

Ojah N, DekaJ HS, Kandimalla R, Gogoi D, Medhi T, Mandal M, Ahmed GA, Choudhury AJ (2019) Chitosan coated silk fibroin surface modified by atmospheric dielectric-barrier discharge (DBD) plasma: a mechanically robust drug release system. J Biomater Sci Polym Ed 30:1–16

Ozkan A, Dufour T, Silva T, Britun N, Snyders R, Bogaerts A, Reniers F (2016) The influence of power and frequency on the filamentary behaviorof a flowing DBD application to the splitting of CO2. Plasma Sources Sci Technol 25:025013

Petlin DG, Tverdokhlebov SI, Anissimov YG (2017) Plasma treatment as an efficient tool for controlled drug release from polymeric materials: a review. J Cont Rel 266:57–74

Pollini M, Paladini F (2020) Bioinspired materials for wound healing application: the potential of silk fibroin. Materials 13:3361

Queen D, Gaylor JDS, Evans JH, Courtney JM, Reid WH (1987) The preclinical evaluation of the water vapour transmission rate through burn wound dressings. Biomaterials 8:367–371

Ray D, Subramanyam C (2016) CO_2 decomposition in a packed DBD plasma reactor: influence of packaging materials. RSC Adv 6:39492

Rezaei F, Shokri B, Sharifian M (2016) Atmospheric-pressure DBD plasma-assisted surface modification of polymethyl methacrylate: a study on cell growth/proliferation and antibacterial properties. App Sur Sci 360:641–651

Ribeiro VP, Almeida LR, Martins AR, Pashkuleva I, Marques AP, Ribeiro AS, Silva CJ, Bonifacio G, Sousa RA, Reis RL, Oliveira AL (2016) Influence of different surface modification treatments on silk biotextiles for tissue engineering applications. J Biomed Mater Res B104:496–507

Saeed SM, Hamid Mirzadeh H, Zandi M, Barzin J (2017) Designing and fabrication of curcumin loaded PCL/PVA multi-layer nanofibrous electrospun structures as active wound dressing. Prog Biomater 6:39–48

Shababdoust A, Ehsan M, Shokrollahi P, Zandi M (2018) Fabrication of curcumin-loaded electrospun nanofiberous polyurethanes with anti-bacterial activity. Prog Biomat 7:23–33

Simor M, Creyghton Y, Wypkema A, Zemek J (2010) The influence of surface DBD plasma treatment on the adhesion of coatings to high-tech textiles. J Adhes Sci Tech 24:77–97

Subia B, Kundu SC (2012) Drug loading and release on tumor cells using silk fibroin–albumin nanoparticles as carriers. Nanotechnology 24:035103

Theapsak S, Watthanaphanit A, Rujiravanit R (2010) Preparation of chitosan-coated polyethylene packagingfilms by DBD plasma treatment. ACS App Mater Interf 4:2474–2482

TomehMhd A, Hadianamrei R, Zhao X (2019) Silk fibroin as a functional biomaterial for drug and gene delivery. Pharmaceutics 11:494

Ujang Z, Rashid AHA, Suboh SK, Halim AS, Lim CK (2014) Physical properties and biocompatibility of oligochitosan membrane film as wound dressing. J Appl Biomater Funct Mater 12:155–162

Wang Y, Kim HJ, Vunjak-Novakovic G, Kaplan DL (2006) Stem cell-based tissue engineering with silk biomaterials. Biomaterials 27:6064–6082

Wang C, Lai PC, Syu SH, Leu J (2011) Effects of CF4 plasma treatment on the moisture uptake, diffusion and WVTR of poly(ethylene terephthalate) flexible films. Sur Coat Tech 206:318–324

Wang C, Zhang G, Wang X (2012) Comparisons of discharge characteristics of a dielectric barrier discharge with electrode structures. Vacuum 86:960–964

Williams KL, Godke RA, Bondioli KR (2011) Isolation and culture of porcine adipose tissue-derived somatic stem cells. Methods Mol Biol 702:77–86

Xiaoping T, Rongde Lu, Hui L (2012) Electrical characteristics of dielectric-barrier discharges in atmospheric pressure air using a power-frequency voltage source. Plasma Sci Technol 14:723

Xu R, Xia H, He W, Li Z, Zhao J, Liu B, Wang Y, Lei Q, Kong Y, Bai Y, Yao Z, Yan R, Li H, Zhan R, Yang S, Luo G, Wu J (2016) Controlled water vapor transmission rate promotes wound-healing via wound re-epithelialization and contraction enhancement. Sci Rep 6:24596

Yoshida S, Hagiwara K, Hasebe T, Hotta A (2013) Surface modification of polymers by plasma treatments for the enhancement of biocompatibility and controlled drug release. Sur Coat Tech 233:99–107

Yucel T, Lovett ML, Kaplan DL (2014) Silk-based biomaterials for sustained drug delivery. J Cont Rel 190:381–397

Zhang Z, Zhao Z, Zheng Z, Liu S, Mao S, Li X, Chen Y, Mao Q, Wang L, Wang F, Wang X, Pan Z, Li G (2019) Functionalization of polyethylene terephthalate fabrics using nitrogen plasma and silk fibroin/chitosan microspheres. App Sur Sci 495:143481

Publisher's Note Springer Nature remains neutral with regard to jurisdictional claims in published maps and institutional affiliations.

Nowgong Girls' College ESTD: 1962 Nagaon :: Assam

Principal
Nowgong Girls' College
Nagaon :: Assam

Dalton Transactions

ROYAL SOCIETY OF CHEMISTRY

PAPER

View Article Online
View Journal

Check for updates

Cite this: DOI: 10.1039/d0dt03054f

Seven-coordinate Ln^{III} complexes assembled from a bulky ^{Mes}acacH ligand: their synthesis, structure, photoluminescence and SMM behaviour†

Pankaj Kalita,[a,b] Prakash Nayak,[a] Naushad Ahmed,[b] Juan Manuel Herrera,[c] Krishnan Venkatasubbaiah,[a,*] Enrique Colacio[*c] and Vadapalli Chandrasekhar[*b,d]

The reaction of a bulky acetyl acetone ligand 1,3-dimesitylpropane-1,3-dione (^{Mes}acacH) with hydrated lanthanide chlorides in the presence of tetramethylammonium hydroxide afforded a new family of neutral mononuclear Ln^{III} complexes $[Ln(^{Mes}acac)_3(DMF)]$ (Ln = Dy (**1**); Tb (**2**); $Y_{0.91}Dy_{0.09}$ (**3**); and Er (**4**)). The molecular structures of these complexes were confirmed by single crystal X-ray diffraction studies. The coordination geometries of the Ln^{III} centre were analysed by SHAPE analysis which revealed a capped octahedral geometry in **1–4**. Photoluminescence studies showed ligand-sensitized green emissions for **2** with an appreciable quantum yield of 0.83%. Static (dc) and dynamic (ac) magnetic studies of complexes **1** and **3** were performed. The dynamic magnetic study revealed that complex **1** exhibits zero-field slow relaxation of the magnetization without showing a clear maximum in the out-of-phase ac susceptibility plots. However, magnetic dilution of **1** with the Y^{III} metal ion (complex **3**) and/or the application of a dc magnetic field induces a strong frequency dependence of the ac susceptibility signals with χ''_M peaks in the 3–10 K temperature range, thus supporting field-induced SMM behaviour of **1**. The relaxation process takes place through a combination of the Orbach and Raman mechanisms. The fitting of the temperature dependence of the relaxation time to the equation $\tau^{-1} = \tau_0^{-1} \exp(-U_{eff}/k_BT) + BT^n$, allows the extraction of the effective energy barrier U_{eff}/k_B = 70 K (48.7 cm^{-1}) and pre-exponential parameter of $\tau_0 = 2.7 \times 10^{-7}$ s for the Orbach mechanism (first term) and the parameters $B = 0.04\ s^{-1}\ K^{-n}$ and $n = 6.11$, for the Raman mechanism (second term).

Received 1st September 2020,
Accepted 7th October 2020
DOI: 10.1039/d0dt03054f
rsc.li/dalton

Introduction

Single-molecule- and single-ion magnets (SMMs and SIMs) have been receiving a lot of attention in recent years.[1] These are molecular systems that once magnetized retain their magnetization for a significantly longer period of time, below certain critical temperatures.[2] While most of the initial efforts were devoted to mainly polynuclear 3d complexes,[3] soon this phenomenon was also observed in heterometallic 3d/4f complexes.[4] In a seminal discovery in 2003, slow magnetic relaxation and magnetic hysteresis were observed for the first time in a mononuclear bis(phthalocyanine)Tb^{III} complex $(TBA)^+[Tb(Pc)_2]^-$ (TBA = tetrabutylammonium).[5] This discovery opened up a new direction for the utilization of 4f-ions in the construction of molecular magnets. Recent advancements in this field reveal that mononuclear complexes could exhibit promising SMM behaviour provided the following two criteria are met: (*a*) the complex should have a bistable spin ground state with a high magnitude of $|m_J|$ *i.e.* an *Ising* ground state, and should possess (*b*) well isolated excited states with magnetic moments co-linear with the ground state.[6] The 4f-ions are considered to be suitable candidates for the design and assembly of molecular magnets due to the fact that many of them possess a fairly large ground state spin, *S*, and also in addition, have intrinsic magnetic anisotropy arising from a large unquenched orbital angular mo[illegible] ground state spin–orbit coupling. One important dra[illegible] of [illegible] 4f complexes, however, is the significa[illegible] the temperature independent zero field quantum tunnelling

[a]School of Chemical Sciences, National Institute of Science Education and Research Bhubaneswar, HBNI, Jatni, Khurda - 752050, Odisha, India. E-mail: krishna@niser.ac.in
[b]Tata Institute of Fundamental Research Hyderabad, Gopanpally, Hyderabad-500 046, India. E-mail: sc@iitk.ac.in, sc@tifr.res.in
[c]Departamento de Química Inorgánica, Facultad de Ciencias, Universidad de Granada, Avenida de Fuentenueva s/n, 18071 Granada, Spain. E-mail: ecolacio@ugr.es
[d]Department of Chemistry, Indian Institute of Technology Kanpur, Kanpur-208016, India

†Electronic supplementary information (ESI) available. CCDC 2023655, 2023662, 2023663 and 2023665. For ESI and crystallographic data in CIF or other electronic format see DOI: 10.1039/d0dt03054f

This journal is © The Royal Society of Chemistry 2020

Nowgong Girls' College ESTD: 1962 Nagaon :: Assam

Principal
Nowgong Girls' College
Nagaon :: Assam

Food Research International 136 (2020) 109599

Contents lists available at ScienceDirect

Food Research International

journal homepage: www.elsevier.com/locate/foodres

An innovative approach for iron fortification of rice using cold plasma

Kumudhini Akasapu[a], Namita Ojah[b], Arun Kumar Gupta[a], Arup Jyoti Choudhury[b], Poonam Mishra[a,*]

[a] Department of Food Engineering and Technology, Tezpur University, Tezpur, Assam 784028, India
[b] Department of Physics, Tezpur University, Tezpur, Assam 784028, India

ARTICLE INFO

Keywords:
Cold plasma
Rice
Surface etching
Fortification
Bioavailability

ABSTRACT

In the present study, an innovative cold plasma treatment was used as a tool to fortify the white rice. The amounts of ferrous sulphate and ascorbic acid were optimized for improving the bioavailability of iron. White rice samples were treated with plasma at a constant voltage of 20 kV for varying time (10 min and 15 min). The exposure time of plasma was selected based on the surface characteristics, hydrophilicity and thermal properties. Significant improvement was observed in the characteristics of hydrophilicity, surface energy, cooking time and hardness of plasma-treated rice. Plasma treated rice was fortified with the optimum concentrations of iron and ascorbic acid solution. Optimum concentrations of iron and ascorbic acid per 100 g of rice (862.93 mg and 1398.27 mg) were found by conducting experiments using Central Composite Design of Response Surface Methodology. Further, rice was blended with untreated rice in the ratio of 1:100 and 1:200 and was packed in LDPE and PP pouches and was stored at ambient temperature for further storage analysis. The in vitro bioavailability of iron was significantly higher in the plasma-treated fortified rice at both 1.35 and 7.5 pH than in the control sample, and plasma treatment significantly reduced the rate of oxidation of iron during storage.

1. Introduction

Anaemia is a condition in which blood lacks enough healthy red blood cells. Iron deficiency anaemia (IDA) is the most common type of micronutrient malnutrition, affecting more than 20% of the world's population (McLean et al., 2009). The major factor responsible for IDA is the consumption of a diet deficient in iron. According to the global data reports for 2018, the prevalence of iron deficiency anaemia is found highest in India, with 39.80% followed by South Africa, China and Japan. To overcome this problem, Governments and the World Health Organisation have initiated programs like food fortification. White rice, which is deficient in iron and B complex vitamins is the most common staple food in the regions where there is a higher prevalence of anaemia. Rice is also the staple food for over 3.5 billion people worldwide who depend on it for more than 20% of their daily calories (FAO, 2001).

Rice is currently being fortified using techniques like dusting, coating, steaming and extrusion. However, these commonly used techniques are observed to have a few drawbacks like loss of heat-sensitive nutrients and oxidation of iron in case of steaming (US Patent No. 3620762), washing off the coated nutrients in the absence of appropriate binding agents (US Patent No. 4446163). Extrusion technique exhibited a disadvantage of the easy separation of fortified kernels from natural rice due to density differences (US Patent No. 5609896). Cold plasma, due to its surface etching and cross-linking properties, was found to alter the amylose content and also improve the texture of the cooked rice with reduced cooking time (Thirumdas et al., 2016). It causes surface fissures, cross-linking of starch, hydroxyl and acidic functional groups on the rice surface, which might help with increased absorption and better binding of iron.

Cold plasma (CP) processing is one of the emerging non-thermal food processing technologies with potential applications in surface decontamination and sterilization (Misra et al., 2011). Non-thermal or cold plasma is the plasma generated under atmospheric or vacuum pressures at temperatures of 30–60 °C and requires low energy. It contains a wide variety of active particles like ions, radicals, electrons,

Abbreviations: CC, Control rice; CP, Plasma treated rice; ANOVA, Analysis of Variance; CCFD, Central Composite Face-centred Design; IDA, Iron Deficiency Anaemia; LDPE, Low density polyethylene; PE, Polyethylene; PP, Polypropylene; RSM, Response Surface Methodology; SEM, Scanning Electron Microscope; CFL, Control rice non-blended packed in LDPE pouch; CFP, Control non-blended packed in PP pouch; CFP100, Control blended in 1:100 ratio packed in PP pouch; CFP200, Control blended in 1:200 ratio packed in PP pouch; PFL, Plasma treated non-blended packed in LDPE pouch; PFP, Plasma treated non-blended packed in PP pouch; PFP100, Plasma treated blended in 1:100 ratio packed in PP pouch; PFP200, Plasma treated blended 1:200 ratio packed in PP pouch

* Corresponding author.
E-mail address: mpoonam1@rediffmail.com (P. Mishra).

https://doi.org/10.1016/j.foodres.2020.109599
Received 3 April 2020; Received in revised form 22 July 2020; Accepted 23 July 2020
Available online 28 July 2020

Principal
Nowgong Girls' College
Nagaon :: Assam

Nowgong Girls' College
ESTD: 1962
Nagaon :: Assam

molecules and metastable excited species which have enough energy to break covalent bonds and initiate some reactions and form volatile compounds. Plasma processing is found to cause surface etching and also increase the surface energy of the samples due to the energetic and reactive species present in the plasma (Thirumdas et al., 2015). Most of these active species disappear once the plasma is turned off. However, few of them react to other reactive species. Plasma processing is environmentally safe, fulfilling all ecological standards (Misra et al., 2011).

In recent years, apart from fruits and vegetables, researchers are working out to find the applications of cold plasma processing on cereals and pulses where cold plasma treatment was found to produce improved textural and nutritional properties with reduced cooking time (Thirumdas et al., 2016). Among these, some studies have been carried out on rice to determine the effect of cold plasma processing on the physicochemical, functional and cooking properties of rice. Low pressure cold plasma treated parboiled rice showed a significant increase in water absorption, and the cooking time was reduced significantly (Sarangapani et al., 2015; Thirumdas et al., 2015). An increase in antioxidant properties and total phenolic content was observed in low temperature plasma-treated basmati rice flour (Thirumdas et al., 2016). These changes in physicochemical and cooking properties are mainly attributed to the surface etching phenomenon caused by cold plasma processing (Thirumdas et al., 2015). But the application of cold plasma for the iron fortification of white rice has not been tried so far.

As the cold plasma creates an acidic environment, therefore it would be suitable for the better binding of iron on the rice surface and also reduce the oxidation of iron during storage. Thus, for the present study, white rice, which can act as a best carrier, is chosen for fortification with iron using cold plasma as a pre-treatment technique. We studied the effect of plasma on the physicochemical properties of raw and cooked rice. We are reporting for the first time the role of plasma treatment in iron fortification of rice and its effect on the bioavailability of iron during storage. An Indian patent is also filed from the outcome of the present investigation.

2. Materials and methods

2.1. Material

Ferrous sulphate confirming to IP standards, ascorbic acid, alpha-dipyridyl reagent and hydroxylamine hydrochloride were of analytical grade and were procured from Merck Millipore, India. Rice was purchased from the local market of Tezpur, Assam, India.

2.2. Cold plasma treatment of rice

For the plasma treatment, Atmospheric Pressure Dielectric Barrier Discharge (DBD) plasma reactor (0–50 kV, 50 Hz, Zenoics Systech, India) was used, and the setup used is shown in Supplementary Fig. S1. The dielectric barrier discharge (DBD) plasma system consists of two square copper electrodes, each having a surface area of 225 cm^2 and a thickness of 5 cm. The upper electrode is connected to a high voltage power supply. The rice samples were subjected to atmospheric cold plasma. Rice samples of 20 g were taken in each petri plate and in one slot, [illegible] petri plates were placed in between the two electrode plates with a gap of [illegible] cm. Voltage was maintained constant at 20 kV [illegible] time of the plasma treatment was varied. The cold plasma parameters were stabilized before on the extent of etching on the surface of rice obtained from the SEM images. All plasma treatments were carried out at room temperature and at 56% relative humidity with atmospheric air as the working gas. The cold plasma treated rice samples were sealed in a petri dish and stored in vacuum desiccators for further analysis.

2.3. Proximate composition of rice

Moisture content (925.10), crude protein contents (990.03) and pH were estimated as per the official methods of AOAC (19th edition). The amylose content of the rice before and after the plasma treatment was determined following the procedure of Juliano (1979).

2.4. Characterization of rice

2.4.1. Scanning Electron Microscope

The surface etching was analysed using a Scanning Electron Microscope (SEM, JEOL, Japan) at an accelerating potential of 5 KV using X-ray Detector-Link Pentafet 7021 (Oxford Instruments Microanalysis Limited, Bucks, England). The rice grains (with and without plasma treatment) were completely dried under low pressure and then were sputter-coated with gold–palladium (60:40) 3 times for the 20 s under vacuum using Desk II Sputter/Etch Unit (Denton Vacuum, LLC, Moorestown, NJ) before viewing.

2.4.2. Water uptake, cooking time, elongation ratio (ER) and width expansion ratio (WER) of rice

Water uptake of the sample was determined as per the method given by Lee et al. (2016), however cooking time, ER and WER of the sample were estimated according to the method of Chen et al. (2012).

2.4.3. Colour characteristics

The colour characteristics of the rice samples before and after plasma treatment were determined using Hunter Lab Colorimeter (Ultra scan VIS, Hunter Lab. Inc., USA). The Hunter colour values L^* (lightness), a^* (redness) and b^* (yellowness) were determined. The whiteness index (WI) and hue (a/b) were determined. WI was calculated using the equation:

$$WI = 100 - \sqrt{[(100 - L*)^2 + (a*)^2 + (b*)^2]} \quad (1)$$

where L^*, a^* and b^* are the lightness, redness and yellowness values, respectively (Mishra and Mahanta, 2014).

2.4.4. Hardness

Texture profile analysis (TPA) of the cooked rice (with and without plasma treatment) was performed using a texture (TAHD- plus, Stable Micro Systems, UK) with a two-cycle compression. A 2 mm radius probe with a test speed of 1 mm/s and a load cell of 5 kg was used for the compression. A deformation ratio of 20% was used. Hardness (N) was determined from the two-cycle curves (Thirumdas et al., 2016).

2.4.5. Pasting properties

Pasting properties of the rice flour suspensions were using Rapid Visco Analyser (Newport Scientific Instrument; Sweden). Powdered sample (3 g) was taken in a canister and added with 25 mL distilled water. The sample was held at 50 °C for 1 min, then heated from 50 °C to 95 °C at the rate of 12 °C/min, and held at 95 °C for 2.4 min followed by cooling to 50 °C at the rate of 11.25 °C/min and finally holding at 50 °C for 1 min. The pasting properties, namely peak viscosity (PV), pasting temperature (PT), final viscosity (FV), breakdown viscosity (BV) and setback (SB) viscosity, were determined following the procedure of Dutta and Mahanta (2014).

2.4.6. Hydrophilicity and surface energy

The effect of plasma on hydrophilicity of the rice grain was determined by water contact angle measurements. The contact angle (θ) was measured by the Contact Angle Measurement System (Data Physics OCA 20, Germany) using the sessile drop method (Sarangapani et al., 2015). Water (2.5 μL) was dispensed on the surface of the rice grain to measure the contact angle between the [illegible] and the grain-water interface. Each image of the drop is then stored via a CCD

Nowgong Girls' College ESTD: 1962 Nagaon :: Assam
C.T.C.
Principal
Nowgong Girls' College
Nagaon :: Assam

Table 1
Effect of cold plasma on proximate, cooking quality characteristics and physicochemical properties of rice.

	UC	UP (15 min)
Moisture content (%)	14.13 ± 0.29^a	13.07 ± 0.07^b
Protein (%)	5.50 ± 0.06^b	5.87 ± 0.10^a
Amylose (%)	25.33 ± 0.32^a	19.52 ± 0.08^b
Cooking time (min)	22.53 ± 0.60^a	12.90 ± 0.60^b
Water uptake (g/g)	2.33 ± 0.10^b	3.22 ± 0.10^a
Elongation ratio	1.24 ± 0.01^b	1.26 ± 0.02^b
Width expansion ratio	1.25 ± 0.01^a	1.22 ± 0.02^a
L*	66.81 ± 2.04^a	68.09 ± 1.40^a
WI	66.38 ± 0.04^a	67.62 ± 0.19^a
Hardness (N)	0.73 ± 0.03^a	0.30 ± 0.18^b
pH	6.51 ± 0.03^a	6.18 ± 0.02^b
Pasting temperature (°C)	65.00 ± 0.58^a	55.00 ± 1.15^b
Peak viscosity (cP)	947.00 ± 0.58^a	872.00 ± 4.93^b
Hold viscosity (cP)	930.00 ± 2.52^a	845.00 ± 5.86^b
Breakdown viscosity (cP)	15.00 ± 0.58^b	21.00 ± 1.00^a
Final viscosity (cP)	1709.00 ± 5.51^a	1614.00 ± 1.15^b
Setback viscosity 1 (cP)	776.00 ± 3.79^a	763.00 ± 3.06^a
Setback viscosity 2 (cP)	754.00 ± 4.73^a	740.00 ± 4.51^a
Contact angle (degree)	70.73 ± 0.10^a	55.05 ± 0.10^b
Surface energy (mJ/m^2)	41.07 ± 0.02^b	50.83 ± 0.01^a

All the data are expressed as mean ± standard deviations. Means with different superscript letters in a row differ significantly ($p < 0.05$; $n = 3$).

video camera, using a PC based acquisition and data processing system. The surface energies were obtained by incorporating the contact angle values in Young's equation. A simplified equation suggested by Deshmukh and Shetty (2008) was used to calculate the surface energy.

$$SE = 2.9 \times 10 - 5(\delta)3 - 0.00652(\delta)2 - 0.1362(\delta) + 72.8 \quad (2)$$

2.4.7. Thermal properties

The thermal properties of the rice flour were analysed using the Differential Scanning Calorimeter (Shimadzu model, TGA50 DSC60). A sample flour of 5 mg was taken in the aluminium pan, and 10 μL distilled water was added. The pan was sealed and kept aside for one h to reach equilibrium. The measurements were performed over the range of 30–150 °C at a heating rate of 10 °C/min. Then the gelatinization temperature (T_g) was obtained using the software TA-60WS (Dutta and Mahanta, 2014).

2.5. Optimization of fortification parameters

Optimization was performed using RSM and Central Composite Face-centred Design (CCFD) (Supplementary Table 1). Samples were prepared with different combinations, according to CCFD, of the two fortification parameters, namely the concentration of iron (ferrous sulphate) (mg) and concentration of ascorbic acid (mg) plasma-treated rice. The models developed were then analysed and optimized based on Fe^{2+} bioavailability in acidic (1.35 pH) and alkaline (7.5 pH) conditions, colour and hardness of fortified rice. Plasma treated rice samples were sprayed with the optimum concentration of ferrous and ascorbic acid solution at a rate of 30 mL 100 g^{-1} of rice. They were then tempered for 1 h at room temperature in an incubator and dried in a tray drier at 40 °C to a moisture content of 12%. These samples were used for further study.

2.6. In vitro bioavailability estimation

The in-vitro bioavailability of iron from plasma-treated fortified rice was determined following the in-vitro method described by Narasinga Rao and Prabhavathi (1978). According to this method, duplicates of an 8% (w/v) homogenate (2 mL) of the food prepared in pepsin- HCl (0.5% pepsin in 0.1 N HCl) solution, pH 1.35 (adjusted with distilled H_2O) were incubated at 37 °C for 90 min, after which the contents of one set were centrifuged at 3000 rpm for 45 min, and the supernatant was filtered and saved for the iron estimation. The pH of the other set was adjusted to 7.5 with 5 N NaOH and was incubated and processed as above to obtain the filtrate. Fe^{2+} form of iron in the filtrates was estimated by the alpha, alpha-dipyridyl method of AOAC. Duplicate aliquots (5 mL) of the filtrates were taken and the volume in one set was made up to 15 mL and served as the extract blank. The other aliquot was treated with 1 mL of 10% hydroxylamine hydrochloride, 5 mL of acetate buffer (pH 4.2), 2 mL of 0.1% of alpha, alpha-dipyridyl reagent, and volume was made up to 15 mL with water. The developed colour was measured at 522 nm against a reagent blank. As micronutrients enter the human body and pass through the stomach, they are exposed to stomach acids with a very low pH around 1.5 and after that they pass to the duodenum (pH 6.5–7) in small intestine. Therefore to determine the absorption of iron (similarly as it takes place in the human body) in both the conditions (i.e., acidic and alkaline), the in vitro bioavailability study was conducted both at pH 1.35 and pH 7.5.

2.7. Storage study

The control (non-plasma treated fortified) rice and plasma-treated fortified rice were packed in two different packaging materials, namely low-density polyethylene (LDPE) pouches and polypropylene (PP) pouches. Also, blended (plasma-treated fortified rice mixed with raw rice in the ratio of 1:100 and 1:200) rice were packed in polypropylene pouches. The packed rice was stored at ambient temperature, and storage study was conducted for 45 days at an interval of 15 days. The samples were analysed for bioavailability of iron, hardness and colour after cooking.

2.8. Statistical analysis

Statistical analysis of the results was performed by ANOVA using SPSS (IBM statistical analysis version 19). Significance among the samples was compared at $p < 0.05$ by post-hoc comparison, SPSS 19 version. Minimum 3 replicates were performed for all the analyses.

3. Results and discussion

3.1. Effect of cold plasma treatment on surface morphology of rice

SEM images at a magnification of 2000X were obtained for rice samples with and without plasma treatment to observe any etching behaviour on the surface of the rice due to the plasma (Fig. 1(i)). Plasma treatment has caused a significant effect on the surface of rice grains. Rice grains without plasma treatment (Fig. 1(i)a) depicted a compact natural structure, whereas rice grains with plasma treatment had significant visible fissures on the surface. The etching on the surface increased with an increase in plasma treatment time. Rice treated with plasma for 10 min had no significant change on the surface morphology (Fig. 1(i) b) compared to that of the control, but after 15 min of plasma exposure (Fig. 1(i)c), a significant surface etching was observed compared to the control. Similar findings were obtained for brown rice (Chen et al., 2012; Chen, 2014), parboiled rice, basmati rice (Thirumdas et al., 2015) and bamboo rice (Pankaj et al., 2018) when treated with plasma. The obtained results are in line with the findings of Yodpitak et al. (2019), who observed plasma treated rice husk depicted a softer and smoother surface with significant fissures on the surface. The surface etching with cavities and roughness of the surface of the rice is mainly due to the breakdown of covalent bonds caused by the bombardment of reactive species present in the plasma with the surface of the rice grain (Thirumdas et al., 2016). Based on the surface etching of rice, 15 min plasma treatment was selected for further analysis.

C.T.C.
Principal
Nowgong Girls' College
Nagaon :: Assam
Nowgong Girls' College ESTD: 1962 Nagaon :: Assam

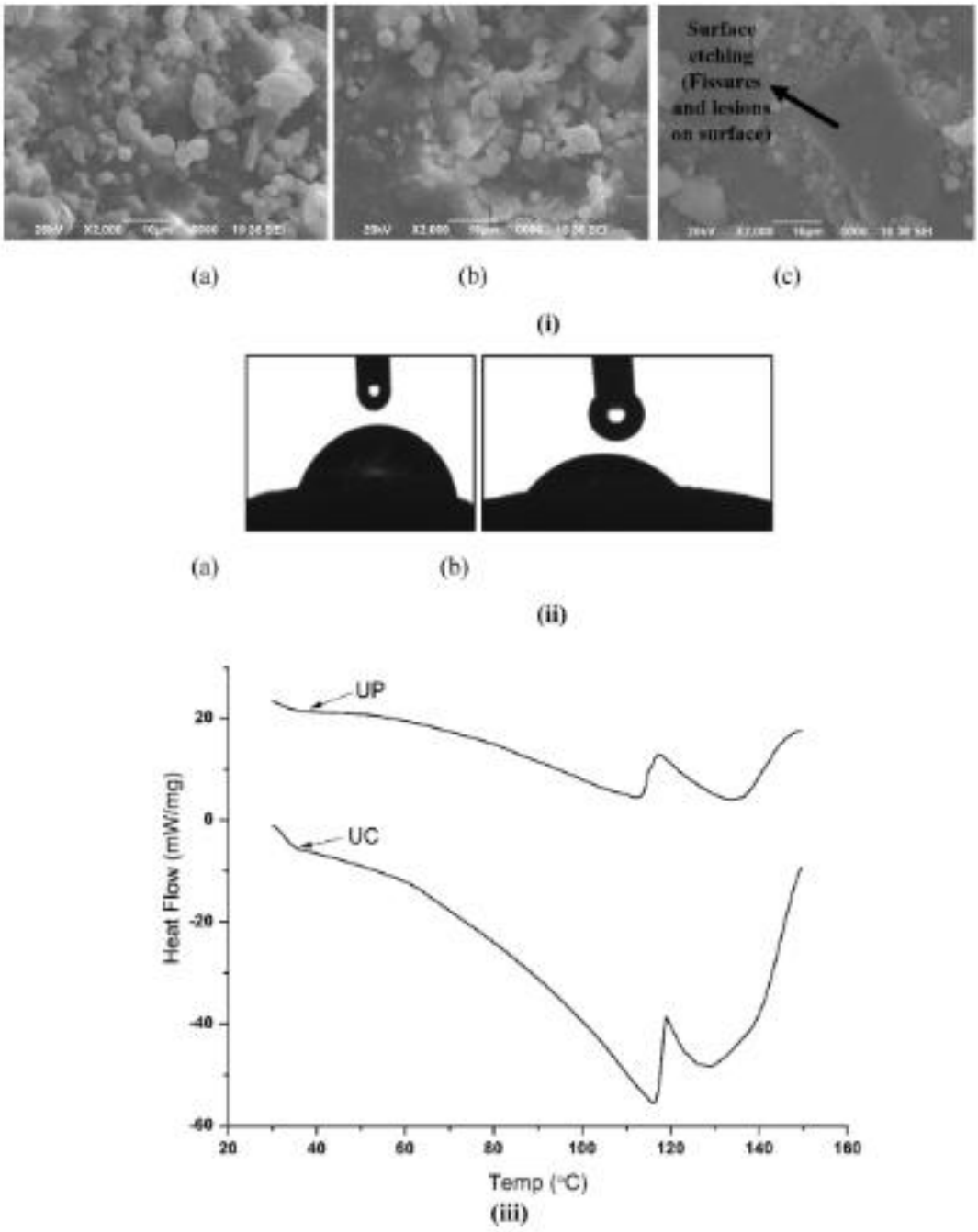

Fig. 1. (i) SEM images at 2000 × (a) control rice (b) plasma treated rice (10 min) (c) plasma treated rice (15 min) (ii) Contact angle images of (a) control rice and (b) plasma treated rice (15 min) (iii) Thermal properties of native and plasma treated rice.

3.2. Effect of cold plasma on proximate composition of rice

Rice samples with and without plasma treatment were tested for moisture content, protein and amylose content (Table 1). The moisture content of rice was reduced from 14.13% to 13.07% after the application of [illegible] plasma. Reduction in moisture content after the plasma treatment was observed in granular starches treated with low pressure cold plasma (Lee et al., 2016). This reduction in moisture content after plasma treatment may be attributed to the decomposition of the water molecules into oxygen radicals (Zou, Liu, & Eliasson, 2004).

Exposure of 15 min of plasma treatment increased the protein content [illegible] (Table 1). These present findings are in line with the results reported by Chen et al. (2012) and Thirumdas et al. (2015). However, this remains unclear and requires further investigations.

The amylose content of plasma-treated rice was reduced significantly from 25.33% to 19.52% (Table 1). This reduction in amylose content might be due to the leaching of amylose fractions due to the depolymerisation (Sarangapani et al., 2015; Thirumdas et al., 2016).

3.3. Effect of cold plasma on characteristics of rice

3.3.1. Effect of cold plasma on cooking quality of rice

Cooking time, water uptake ratio, elongation ratio (ER) and volume expansion ratio (VER) were the parameters analysed (Table 2). After the plasma treatment, a significant reduction in the cooking time was observed for the same degree of hardness. The formation of cooking

CTC
Principal
Nowgong Girls' College
Nagaon :: Assam
Nowgong Girls' College ESTD:1962 Nagaon :: Assam

time can be attributed due to the easy penetration of water into the plasma-treated samples through the fissures caused on the rice surface which were not found in untreated samples (Chen et al., 2012). Similar findings were found in the research conducted by Sarangapani et al. (2015) on parboiled rice treated with low pressure plasma. The water uptake ratio of control rice was 2.33 g/g however, plasma-treated rice had 3.22 g/g of rice. An increase in the water uptake ratio may be credited to the change in the surface morphology of the rice due to fissures caused during plasma treatment which resulted in increased water absorption (Lee et al., 2016; Zargarchi and Saremnezhad (2019)).

ER is the increase in the length of the kernel upon swelling of starch granules due to an increase in the water uptake (Juliano, 1979). ER increased from 1.24 to 1.26 after the plasma treatment while the WER for plasma-treated samples reduced from 1.25 to 1.22. The changes in both ER and WER due to plasma treatment were found insignificant.

3.3.2. Effect of cold plasma on colour characteristics of rice

The colour values of rice with and without plasma treatment were measured in terms of Hunter L^*, a^*, b^* and whiteness index (WI). Though the L^* values of plasma-treated samples were found to be increased compared to the untreated samples, but the difference was not significant (Table 1). WI of plasma-treated samples increased from 66.38 to 67.62. These findings are in line with the findings of Pal et al. (2016).

3.3.3. Effect of plasma on hardness & pH of rice

Hardness is one of the most important parameters which play a significant role in determining the texture of cooked rice and consumer acceptability (Chen et al., 2012). The hardness of rice was significantly reduced from 0.73 N to 0.30 N after 15 min of plasma treatment (Table 1). Reduction in hardness after plasma can be correlated to the reduction in the amylose content of plasma-treated samples (Sarangapani et al., 2015). Also, the easy penetration of water resulted in plasma treatment may be one of the possible reason for the decrease in hardness (Lee et al., 2016).

The pH of rice was reduced from 6.51 (control sample) to 6.18 after the plasma treatment which may be due to the formation of acidic functional groups like carboxyl, carbonyl and peroxides during the plasma (Thirumdas et al., 2017).

3.3.4. Effect of cold plasma on pasting properties of rice

Pasting temperature is the temperature at which there is a sudden rise in the viscosity during the continuous heating process (Thirumdas et al., 2016). Pasting temperature and peak viscosity of rice reduced significantly after plasma treatment, which can be linked with the decrease in amylose content and cooking time due to the plasma treatment. Reduction in the final viscosity of plasma treated rice can be correlated to the chemical modification of the rice starch due to the reactive species generated during plasma treatment (Potluri et al., 2018). However, the decrease in peak viscosity may be due to the disintegration of some of the fragile starch granules (Chen et al., 2012). Setback viscosity is one of the useful parameters which help in determining the storage quality and hardness of the rice (Zaidul et al., 2007). Though there was a reduction in the setback viscosity after the plasma treatment, the change was not significant (Table 1).

3.3.5. Effect of cold plasma on hydrophilicity and surface energy

The measure of the contact angle determines the hydrophilicity of the rice. The contact angle images of the samples are shown in Fig. 1 (ii). Plasma treatment has resulted in a substantial difference in both contact angle and surface energies of the treated rice samples. The contact angle of control rice and treated rice were 70.7° and 55.0° respectively. The surface energy of these samples has increased from 41.07 to 50.83 (Table 1). The reduction in the contact angle of plasma-treated samples can be associated with the increased water absorption due to the surface etching and fissures caused by the plasma (Sarangapani et al., 2015).

3.3.6. Thermal properties

The DSC plots for both the plasma-treated and untreated samples are shown in Fig. 1(iii). Decrease in glass transition temperature from 104.40° (control) to 89.40° (plasma-treated) is mainly corresponding to the peak temperature observed in rice samples after the plasma treatment. A decrease in the glass transition temperature may be attributed to the early conversion of the crystalline phase to amorphous due to the de-crystallization of starch caused by the reactive plasma species (Lii et al. 1996).

3.4. Optimization of fortification parameters of plasma-treated rice

Samples with different combinations of amounts of ferrous sulphate and ascorbic acid solution were prepared using RSM-CCFD. These samples were analysed for in vitro bioavailability of Fe^{2+} as measured by Fe^{2+} BA 1.35 (mg/100 g of rice) and Fe^{2+} BA 7.5 (mg per 100 g of rice). Using the data obtained, second-order polynomial models were fitted for Fe^{2+} BA 1.35, Fe^{2+} BA 7.5, a/b and hardness (N), the however the linear model was found suitable for Fe^{2+} BA 7.5. The weighted average of Fe^{2+} BA 1.35 and Fe^{2+} BA 7.5 was taken as objective while considering a/b and N as constraints with lower and upper bounds.

The results obtained for each response variable after fortifying the plasma-treated rice samples as per the model generated experimental runs are given in Table 2 and the ANOVA results for each response are

Table 2
CCFD results for plasma treated fortified rice.

Sl. No.	Coded values		Independent variables (Actual values)		Responses			
	Factor A	Factor B	Iron(mg)	Ascorbic acid (mg)	Fe^{2+} BA 1.35 (mg/100 g)	Fe^{2+} BA 7.5 (mg/100 g)	Colour (a/b)	Hardness (N)
1	−1	−1	500	0	46.00	12.92	−0.03	0.12
2	+1	−1	900	0	98.28	8.37	0.04	0.13
3	−1	+1	500	1500	85.91	90.35	0.28	0.09
4	+1	+1	900	1500	130.21	97.24	0.23	0.06
5	−1	0	500	750	84.23	81.61	0.[illegible]	0.[illegible]
6	+1	0	900	750	122.00	48.85	0.[illegible]	0.[illegible]
7	0	−1	700	0	72.61	3.37	0.[illegible]	0.[illegible]
8	0	+1	700	1500	110.63	90.89	0.[illegible]	0.[illegible]
9	0	0	700	750	105.50	63.50	0.09	0.09
10	0	0	700	750	109.40	62.83	0.08	0.10
11	0	0	700	750	101.40	70.50	0.[illegible]	0.09
12	0	0	700	750	108.50	60.83	0.07	0.[illegible]
13	0	0	700	750	109.00	48.83	0.08	0.[illegible]

Results were shown as per standard order. However, experiments were conducted in random order.
Centre points are replicated 5 times to get the pure error and thereby to assess the lack of fit.

C.T.C.
Principal
Nowgong Girls' College
Nagaon :: Assam
Nowgong Girls' College ★ ESTD: 1962 ★ Nagaon :: Assam

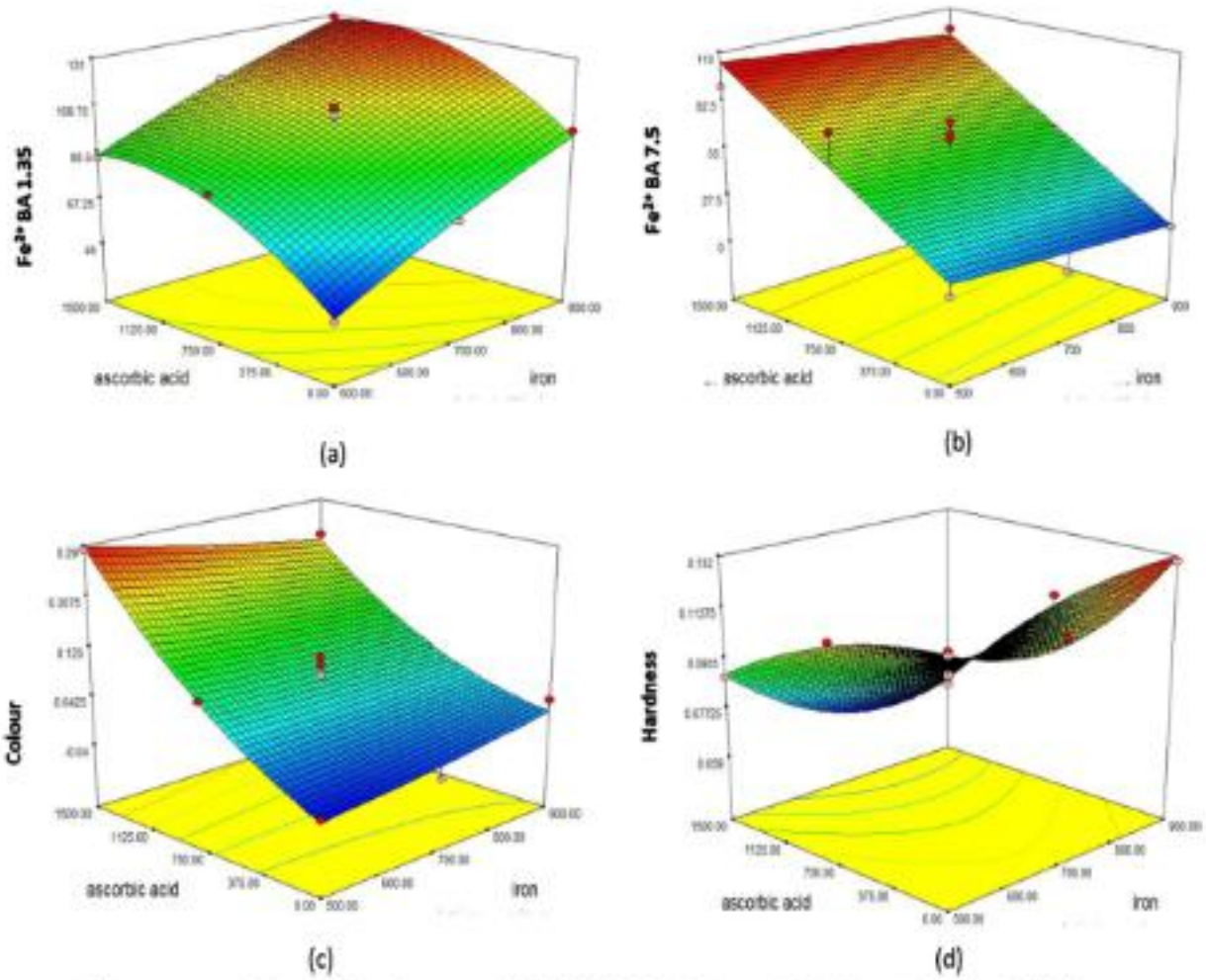

Fig. 2. Response surface graphs for plasma treated fortified rice (a) Fe^{2+} BA 1.35 (b) Fe^{2+} BA 7.5 (c) colour (d) hardness.

shown in Supplementary Table S1.

The 3D graph shows that the Fe^{2+} in vitro bioavailability at pH 1.35 has increased with an increase in the concentration of ferrous sulphate and ascorbic acid (Fig. 2a). With increasing ascorbic acid concentration, the Fe^{2+} in vitro bioavailability at pH 7.5 increased significantly. However, increasing the iron content did not affect the Fe^{2+} bioavailability at pH 7.5 (Fig. 2b). This might be probably due to the poor solubility of iron in the non-acidic environment (Bezwoda et al., 1978); therefore, the solubility of iron reduced when the concentration of iron is increased at pH 7.5 and subsequently reduced the in vitro bioavailability. The presence of ascorbic acid reduced the rate of oxidation of Fe^{2+} and improved the bioavailability of iron even at pH 7.5. There was no obvious effect of the iron on the redness of the fortified rice, however, ascorbic acid showed a significant effect on the redness of the rice (Table S1; Fig. 3c). The probable reason for the same may be that the presence of a higher level of ascorbic acid improves the solubility of iron, which helps in proper adsorption and binding of iron on the surface. Any systemic effect of iron and ascorbic acid on the hardness of rice could not be noticeable in the present investigation (Fig. 2d).

Optimum values for ferrous sulphate and ascorbic acid were found to be 862.5 mg and 1196.5 mg/100 g of rice respectively. The sample was prepared at the optimal combination and actual values for the responses were found out. The predicted model was validated by conducting a chi-square test (Supplementary Table S2) at a probability of 0.05. Accordingly, predicted values for each response obtained from model equations were compared with the actual values obtained. As the chi-square value for the responses is less than the tabulated chi-square value at $p = 0.05$ for actual and predicted responses thus, the predicted model was found significant.

3.5. Storage study

3.5.1. Storage stability of plasma-treated fortified non-blended rice and blended rice

For the storage stability study, apart from only fortified rice samples, blended samples were also prepared and stored at ambient temperature. Blended samples were prepared by mixing fortified rice with unfortified rice in the ratios of 1:100 (w/w) and 1:200 (w/w). The Non-blended samples were packed in LDPE and PP pouches, whereas blended samples were packed in PP pouches only. Stored rice was analysed at an interval of 15 days for Fe^{2+} in vitro bioavailability at pH 1.35 and 7.5, a/b and hardness in the cooked sample.

Rice treated with plasma retained approximately 120 mg/100 g and 80 mg/100 g after cooking at 1.35 and 7.5 pH, respectively. However, control had 50 mg and 38 mg/100 g of Fe^{2+} at 1.35 and 7.5 pH, respectively (Fig. 3a and b). Pre-treatment with plasma increased the surface energy of rice and modified the [illegible] which facilitate the binding and adsorption of Fe^{2+} [illegible]. In contrast, low surface energy of control sample favoured [illegible] Fe^{2+} which subsequently leached out [illegible] during washing and cooking and hence reduced the in vitro bioavailability of iron. A similar reduction in oxidation of Fe^{2+} in red [illegible] is reported by [illegible] et al. (2018), where the oxidation rate of Fe^{2+} in plasma treated sample was found to be very less as compared to that of sample without plasma treatment. The comparatively low concentration of Fe^{2+} at pH 7.5 might be due to the high rate of oxidation and [illegible] solubility of

Principal
Nowgong Girls' College
Nagaon :: Assam
Nowgong Girls' College ESTD. 1962 Nagaon :: Assam

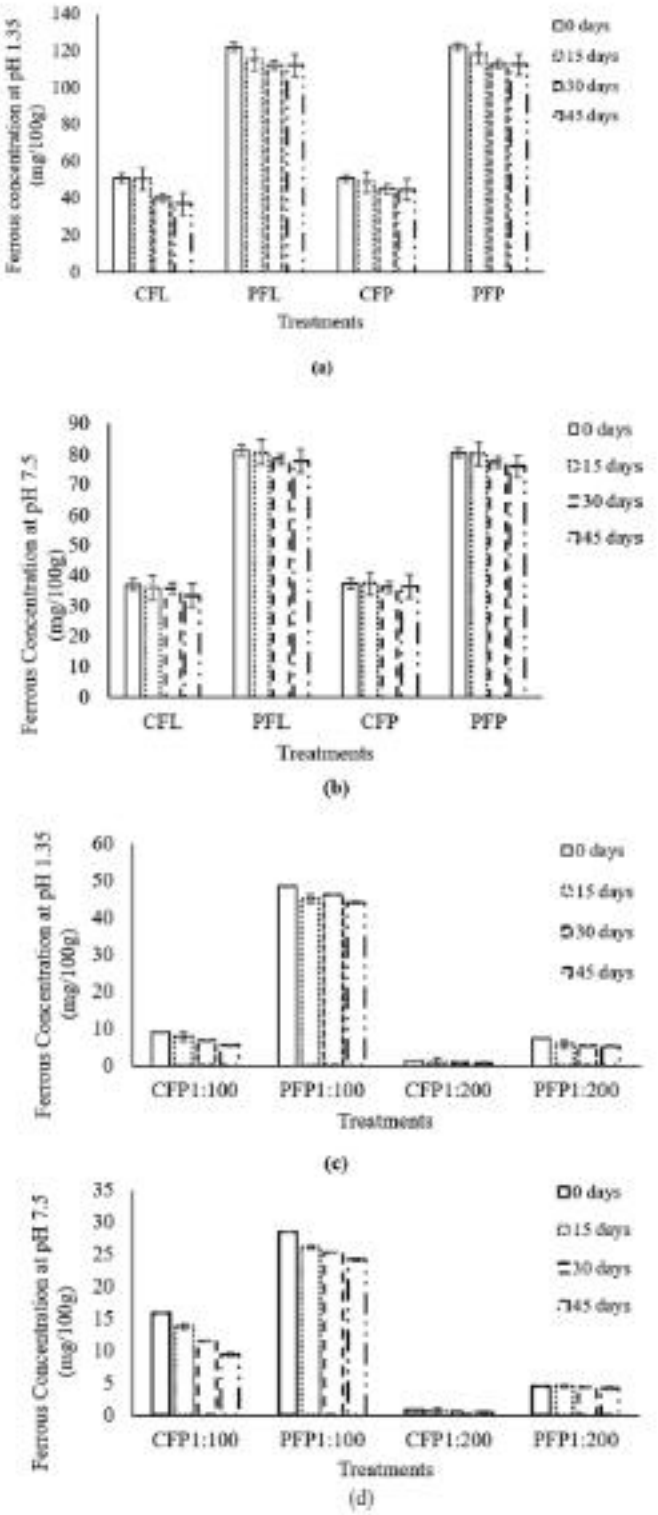

Fig. 3. Effect of storage at ambient temperature on the bioavailability of (a) Iron concentration at pH 1.35 in non-blended rice (b) Iron concentration at pH 7.5 in non-blended rice (c) Iron concentration at pH 1.35 in blended rice (d) Iron concentration at pH 7.5 in blended rice.

Fe^{2+} in an alkaline environment (Bezwoda et al., 1978). Due to poor oxygen barrier properties of LDPE, the rate of oxidation of Fe^{2+} was reasonably high which reduced the solubility of iron and consequently the sample stored in LDPE pouches had a lower in vitro bioavailability of both pH 1.35 and 7.5 than the sample stored in PP pouches (Fig. 3a and b).

Fig. 3c presents the in vitro bioavailability of blended fortified rice samples (at two different ratios, i.e., 1:100 and 1:200) at pH 1.35. In vitro bioavailability of Fe^{2+} was comparatively lower in the control sample than in the plasma-treated sample. At pH 1.35, in vitro bioavailability of Fe^{2+} in plasma-treated blended rice in the ratio of 1:100 and 1:200 was found to be 50 mg/100 g and 10 mg/100 g of rice respectively, which was relatively more than the ratio of 1/100 or 1/200 that was observed in non-blended sample. A similar trend was observed when analysed at pH 7.5 (Fig. 3d). Blending with unfortified rice at 1:100 or 1:200 ratios have reduced the leaching losses of iron during washing and cooking and therefore improved the bioavailability of iron. We estimated the in-vitro bioavailability of the iron through analyzing its solubility at different pH, i.e., 1.35 and 7.5 (Bezwoda et al., 1978). The solubility of iron is higher in acidic pH than in alkaline pH (Bezwoda et al., 1978). The presence of ascorbic acid might have reduced the rate of oxidation of Fe^{2+} into Fe^{3+} and therefore improved the bioavailability of iron. But when the ratio of unfortified rice was increased from 1:100 to 1:200, then there might be a possibility that the level of ascorbic acid used to fortify the rice was not as effective as in the case of 1:100 to prevent the oxidation. Hence, the bioavailability reduced (in 1:200) not because of leaching losses, but due to oxidation of the iron also. However, further studies may be required to support the findings of the present investigation. The in vitro bioavailability of the iron at both pH in plasma-treated rice was retained effectively up to 45 days of storage compared to the control sample.

Reduction in the hardness of plasma-treated rice is observed in non-blended fortified samples (Fig. 4a); the hardness of non-blended plasma-treated rice was comparatively low (Thirumdas et al., 2016) as it was evident from the significant reduction in the cooking time also. When we blended in 1:100 or 1:200 ratios, the overall hardness may be dominated by the attributes of untreated rice and therefore, we have not observed a similar trend in blended and non-blended rice. Control samples stored in LDPE pouches had comparatively more hardness after 15 days of storage than samples stored in PP pouches. The redness of the fortified rice without plasma treatment was reasonably higher than the plasma-treated fortified sample (Fig. 4b), which supports our findings that the plasma treatment may be helpful to reduce the rate of oxidation of Fe^{2+} into Fe^{3+}. Packaging material showed no significant impact on the colour of the stored rice (Fig. 4b). A similar kind of trend was observed in the blended sample also (Fig d).

4. Conclusions

Plasma treatment resulted in a significant change in the surface of the rice by creating a surface etching. The etching on the surface was observed in the SEM images and it was found that the extent of etching increased with an increase in the plasma treatment time. Plasma also increased the hydrophilicity and surface energy of the rice, which helped in reducing the cooking time by almost 10 min compared to that of the rice without plasma treatment. For rice, the cooking time was reduced further with an increase in the plasma treatment time to 15 min. This reduction in cooking time can be used for the preparation of instant rice. Rice fortified after the plasma treatment showed a significant increase in the bioavailability of Fe^{2+} in cooked rice compared to the rice without plasma treatment. Plasma may have resulted in an acidic environment on the rice surface may have resulted in the formation of acidic functional groups, which helped in reducing the cooking time, leaching of iron and more stable Fe^{2+} form. The in vitro bioavailability of iron was significantly higher in the case of plasma treated rice at both pH and 7.5 pH than the control. Still, further studies will be required to deal with changes in the functional groups due to the plasma treatment on the surface of the rice and also the interaction of iron with these functional groups.

C.T.C.
Principal
Nowgong Girls' College
Nagaon :: Assam
Nowgong Girls' College ESTD. 1962 Nagaon :: Assam

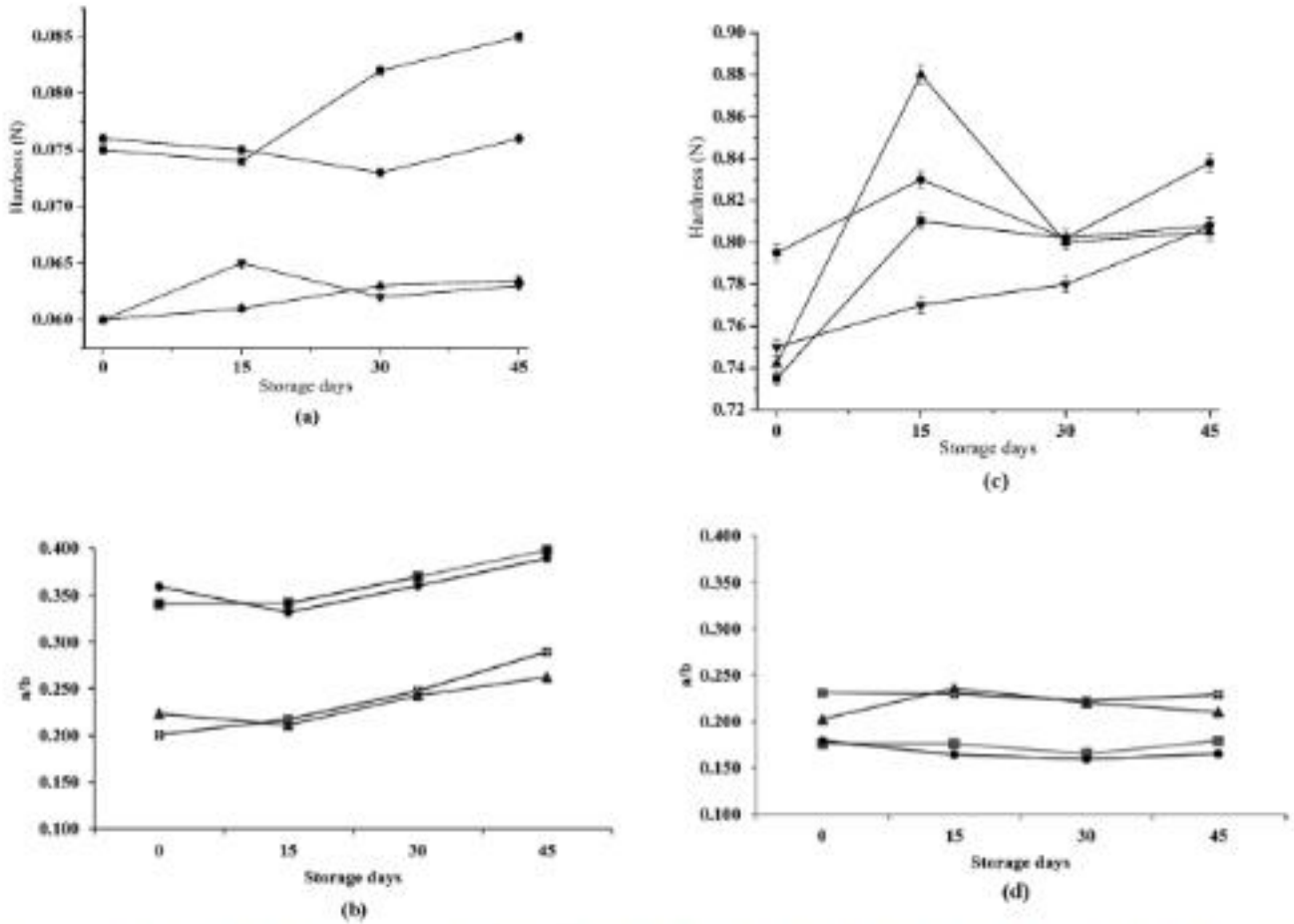

Fig. 4. Effect of storage at ambient temperature on (a) Hardness of non-blended iron fortified rice (■ = CFL, ● = CFP, ▲ = FFP, ▼ = PFL) (b) colour of non-blended iron fortified rice (■ = CFL, ● = CFP, ▲ = FFP, + = PFL) (c) Hardness of blended iron fortified rice (● = CFP 1:100, ▼ = PFP 1:100, ■ = CFP1:200, ▲ = PFP1:200) (d) colour of blended iron fortified rice (● = CFP 1:100, ▲ = PFP 1:100, ■ = CFP1:200, + = PFP1:200).

Appendix A. Supplementary material

Supplementary data to this article can be found online at https://doi.org/10.1016/j.foodres.2020.109599.

References

Bezwoda, W., Charlton, R., Bothwell, T. H., Torrance, J., & Mayet, F. (1978). The importance of gastric hydrochloric acid in the absorption of non heme food iron. *Journal of Lab Clinical Medicine, 92*, 108–116.

Chen, H. H., Chen, Y. K., & Chang, H. C. (2012). Evaluation of physicochemical properties of plasma treated brown rice. *Food Chemistry, 133*(1), 74–79.

Chen, H. H. (2014). Investigation of properties of long-grain brown rice treated by low-pressure plasma. *Food and Bioprocess Technology, 7*(9), 2484–2491.

Deshmukh, R. R., & Shetty, A. R. (2008). Comparison of surface energies using various approaches and their suitability. *Journal of Applied Polymer Science, 107*(6), 3707–3717.

Dutta, H., & Mahanta, C. L. (2014). Traditional parboiled rice-based products revisited: Current status and future research challenges. *Rice Science, 21*(4), 187–200.

Zou, J. J., Liu, C. J., & Eliasson, B (2004). Modification of starch by glow discharge plasma. *Carbohydrate polymer, 55*(1), 23–26.

FAO. (2001). The state of food and agriculture 2001 (No. 33). Food & Agriculture Organization.

Juliano, B. [illegible] 97[illegible]. [illegible]ain of rice grain quality. *Chemical Aspects of Rice Grain Quality*, 69–9[illegible]

Lee, K. [illegible] Choe, J. H., Choi, H. W., Jung, K. S., Jeong, J. Y., Kim, S. H., ... Kim, W. H. (2016). Extracellular [illegible] plasma mechanisms for improved microbial and physicochemical quality of brown rice. *LWT-Food Science and Technology, 73*, 442–447.

Li, C. [illegible] Th[illegible] Hwang, [illegible] (1996). Effect of amylose content on the rheological properties of [illegible] starch. *Cereal Chemistry, 73*(4), 415–420.

McLean, E., Cogswell, M., Egli, I., Wojdyla, D., & De Benoist, B. (2009). Worldwide prevalence of anaemia, WHO vitamin and mineral nutrition information system, 1993–2005. *Public Health Nutrition, 12*(4), 444–454.

Mi[illegible] [illegible] comparative analysis of functional and nutritive [illegible] [illegible] seed and seed coat powder. *American Journal of Food Technology, 9*(3), 159–166.

Misra, N. N., Tiwari, B. K., Raghavarao, K. S. M. S., & Cullen, P. J. (2011). Nonthermal plasma inactivation of food-borne pathogens. *Food Engineering Reviews, 3*(3–4), 159–170.

Narasinga Rao, B. S., & Prabhavathi, T. (1978). An in vitro method for predicting the bioavailability of iron from foods. *The American Journal of Clinical Nutrition, 31*(1), 169–175.

Pal, P., Kaur, P., Singh, N., Kaur, A., Misra, N. N., Tiwari, B. K., ... Virdi, A. S. (2016). Effect of nonthermal plasma on physico-chemical, amino acid composition, pasting and protein characteristics of short and long grain rice flour. *Food Research International, 81*, 50–57.

Pathuri, S., Sangeetha, K., Santhosh, B., Nivas, G., & Mahendran, R. (2018). Effect of low-pressure plasma on bamboo rice and its flour. *Journal of Food Processing and Preservation, 42*(12), Article e13846.

Sarangapani, C., Devi, Y., Thirumdas, R., Annapure, U. S., & Deshmukh, R. R. (2015). Effect of low-pressure plasma on physico-chemical properties of parboiled rice. *LWT-Food Science and Technology, 63*(1), 452–460.

Thirumdas, R., Sarangapani, C., & Annapure, U. S. (2015). Cold plasma: A novel non-thermal technology for food processing. *Food Biophysics, 10*(1), 1–11.

Thirumdas, R., Saragapani, C., Ajinkya, M. T., Deshmukh, R. R., & Annapure, U. S. (2016). Influence of low pressure cold plasma on cooking and textural properties of brown rice. *Innovative Food Science and Emerging Technologies, 37*, 53–60.

Thirumdas, R., Trimukhe, A., Deshmukh, R. R., & Annapure, U. S. (2017). Functional and rheological properties of cold plasma treated rice starch. *Carbohydrate Polymers, 157*, 1723–1731.

Yang, R., Liu, Y., Meng, D., Wang, D., Blanchard, C. L., & Zh[illegible] (2018). Effect of atmospheric cold plasma on structure, activity, [illegible] reversible unfolding of the phytoferritin. *Food Chemistry, 264*, 41–48.

Yodpinit, S., Mahatheeranont, S., Boonyawan, D., Sookwong, P., [illegible] Norkaew, O. (2019). Cold plasma treatment for [illegible] elimination and [illegible] bioactive physicochemical content of germ[illegible] rice. *Food Chemistry, 289*, 328–339.

Zaidul, I. S. M., Norulaini, N. N., Omar, A. M. [illegible] & Noda, T. (2007). [illegible] analysis of mixtures of wheat flour and [illegible] potato, and cassava starches. *Carbohydrate Polymers, 69*(4), [illegible]

Zargarchi, S., & Sarmurzehad, S. (2019). Ga[illegible] aminobutyric acid, phenolic and antioxidant capacity of germinated indica pa[illegible] affected by low-pressure plasma treatment. *LWT, 102*, 291–294.

CTC
Principal
Nowgong Girls' College
Nagaon :: Assam

Nowgong Girls' College
ESTD: 1962
Nagaon :: Assam

magnetochemistry

MDPI

Review

High-Coordinate Mononuclear Ln(III) Complexes: Synthetic Strategies and Magnetic Properties

Joydev Acharya [1,2,†], Pankaj Kalita [1,†] and Vadapalli Chandrasekhar [1,2,*]

[1] Tata Institute of Fundamental Research Hyderabad, Gopanpally, Hyderabad 500107, India; joydev@tifrh.ac.in (J.A.); pankajkalita14@iiser.ac.in (P.K.)
[2] Department of Chemistry, Indian Institute of Technology Kanpur, Kanpur 208016, India
* Correspondence: vc@tifrh.ac.in
† Authors contributed equally.

Abstract: Single-molecule magnets involving monometallic 4f complexes have been investigated extensively in last two decades to understand the factors that govern the slow magnetization relaxation behavior in these complexes and to establish a magneto-structural correlation. The prime goal in this direction is to suppress the temperature independent quantum tunneling of magnetization (QTM) effect via fine-tuning the coordination geometry/microenvironment. Among the various coordination geometries that have been pursued, complexes containing high coordination number around Ln(III) are sparse. Herein, we present a summary of the various synthetic strategies that were used for the assembly of 10- and 12-coordinated Ln(III) complexes. The magnetic properties of such complexes are also described.

Keywords: high-coordinate Ln(III) complexes; multi-dentate ligands; single-ion magnets; quantum tunneling of magnetization

check for updates

Citation: Acharya, J.; Kalita, P.; Chandrasekhar, V. High-Coordinate Mononuclear Ln(III) Complexes: Synthetic Strategies and Magnetic Properties. *Magnetochemistry* **2021**, *7*, 1. https://dx.doi.org/10.3390/magnetochemistry7010001

Received: 30 November 2020
Accepted: 17 December 2020
Published: 22 December 2020

Publisher's Note: MDPI stays neutral with regard to jurisdictional claims in published maps and institutional affiliations.

Copyright: © 2020 by the authors. Licensee MDPI, Basel, Switzerland. This article is an open access article distributed under the terms and conditions of the Creative Commons Attribution (CC BY) license (http://creativecommons.org/licenses/by/4.0/).

1. Introduction

The seminal discovery by Sessoli et al. that a Mn_{12} cluster can show slow relaxation of magnetization reversal at very low temperatures has ignited the interest of both theoretical and experimental researchers from disciplines such as coordination chemistry, molecular magnetism and molecular materials [1]. This area of work, which is now very active, includes different systems such as single-molecule magnets (SMMs), single-ion magnets (SIMs) and single-chain magnets (SCMs). These systems are receiving attention due to the possibility of their potential to be utilized in various areas including data storage, quantum computation and spintronics [2–6]. In addition, the field of molecular magnetic refrigerants based on the principle of magneto caloric effect (MCE) also has been receiving wide research interest [7].

Single-molecule magnets (SMMs), of which SIMs are a sub-set, are characterized by a well-defined magnetically bi-stable ground electronic state and can remain magnetized below certain temperatures showing a slow relaxation of magnetization. Through experimental and theoretical work carried out over several years it has now been established that one of the characteristics of SMMs is the effective energy barrier (U_{eff}) that separates the two lowest energy spin states. This is the energy required to flip the direction of the magnetization and has been shown in polynuclear transition metal complexes to be dependent on the *Ising* type magnetic anisotropy as characterized by the zero-field splitting parameter, D and the total spin: $U_{eff} = |D|S^2$ for integer spin and $|D|(S^2-\frac{1}{4})$ for half-integer spin. In contrast to what this relationship suggests—that increasing the total spin would continuously cause an increase of U_{eff}—it has been shown that the magnetic anisotropy, in fact, is more important. This has led to a focus on 4f metal complexes [8–10]. The 4f orbitals of the lanthanide ions are deeply buried and therefore do not interact strongly with an external ligand field. Thus, even in their complexes, lanthanide ions can possess large

C.T.C.
Principal
Nowgong Girls' College
Nagaon :: Assam

Pankaj Kalita

Nowgong Girls' College ★ ESTD: 1962 ★ Nagaon :: Assam

Dalton Transactions

ROYAL SOCIETY OF CHEMISTRY

PAPER

View Article Online
View Journal

Check for updates

Cite this: DOI: 10.1039/d0dt03054f

Seven-coordinate Ln^{III} complexes assembled from a bulky ^{Mes}acacH ligand: their synthesis, structure, photoluminescence and SMM behaviour†

Pankaj Kalita, [a,b] Prakash Nayak,[a] Naushad Ahmed, [b] Juan Manuel Herrera, [c] Krishnan Venkatasubbaiah, *[a] Enrique Colacio *[c] and Vadapalli Chandrasekhar *[b,d]

The reaction of a bulky acetyl acetone ligand 1,3-dimesitylpropane-1,3-dione (^{Mes}acacH) with hydrated lanthanide chlorides in the presence of tetramethylammonium hydroxide afforded a new family of neutral mononuclear Ln^{III} complexes $[Ln(^{Mes}acac)_3(DMF)]$ (Ln = Dy (**1**); Tb (**2**); $Y_{0.91}Dy_{0.09}$ (**3**); and Er (**4**)). The molecular structures of these complexes were confirmed by single crystal X-ray diffraction studies. The coordination geometries of the Ln^{III} centre were analysed by SHAPE analysis which revealed a capped octahedral geometry in **1–4**. Photoluminescence studies showed ligand-sensitized green emissions for **2** with an appreciable quantum yield of 0.83%. Static (dc) and dynamic (ac) magnetic studies of complexes **1** and **3** were performed. The dynamic magnetic study revealed that complex **1** exhibits zero-field slow relaxation of the magnetization without showing a clear maximum in the out-of-phase ac susceptibility plots. However, magnetic dilution of **1** with the Y^{III} metal ion (complex **3**) and/or the application of a dc magnetic field induces a strong frequency dependence of the ac susceptibility signals with χ''_M peaks in the 3–10 K temperature range, thus supporting field-induced SMM behaviour of **1**. The relaxation process takes place through a combination of the Orbach and Raman mechanisms. The fitting of the temperature dependence of the relaxation time to the equation $\tau^{-1} = \tau_0^{-1} \exp(-U_{eff}/k_BT) + BT^n$, allows the extraction of the effective energy barrier U_{eff}/k_B = 70 K (48.7 cm^{-1}) and pre-exponential parameter of $\tau_0 = 2.7 \times 10^{-7}$ s for the Orbach mechanism (first term) and the parameters $B = 0.04\ s^{-1}\ K^{-n}$ and $n = 6.11$, for the Raman mechanism (second term).

Received 1st September 2020,
Accepted 7th October 2020
DOI: 10.1039/d0dt03054f
rsc.li/dalton

Introduction

Single-molecule- and single-ion magnets (SMMs and SIMs) have been receiving a lot of attention in recent years.[1] These are molecular systems that once magnetized retain their magnetization for a significantly longer period of time, below certain critical temperatures.[2] While most of the initial efforts were devoted to mainly polynuclear 3d complexes,[3] soon this phenomenon was also observed in heterometallic 3d/4f complexes.[4] In a seminal discovery in 2003, slow magnetic relaxation and magnetic hysteresis were observed for the first time in a mononuclear bis(phthalocyanine)Tb^{III} complex $(TBA)^+[Tb(Pc)_2]^-$ (TBA = tetrabutylammonium).[5] This discovery opened up a new direction for the utilization of 4f-ions in the construction of molecular magnets. Recent advancements in this field reveal that mononuclear complexes could exhibit promising SMM behaviour provided the following two criteria are met: (*a*) the complex should have a bistable spin ground state with a high magnitude of $|m_J|$ *i.e.* an *Ising* ground state, and should possess (*b*) well isolated excited states with magnetic moments co-linear with the ground state.[6] The 4f-ions are considered to be suitable candidates for the design and assembly of molecular magnets due to the fact that many of them possess a fairly large ground state spin, *S*, and also in addition, have intrinsic magnetic anisotropy arising from a large unquenched orbital angular momentum and strong spin–orbit coupling. One important drawback of some of the 4f complexes, however, is the significant contribution from the temperature independent zero field [illegible]

[a]School of Chemical Sciences, National Institute of Science Education and Research Bhubaneswar, HBNI, Jatni, Khurda - 752050, Odisha, India. E-mail: krishna@niser.ac.in
[b]Tata Institute of Fundamental Research Hyderabad, Gopanpally, Hyderabad-500 046, India. E-mail: sc@iitk.ac.in, sc@tifr.res.in
[c]Departamento de Química Inorgánica, Facultad de Ciencias, Universidad de Granada, Avenida de Fuentenueva s/n, 18071 Granada, Spain. E-mail: ecolacio@ugr.es
[d]Department of Chemistry, Indian Institute of Technology Kanpur, Kanpur-208016, India

†Electronic supplementary information (ESI) available. CCDC 2023655, 2023662, 2023663 and 2023664. For ESI and crystallographic data in CIF or other electronic format see DOI: 10.1039/d0dt03054f

CTC
Principal
Nowgong Girls' College
Nagaon :: Assam
Nowgong Girls' College ESTD: 1962 Nagaon :: Assam

ISSN 2278-2281 (Online Version)
ISSN 0976-3597 (Print Version)

NeBIO

www.nebio.in

A Journal of Environment and Biodiversity

Volume XII Issue 1 March 2021

NECEER

North East Centre for Environmental Education & Research, Imphal

C.T.C.
Principal
Nowgong Girls' College
Nagaon :: Assam

Nowgong Girls' College
ESTD: 1962
Nagaon :: Assam

nebio.in

Gotruvalli M. Prashanth Kumar

Abstract I Full Text PDF I

Research Article

Microfungal diversity of rice field at different altitudes in Bishnupur district of Manipur

Heisnam Loidang Devi & Anjan Kumar Sarma

Abstract I Full Text PDF I

Research Article

Ethnomedicinal uses of some wild edible plants used by the Tiwa Tribe of Nagaon district, Assam

Puspa Komor & Rakhi Bhattacharyya

Abstract I Full Text PDF I

C.T.C.

Principal
Nowgong Girls' College
Nagaon :: Assam

Nowgong Girls' College
ESTD: 1962
Nagaon :: Assam

Coordination Chemistry Reviews 432 (2021) 213707

Contents lists available at ScienceDirect

Coordination Chemistry Reviews

journal homepage: www.elsevier.com/locate/ccr

Review

Heterometallic Cu^{II}–Ln^{III} complexes: Single molecule magnets and magnetic refrigerants

Atanu Dey [a,*], Prasenjit Bag [a,1], Pankaj Kalita [a,1], Vadapalli Chandrasekhar [a,b,*]

[a] Tata Institute of Fundamental Research Hyderabad, Gopanpally, Hyderabad 500046, India
[b] Department of Chemistry, Indian Institute of Technology Kanpur, Kanpur 208016, India

ARTICLE INFO

Article history:
Received 20 August 2020
Accepted 5 November 2020
Available online 22 January 2021

Keywords:
Heterometallic $3d$–$4f$ complexes
Ferromagnetic interaction
Single molecule magnets
Magnetocaloric effect
Single chain magnets

ABSTRACT

Molecular nanomagnets containing heterometallic 3d–4f complexes have been investigated extensively for the past few years realizing the role of exchange interaction to minimize the QTM effect. In this context, heterometallic complexes particularly containing Cu^{II}-Ln^{III} have encompassed a pivotal role due to the ferromagnetic exchange interaction. Herein we review the Cu/Ln complexes that exhibit single molecule magnet (SMM)/magnetocaloric effect (MCE) in a comprehensive way.

© 2020 Elsevier B.V. All rights reserved.

Contents

1. Introduction 2
2. Cu^{II}-Ln^{III} exchange coupling 3
   2.1. Impact of Cu^{II}-Ln^{III} exchange coupling on SMM behavior 7
3. Heterometallic $Cu^{II}Ln^{III}$ complexes of varying nuclearities, showing SMM behavior 8
   3.1. Dinuclear $Cu^{II}Ln^{III}$ complexes 8
   3.2. Trinuclear $Cu^{II}Ln^{III}$ complexes 15
   3.3. Tetranuclear $Cu^{II}Ln^{III}$ complexes 21
   3.4. Pentanuclear $Cu^{II}Ln^{III}$ complexes 32
   3.5. Hexanuclear $Cu^{II}Ln^{III}$ complexes 33
   3.6. Heptanuclear $Cu^{II}Ln^{III}$ complexes 34
   3.7. Octanuclear $Cu^{II}Ln^{III}$ complexes 35
   3.8. Nonanuclear $Cu^{II}Ln^{III}$ complexes 36
   3.9. Decanuclear $Cu^{II}Ln^{III}$ complexes 41
   3.10. Higher nuclearity $Cu^{II}Ln^{III}$ complexes 42
   3.11. Heterotrimetallic/tetrametallic complexes containing $\{Cu^{II}$-$Ln^{III}\}$ moieties 46
   3.12. $\{Cu^{II}$-$Ln^{III}\}$ complexes containing radical ligands 48
4. Magnetocaloric effect of $Cu^{II}Ln^{III}$ complexes 51
   4.1. Cu^{II}-Gd^{III} complexes possessing extended structures 54
   4.2. MCE of discrete Cu^{II}-Gd^{III} complexes 56
5. Conclusion and perspectives 64
   Declaration of Competing Interest 64
   Acknowledgements 64
   References 64

* Corresponding authors.
E-mail addresses: [illegible]50@gmail.com (A. Dey), vc@iitk.ac.in, vc@tifr.res.in (V. Chandrasekhar).
[1] These authors contributed equally.

https://doi.org/10.1016/j.ccr.2020.213707
0010-8545/© 2020 Elsevier B.V. All rights reserved.

Principal
Nowgong Girls' College
Nagaon :: Assam

Nowgong Girls' College
ESTD: 1962
Nagaon :: Assam

ISSN: 2454-3837 Vol.-VII Issue-I March 2021

সম্প্রীতি
sampriti

ৰাষ্ট্রীয় গৱেষণা পত্রিকা

Double Blind Peer Reviewed National
Research Journal of Humanities and Social Sciences

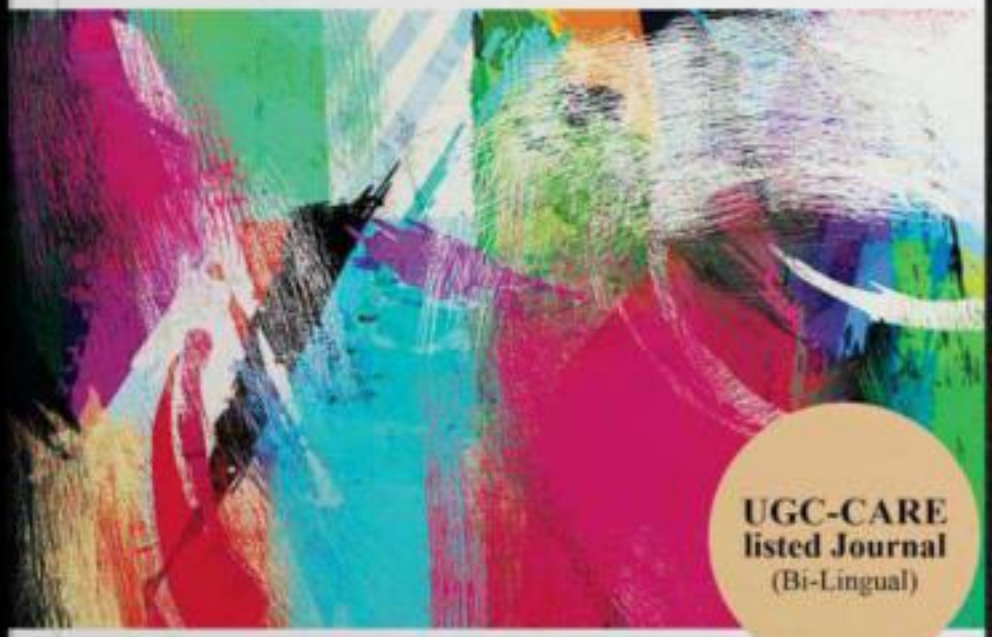

UGC-CARE
listed Journal
(Bi-Lingual)

Editor in Chief
Dr. Dhiraj Patar

Assistant Editor
Dr. Rumi Patar

C.T.C.
Principal
Nowgong Girls' College
Nagaon :: Assam

Nowgong Girls' College
ESTD: 1962
Nagaon :: Assam

সম্প্রীতি ISSN : 2454-3837

বাষ্ট্রীয় গবেষণা পত্রিকা

SAMPRITI

DOUBLE BLIND PEER REVIEWED NATIONAL RESEARCH JOURNAL OF HUMANITIES AND SOCIAL SCIENCES

Vol.-VII, Issue-I, March 2021

UGC-Care listed Journal

(Bi-Lingual)

Editor in Chief

Dr. Dhiraj Patar

Assistant Editor

Dr. Rumi Patar

SAMPRITI PUBLICATION

NEAR GAUHATI UNIVERSITY

ASSAM FOREST SCHOOL-781014

Principal

Nowgong Girls' College

Nagaon :: Assam

Nowgong Girls' College ESTD: 1962 Nagaon :: Assam

Content

আঞ্চ সাংকেতিক অনুবাদকৰূপে ভবেন্দ্রনাথ শইকীয়াৰ অন্তৰ্দীপ উপন্যাসৰ চলচ্চিত্ৰ ৰূপ অভিযান : এটি আলোচনা।
শেষাদ্রী গোস্বামী 11-17

অসমীয়া ডাকৰ বচন, প্ৰবাদ-পতিয়ন, ফকৰা-যোজনা, সাঁথৰ আদিত ভৌগোলিক্যৰ প্ৰতিফলা পাৰিপাৰ্শ্বিক সচেতনতা : এটি বিশ্লেষণাত্মক অধ্যয়ন
ড° বিশ্বজিৎ দাস, আনিতা শইকীয়া 18-29

অসমীয়া শিশুসাহিত্য আৰু হোমেন বৰগোহাঞিঁ : এক সমীক্ষা
ড° আখতাৰুল ইছলাম 30-38

ডাইনী হত্যা : এক সামাজিক ব্যাধি
অমল চন্দ্ৰ দাস 39-44

মিচিং লোক-জীৱনৰ বাঁহ-বেতশিল্পৰ ব্যৱহাৰ : এক ক্ষেত্ৰভিত্তিক অধ্যয়ন
ড° বিজয়কৃষ্ণ দলৈ 45-68

অসমীয়া ভাষাৰ শব্দ-সম্ভাৰ : এটি বিশ্লেষণাত্মক অধ্যয়ন
ড° বন্দেশ্বৰ মিলি 69-90

সাধুকথাৰ কথাঙ্গ বিচাৰ : এক বৈজ্ঞানিক চমু অধ্যয়ন
ড° জ্যোতি গগৈ 91-101

সাধুকথাৰ প্ৰায়োগিক দিশ : এটি বিশ্লেষণাত্মক অধ্যয়ন
দীপক নাথ 102-[illegible]

Principal
Nowgong Girls' College
Nagaon :: Assam

Nowgong Girls' College
ESTD: 1962
Nagaon :: Assam

Sampriti
Vol : Vol.-VII, Issue-I, March 2021
ISSN : 2454-3837
pages:18-29

অসমীয়া ডাকৰ বচন, প্ৰবাদ-পটন্তৰ, ফকৰা-যোজনা, সাঁথৰ আদিত জৈৱবৈচিত্ৰ্যৰ প্ৰতিথকা পাৰিপাৰ্শ্বিক সচেতনতা : এটি বিশ্লেষণাত্মক অধ্যয়ন

ড° বিশ্বজিৎ দাস
সহযোগী অধ্যাপক, নগাঁও ছোৱালী মহাবিদ্যালয়

আদিত্য শইকীয়া
গবেষক, (Correspondent author) *অসমীয়া বিভাগ,গুৱাহাটী বিশ্ববিদ্যালয়*
adityasaikia305@gmail.com

সংক্ষিপ্তসাৰ

অসমীয়া জাতীয় জীৱনত ডাকৰ বচন, ফকৰা-যোজনা, প্ৰবাদ-পটন্তৰ, সাঁথৰ আদিৰ গুৰুত্ব অপৰিসীম। প্ৰকৃতিৰ অনুগ্ৰহত বিভিন্ন পৰিবেশমিত্ৰ লোকবিশ্বাসৰ গইনা লৈ সৃষ্ট অসমীয়া ডাকৰ বচন, ফকৰা-যোজনা, প্ৰবাদ-পটন্তৰ, সাঁথৰ আদিত পৰিবেশৰ বিভিন্ন ৰহস্য থকাটো স্বাভাৱিক। এটা জাতি দীৰ্ঘজীৱি হোৱাৰ ক্ষেত্ৰত ডাকৰ বচন, ফকৰা-যোজনা, প্ৰবাদ-পটন্তৰ, সাঁথৰ আদিৰ মাজত পঞ্জীভূত পাৰিপাৰ্শ্বিক সচেতনতাৰ দিশবোৰ অধ্যয়ন হোৱাটো নিতান্তই প্ৰয়োজনীয়। ইয়াৰ লগতে, বিশ্বায়নৰ যুগত বহনক্ষম উন্নয়নৰ স্বাৰ্থত এই বিষয়টি অধ্যয়নৰ যথেষ্ট গুৰুত্ব আছে। সেয়েহে, অসমীয়া ডাকৰ বচন, ফকৰা-যোজনা, প্ৰবাদ-পটন্তৰ, সাঁথৰ আদিৰ মাজত জৈৱবৈচিত্ৰ্যৰ প্ৰতি থকা পাৰিপাৰ্শ্বিক [illegible] কেনেদৰে আছিল, সেই সময়ৰ অসমীয়া জনসমাজে কেনেদৰে [illegible]

Principal
Nowgong Girls' College
Nagaon :: Assam

Nowgong Girls' College
ESTD: 1962
Nagaon :: Assam

বাখিছিল সেই সম্পর্কে অধ্যয়ন কৰাই এই গৱেষণা পত্ৰৰ উদ্দেশ্য। এনে ধৰণৰ অধ্যয়ন পৃথিৱীৰ প্ৰায়বোৰ জাতিৰ লোকসাহিত্যতে হেছে আৰু তাৰ পৰা বহুতো সুফলো লাভ কৰা দেখা গৈছে। অসমীয়া লোকসাহিত্যৰ অন্তৰ্গত ডাকৰ বচন, ফকৰা-যোজনা, প্ৰবাদ-পটন্তৰ, সাঁথৰ আদিত এই বিষয়ে অধ্যয়নৰ এক বিশাল ক্ষেত্ৰ আছে।

সূচক শব্দ : প্ৰবাদ, জৈৱবৈচিত্ৰ, লোকসাহিত্য

১.০০ অৱতৰণিকা

ডাকৰ বচন, ফকৰা-যোজনা, প্ৰবাদ-পটন্তৰ, সাঁথৰ আদি অসমীয়া লোকসাহিত্য তথা ভাষা সাহিত্যৰ অমূল্য ৰত্ন। এইবোৰ অসমীয়া লোকসাহিত্যৰ যুগ-যুগান্তৰৰ অভিজ্ঞতা আৰু জ্ঞানলব্ধ স্তম্ভ। ইয়াৰ মাজেৰে প্ৰতিফলিত হয় অনেক যুগ যুগ ধৰি আৰ্জিত মানৱ জীৱনৰ ভাবানুভূতি, লোকসমাজৰ চিন্তা-চৰ্চা, সামূহিক ধ্যান-ধাৰণা আদি। ইয়াৰ প্ৰধান গুণগত বৈশিষ্ট হৈছে কম কথাৰ মাজেৰে অধিক প্ৰকাশ কৰা।

অসমীয়া লোকসাহিত্যৰ সৌন্দৰ্য উপলব্ধিৰ অনন্য অলংকাৰ ডাকৰ বচন, ফকৰা-যোজনা আদিৰ লগত অসমীয়া জাতীয় জীৱনৰ নিবিড় সম্বন্ধ আছে। মুখে মুখে বাগৰি অহা, জাতিৰ সমুহীয়া, ব্যৱহাৰিক আৰু নৈতিক জ্ঞানৰ সঞ্চয়পুঁজি হোৱা হেতুকে লোকসাহিত্যৰ এই বিভাগটোত অসমীয়া লোকজীৱনৰ লগত জড়িত ৰাজনীতি, অৰ্থনীতি, কৃষি, শিল্প, গৃহস্থালি, আচাৰ-ব্যৱহাৰ আদি সকলো বিষয়ৰ সাৰুৱা উপদেশ পোৱা যায়। এইক্ষেত্ৰত আলোচ্য 'পাৰিপাৰ্শ্বিক সচেতনতা' বা 'পৰিৱেশ বিষয়ক সাৰুৱা উপদেশ' অন্যতম। লোকসাহিত্যৰ এই বিভাগৰ 'ডাকৰ বচন, ফকৰা-যোজনা, প্ৰবাদ-বাক্য' এই তিনিটা ভাগতেই পাৰিপাৰ্শ্বিক সচেতনতা সম্পৰ্কীয় সাৰুৱা উপদেশসমূহ সঞ্চিত হৈ আছে। সেয়েহে, আলোচনাৰ সুবিধাৰ্থে এইবোৰক পৃথকে পৃথকে ধৰা নাই।

১.০১ গৱেষণা পদ্ধতি

"অসমীয়া ডাকৰ বচন, প্ৰবাদ- পটন্তৰ, ফকৰা-যোজনা, সাঁথৰ আদিত প্ৰতিফলিত জৈৱবৈচিত্ৰ্যৰ প্ৰতি থকা পাৰিপাৰ্শ্বিক সচেতনতা" শীৰ্ষক গৱেষণা পত্ৰখনি অধ্যয়নৰ বাবে প্ৰধানকৈ বিশ্লেষণাত্মক পদ্ধতি গ্ৰহণ কৰা হৈছে। গৱেষণা বিষয়টি অধ্যয়নৰ ক্ষেত্ৰত বিভিন্ন ধৰণৰ তথ্যৰ উৎস হিচাপে মুখ্য, গৌণ আৰু অন্যান্য উৎসৰ ওপৰত গুৰুত্ব দিয়া হৈছে।

১.০২ প্ৰমেয়

গৱেষণা কৰ্মত নিম্নলিখিত সিদ্ধান্তসমূহ প্ৰতিপাদ্য বিষয়ৰূপে উপস্থাপিত হ'ব বুলি আশা কৰা হৈছে—

(ক) অসমীয়া ডাকৰ বচন, ফকৰা-যোজনা, প্ৰবাদ-পটন্তৰ, সাঁথৰ আদিত পৰম্পৰাগতভাবে পৰিৱেষ্টিত জৈৱবৈচিত্ৰ্যৰ বিভিন্ন দিশৰ ওপৰত বিজ্ঞানসম্মত বিশ্লেষণেৰে আমাৰ বিচাৰ্য পাৰিপাৰ্শ্বিকভাৱে সচেতনতামূলক তথা পৰিৱেশমিত্ৰ দিশ সম্পৰ্কে জানিব পৰা যাব।

(খ) পুৰণি অসমীয়া সমাজৰ জৈৱবৈচিত্ৰ্য সম্পৰ্কে থকা জ্ঞান, দায়বদ্ধতা আৰু সচেতনতা সম্পৰ্কে উচিত মূল্যায়ন হ'ব।

C.T.C.
Principal
Nowgong Girls' College
Nagaon :: Assam

Nowgong Girls' College
ESTD: 1962
Nagaon :: Assam

(গ) বিশ্বায়নৰ যুগত সমগ্ৰ বিশ্বতে পৰিবেশৰ প্ৰভাৱ অপৰিসীম। সেয়েহে বিষয়টোৰ উপৰিও অধ্যয়ন বৰ্তমানৰ সমাজ আৰু সাহিত্যৰ লগতে বিজ্ঞানৰ জগতখনিলৈ অন্যতম আহৰণ হিচাপে পৰিগণিত হ'ব।

২.০০ গছ-গছনি সংৰক্ষণ আৰু প্ৰতিপালন

এ. পি. জে. আব্দুল কালামে কৈছিল 'মই চৰাই পুহিছিলো উৰি গ'ল। মই বান্দৰ পুহিছিলো, পলাই গ'ল। যেতিয়া মই গছ এজোপা ৰুপৌ, তেতিয়া চৰাই আৰু বান্দৰ দুয়োটিই ঘূৰি আহিল।' পাৰিপাৰ্শ্বিক সচেতনতাৰ ই এক ডাঙৰ উদাহৰণ। বিশ্বব্ৰহ্মাণ্ডত পৃথিবী হৈছে একমাত্ৰ গ্ৰহ যিটো জীৱৰ আবাসভূমি। পৃথিবীৰ গছ-গছনি, প্ৰাণী আদি সকলো সম্পূৰ্ণ পাৰস্পৰিক নিৰ্ভৰশীলতাৰ ফলশ্ৰুতি আৰু এই নিৰ্ভৰশীলতাৰ মূল শুৰিটো হ'ল 'গছ-গছনি'।

প্ৰাণীজগত বৰ্ত্তি থকাত গছ-গছনিৰ গুৰুত্ব অপৰিসীম। সভ্যতাৰ আৰম্ভণিৰে পৰা মানুহ এইক্ষেত্ৰত সচেতন। পৰিবেশ অনুযায়ী পৃথিবীৰ যি যি অংশত প্ৰাণীবাশিৰ বাসস্থলী, সেই অংশে উদ্ভিদবাশিৰো উৎপন্নস্থলী। বিভিন্ন ধৰণৰ শৃংখলৰ জৰিয়তে উদ্ভিদ আৰু প্ৰাণী পৰস্পৰে পৰস্পৰৰ ওপৰত নিৰ্ভৰশীল। অকল খাদ্য শৃংখলৰ প্ৰাথমিক উপাদান বা উপভোক্তা হিচাপে খাদ্য শৃংখলৰ যোগেদি উদ্ভিদ আৰু প্ৰাণীজগত পৰস্পৰে পৰস্পৰৰ ওপৰত নিৰ্ভৰশীল এনে নহয়। জলবায়ু, অ'জেন, জৈৱবৈচিত্ৰ্য, বায়ু প্ৰদূষণ, গৰাখহনীয়া ইত্যাদি বিভিন্ন দিশত ই ক্ৰিয়াশীল। সেয়েহে কৃষ্টি সভ্যতাৰ প্ৰতিষ্ঠাপক মানুহ বা পৰম্পৰাগত অসমীয়া সমাজখনে উদ্ভিদজোপাৰ মূল্য সুন্দৰকৈ বুজি পাইছিল। সেই অনুসাৰে পৰিবেশ বিজ্ঞানৰ অনুষ্ঠানিক জ্ঞান নথকা সময়তো পৰম্পৰাগত কৃষিজীৱী অসমীয়া সমাজখনে পৰিবেশমিত্ৰ বহুতো কাম-কাজ কৰি গৈছিল। এইক্ষেত্ৰত—

"এক জুপি বৃক্ষ আছে জগতক জুৰি।
তলে আছে ডাল পাত ওপৰে আছে গুৰি।।" (গগৈ ৩৪)

"যেবেসে ধৰ্ম কৰিব জানি।
পুখুৰী খানিয়া ৰাখিব পানী।।
বৃক্ষ ৰোপণে অধিক ধৰ্ম।
মঠ-মণ্ডপত অধিক কৰ্ম।।" (গগৈ ৩০)

বেদান্ত, উপনিষদ আদিৰ তত্ত্বেৰে সম্মলিত ফকৰাৰ বুকুত সাঁথৰৰ সাঁচত সোমাই থকা প্ৰথমৰ ফকৰাটিত গছ-পাত। এনেদৰে ডাকৰ বচনৰ পৰম্পৰাগত অসমীয়া সমাজ জীৱনে পাকে-পকাৰে গছজোপাক অদ্বৈতবাদৰ লগত তুলনা কৰি অসমীয়া সমাজত গছৰ মহিমা তথা তাৰ উপকাৰিতা আৰু লগতে প্ৰয়োজনীয়তাৰ কথা ব্যক্ত কৰিছে।

দ্বিতীয় ডাকৰ বচনটিত, বৃক্ষৰোপণক ধৰ্মৰ শাৰীত স্থান দিছে। ধৰ্মই মানুহক কৰ্মী কৰি তোলে আৰু সংসাৰৰ অন্যান্য মায়া-মোহৰ পৰা আঁতৰাই প্ৰাপ্যখিনি গ্ৰহণ কৰি শান্তিৰে মোক্ষ-প্ৰাপ্তিৰ পথত আগুৱাই লৈ যায়। কোৱা হয়, এজোপা গছ হাজাৰটা মানুহৰ সমান। এনে মহান কৰ্ম [illegible] বৃক্ষৰোপণ কৰিটো গোনপটীয়াকৈ মোক্ষপ্ৰাপ্তিৰ প্ৰশস্ত [illegible] সেই ৰাতিয়াৰ দিনতে পাৰিপাৰ্শ্বিকভাৱে ইমান [illegible] আছিল [illegible]

CTC
Principal
Nowgong Girls' College
Nagaon :: Assam
Nowgong Girls' College ESTD: 1962 Nagaon :: Assam

অসমৰ সমাজ একবিংশ শতিকাতো গছ-গছনি জঙ্গলে-মধে কাটি ধ্বংস কৰাত ব্যস্ত।

গছ-গছনিৰ প্ৰয়োজনীয়তাৰ কথা দাঙি ধৰি তাক ৰোপণ কৰিলে নহয় তাৰ বংশবৃদ্ধি কৰা, প্ৰতিপালন কৰা আদি কথাও লোকসাহিত্যৰ এই শাখাত প্ৰতিফলিত হয়। ক'বৰাত গছৰ গুটি পালে নিজৰ বাৰীত কই থবৰ দিহা দিছে। গছ-গছনি খাদ্য উৎপাদনত একমাত্ৰ স্বনিৰ্ভৰশীল হীয় আৰু গছ-গছনিক জীয়াই বখাৰ দায়িত্ব প্ৰাণীজগতৰ অৰ্থাৎ মানুহৰ। সেয়েহে গুটি সিঁচৰণ কৰা, কীট-পতংগ নিয়ন্ত্ৰণ, তৃণ-তৰুৰ অতিবৃদ্ধি ৰোধ আদিত মানৱ জাতিৰ সক্ৰিয় ভূমিকা সমৰ্কীয় বিভিন্ন তথ্য ডাকৰ বচনত পোৱা যায়। ইয়াৰ লগতে কোনজোপা গছ কেনেদৰে কৰ লাগে, কেনেদৰে কলে তাৰ সুফল পোৱা যায় সেই বিষয়সমূহো ডাকৰ বচনত বিদ্যমান।

"বাটত পালে গুটি,
বাৰীত থবা গুজি।
সময়ত লাগিব গুটি,
তেতিয়াহেপাবা জুতি।" (সং- নৰকান্ত শইকীয়া, গোলাঘাট)

"জালুকত গোবৰ, পানত মাটি,
কল ৰুবা তিনিবাৰ কাটি।" (গগৈ ১৯)
"লাগে তামোল নালাগে
নালাগে তামোল লাগে।" (কোঁচ ২৮০)
"সাতে পাতল পাঁচত ঘন,
ছয়ত তামোল নদন বদন।" (কোঁচ ৩১০)
"তামোলত গোবৰ মাহত মাটি
নফলিলে নাৰিকল শিপা কাটি। (কোঁচ ১৫২)

কলগছজোপাৰ বিষয়ে কৈছে—

"এহাত এমুঠন দিবা পোত,
তেহে চাবা কলৰ গোট। (শর্মা ৪২)
"আঠীয়াত গোবৰ, পানত মাটি,
পুৱাত ছায়, মালভোগত খায়।" (শর্মা ৪৯)
"তিনিশ যাঠি জোপা ৰুবা ক'ল,
মাহেকে পহেকে চিকুণাবা তল।
পাত-পচলা লাভত খাবা,
লংকাৰ বণিজ ঘৰতে পাবা। (কোঁচ ১৫৯)
"নতুন কলৰ নাকাতিবা পাত,
তেতিয়াহে কলৰ নাযায় জাত। (সং -ত্ৰিলোচন গগৈ, গোলাঘাট)

অসমীয়া সমাজ জীবনত কলগছৰ ভূমিকা গুৰুত্বপূৰ্ণ। পাৰিপাৰ্শ্বিক [illegible] কলগছজোপাৰ [illegible] ভূমি অবক্ষয়, বৰষুণৰ পানী ধৰি ৰখা, [illegible] লগতে অন্যান্য চৰাই-চিৰিতিৰ [illegible] বাসস্থল হিচাপে ইয়াৰ পাৰিপাৰ্শ্বিক গুণ [illegible] পুৰণি [illegible]

C.T.C.
Principal
Nowgong Girls' College
Nagaon :: Assam
Nowgong Girls' College ESTD: 1962 Nagaon :: Assam

সমাজখন এই গুণবোৰৰ বিষয়ে জ্ঞাত আছিল আৰু সেইহেতুকে ইয়াৰ বিষয়ে উপৰিউক্ত কথাসাৰ ডাকৰ বচনত সন্নিবিষ্ট কৰি থৈ গৈছে। ডাকৰ বচন অনুযায়ী ঘৰতে পোৱা সহজলভ্য জৈবিক সাৰ 'গোবৰ, জাবৰ' আৰু জৈবিক কীটনাশক 'ছাই' আদিৰ পাৰিপাৰ্শ্বিক মূল্য কৃত্রিম সাৰতকৈ বেছি। কৃত্রিম সাৰ তথা কীটনাশক ঔষধবোৰ ভাল যিমান, বেয়াও সিমান। এইবোৰ ব্যৱহাৰ কৰিলে মাটিৰ গুণাগুণ প্ৰথম অৱস্থাত বৃদ্ধি পালেও পাছলৈ সাৰ নিদিলে সম্পূৰ্ণৰূপে বেয়া হৈ যায়। পুৰণ পদ্ধতিত মাটিৰ গুণাগুণ ভালে থাকে তথা অন্য জীৱকুলবোৰো অপকাৰ নহয়।

"ৰাসায়নিক সাৰৰ পৰিৱৰ্তে জৈবিক সাৰ ব্যৱহাৰ কৰি আৰু কীটনাশক দ্ৰব্যৰ সলনি জৈবিক পদ্ধতিৰে শস্যৰ অনিষ্টকাৰী কীট-পতংগ ধ্বংস কৰাৰ ব্যৱস্থা কৰি মাটি প্ৰদূষণ ৰোধ কৰিব পাৰি।" (পাঠক ১০০)

ডাকৰ বচনৰ লগতে অসমীয়া সমাজত প্ৰচলিত 'প্ৰবাদ' কিছুমানতো পৰম্পৰাগত অসমীয়া সমাজ জীৱনৰ গছ-গছনি সম্পৰ্কীয় সচেতনতা দেখা যায়। এইক্ষেত্ৰত—

"গছ থাকিলেহে মানুহ থাকিব।"
"আঁহতগছ, ৰৱগছ কাটিব নাপায়।"
"উঠি অহা গছ পুলি কাটিব নাপায়।"
"তুলসীৰ আগত চাকি জ্বলোৱা হয়।"
"বেলগছৰ তলত চাকি জ্বলাই পূজা কৰা হয়।"
"সিজু গছৰ গুৰিত পূজা কৰা হয়।"

ডাঙৰ ডাঙৰ গছ বা ৰৱগছবোৰ কাটিব নাপায় বুলি অসমীয়া সমাজত যি প্ৰবাদ আছে সি সম্পূৰ্ণ বৈজ্ঞানিক। ৰৱগছজোপাই বায়ুমণ্ডলৰ অ'জেন, নাইট্ৰজেন আদিৰ ভাৰসাম্য সুচাৰুৰূপে চলাই থাকে। সাধাৰণতে ৰৱগছজোপাৰ পাতৰ সংখ্যা অন্যান্য গছৰ তুলনাত বেছি ফলস্বৰূপে, জীৱজগত বৰ্তি থাকিবৰ বাবে কাৰ্বন-ডাই-অ'ইড সেৱন আৰু অ'জেন বৰ্জনৰ পৰিমাণ বেছি।

ইয়াৰ লগতে অন্যান্য গছৰ তুলনাত ৰৱগছজোপাই মানুহকে ধৰি অন্যান্য চৰাই-চিৰিকটি জীৱ-জন্তু সকলোৰে আশ্ৰয়স্থল হিচাপে কাম কৰে। চিলনী, কাউৰী আদি চৰাইয়ে এনেধৰণৰ ৰৱগছক বংশবৃদ্ধি তথা আশ্ৰয়ৰ স্থল হিচাপে ব্যৱহাৰ কৰে। পৰিৱেশৰ লগত অৰ্থাৎ পুৰণি কালৰে পৰা প্ৰকৃতিৰ ওচৰত থকা বাবে এনেবোৰ দিশ তেওঁলোকৰ সুন্দৰভাৱে দৃষ্টিগোচৰ হৈছিল আৰু তেওঁলোকে তাৰ সংৰক্ষণৰ হেতুকে 'বৃক্ষপূজা' তথা 'কাটিব নাপায়, 'গছত দেৱতা থাকে' ইত্যাদি পৰম্পৰাৰ সৃষ্টি কৰিছিল। ইয়াৰ মূলতে আছিল বিশেষকৈ বায়ু প্ৰদূষণ ৰোধ আৰু জৈৱবৈচিত্ৰ্য অটুত ৰখা। 'বিহু'ৰ সময়ত ৰৱগছৰ তলত বিহু মৰাৰ অন্তৰালত ওপৰঃ কোৱাৰ দৰে বৈজ্ঞানিক কাৰণ আছে। প্ৰাথমিক কাৰণ হিচাপে ৰৱগছৰ তলত ছাঁ পোৱা যায়।

এনেবোৰ পাৰিৱেশিক দিশৰ লগতে উপৰিউক্ত প্ৰতিজোপা গছৰ ঔষধি গুণ আছে। অসমীয়া লোকসমাজৰ লগত জড়িত প্ৰায় সকলো গছ ঔষধি গুণসম্পন্ন। পুৰণি অসমীয়া সমাজখনে অতি প্ৰাচীন কালৰেপৰা ৰোগ নিৰাময়ৰ কাৰণে উদ্ভিদৰ ওপৰত নিৰ্ভৰ কৰি আহিছে। সেয়েহে, বিশ্বৰ প্ৰতিটো জাতি, সম্প্ৰদায়ৰ অতি পুৰণি পৰম্পৰাগত [illegible] দৰে অসমীয়া [illegible] অসমীয়া লোকসমাজত তাহানি দিনৰে [illegible]

C.T.C.
Principal
Nowgong Girls' College
Nagaon :: Assam
Nowgong Girls College ESTD: 1962 Nagaon :: Assam

আঁহত, জৰী আদি গছৰ লগতে নিম গছ অসমীয়া ঔষধি ব্যৱস্থাৰ অধীনৰ অন্যতম এজোপা গছ। নিম গছ মানৱ সমাজলৈ প্ৰকৃতিৰ অনবদ্য অৱদান। অসমীয়া লোক সংস্কৃতি, লোকবিশ্বাসত নিম গছৰ স্থান অনন্য। বসন্ত জ্বৰত শুকান নিমৰ পাত বিছনাৰ তলত থোৱা, নিম পাত খালে বসন্ত হোৱা নহয়, বহাগ বিহুৰ মানুহ বিহুৰ দিনা গুলাপেটত মুখত নিম পাত লোৱা, নিম পাত ৰাখেক্ষৰ মাজত থোৱা, পথাৰত নিমৰ ডাল পোতা আদি অনেক পৰম্পৰা অসমীয়া লোকসমাজত প্ৰচলিত। অসমীয়া লোকসমাজৰ লগত নিম, বেল, সিজু, আঁহত আদি গছ জড়িত হোৱাৰ অন্তৰালত বৈজ্ঞানিক কাৰণ নিহিত হৈ আছে।

"এবিধ অতি মূল্যবান ঔষধি গুণেৰে সমৃদ্ধ উদ্ভিদ হ'ল 'নিমগছ'। নিম গছৰ পাতবোৰ তিতা। নিম পাতৰ ব্যৱহাৰে ডায়বেটিছ, বেক্টেৰিয়া আদি প্ৰশমনত সহায় কৰে। নিম গছৰ পাতবোৰ পেটৰ ঘাঁ আৰু আলচাৰ নিৰাময়ৰ বাবে অত্যন্ত সুফলদায়ক। পাতৰ লগতে গছজোপাৰ শিপা, বাকলি, ডাল, ঠাৰি, ফল-মূল আদি বিভিন্ন দৰৰত ব্যৱহাৰ কৰা হয়। নিম গছৰ শিপাৰ ব্যৱহাৰ বাকলি, ফল আদিতকৈ বেছি। ইয়াৰ উপৰিও, মেলেৰিয়াকে আদি কৰি পালজ্বৰ, নিউমোনিয়া, কলাজ্বৰ আদি ৰোগত নিম গছৰ বাকলিৰ ব্যৱহাৰে সুফল দিয়ে। এই গছজোপাৰ পাতবোৰ কিছুমান জীৱ-জন্তুৰ প্ৰিয় খাদ্য। 'উট' এই ক্ষেত্ৰত অন্যতম। অন্ধ্ৰপ্ৰদেশত গৰুক নিমগছৰ পাত খাদ্য হিচাপে দিয়া হয়। ইয়াৰ মূলতে হ'ল গৰুৰ গাখীৰৰ ক্ষৰণ বা গাখীৰৰ পৰিমাণ বৃদ্ধি কৰা। বিভিন্ন প্ৰসাধন সামগ্ৰী প্ৰস্তুতকৰণত যেনে, চুলিৰ তেল, চাবোন, তেল, দন্তমঞ্জন আদিত ইয়াৰ ব্যৱহাৰ অধিক। বিভিন্ন ব্যাসায়িক দ্ৰব্য প্ৰস্তুত কৰোঁতে নিমপাতৰ ব্যৱহাৰ কৰা হয়।"[১]

ভাৰতবৰ্ষত সহজলভ্য এবিধ ঔষধি গুণসম্পন্ন উদ্ভিদ হ'ল 'বেলগছ'। বেলৰ ফল ঔষধি গুণসম্পন্ন। অতি প্ৰাচীন কালৰেপৰা ঔষধি ফল হিচাপে ইয়াৰ ব্যৱহাৰ হৈ আহিছে। পেটৰ সমস্যাৰ পৰা পৰিত্ৰাণ পাবলৈ বেলগছৰ ফল ব্যৱহাৰ কৰা হয়। ডায়েৰিয়া, কোষ্ঠকাঠিন্য আদি ৰোগৰ নিৰাময় বাবে বেলগছৰ ফল অত্যন্ত সুফলদায়ক। বিভিন্ন পানীয় প্ৰস্তুতকৰণত বেলৰ ফল ব্যৱহাৰ কৰা হয়। গৰম দিনত দেহৰ উষ্ণতাৰ ভাৰসাম্য বাবে এইবিধ ফলৰ ব্যৱহাৰ অতি গুৰুত্বপূৰ্ণ।[২]

"বিভিন্ন সংক্ৰমণ ৰোধ আৰু অস্থিভংগ নিৰাময়ৰ বাবে আঁহত গছৰ পাত ব্যৱহাৰ কৰা হয়। আঁহত গছৰ পাতৰ ব্যৱহাৰে হাপানি, কাঁহ, ডায়েৰিয়া, পেষ্টিকৰ সমস্যা আদি দূৰ কৰে। আঁহতৰ কোঁহ (কুমলীয়া পাত) চৰ্মৰোগ নিৰাময়ৰ বাবে অত্যন্ত গুৰুত্বপূৰ্ণ। প্ৰস্ৰাব আৰু হজমৰ সমস্যা দূৰীকৰণৰ বাবে আঁহত গছৰ ঠাৰি ব্যৱহাৰ কৰা হয়। আঁহতগছৰ ফলৰ পৰা প্ৰস্তুত কৰা শুকান পাউদৰ শ্বাস-প্ৰশ্বাসৰ সমস্যা তথা হাপানিৰ কাৰণে অত্যন্ত সহায়ক। বৰ্তমান [illegible] ব্যৱহাৰ প্ৰস্তুত কৰোঁতে আঁহতৰ পা[illegible]

C.T.C.
Principal
Nowgong Girls' College
Nagaon :: Assam
Nowgong Girls' College
ESTD: 1962
Nagaon :: Assam

হয়। আঁহত গছক পৰম্পৰাগতভাৱে এজোপা পবিত্ৰ গছ হিচাপে গণ্য কৰা হয়। নাকৰ তেজ গুলোৱা, হৃদপিণ্ডৰ ৰোগ, ডাইবেটিছ, কোষ্ঠকাঠিন্য, জ্বৰ, জণ্ডিছ আদি ৰোগৰ নিৰাময়ত পৰম্পৰাগতভাৱে আঁহত গছৰ পাত ব্যৱহাৰ হৈ আহিছে।"

পাৰিপাৰ্শ্বিকভাৱে সচেতন পুৰণি অসমীয়া লোকসমাজখনে প্ৰকৃতিৰ অনাবদা এই গছ-গছনিবোৰৰ বিষয়ে সম্পূৰ্ণ জ্ঞাত আছিল আৰু সেয়েহে, এই গছ-গছনিবোৰক অসমীয়া লোকবিশ্বাস তথা লোকসাহিত্যত স্থানাংকৃত কৰিছিল। অসমীয়া লোকসাহিত্যৰ অন্তৰ্গত ডাকৰ বচনত এই গছ-গছনিবোৰৰ লগত জড়িত ঔষধি ব্যৱস্থাৰ প্ৰত্যক্ষ ব্যৱহাৰ সম্বন্ধে সুন্দৰ নিদৰ্শন পোৱা যায়। ডাকৰ বচনত —

"ত্ৰিফলা দিয়া নিমৰ ছাল।
ছাগ দুগ্ধৰে বাটিব ভাল।।
নিশাভাগে তাক নিয়ৰে থৈব।
প্ৰভাত সময়ে মাথাত লৈব।।
হাতে ঘঁহি ঘঁহি মাথাত দিব।
শুকালে পাছে স্নান কৰিব।।
যিজনে কৰিব এহি প্ৰকাৰ।
ক্ৰোশেকৰ পথলৈ দৃষ্টি তাহাৰ।। (গগৈ ২৫)
"জালুক পিপলী আদা খায়।
ডাকে বোলে তাৰ কাঁহ পলায়।।(গগৈ ২৫)
"ভাত খায় উঠি তিনি শিলিখা।
তাক কি কৰিবে ৰোগ পিলিকা।।
ভোগজিৰা পোটকৰা তক মূল।
বেলপাত খাইলে নাখ হৰে শুল।।(শৰ্মা ৬৬)

ডাকৰ বচনত সন্নিবিষ্ট ঔষধি গছ-গছনিৰ প্ৰত্যক্ষ ব্যৱহাৰৰ লগতে পৰোক্ষ ব্যৱহাৰৰ দ্বাৰা বিভিন্ন ৰোগ নিৰাময় হয়। তুলসী, নিম ইত্যাদি পৰিবেশৰ কাৰণে অত্যন্ত জৰুৰী। এই গছ-গছনিবোৰে বায়ু প্ৰদূষণ ৰোধ কৰাৰ লগতে গছবোৰৰ অক্সিজেন প্ৰস্তুত কৰিব পৰা ক্ষমতা অন্যান্য গছতকৈ বহু বেছি। ইয়াৰ লগতে, এই গছ-গছনিবোৰ যদি মানুহৰ ঘৰত থাকে তেতিয়াহলে স্বতঃস্ফূৰ্তভাৱে মানুহ কিছুমান ৰোগৰ পৰা পৰিত্ৰাণ পায়। পুৰণি অসমীয়া সমাজখন এই গছ-গছনিবোৰৰ প্ৰত্যক্ষ আৰু পৰোক্ষ ব্যৱহাৰৰ উপকাৰিতা সম্পৰ্কে সম্পূৰ্ণ জ্ঞাত আছিল আৰু সেয়েহে তেওঁলোকে এই গছ-গছনিবোৰ সুন্দৰভাৱে সংৰক্ষণ কৰি ৰাখিছিল।

"নিম গছৰ সালোক-সংশ্লেষণ কৰিব পৰা ক্ষমতা অতি বেছি আৰু আন যিকোনো গছৰ প্ৰজাতিতকৈ অধিক অক্সিজেন প্ৰস্তুতেৰে বায়ুমণ্ডল বিশুদ্ধ কৰি ৰাখে। ভাৰতবৰ্ষৰ উত্তৰ অংশত, গৰম গ্ৰীষ্মকালত চাৰিওফালৰ পৰিবেশৰ [illegible] নিমগছৰ তলৰ তাপমাত্ৰা ১০° চেলচিয়াছ [illegible]

C.T.C.
Principal
Nowgong Girls' College
Nagaon :: Assam
Nowgong Girls' College ESTD: 1962 Nagaon :: Assam

যায়। কম ঘনত্বযুক্ত আৰু উচ্চ ৰতাহযুক্ত এলেকাত নিম গছে ৰতাহ ৰন্ধকৰণত যথেষ্ট সহায় কৰে। পৰিপক্ক এজোপা নিমগছে প্ৰায় ১০-১০০ টন পাত, ফল আৰু কাঠ যোগান ধৰিব পাৰে। ঋতুগতভাৱে শুকান স্থানৰ বাবে নিমগছ এক অভিযোজন। এইবোৰৰ লগতে, নিম গছে শব্দ প্ৰদূষণ ৰোধ কৰাত গুৰুত্বপূৰ্ণ ভূমিকা পালন কৰে।"*

৩.০০ জীৱ-বৈচিত্ৰ্য সংৰক্ষণ

আদিম যুগৰে পৰা হাবিয়ে বনিয়ে ঘূৰি ফুৰি জীৱন অতিবাহিত কৰি প্ৰকৃতিৰ বিভিন্ন নিয়মক সাৰোগত কৰি 'মানুহ' হিচাপে নিজকে চিনাকি দিবলৈ সক্ষম হোৱা মানৱ জাতি প্ৰকৃতিৰ সকলো উপাদানৰ লগত চিৰপৰিচিত। প্ৰকৃতিৰ প্ৰতিটো জীৱৰ প্ৰাকৃতিক ভাৰসাম্য ৰক্ষাৰ ক্ষেত্ৰত সুকীয়া ভূমিকা আছে। জীৱ-জন্তু সংৰক্ষণৰ ক্ষেত্ৰত অসমীয়া সমাজখন যথেষ্ট সচেতন আছিল। এই সচেতনতাৰ হেতুকে প্ৰকৃতিৰ কিছুমান জীৱ জনসমাজত সুকীয়া আসন লাভ কৰি 'ঘৰচীয়া' হিচাপে চিহ্নিত হ'ল। সেয়েহে ডাকৰ বচন, প্ৰবাদ বাক্য আদিত ঘৰচীয়া আৰু বনৰীয়া সকলো জীৱৰ প্ৰতি মানুহ দয়াশীল হোৱাৰ কথা পোৱা যায়। আনহে নালাগে সেই সমাজখনে মানুহৰ প্ৰত্যক্ষভাৱে অপকাৰী কিছুমান জীৱকো গছ-গছনিৰ দৰে ভগৱানৰ মহিমা সানি জীৱ-বৈচিত্ৰ্য সংৰক্ষণৰে সুন্দৰ পাৰিপাৰ্শ্বিক সচেতনতাৰ পৰিচয় দিছিল।

"দুঠেঙীয়াক গোৰ মাৰি পেলাবা,
চাৰিঠেঙীয়াক ডাঙি ধৰিবা।" (গঁগে ৬৩)
"পশু নকৰিবা শৰ
মৰাও নানিবা জীয়াও নানিবা
শুদা হাতে নপশিবা ঘৰ।" (কোঁচ ৩৫৫)
"যাৰ নাই গৰু,
সি সবাতোকৈ সৰু।।"(কোঁচ ২৬৫)
"চাৰিঠেঙীয়া পালে ডাঙি ধৰিবা।
দুঠেঙীয়া পালে হেঁচা মাৰি ধৰিবা।।"(কোঁচ ১২৪)
"মেকুৰী মাৰিব নেপায়।"
"সাপ মাৰিব নেপায়।"
"সাপে লেখিলেহে খুটে, দেখিলে নুখুটে।"
"যোৱা সাপ দেখিলে গামোচা দলিওৱা"
"বহাগ বিহুত গৰু গা ধুওৱা আৰু পূজা কৰা।"

অসমীয়া লোকসমাজত প্ৰচলিত লোকসাহিত্যৰ এই বিভাগৰ ওপৰৰ প্ৰতিটো পংক্তি জীৱ-বৈচিত্ৰ্য সংৰক্ষণৰ লগতজড়িত। এইবোৰৰ মাজেৰে প্ৰত্যক্ষ ৰূপত পাৰিপাৰ্শ্বিক সচেতনতা প্ৰকাশ নাপালেও পৰোক্ষভাৱে ওপৰৰ প্ৰতিটো পংক্তি পাৰিপাৰ্শ্বিক সচেতনতাৰে আপ্লাবিত। সেয়েহে পংক্তিবোৰৰ মাজেৰে 'মানুহতকৈ জীৱ-জন্তু বেছি [illegible] অনিষ্ট নকৰা, [illegible] সম্পৰ্ক নিৰূপণ, মেকুৰী [illegible] প্ৰাণীৰ [illegible]

CTC
Principal
Nowgong Girls' College
Nagaon :: Assam
Nowgong Girls' College ★ ESTD: 1962 ★ Nagaon :: Assam

'মাৰিব নেপায়' বুলি ধাৰ্মিক দিশৰ সংযোজন' আদি পাৰিপাৰ্শ্বিকভাৱে সচেতন দিশ অসমীয়া সমাজত প্ৰতিষ্ঠা কৰা হৈছে। অসমীয়া সমাজত সৰীসৃপ জাতীয় প্ৰাণী সাপৰ সৈতে বহুতো ভ্ৰান্ত ধাৰণা জড়িত হৈ আছে। অসমীয়া সমাজত সততে সাপ এবিধ অপকাৰী জীৱ আৰু ইয়াক দেখিলে মাৰিব লাগে নহয় পলাব লাগে বুলি ভবা হয়। সাপ এডাল দেখিলে কেৱল মৰাৰ কথা ভাবে; ভাবি নাচায়, ই অপকাৰী নে উপকাৰী।

> "প্ৰাপ্ত তথ্য মতে আমাৰ দেশত ২৭৫ বিধ প্ৰজাতিৰ সাপ আছে। তাৰে ভিতৰত উত্তৰ পৰত ১০২ বিধ সাপ পোৱা যায়। ইয়াৰ ভিতৰত ৫০ বিধ সাপহে বিভিন্ন প্ৰকাৰে বিষাক্ত। এই ৫০ বিধ সাপৰ ভিতৰত আকৌ ভালেমান বিষধৰ সাপৰ পৰা মানুহৰ ক্ষতি কৰা বা মৃত্যু ঘটাব পৰাৰ আশংকা কম। কিয়নো বহুতৰে বাসস্থান গভীৰ অৰণ্যত। বহু বিষাক্ত সাপ আমাৰ ওচৰে পাজৰে থাকে, যিবোৰৰ এজন মানুহৰ মৃত্যু ঘটাব পৰা বিষ নাই। মানুহৰ সৈতে সততে সংস্পৰ্শলৈ আহিব পৰা আৰু অপকাৰ সাধিব পৰা সাপ কেইবিধ হ'ল— ৰজাফেঁটী, ফেঁটীগোম, চকৰী ফেঁটী। সাগৰীয় সাপৰ বিষ অতি বিষাক্ত হয় লুণীয়া পানীৰ কাৰণে। অলুণীয়া পানীত বাস কৰা সকলো সাপেই অবিষাক্ত। আমাৰ প্ৰায়বোৰ মানুহৰে ধাৰণা যে সাপে মানুহ দেখিলেই খুটিবলৈ আহে বা ফেঁট তোলে। আচলতে সাপে ভয় খালে বা আঘাত পালেহে আত্মৰক্ষাৰ বাবে খুট মাৰে। ইয়াৰ উপৰিও সাপে কাৰোবাক বিচাৰি প্ৰতিশোধ লোৱা কাহিনী অমূলক।" (ৰাজবংশী ১১৭)

প্ৰকৃততে, সাপ পৃথিৱীৰ বিভিন্ন পৰিৱেশৰ লগত খাপ খোৱাই চলিব পৰা এক সৰীসৃপ শ্ৰেণীৰ প্ৰাণী। বিভিন্ন ৰঙেৰে, বিভিন্ন আচৰণেৰে এন্দুৰ, নিগনি নিয়ন্ত্ৰণেৰে শস্য সুৰক্ষাৰ লগতে মানৱ সমাজৰ উপকাৰ তথা প্ৰকৃতিৰ ভাৰসাম্য ৰক্ষাৰ ক্ষেত্ৰত সাপে গুৰুত্বপূৰ্ণ ভূমিকা পালন কৰে। পুৰণি অসমীয়া সমাজখন এইবোৰ দিশত যথেষ্ট সচেতন আছিল আৰু সেয়েহে অসমীয়া সমাজত প্ৰবৰ্তিত ভ্ৰান্ত ধাৰণাৰ বিপৰীতে অসমীয়া সমাজ তথা লোকসাহিত্যৰ এই শাখাত 'মাৰিব নেপায়', 'যজা সাপ দেখিলে গামোচা দিব লাগে', 'সাপে কপালত লেখিলেহে খুটে' ইত্যাদি ধাৰণা সৃষ্টি কৰি থৈ গৈছে। অসমীয়া সমাজত 'যজা সাপ দেখিলে গামোচা দিব লাগে' বুলি থকা প্ৰবাদটি এই সকলোবোৰৰ উৰ্ধত। প্ৰবাদটিত সুশৃংখলিত পৰিস্থিতিতন্ত্ৰৰে সাপৰ বৈচিত্ৰ্য অটুত ৰাখিব বিচৰা হৈছে। প্ৰজননৰ উদ্দেশ্যে মিলিত যজা সাপ দুটি যাতে অসমীয়া সমাজত প্ৰবৰ্তিত ভ্ৰান্ত ধাৰণাৰ বশবৰ্তী নহয় সেইহেতুকে পুৰণি অসমীয়া সমাজখনে যজা সাপ দেখিলে গামোচা দিব লাগে বুলি পৰিবেশমিত্ৰ ধাৰণাৰ সৃষ্টি কৰি থৈ গৈছে।

৪.০০ সিদ্ধান্ত আৰু সামৰণি

এটা জাতি সামাজিক, সাংস্কৃতিক, অৰ্থনৈতিক আৰু পাৰিপাৰ্শ্বিকভাৱে সবল হোৱাৰ ক্ষেত্ৰত লোকসাহিত্যৰ এই বিভাগটিৰ ভূমিকা অত্যন্ত গুৰুত্বপূৰ্ণ। অসমীয়া লোকসাহিত্যৰ এই বিভাগটিয়ে প্ৰাকৃতিক পৰিৱেশ অবিহনে জীবন বাটত আগুবাই যোৱা [illegible] সময়ত

Principal
Nowgong Girls' College
Nagaon :: Assam
Nowgong Girls' College ESTD: 1962 Nagaon :: Assam

পৰিবেশ বিষয়ক জ্ঞান আৰু তথ্য প্ৰদানত অসমীয়া লোকসাহিত্যৰ এই বিভাগটিৰ ভূমিকা অত্যন্ত গুৰুত্বপূৰ্ণ। অসমীয়া লোকসাহিত্যৰ অন্যান্য ভাগ কেইটাৰ তুলনাত 'ডাকৰ বচন, ফকৰা-যোজনা, প্ৰবাদ বাক্য' আদি প্ৰত্যক্ষ ৰূপত পুৰণি অসমীয়া সমাজৰ পাৰিবেশিক দায়বদ্ধতা আৰু ভবিষ্যৎ প্ৰজন্মৰ কৰ্তব্য সম্পৰ্কীয় বিভিন্ন তথ্যৰ বাটকটীয়া। অসমীয়া লোকসাহিত্যৰ এই বিভাগটিৰ প্ৰায় প্ৰতিটো পংক্তিতে পাৰিপাৰ্শ্বিক সচেতনতা অন্তৰ্নিহিত হৈ আছে। সামাজিক আৰু পাৰিবেশিক অনাময়ৰ সকলো দিশ লোকসাহিত্যৰ এই বিভাগটিত বিদ্যামান। অসমীয়া লোকসমাজৰ বিভিন্ন দিশৰ সমান্তৰালকৈ জৈৱবৈচিত্ৰ্যৰ প্ৰতি থকা পাৰিপাৰ্শ্বিক সচেতনতাৰ বিভিন্ন দিশ লোকসাহিত্যৰ এই বিভাগত প্ৰতিফলিত হয়।পুৰণি অসমীয়া সমাজখন জৈৱবৈচিত্ৰ্য সম্পৰ্কে যথেষ্ট জ্ঞানী, দায়বদ্ধ আৰু সচেতন আছিল। গৱেষণা পত্ৰত প্ৰাপ্ত এই সিদ্ধান্তসমূহৰ ভেটিতে বৈচিত্ৰ্যময় অসমীয়া জাতি, বৈচিত্ৰ্যময় অসম বা অসমৰ প্ৰাকৃতিক সৌন্দৰ্য্য, জীবন নিৰ্বাহৰ উপযুক্ত বাতাবৰণ আদি দিশৰ উন্মেষ ঘটি; সেই দিশাবোৰৰ মাজত সুসমন্বয় ঘটি 'অসম' ৰাজ্যখন অন্যান্য ৰাজ্যৰ তুলনাত তাহানিদিনৰে পৰা জাকত-জিলিকা হৈ আছে। এনেদৰে অসমীয়া লোকসাহিত্যৰ সমান্তৰালকৈ অসমীয়া জাতি পাৰিপাৰ্শ্বিক সচেতনতাৰ দিশত দোপত -দোপে আগবাঢ়ি যায় সেই উদ্দেশ্যে পাঁচশ বছৰৰ পূৰ্বে মহাপুৰুষ শ্ৰীমন্ত শংকৰদেৱে কৈ যোৱা এষৰি উপদেশবাণীৰে গৱেষণা পত্ৰৰ সামৰণি মৰা হৈছে—

"কুকুৰ শৃগাল গদৰ্ভৰো আত্মাৰাম।
জানিবা সবাকো পৰি কৰিবা প্ৰণাম।।"

টোকা

১। Almost every part of the tree is bitter and finds application in indigenous medicine. Neem extracts have been reported to possess anti-diabetic, anti-bacterial and antiviral properties and they have been used successfully in case of stomach worms and ulcers. The stem, root bark and young fruits are reported to possess astringent, tonic and anti-periodic properties. The root bark is reported to be more active than the stem bark and young fruits. The bark is reported to be benificial in malarial fever and useful in cutaneous diseases. The twigs and leaves can be fed to cattle in conjunction with other feeds, camels also eat the leaves. In Andhra Pradesh, they are regularly fed to cattle and goats to increase the secretion of milk and manure. Considerable quantities of the oil are employed in cosmetic preparation such as hair-lotions, medicated soaps, washing soaps and tooth pastes; it can be mixed for the production of olein and stearin and high melting sterin after hydrogenation. Regular application of hair oil containing oil of Margosa is reported to prevent baldness and greying of hair. The seeds also contain an essential oil which has been found to possess anti-microbial activity. [Shrivastava Manu, P. 4]

২। The impotance of bael fruit also lies in curative properties which makes the tree one of the useful midicinal plants of India. The fruit is hard shelled berry and [illegible] medicinal properties due to marmelosin content it has

C.T.C.
Principal
Nowgong Girls' College
Nagaon :: Assam

Nowgong Girls' College
ESTD: 1962
Nagaon :: Assam

been known in India from prehistoric times. It is very popular because of its rich nutritive, sweet, aromatic mucilage and protien contents and good for all kinds of stomach disorders. Bael fruits are very useful in chronic diarrhoea, altrnating with the spells of constipation. The ripe fruits are used for preparation of high quality soft drink and beverages. It has very cooling effect and protects the body system for maintaining of body temperature during hot summer. The mature fruit is used for preparation of murrabba, candy, toffee and bael powder. The fruit is rich in Vitamin B (Riboflivin) and also has fair amount of Vitamin A ,Vitamin C and minarals such as calcium, phosphorus potassium and protein content in ripe fruits is very high. (Jitendra Kumar Singh, Introduction, Chapter 1)

৩। Ficus religiosa is being used to cure various infections and bone fracture. Leaves are used in conditions like asthma, cough,diarrhoea, gastric problems. Shoots are used in treating skin problems (Singh and Jaiswal,2014). Stem can be used in treatment of urinary disorders and problems of digestive system. The dried powder of fruits has been used in treatment of respiratory problems like asthma(Panchawat,2014). Many present day herbal medicines contain parts of Ficus religiosa as an ingredient. Different parts can be consumed either in raw form (powder, extract) or in form of indigenous medicines (either alone or in combination with other herbs) for specific ailments. Ficus religiosa is a traditional religious plant in India and is used in treament of several health ailments as a home based remedy either singly or in combination with other herbs. It has been traditionally used in the treatment of heart ailments, nose bleeding, diabetes,constipation, fever, jaundice etc. [Sandeep and etc., P.15]

৪। Neem has high rate of photosynthesis and liberate more O_2 than many other tree species, thus purify the atmosphere. In the northern part of India, the temperature under the neem has been found to be 10^0c less than the surrounding temperature during the hot summer months. In areas of low rainfall and high wind speed, neem is useful as wind breaks. Completely grown neem tree yield about 10-100 tons of biomass/comprised of leaves (50%) and fruits and wood (25% each; Anonymous, 2006). Its extensive deep root system is presumably an adaption to seasonally dry sites. Neem is also help in to reducing sound pollution at their adverse effect on the loudly places.[Manoj Kumar Jhariya and etc., P. 2]

গ্রন্থপঞ্জী ঃ

কোঁচ, জীৱনচন্দ্র। *অসমীয়া ভাষাৰ অলংকাৰ ফকৰা-যোজনা*। পঞ্চম প্রকাশ। ডিব্রুগড় ঃ কুমাৰণীছীগা, ২০১১। প্রকাশিত।

গগৈ, লীলা। *অসমীয়া লোকসাহিত্যৰ ৰূপৰেখা*। প্রথম প্রকাশ। ডিব্রুগড় ঃ বনলতা, ২০০৭। প্রকাশিত।

পাঠক, মহানন্দ। *একৈশ শতিকাৰ পৰিবেশ গৱেষণাত ভূত*। প্রথম প্রকাশ। গুৱাহাটী ঃ [illegible] ২০১৫। প্রকাশিত।

C.T.C.
Principal
Nowgong Girls' College
Nagaon :: Assam
Nowgong Girls' College ESTD: 1962 Nagaon :: Assam

বাজবংশী, ঘনশ্যাম। *অৱণ্যৰ ভিতৰচ'ৰা*। প্ৰথম প্ৰকাশ। গুৱাহাটী : অসম বুক ট্ৰাষ্ট, ২০১৬। প্ৰকাশিত।

শৰ্মা, নবীন চন্দ্ৰ। *ডাক-প্ৰবচন আৰু ডাক-পৰম্পৰা*। দ্বিতীয় প্ৰকাশ। গুৱাহাটী : জ্যোতি প্ৰকাশন, ২০১২। প্ৰকাশিত।

বিশেষ সহায়ক নিবন্ধ

Shrivastava Manu. *Screening of Neem Tree for Maximum Utilization of its Constituents*. Department of Chemistry. Dr. Rammanohar Lohia Avadh University. Faridabad. P. 4.

Jitendra Kumar Singh. *Studies on integrated nutrient management in Bael Aegla Marmelos Marmetos cv Narendra Bael 09*. Department of Horticulture. V.B.S.. Introduction. Chapter 1.

Sandeep and etc.. *Ficus religiosa : A wholesome medicinal tree*. Journal of Pharma cognosy and Phytochemistry. P. 35.

Monoj Kumar Jhariya and etc.. *Neem- A Tree for Solving Global Problem*. Vol. 3. Issue:10.Oct. 2013. P. 2.

C.T.C.
Principal
Nowgong Girls' College
Nagaon :: Assam

Nowgong Girls' College
ESTD: 1962
Nagaon :: Assam

Papers published per teacher in the Journals notified on UGC website during the Academic Session: 2021-22

Submitted to the NAAC for 3rd Assessment Cycle of Assessment & Accreditation

NOWGONG GIRLS' COLLEGE

Re-accreditated at A Grade by the NAAC (2nd Cycle)

J. Chem. Sci. (2021) 133:82
https://doi.org/10.1007/s12039-021-01920-7

© Indian Academy of Sciences

REGULAR ARTICLE

Special Issue on Beyond Classical Chemistry

Octanuclear {Ln_8} complexes: magneto-caloric effect in the {Gd_8} analogue

PANKAJ KALITA[a,b], JOYDEB GOURA[a,d], PRAKASH NAYAK[a], ENRIQUE COLACIO[c,*] and VADAPALLI CHANDRASEKHAR[b,d,*]

[a]School of Chemical Sciences, National Institute of Science Education and Research, HBNI, Bhubaneswar, Jatni, Khurda 752 050, Odisha, India
[b]Centre for Interdisciplinary Sciences, Tata Institute of Fundamental Research, Gopanpally, Hyderabad 500 046, India
[c]Departamento de Química Inorgánica, Facultad de Ciencias, Universidad de Granada, Avenida de Fuentenueva s/n, 18071 Granada, Spain
[d]Department of Chemistry, Indian Institute of Technology Kanpur, Kanpur 208 016, India
E-mail: ecolacio@ugr.es; vc@tifrh.res.in; vc@iitk.ac.in

MS received 8 March 2021; revised 31 March 2021; accepted 31 March 2021

Abstract. Two neutral, isostructural, octanuclear, Ln^{III} complexes, $[Ln_8(HL)_6(L)_2(\mu_3\text{-}OH)_4(\mu_2\text{-}OH)_2(H_2O)_6]$.solv (Ln = Gd(III), ($\mathbf{1}^{Gd}$) and Dy(III), ($\mathbf{2}^{Dy}$) have been synthesized using Ln^{III} nitrate salts and a *o*-vanillin-supported multi-dentate ligand, *N*′-(2-hydroxy-3-methoxy-5-nitrobenzylidene)-2-(hydroxyamino) propanehydrazide (H_3L) in the presence of tetramethyl ammonium hydroxide. The complexes were structurally characterized by single crystal X-ray diffraction studies. The complexes are held by the cumulative coordination action of six $[HL]^{2-}$, two $[L]^{3-}$ chelating ligands, H_2O and hydroxide ligands. Magneto-structural analysis of complexes $\mathbf{1}^{Gd}$ and $\mathbf{2}^{Dy}$ reveals the presence of intramolecular antiferromagnetic interactions between the Ln^{III} ions. Magneto-caloric effect was analysed for the complex $\mathbf{1}^{Gd}$ which shows a maximum in the change of molar entropy ($-\Delta S_m$) of magnitude 25.5 J kg^{-1} K^{-1} at T = 3 K and an applied field change ΔB = 5 T.

1. Introduction

Lanthanide complexes have been of considerable research interest in recent years owing to their interesting magnetic,[1–10] optical,[11–20] and catalytic properties.[21–28] Among these systems, polynuclear complexes are formed usually as a result of the bridging ligands such as the hydroxide ligand.[29–39] Such complexes are also of interest in the field of molecular magnetism.[30,31,40–45] However, the synthesis of such complexes is fraught with some challenges. One difficulty is the formation of intractable polymeric complexes because of the ready de-protonation of the coordinated water molecules around the lanthanide ions. The formation of discrete complexes becomes feasible if controlled de-protonation of the coordinated water molecules can be achieved.[29] This is often possible by having an appropriate multi-site coordinating ligand to bind to the lanthanide ions so that the available coordination sites are reduced and the chances for the formation of a discrete complex are increased. In our lab, multi-pocket, multidentate hydrazone ligands have been extensively used for the synthesis of discrete polynuclear lanthanide complexes.[46–50] In this regard, we have designed a multi-pocket hydrazone ligand which was used to isolate dinuclear Ln^{III} complexes.[51] In these complexes, we have observed uncoordinated free oxime –OH groups which could be potentially deprotonated so that these can proliferate to form multinuclear complexes.

*For correspondence

Supplementary Information: The online version contains supplementary material available at https://doi.org/10.1007/s12039-021-01920-7.

Published online: 03 August 2021

Principal
Nowgong Girls' College
Nagaon :: Assam

Nowgong Girls' College
ESTD: 1962
Nagaon :: Assam

NJC

ROYAL SOCIETY OF CHEMISTRY

PAPER

Check for updates

Cite this: *New J. Chem.*, 2021, 45, 12848

Tantalum(v) peroxido complexes as phosphatase inhibitors: a comparative study *vis-a-vis* peroxidovanadates†‡

Gangutri Saikia,* Hiya Talukdar, Kabirun Ahmed, Nand Kishore Gour and Nashreen S. Islam*

The present work illustrates the synthesis and comprehensive characterization of novel peroxidotantalum(v) complexes anchored to water soluble polymer (WSP) matrices *viz.*, $[Ta_2(O_2)_4(carboxylate)_2]$–PA (PA = polysodium acrylate) (**PATa**) and $[Ta(O_2)_2(sulfonate)_2]$–PSS (PSS = polysodium 4-styrene sulfonate) (**PSSTa**) and their identification as potent inhibitors of acid phosphatase (ACP) activity. Using a set comprising tantalum(v) and vanadium(v) peroxides in similar macro ligand environments, and wheat thylakoid acid phosphatase as a model enzyme, it has been demonstrated for the first time that peroxidotantalum (pTa) derivatives are 2–3 fold more active as ACP inhibitors (IC_{50}: 0.34 μM for **PSSTa**) compared to their V containing analogues (IC_{50}: 1.22 μM). Enzyme kinetics analysis further revealed that the pTa and peroxidovanadate (pV) compounds tested, irrespective of the nature of their ligand environment, inhibit ACP function exclusively *via* a non-competitive pathway with K_i and K_{ii} values ranging between 0.2 and 4.7 μM. Importantly, under the effect of the enzyme catalase, the pTa compounds with a rate of peroxide loss as low as 0.92 μM min^{-1} (**PATa**) emerged to be remarkably more resistant to degradation relative to the corresponding pV compound, which degraded at a significantly faster rate (5.80 μM min^{-1}).

Received 28th February 2021,
Accepted 3rd June 2021

DOI: 10.1039/d1nj01005k

rsc.li/njc

Introduction

Interest in the peroxido species of d^0 metal ions of group 5 seems to be never diminishing over the past decades.[1] Vanadium and its peroxido complexes in particular continue to have tremendous importance mainly owing to several significant discoveries relating to their biological and pharmacological role in the treatment of diabetes mellitus, malignancy and diseases caused by parasites.[1a,c–g] A few reports are also available on the biological activity of Nb compounds such as anticancer activity[2] and enzyme inhibitory activity.[3] On the other hand, the potential of peroxido compounds of tantalum, another group V element, as bioactive agents remains yet to be explored although tantalum and its compounds are not new in the field of medicinal chemistry. Being a bio-inert element with excellent biocompatibility and relatively non-toxic to animals, compounds of tantalum and its oxide based nanoparticles have been used as inert materials for implants[4] and various other therapeutic applications.[5,6] Recently, Starha *et al.* reported a new Schiff base–Ta complex, which exhibited strong cytotoxicity in cancer cells.[7] Notwithstanding these important findings, the contemporary interest in peroxidotantalum (pTa) compounds still mostly remains restricted to their utility as effective water soluble precursors to obtain Ta-based oxide materials for advanced technology applications.[8f] The aqueous chemistry of Ta is known to be limited to a very few available water soluble precursors.[8d,9]

It is pertinent to mention that our group has previously introduced a series of structurally defined and stable macrocomplexes by incorporating peroxide derivatives of d^0 metal ions *viz.*, V(v), Mo(vi), W(vi) and Nb(v) on water soluble polymers (WSPs) and explored their various bio-relevant aspects including their activity as inhibitors of enzyme phosphatases.[3c,9] Very recently, we have shown that peroxido compounds of V and Nb can effectively inhibit the activity of calcineurin, a serine/threonine phosphatase, *via* an uncompetitive pathway.[3c] The poly(acrylate) anchored pV species (PAV) also inhibited growth of lung carcinoma cells (A549)[10] in addition to displaying a vasomodulatory effect on rat aorta[11] and antibacterial[9a] properties. Importantly, the immobilized peroxidometallates

Department of Chemical Sciences, Tezpur University, Napaam, Tezpur 784028, Assam, India. E-mail: sai@tezu.ernet.in, nashreen.islam@rediffmail.com; Fax: +91-3712-267006; Tel: +91-9435180222, +91-3712-267007

† This paper is dedicated to the memory of Professor T. Ramasarma. We shall remain ever grateful to late Professor T. Ramasarma, Department of Biochemistry, Indian Institute of Science, Bangalore, India for valuable suggestions and discussions.

‡ Electronic supplementary information (ESI) available: TGA data of **PATa** and **PSSTa**, experimental and theoretical IR spectral data of **PATa**, ^{13}C NMR spectral data of **PATa** for the stability study, L–B plots for inhibition of ACP activity in the presence or absence of (A) **DPV**, (B) **PAV** and (C) **PATa**. See DOI: 10.1039/d1nj01005k

 This journal is © The Royal Society of Chemistry and the Centre National de la Recherche Scientifique

Principal
Nowgong Girls' College
Nagaon :: Assam

Nowgong Girls' College ESTD: 1962 Nagaon :: Assam

Molecular Catalysis 516 (2021) 111988

Contents lists available at ScienceDirect

Molecular Catalysis

journal homepage: www.journals.elsevier.com/molecular-catalysis

A sustainable approach towards solventless organic oxidations catalyzed by polymer immobilized Nb(V)-peroxido compounds with H_2O_2 as oxidant

Hiya Talukdar, Sandhya Rani Gogoi, Gangutri Saikia, Sazida Yasmin Sultana, Kabirun Ahmed, Nashreen S. Islam *

Department of Chemical Sciences, Tezpur University, Tezpur 784028, Assam, India

ARTICLE INFO

Keywords:
Supported peroxidoniobium(V) complexes
Olefin epoxidation
Sulfide oxidation
Solvent free reaction
Heterogeneous catalyst

ABSTRACT

New heterogeneous catalysts comprising of peroxidoniobium(V) complexes immobilized on amino acid grafted cross-linked poly(styrene-divinylbenzene) resin has been developed. Results of FTIR, Raman, NMR, XPS, XRD, EDX, SEM, BET, TGA, and elemental analysis confirmed the successful anchoring of triperoxidoniobium(V), $[Nb(O_2)_3]^-$ species to the host polymer *via* the pendant amino acid groups. The supported catalysts exhibited excellent performance in epoxidation of styrene and a range of cyclic and terpenic compounds under environmentally acceptable solvent-free condition, with aqueous H_2O_2 as oxidant. The catalytic protocols provided excellent conversion to the desired epoxide (up to 100%) with selectivity > 99%, TON as high as 1000, and high H_2O_2 utilization efficiency (93–97%). Moreover, the catalysts efficiently facilitated chemoselective solvent-free oxidation of a variety of thioethers to sulfones at room temperature. Simple operational strategy, easy recyclability for multiple reaction cycles with the consistent activity selectivity profile are the additional significant attributes of the developed catalytic processes.

1. Introduction

Among the vast range of organic oxidations, epoxidation of olefins, as well as oxidation of organosulfur compounds to sulfoxide or sulfone, are outstanding industrial transformations representing the basis of a variety of chemical processes for the production of commodity and fine chemicals [1–7]. Moreover, the sulfide-oxidation based procedure of oxidative desulfurization has been recognized as a greener alternative method for the removal of sulfur from fuel feedstock [8,9]. The mounting environmental concerns in recent times have triggered a dramatic upsurge in interest in the development of safer and sustainable alternative synthetic routes to target compounds [10–13]. The use of heterogeneous catalysts that support clean and energy-efficient transformations and can perform optimally in absence of hazardous organic solvents, are emerging as issues of paramount importance in green synthetic strategy.

Solvent-free organic synthesis in addition to being cost-effective, contributes significantly towards waste minimization and environmental protection and thus displays tremendous application potential for larger-scale chemical processes [14–19]. Scores of innovative and promising supported transition metal heterogeneous catalysts have been reported over the recent years for olefin epoxidation under solvent less condition [14–19]. However, in order to attain high activity, the majority of these protocols required to employ organic hydroperoxides e.g., tert-butyl hydroperoxide (TBHP) and cumene hydroperoxide (CHP) as oxidants under anhydrous condition [14–17]. It is intriguing to note that, niobium-based solid catalysts so far have rarely been tested in solvent free organic oxidations, although such systems were often reported to display superior activity when aqueous hydrogen peroxide was used as a terminal oxidant [3,20–26]. This feature offers a significant advantage as catalytic epoxidation of olefins with aqueous H_2O_2, an ideal non-polluting, and cost-effective oxidant, is the focus of much contemporary research [10–13].

Work from several laboratories has demonstrated that silica supported Nb(V) catalysts are highly stable towards hydrolysis and metal leaching and such systems were observed to provide faster rates of oxidation compared to the more standard Ti-SiO_2 catalysts [20–26]. The advancement in liquid phase olefin epoxidation over niobium and tungsten-based catalysts has been comprehensively reviewed by Yan *et al.* recently [3]. It has been noted that notwithstanding the considerable progress in improving the activity of nanostructured Nb and W catalysts, poor selectivity and stability of such systems are still major issues to

* Corresponding author at: Department of Chemical Sciences, Tezpur University, Napaam, Tezpur 784028, Assam, India.
E-mail address: nsi@tezu.ernet.in (N.S. Islam).

https://doi.org/10.1016/j.mcat.2021.111988
Received 16 August 2021; Received in revised form 25 October 2021; Accepted 26 October 2021
2468-8231/© 2021 Elsevier B.V. All rights reserved.

Principal
Nowgong Girls' College
Nagaon :: Assam

Nowgong Girls' College
ESTD: 1962
Nagaon :: Assam

Advanced Engineering Informatics 50 (2021) 101362

Contents lists available at ScienceDirect

Advanced Engineering Informatics

journal homepage: www.elsevier.com/locate/aei

Full length article

Teaching and Learning Crystal structures through Virtual Reality based systems

Vishawash Kumar [a], Sahil Gulati [a], Bhargab Deka [b,c], Himangshu Sarma [d,*]

[a] Department of Computer Science & Engineering, Indian Institute of Information Technology Senapati, Manipur 795002, India
[b] Department of Physics, Indian Institute of Information Technology Senapati, Manipur 795002, India
[c] Department of Physics, Nowgong Girls' College, Nagaon 782002, India
[d] Department of Computer Science & Engineering, Indian Institute of Information Technology, Sri City, Chittoor, 517646, India

ARTICLE INFO

Keywords:
Virtual Reality
Crystal
Crystallography
Physics
XRD
Virtual lab

ABSTRACT

Teaching and learning through Virtual Reality(VR) is an emerging technology in the last few years. In this article, the development and use of a VR based teaching–learning system for crystal structures are discussed. The VR system is designed as a lab environment where a user can do experiments related to crystal structures. The VR system is designed in Unity,[1] and Oculus Rift S[2] is used as a VR headset. Currently, the system consists of three phases; in the first phase user can visualize the crystal lattice structures, wherein the second one a user can visualize the light interaction with the crystal lattice structure using a virtual torch ray. The third phase is the X-ray Diffraction (XRD) experiment. In this phase, users can perform the XRD experiment in the lab environment by taking a random crystal from a crystal dispenser machine and placing it in the X-ray machine which identifies the chosen crystalline material and analyses the unit cell. The incident ray colour changes when there is a peak found in the crystal for a better understanding of the user. There is also an interactive display where users can increase/decrease the angles of the radiation and also lock and unlock the experiment to view the diffraction plot for the crystal structure. In many cases, it was found that XRD and the crystal structure is available in the course syllabus but there are no experiments to enhance their learning. Therefore an experiment with 39 participants was performed where the maximum participants are new to crystallography. The study was conducted in two phases; in the first phase, participants are asked to watch video tutorials of the topic followed by questionnaires; in the second phase participants are asked to do the VR based experiment and followed by questionnaires related to overall study and experiment. From the analysis of the study we found that everyone found VR based teaching methods are better than traditional book/video studies. Study results give an average score of 56.74% in comparison to VR based learning approach with an average score of 93.81%. Participants who took part in the experiment found the experience interactive and motivating and found it helpful to learn elusive concepts, which can be learned when simulated. For example, one participant wrote: "The VR experience was surreal and was easy to control. Lucid user experience. Got a view of XRD like never seen before".

1. Introduction

Virtual Reality (VR) is a rapidly propelling innovation with numerous different applications fields, for example, engineering, industrial maintenance and assembly, business, medicine and healthcare or communication. VR is used to create a virtual world where users can feel the real world experience with body movement and three dimensional (3D) multimedia. In VR, a user can interact through all five senses [1] where the user can visualize a 3D object in the same way that they interact with a physical object in the real world. In recent years,

* Corresponding author.
E-mail addresses: himangshu.iiitu@gmail.com, himangshu.sarma@iiits.in (H. Sarma).

[1] https://www.unity.com/
[2] https://www.oculus.com/rift-s/
[3] https://www.vive.com/eu/
[4] https://www.playstation.com/en-us/explore/playstation-vr/
[5] https://www.samsung.com/global/galaxy/gear-vr/
[6] https://vr.google.com/cardboard/
[7] https://vr.google.com/daydream/

https://doi.org/10.1016/j.aei.2021.101362
Received 14 January 2021; Received in revised form 2 July 2021; Accepted 13 July 2021
1474-0346/© 2021 Elsevier Ltd. All rights reserved.

Principal
Nowgong Girls' College
Nagaon :: Assam

Nowgong Girls' College ESTD: 1962 Nagaon :: Assam

after introducing Head-Mounted Display (HMD) [2] such as Oculus Rift, HTC vive,[3] PlayStation VR,[4] Samsung Gear VR,[5] Google Cardboard,[6] Google DayDream[7] bring VR into a level in which it more realistically represents real life than ever [3]. Over the years, a range of innovations has been introduced to improve teaching and learning approaches in the educational field. Learning and instructing is an exceptionally encouraging field of VR applications. VR platforms serve as a potentially disruptive learning and teaching medium. As per the study, students are more positive and interactive in teaching and learning through VR as compared to other traditional learning tools [4]. VR will play a key role in upcoming days in the domain of teaching and learning, especially when in the pandemic situation traditional teaching and learning methods are transforming to digital education. In traditional online teaching and learning has a lots of limitations which restrict the teaching and learning to theoretical study only. Practical or Laboratory is one of the important methodology without which it is incomplete. It also says that people can easily understand and learn things through practical teaching as compared to only theoretical teaching and learning [5]. VR can play an important role in Science, Technology, Engineering, and Mathematics (STEM) subjects where practical or laboratory is one of the major parts of the subjects, specifically physics, chemistry and engineering subjects [6]. VR based experiments are having a lot of benefits such as

- Entertaining as working in a game environment
- It can be run multiple times until one understand properly
- Cost effective as its having virtual objects

The utilization of gamification in training assists with improving the student's inspiration to learn, using game components in learning situations with the objective of augmenting engagement of the student, which causes them to keep learning. Students can learn about a subject by living it thanks to the sense of presence VR delivers. The body believes it is in a different location and this sensation interests the mind in a remarkable way. Students visualize the things they are learning about rather than reading about them. VR can enhance visual learning methods making it easier to comprehend complex operations or mechanisms. Also, since memories are formed mostly through emotional responses to what we are witnessing, virtual reality makes it simple to memorize concepts by keeping students engaged throughout the event.

In chemistry, intelligent recreations and perceptions and virtual research centres have appeared as encouraging strategies to show complex ideas and can upgrade the comprehension of these ideas by making concealed ideas noticeable and lead unthinkable analyses. "The atomic structure of substances" is a crucial concept of chemistry. It is the establishment of further findings about the chemical compounds and their properties.

1.1. Crystallography

Solid materials are broadly classified as crystalline and non crystalline depending on the arrangements of the constituent atoms or molecules. Crystalline solids are characterized by regular or periodic arrangements of atoms or molecules. Crystallography is the branch of science dealing with the determination of the arrangement of atoms in crystalline solids and with the geometric structure of crystal lattices. The study of crystallography is necessary to understand the strong correlation between the structure of a material and their physical properties [7,8].

To describe the arrangements of atoms in a crystal, it is convenient to describe the arrangements of imaginary points in space which have a definite relationship with the atoms of the crystal. Such an arrangement of an infinite number of imaginary points having identical surroundings is known as lattice [7]. The smallest unit of the lattice which on continuous repetition generates the complete lattice is defined as a primitive unit cell. However, sometimes a unit cell with a larger volume is taken into account as the building unit due to its higher symmetry than

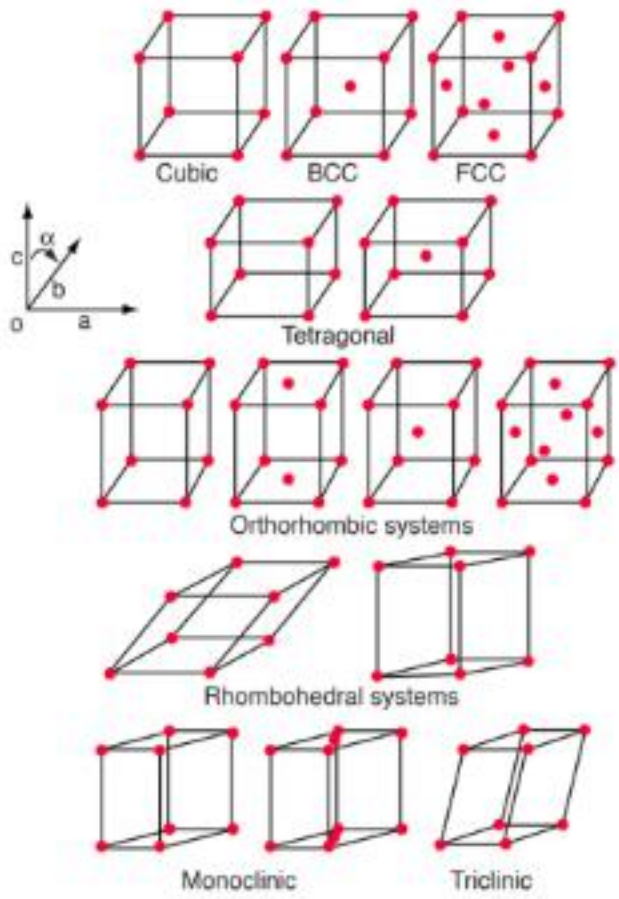

Fig. 1. Bravais lattices in three dimensions.[8]

the primitive unit cell for the particular lattice. This type of unit cell is known as a non-primitive lattice. Lattice is a mathematical concept whereas crystal structure is a physical picture and is formed by associating a structural or building unit identically with every lattice point. This structural unit is called a basis consisting of an atom or a group of atoms.

$$Lattice + Basis = crystal\,structure$$

Symmetry is one very important aspect of study in crystallography. A symmetry operation transforms the crystal to itself, i.e. a crystal remains invariant under symmetry operation. These operations are translation, rotation, reflection and inversion. These symmetry operations are collectively known as point symmetry operations. There are total of 32 point groups in three dimensional lattices. Only those lattices are permissible which are consistent with the point group operations. Such lattices are known as Bravais lattices. A Three Dimension (3D) structure of Bravais lattices is shown in Fig. 1. The 32 point groups produce a total number of 14 Bravais lattices in three dimensions. These Bravais lattices may further be classified into 7 distinct crystal systems as analysed in Table 1.

The lattice points forming a lattice may be thought of as occupying various sets of parallel planes. The scheme to represent the orientation of planes in a lattice was first introduced by Miller [7]. The indices of planes are therefore known as Miller indices and conventionally denoted as the three indices enclosed in parentheses: (hkl) e.g. (100), (111) etc. A structure of the same for a simple cubic [illegible] as shown in Fig. 2. The interplanar spacing between the [illegible]

[8] http://hyperphysics.phy-astr.gsu.edu/hbase/Sol[illegible]

Principal
Nowgong Girls' College
Nagaon :: Assam
Nowgong Girls' College
ESTD: 1962
Nagaon :: Assam

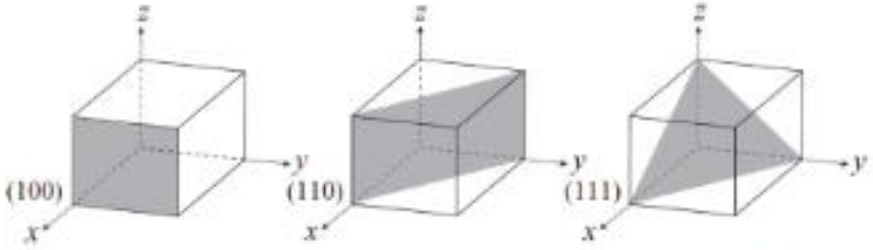

Fig. 2. Three lattice planes and their Miller indices in a simple cubic Bravais lattice [9].

Table 1
Crystal systems and Bravais lattices in three dimensions; P: Simple, I: Body Centred, F: Face Centred, B: Base Centred.

Crystal Systems	Bravias Lattice symbols	Lattice parameters
Cubic	3 (P,I,F)	$a = b = c$ $\alpha = \beta = \gamma = 90°$
Tetragonal	2 (P,I)	$a = b \neq c$ $\alpha = \beta = \gamma = 90°$
Orthorhombic	4 (P,I,F,C)	$a \neq b \neq c$ $\alpha = \beta = \gamma = 90°$
Hexagonal	1(P)	$a = b \neq c$ $\alpha = \beta = 90°, \gamma = 120°$
Trigonal	1(P)	$a = b = c$ $\alpha = \beta = \gamma < 120°, \neq 90°$
Monoclinic	2 (P,B)	$a \neq b \neq c$ $\alpha = \beta = 90° \neq \gamma$
Triclinic	1(P)	$a \neq b \neq c$ $\alpha \neq \beta \neq \gamma$

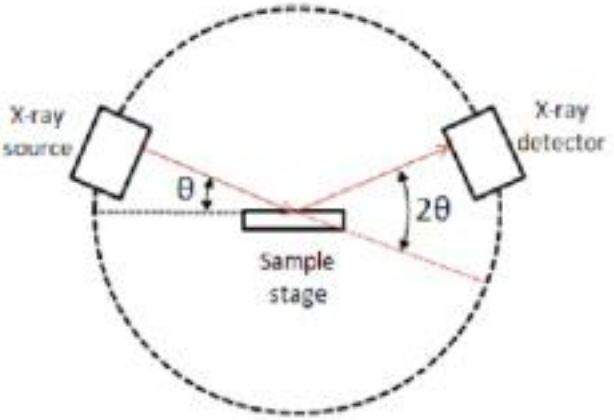

Fig. 3. Schematic diagram of a XRD setup. The obtained data set contains information of 2θ value where the constructive interference occurs and the corresponding intensity of the diffracted beam [10].

Table 2
Selection rule for miller indices for cubic lattice.

Bravais Lattice	Allowed Reflection	Forbidden Reflection
Simple	All	None
Body centred	$(h + k + l)$ even	$(h + k + l)$ odd
Face centred	h, k and l unmixed (i.e. all even or all odd)	h, k and l mixed

a family of parallel (hkl) planes is denoted by "d" and can be expressed in terms of Miller indices and the lattice constants. For example, the distance d between adjacent planes in a cubic crystal is given by:

$$d = \frac{a}{\sqrt{h^2 + k^2 + l^2}}$$

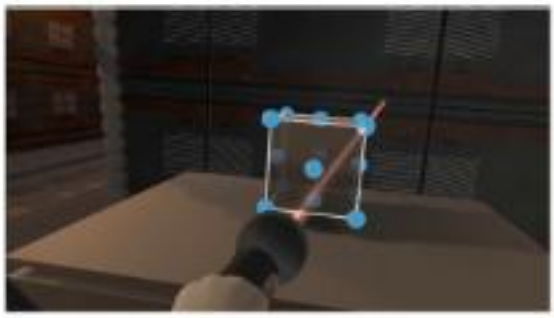

Fig. 4. X-ray(light) passing through atom in FCC model.

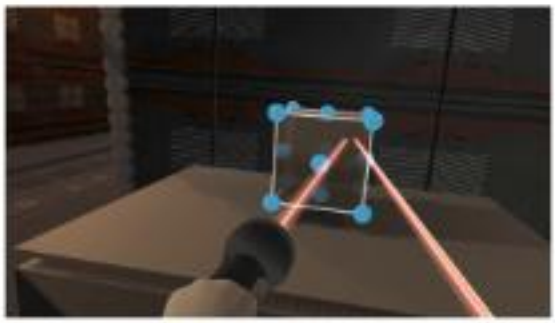

Fig. 5. X-ray(light) reflecting from plane in FCC model.

Modern crystallography is largely based on the analysis of the diffraction of X-rays by crystals. A crystal acts as a three dimensional grating for X-rays of wavelength of the order of atomic diameter. The position of diffraction lines determines the space lattice and their intensity determines the basis [7]. X-ray diffraction can be considered as a phenomenon of reflection from parallel atomic planes followed by constructive interference of reflected radiation. The condition under which reflection occurs is given by Bragg's law:

$$2d \sin\theta = n\lambda$$

[11], where d is the interplanar spacing, n is the order of diffraction and θ is the glancing angle at which the X-ray of wavelength λ is falling on a particular lattice plane. Bragg's reflection condition is concerned with the scattering of X-rays from point scattering centres arranged on the space lattice. However, in actual crystals, these lattice points are occupied by atoms or a group of atoms. Therefore the intensity of an X-ray beam diffracted from a crystal depends on the number, type and distribution of atoms within the unit cell. By studying the intensity of the diffraction lines or their presence or absence, the corresponding structure of a crystal can be determined. For example, selection rules for cubic crystals are mentioned in Table 2.

2. Background

Virtual Reality applications are used in different teaching and learning approaches; however maximum applications are video based instead of interactive. There are also a lot of health based applications designed through VR platforms where users can improve their health condition through a game based entertainment method instead of traditional approach [12,13].

A group of researchers from Ireland did a school level virtual Physics experiment as part of the European Horizon 2020 NEWTON Project. In the project a computer based VR application designed which teaches water cycle in nature and precipitation formation concepts. They did the study on 27 school students where the result says it was very enjoyable [6]. The system consists of two parts: (a) Nature VR Environment (b) Experimental Virtual Laboratory (VL) Environment. Nature VR environment describes of the natural water cycle definitions, such as vaporization, evaporation, boiling and condensation and examples of these phenomena occurring in nature. In the second part water cycle in nature was scientifically described in the Experimental VL Environment. In the domain of Mathematics, a VR based 3D robot was designed to describe two dimensional Cartesian coordinates. The study was done on 28 students and the analysis says students' interests and liking toward Mathematics increased [14]. A different study was aimed to understand the parameters that affect the sense of presence in VR among undergraduate healthcare students and postgraduate (PG). 42 Undergraduate healthcare students and 19 PG were immersed in a mass casualty incident-immersive simulation. The result indicated that the sense of presence was high among both groups but higher among PG and was positively correlated to immersion propensity [15]. Another study was done in the field of conic sections of geometry where a virtual world was built and students are asked to use tangible interfaces to manipulate geometrical figures to learn different geometrical concepts. The results say that the virtual environment helped students to understand it in a more meaningful way [16]. A group of researchers designed a virtual chemistry experiment to build molecules for pre-college students, where the user fixes an atom in a 3D environment. The study was done by over 50 people and the result showed that it was very positive. Also, people felt that the 3D building molecules interface was very intuitive and enjoyable [17]. However, it is not a VR, it is designed in OpenGL[9] [18]. Another similar system for feedback haptic applications in virtual reality about chemical bonds (ionic and covalent bonds) was developed where a target group of users are school students and designed in OpenGL where a 3D 6 DOF (Degree of Freedom) haptic device was used. In the experiment, users need to study the chemical bonds of the atoms. The study was done by 52 students who are from the 6th and 7th standard. To determine the quality and effectiveness of this program, the students are split into two classes as survey and control. From the findings, students in the study group who claimed that haptic devices are a resource for education were more optimistic than the control group trained by conventional educational methods [19]. A further interactive virtual science laboratory was developed using human computation for people without the equipment required in their scientific laboratories. The virtual lab was a recreation of the school laboratory which was designed in Unity 3D and Oculus Rift and Microsoft Kinect[10] [20] devices where a student can virtually interact with the lab equipment through different hand gestures. The experiment was done through the interaction of teachers [21]. A VR multi-sensory classroom was built in another Chemistry project to create hydrocarbon molecules, in which customers have to experiment with a combination of HMD and Leap Motion[11] [22] with supporting gloves which have integrated sensors. The system was designed as an Android application. In the virtual experiment, users can grab and bring atoms to form multiple bonds. The result shows that this type of virtual classroom is useful for learning, interaction and motivation, but only 13 participants, who come from different classes, participated in the study [23]. In this project, the author developed a VR system through which users can visualize atomic-level precision, the structures and dynamics of complex molecular structures in a virtual environment. The VR environment can be visualized using HTC Vive. In the analysis, immersive VR environments were found to be able to conduct more complex molecular simulation work faster than traditional interfaces [24]. To learn the crystallography concepts, a group of researchers developed a virtual laboratory based on VR, where a student can learn crystallography by analysing 14 Bravais lattices, i.e., unit cells, interstitial sites, crystallographic planes, directions [25].

3. VR system

Usually, in a traditional approach students learn crystal lattice through 2D images, therefore giving an alternate 3D VR visualization will be better for students to understand it properly. Also, for XRD experiments laboratory infrastructure is not found in the majority of the teaching institute, therefore a VR based learning environment for the XRD experiment can be helpful to the student community. Therefore, in this article we proposed a system consists of a three-dimensional extensible virtual laboratory developed in Unity3D which includes three crystallographic simulations, the crystal lattice visualization, the interaction of X-ray of arbitrary wavelengths with the planes of crystal structures and the XRD experiment. For visualization of X-ray we are using different coloured lights. The Unity Physics Engine allows objects to simulate natural universal forces like gravity, velocity, acceleration, and friction. It enables a wide range of objects with different physical qualities to interact dynamically with other objects in a scene. The physics engine enables our experiment to simulate in a realistic environment which may be difficult to implement in traditional multimedia teaching methods.

3.1. Crystal lattice visualization

The first room consists of interactive wireframe models of all the fourteen Bravais lattices crystal structures. These models can be grabbed using the VR handset by either pointing towards them or by moving closer and picking them up similar to a real world object. Users can pick up the structures and visualize the various aspects of a unit cell for example the length of sides, the angles between sides and their relation with each other.

3.2. Crystal X-ray interaction

The second room contains models of three cubic structures, namely, the "Face-Centered-Cubic" (FCC), the "Body-Centered-Cubic" (BCC), and the primitive cubic structure (simple cubic). These are "Ball and Stick" models with atoms at corners, faces and at the centre of the unit cell and the planes formed by these atoms in the planes corresponding to the X, Y, & Z axes. A grabbable 3D model of a torch is used as a X-ray(light) source for interaction between X-ray(light) waves and crystal structures. This room aims to study the interaction between X-ray(light) waves and the planes formed in the crystal structures by following a simple rule that planes with an atom at their centre will not reflect any light as shown in Fig. 4. While the planes which have no atoms at their centre will reflect some X-ray(light), and the rest will pass through the plane. Resulting in all the planes in the primitive cubic structure to reflect the X-ray(light), while for FCC, only the planes in the inside ($x = 0$, $y = 0$, and $z = 0$) will reflect the X-ray(light) as shown in Fig. 5 and for the BCC, only the planes on the outer surface will do so as shown in Fig. 7. The simulation uses a line-[illegible] that traces the path taken by the ray originated from [illegible] storing the coordinates of "Hits" or turns/collisions and draws out the path for the users to see how the X-ray(light) is interacting with the crystal structures.

[9] https://www.opengl.org/
[10] https://developer.microsoft.com/en-us/windows/kinect/
[11] https://www.ultraleap.com/product/leap-motion-controller/

CTC
Principal
Nowgong Girls' College
Nagaon :: Assam
Nowgong Girls' College
ESTD: 1962
Nagaon :: Assam

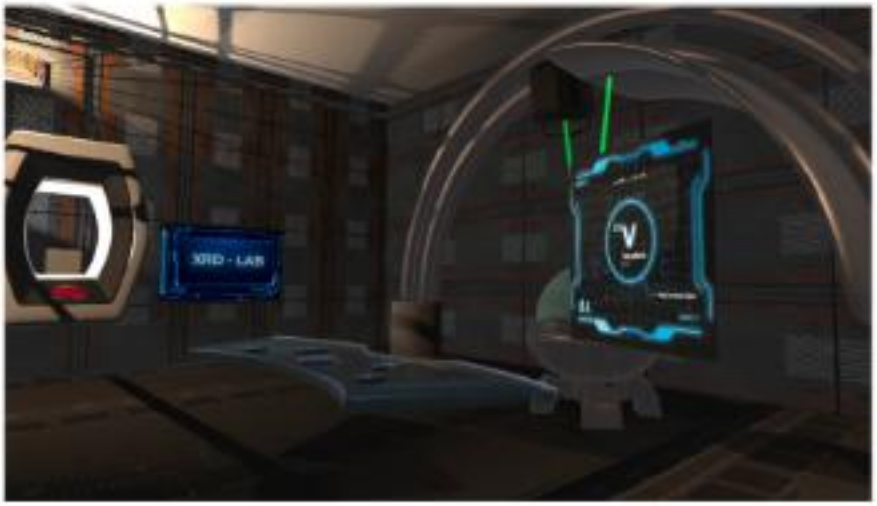

Fig. 6. View of XRD lab.

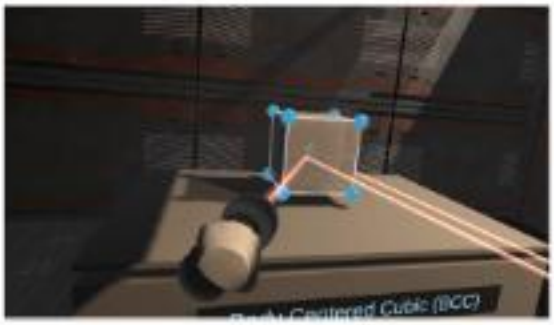

Fig. 7. X-ray(light) reflecting from plane in BCC model.

Fig. 8. X-ray changing its colour to red depicting maxima at that angle. (For interpretation of the references to colour in this figure legend, the reader is referred to the web version of this article.)

3.3. XRD

The third room has a model of an XRD analyzer machine, a machine that generates random D-Block elements, a screen to plot out the X-ray diffraction chart, and a table with buttons to control the XRD machine. An image of the lab is shown in Fig. 6

To start the experiment, users first head to the element generator which instantiates a game object which is a random D-Block element unknown to the user. This element is grabbed and placed at the centre of the XRD analyzer for examination. The analyzer scans the element by emitting an X-ray which is colourized green for easy visualization. This X-ray is emitted from the tip of the scanner which can move from 0 to 90 degrees and this angle can be increased or decreased by the user using the controls on the table. The X-ray when incident on the element gets reflected and the analyser reads the reflected ray for maximum or minimum intensity. In the case of maxima, the ray turns from green to red indicating the user that maximum intensity was recorded at that particular angle as shown in Fig. 8. The analyser records all the angles at which maximum intensity was achieved by moving the scanner tip from 0 to 90 degree. This recorded data (maximum intensities points) is now compared to every D-block element in the periodic table and matches it with the correct element. The plot button on the control table displays a pre-recorded Intensity vs 2θ graph including the maxima peaks for that randomly generated D-block element as shown in Fig. 9. The predict button on the table displays the name, atomic number and atomic mass of the D-block element which was unknown to the user in the first place as shown in Fig. 10. In this XRD simulation, the user can visualize how the XRD experiment works in general and preliminarily interact with the lab using two haptic touch controllers.

Fig. 9. Intensity versus 2θ graph showing peak intensities for the element.

Fig. 10. Results of the experiment.

Principal
Nowgong Girls' College
Nagaon :: Assam

Nowgong Girls' College
ESTD: 1962
Nagaon :: Assam

Table 3
A list of comments and feedback.

Sl No	Comments/Feedback
1	The application is awesome.
2	We can examine the crystals in the real world through the VR experiment and it feels very simple.
3	Got a view of XRD like have not did before, cool!!
4	I was able to understand concept more clearly
5	It is very good for learning new thing
6	Yes, The XRD diffraction was easily understandable through graph and Diffraction
7	The visualization of crystal lattices makes the textbook explanations lucid and far more understandable.
8	It was exciting to view lectures on solid state in CR.
9	The vr study was surreal and i really liked it.
10	Its excellent, more feature adding is also be good in future
11	I think it is great.
12	Better way of learning
13	Camera movement should be smoother
14	When button push on the controller in the X-ray room button colour should change with a different colour.
15	For now it is great.
16	You can record audio for every element so that there is no need to watch video prior to the experiment.
17	Its good and excitable.
18	Please add other concepts of basic science in future.
19	It would be more efficient, if demonstration of steps is available in VR itself.

4. Participants

For the user experience based study, 39 participants were selected from our institution (5 female, 34 male, 0 other) with a mean age of 20.30 (SD = 4.09). All the participants reported normal or corrected to normal vision. To evaluate participant learning choice, we used a pre-post model. Total 36 participants reported having prior knowledge about crystal structures, 21 participants reported having prior knowledge on miller indices and XRD experiment. The pre and post VR experience questionnaire consisted of 3 and 7 questions respectively. The experiment was performed in a normal room environment on a high-end PC with attached external speakers.

5. Study/experiment

To carry out the study participants were introduced to two different learning methods for understanding crystallography; a video lecture as close to traditional as possible and a fully featured VR simulation.

The video explained the crystallography concepts such as lattice structure and XRD experiment through 2D representations. The participants were asked to fill out a questionnaire based on their learning experience with the video lecture.

Participants were then informed about the VR experience and usage of VR headset and controllers before starting the experiment. They were initially placed in the crystal lattice visualization room but could move to other rooms. They used hand controllers to move around using the instruction charts in the VR lab. The controls were designed similar to an interaction with keyboard and mouse. Throughout the experiment, the participants were in contact with a research supervisor who also guided them through different VR simulations. Different VR simulations have different interactivity experience and endorse different scenarios. In the VR version of the activity, participants saw immersive and interactive visualizations of crystal structures, XRD lab and machines.

The objective of this experiment was to showcase the possibilities of VR based learning systems and to evaluate the future potential of this VR simulation for understanding concepts of crystallography. After the VR activity, participants filled-out a post-questionnaire. The post-questionnaire was divided into two parts: (1) learning experience with VR on a Likert scale of 1 (Strongly disagree) to 5 (Strongly agree). (2) questions about what they liked/disliked and feedback regarding the experiment. The objective of this experiment was to showcase the possibilities of VR based learning systems and to evaluate the future potential of this VR simulation for understanding concepts of crystallography.

6. Results

Participants were asked to rate both of the learning experiences (traditional and VR) based on three topics; crystal structures, miller indices and XRD experiment. The traditional video lecture method received an average score of 56.74% in comparison to the VR method which received an average score 93.81%. From the study, the results say that in all three topics participants highly rated VR based learning where video based learning got a mixed response as shown in Figs. 11–13. Also after the VR experiment, during post VR questionnaire the participants were asked a direct question "Was VR based learning better than the traditional method of learning through video lectures?", where participants rated 94.8% in the support of Strongly Agree (74.4%) and Agree (20.4%) as shown in Fig. 14. Participants found the experience interactive and motivating and found helpful to learn elusive concepts, which can be learned when simulated. The VR-based teaching and learning experiment received very positive comments and feedback from the participants. A list of comments and feedback are shown in Table 3

To evaluate the user experience and identify the issues in the system participants were asked to give feedback. While the overall experiment was described as exciting and immersive some participants mentioned that the camera movement could have been smoother. While some of the participants found the controls overwhelming due to lack of experience in using VR technology.

7. Conclusion & future work

Teaching and learning STEM through VR or in a virtual environment is going to be very popular and one of the major research areas. Usually, laboratories for these subjects are very expensive as well as very difficult to teach through online education. Therefore, teaching through a virtual environment can boost the teaching and learning as well as very cost-effective too. Usually the idea of crystals and the periodic arrangements of their constituents is introduced in higher classes of the school, mainly in the science curriculum of class 11 or 12. Elaborate description of the same and techniques to determine the crystal structure of a given material like XRD are included in the course curriculum like bachelor and master degree in basic sciences viz physics, chemistry and biology or various technical programmes involving material characterization (courses like Solid State Physics, Solid State Chemistry, Biochemistry, Biophysics etc.). However, the study said that the practical syllabus of the courses does not give any scope of using an XRD machine due to both financial and space limitations. Hence, we proposed different virtual laboratories where a detailed view of the different crystal structure is shown in Lab 1, Lab 2 contains the theory behind it and the use of the XRD in the Lab 3 to enhance their concepts obtained from 2D diagrams of the text books. The lab presented a detailed analysis about the impact of VR on student learning, particularly for the topic crystallography. With this system a user can learn and visualize all these features within 15–20 min, whether to learn the same thing through a traditional video based approach a user needs to follow multiple videos and it will cost more time as well as not able to visualize like a VR system. A high majority of students (93.81%) found VR learning more effective and immersive as compared to traditional teaching methods. A few participants who were not familiar with VR sets and controls and using [illegible] some kind of motion sickness after using the [illegible] for a longer period. However, higher frame rates can solve the issue of motion sickness. Moreover, we are working on scaling the application to make it accessible on cheaper VR headsets like google cardboard.

Principal
Nowgong Girls' College
Nagaon :: Assam

Nowgong Girls' College
ESTD: 1962
Nagaon :: Assam

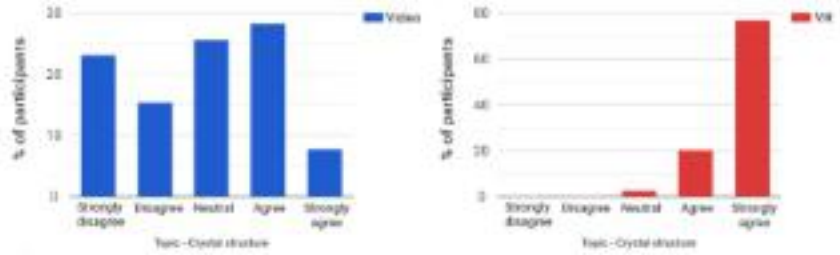

Fig. 11. Participants rating on Video vs VR based learning topic crystal structure.

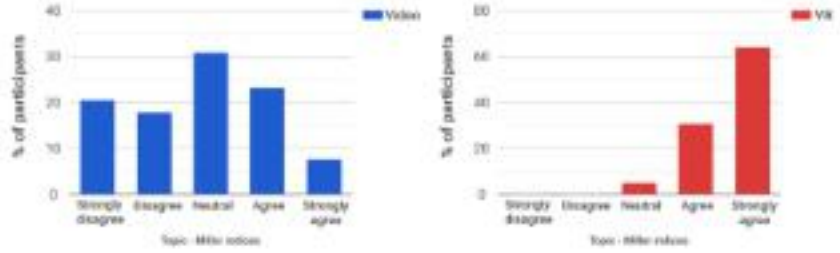

Fig. 12. Participants rating on Video vs VR based learning miller indices.

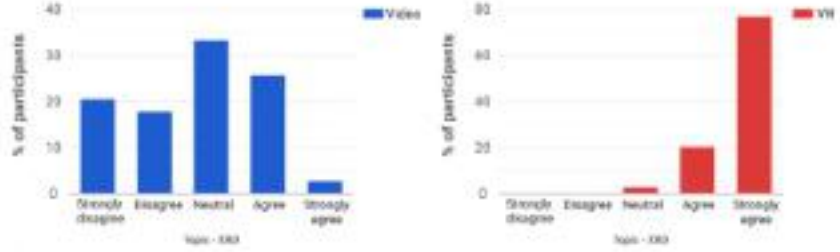

Fig. 13. Participants rating on Video vs VR based learning topic xrd.

Fig. 14. Comparative rating on VR over video.

conclusion, we found concrete proof of change in participants' ability to grasp concepts of crystallography using VR setup as compared to video lectures through this study.

There were no differences found in student learning in VR, video and static images as per previous work [20]. However, the results from our study indicated that students prefer VR setup for learning about crystallography as they found the interactions more engaging and immersive. In the present work, we concentrated on user experience with a focus on interaction and learning value. However, to exceed human performance in teaching, various new approaches will be implemented in the next few years. Future work will give more focus on population, methods and results. We also aim to further optimize the simulation for smoother camera movements and add audio instructions in the lab. In the future, implementing an AR version can generate more satisfying results because it will be portable, cost-effective and solve hardware issues such as field of view in the HMD. Future publications will consider VR applications for a broader range of STEM subjects and focus on retention of elusive concepts.

Declaration of competing interest

The authors declare that they have no known competing financial interests or personal relationships that could have appeared to influence the work reported in this paper.

Acknowledgement

The research reported in this paper has been supported by the Third phase of Technical Education Quality Improvement Programme (TEQIP-III), India.

References

[1] G.C. Burdea, P. Coiffet, Virtual Reality Technology, John Wiley & Sons, 2003.
[2] Z. Chen, W. Peng, B. Peiris, K. Minamizawa, ThermoReality: Thermally enriched head mounted displays for virtual reality, in: ACM SIGGRAPH 2017 Posters, 2017, pp. 1–2.
[3] S. Günther, F. Müller, D. Schön, O. Elmoghazy, M. Mühlhäuser, T. Schmitz, Therminator: Understanding the interdependency of visual and on-body thermal feedback in virtual reality, in: Proceedings of the 2020 CHI Conference on Human Factors in Computing Systems, 2020, pp. 1–14.
[4] G. Cooper, H. Park, Z. Nasr, L. Thong, R. Johnson, Using virtual reality in the classroom: preservice teachers' perceptions of its use as a teaching and learning tool, Educ. Media Int. 56 (1) (2019) 1–13.

Principal
Nowgong Girls' College
Nagaon :: Assam
Nowgong Girls' College ESTD: 1962 Nagaon :: Assam

[5] K.S. Nováková, Z. Gierlinová, New models of theoretical and practical education in urban environment (On example of experience-based pedagogy in Slovak Towns), Procedia-Soc. Behav. Sci. 228 (2016) 305–310.
[6] D. Bugnaevschi, C. Mamman, G.-M. Munteau, Teaching and learning physics using 3D virtual learning environment: A case study of combined virtual reality and virtual laboratory in secondary school, J. Comput. Math. Sci. Teach. 39 (1) (2020) 5–18.
[7] N.W. Ashcroft, N.D. Mermin, et al., Solid State Physics [by] Neil W. Ashcroft [and] N. David Mermin, Holt, Rinehart and Winston, New York, 1976.
[8] H. Meyers, H. Myers, Introductory Solid State Physics, CRC Press, 1997.
[9] J. Yamamoto, T. Okamoto, A. Toyotama, Colloidal crystals, in: Pattern Formations and Oscillatory Phenomena, Elsevier, 2013, pp. 165–198.
[10] M. Mulder, Synthesis of LiNi0.5Mn1.5O4 Nanofibers by Electrospinning, 2016.
[11] W.H. Bragg, W.L. Bragg, The reflection of X-rays by crystals, Proc. R. Soc. Lond. Ser. A, Containing Papers of A Mathematical and Physical Character 88 (605) (1913) 428–438.
[12] H. Sarma, R. Porzel, J. Smeddinck, R. Malaka, Towards generating virtual movement from textual instructions, in: Conference on Human Computation & Crowdsourcing (HCOMP 2015), 2015.
[13] H. Sarma, R. Porzel, J.D. Smeddinck, R. Malaka, A.B. Samaddar, A text to animation system for physical exercises, Comput. J. 61 (11) (2018) 1589–1604, http://dx.doi.org/10.1093/comjnl/bxy014.
[14] I. Simsek, The effect of 3D virtual learning environment on secondary school third grade students' attitudes toward mathematics, Turk. Online J. Educ. Technol. 15 (2) (2016) 162–168.
[15] J.-C. Servotte, M. Goosse, S.H. Campbell, N. Dardenne, B. Pilote, I.L. Simoneau, M. Guillaume, I. Bragard, A. Ghuysen, Virtual reality experience: Immersion, sense of presence, and cybersickness, Clin. Simul. Nurs. 38 (2020) 35–43, https://doi.org/10.1016/j.ecns.2019.09.006, URL: https://www.sciencedirect.com/science/article/pii/S1876139918303244.
[16] G. Guerrero, A. Ayala, J. Matos, L. Casades, X. Alamán, Integrating virtual worlds with tangible user interfaces for teaching Mathematics: A pilot study, Sensors 16 (11) (2016) 1775.
[17] C.M. Sauer, W.A. Hastings, A.M. Okamura, Virtual environment for exploring atomic bonding, in: Proc. of EuroHaptics, Citeseer, 2004, pp. 5–7.
[18] M. Woo, J. Neider, T. Davis, D. Shreiner, OpenGL Programming Guide: The Official Guide To Learning OpenGL, Version 1.2, Addison-Wesley Longman Publishing Co., Inc., 1999.
[19] E. Ucar, H. Ustunel, T. Civelek, I. Umut, Effects of using a force feedback haptic augmented simulation on the attitudes of the gifted students towards studying chemical bonds in virtual reality environment, Behav. Inf. Technol. 36 (5) (2017) 540–547.
[20] Z. Zhang, Microsoft kinect sensor and its effect, IEEE Multimedia 19 (2) (2012) 4–10.
[21] F. Torres, L.A.N. Tovar, M.C. Egresy, Virtual interactive laboratory applied to high schools programs, Procedia Comput. Sci. 75 (2015) 233–238.
[22] F. Weichert, D. Bachmann, B. Rudak, D. Fisseler, Analysis of the accuracy and robustness of the leap motion controller, Sensors 13 (5) (2013) 6380–6393.
[23] B.I. Edwards, K.S. Bielawski, R. Prada, A.D. Cheok, Haptic virtual reality and immersive learning for enhanced organic chemistry instruction, Virtual Real. 23 (4) (2019) 363–373.
[24] M. O'Connor, H.M. Deeks, E. Dawn, O. Metatla, A. Roudaut, M. Sutton, L.M. Thomas, B.R. Glowacki, R. Sage, P. Tew, et al., Sampling molecular conformations and dynamics in a multiuser virtual reality framework, Sci. Adv. 4 (6) (2018) eaat2731.
[25] J. Extremera, D. Vergara, L.P. Dávila, M.P. Rubio, Virtual and augmented reality environments to learn the fundamentals of crystallography, Crystals 10 (6) (2020) http://dx.doi.org/10.3390/cryst10060456, URL: https://www.mdpi.com/2073-4352/10/6/456.
[26] J.R. Smith, Physics Education Research Conference, 2017, p. 276.

Principal
Nowgong Girls' College
Nagaon :: Assam

Nowgong Girls' College
ESTD: 1962
Nagaon :: Assam

Journal of Magnetism and Magnetic Materials 546 (2022) 168913

Contents lists available at ScienceDirect

Journal of Magnetism and Magnetic Materials

journal homepage: www.elsevier.com/locate/jmmm

Effects of composition variation and site disorder on the magnetic interactions in $Ru_2Fe(Si_{1-x}Ge_x)$ alloys

Bhargab Deka [a,c,*], Ashis Kundu [b,c], Subhradip Ghosh [c], A. Srinivasan [c]

[a] Department of Physics, Nowgong Girls' College, Nagaon 782002, India
[b] Institute for Advanced Study, Shenzhen University, Shenzhen 518060, China
[c] Department of Physics, Indian Institute of Technology Guwahati, Guwahati 781039, India

ARTICLE INFO

Keywords:
Full Heusler alloys
Antiferromagnet
Ferromagnet
Ab initio calculations
Heisenberg exchange integral

ABSTRACT

X-ray diffraction studies on arc melted $Ru_2Fe(Si_{1-x}Ge_x)$ ($0 \leq x \leq 1$) alloys did not show the characteristic (111) and (200) super-lattice peaks of the stable $L2_1$ structure of full Heusler alloys. The alloy with $x = 0$ exhibited antiferromagnetic behaviour. However, with increase in x, the alloys became ferromagnetic. In order to understand the origin of the novel magnetic behavior of these alloys and its correlation with their crystal structure, ab initio study was carried out using spin-polarized relativistic Korringa-Kohn-Rostoker Green's function method. The study shows that the antiferomagnetism in the alloy with $x = 0$ is due to the presence of B2 disorder. Due to this, the 2nd nearest neighbour (NN) exchange interaction between the Fe atoms at proper and improper sites, respectively, becomes strongly antiferromagnetic which dominates over the 1st NN ferromagnetic exchange interaction. With increase in x, the alloys become ferromagnetic with an improvement in $L2_1$ ordering which in turn makes the 1st NN interaction strongly ferromagnetic. The electronic structure calculations show no half metallic gap in either spin direction for all the alloys. Comparison of experimental and theoretically estimated properties of $Ru_2Fe(Si_{1-x}Ge_x)$ alloys provides insight to the variation in the magnetic interaction with the composition and the disorder present in the alloys.

1. Introduction

Discovery of half-metallicity with high spin polarized current in Co_2MnSi [1,2] and other full Heusler alloys [3-5] has been instrumental in the development of spin valve based giant magneto-resistance (GMR) devices with full Heusler alloys as ferromagnetic electrodes. However, such spin valves usually use Ir-Mn as an antiferromagnetic (AFM) layer to pin the magnetization of one of the ferromagnetic layers [6,7]. If all the layers in a spin valve could be realized using Heusler alloys with matching lattice constant, it would improve the functionality with superior interfacial properties. In this regard, an AFM full Heusler alloy with high Neel temperature (T_N) is essential. Very few AFM full Heusler alloys such as Ru_2MnZ (Z = Si, Ge, Sn, Sb) [8,9] and Ru_2FeSi [10-12] have been reported so far. Among these, Ru_2FeSi with T_N (=280 K [10], = 270 K [12]) close to room temperature appears to be promising. However, not much studies have been reported on Ru based alloys; both theoretically and experimentally. Fully ordered Heusler alloys with the chemical formula of X_2YZ exhibit $L2_1$ structure, where X and Y are usually transition metals and Z is an element with *sp* valence electrons [13,14]. The stable $L2_1$ structure of these alloys consists of four interpenetrating FCC sub-lattices with X atoms at 8c (¼,¼,¼ and ¾,¾,¾), Y atoms at 4b (½,½,½) and Z atoms at 4a (0,0,0) Wyckoff positions. Intermixing of Y and Z atoms leads to *B2* type disorder and intermixing between X, Y and Z atoms result in *A2*-type disorder in these alloys. The presence of these disorders have considerable impact on the properties of the alloys [11,15]. Moreover, it has been found that substitution of a fourth element for any of the three elements in X_2YZ alloys can tailor their electronic structure and magnetic properties. Proper choice of a fourth element and its concentration such as $Ru_2Y(Z_{1-x}Z'_x)$ provide a means of obtaining ferromagnetic and antiferromagnetic materials in the same quaternary system. In an earlier work, we had reported the crystallographic and magnetic properties of quaternary $Ru_2Fe(Si_{1-x}Ge_x)$ alloys with $0 \leq x \leq 1$ [12]. X-ray diffraction and magnetization studies on $Ru_2Fe(Si_{1-x}Ge_x)$ alloys showed (a) absence of characteristic superlattice $L2_1$ peaks in all the alloys and (b) alloy with $x = 0$ was found out to be antiferromagent with T_N of 270 K. However, with increase in x, ferromagnetic interaction appeared in the samples. Though the reason for this change in magnetic interaction in this alloy system with Ge

* Corresponding author.
E-mail addresses: bdeka85a@gmail.com (B. Deka), subhra@iitg.ac.in (S. Ghosh), asrini@iitg.ac.in (A. Srinivasan).

https://doi.org/10.1016/j.jmmm.2021.168913
Received 27 July 2021; Received in revised form 2 November 2021; Accepted 29 November 2021
Available online 7 December 2021
0304-8853/© 2021 Elsevier B.V. All rights reserved.

Principal
Nowgong Girls' College
Nagaon :: Assam

Nowgong Girls' College
ESTD: 1962
Nagaon :: Assam

substitution is not known, the Curie temperature T_C increases well above room temperature with Ge substitution (T_C increased from 354 K to 460 K as x was increased from 0.25 to 1.00 [12]). There are several publications which have established the crystal structure and possible structural disorders in Ru_2FeZ alloys and the effect of disorder on their magnetic properties have been discussed in earlier works from a different perspective. In the XRD study of Ru_2FeSi, Mishra et al [10] depict a structure with a small amount of Ru-Fe/Si (X-Y/Z) disorder but a dominating Fe-Si (Y-Z or B2-type) disorder. Szytula et al [11] conducted magnetic susceptibility and (X-ray and neutron) diffraction studies on Ru_2FeSi alloys and found the alloy to be formed in B2 structure (Fe-Si-disordered). Hyperfine field investigations carried out by Patil et al [16] on Ru_2FeGe indicate the presence of Ru-Ge (X-Z) disorder with the alloy. Yin et al [17] reported the B2 structure for the Ru_2FeSi and $L2_1$ structure with a very low intensity (1 1 1) peak for the Ru_2FeGe alloy respectively. The effect of the B2 disorder on the Ru_2FeSi alloy is quite interesting as this alloy shows antiferromagnetic nature instead of the more dominant ferromagnetism exhibited by the majority of Heusler alloys. Considering the importance of antiferromagnetic full Heusler alloys and the lack of understanding of the magnetic interaction in these alloys, *ab initio* calculations and magnetization measurements have been carried out on $Ru_2Fe(Si_{1-x}Ge_x)$ alloys. In this report, variation in magnetic interaction with composition is studied and the effect of chemical disorder on the type of interaction deduced from these calculations has been compared with experimental results.

2. Methodology

$Ru_2Fe(Si_{1-x}Ge_x)$ alloys were prepared by arc melting method as described earlier [12]. The processed alloy samples were characterized using X-ray diffractometer (Rigaku TTRAX III) with Cu K_α X-rays (λ = 0.15406 nm) and vibrating sample magnetometer (VSM, Lakeshore 7410) coupled with a variable temperature sample holder. Overall alloy composition was estimated from energy dispersive spectrometer (EDS, Oxford) was within 1% of the nominal composition.

The electronic structure of the alloys has been calculated using full-potential based spin polarized relativistic Korringa-Kohn-Rostoker (SPR-KKR) Green's function method [18]. The Generalized Gradient Approximation (GGA) was used for exchange and correlation to solve the Kohn-Sham equation [19,20]. The angular moment cut-off to the plane wave (l_{max}) was taken as 3. The Brillouin zone integrations have been carried out on a uniform 24 × 24 × 24 k-mesh. The Green's function was calculated for 30 complex energy points distributed exponentially on a semi-circular contour. The energy convergence criterion was set to 10^{-6} Ry for the self-consistent cycles. The coherent potential approximation (CPA) was used to incorporate the effect of atomic disorder. *B2* disorder is achieved by assigning (50% occupancy of Fe and 50% occupancy of Z) to both 4a and 4b Wyckoff positions. In what follows, we shall designate Fe atoms on the sites of the nominal (original) Fe sub-lattice as Fe_{4b}, whereas those on the sites of the nominal Z sub-lattice as Fe_{4a}. The magnetic properties of the Ru_2FeZ Heusler compounds can be well described by the classical Heisenberg Hamiltonian, $H = -\sum_{<ij>} J_{ij} e_i e_j$ where J_{ij} is the Fe-Fe exchange interaction, the sum runs over all the different Fe-Fe pairs and e_i represents the unit vector pointing along the magnetic moment of the i^{th} Fe site [20,21]. In the case of chemical disorder between the Fe and Z sub-lattices, the sum in Hamiltonian equation also includes sites on the Z sub-lattice occupied by Fe atoms.

3. Results and discussion

Fig. 1 shows the comparison between the room temperature experimental X-ray diffraction (XRD) patterns (represented by black colour lines) and simulated $L2_1$ (red colour lines) and B2 (blue colour lines) structured $Ru_2Fe(Si_{1-x}Ge_x)$ alloys. The structure factor of the first three reflections are given by the relations,

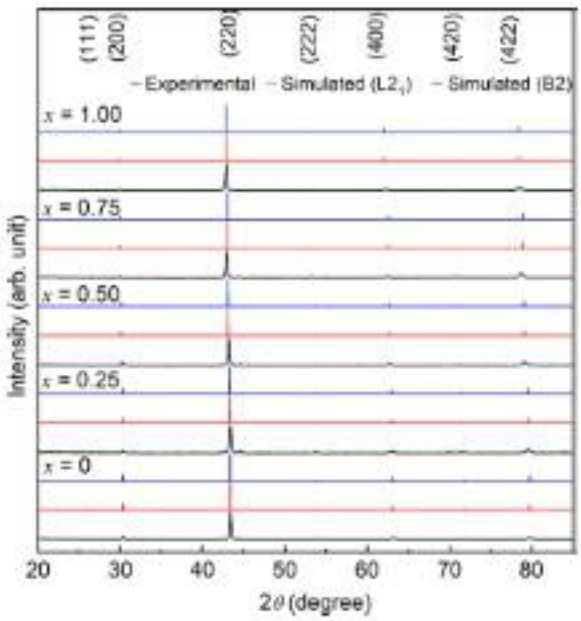

Fig. 1. Simulated XRD patterns of $L2_1$ and B2 structured $Ru_2Fe(Si_{1-x}Ge_x)$ alloys along with the experimental XRD patterns.

$$\begin{aligned} F(111) &= 4(f_x - f_z) \\ F(200) &= 4\left(2f_y - (f_x + f_z)\right) \\ F(220) &= 4\left(2f_x + f_y + f_z\right), \end{aligned} \tag{1}$$

where f_x, f_y and f_z are average scattering amplitudes for respective sub-lattices. The XRD pattern in Fig. 1 reveals that the peaks with all odd Miller indices, including (1 1 1), are absent which indicates a transition from $L2_1$ to *B2* structure due to intermixing of Y and Z atoms. However, since Fe and Ge are from the same period, nearly equal scattering factors of Fe (f_{Fe}) and Ge (f_{Ge}) could also result in such XRD patterns devoid of this super-lattice peak as suggested by F(1 1 1) relation in Eq. (1) [22]. Absence of the (1 1 1) peak even in the theoretically generated XRD pattern for alloys with high Ge concentration confirms the above argument. Although simulated XRD pattern for x = 0.25 shows the (1 1 1) peak, its intensity is very small. With increase in x, lattice constant increases because of larger atomic radius of Ge compared to Si. The lattice constant for x = 0, 0.25, 0.50, 0.75 and 1.00 are 5.89 Å, 5.89 Å, 5.92 Å, 5.96 Å and 5.98 Å respectively [12]. Table 1 shows the peak height of the three major peaks of Heusler alloy (1 1 1), (2 0 0) and (2 2 0) for alloys having 0% ($L2_1$), 25% and 50% Ru-Ge disorder. It can be seen that the height of the super lattice peak (1 1 1) increases with increase in Ru-Ge disorder. Simulated results show similar behaviour exhibited by the alloys containing Si as well. Since the (1 1 1) peaks are not clearly discernible in the experimental XRD patterns, the simulations on disordered structures is limited to B2 type disorder only.

Thermo-magnetization measurements show that the alloy with x = 0 is antiferromagnetic with T_N = 270 K. Substitution of Ge in Si sites resulted in the development of ferromagnetism, resulting in increase in both T_C and magnetization of the alloys [12]. In order to identify the

Table 1
Peak height of the three major XRD peaks of Heusler alloy (1 1 1), (2 0 0) and (2 2 0) for alloys having 0% ($L2_1$), 25% and 50% Ru-Ge disorder for Ru_2FeGe alloy.

Peak	0% Ru-Ge disorder	25% Ru-Ge disorder	50% Ru-Ge disorder
(1 1 1)	0.581047	1.695980869	2.[illegible]8963
(2 0 0)	6.538965	6.675180182	2.417590[illegible]
(2 2 0)	100	100	100

Principal
Nowgong Girls' College
Nagaon :: Assam
Nowgong Girls' College ESTD: 1962 Nagaon :: Assam

composition at which the antiferromagnetic to ferromagnetic transition occurs, additional alloy compositions, viz., x = 0.10, 0.15 and 0.20 were prepared. Of these, x = 0.10 and 0.15 exhibited antiferromagnetic behaviour and $x = 0.20$ showed ferromagnetic behaviour. This experimental data reveals that the antiferromagnetic to ferromagnetic transition occurs between $x = 0.15$ and $x = 0.20$ in this system as illustrated in Fig. 2.

To investigate the change in magnetic interaction with Ge substitution and the effect of *B*2 disorder on these interactions, *ab initio* calculations were carried out on $Ru_2Fe(Si_{1-x}Ge_x)$ alloys using SPR-KKR Green's function method. The experimental lattice parameters of the alloys were used in these calculations. Fig. 3 shows the variation of the exchange interactions (J_{ij}) representing the magnetic interaction between Fe atoms as a function of interatomic distance in units of lattice parameter (a) for $Ru_2Fe(Si_{1-x}Ge_x)$ alloys with a fully ordered $L2_1$ structure. Magnetic interaction that was ferromagnetic at $0.707a$ (*i.e.* $a/\sqrt{2}$), turned antiferromagnetic at $1.0a$ and the interactions died out at large ($\geq 2.25a$) interatomic distances. This damped oscillatory behaviour exhibited by J_{ij} in Fig. 3 is similar to Ruderman–Kittel–Kasuya–Yosida. (RKKY) type of interaction mediated by *sp* atoms. It can be observed from Fig. 3 that the first nearest neighbour (NN) magnetic interactions between these atoms is strongly ferromagnetic, leading to ferromagnetism in all the alloys including $x = 0$ alloy. Since this contradicts the experimental results depicted in our previous work [12] and the *B*2 structure shown by the XRD pattern of this compound, *ab initio* calculations were carried out on all these alloy compositions by introducing *B*2 disorder in the $L2_1$ unit cell.

Fig. 4 shows both intra sub-lattice and inter sub-lattice exchange interactions between the Fe atoms with interatomic distance for *B*2 disordered $Ru_2Fe(Si_{1-x}Ge_x)$ alloys. As we can see, the second NN inter sub-lattice exchange interaction between the Fe_{4b} atom in the proper (4b) position and the Fe_{4a} atom in the improper position (4a) becomes antiferromagnetic due to decrease in the distance between Fe atoms. Hence, in alloys with considerable amount of *B*2 disorder, antiferromagnetism is expected to dominate. A similar trend in the exchange interactions is also observed for Ru_2MnSi with *B*2 disorder [23]. XRD pattern of Ru_2FeSi alloy reveals a disordered *B*2 structure and so this alloy is expected to be an antiferromagnet as confirmed by experimental report [12]. However, magnetic measurements show that alloys with $x = 0.25$, 0.50, 0.75 and 1.00 are ferromagnetic despite the absence of the characteristic (111) reflection of $L2_1$ structure in their XRD patterns. Hence, this observation can be reasoned out that the intensity of (111) reflection is reduced below the detectable limit for the alloys with $x > 0$ due to nearly equal scattering factor f_{Fe} and f_{Ge}, despite their $L2_1$ structure.

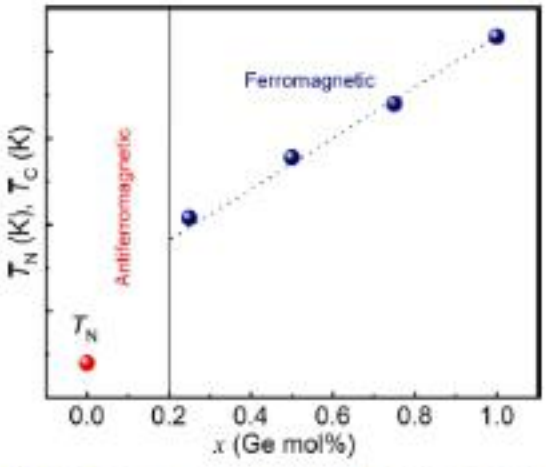

Fig. 2. Variation of transition temperature of $Ru_2Fe(Si_{1-x}Ge_x)$ alloys as a function of Ge at.%.

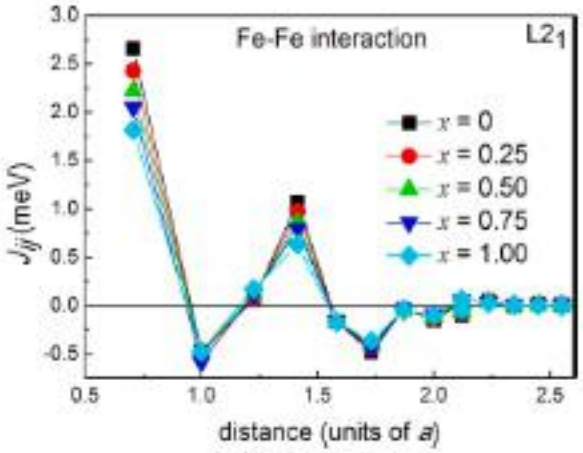

Fig. 3. Calculated Fe-Fe exchange interactions, J_{ij} in $Ru_2Fe(Si_{1-x}Ge_x)$ alloys with $L2_1$ structure as a function of the interatomic distance, measured in the units of lattice constant.

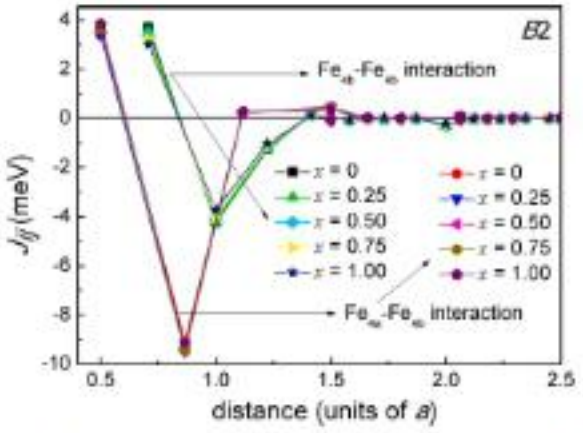

Fig. 4. Calculated Fe-Fe exchange interactions, J_{ij} in $Ru_2Fe(Si_{1-x}Ge_x)$ alloys with *B*2 disorder as a function of the interatomic distance, measured in the units of lattice constant.

In order to examine the electronic structure of these alloys with both $L2_1$ and *B*2 structures close to the Fermi energy level (E_F), their density of states (DOS) was calculated and shown in Fig. 5(a) and Fig. 5(b), respectively. It is immediately evident from these figures that there is no gap at E_F for either spin direction for both $L2_1$ and *B*2 phases. So, half-metallicity is not expected in any of the $Ru_2Fe(Si_{1-x}Ge_x)$ alloys. It is worthy to point out here that previous theoretical calculation performed on the alloy with $x = 1$ [24] yielded similar result. However, a minimum (or a pseudo gap) is observed at E_F for the alloys in the minority channel of the DOS. Moreover, the position of this minimum shifts to lower energy when *B*2 disorder is introduced. Fig. 6 shows the value of the spin polarization as a function of x calculated from the DOS for both the ordered ($L2_1$) and (B2) disordered alloys. In both the cases, all the alloys show very low spin polarisation. Spin polarisation increases with increase in Ge substitution. Spin polarisation of the ordered $L2_1$ alloys is higher than the corresponding alloys with B2 disorder. Moreover, the rate of increase of spin polarisation with x is relatively higher for B2 alloys.

Fig. 7(a) and Fig. 7(b) show the atom resolved DOS for the alloys with $x = 0.5$ with ordered $L2_1$ and disordered *B*2 structures respectively. The Fe atom is more affected by the disorder as compared to Ru as shown by the DOS. Similar behaviour in DOS has also been observed in the isoelectronic ferromagnetic compound Fe_3Si [25]. The atom resolved DOS for other compositions of $Ru_2Fe(Si_{1-x}Ge_x)$ alloys also shows similar

Principal
Nowgong Girls' College
Nagaon :: Assam

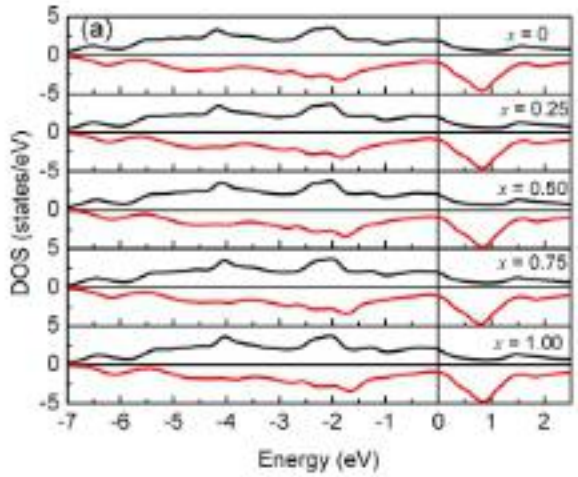

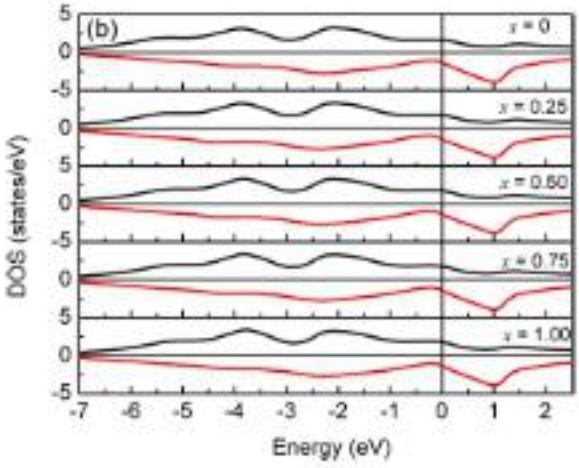

Fig. 5. Total DOS for $Ru_2Fe(Si_{1-x}Ge_x)$ alloys with (a) $L2_1$, and (b) $B2$ structures. The zero of the energy is set at Fermi energy (E_F).

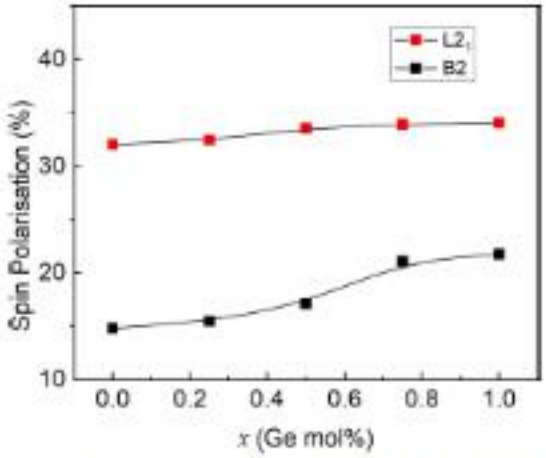

Fig. 6. Spin polarization as a function of x calculated from the DOS for both $L2_1$ and $B2$ disordered alloys.

behaviour.

Rhodes-Wohlfarth (R-W) ratio (p_c/p_s), was estimated from the saturation magnetic moment p_s expressed in units of μ_B and p_c (effective magnetic moment per magnetic atom). p_c can be deduced from the Curie constant, C using the relation [26-28],

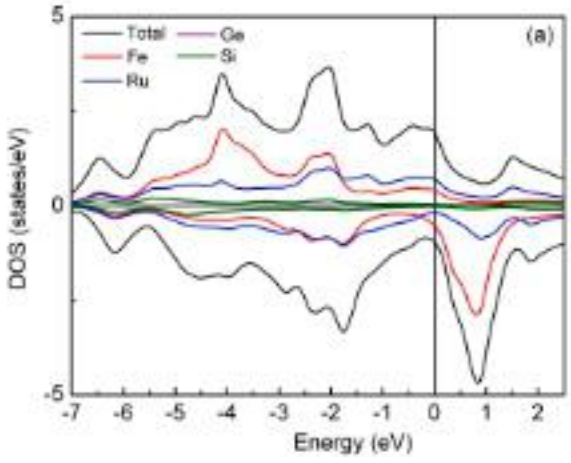

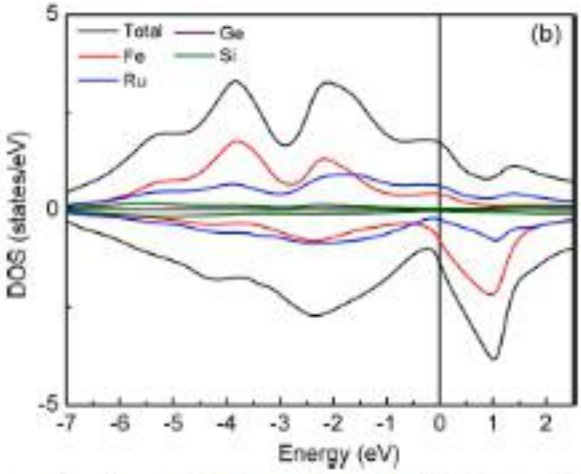

Fig. 7. Total and atom resolved DOS for the alloys with (a) $L2_1$ and (b) $B2$ structures for the alloy with $x = 0.5$. The zero of the energy is set at Fermi energy (E_F).

$$C = \frac{N_A \mu_B^2 P_c (P_c + 2)}{3k_B} \tag{2}$$

C was estimated from the inverse magnetic susceptibility versus temperature data for $T > T_C$ for all the alloys according to Curie-Weiss law,

$$\chi^{-1} = C^{-1}T - C^{-1}\theta_p \tag{3}$$

where θ_p is paramagnetic Curie temperature. p_c/p_s is expected to be unity for local moment ferromagnets and larger than unity for itinerant ferromagnets. On the other hand, for half-metallic ferromagnets R-W ratio can have value less than unity [27,28]. The calculated R-W ratio for

Table 2
Magnetic moment at an applied field of 10 kOe [12], effective moment per magnetic atom (p_c) [12], R-W ratio p_c/p_s, and M_t calculated using nominal composition (M_{Nom}) and EDS measured composition (M_{EDS}) for $Ru_2Fe(Si_{1-x}Ge_x)$ alloys. Total magnetic moment (M_{tb}) of the alloys with $L2_1$ and $B2$ structures obtained from *ab initio* calculations are also shown.

x	$M_{10\,kOe}$ (μ_B)	p_c (μ_B)	p_c/p_s	M_{Nom} / M_{EDS} (μ_B)	M_{tb} ($L2_1$) (μ_B)	M_{tb} ($B2$) (μ_B)
0	0.03	4.4	–	4.0 / 4.0	3.81	3.80
0.25	0.40	4.8	12	4.0 / 4.0	3.84	3.80
0.50	1.21	4.9	4.04	4.0 / 3.9	3.89	3.80
0.75	2.04	3.7	1.81	4.0 / 3.9	3.89	3.80
1.00	2.69	3.7	1.38	4.0 / 3.9	3.91	3.80

all the alloys have value greater than unity as shown in Table 2. Moreover, non-integer value of saturation magnetization (M_s) for both experimental and theoretically calculated results (Table 2) confirms the absence of half-metallic nature in the alloys. In Table 2, M_{Nom} refers to the calculated value of the magnetic moment from Slater-Pauling rule using the nominal composition whereas M_{EDS} is the same calculated from Slater-Pauling rule using the measured composition of the synthesized alloys using EDS.

4. Conclusion

Detailed *ab-initio* calculations using SPR-KKR Green's function method have been performed for quaternary $Ru_2Fe(Si_{1-x}Ge_x)$ alloys. The calculations attribute the antiferromagntism of the alloy with $x = 0$ to the *B*2 disorder present in this alloy. Due to this disorder, the 2^{nd} NN interaction between the Fe atoms at proper and improper sites, respectively, becomes strongly antiferromagnetic and dominates over the 1st NN ferromagnetic interaction. With increase in x, ferromagnetic interaction appears in $Ru_2Fe(Si_{1-x}Ge_x)$ alloys and T_C increases with increase in x, due to improvement in their $L2_1$ ordering. These studies show that alloys with antiferromagnetic as well as ferromagnetic interactions of different strengths could be achieved in this alloy system depending on the composition as well as chemical ordering. The electronic structure of these alloys with both $L2_1$ and *B*2 structures shows the absence of half-metallicity in the alloys which is confirmed by the R-*W* ratio of the alloys having values greater than unity. Despite the lack of half-metallicity, the potential of the antiferromagnetic alloy is significant due its application as the pinning layer in all Heusler spin valve structures.

Declaration of Competing Interest

The authors declare that they have no known competing financial interests or personal relationships that could have appeared to influence the work reported in this paper.

Acknowledgement

Financial assistance from the Council of Scientific and Industrial Research, India vide project no: 03(1431)/18/EMR-II and computational facilities provided to Department of Physics, IIT Guwahati under DST-FIST programme are gratefully acknowledged.

References

[1] S. Ishida, S. Fujii, S. Kashiwagi, S. Asano, J. Phys. Soc. Jpn. 64 (1995) 2152.
[2] L. Ritchie, G. Xiao, M. Zhang, Z. Chen, Z. Liu, G. Wu, X.X. Zhang, Phys. Rev. B 68 (2003), 104430.
[3] I. Galanakis, P.H. Dederichs, N. Papanikolaou, Phys. Rev. B 66 (2002), 174429.
[4] I. Galanakis, P.H. Dederichs, Half-Metallic Alloys: Fundamentals and Applications, Springer, Berlin, 2005.
[5] B.S.D.C.S. Varaprasad, A. Srinivasan, Y.K. Takahashi, M. Hayashi, A. Rajanikanth, K. Hono, Acta Mater. 60 (2012) 6257e6265.
[6] K. Nikolaev, P. Kolbo, T. Pokhil, X. Peng, Y. Chen, T. Ambrose, O. Mryasov, Appl. Phys. Lett. 94 (2009), 222501.
[7] T.M. Nakatani, N. Hase, H.S. Goripati, Y.K. Takahashi, T. Furubayashi, K. Hono, IEEE Trans. Magn. 48 (2012) 1751.
[8] T. Kanomata, M. Kikuchi, H. Yamauchi, J. Alloys Compd. 414 (2006) 1.
[9] S. Mizusaki, A. Doumoto, T. Ohnishi, Y. Nagata, T.C. Ozawa, H. Sawata, Y. Noro, J. Phys. Conf. Ser. 200 (2010), 052017.
[10] S.N. Mishra, B. Rambabu, A.K. Grover, P.N. Tandon, J. Magn. Magn. Mater. 51 (1985) 350.
[11] A. Szytuła, H. Przewoźnik-Bak, J. Leciejewicz, J. Magn. Magn. Mater. 80 (1989) 195.
[12] B. Deka, R. Das, A. Srinivasan, J. Magn. Magn. Mater. 347 (2013) 101.
[13] F.J. Webster, K.R.A. Ziebeck, J. Phys. Chem. Solids 34 (1973) 1647.
[14] R.A. de Groot, F.M. Mueller, P.G. van Engen, K.H.J. Buschow, Phys. Rev. Lett. 50 (1983) 2024.
[15] P.J. Webster, Contemp. Phys. 10 (1969) 559.
[16] V.S. Patil, et al., Phys. Stat. Sol. (b) 118 (1983) 57.
[17] M. Yin, P. Nash, J. Alloys Compd. 634 (2015) 70.
[18] H. Ebert, D. Ködderitzsch, J. Minar, Rep. Prog. Phys. 74 (2011), 096501.
[19] J.P. Perdew, K. Burke, M. Ernzerhof, Phys. Rev. Lett. 77 (1996) 3865.
[20] A. Kundu, S. Ghosh, S. Ghosh, Phys. Rev. B 174107 (2017).
[21] A. Liechtenstein, M. Katsnelson, V. Antropov, V. Gubanov, J. Magn. Magn. Mater. 67 (1987) 65.
[22] B. Balke, S. Wurmehl, G.H. Fecher, C. Felser, C. Maria, M. Alves, F. Bernardi, J. Morais, Appl. Phys. Lett. 90 (2007), 172501.
[23] S. Khmelevskyi, E. Simon, L. Szunyogh, Phys. Rev. B 91 (2015), 094432.
[24] A. Hamri, Z. Driss, B. Hamri, A. Hallouche, Int. J. Modern Phys. B 29 (2015) 1550057.
[25] B. Ma, Q. Xie, J. Huang, Intermetallics 46 (2014) 12e17.
[26] E.P. Wohlfarth, J. Magn. Magn. Mater. 7 (1978) 113.
[27] M.J. Otto, R.A.M. van Woerden, P.J. van der Valk, J. Wijngaarrll, C.F. van Bruggeni, C. Haas, K.H.J. Buschow, J. Phys.: Condens. Matter 1 (1989) 2341.
[28] N.P. Duong, L.T. Hung, T.D. Hien, N.P. Thuy, N.T. Trung, E. Brück, J. Magn. Magn. Mater. 311 (2007) 605.

Principal
Nowgong Girls' College
Nagaon :: Assam

Nowgong Girls' College
ESTD: 1962
Nagaon :: Assam

Volume 29
2020-21

ISSN : 0975-5659
UGC CARE List Group I
Sr. No. 67 (Arts and Humanities)

DIBRUGARH UNIVERSITY JOURNAL OF ENGLISH STUDIES

A Peer-Reviewed Journal

DUJES

Editors

Lakhipriya Gogoi

Deeptangshu Das

Department of English, Dibrugarh University
Dibrugarh, Assam

Nowgong Girls' College ESTD: 1962 Nagaon :: Assam

Principal
Nowgong Girls' College
Nagaon :: Assam

Volume 29
2020-21

ISSN : 0975-5659 [Print]
: 2581-7833 [Online]
www.dujes.co.in

DIBRUGARH UNIVERSITY JOURNAL OF ENGLISH STUDIES

(A UGC-CARE Listed Peer-Reviewed Journal)

Editors

Lakhipriya Gogoi **Deeptangshu Das**

Department of English
Dibrugarh University
Dibrugarh, Assam

Principal
Nowgong Girls' College
Nagaon :: Assam

Nowgong Girls' College
ESTD: 1962
Nagaon :: Assam

Dibrugarh University Journal of English Studies
Volume 29, 2020-21

ADVISORY BOARD

Ashok K. Mohapatra
Professor of English, Department of English, Sambalpur University, Jyoti Vihar, Sambalpur, Odisha - 768019. e-mail : mohaashok@gmail.com

B. K. Danta
Professor of English, Department of English and Foreign Languages, Department of English & Foreign Languages, Tezpur University, Tezpur, Assam - 784028. e-mail : bkdanta@tezu.ernet.in/bkdanta@gmail.com

Nandana Dutta
Professor of English, Department of English, Gauhati University, Guwahati, Assam-781014. e-mail : nandana@gauhati.ac.in

Sukalpa Bhattacharjee
Professor of English, Department of English, North-Eastern Hill University, Shillong-793022. e-mail : bsukalpa@hotmail.com

N. Rama Devi Murru
Professor of English, Department of Indian and World Literatures, English and Foreign Languages University, Hyderabad - 500007. e-mail : nramadevieflu@gmail.com

Ananda Bormudoi
Associate Professor of English, Department English, Dibrugarh University, Dibrugarh, Assam, PIN- 786004. e-mail : ananda.bormudoi@gmail.com

EDITORIAL BOARD

Mridul Bordoloi
Anurag Bhattacharyya
Dipak Kumar Doley
Basil N. Darlong Diengdoh
Nasmeem F. Akhtar
Meena Sharma
Khandakar Shahin Ahmed

EDITORS

Lakhipriya Gogoi
Assistant Professor, Dept. of English, Dibrugarh University, Dibrugarh-04.
e-mail : lakhipriya_gogoi@dibru.ac.in

Deeptangshu Das
Assistant Professor, Dept. of English, Dibrugarh University, Dibrugarh-04.
e-mail : deeptangshudas@dibru.ac.in

Price of one copy : ₹ 200.00 (for Individuals)
₹ 300.00 (for Institutions)
US $ 10 (Overseas)

Website : www.dujes.co.in
Published in : June, 2021
Published by : The Registrar, Dibrugarh University, Dibrugarh
Printed at : INSUI INFOTECH, Dibrugarh

Principal
Nowgong Girls' College
Nagaon :: Assam

Nowgong Girls' College
ESTD: 1962
Nagaon :: Assam

CONTENTS

	Pages
Of Growth and Development: Appropriating the Pedagogical Significance of Science Fiction- A Case Study of H.G. Wells's *The Time Machine* and Michael Crichton's *Jurassic Park* **Goutam Karmakar**	1-11
Subaltern Lives and Utopian Potentialities in Hansda Sowvendra Shekhar's *Jwala Kumar and the Gift of Fire: Adventures in Champakbagh* **Abin Chakraborty**	12-21
Migration and the Struggle with Choices in an Increasingly Unstable World : A Reading of Mohsin Hamid's *Exit West* and Amitav Ghosh's *Gun Island* **Rimi Nath**	22-30
Writing Kashmir, Writing the End of Empire : A Study of Two Post-War British Novels **Somjyoti Mridha**	31-40
The Depiction of Dalit Women in Indian Women's Poetry in English **Shruti Sareen**	41-54
What Makes You A "Bride": A Comparative Study of Assamese Folk Balladic Bride Jona Gabharu and Chaucerian Bride in *The Wife of Bath's Tale* **Gutimali Goswami**	55-63
A Postmodern Feminist Interpretation of *Half of a Yellow Sun* and *Front Lines* **Punyashree Panda, Trina Bose**	64-74
Transformed Role of Jewish American Women in Judaism: Reading Rebecca Goldstein's *Mazel* **Bhaskar Lama**	75-86
Being to Becoming: The Discourse of Self in Doris Lessing's *The Golden Notebook* and *Love, Again* **Sanghamitra Sadhu**	

Principal
Nowgong Girls' College
Nagaon :: Assam

Nowgong Girls' College ESTD: 1962 Nagaon :: Assam

Afghanistan in Post-9/11 American Poetry: A Creative Response to *Orientalism*
Joydeep Chakraborty 100-115

Stranger Gods, Untouchable Offspring: The Politics of Space and Hegemonic Masculinity in Perumal Murugan's *One Part Woman*
Damini Kashyap 116-124

Aesthetics of the Grotesque Body : The Dismemberment Metaphor in the Assamese Folktale "Tejimola"
Jharna Choudhury 125-134

Subversion of Post-Truth Discourse and Data Politics in Indian Agrarian Crisis : Kota Neelima's *Shoes of the Dead*
Miruna George, Jaya Selvi D 135-144

Theorizing the Ontology of 'Home' in Diaspora Imagination
Bhagabat Nayak 145-155

Masquerading Gelotophobia through Self-Evasive Laughter : Exploring the Link Between the Ridiculous Bangal in Select Popular Bengali Cinema of the 60s and His Ghoti Bhadralok and Bangal Refugee Viewer in The Entrenous(?) of the Movie Hall
Ashes Gupta 156-170

"Walking with the Gods": Writing Body and Land in India's Northeast
Rakhee Kalita Moral 171-187

The Postfeminist World-View and Superheroines : Critiquing Female Representations within the Superhero Genre
Anindya Syam Choudhury, Kinshuk Chakraborty 188-204

Muslin in their Mouths : Identifying Conflict in Sophie Mackintosh's *The Water Cure*
Chaandreyi Mukherjee 205-213

Altered States: A Reading of Cesar Aira's *An Episode in the Life of a Landscape Painter*
Mubashir Karim 214-223

Gender and Disguise: Representation of *Bacha Posh* in Nadia Hashmi's *One Half from the East* and *The Pearl that Broke its Shell*
Mridula Kashyap 224-236

Principal
Nowgong Girls' College
Nagaon :: Assam

Nowgong Girls' College ★ ESTD: 1962 ★ Nagaon :: Assam

The Order of Extra-Terrestrials– Researching the Dynamics of Alien Forms in Science Fiction
Ruchita Machal 237-249

Cry Witch : Representation of German Witch-Lore and Persecution of Dispossessed Women in Oliver Potzsch's *The Hangman's Daughter* and Erika Mailman's *The Witch's Trinity*
Isha Biswas 250-261

"Shifting Landscapes of Childhood": Situating the Identity of Ila in Terms of Place and Space in Amitav Ghosh's *The Shadow Lines*
Pratik Chowdhury 262-274

"The Picture of Oryx Looking": The Returned Gaze as Feminist Resistance against the Male Gaze in Margaret Atwood's *Oryx and Crake*
Cr Patricia Mary Hodge 275-287

The Unclean Female Body and the Discourse of Sanitation in three Cinematic Texts
Sugandha Sehgal 288-299

The City of Colombo in Carl Muller's *Colombo* and Shyam Selvadurai's *The Hungry Ghosts*
Esther Daimari 300-312

To be or Not to be? The Dichotomy of being Oneself in Jhumpa Lahiri's *The Namesake*
Priyanka Sharma 313-325

The Image of Mahatma Gandhi in Advertisement : Subverting its Conventional Semiotics
Saba Anish, Dwijen Sharma 326-342

Revisiting Gender Narratives : A Critical Study of Nee Devi's Short Stories
Gurumayum Deepika 343-354

Revisiting Bhadralok: "Dangoriya" as the Term for Assamese Masculinity
Parikshit Sarmah 355-364

The Gaze of the 'Other': A Study of Frederick Douglass's *Narrative of the Life of Frederick Douglass: An American Slave* (1845)
Pronami Bhattacharya [illegible]

Principal
Nowgong Girls' College
Nagaon :: Assam

Nowgong Girls' College
ESTD: 1962
Nagaon :: Assam

The Cyborg Lives of the Frankenstein Myth : A Study of Re/presentation and Consumption of *Frankenstein* in Select 21st Century Pop Culture Adaptations
Sango Bidani, Zahra Rizvi 380-390

The Neomonsters Thesis: Dystopias, Ideologies and Monsters in *Ghoul* and *Betaal*
Sami Ahmad Khan 391-404

Hunger, Representation, and the Gorkhaland Movement
Samiran George Ghissing 405-416

The Pastoral Power Dialectic : A Foucauldian Reading of *The Slayer Slain*
Mini M Abraham 417-426

Fandry : A Cinematic Journey from Rejection to Resistance
Jaishree Kapur 427-438

Locating Hotel as a Postmodern Trope of Homelessness and A Microcosm of Segregationist Society of London in Monica Ali's *In the Kitchen*
Shafayat Hussain Bhat, Amandeep Singh 439-447

The Flora and Fauna in Karnad : A Study of *Nāga-Mandala* and *The Fire and The Rain*
Devamitra Chakraborty 448-460

"*A-Death-Within-The-Self*— The Phenomenal Expulsion of Expectation": Reading Narratives of Miscarriage
Bonjyotshna Saikia 461-472

Bi Now, Gay Later or *Gay Now, Bi Later* : A Close Reading of *Cinnamon Gardens*
Monoj K. Hazarika 473-481

Rereading 'Mahatma' in Indian History through a Reading of *Bhimayana : Experiences of Untouchability*
Mushrifa Ibrahim 482-490

The Colonial/ Postcolonial Gaze : A Feminist Analysis of Malek Alloula's *The Colonial Harem*
Nazrana Haque 491-501

Principal
Nowgong Girls' College
Nagaon :: Assam

Nowgong Girls' College ESTD: 1962 Nagaon :: Assam

Representation and Nuances : Interrogating Representation of the Tribal in Mamang Dai's *The Legends of Pensam* and Gopinath Mohanty's *Paraja*
Lakshminath Rabha 505-517

Striking a Balance between the Male and the Female Principles : A Reading of Achebe's *Things Fall Apart* and *Anthills of the Savannah*
Lakshminath Kagyung 518-527

BOOK REVIEW :

Tazmeen Amna's "*Goner*" – An Onerous Achievement
Anubhav Pradhan 528-530

Rakhshanda Jalil's "*Preeto and Other Stories*"
Harshit Nigam 531-533

Principal
Nowgong Girls' College
Nagaon :: Assam

Nowgong Girls' College ESTD: 1962 Nagaon :: Assam

pp. 224-236

GENDER AND DISGUISE: REPRESENTATION OF *BACHA POSH* IN NADIA HASHMI'S *ONE HALF FROM THE EAST* AND *THE PEARL THAT BROKE ITS SHELL*

Mridula Kashyap

Abstract

The notion of *bacha posh* refers to the cross-dressing of a girl as a boy which is deployed as a way of disguising gender roles. It is a cultural practice that was widespread in Afghanistan and parts of Pakistan whereby girls were raised as boys during their childhood till they attain the age of puberty so that they could have access to educational opportunity, mobility, economic and public spaces from which they were being deprived because of their gender. But can such cross-dressing truly allow girls to receive the benefits of patriarchy– the freedom that is limited only for the dominant gender? Is the disguise of gender role a means of empowerment for girls or a form of oppression? Is freedom only a kind of illusion? Keeping these questions in mind, the paper will examine the practice of *bacha posh* as depicted in Nadia Hashmi's novels. One can argue that while *bacha posh* is practised with a purpose of liberating the girls from the codes of restriction and subjugation attached to the female body, it further complicates the subject position of the person who disguises into *bacha posh*. *Bacha posh* is never a liberating force, rather it reflects the sordid position of the female body in a socio-cultural space. This is due to the gender dysphoria experienced by the *bacha posh* as a result of the incongruity between biological sex and the masculine gender role that the girls have to perform.

Keywords : Bacha posh, Gender dysphoria, subjectivity, body, masculinity

Masculinity is not a fixed entity embedded in the body or personality traits of individuals. Masculinities are configurations of practice that are accomplished in social action and, therefore, can differ according to the gender relations in a particular social setting.

(Connell and Messerschmidt 836)

The idea of *bacha posh* is one of the constructions of masculinity and the product of rigid patriarchy where there is a complex interplay between the [illegible] and the social system that eventually leads to perplexing ideas of [illegible] and gender identity. Women's body and space in Afghanistan have been caught up in

Nowgong Girls' College ESTD: 1962 Nagaon :: Assam

Principal
Nowgong Girls' College
Nagaon :: Assam

the mire of the turbulent history of state-society relations, the economic situation and the discontent between religious and political status quo that has led to unequal gender relations and dominant modes of 'hegemonic masculinity'[4]. These states of affairs have had their impact over women's mobility, dress code and sexuality. The oppressive state apparatus allows men to police women's mobility thereby constraining their space in the Afghan society. The Mujahideen regime (1992-1996) and the Taliban regime (1996-2001) have established hegemonic masculinity that legitimizes the subordination of women, specifically the latter institutionalizes gender inequality and policing of women's mobility to the extent that they could not enter the public space without being accompanied by a *mahram* (male relative). Restriction of women to enter the public space also limits their economic opportunities and their ability to access public services. Masculine dominance becomes normative in every institution. In the family, the birth of a boy child becomes the most essential and women are held responsible for giving birth to boys. Associated with the importance of the birth of a boy child or the presence of a male member in the family is the question of economic productivity as girls/women are debarred from that space. Jenny Nordberb in her seminal work on *bacha posh* entitled *The Underground Girls of Kabul: The Hidden Lives of Afghan Girls Disguised as Boys* (2014) claims that every Afghan family must have at least one son, without which the family would be considered incomplete, weak and vulnerable. So, every Afghan married woman is obliged to bear a son and it becomes her sole purpose in life, failing to do so she is stigmatized as *dokhtar zai* or "she who only brings daughters" and her husband, in turn, is defamed as *mada post* or "he whose woman will only deliver girls." Thus, in a society where hegemonic masculinity prevails, it is the woman who always becomes accountable for the failure to bear the boy child. Against this backdrop of masculine dominance and absence of space for the woman that the custom of *bacha posh* develops. The notion of *bacha posh* refers to the cross-dressing of the girl as a boy which is deployed as a way of disguising gender roles. It is a cultural practice that was widespread in Afghanistan and parts of Pakistan whereby girls were raised as boys during their childhood till they attain the age of puberty so that they could have access to educational opportunity, mobility, economic and public spaces from which they were being deprived because of their gender. But can such cross-dressing truly allow girls to receive the benefits of patriarchy— the freedom that is limited only for the dominant gender? Is the disguise of gender role a means of empowerment for girls or a form of oppression? Is freedom only a kind of illusion? Keeping these questions in mind, the paper will examine the practice of *bacha posh* as depicted in Nadia Hashmi's novels. One can argue that while *bacha posh* is practised with a purpose of liberating the girls from the codes of restriction and subjugation attached to the female body, it further complicates the subject position of the person who disguises into *bacha posh*. *Bacha posh* is never a liberating force, rather it reflects the sordid position of the female body in a socio-cultural space. This is due to the gender dysphoria experienced by the *bacha posh* as a result of the [illegible] between biological sex and the masculine gender role that the [illegible] have to

Principal
Nowgong Girls' College
Nagaon :: Assam

Nowgong Girls' College ESTD: 1962 Nagaon :: Assam

perform.

These issues and complexities associated with the custom of *bacha posh*, set against the backdrop of a perplexing Afghan history, are intricately interwoven by Nadia Hashmi in her novels *One Half from the East* (2016) and *The Pearl that Broke its Shell* (2014). In both the novels, Hashmi exposes the vulnerability of woman as a result of the rigid patriarchal structure that has constrained their lives altogether. Obayda in *One Half of the East* is made into a boy with the belief that she would bring good luck to the family and also render economic support because of her father's wretched condition when he loses one of his legs in a bomb explosion. After the catastrophe, the family shifts from the city of Kabul to a small village where Obayda is compelled by her mother and her aunt to cross-dress as a boy and take up the new identity of Obayd. This new identity at the age of ten leaves her in a baffled state as she was always comfortable being a girl. She realizes that she could not fit into the straitjacket of any of the gender roles and suffers from a kind of gender dysphoria. Hence, the novel centers on Obayda's labyrinthine quest for identity as the *bacha posh* identity that is thrust upon her does in no way liberate her, further it aggravates her dilemma and leads her to an abyssal position. In *The Pearl that Broke its Shell*, Hashmi intertwines the intergenerational tales of two Afghan women who had to change their gender roles under different circumstances. Like Obayda, Rahima is made into a boy so that she could access the benefits of patriarchy and support the family as she has no brothers and left with a father who self-medicates with opium. Rahima adores her *bacha posh* life as it provides her with the opportunity to relish the fruits of patriarchy which are otherwise denied to girls because of their gender. However, the freedom that Rahima enjoys is cut short when her opium-addict father arranges her marriage with an elderly and powerful warlord in exchange for a huge bride-price and the supply of opium. At once Rahima's life metamorphoses from a carefree *bacha posh* to the fourth wife of Abdul Khaliq, the warlord. Hashmi juxtaposes the story of Rahima with her great-great-grandmother Shekiba, born a century ago, who had to perform the role of a boy and work in the farm after the cholera epidemic killed her mother and the other siblings. As Shekiba was Herculean build, she was also assigned the job of a guard in King Habibullah's harem, dressed as a man. *The Pearl that Broke its Shell* projects how Rahima and Shekiba break up from their claustrophobic gender identities to adopt a variation that would provide them liberation, only to realize that such liberation is simply an illusion and therefore, the quest for their identities continue.

Though the body of literature produced in this area is limited, yet there are a few fiction writers apart from Hashmi, who has dealt with the practice of *bacha posh* in their works. Canadian writer and activist Deborah Ellis' acclaimed novel, *The Breadwinner* (2001), is about an eleven-year-old girl Parvana who has to become a *bacha posh* in the land of Kabul where "bombs had been [illegible] of Parvana's whole life" (11). When the Taliban militia has confiscated [illegible] asserted their hegemony, Parvana's father is arrested, her educa[illegible] stopped

Nowgong Girls' College ESTD: 1962 Nagaon :: Assam
C.T.C.
Principal
Nowgong Girls' College
Nagaon :: Assam

and in the absence of any male member, there is none to run the family. Under such circumstances Parvana is cross-dressed as a boy so that she could become the breadwinner of the family, "As a boy, you'll be able to move in and out of the market, buy what we need and no one will stop you..." (27). The novel, thus, captures Parvana's struggle not only to search her father but also to sustain her family. Ukmina Manoori's memoir *I am a Bacha Posh: My Life as a Woman Living as a Man in Afghanistan* (2014) narrates her story of undaunted determination in her decision to remain a *bacha posh* throughout her life, resisting family and social pressures of resuming to womanhood after puberty. Once a *bacha posh* is on the brink of womanhood, she is expected to discard her man's clothing and take recourse to veil and think about her marriage. Ukmina writes:

> At this age, the other girls veiled themselves. Those who had, like me, lived their childhood as a boy, gave up their shalwar kameez and the freedom that it conferred, little by little. They abandoned their fields and their games to integrate into the framework of their whole life from this point forward: the walls of their home. They learned how to sew, take care of the children, help their mothers. It took a few months before they embraced their destiny as women: at twelve years old, they wore burqas and did not leave the house anymore without the presence of a man. (15)

However, Ukmina decides to deviate from such social norms and destine her life for the cause of her country by waging war against the Soviets, entering into politics and working diligently for the upliftment of the rights of the Afghan woman. Alike Ukmina, Maria Toorpakai is another valiant figure whose *A Different Kind of Daughter: The Girl Who Hid from the Taliban in Plain Sight* (2016) is a sports memoir where she narrates her harrowing journey as a *bacha posh* to become an athlete hailing from an oppressive region of Pakistan called Waziristan, dominated by the Talibans. Toorpakai's father always considers her to be a "different kind of daughter" (7) as he could perceive that she is a born athlete. She loathed dolls and wearing fancy dresses, instead preferred boy's clothing and playing outside in the dirt which "in my part of the world, for a girl to venture out uncovered was *haram*— forbidden, a sin against God" (7). In her part of the country women playing squash or any other sports is considered *haram*. But squash is not simply a sport for her, but a matter of life and death: ""It's not about playing anymore, Maria. It's about staying alive"" her father tells her (164). It is only through adopting the role of a *bacha posh* or in other words, masquerading as a boy, that Maria Toorpakai was able to escape the death threats of the Talibans and flee to Canada to pursue her dream.

The word *bacha posh* etymologically means 'dressed as a boy' which is Dari origin. The transformation of the gender identity of girls is decided by the parents at a very tender age, often at birth. As decided by the parents, the girls have to perform the assigned gender role till the time of puberty which is considered to be their marriageable age. Although the community members are aware that the *bacha posh* children are born as girls, but they treat them according to the roles

Principal
Nowgong Girls' College
Nagaon :: Assam

Nowgong Girls' College
ESTD: 1962
Nagaon :: Assam

performance. As Nordberg writes : "These girls are hidden, and that is exactly the point. To everyone on the outside, they are just *bachas*" (48). But as they grow older and reach the age of puberty, their role-playing becomes difficult to sustain, although some *bacha posh* refuse to revert to their biological gender identity. The practise of *bacha posh* developed against the backdrop of a hegemonic masculine society where "men have all the privileges" (61). Among the various reasons discussed by Nordberg in her book *The Underground Girls of Kabul* for the practice of disguising girls as boys in Afghanistan are the predominantly patrilineal structure where sons are more valued than daughters, the social stigma a family has to experience for having no son and the pressure perpetuated upon families to bear at least one son. Because of such social stigma and pressure girls are masqueraded as boys soon after their birth, and the hoax sons are considered to be better than having no sons. There is also a superstitious belief that the *bacha posh* in the family would bring good luck to the future birth of boys in the family. As it is believed that "through visual manifestation, when a woman looks at the image of a male child every day, her body will eventually conceive a son" (69). Thus, till the birth of the actual son, the *bacha posh* serves the family intention. However, the intention varies as seen in the case of upper or middle-class families where girls are cross-dressed as boys to keep intact the family honour and prestige. Although the girls do not choose their enforced boyhood willingly but in many cases "they enjoy their borrowed status" (67). The *bacha posh* belonging to upper or middle-class families enjoy the privileges of going to school and playing outdoor games with boys, which otherwise, they have been deprived of because of their gender. But those belonging to underprivileged families need to engage in forced child labour for economic sustenance of the family. Nordberg observes:

> Among street children in the merchant business, selling chewing gum, polishing shoes, or offering to wash car windows on the streets, some are actual boys, and others are girls in disguise. They are all part of Kabul's underbelly and, to those who pass them by, mostly just invisible. (67)

Nordberg further observes that irrespective of the families being rich, poor, educated, uneducated, Pashtuns, Tajiks, Hazara or Turkoman, what is indistinguishable amongst them is their need for a son. The made-up son supports the family as a breadwinner, plays the role of a *mahram* by accompanying the female members of the family to public spaces where women's mobility is restricted, the one who can have access to education and finally facilitates the family to be complete as the lack of son makes the family incomplete. It is the clothing and the haircut that differentiates a boy from a girl and permits the *bacha posh* to have access to all the privileges and spaces that are otherwise restricted only to the male members in a hegemonic masculine Afghan society. In this context clothing and haircut act as a means of camouflage to conceal the female body while evoking the masculine persona.

Though a *bacha posh* feels empowered as a result of her entrée into the masculine domain, this phase is transitory. The dilemma of these girls when they

Principal
Nowgong Girls' College
Nagaon :: Assam

Nowgong Girls' College
ESTD: 1962
Nagaon :: Assam

have to revert to their feminine selves is analysed by Corboz, Gibbs and Jewkes in their essay "Bacha posh in Afghanistan: factors associated with raising a girl as a boy" (2019):

> When girls raised as boys reach puberty, they are usually 'converted' back into girls. This often poses a dilemma for those girls who had more freedom and mobility during childhood, only to have this freedom restricted when being required to re-adopt a feminine identity and sometimes being prepared for marriage a short time after becoming a girl again. Conversion back to being a girl may be particularly difficult for those *bacha posh* who identify as male and want to continue living as a boy. (3)

The reversion to womanhood involves a constant struggle as years of performance makes it difficult to reappropriate the body into the feminine persona. After switching to the feminine persona, she has to unlearn the things that she has mastered as a boy and adopt the feminine body language. The overt appearance becomes easy to convert but the psychological impact left by years of performance is difficult to wipe out. Shukria, a former *bacha posh* narrates her experience in Nordberg's *The Underground Girls of Kabul:* "With time, nurture can become nature...Becoming a man is simple. The outside is easy to change. Going back is hard. There is a feeling inside that will never change" (178). It is then that a *bacha posh* suffers from gender dysphoria. Gender dysphoria results from the experience of gender incongruence that causes uneasiness in the *bacha posh* after she switches to her biological identity. Mark A. Yarhouse in his book *Understanding Gender Dysphoria: Navigating Transgender Issues in a Changing Culture* (2015) defines gender dysphoria as thus:

> Gender dysphoria refers to the experience of having a psychological and emotional identity as either male or female, and that your psychological and emotional identity does not correspond to your biological sex—this perceived incongruity can be the source of deep and ongoing discomfort. Specifically, gender dysphoria is on the one hand the experience of being born male (biological sex) but feeling a psychological and emotional identity as female. Similarly, gender dysphoria is the experience of being born female (biological sex) but feeling a psychological or emotional identity as male. (19)

However, Mark A. Yarhouse's concept of gender dysphoria is different from the kind of dysphoria experienced by a *bacha posh*. Yarhouse examines gender dysphoria as a transgendered concept. But the gender dysphoria that a *bacha posh* suffers from is not a genetic disorder as *bacha posh* is an imposed identity upon the girl to perform the role of maleness: "Her identity develops from a mere biological female to becoming a culturally defined boy through social interaction, within the family and outside" (Sawitri 16). The *bacha posh* is reared in an altogether different cultural setting where rather than the fostering of feminine qualities such as compliance and submissiveness, excessively aggressive masculine attitudes are encouraged. The momentary liberty they experience as a result of the isolation from their birth gender creates gender identity conflict in them.

Principal
Nowgong Girls' College
Nagaon :: Assam
Nowgong Girls' College ESTD: 1962 Nagaon :: Assam

Bacha posh is not a novel tradition but can be traced back to twentieth-century Afghanistan. King Habibullah Khan who reigned Afghanistan from 1901 to 1919 devised the concept of appointing women sentinels, dressed in men's apparel to guard the king's harem. He designated his youngest daughter to stand as the guard of the harem garbed in man's uniform. Assigning male sentinels to watchdog the harem could be hazardous to women's chastity and the royal bloodline. Before appointing women guards, eunuchs stood as sentries to guard the king's mistresses. But, by his novel idea, women replaced the eunuchs to stand as sentries of the harem, thereby marking the initiation of the presence of cross-dressed women in the history of the royal stratum of Afghan society. However, the presence of such cross-dressed women is not confined to Afghanistan alone. Such women could be traced in different eras of the Western and Eastern history who mostly performed the role of warriors. Nordberg cites a number of such woman warriors who dressed as men:

> In the first century, Triaria of Rome joined her emperor husband in war, wearing men's armor. Zenobia was a third-century queen in Syria who grew up as a boy and went on to fight the Roman empire on horseback. Around the same time in China, Hua Mulan took her father's place in battle, wearing his clothes. Joan of Arc was famously said to have seen an archangel in 1424, causing her to adopt the look of a male soldier and help fight France's war against England. (198)

Nordberg further states that the Catholic Church not only approves woman cross-dressed as a man but honours them for their bravery and demonstration of masculine traits. Valerie Hotchkiss observes that in medieval Europe, the women who cross-dressed as men preferred to remain celibate throughout their lives. One also finds references in the twelfth-century religious texts such as - *Scivias* by Hildegard von Bingen and *Summa Theologica* by Thomas Aquinas- about engaging such women during wars and other emergency situations. Dutch historians Lotte C. van de Pol and Rudolf M. Dekker in their research on the experiences of these women discovered that between the sixteenth to nineteenth centuries in Europe, there lived more than a hundred women who either took the profession of sailors or soldiers disguised in men's clothing. Their gender identities were revealed only after their death when their bodies were carried off the battleground. These women adopted male identity for reasons similar to that of *bacha posh* in Afghanistan. Some undertook male identity to support themselves and their families, some masqueraded as men to travel or evade forced marriages, while others went for higher education as it was forbidden for women. Unfortunately, they had to face trial when their disguise was unmasked, though the punishment became lenient for those women who took part in wars for the cause of their lands. However, by the nineteenth century, the phenomenon of women cross-dressing as men gradually declined. Perhaps, it might be due to the rise of an organized society based on a civil registration system where certain measures like border controls and medical inspections were made obligatory for soldiers as a result of which it became difficult for women to disguise as men. Similar to the *bacha posh* practise in Afghanistan,

Nowgong Girls' College ESTD: 1962 Nagaon :: Assam
Principal
Nowgong Girls' College
Nagaon :: Assam

in Northern Albania and Montenegro an age-old practice known as 'sworn-virgins' as a consequence of a highly patriarchal and patrilineal tribal society "where children are thought to stem directly from the blood of the father, and the woman is considered merely a carrier" (199). Thus, the *bacha posh* is not an exclusively Afghan practice but exists in other parts of the world throughout the history of women.

This age-old cultural practice is the core issue upon which Nadia Hashmi has set her novels. In *One Half from the East*, Obayda becomes a victim of this cultural practice at the age of ten when her father has been maimed for life by the bomb blast and the family has to shift from Kabul to settle in the village. Her aunt concocts the idea of transforming Obayda into a boy assuring her mother that such a practice would herald good luck to the family.

> Make Obayda into a boy. With her as a son, she will bring good luck to your home. You'll see your husband cheer up. Then you plan for another baby in the family. Having a bacha posh at home brings boy energy into your household. The next baby that comes will be a boy. And once you have a real son, watch what happens. Your husband will come back to life. I've seen this work in the families around us. It's not magic—it's just how it is. And that's when Obayda can go back to being a girl. (14)

The new identity imposed upon Obayda makes her world topsy-turvy. She always liked being a girl, doing "girl things" (2016:14) and had a great fascination for dancing. The *bacha posh* identity becomes problematic for Obayda as she has to unlearn the things that she has learned as a girl for ten years and adopt the new language and behaviour of boys. She is debarred from household chores and is expected to play outdoor games with boys and go out to the market. A sense of insecurity and the fear of being exposed looms large in her mind. Her sense of insecurity becomes more acute when she goes to school and finds herself amid boys in the school playground: "I watch the boys drift one way and the girls another. I am now in the weird place between both worlds" (2016: 24). Her *bacha posh* identity leads her to an awkward situation where she is neither able to assimilate with boys nor with girls. Through Obayda's complex state of mind, Hashmi projects that the dubious identity of a *bacha posh* results from the fact that she has to enact masculinity with a female body. Obayda struggles hard to perform the role of Obayd but "still haven't fully got used to it" (2016: 25). She finds that the masculine gender behaviour is indeed different from that of the female and strives to tackle the sex-gender dichotomy. However, Obayda's struggle to appropriate herself to the masculine gender role becomes less complicated when she meets another *bacha posh* in her school. Rahim/Rahima tells Obayda that to perform the role of *bacha posh* efficiently, she must stop thinking herself as a female garbed in male clothing, but consider herself a boy: "You're a boy, not a *bacha posh*, Obayd. If you get that, there is nothing else" (2016: 36). Rahima has competently adopted the masculine body language and loves her *bacha posh* identity as it provides her with the freedom that she has been deprived of as a female. Though 'Rahim' is an imposed identity, she does

Principal
Nowgong Girls' College
Nagaon :: Assam

Nowgong Girls' College
ESTD: 1962
Nagaon :: Assam

been able to naturalise her body to the masculine gender role because she has learned that "Being a boy is not all in your pants. It's in your head" (36). The body must adjust to the mind.

Renouncing the feminine gender indeed provides Rahima and Obayda with the benefits of male privilege but they know very well that such freedom is illusory. They can enact masculinity but can never be a man since the *bacha posh* is socially perceived as a subordinated masculinity. The subordinated masculinity can in no way be a liberating force, rather it complicates the subject position of the body. They are both "one half from the east and one half from the west" (2016: 36) as Obayda's mother describes them. They want to get rid of their dubious identity as it prevents them from being neither fully male nor fully female. The interplay between the body and the social process results in complex gender role leaving them in an in-between position. Rahima confesses: "That's the problem with being half things...it's hard if you think you're missing something. I don't want to be a half thing. I just want to be one whole normal me." (2016: 55). Obayda agrees with her. With time Obayda becomes complacent in her role as a *bacha posh* and is unwilling to retrogress to her birth sex. She desires to take up the masculine identity in perpetuity, thereby dispelling the 'half thing' to become 'one whole normal' being. But she is aware that like the *bacha posh* identity thrust upon her, the parents would again transform her into a girl. Her sense of insecurity rises when she comes to know about her mother's pregnancy. If it's a girl, she would also be a victim of the tradition of *bacha posh*, but if it's a boy her role as *bacha posh* would come to an end: "If it is a boy, I'm finished. My parents will have the son they need and my work as a *bacha posh* will be complete" (2016: 60). To get rid of her contradictory position, and live as unitary subject Obayda becomes possessed by the rainbow myth and heads towards the mountain range in search of the rainbow with the belief that walking under the rainbow would metamorphose her into a boy forever. Nordberg discusses in her book how the rainbow myth of gender-changing is widespread in Afghanistan:

> The rainbow, a favourite element in every mythology from the Norse to the Navajo people, often symbolizes wish fulfilment. In Afghanistan, finding a rainbow promises a very special reward: It holds magical powers to turn an unborn child into a boy when a pregnant woman walks under it. Afghan girls are also told that they can become boys by walking under a rainbow, and many little girls have tried. (Nordberg 229)

Obayda's disappearance in the quest for the rainbow causes much tension in the family and to her utter dismay, she finally learns from her mother that the rainbow is only a legend told to children. Dejected, she questions her mother: "Why would you want me to be a boy only for now? If being a boy now is good, isn't being a boy forever even better?" (Hashmi 2016: 91). Obayda was content with her identity as a girl before the *bacha posh* identity had been imposed upon her. With the imposition of *bacha posh* identity, she begins to grow with altogether different psychosocial expectation which in turn creates confusion

Principal
Nowgong Girls' College
Nagaon :: Assam

Nowgong Girls' College
ESTD: 1962
Nagaon :: Assam

about her own identity. This acute sense of discomfort results from the non-conformity between her female body and the masculine gender role that she has to enact which develops a kind of gender dysphoria in her. The experience of gender dysphoria resulting from the imposed identity triggers unease by isolating her not only from the family but also from the larger mainstream society. Thus, Hashmi demonstrates the nuances and complexities associated with the practice of *bacha posh* which proves problematic for girls to assimilate back into their culture as they become baffled about their identity.

Hashmi's critical stance on the practice of *bacha posh* is also reflected in her novel *The Pearl that Broke its Shell*. When the Taliban ruled over the streets of Afghanistan asserting domination through force and noxious practices, it became difficult for Rahima and her sisters to attend school and leave the house as they had no brother but an inept father who was a narcotist. Under such circumstances, Madar-*jan* (a term of endearment for mother) transforms Rahima into a *bacha posh* as she needs help with the errands and it has seemed unfeasible for her to depend on Padar-*jan* for anything. "*Bachem*, from now on we're going to call you Rahim instead of Rahima" Madar-*jan* tells her (2014: 35). Once the *bacha posh* identity has been thrust upon her, Rahima has to adjust her body to accommodate herself into the new gender role. To maintain the charade, she has to learn the new language and behaviour of boys like Obayda. Like most of the *bacha posh*, it becomes problematic for Rahima to enter into the new territory: "My instincts were to jerk back, to run away and never to look them (the boys) in the eye again" (2014: 67). Rahima has to readjust her body to a completely different psychosocial expectation and is indeed perplexed to observe the transformation in her mother's behaviour towards her. Her mother constantly orients her to acclimatize her body to the masculine gender behaviour and she is constantly apprehensive about the masquerade being exposed:

> "Listen, Rahim-*jan*. You should be out with the boys, playing. That's what *boys* do— do you understand what I'm saying?" ...
>
> ... "Yes Madar-*jan*, but sometimes I just don't want to. They... they push each other a lot."
>
> "Then push back."
>
> I was surprised by her advice but the look on her face told me she was serious. Here sat my mother telling me the exact opposite of what she'd always said. I would have to toughen up." (68)

Rahima's cross-gender identification as a result of the imposed identity altered her mother's response to facilitate her to adopt the cultural expectations of maleness. As already referred, Rahima is not the only member in the family to have adopted the practice of cross-dressing. Rahima hears from her aunt Khala Shaima the account of her great-great-grandmother who was a son to her father and worked in the farm like a boy and who also worked as a harem-guard in King Habibullah's palace, dressed in man's uniform. Resisting the tradition of reverting to the birth sex once a *bacha posh* attains the age of puberty, Rahima nevertheless continues to cross-dress as a boy till Padar-*jan* arranges her

Principal
Nowgong Girls' College
Nagaon :: Assam

Nowgong Girls' College ★ Nagaon :: Assam ★ ESTD: 1962

marriage with Abdul Khaliq, a dominant warlord. Padar-*jan* decides to marry off Rahima and her two sisters with Abdul Khaliq and his cousins in exchange for a large bride price and a supply of opium. Madar-*jan* resists but to no avail. Padar-*jan* is obstinate in his decision. Nordberg discusses how at this moment daughters are discernibly the cards played by Afghan fathers:

> Men make alliances, and not necessarily in the best interest of their daughters. These alliances are related to the social prestige and honour of the family. But it may also be opportunism. They want to marry up to create more security— financial or physical— for the family in a time of need. (Nordberg 152)

Through the predicament of Rahima, Hashmi projects that in a hegemonic masculine society woman are repressed at every stage. *Bacha posh* and marriage act as restrictive mechanisms that threaten the subjectivity of women. Firstly, she is transformed into a boy by the imposition of the *bacha posh* practise to absolve the family from stigma and undertake the family responsibility, next, she is regressed to a girl by the imposition of marriage for the financial security of her family. Deniz Kandiyoti describes the marriages of young girls to older men as "distress sales to food or cash" (Kandiyoti 180). Rahima and her sisters become victims of such forced marriages but in case of Rahima things become more problematic because of the frequent reversal of roles imposed upon her.

At the age of thirteen, Rahima becomes the fourth wife of the warlord Abdul Khaliq. Years of performing the masculine role have left certain permanent marks in her which prevents her from accommodating wholly into her new role as Abdul Khaliq's wife. Her marital life becomes highly dissatisfying. She loathes her husband as he dehumanizes her by inflicting violence upon her to assert his dominance:

> The thought of him made me queasy. I hated the feeling of it. I hated his breath, his whiskers, his callused feet. But there would be no escape. He called for me when he pleased and made me do what he wanted. (Hashmi, 2014, p.169)

Abdul Khaliq's oppressive nature restricts Rahima's autonomy and space in her new environment. Ever since Rahima was converted into a *bacha posh* she was debarred from household chores, and now reframing her life to feminine obligations has been difficult for her. Her mother-in-law asks Abdul Khaliq's first wife, Badriya to keep Rahima under constant surveillance so that she gets acquainted with her feminine duties and can perform appropriately the role of a wife:

> "Make sure she does a good job, Badriya. This girl has a lot to learn. She was a *bacha posh*, don't forget. Can you believe that? A *bacha posh* at this age! No wonder she has no clue how to carry herself as a woman. Look at the way she walks, her hair, her fingernails! Her mother should be ashamed of herself." (176)

Her mother-in-law not only condemns her for lacking femini[illegible]

Principal
Nowgong Girls' College
Nagaon :: Assam

Nowgong Girls' College ESTD: 1962 Nagaon :: Assam

but also accuses her mother of allowing her to continue with her *bacha posh* identity even after puberty. Rahima's only salvation in her miserable life is her son, Jahangir. Being able to bear a son Rahima's position in the family becomes somewhat better as Jahangir becomes one of Abdul Khaliq's favourites. But any reprieve for Rahima is momentary. When the new government comes to power and demands women to be members of the parliament, Abdul Khaliq promotes Badriya as one of the members to exert his influence over government affairs. As Rahima knows to read and write, she offers to help Badriya in Kabul. Though she seems uncertain to leave Jahangir behind but grabs the opportunity when Abdul Khaliq permits her to assist Badriya in Kabul. While she is in Kabul, Jahangir becomes ill and by the time she returns home, to her utter dismay he passes away. Rahima could not believe her destiny. Jahangir was her only solace in her wretched life. The demise of her son leaves her dejected and devastated. Rahima bemoans her lot:

> I was a little girl and then I wasn't.
> I was a *bacha posh* and then I wasn't.
> I was a daughter and then I wasn't.
> I was a mother and then I wasn't.
> Just as soon as I could adjust, things changed. I changed. This last change was the worst. (2014: 384)

Life provides Rahima with such diverse ephemeral roles that each time she attempts to accommodate herself to a particular role it alters and then she is assigned to another new role. The death of her son steals the very breath of her existence. When Rahima is still not able to overcome the grief at the loss of her son, Abdul Khaliq accuses her of their son's death: "A *bacha posh*. I should have known better. You still don't know what it is to be a woman" (2014: 408). At every blow, he curses her for being an irresponsible mother. He cuts off her hair and assaults her brutally, causing Rahima to miscarry her unborn child: "Fresh tears for a new loss. I may have killed one of Abdul Khaliq's children. But he has just killed another" (2014: 409). Nevertheless, Rahima does not abandon hope as her aunt Khala Shaima's words ring in her ears. She often used to say her that everyone needs an 'escape.' Inspired by Khala Shaima's words Rahima make plans to escape from her state of wretchedness. When she goes to Kabul with Badriya to assist her, she narrates her whole story to Hamida and Sufia, the women parliamentarians with whom she befriends and makes plans to escape by feigning sickness. Finally, she cuts off her hair, cross-dresses herself in men's attire to transform from Rahima to Rahim and escapes from her restrictive life.

Hashmi's novels project the complexities faced by the feminine body through participating in the social practice of *bacha posh*. The practice of *bacha posh* is the outcome of a dysfunctional society and a reflection of its vulnerability. Though by feigning masculinit,y girls can have access to freedom yet such a notion of agency proves to be evanescent. Hashmi demonstrates how her characters suffer from gender dysphoria because of the imposition of *bacha posh* identity upon them. Both Obayda and Rahima want to get rid of the subordinated

Principal
Nowgong Girls' College
Nagaon :: Assam

Nowgong Girls' College ESTD: 1962 Nagaon :: Assam

masculinity of *bacha posh* at it complicates their subject position and leads to complex gender relations. Their quest to initiate themselves into masculine gender roles and their despise against their birth gender grows from the subordinate position of women in the hegemonic masculine Afghan society. But they also come to terms with the fact that that by enacting masculinity through the practice of *bacha posh*, they can never truly liberate themselves from subjugation, rather it results in further subordination of their bodies.

Notes :

[1] The concept of 'hegemonic masculinity' which has influenced gender studies across diverse academic fields has been discussed by Connell and Messerschmidt in their essay "Hegemonic Masculinity: Rethinking the Concept"

Works Cited :

Connell, R. W. and James W. Messerschmidt. "Hegemonic Masculinity: Rethinking the Concept" *Gender and Society*, vol. 19, no. 6, Dec. 2005, pp. 829-859.

Corboz, Julienne, Andrew Gibbs and Rachel Jewkes. "Bacha posh in Afghanistan: factors associated with raising a girl as a boy." *Culture, Health & Sexuality*, 17 June 2019, https://doi.org/10.1080/13691058.2019.1616113Apply/45022.

Ellis, Deborah. *The Breadwinner*. House of Anansi Press, 2001.

Hashmi, Nadia. *The Pearl that Broke its Shell*. Harper Collins Publisher, 2014.

---. *One Half from the East*. Harper Collins Publisher, 2016.

Kandiyoti, Deniz. "Old Dilemmas or New Challenges? The Politics of Gender and Reconstruction in Afghanistan." *Development and Change*, vol. 38, no. 2, 2007, pp. 169–199.

Manoori, Ukmina and Stephanie Lebrun. *I am a Bacha Posh: My Life as a Woman Living as a Man in Afghanistan*. Translated by Peter Chianchiano, Skyhorse Publishing, 2014.

Nordberg, Jenny. *The Underground Girls of Kabul: The Hidden Lives of Afghan Girls Disguised as Boys*. Virago Press, 2014.

Sawitri, Made Yaya. "Cultural and International Dissonance on Girls Empowerment: the Case of Afghanistan's Female Son." *Aegis*, vol. 2, no. 1, Sep. 2017, pp. 11-25.

Toorpakai, Maria and Katharine Holstein. *A Different Kind of Daughter: The Girl Who Hid from the Taliban in Plain Sight*. Bluebird, 2016.

Yarhouse, Mark A. *Understanding Gender Dysphoria: Navigating Transgender Issues in a Changing Culture*. Inter Varsity Press, 2015.

Principal
Nowgong Girls' College
Nagaon :: Assam

Nowgong Girls' College
ESTD: 1962
Nagaon :: Assam

> She who could not eat with her hands;...never chewed a *paan* and had not tried most sweets in the *mithaishop*, for they made her retch;....felt happier with so-called English vegetables, snap peas, French beans, spring onions, and feared—*feared*—*loki, tinda, kathal, kaddu, patrel* and the local *saag* of the market. Eating together they had always felt embarrassed—he, unsettled by her finickiness and her curbed enjoyment, and she, revolted by his energy and his fingers working the dal, his slurps and smacks. The judge ate even his chapattis, his *puris* and *paranthas*, with knife and fork (Desai 176)

As Gyan and Sai's romantic bubble cracks the political unrest impinges upon their lives, the Gorkhaland posters proliferate the landscape, ranging from "we are stateless" to "we are constitutionally tortured. Return our land from Bengal". Marx positsthis gnawing need of hunger as "a natural need; it therefore needs a nature outside itself, and object outside itself, in order to satisfy itself, to be stilled. Hunger is an acknowledged need of my body for an object which exists outside it, indispensable to its integration and to the expression of its essential being" (Ellman 32). Marx is talking about physical hunger as well as what I call metaphorical hunger; which is a mixture of affect and need. The demand is for recognition of the hybrid status of the Indian-Nepalis. It isn't just about self articulation but how others view you as well. This hungering can be satiated only through action. Rather than ignoring this affective hunger and focusing only on the physical hunger, it is the combination of both which is articulated, in what it means to be a hyphenated subject—to be an Indian-Nepali. Both kinds of hunger in all the three texts aren't just about sustenance but also of satisfaction, it moves towards remedying wrong.

In "Beyond Sausages and Poached Eggs" the narrator mentions how the "Gorkha" in him was created. It is on his trip to Kolkata where he is introduced by the Burra sahib as his "Man Friday"—which has racist connotations derived from Daniel Defoe's *Robinson Crusoe*, theprimitive man, the popular stereotype of the loyal Gorkha servant/soldier. A stranger in the city asks him "where I was from" and then more explicitly "where in Nepal my home was" this casual branding as foreigner is implicit in the construction of the national imaginary, there is constriction on who it conferred as an "authentic" citizen and consequently who isn't. The identity crisis of the Indian-Nepalis is when the term Nepali has connotation of nationality over ethnicity. This innocuously asked question is however loaded with meanings; it elicits "origins" and relegates the protagonist to "margin". He is marked as a stranger and Butler calls it as being marked as "unreal", this unreality is a violence in itself, "whose lives are real? How might reality be remade? Those who are unreal have, in a sense, already suffered the violence of derealization" (Butler 33) and this "derealization" of the other means that they are neither citizens nor foreigners, subjects nor objects and exist as abject beings.

The political speech in Desai's text in chapter Twenty Six again discusses hunger, describing the India-Nepali's continuous oppression from the colonial to the neo-colonial one. The government's apathy and under develop[illegible]

Principal
Nowgong Girls' College
Nagaon :: Assam

Nowgong Girls' College ESTD: 1962 Nagaon :: Assam

ISSN: 0974-5823 Vol. 6 No. 3 December, 2021

International Journal of Mechanical Engineering

Assessment of Urban Growth and its impact on Groundwater Quality using Remote Sensing and GIS techniques in GMDA Area, Assam, India

Parimita Saikia, Keemee Das, Chandan Bhuyan, Ashish Saikia, Ranjeeta Kar

Royal School of Environmental and Earth Sciences, Assam Royal Global University, Guwahati-35

Abstract* - Land use/ Land cover (LU/ LC) monitoring is essential for water conservation and management. In the GMDA area, uncontrolled urban growth has led to the deterioration of groundwater quality, with around 70% of the population relying on groundwater for drinking and other household purposes. An attempt has been made in this study to comprehend the influence of LU/LC on groundwater quality in the Guwahati Metropolitan Authority (GMDA) area. Landsat 5 TM and OLI satellite data for 2000 and 2019 were used to prepare LU/ LC maps using different interpretation elements like tone, size, texture, pattern and association. Using supervised classification, LU/ LC classes identified were recognised such as vegetation, built-up areas, water bodies, sandbar and fallow land. The groundwater quality data collected from Central Ground Water Board (CGWB) were used to analyse the distribution of groundwater quality parameters like pH, Ca, $CaCO_3$, F, Cl, HCO_3, K, SO_4, Mg, Na, NO_3 and TDS using Inverse Distance Weightage (IDW). Comparing the LU/LC of the years 2000 and 2020, a significant change was observed in the built-up areas, and vegetation by around 32% and 13% whereas, a decrease in areas with waterbody and fallow land by 11.5% and 45% was calculated. Additionally, a change in the increase in the concentration of some of the parameters like F, K, Mg and SO_4 from 2014 to 2019 was also recorded.

Index Terms - Groundwater quality, urban growth, remote sensing, GIS

INTRODUCTION

Urbanisation has sustainable consequences for changes in demographic features and physical landscape. Unplanned and rapid urbanisation can have a negative impact on different environmental components particularly, land and water. Water is a significant resource and a fundamental necessity for the sustenance of the life of flora and fauna. According to UNEP, 2001, the issue is aggravated in India as 16% of the world's human population is occupying only 2.5 % of the total geographical territory. Therefore, to cope with environmental changes and facilitate sustainability, a thorough understanding of the processes of urbanization-induced land-cover change is required (Patra et al., 2018; Jhariya & Khan, 2018). Approximately 1.5 billion people rely on groundwater resources withdrawing 20% of global water withdrawals. Topography, lithology, geological structures, depth of weathering, the extent of fractures, secondary porosity, slope, drainage pattern, landforms, land use/land cover, elevation, rainfall, and other climatic conditions, as well as the interrelationship between these factors, govern the occurrence and movement of groundwater in an area. Unplanned urbanisation and rising human demand on the hydrogeomorphologic system frequently lead to changes in the groundwater recharge mechanism (Prabir et al, 2012).

Anthropogenic activities are the primary cause of changes in land use and land cover (LULC). Many studies have been conducted to investigate land use/ land cover (LU/LC) change and its effects on groundwater quality and quantity utilising remote sensing (RS) and geographic information systems (GIS) (Prabir et al, 2012). Elmahdy et al., 2020 and Singh et al., 2010 emphasised the impact of change in LU/LC on groundwater quantity and quality. Various studies integrated the impact of LU/LC changes on groundwater quality (Singh et al, 2011; Venkateswarlu et al., 2014; Khan & Jhariya, 2018, Karimian et al., 2019).

RS/GIS are a useful tool for studying LU/LC changes because of its spatio-temporal coverage capabilities. The rationale of the study lies in understanding the spatio-temporal land use and land cover dynamics and their impact on groundwater quality in the area. Changes in land-use patterns and subsequent inability to enforce land-use regulations have resulted in arbitrary housing building in GMDA, which has increased surface run-off and reduced groundwater recharge. Another issue of groundwater quality degradation due to anthropogenic activities that have been observed is leachate from improperly disposed of solid waste, which causes higher contamination of shallow aquifers, and as a result, extraction pressure is increasing in deeper aquifers for relatively better water quality, illustrating the exploitative perspective toward the most widely used water resource once again (Hazarika et al., 2016).

STUDY AREA

Guwahati Metropolitan Development area (GMDA) is the gateway of North-East India. It is bounded by 26°5'39" N to 26°12'39" N latitudes and 91°34'39" E to 91°51'39" E longitudes. Situated on the southern bank of the river Brahmaputra, the southern and the eastern sides of the area are bounded by hills that are extensions of the [illegible] Hills of Meghalaya. The location map is illustrated in [illegible].

Principal
Nowgong Girls' College
Nagaon :: Assam

Nowgong Girls' College ESTD 1962 Nagaon :: Assam

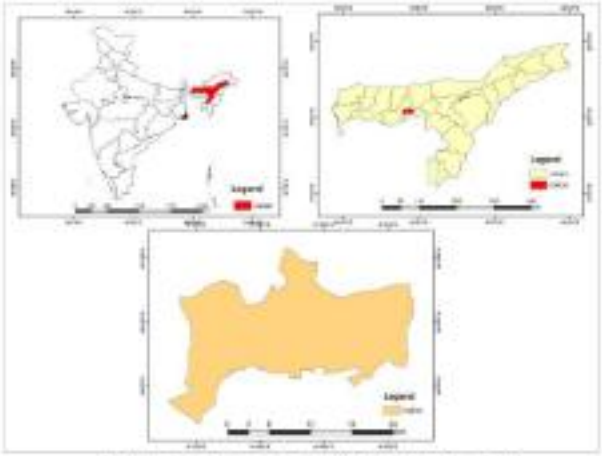

Fig. 1: Location map showing GMDA boundary
Source: Census of India & Guwahati Metropolitan Development Authority

Geologically, Guwahati rests upon the typical Precambrian rock units which are overlain by young and recent alluvium. The region is located at an elevation of about 54 meters above mean sea level. Major streams and rivers of the region originate from the southern and northeastern highlands and flow through natural slope gradients. These include Amchang, Bahini, Basistha Bahini, Bharalu, Khanajan and Mora Bharalu. The river Bharalu dissects the region for a length of about 9 km. Wetlands are located in parts of the central, southeastern and western regions of the city. These are primarily depressed valley areas with remnants of palaeo-channels of Brahmaputra.

Guwahati is underlain by the geological formation of the Achaean / Pre-Cambrian age followed by Quaternary formation. The Achaean and Pre-Cambrians are represented by inselbergs, denudational hills, compound gneissic rocks, granite, schists, amphibolites, pegmatites and basic/acidic intrusions. The Quaternary formation is represented by loose sands of various grades, pebbles, cobbles, gravels, clay and silts. In these rock groups, groundwater is stored in various conditions. In the loose Quaternary foothills, it is stored in porous sand fractures and in the case of hard consolidated foothills, it is stored in the fraction fissures, joints and structurally weak formations. The geological map has been shown in Fig. 2.

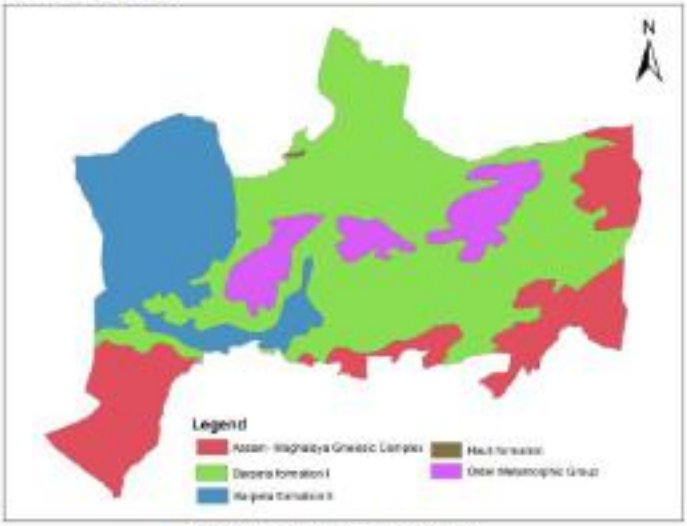

Fig. 2: Geological map of GMDA
Source: Geological Survey of India

Hydrogeological studies revealed the presence of groundwater just under water table conditions in the case of shallow aquifers; however, in the case of deeper aquifers, it is available within the semi-confined to confined conditions. In the loose unconsolidated formations depth to water in the open dug wells ranges from 2 to 4 meters below ground level during the pre-monsoon period. Dug wells located in the foothills zone however show deeper groundwater levels ranging between 5 to 10 meters below ground level during the pre-monsoon period. Shallow tube wells are constructed in the loose formation down to 30 m. The natural drainage system of the city is not uniform and is very much influenced by the landscape pattern of the city.

METHODOLOGY

To assess the LU/LC change and its impact on groundwater quality, Landsat TM and OLI satellite imageries have been used from the USGS website (www.earthexplorer.com) for the years 2000 and 2020. A geological map has been prepared using Geological Survey of India (GSI) data. The data were geo-rectified into World Geodetic System 1984 and datum 46 North. Groundwater quality data for the period of 2014-2019 have been obtained from Central Ground Water Board (CGWB) website. The preparations of groundwater quality maps were prepared using the Inverse Distance Weightage (IDW) raster interpolation technique of various groundwater quality parameters. The groundwater sampling locations were imported into ArcGIS and used to prepare maps for selected parameters namely, pH, Ca, $CaCO_3$, Cl, HCO_3, F, K, SO_4, Mg, NO_3 and TDS.

RESULTS AND DISCUSSION

Spatial distribution map

Groundwater quality maps are useful in determining the suitability of water for various reasons, primarily drinking. Selected parameters namely, pH, Ca, $CaCO_3$, Cl, HCO_3, F, K, SO_4, Mg, NO_3 and TDS for the years 2014 and 2019 have been presented in figures 3, 4 and 5 and change in the occurrence has been shown in Table 1.

pH: pH is one of the most significant water quality parameters with the optimum which ranges from 6.5-8.5. It is a measure of hydrogen ion concentration in the water. The pH values indicate the acidic, basic and alkaline nature of water (Singha et al., 2015, Khan and Jhariya, 2018). According to the data, pH in the study area ranges from 7.38 mg/L to 8.78 mg/L, which is within acceptable limits. Spatial distribution for the mentioned parameter has been depicted in Fig. 1(a). It can be observed that there has been an increase in the pH level spatially in 2019 in the range of 8.41 to 8.78 mg/L as shown in Table 1 and Fig. 3(a).

TDS: The concentration of mineral compositions dissolved in water are known as total dissolved solids (TDS). Desirable limit within the permissible limit ranges [illegible] mg/L. Fig. 1(b) shows the spatial distribution of TDS in the study

Principal
Nowgong Girls' College
Nagaon :: Assam

Nowgong Girls' College
Estd. 1962
Nagaon :: Assam

area which range from 114.46 to 339.47 mg/L. Table 1 and Fig. 3(b) shows a maximum increase in the variation of TDS in the range 204.47 - 249.47 mg/L in the period.

Chloride (Cl-): Water contains various amounts of chloride, depending on the geochemical circumstances. Industrial waste, sewage disposal, and the leaching of saline residues into the soil can all cause chloride concentrations. Drinking water with a high chloride percentage has a salty taste to it. The permissible limit for chloride concentration ranges between 1000 mg/L. It can be observed that there has been an increase in the chloride concentration spatially in 2019 in the range 24.81 – 48 mg/L as shown in Table 1 and Fig. 3(c). Overall, the water samples are within the permissible limit in both years.

Total Hardness (as $CaCO_3$): Hardness is caused due to the presence of carbonates and bicarbonates of calcium and magnesium, chlorides, nitrates and sulphates of calcium and magnesium. The permissible limit of $CaCO_3$ is 200 mg/L. The total hardness of the water samples in the study area varies from 69-267 mg/L in the time period. There has been a maximum increase in the area under the range 108 – 148 mg/L since 2014 as shown in Fig. 3(d) and Table 1.

Alkalinity (HCO3-): It is the main alkaline factor in almost all water. Generally, for most water systems, carbonates (CO3 2-) are the least predominant ions whereas bicarbonates (HCO3-) are the dominant anions. The permissible limit of alkalinity is 200 mg/L. Table 1 and Fig. 4(a) shows the spatial distribution of alkalinity in the study area. It has been observed there is a maximum increase in the variation of alkalinity in the range 81- 111 mg/L in the period.

Fluoride (F): It is a natural pollutant of water commonly found in the form of fluorine. Groundwater usually contains fluoride dissolved by geological formations. The permissible limit for fluoride is 1.5 mg/L. Excessive fluoride concentration can cause skeletal fluorosis or fluorosis. The concentration of F in the water samples in the study area varies from 0.2 to 6.2 mg/L in the time period. There has been a maximum increase in the area under the range of more than 1.5 mg/ L spatially since 2014 which are beyond the permissible limit as shown in Fig. 4(b) and Table 1.

Potassium (K+): The majority of species require potassium in their diet. Potassium also plays an important part in plant growth. Excess potassium, on the other hand, is dangerous in water because it spreads quickly due to its great mobility. Table 1 and Fig. 4(c) show the spatial distribution of potassium concentration in the study area. Overall the water samples are within the permissible limit in both years.

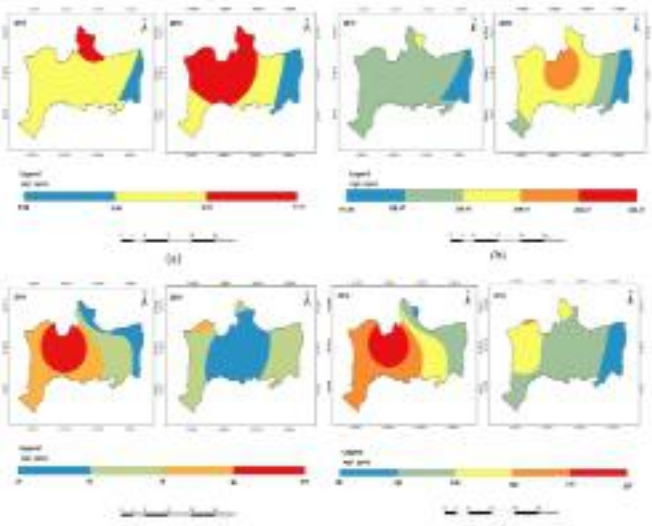

Fig. 3: Spatial distribution for the year 2014 and 2019: (a)pH (b)TDS (c)Cl (d)$CaCO_3$
Source: Central Ground Water Board

Magnesium (Mg2+): Magnesium is prevalent in groundwater. Magnesium ion is required for cell activity during enzyme activation. However, water has an unpleasant taste when the concentration exceeds the allowed limits. The permissible limit of the concentration of Mg is 100 mg/L. Table 1 and Fig. 4(d) show the spatial distribution of the concentration of magnesium in the study area. Overall, the water samples are within the permissible limit in both years.

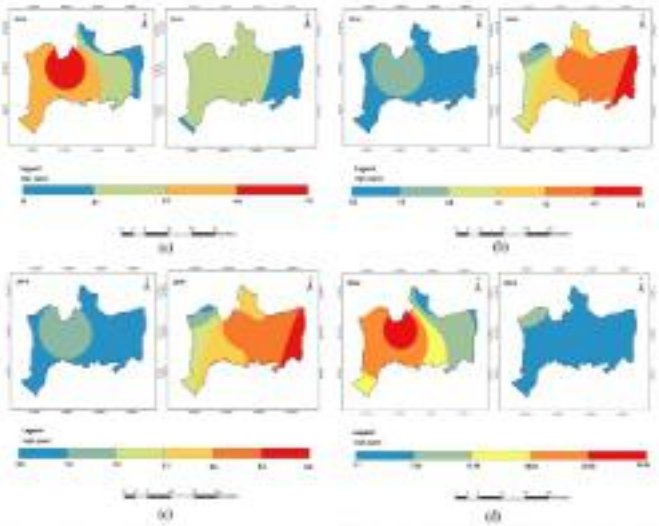

Fig. 4: Spatial distribution for the year 2014 and 2019: (a) HCO_3- (b) F (c)K+ (d) Mg2+
Source: Central Ground Water Board

Calcium (Ca++): Calcium is formed in water mostly as a result of the presence of minerals such as limestone, dolomite, gypsum, and gypsiferous. The BIS specifies a calcium acceptable limit of 75-200 mg/l. The spatial distribution of the concentration of calcium in the study area for the time period has been shown in Table 1 and Fig. 5(a). Overall, the water samples are within the permissible limit in both years.

Sodium (Na+): Sodium is abundant in most natural streams. The highest sodium allowable value is 200 mg/L. High sodium intake can cause increased blood pressure, [illegible] oedema, and hyperosmolarity. Groundwater with a high concentration of sodium is unsuitable for agricultural usage

Principal
Nowgong Girls' College
Nagaon :: Assam

Copyrights @Kalahari Journals

Nowgong Girls' College
ESTD 1962
Nagaon :: Assam

because it degrades the soil. The concentration of sodium in the study area ranges between 11.73-83.38 mg/L as shown in Fig 5(b) and Table 1 are within the permissible limit in both years.

Nitrate (NO_3): Atmosphere legumes, plant debris, and animal excreta are the main sources of nitrate in water. Nitrate levels in water over 100 mg/l are harsh to the taste and cause physiological irritation in humans. In humans, water from shallow wells containing more than 45 mg/L produces methemoglobinemia, often known as a blue baby syndrome. Higher nitrate concentrations are found mainly due to the application of fertilizers, septic tanks, open dumpsites, inadequate manure management, etc. Nitrate concentration in the study area as shown in Fig. 5(c) is within the permissible limit in both years but Table 1 shows there is an increase in the concentration in 2019.

Sulphate (SO_4--): Sulphur in groundwater is usually in the form of sulphate. The weathering of sulphide-bearing rocks like granite, fertiliser, and rainfall can all cause sulphate to infiltrate groundwater. The permissible limit of concentration of sulphate is 200 mg/L. The spatial distribution of the concentration of sulphate in the study area for the time period has been shown in Table 1 and Fig. 5(d). Overall, the water samples are within the permissible limit in both years.

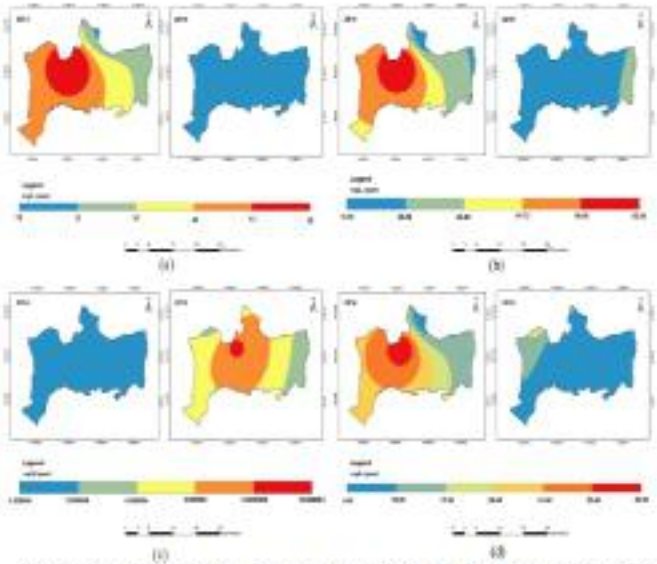

Fig. 5: Spatial distribution for years 2014 and 2019 for (a) Ca (b)Na (c)NO_3 (d) SO_4

Source: Central Ground Water Board

Parameters	Range	2000(Area in km²)	2020(Area in km²)	Change (Area in km²)
Ca	12-22	1.9188	0	-1.918
	22-32	73.9719	382.548	308.576
	32-42	77.8617	0	-77.861
	42-52	152.141	0	-152.141
	52-62	76.6548	0	-76.654
$Caco_3$	69 - 108	2.8035	60.1371	57.333
	108 - 148	81.7209	230.363	148.642
	148 - 188	71.1495	89.8902	18.740
	188 - 228	151.643	2.1573	-149.486
	228 - 267	75.231	0	-75.231
Cl	24.81 - 48	53.7831	183.1	129.316
	48 - 71	92.6424	190.168	97.525
	71- 94	140.65	9.279	-131.371
	94 - 117	95.472	0.0009	-95.471
Fluoride	0.23 - 1.2	260.736	3.7845	-256.952
	1.2 - 2.2	121.811	18.9981	-102.813
	2.2 - 3.2	0	56.0574	56.057
	3.2 - 4.2	0	99.8739	99.873
	4.2 - 5.2	0	163.056	163.056
	5.2 - 6.2	0	40.7781	40.778
HCO_3	51.21 - 81	5.05512	99.5382	94.483
	81 - 111	9.88281	283.009	273.126
	111- 141	16.09829	0	-16.098
	141- 171	7.21854	0	-7.218
K	2.13 - 7.58	17.2314	361.151	343.919
	7.58 - 13.06	106.759	21.3966	-85.362
	13.06 - 18.54	63.4869	0	-63.486
	18.54 - 24.02	142.04	0	-142.04
	24.02 - 29.5	53.0307	0	-53.030
Mg	7.81 - 13.12	10.1421	280.355	270.212
	13.12 - 18.43	95.2065	93.2067	-1.999
	18.43 - 23.74	48.1509	8.9847	-39.166
	23.74 - 29.05	93.9114	0	-93.911
	29.05 - 34.36	105.429	0	-105.42
	34.36 - 39.67	29.7081	0	-29.708
NO_3	0.00000401 - 3	0		0
	3 - 6	382.5479	56.8[illegible]	[illegible]

Copyrights @ Kalahari Journals

Principal
Nowgong Girls' College
Nagaon :: Assam

Nowgong Girls' College
Estd. 1962
Nagaon :: Assam

	6 - 9	0	162.229	162.229
	9 - 12	0	153.338	153.338
	12 - 15	0	10.458	10.458
pH	7.67 - 8.04	34.5213	62.2287	27.707
	8.04 - 8.41	316.922	125.177	-191.745
	8.41- 8.78	31.1049	195.1419	164.037
SO_4	3.49 - 10.49	9.9036	332.433	322.529
	10.49 - 17.49	93.6567	44.9631	-48.693
	17.49 - 24.49	49.8879	5.1516	-44.736
	24.49 - 31.49	96.1344	0	-96.134
	31.49 - 38.49	105.121	0	-105.121
	38.49 - 45.49	27.8442	0	-27.844
TDS	114.46 - 159.47	47.511	43.0812	-4.429
	159.47 - 204.47	329.861	70.6158	-259.245
	204.47 - 249.47	5.1759	206.447	201.271
	249.47 - 294.47	0	62.4033	62.403
	294.47 - 339.47	0	0	0
Na	11.72 - 26.06	19.2519	330.024	310.772
	26.06 - 40.39	102.151	52.524	-49.627
	40.39 - 54.72	58.7736	0	-58.773
	54.72 - 69.05	136.605	0	-136.605
	69.05 - 83.38	65.7666	0	-65.766

Table 1: Change in the groundwater quality from 2014 to 2019.
Source: Central Ground Water Board, Guwahati

EVALUATION OF LU/LC MAP

LU/LC map was prepared using supervised classification using Landsat datasets. From 2000 to 2020, there were significant changes in LULC, according to the current study (Table 2 and Fig. 6). Fig. 6 shows the land use/land cover map from 1999 to 2016, as well as the change analysis rate from Table 2. According to this study, the highest LULC changes were reported in the built-up areas, vegetation, by around 32% and 13% while there has been a decrease in areas with waterbody and fallow land by 11.5% and 45% in the time period.

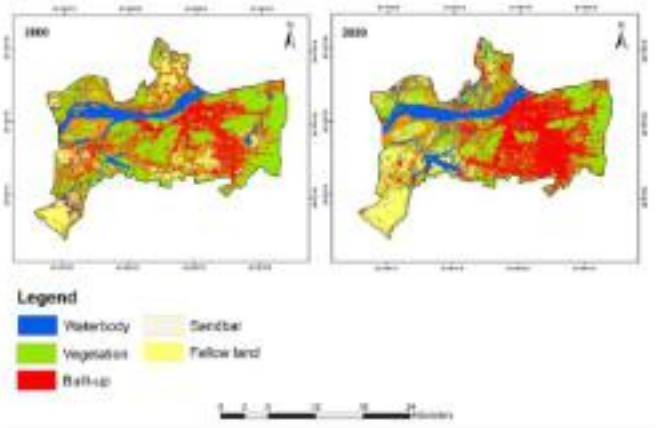

Fig. 6: LU/LC analysis for years 2000 and 2020,
Source: Landsat TM and OLI

LU/LC	2000	2020	Change (%)
Waterbody	33.1119	29.286	-11.55
Veg	518.411	586.225	13.08
BU	183.371	242.243	32.10
Sandbar	4.959	30.3336	511.68
Fallow land	329.971	181.736	-44.92

Table 2: LU/LC changes during 2000 to 2020.
Source: Landsat TM and OLI

CONCLUSION

Because land use and land cover change have a big impact on groundwater quality, it's important to assess it to make sure it's safe to drink. Landsat satellite imageries were used to measure LULC for the years 2000 and 2020. In this study, it is found that there is a drastic change in the settlement area.

LULC analyses reported changes in the built-up areas, vegetation, by around 32% and 13% during the time period. On the other hand, there is a decrease in areas with waterbody and fallow land by 11.5% and 45% between 2000 and 2020. The association between LULC change and groundwater quality has been subjectively established, and it has been discovered that fluoride contamination is primarily concentrated in the GMDA settlement areas. Fluoride concentrations in groundwater increased in 2019, especially in the settlement area, showing that anthropogenic activities in the study region caused the groundwater to surpass the BIS permissible limit.

Copyrights @Kalahari Journals

Principal
Nowgong Girls' College
Nagaon :: Assam
Nowgong Girls' College ESTD: 1962 Nagaon :: Assam

REFERENCES

Elmahdy, S., Mohamed, M., & Ali, T. (2020). Land Use/Land Cover Changes Impact on Groundwater Level and Quality in the Northern Part of the United Arab Emirates. Remote Sensing, 12(11), 1715. MDPI AG. Retrieved from http://dx.doi.org/10.3390/rs12111715

Hazarika, Natasha & Nitivattananon, Vilas. (2016). Strategic assessment of groundwater resource exploitation using DPSIR framework in Guwahati city, India. Habitat International. 51. 79-89. 10.1016/j.habitatint.2015.10.003.

Karimian, K., Amini, A., Ghaiumi Mohammadi, H. (2019). The Impact of Land Use/Land Cover Changes on Groundwater Resources Using Remote Sensing & GIS (Case Study: Khan-Mirza Plain). Desert, 24(2), 319-330. doi: 10.22059/jdesert.2019.76388

Khan, Rubia & Jhariya, Dalchand. (2018). Assessment of Land-use and Land-cover Change and its Impact on Groundwater Quality Using Remote Sensing and GIS Techniques in Raipur City, Chhattisgarh, India. Journal of the Geological Society of India. 92. 59-66. DOI: 10.1007/s12594-018-0953-3.

Singh, C.K., Shashtri, S., Mukherjee, S. et al. (2011). Application of GWQI to Assess Effect of Land Use Change on Groundwater Quality in Lower Shiwaliks of Punjab: Remote Sensing and GIS Based Approach. Water Resour Manage 25, 1881–1898. https://doi.org/10.1007/s11269-011-9779-0

Singh, Sudhir & Singh, Chander. (2010). Impact of land-use and land-cover change on groundwater quality in the Lower Shiwalik hills: A remote sensing and GIS based approach. Central European Journal of Geosciences. 2. DOI: 10.2478/v10085-010-0003-x.

Singha, Soumya & C P, Devatha & Singha, Sudhakar & Verma, Mukesh. (2015). Assessing Ground Water Quality using GIS. International Journal of Engineering Research and. V4. 10.17577/IJERTV4IS110604.

Venkateswarlu, Gogana & Jayasankar, G & Saradhi, B.V. (2014). Impact Assessment of Land Use Change on Ground Water Quality Using Remote Sensing & GIS for Zone V under Municipal Corporation Hyderabad. IOSR Journal of Mechanical and Civil Engineering. 11. 36-42. DOI: 10.9790/1684-11153642.

AUTHOR INFORMATION

Parimita Saikia, PhD Research Scholar, Department of Geography, Royal School of Environmental and Earth Sciences, Assam Royal Global University.

Dr. Keemee Das, Assistant Professor, Department of Geography, Royal School of Environmental and Earth Sciences, Assam Royal Global University.

Chandan Bhuyan, Assistant Professor, Department of Geography, Royal School of Environmental and Earth Sciences, Assam Royal Global University.

Ashish Saikia, Assistant Professor, Department of Geography, Royal School of Environmental and Earth Sciences, Assam Royal Global University.

Dr. Ranjeeta Kar, Assistant Professor, Department of Geology, Royal School of Environmental and Earth Sciences, Assam Royal Global University.

Principal
Nowgong Girls' College
Nagaon :: Assam

Nowgong Girls' College
ESTD: 1962
Nagaon :: Assam

ISSN: 0974-5823 Vol. 6 No. 3 December, 2021

International Journal of Mechanical Engineering

Spread of COVID-19 and the Role of Distance-decay: A Case Study of West Bengal, India

Ashish Saikia*[1], Chandan Bhuyan[1], Dr. Keemee Das[1], Dr. Ranjeeta Kar[2], Arundhuti Patangia[3]

[1]*Assistant Professor, Department of Geography, Royal Global University, Guwahati-35, Assam, India*

[2]*Assistant Professor, Department of Geology, Royal Global University, Guwahati-35, Assam, India*

[3]*Research Scholar, Department of Geography, Gauhati University, Guwahati-14, Assam, India*

Abstract

Geographical phenomena are widely spread across space. Spatial distribution of such phenomena can be well understood by using various statistical methods. COVID-19 pandemic has also attained global recognition after its spatial diffusion through various mediums. The present paper tries to analyze the geographical spread of COVID-19 disease in West Bengal, India in terms of distance-decay function. The analysis has been carried out using multiple ring buffer in ArcGIS 10.8 and simple linear regression analysis which discloses that the density of COVID-19 cases is very high in the Central Business District (CBD) and diminishes while one moves from the CBD towards periphery.

Keywords: Distance-decay, COVID-19, Regression Analysis, West Bengal, Multiple ring buffer

1. Introduction

The outbreak of novel Coronavirus disease in 2019 (COVID-19) spread rapidly in China from its origin in Wuhan, Hubei Province, China (Chen et al., 2020) and eventually spread throughout the world. It has been recognized as a Global Pandemic by the World Health Organization (WHO). Several studies related to the spread of the disease suggests that the cities are more vulnerable to such pandemics (Khavarian-Garmsir et al., 2020), (Dettilo et. al., 2020), (Muggah et al., 2020), (Diez et al., 2020). "The high concentration of people and activities in cities make them vulnerable to various stressors such as natural and man-made disasters." (Sharifi & Khavarian-Garmsir, 2020). Spread of COVID-19 and its outbreak has been analyzed in relation to various factors such as environmental (Carteni et al., 2020), socio-economic, demographic, healthcare resources (Buja et al., 2020), infrastructures (Nakada & Urban, 2020) etc. Its spread and impacts are concerned with the composition of the population, specially, population age structure (Dowd et al., 2020). In addition, its impacts and progression can also be correlated with population density, since living in closer proximity to one another is likely to imply a higher infection rate (Desmet & Wacziarg, 2021). Kolkata is one of the most densely populated cities in the world with 24,306 persons per sq. km.The first case of COVID-19 in the state of West Bengal had been found in Kolkata in 17 March, 2020 as a student who returned from United Kingdom (The Hindu, 17 March, 2020). Till the last weeks of April, the spread of COVID-19 was restricted to the airports only. But the community transmission has occurred in various district from the last two weeks of April 2020. Till 28th September, the state has reported a total of 1,567,573 cases out of which 18,764 persons were succumbed to death.

In the current study, an attempt has been made to analyze the spread of the COVID-19 pandemic in terms of distance from the city center. Waldo Tobler's first law of Geography rightly explains distance- decay as, "Everything is related to everything else, but near things are more related than distant things" (Tobler, 1970). Distance plays crucial role in the distribution of ideas, technology, population, and interaction (Eldridge, 1991). Colin Clark (1951) devised a negative exponential model, where he revealed that the residential density of an area is negatively correlated to distance from the city center. Notably, as one moves away from the city center, the population density goes on decreasing. This proposition gave us the concept of concentric development of a city or a residential area where the rate of population density decreases similarly in all the directions, results in the growth of a circular city with Central Business District (CBD) at the center (Clark, 1951). The relationship devised by Clark has been applied in the context of the Density of COVID-19 infected persons that has been detected in the state of West Bengal by taking Kolkata district as the CBD. This paper is therefore an attempt to examine the applicability of Distance-decay model in the distribution of COVID-19 cases across West Bengal, India.

2. Study Area

In this study, the aim is to investigate the applicability of Distance-Decay model envisaged by Colin Clark (1951) in the event of the density of COVID-19 cases that have been detected in the state of West Bengal. For this purpose, we have taken West Bengal as our study area. The districts of West Bengal have been considered as the spatial units on which the whole analysis process depends. Clark has taken the area around a Central Business District as the study area. But we have considered the districts as the periphery urban areas and the Kolkata district as the Central Business District.

West Bengal is situated in the Eastern part of India covering up an area of 88,752 sq. km extending from the foothills of the Himalayas to the Bay of Bengal. It lies between 85°50′E to 89°50′ E longitude and 21°25′N to 27°13′N latitude (Fig 1). The [illegible] boundary of West Bengal is covered by Bangla[illegible] and Assam. [illegible] the

Principal
Nowgong Girls' College
Nagaon :: Assam

Nowgong Girls' College
ESTD: 1962
Nagaon :: Assam

north, Sikkim and Bhutan covers the boundary. In the western boundary, there lies Bihar, Jharkhand and Orissa and the southern part is covered up by the Bay of Bengal. The state enjoys tropical hot, humid and monsoon climate. 13.93% area out of the total area is covered by natural vegetation. (Biswas et al., 2021)

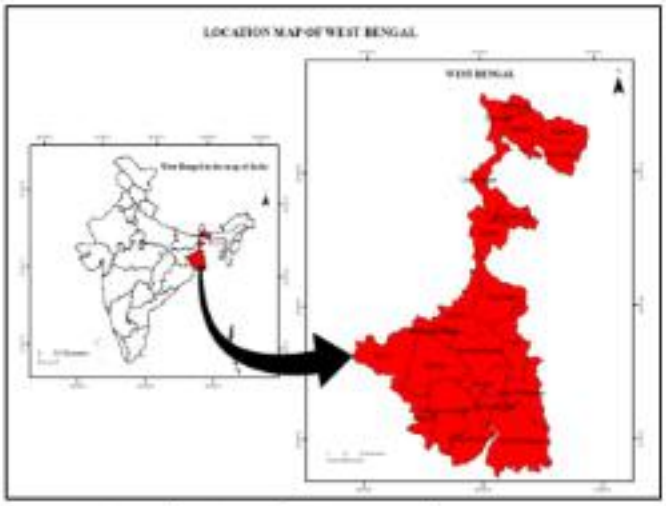

Figure 1 Location Map of West Bengal

Source: Authors' own work

The state has 23 districts, out of which South 24 Parganas is the largest and Kolkata is the smallest. The total population of the state is 91,347,736 according to Census of India, 2011 with a population density of 950 persons per sq. km. The capital of the state, Kolkata is the third-largest urban agglomeration in India. Kolkata districts have a 100% urbanization level. The average urbanization level of the state is 28.78%. The sex ratio is 934 and the literacy rate is 74.04%.

3. Methodology

3.1 Data Collection

As the collection of primary data is not possible in the current situation. So, the study has to be completed on the basis of secondary data collected from various online sources. Both, Central and the State government of West Bengal has been publishing COVID-19 related data in their websites. Data from February 2020 to 15 May 2021 has been collected from the Health and Family Welfare Department, Government of West Bengal. The websites that have been visited for collecting COVID-19 data are:

1. https://www.covid19india.org/state/WB
2. https://www.covid19india.org

Data on population has been collected from Census of India website:

1. https://censusindia.gov.in/DigitalLibrary/MFTableSeries.aspx (Primary Census Abstract Tables)

3.2 Methods

Colin Clark (1951) propounded an exponential model for describing the pattern of population density distribution (Tse, 1976). His model has been further utilized by various researchers in various fields of knowledge. Clark's model is:

$$Dx = Do\, e^{-bx}$$

(Clark, 1951)

Where, Dx is the population density at distance x, Do is the assigned central population density, e is the exponent of distance and b is the density gradient. Clark had used two generalisations for his study of population density and distance in various cities around the world. These are:

a. In every large city, excluding the central business zone, which has few resident inhabitants, we have districts of dense population in the interior, with density falling off progressively as we proceed to the outer suburbs.

b. In most (but not all) cities, as time goes on, density tends to fall in the most populous inner suburbs, and to rise in the outer suburbs, and the whole city tends to "spread itself out."

"The model shows a non-linear relationship between the distance and population density. In order to find out a linear relationship, a logarithmic transformation of the distance-decay equation is necessary". (Das, 2020)

Thus,

$$\log_e d(x) = \log_e (d_0 e^{-bx})$$

Or

$$\log_e d(x) = \log e d_0 - bx \cdot \log_e e \text{ (Since } \log_e e = 1)$$

Thus,

$$\log_e d(x) = \log e d_0 - bx$$

Now, if we write $\log_e d(x)$ as $\hat{y}$ and $\log e d_0$ as a. Then, $\hat{y} = a + bx$, and it is a linear equation of distance-decay Model. Clark envisaged that the population density of a city decreases as the distance increases from the city centre. The steepness of the decline in density changes over time. The decline of density from the city centre largely depended upon the co-efficient b. A high value of b results in sharp decline of density with the increase in distance from the centre which is often called as a compact city. A low value means gradual decline in density resulting in the city to be more spread out. Clark has indicated transport as one of the basic factors for which the decline in density changes (Tse, 1976).

In his methodology, Clark had drawn a series of concentric rings about the centre of the city at an interval 1 mile of radius. Where these circles cut the census tracts, he made arbitrary apportionments of the population. This was done by considering the proportion of land area lying in each ring exclusive of the open spaces. The total population and the average density for each ring had been calculated then. A diagram was then prepared where the horizontal axis represented the distance from the city centre and the vertical axis represented the measured density in a natural logarithm. The parameters D_0 and b were obtained by using regression analysis using the logarithmic form of equation (Tse, 1976).

In this study, data collected from various sources have been classified to fulfil the demand of the analysis process. We have followed the methodology used by Clark. Recent map of West Bengal with its newly formed districts has been digitized in ArcMap 10.8. The data related to COVID-19 and population has been classified in MS excel 2013. It is worth mentioning that new districts have been formed after 2011 census. Therefore, the population data for the new districts are not readily available. To compensate [illegible] have estimated the population data of the old districts into two separate new

Copyrights @Kalahari Journals

Principal
Nowgong Girls' College
Nagaon :: Assam
Nowgong Girls' College
ESTD: 1962
Nagaon :: Assam

districts which have been formed in the later period. All other map works have been done using ArcMap 10.8. Concentric circles around Kolkata district have been created using Multiple Buffer Ring analysis (Fig 2). The plotting of the case density for each ring against average distance of each ring has been done in MS excel 2013. Case density has been found out by dividing the total cases (sum of the number cases found in the census tracts which fall under a particular ring) of each ring by the total area of the ring. (Table 1).

Figure 2. Concentric zones around Kolkata district

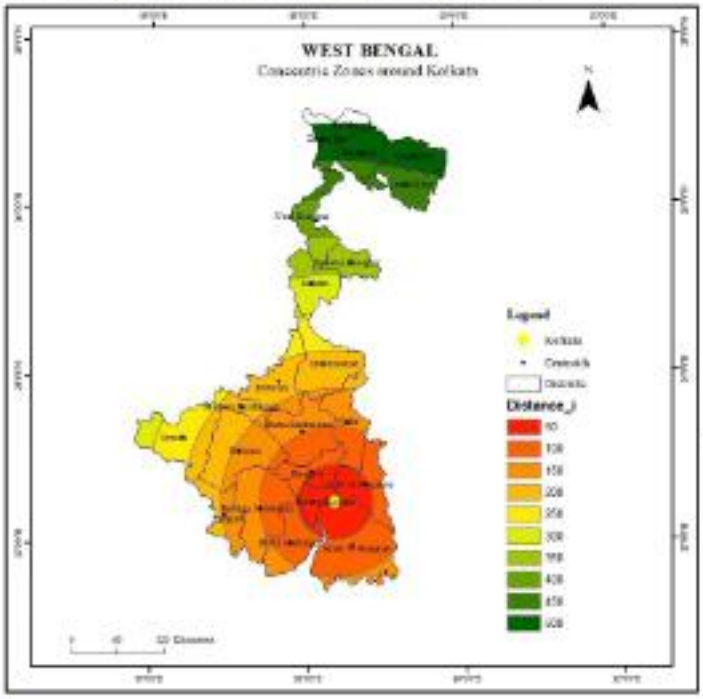

Source: Authors' own work

Table 1. Zone wise density of COVID-19 infected persons

Zones	Distance in KM	Average Distance	Districts Under the zones	Total Population affected by COVID-19	Total Area	Density of Infected Population (Persons/sq. km)
1	0	0	Kolkata	316229	185	1709
2	0-50	41.66	North 24 Parganas, Howrah, Hooghly	506060	8640	59
3	50-100	79.62	Purba Medinipur, South 24 Parganas, Paschim Medinipur	214254	16299.17	13
4	100-150	125.3	Nadia, Purba Bardhaman, Bankura, Jhargram	160771	19279.33	8
5	150-200	178.13	Murshidabad, Birbhum, Paschim Bardhaman	131758	11472.17	11
6	200-250	218.09	Purulia	19340	6259	3
7	250-300	290.8	Maldah	33124	3733	9
8	300-350	317.1	Dakshin Dinajpur	17429	2219	8
9	350-400	372.1	Uttar Dinajpur	19698	3140	6
10	400-450	429.9	Cooch Bihar	28863	3387	5
11	450-500	477.57	Alipurduar, Jalpaiguri, Kalimpong, Darjeeling	119963	9363.5	13

Source: Census of India, https://www.covid19india.org/state/WB and Author's own calculation (as of 28th September 2021)

4. Results and Discussion

The graph obtained by plotting the average density of COVID-19 cases against the average distance of each ring shows a negative correlation trend. In the linear model, the *a* value is 255.74 and the *b* value is -0.1534 and the value of R^2 is 0.2391 which suggests that 23.91 per cent of variation of COVID-19 cases is explained by the distance from the Central Business District i.e., Kolkata District (table 2).

Table 2. Density gradient statistics

Independent Variable	Explanatory Variable: Density of COVID-19 cases		
	Model	Correlation coefficient	R^2 value
Average distance	y = -1.5585x + 526.12	-0.4889	0.2391

Source: Author's own work

The trend line so obtained, slopes towards its right (figure 3). The maximum expected density of cases is at the Kolkata district which is 526 persons per sq. km whereas the minimum expected density is found to be in the farthest point which shows a negative value of -218 persons per sq. km. The observed density in the Kolkata is much higher than the expected density which signifies a very high interaction among the people living there. This high interaction is due to good transportation and communication networks, overcrowding in markets etc. on the other hand peripheral regions show values higher than the expected values because these regions lie in the areas where the transportation is quite developed due to interstate connectivity facility. But the middle areas show values which are much lower than the expected values. In these regions, transport connections are not well developed. Remote areas such as, delta, wetlands, forests, villages are largely located in these zones. It clearly proofs that the outbreak of COVID-19 disease is higher in those areas where the transportation system is well developed, where the interaction between people is much higher.

Figure 3. Density Gradient of COVID-19 cases in West Bengal, India

Nowgong Girls' College ★ ESTD 1962 ★ Nagaon :: Assam

Principal
Nowgong Girls' College
Nagaon :: Assam

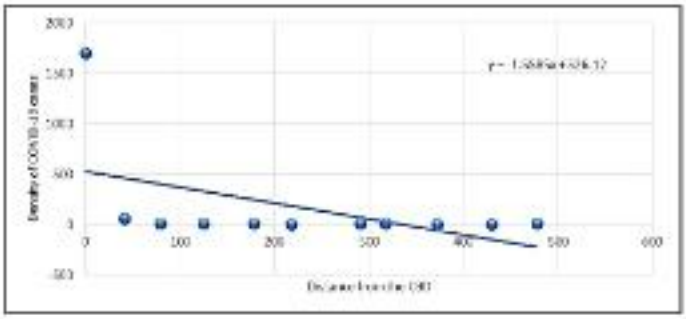

Source: Author's own work

5. Conclusion

As mentioned earlier, this paper aims at giving a distance-decay model-based description of COVID-19 outbreak in the state of West Bengal. The disease reaches every district in the state although there is much disparity in terms of frequency of occurrence of cases across districts. The model aptly defines its prospective of decay of a geographical phenomenon with increase in distance. More an area is well connected with transport lines, greater is the chance of outbreak of COVID-19 disease. Therefore, it is suggested to restrict the inter-district flows i.e., movement of people to avoid further spread of the pandemic. The state governments have taken bold steps like lockdown and curfew in various states. These measures will surely reduce the rate of spread of the disease. Reducing the level of interaction between people is the sole measure that can be initiated by any type of administrative unit.

REFERENCES

1. Biswas, B., Roy, R., Roy, T., & Chowdhury, S. (2021). Geographical Appraisal of COVID-19 in West Bengal , India. *GeoJournal*, *4*. https://doi.org/10.1007/s10708-021-10388-4
2. Buja, A., Paganini, M., Cocchio, S., Scioni, M., Rebba, V., & Baldo, V. (2020). Demographic and socio-economic factors, and healthcare resource indicators associated with the rapid spread of COVID-19 in Northern Italy: An ecological study. *PLoS ONE*, *15*(12 December), 1–13. https://doi.org/10.1371/journal.pone.0244535
3. Carteni, A., Di Francesco, L., & Martino, M. (2020). How mobility habits influenced the spread of the COVID-19 pandemic: Results from the Italian case study. *Science of the Total Environment*, *741*, 140489. https://doi.org/10.1016/j.scitotenv.2020.140489
4. Chen, S., Yang, J., Yang, W., Wang, C., & Bärnighausen, T. (2020). COVID-19 control in China during mass population movements at New Year. *The Lancet*, *395*(10226), 764–766. https://doi.org/10.1016/S0140-6736(20)30421-9
5. Dattilo, Wesley, et al. "COVID-19 most vulnerable Mexican cities lack the public health infrastructure to face the pandemic: a new temporally-explicit model." *MedRxiv* (2020).
6. Desmet, K., & Wacziarg, R. (2021). Understanding spatial variation in COVID-19 across the United States. *Journal of Urban Economics*, *July 2020*, 103332. https://doi.org/10.1016/j.jue.2021.103332
7. Diez Roux, Ana V., et al. "Urban health and health equity in Latin American cities: what COVID-19 is teaching us." *Cities & Health* (2020): 1-5.
8. Dowd, J. B., Andriano, L., Brazel, D. M., Rotondi, V., Block, P., Ding, X., Liu, Y., & Mills, M. C. (2020). Demographic science aids in understanding the spread and fatality rates of COVID-19. *Proceedings of the National Academy of Sciences of the United States of America*, *117*(18), 9696–9698. https://doi.org/10.1073/pnas.2004911117
9. Eldridge, J. D., & Jones III, J. P. (1991). Warped space: A geography of distance decay. *The Professional Geographer*, *43*(4), 500-511.
10. Khavarian-Garmsir, A. R., Ayyoob Sharifi, and Nabi Moradpour. "Are high-density districts more vulnerable to the COVID-19 pandemic?" *Sustainable Cities and Society* 70 (2021): 102911.
11. Muggah, Robert, and R. Katz. "How cities around the world are handling COVID-19-and why we need to measure their preparedness." *World Economic Forum*. 2020.
12. Nakada, L. Y. K., & Urban, R. C. (2020). COVID-19 pandemic: environmental and social factors influencing the spread of SARS-CoV-2 in São Paulo, Brazil. *Environmental Science and Pollution Research*. https://doi.org/10.1007/s11356-020-10930-w
13. Nekola, Jeffrey C., and Peter S. White. "The distance decay of similarity in biogeography and ecology." *Journal of biogeography* 26.4 (1999): 867-878.
14. Rengert, G. F., Piquero, A. R., & Jones, P. R. (1999). Distance decay reexamined. *Criminology*, *37*(2), 427-446.
15. Sharifi, A., & Khavarian-Garmsir, A. R. (2020). The COVID-19 pandemic: Impacts on cities and major lessons for urban planning, design, and management. *Science of the Total Environment*, *749*, 1–3. https://doi.org/10.1016/j.scitotenv.2020.142391
16. Tobler, W. (1970). A Computer Movie Simulating Urban Growth in the Detroit Region. *Economic Geography*, *46*, 234-240. Doi: 10.2307/143141
17. Tse, M.-L. (1976). *Urban Population Density Distribution : a Contribution From the Vancouver Case*.
18. Singh, S. S. (2021). Coronavirus: Kolkata reports first case. Coronavirus | Kolkata reports first case. Retrieved December 5, 2021, from https://www.thehindu.com/news/national/other-states/coronavirus-west-bengal-reports-first-case/article31093265.ece

Principal
Nowgong Girls' College
Nagaon :: Assam

Nowgong Girls' College ESTD: 1962 Nagaon :: Assam

ISSN: 2319-8893
RNP/GH-165/2021-2023

সপ্তদশ বছৰ, ষষ্ঠ সংখ্যা, জানুৱাৰী ২০২১

সাতসৰী

₹ ৩০.০০

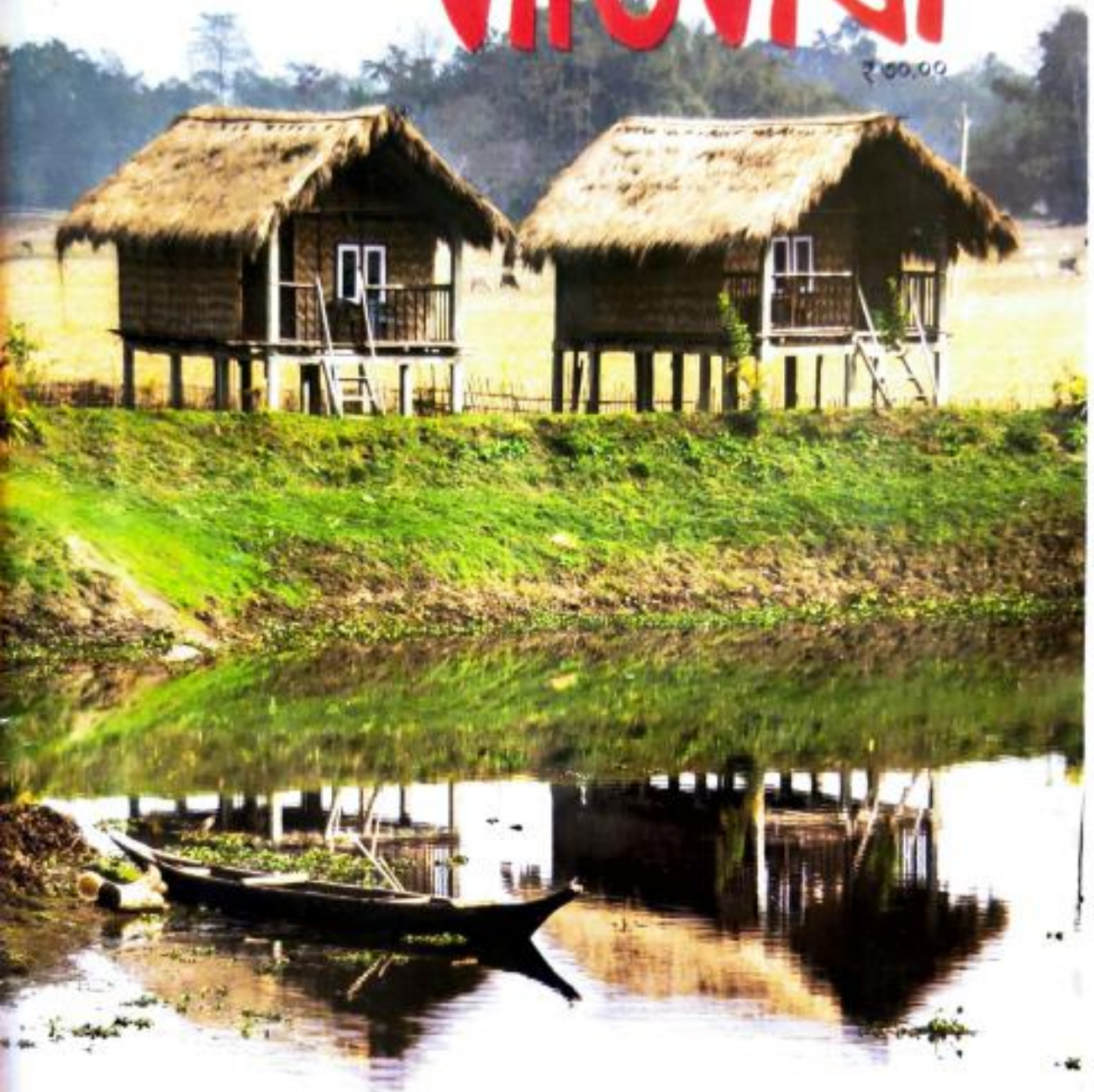

জ্ঞানপীঠ বঁটাপ্রাপ্তিৰ আনন্দময় মুহূর্তটো

সামাজিক নেতৃত্বৰ গুণেৰে যুগপুৰুষ শংকৰদেৱ

বিশ্বব্রহ্মাণ্ডৰ ৰহস্য ভেদিবলৈ মহাকাশত নতুন দূৰবীক্ষণ

C.T.C.
Principal
Nowgong Girls' College
Nagaon :: Assam

Nowgong Girls' College
ESTD: 1962
Nagaon :: Assam

সাতসৰী

সপ্তদশ বছৰ, ষষ্ঠ সংখ্যা • জানুৱাৰী, ২০২২

SATSARI

Vol. No.: 17, Issue No. 6 • January, 2022 • Pages : 12x

Reg. No. : ASSASS/2011/35776

ISSN: 2319-8893 • Rs.30.00

অভিমত | মৃণাল কান্তি চক্রৱর্তী • অবিভক্ত গোৱালপাৰা জিলা : কল্প, সাক্ষ্য, ইতিহাস • ১৩

বিশেষ লেখা | অমিতাভ ফুকন • জ্ঞানপীঠ বঁটাপ্রাপ্তিৰ আনন্দময় মুহূর্তটো • ১৭

প্রবন্ধ নিবন্ধ | সমুদ্র গুপ্ত কাশ্যপ, ড° মুনীন্দ্র কাকতি • সামাজিক নেতৃত্বৰ গুণেৰে যুগপুৰুষ শংকৰদেৱ • ২৮
উপেন্দ্র বৰকটকী • ড° নগেন শইকীয়া : ধূলিৰ ধেমালিৰ পৰা খ্যাতিৰ ফুলনিলৈ • ৩৩
কুশল দত্ত • সন্ত তাঁতিৰ কবিতা • ৩৭
ড° প্রাঞ্জল শর্মা বশিষ্ঠ • রুদ্র কন্দলীৰ 'সাত্যকী-প্রবেশ' • ৪১
ড° জুবি দত্ত • অসমীয়া উপন্যাসত কুইয়াৰ চেতনা • ৪৭
ড° অংকুৰণ দত্ত • তথ্যচিত্রৰ নান্দনিকতা আৰু গৱেষণাত্মক চিত্রায়ণ • ৫২
ভার্গৱ বৰঠাকুৰ • বিশ্বব্রহ্মাণ্ডৰ ৰহস্য ভেদিবলৈ মহাকাশত জেম্‌ছ্‌ ৱেব দূৰবীণ • ৫৫
লোকনাথ গোস্বামী • 'আমাৰ প্রতিনিধি'ৰ স্বর্ণিল কুৰিটা বর্ষ • ৫৭
ড° বিশ্বজিৎ দাস, আদিত্য শইকীয়া • অসমৰ জলবায়ু, পৰম্পৰাগত গৃহ নির্মাণ আৰু ডাকৰ বচন • ৬০
মূল : গোপালকৃষ্ণ দে, অনুবাদ : গীতাশ্রী তামুলী • সতী জয়মতী • ৬৩
পুলিন কলিতা • বন্ধুৰাৰ সংগীতময় সংসাৰ • ৬৭

কবিতা | ৰফিকুল হোছেইন • ৭২
ড° যতীন কোঁৱৰ, নীলিম কুমাৰ • ৭৩
দেৱানন্দ ভট্টাচার্য্য, উৎপল কলিতা • ৭৪
ককেনা ঠাকুৰীয়া, অজ্ঞানজ্যোতি দেউৰী • ৭৫
চন্দন গোস্বামী, সপোনজ্যোতি মৰিগগ্রা • ৭৬

গল্প | কল্পলোচন পাঠক • খোজ • ৭৮
মণিকা দেৰী • জোৰা লগা ঘৰ • ৮২
ডাঃ নয়নজ্যোতি শর্মা • ৰে-ঘ-নী-সে-হা-সু-ৰ • ৮৫
অপু ভৰদ্বাজ • মাংস • ৯০

অনুবাদ গল্প | মূল : দামোদৰ মউজু, অনুবাদ : উৎপল বৰুৱা • মহাজীৱনৰ বস্তি
মূল : কিনফাম্ সিং নংকিন্‌ৰি, অনুবাদ : ড° স্বাতী কিৰণ • জাপি

কোংকনী সাহিত্যিক দামোদৰ মউজুৰ সৈতে কথোপকথন হিল্লোল কুমাৰ পাঠক আৰু মৃণ্ময় ভূঞা ২০

C.T.C. Copy

Principal
Nowgong Girls' College
Nagaon :: Assam

Nowgong Girls' College
ESTD: 1962
Nagaon :: Assam

অসমৰ জলবায়ু, পৰম্পৰাগত গৃহ নিৰ্মাণ আৰু ডাকৰ বচন

ড° বিশ্বজিৎ দাস
আদিত্য শইকীয়া

শক্তি, স্থাপত্যবিদ্যা আৰু পৰিবেশ— এই তিনিওটাৰ মাজত অনন্য সম্পৰ্ক বিদ্যমান। শক্তি আৰু স্থাপত্যবিদ্যাৰ সমান্তৰালকৈ পৰিবেশৰ উন্নয়ন হোৱাটো নিতান্তই প্ৰয়োজনীয়। বিজ্ঞানৰ ঋণাত্মক প্ৰয়োগ, অবহনক্ষম উন্নয়ন আদিৰ লগত সংগতি ৰাখি আধুনিক মানুহে উন্নত আৰু অত্যধিক বৈষয়িক মান বৃদ্ধিৰ কাৰণে আধুনিক স্থাপত্যবিদ্যাৰে সৃষ্টি কৰা ঘৰসমূহে শক্তি অপচয়ৰ জৰিয়তে গোলকীয় উত্তাপ বৃদ্ধি কৰি পৰিবেশৰ ওপৰত বিৰূপ প্ৰভাৱ পেলায়।

> 'US energy information administration illustrates that buildings are responsible for almost 48% of total energy consumption and responsible for sustantial amount of green house gas emission.'

গৃহ নিৰ্মাণৰ ক্ষেত্ৰত জলবায়ু, আৰ্দ্ৰতা, ৰতাহৰ গতিবেগ, ৰতাহৰ দিশ, ৰৰষুণ, সৌৰতাপ বিকিৰণ, বায়ুৰ উষ্ণতা আদি বিষয়ে গুৰুত্বপূৰ্ণ ভূমিকা গ্ৰহণ কৰে। এইবোৰৰ ওপৰি পৰিবেশমিত্ৰ গৃহ নিৰ্মাণ কৰিবলৈ হ'লে সেই নিৰ্দিষ্ট এলেকাত বসবাস কৰা সেই জাতিটোৰ সামাজিক-সাংস্কৃতিক-শাৰীৰিক গঠন, জীয়াই থকাৰ প্ৰণালী, নিৰ্দিষ্ট এলেকাত প্ৰাপ্ত গৃহ নিৰ্মাণৰ সামগ্ৰী আৰু অতীজৰে পৰা জাতিটোৱে সম্মুখীন হৈ অহা বিভিন্ন প্ৰাকৃতিক দুৰ্যোগ আদিৰ ইতিহাস জনাটো অতি প্ৰয়োজনীয়। অসমীয়া জাতি এনেধৰণৰ ইতিহাসেৰে সমৃদ্ধ এটা জাতি। সেই অনুসাৰে পাৰিপাৰ্শ্বিকভাৱে সচেতন অসমীয়া জাতিয়ে এই সকলো [illegible] অসমৰ জলবায়ুৰ লগত খাপ খুৱাই ডাকৰ বচনত গৃহ নিৰ্মাণৰ পৰিবেশ [illegible] দাঙি থৈ গৈছে।

C.T.C.
Principal
Nowgong Girls' College
Nagaon :: Assam

Nowgong Girls' College
ESTD: 1962
Nagaon :: Assam

'পুবা-পশ্চিমাকৈ সাজিবা ঘৰ
অকাল মৃত্যুক নাহিকে ডৰ।
পুবে ভঁৰাল দক্ষিণে গঁৰাল
উত্তৰে চৰু দক্ষিণে গৰু।
পশ্চিমে বাঁহ পুবে বেত
উত্তৰে তামোল-পাণ, দক্ষিণে খেত।।'

ঘৰৰ লগত বাৰীত থকা বিভিন্ন উপাদান—

'পুবে ভঁৰাল পশ্চিমে গঁৰাল।
উত্তৰে চৰু দক্ষিণে গৰু
উত্তৰে বাঁহ, দক্ষিণে হাঁহ।।
দাঁতিত কঁঠাল, মাজত আম।
তেৰে জানিবা বাৰীৰ কাম।।
পুবে ভানু পশ্চিমে ছায়া।
তেৰে জানিবা বাৰীৰ কাথা।।'

'নৱে দেৰে সাজিবা ঘৰ।
এখানি নাটে দুখানি কৰ।।
চাল সম কৰি মাড়লি দিবা।
লংকাৰ বণিজ হাততে পাবা।।
জতেক ৰুয়া ততেক লবা।
তাৰ তিনি জোখা মাগুলি দিবা।।'

পৰম্পৰাগত অসমীয়া সমাজত ঘৰ-দুৱাৰ নিৰ্মাণ কৰোঁতে ডাকৰ বচনৰ ৰীতি-নীতিবোৰ সসম্ভ্ৰমে মানি চলা হয়। ডাকৰ বচনত সন্নিবিষ্ট এই ৰীতি-নীতিসমূহ মানি চলাৰ জৰুৰালত প্ৰাকৃতিক শক্তিৰ সুব্যৱহাৰৰ প্ৰসংগ জড়িত হৈ আছে। অসমীয়া সমাজখনে সূৰ্যৰ বশ্মিৰ লগত সংগতি ৰাখি ঘৰৰ স্থিতি নিৰূপণ কৰিছিল। অসমৰ জলবায়ুৰ লগত খাপ খুৱাই প্ৰকৃতিৰ পৰা অনায়াসে লাভ কৰিব পৰা সৌৰশক্তি সাধ্যানুসাৰে যাতে ব্যৱহাৰ কৰিব পৰা যায় সেই উদ্দেশ্যে পৰম্পৰাগত অসমীয়া সমাজখনে ঘৰ-দুৱাৰ পুবা-পশ্চিমাকৈ আৰু দক্ষিণমুৱাকৈ নিৰ্মাণ কৰিছিল। সৌৰশক্তি বা সূৰ্যৰ বশ্মিয়ে ঘৰ এটা আলোকিত কৰাৰ লগতে প্ৰাকৃতিকভাবে নিৰাময় আৰু সজীৱ কৰাত গুৰুত্বপূৰ্ণ ভূমিকা পালন কৰে।

'Natural lighting will reduce the production of harmful bacteria and organism that can grow in any house. Natural light is terrific for a healthy complexion.'

সূৰ্যৰ বশ্মি ঘৰৰ সমান্তৰালকৈ মানুহৰ কাৰণেও উপকাৰী। বিভিন্ন বেমাৰ-আজাৰৰ পৰা এই বশ্মিয়ে মানুহক ৰক্ষা কৰে।

'The sun is the best source of vitamin D. When your skin is exposed to sunlight it makes vitamin D from cholesterol. The sun's ultraviolet B(UVB) rays hit cholesterol in the skin cells, providing the energy for vitamin D synthesis to occur. Vitamin D has many roles in the body and essential for optimal health.'

পুৰণি অসমীয়া সমাজৰ পৰম্পৰাগত ঘৰবোৰত বাঁহৰ বেৰ দিয়া, বেৰত পাতলীয়াকৈ মাটি লেপা, বাঁহেৰে ঘৰ বনোৱা আদিৰ মূলতে এই সূৰ্যৰ বশ্মি যাতে সেই উপাদানবোৰৰ মাজেৰে অনায়াসে প্ৰতিসৰণ হয়। ডাকৰ বচনৰ উল্লিখিত গৃহ নিৰ্মাণ প্ৰণালীৰ লগত জড়িত ৰীতি-নীতি আৰু ব্যৱহৃত প্ৰাকৃতিক উপাদানসমূহে অসমৰ নাতিশীতোষ্ণ জলবায়ুৰ বিষয়েও নিদৰ্শন দাঙি ধৰে। প্ৰকৃততে পাৰিপাৰ্শ্বিকভাৱে সচেতন পুৰণি অসমীয়া সমাজে অসমৰ জলবায়ুৰ লগত সংগতি ৰাখিবলৈ গৈ প্ৰকৃতিৰ পৰা এই সম্পদবোৰ নিৰ্বাচন কৰি ঘৰ নিৰ্মাণত ব্যৱহাৰ কৰিছিল। পৰম্পৰাগত পুৰণি অসমীয়া সমাজত ঘৰৰ লগতে ভঁৰাল, গোহালি, গঁৰাল আদিৰ স্থিতি সূৰ্যৰ বশ্মিয়ে নিৰূপণ কৰিছিল। সূৰ্যৰ বশ্মিয়ে যাতে নিৰ্দিষ্ট জোখত ঘৰ, ঘৰৰ লগত লাগি থকা বাৰী, ভঁৰাল, গোহালি আদি স্পৰ্শ কৰিব পাৰে সেই উদ্দেশ্যে পুৰণি অসমীয়া সমাজখনে ডাকৰ বচনৰ মাজেৰে ঘৰৰ পুবফালে বেতগছ, উত্তৰে

Principal
Nowgong Girls' College
Nagaon :: Assam

ণ-পাণ আৰু বাঁহ, পশ্চিমে বাঁহ, দক্ষিণে খেতি, দাঁতিত কঁঠাল, বাৰীৰ মাজত আম আদি ৰোপণ দিহা দিছে।

ডাকৰ বচনত উল্লিখিত পৰম্পৰাগত অসমীয়া ঘৰ নিৰ্মাণ প্ৰণালীত ব্যৱহাৰ কৰা সামগ্ৰী ন— ইকৰা, নৰা, খেৰ, বাঁহ আদি অসমৰ প্ৰকৃতি তৰ অৱদানীকৃত অতিকে সহজলভ্য স্থানীয় সম্পদ। তীজৰে পৰা এই সম্পদবোৰে সময়ৰ লগত সংগতি ৰাখি মসাধাৰণৰ অভাৱ পূৰণ কৰি আহিছে। পৰম্পৰাগত সমীয়া সমাজখনে ঘৰ নিৰ্মাণ কৰোঁতে ব্যৱহাৰ কৰা এই ামগ্ৰীবোৰ পাৰিপাৰ্শ্বিক সচেতনতাৰ ফালৰ পৰা যথেষ্ট ুৰুত্বপূৰ্ণ। প্ৰথম হৈছে, ঘৰ নিৰ্মাণ কৰোঁতে প্ৰয়োজনীয় ামগ্ৰীবোৰ প্ৰকৃতিৰ পৰা সংগ্ৰহ কৰি পৰম্পৰাগত অসমীয়া সমাজখনে প্ৰকৃতিৰ লগত পাৰিপাৰ্শ্বিকভাৱে সহযোগিতা কৰাৰ লগতে প্ৰকৃতিৰ প্ৰতি সম্মান প্ৰদৰ্শন কৰিছিল। দ্বিতীয়তে এই সম্পদবোৰ অৰ্থনৈতিকভাৱে অতি সহজলভ্য নবীকৰণযোগ্য আৰু পৰিবেশৰ লগত খাপখোৱা। নৰা, ইকৰা, খেৰ, বাঁহ আদি প্ৰাকৃতিক সম্পদবোৰে প্ৰকৃতিৰ ওপৰত বেয়া প্ৰভাৱ নেপেলায়। ইয়াৰ বিপৰীতে আধুনিক যুগৰ ঘৰ নিৰ্মাণ প্ৰণালীত ব্যৱহৃত ৰড, চিমেণ্ট, শিল, বালি আদি সামগ্ৰীয়ে পৰিবেশৰ ওপৰত সদায় বিৰূপ প্ৰভাৱ পেলায়।

'In modern times building materilals like cement, steel and bricks are highly energy intensive. Different study reported that the embodied energy cost as well as running cost can be significantly reduced is climate responsive building design. Energy effecient building has potential to translate to 1.35 billion tones of carbon.'

তৃতীয়তে ভূমিকম্পকে আদি কৰি অন্যান্য প্ৰাকৃতিক দুৰ্যোগৰ লগত মোকাবেলা কৰাত এই প্ৰাকৃতিক সম্পদবোৰে গুৰুত্বপূৰ্ণ ভূমিকা পালন কৰি আহিছে। এইক্ষেত্ৰত ১৮৯৭ আৰু ১৯৫০ চনত হোৱা প্ৰবল ভূমিকম্প দুটা উল্লেখযোগ্য।

ইকৰা, নৰা, খেৰ, বাঁহ আদি প্ৰাকৃতিক উপাদান শিল, ৰড, ইটা আদিতকৈ যথেষ্ট পাতল আৰু ভূমিকম্পৰ জোকাৰণিৰ লগত মোকাবেলা কৰিব পৰাকৈ নমনীয় গুণ বহুত বেছি। পাৰিপাৰ্শ্বিকভাৱে সচেতন পুৰণি অসমীয়া সমাজখনে প্ৰকৃততে, প্ৰাকৃতিক দুৰ্যোগৰ লগত মোকাবেলা কৰাৰ কাৰণেহে এনেধৰণৰ সামগ্ৰীবোৰ প্ৰকৃতিৰ পৰা সংগ্ৰহ কৰিছিল। সেই অনুসাৰে এই সম্পদবোৰে সময়ৰ লগত সংগতি ৰাখি অসমৰ জলবায়ুৰ লগত খাপ খাই ভূমিকম্পৰ লগতে অন্যান্য প্ৰাকৃতিক দুৰ্যোগৰ পৰা অসমীয়া জাতিক ৰক্ষা কৰি আহিছে।

'Performance of traditional houses has been extremely good in several part eartquakes in the region. In the recent 18 september 2011 earthquake (M.6.9), severe damge was observed in reinforced concrete construction. On the other hand, the only damage was observed in Ikara houses due to earthquake shaking alone (not due to lanslide) was to additional classrooms of Ikara type constructed on the thired storey of Govt. secondary school building.'

যুগ যুগ ধৰি জলবায়ু পৰিবৰ্তনে নিজৰ বিশেষ পৰিবৰ্তনৰ চক্ৰত প্ৰকাশ হৈ আহিছে আৰু মানুহ আদিম যুগৰে পৰা তাৰ সাক্ষী হৈ আহিছে। জলবায়ুৰ এনে চক্ৰত অতীতৰ পৰিবৰ্তনৰ বুৰঞ্জী বিষয়ে বুজি পোৱাত আৰু অদূৰ ভৱিষ্যতৰ জলবায়ু সম্পৰ্কে আভাস দিয়াত ডাকৰ বচনে যথেষ্ট অবিহণা দিব পাৰে। সেই অনুসাৰে ডাকৰ বচনত পশ্চিম, উত্তৰ আৰু দক্ষিণে মেঘে গাজিলে ধুমুহা আৰু ববষুণ দুয়োটা অহাৰ সম্ভাৱনা ব্যক্ত কৰিছে। ইয়াৰ বিপৰীতে পুবফালে গাজনি মাৰিলে বিপদৰ আশংকা কম বুলি কৈছে। ডাকৰ বচনত এইবোৰ দিশৰ আঁৱত দীৰ্ঘদিনৰ অভিজ্ঞতাই সক্ৰিয় ভূমিকা পালন কৰে আৰু ইয়াৰ দ্বাৰা সম্ভাব্য ধ্বংসকাৰী প্ৰাকৃতিক দুৰ্যোগৰ ফলত হ'ব পৰা বিপৰ্যয়, মৃত্যু আদি ৰোধৰ কাৰণে বহুতো ব্যৱস্থা ল'ব পৰা যায়। এনেদৰে আগলি ৰতৰা দিয়াত ডাকৰ বচনে অসমীয়া সমাজত প্ৰচুৰ সম্ভাৱনা ব্যক্ত কৰি আহিছে।

'পশ্চিমে গাজিলে নুমাবা জুই,
পুবে গাজিলে থাকিবা শুই।'
'উত্তৰে গাজিলে জানিবা খৰ
দক্ষিণে গাজিলে মাৰিবা লৰ।'
'পুহৰ আদি মাঘৰ শেষ
তেহে চাবা জাৱৰ ঠেহ।'

জলবায়ুৰ লগতে নৈৰ প্ৰকৃতিৰ কথাও ডাকৰ বচনত উল্লেখ আছে—

'নদীৰ কাষত ল'লে ঘৰ,
অ'ৰ পৰা ত'লৈ লৰ।'
'নৈৰ বন নাই খাদে আৰু পোতে,
বিষয়াৰ বন নাই ভাতে আৰু পাতে।'

এনেদৰে পৰিবেশবিজ্ঞানৰ আনুষ্ঠানিক জ্ঞান নথকা সময়ত পৰম্পৰাগত কৃষিজীৱী সমাজত পৰিবেশমিত্ৰ বহুতো কাম-কাজ মানুহে কৰিছিল। সাধাৰণ মানুহবোৰ অশিক্ষিত আছিল যদিও পৰম্পৰাগত বিধি-বিধান তেওঁলোকে পালন কৰিছিল আৰু এনেধৰণৰ বিধি-বিধানৰ দ্বাৰা প্ৰত্যক্ষ বা পৰোক্ষভাৱে পৰিবেশ সংৰক্ষণ হৈছিল।

লেখকদ্বয়ৰ ঠিকনা : [illegible]
ছোৱালী মহাবিদ্যালয়ৰ [illegible] ছাত্ৰ, অসম
[illegible] বিশ্ববিদ্যালয়

Nowgong Girls' College
ESTD: 1962
Nagaon :: Assam
Principal
Nowgong Girls' College
Nagaon :: Assam

ISSN 2278-4004
UGC CARE List

प्राच्या
PRĀCYĀ

(A Peer Reviewed (Refereed) Journal on
Sanskrit & Related Studies)

Vol. XIII

SĀṀKHYA-YOGAVIŚEṢĀṀKAḤ

सांख्य-योगविशेषांकः

Principal
Nowgong Girls' College
Nagaon :: Assam

Department of Sanskrit
M.D.K. GIRLS' COLLEGE
DIBRUGARH
2021

Nowgong Girls' College
ESTD: 1962
Nagaon :: Assam

CONTENTS

1. Early Tamil Schools of Yoga
   — Dr. K. S. Balasubramanian

2. Yama : From Yogi to Common Man-A Hermeneutic Study on the Moral Restraint of Yoga
   — Dr Anamika Sarmah

3. Sāṁkhyatattvakaumudī -Commentary or Sāṁkhyakārikā-Theistic approach to Sāṁkhy
   — Dr.K.Vimuna Devi

4. A Comparative Study of the Concept of Self Revealed in the Kaṭhopaniṣad and Bhagavadgītā from the Perspective of The Sāṁkhya Philosophy
   — Dr Subhra Sabhapandit

5. योगसाधिताद्भुतप्रभावसम्बन्धात्मकप्रकृतिविचारः
   (Principle of Chaityoga as approved by Hathayoga- A Study in the light of Gherandasaṁhitā)
   — Dr. Swapan Nath, & Arpita Nath

6. Awakening of Viveka Through Ākhyāyikās in the Sāṁkhyapravacanabhāṣya
   — A. Chitra

7. Concept of Prakṛti in the Sāṁkhya Philosophy and in the Nāradīyapurāṇa : - A Comparative Study
   — Dr.Aniruddh Adhyaru

8. Dualism in Sāṁkhya and Cartesian Philosophy : An Appraisal
   — Silpi Sikha Mahanta

9. Rāmānujācārya and Aṣṭāṅgayoga
   — Dr. P. C. Muralidharan

10. Space and Time in the Sāṁkhya-Yoga Philosophy : An Analytical Study with Special Reference to Radhanath Phukan's View
    — Dr. Rashmi Dixit

11. YOGAPĀDA of Nīlamekha Āgama
    — Ms. Lakshmya. V. Iyengar

12. Sāṁkhya Philosophy and Science : An Exposition by Radhanath Phukan
    — Kusumlata Nath

13. Principle in Sāṁkhya Philosophy : A Critical Exposition
    — Jyotsna Deka

14. Tri Prakṛti, Puruṣatattva of Sāṁkhya as Reflected in the Viṣṇupurāṇa in the light of Sāṁkhyakārikā
    — Dr. Mitali Goswami

15. 'प्रकृति — स्वरूपविवेचन विशेष सन्दर्भ : सांख्यकारिका' An Analysis
    Prakṛti – with special reference to 'Sāṁkhyakārikā' An Analysis
    — Dr. Chandan Hazarika

16. The Sāṁkhya Philosophy As Reflected in The Manūkāvyam and The Puṣkara
    — Dr Mousumi Sharma

17. Concept of Mokṣa in Sāṁkhya Philosophy A Study in the light of Sāṁkhya Kārikā
    — Kabita Deka

18. Sāṁkhya-Yoga Concepts Reflected in The Śivapurāṇa
    — Dr. Sanasiree Saikia

19. A Comparative Study On The Concept of Mokṣa Liberation in Sāṁkhya and Advaita Vedānta
    — Anshuman Adhyaru

20. Yoga And Peace of Mind: Applying Yo... Student
    — Dr. Jayda Begum & Mr. Kusumg...

Principal
Nowgong Girls' College
Nagaon :: Assam

Nowgong Girls' College
ESTD: 1962
Nagaon :: Assam

The Prakṛti and Puruṣatattva of Śaṅkara as Reflected in the Vivaṇapariṇāma in the light of Sāṅkhyakārikā

Dr. Mitali Goswami

CTC
Principal
Nowgong Girls' College
Nagaon :: Assam

Nowgong Girls' College
ESTD: 1962
Nagaon :: Assam

Journal of Applied Biology & Biotechnology Vol. 10(01), pp. 62-67, January, 2022
Available online at http://www.jabonline.in
DOI: 10.7324/JABB.2021.100108

The ITS2 DNA sequence analysis in six species of barbin fishes with phylogenetic insights

Sandip Choudhury[1]*, Briyanka Kashyap[2], Karabi Dutta[2]
[1]Department of Zoology, Nowgong Girls' College, Nagaon, India.
[2]Department of Zoology, Gauhati University, Guwahati, India.

ARTICLE INFO

Article history:
Received on: August 15, 2021
Accepted on: October 04, 2021
Available Online: January 07, 2022

Key words:
ITS2, nuclear DNA, barbin fishes, genetic distance, phylogenetic relationship

ABSTRACT

The internal transcribed spacer 2 (ITS2) nuclear DNA was sequenced for six species of barbin fishes from Assam in the North Eastern region of India. The variations in the sequences were investigated to estimate nucleotide composition, nucleotide diversity, transition-transversion bias, genetic distance, and phylogenetic relationship. From the sequence analysis, it was found that the average *G* + *C* content (64.8%) was more than *A* + *T* content (35.2%). The nucleotide diversity (Pi) was found to be 0.04737. The number of transition substitutions was more than transversion substitutions and the transition–transversion bias was 1.16. Overall mean genetic distance was found to be 0.050 with a range from 0.005716 (between *Puntius sophore* and *Puntius chola*) to 0.084536 (between *Pethia gelius* and *Systomus sarana*). The phylograms constructed by neighbor-joining and maximum likelihood methods resulted in a similar topology where the monophyly of the *Pethia* group was recovered which consists of *P. gelius*, *Pethia ticto*, and *Pethia conchonius*. The two *Puntius* species (*P. sophore* and *P. chola*) were not clustered together and *S. sarana* remained a distinct taxon. The results of the present study partially validated the utility of the ITS2 DNA sequence in genetic diversity and phylogenetic studies in the barbin fishes.

1. INTRODUCTION

The eukaryotic ribosomal DNA genes are arranged in tandemly repeated clusters with each cluster containing the genes for the 18S, 5.8S, and 28S ribosomal RNA (rRNA). The genes are separated by several spacers, the intergenic spacer or non-transcribed spacer, the external transcribed spacer, and the internal transcribed spacer (ITS). Availability of universal Polymerase Chain Reaction (PCR) primers designed from highly conserved regions flanking the ITS, its relatively small size and high copy number enable easy amplification of ITS regions and this makes the ITS regions an interesting subject for evolutionary/phylogenetic investigations [1]. The ITS2 which is flanked by 5.8S rRNA gene and 28S rRNA gene is a phylogenetic marker that has been of broad use in generic and infrageneric level classifications as its sequence evolves comparably fast [2]. Indeed after its first application in 1991 [3], it has been on a rapidly growing number of publications and most extensively it is used in fungal phylogenetics. In spite of its high use in phylogenetic analyses, the number of publications using this marker in phylogenetic studies in fishes is very less and thus provides great opportunity to test the potential of this genetic marker in fish phylogenetics.

The fishes of genus *Puntius* (Cypriniformes: Cyprinidae) which are commonly known as barbs are oriental and widely distributed in South Asia [4]. Because of their wide distribution in the world, these species are of great interest to fish biologists, ecologists, and evolutionary biologists. The status of *Puntius* is unclear, the demarcation and nomenclatural validity of the genus have remained unsettled [5–7]. Scantiness in the knowledge of intergeneric and infrageneric relationships has made the status of this group obscure [8]. Kottelat described *Puntius* as a "catch-all" genus in which a large number of unrelated small barbs have been placed [9]. Pethiyagoda *et al.* [10] recognized five valid [illegible] clades as distinct genera until then it was in use that *Puntius* genus and their work was re-evaluated and supported [11] with

*Corresponding Author
Sandip Choudhury, Department of Zoology, Nowgong Girls' College, Nagaon, India. E-mail: [illegible]choudhury@gmail.com

© 2022 Choudhury et al. This is an open access article distributed under the terms of the Creative Commons Attribution License -NonCommercial-ShareAlike Unported License (http://creativecommons.org/licenses/by-nc-sa/3.0/).

Principal
Nowgong Girls' College
Nagaon :: Assam

Nowgong Girls' College ESTD: 1962 Nagaon :: Assam

some modifications. There are still so many species under genus *Puntius* whose status is still uncertain.

Different forces have led to the evolution of various molecular markers or gene regions with varying degrees of sequence variation. Thus, appropriate molecular markers or gene regions could be chosen with every caution to deduce a true phylogenetic relationship over a broad taxonomic spectrum. Most of the studies on phylogenetics of *Puntius* and related genus were based on morphology and mitochondrial DNA sequences but very few studies were based on nuclear DNA sequences. There is no report on the utility of ITS2 nuclear DNA on phylogenetic study of puntid and allied species. In the present study, we focussed on the variations of the ITS2 DNA sequences among the selected species and investigating this DNA marker's feasibility in inferring phylogenetic relationship among the selected taxa.

2. MATERIALS AND METHODS

2.1. Taxon Sampling

A total of 60 samples, 10 for each of the 6 barbin fishes under family Cyprinidae *viz. Puntius chola, Puntius sophore, Pethia gelius, Pethia conchonius, Pethia ticto,* and *Systomus sarana* were collected from Kamrup Metropolitan and Golaghat districts of Assam by random sampling. The GenBank accession numbers of the genetic markers used for the specified samples are given (Table 1). The species were identified by the use of taxonomic keys prepared by [4,12-14].

2.2. Extraction of Genomic DNA

For genomic DNA extraction, the phenol/chloroform extraction procedure [15] was used with some modifications. Quantity and quality assessment of extracted genomic DNA was done by spectrophotometry by reading the absorbance at 260 nm of wavelength [16,17] and ethidium—bromide-stained agarose gel electrophoresis technique [16].

2.3. Amplification and Sequencing

For amplification of the nuclear ITS2 DNA marker, the following universal primers were used—Forward primer ITS2 F1 (5'-gcaggacacattgatcatcgacac-3') and Reverse primer ITS2 F2 (5'-ggctcttcctcttcgctcgc-3'). Amplification was done in 30 µl volume in each 0.2 ml labeled PCR tubes containing 30 pmol of each forward and reverse primers, 2.5 µl of 2.5 mM deoxyribonucleotide triphosphate (dNTPs), 3 µl of taq buffer (10×), 1.5 µl of $MgCl_2$ (50 mM), 0.5 µl of taq polymerase (5 µ/µl), 11.5 µl nuclease-free double distilled water, and 5 µl template DNA (10 ng/µl). The thermal profile consisted of an initial denaturation step of 5 minutes at 95°C followed by 35 cycles at 94°C for 30 seconds, 65°C for 30 seconds, 72°C for 1 minute and a final elongated extension at 72°C for 10 minutes. The PCR products were kept in hold at 4°C. After this 1/10 volume (3 µl) of 6× gel loading dye was added to each labeled PCR tube and given brief spin. The PCR products were visualized on 1.2% Low melting (LM) agarose gel containing ethidium bromide and the elution was done using HiPurA Agarose gel DNA purification Spin kit (Himedia) following the manufacturer's protocol. The purified products of PCR were used for sequencing. The same PCR primers were used for sequencing. The PCR products were labeled using the BigDye Terminator v.3.1 cycle sequencing kit (Applied Biosystems). Sequencing was run bidirectionally and visualized on an ABI 3730 XL automated DNA Sequencer following the manufacturer's instructions.

Table 1: GenBank accession numbers of the ITS2 DNA sequence of the species.

Sl. No:	Taxon	GenBank accession no.
1	*Puntius chola*	KJ509175
2	*Pethia conchonius*	KJ509176
3	*Pethia gelius*	KJ509177
4	*Systomus sarana*	KJ509178
5	*Puntius sophore*	KJ509179
6	*Pethia ticto*	KJ509180

2.4. Sequence Analysis

The raw sequences were edited using BioEdit software version 5.0.9 [18]. The bad reads (noises) were removed from the sequences (as examined from the electropherogram) and then searched for homology alignment/similarity using Basic Local Alignment Search Tool (BLAST) program of National Center for Biotechnology Information (NCBI) [19]. The edited sequences were submitted to GenBank (NCBI) through Bankit submission tool (NCBI) following the instructors' protocol. The sequences were aligned using the Clustal X 2.1 sequence alignment software [20]. The extent of sequence differences between species was calculated by averaging pair-wise Kimura-2-parameter [21] comparisons of the sequence difference across all the individuals using the Dnadist program of PHYLIP 3.69 package [22]. The number of polymorphic sites, total number of sites, conserved sites, parsimony informative sites, total number of mutations, and nucleotide diversity were estimated using the DnaSp 5.10.01 software [23]. The nucleotide compositions/frequencies, $G + C$ and $A + C$ content, rate of transitions and transversions, transition: transversion bias were calculated by the software MEGA6 [24]. In all analyses, gaps were considered as missing data.

2.5. Phylogenetic Analysis

Phylogenetic relationships were estimated using (1) Distance-based Neighbour Joining (NJ) method and (2) Character-based Maximum Likelihood (ML) method using the PHYLIP package version 3.69 [22]. The distance matrix for the sequences was constructed by the Kimura 2 parameter method [21]. The transition: transversion ratio was taken to be 2.0 and the sites assigned unweighted. Empirical base frequencies were also used. The distance matrix was then used to reconstruct the phylogenetic tree using NJ method in the Neighbour program of PHYLIP 3.69. For the ML method, the Dnaml program of PHYLIP [illegible] used. The transition: transversion ratio was taken to be [illegible] and the sites assigned unweighted. Empirical base frequencies were also used. [illegible] and slow but accurate analysis were employed. The statistical significance of the branching order was assessed by bootstrap resampling

C.T.C.
Principal
Nowgong Girls' College
Nagaon :: Assam
Nowgong Girls' College ESTD: 1962 Nagaon :: Assam

Table 2: Summary of the nucleotide compositions of ITS2 DNA marker sequences of the species under analysis.

Species	T%	C%	A%	G%	Total	(*G* + *C*) %	(*A* + *T*) %
Systomus sarana	18.7	35.6	16.0	29.7	357	65.3	34.7
Puntius chola	19.0	34.7	16.0	30.3	357	65.0	35.0
Puntius sophore	19.0	34.7	15.7	30.5	357	65.3	34.7
Pethia conchonius	18.0	34.4	17.5	30.1	355	64.5	35.5
Pethia ticto	17.5	35.6	17.5	29.4	354	65.0	35.0
Pethia gelius	19.5	34.3	16.8	29.4	364	63.7	36.3
Average	18.6	34.9	16.6	29.9	357	64.8	35.2

technique [25] considering 1,000 pseudo replicates using the Seqboot program of PHYLIP 3.69. The random dataset was analyzed in exactly the same way the original dataset was analyzed and the results from the random datasets were summarized by constructing an extended majority rule consensus tree using the Consense program of PHYLIP 3.69. The consense outtree files were then transferred to the TreeView 1.6.6 software [26] to draw the phylogenetic trees/phylograms with internal edge labels which represent the bootstrap values.

3. RESULTS

The ITS2 DNA sequences which also contain small partial sequences of 5.8S and 28S rRNA genes obtained from the six fish samples ranged in size from 412 bp for *P. sophore* to 375 bp for *P. gelius*. The BLAST search results were found to be good as revealed by the maximum scores and percentage similarity but for a limited number of species. It was found that there were very few available ITS2 sequences at the GenBank database for species under Cyprinidae family which possess significant similarity to the six new sequences. The frequency/composition of nucleotides, *G* + *C* and *A* + *T* content has been listed (Table 2). The multiple sequence alignment used for analyses of the six sequences resulted in 371 nucleotide sites. After excluding the indels/gaps/missing data, the net number of sites equals 349 nucleotides. Sites with alignment gaps/indels/missing data = 22. Invariable (monomorphic)/conserved sites = 308, variable (polymorphic) sites (S) = 41, total number of mutations (Eta) = 42, singleton variable sites = 29, parsimony informative sites = 12, singleton variable sites (two variants) = 29. Parsimony informative sites for two variants = 11 and for three variants = 1. Average number of nucleotide differences ($\hat{K}$) = 16.533 and nucleotide diversity (Pi) = 0.04737.

Table 3: ML estimates of substitution matrix for ITS2 DNA marker sequences. Each entry is the probability of substitution (*r*) from one base (row) to another base (column).

	A	T	C	G
A	-	4.00	7.71	**15.61**
T	3.74	-	**20.72**	6.59
C	3.74	**10.74**	-	6.59
G	**8.85**	4.00	7.71	-

ML estimate of substitution matrix (Table 3) revealed that transition substitutions were more than transversion substitutions. Overall transition and transversion were found to be 55.92 and 44.08, respectively. The estimated transition/transversion bias (*R*) was found to be 1.16. Pairwise nucleotide differences and genetic distance values (K2P) based on ITS2 DNA sequences are listed (Table 4). The overall mean distance was found to be 0.050 with a range from lowest 0.005716 (between *P. sophore* and *P. chola*) to highest 0.084536 (between *P. gelius* and *S. sarana*).

An extended majority rule consensus phylogram/tree was obtained (Fig. 1). No outgroup was used for the tree construction because of unavailability of ITS2 sequences to be appropriate as to be considered as outgroup species. The bootstrap values were indicated at branch nodes. The bootstrap supports were found to be strong for maximum branch nodes. The monophyly of genus *Pethia* was recovered with bootstrap support of 91.8%. The genus *Puntius* represented by *P. chola* and *P. sophore* was found to be non-monophyletic. *P. sophore* was found to be a close relative to the *Pethia* group. *Puntius chola* and *S. sarana* (the only representative of genus *Systomus*) did not show any clustering. The extended majority rule consensus NJ phylogram/

Table 4: Pairwise genetic distance matrix (K2P) based on ITS2 DNA sequences of the analysed taxa.

	Systomus sarana	*Puntius chola*	*Puntius sophore*	*Pethia conchonius*	*Pethia ticto*	*Pethia gelius*
Systomus sarana	0.000000	*	*	*	*	*
Puntius chola	0.014460	0.000000	*	*	*	*
Puntius sophore	0.014460	0.005716	0.000000	*	*	
Pethia conchonius	0.051291	0.041715	0.035639	0.000000	*	
Pethia ticto	0.080035	0.069898	0.063608	0.051348	0.000000	
Pethia gelius	0.084536	0.080956	0.0[illegible]	0.078316	0.071176	0.00[illegible]

Principal
Nowgong Girls' College
Nagaon :: Assam

Nowgong Girls' College
ESTD: 1962
Nagaon :: Assam

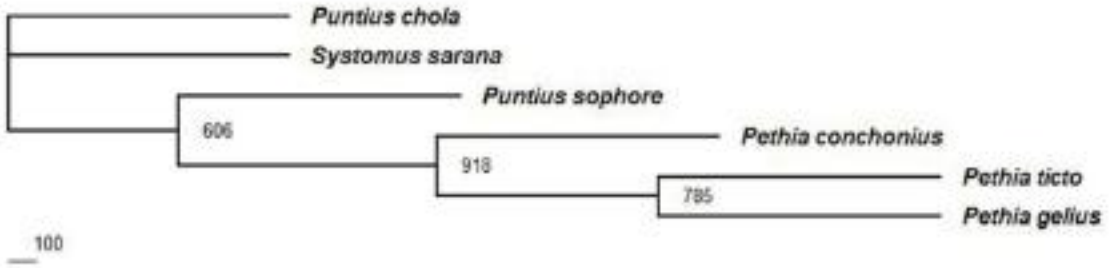

Figure 1: Extended majority—rule consensus ML phylogram (ITS2 DNA sequence datasets). Numbers at branch nodes = bootstrap values (out of 1,000 pseudo replicates).

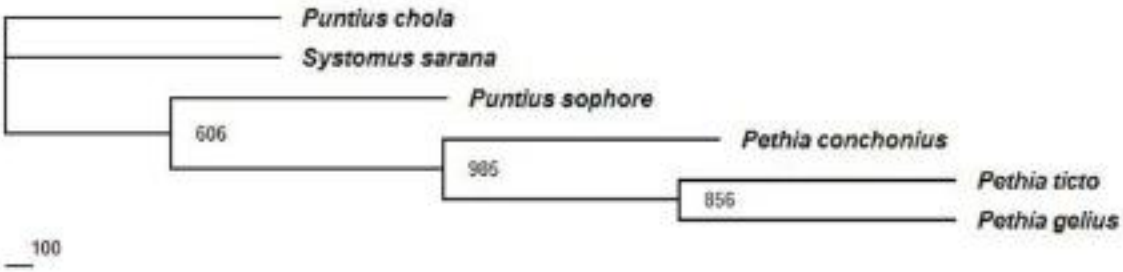

Figure 2: Extended majority—rule consensus NJ phylogram (ITS2 DNA sequence datasets). Numbers at branch nodes = bootstrap values (out of 1,000 pseudo replicates).

tree (Fig. 2) was found to be nearly identical to the ML tree/ phylogram.

4. DISCUSSION

From the sequence analyses of the nuclear ITS2 DNA sequences, it was found that the mean ($G + C$) content (64.8%) of all the species analyzed was more than the mean ($A + T$) content (35.2%) and much higher ($G + C$) content for ITS2 DNA sequences than ($A + T$) content was reported in Brown Trout [27] and Pearl Oyster [28] also. The overall observed transition/transversion bias that was found to be 1.16 indicated the occurrence of transitions more than transversions. Marinho *et al*. [29] also found that for ITS2 DNA sequences transitions were more than transversions. Overall transition (55.92%) which was more than overall transversions (44.08%) is characteristic of the species that have diverged recently from a common ancestor [30]. Transition events more than transversion events were also reported in *Salmo trutta* [27] and five species of fishes of the subfamily Schizothoracinae [31]. The average value of genetic distance (0.050) was found to be low inferring that the species which were analyzed are closely related and are descendants of a near common ancestor. The genetic distance values of the ITS2 DNA sequences of the species analyzed indicate the ability of this marker in describing the interrelationships of the species of fishes studied up to some extent. The nucleotide diversity value of 0.04737 also indicates the closeness of the species analyzed.

In both the ML and NJ methods for the ITS2 DNA sequence analyses, the bootstrap values were satisfactory. This genetic marker was able to distinguish the *Pethia* group as a monophyletic one, which was also found in the previous studies [32,10,33–35,11]. Among the three *Pethia* species in the present study, *P. ticto* and *P. gelius* were found to be more closely related than they are to *P. conchonius*, and *P. sophore* was found to be more closely related to the *Pethia group* than *P. chola*. Based on the Recombination activating gene 2 (RAG2) nuclear gene [36], 16S rRNA gene and cytb gene [10,11], genus *Puntius* was recovered as non-monophyletic and in the present study also, the genus *Puntius* was recovered as non-monophyletic as *P. chola* and *P. sophore* were not clustered together. So, the status of *Puntius* genus from the above and the present study is found to be obscure. The results of the nuclear ITS2 DNA sequence analyses somewhat resembled previous studies but to validate its potential and to test the robustness of this genetic marker for phylogenetic studies in fish, further studies using ITS2 secondary structure, larger sampling size are required. There are evidences that usually support increasing taxon sampling [illegible] at the expense of great quantities of character data [illegible] accuracy of topologies [37].

Principal
Nowgong Girls' College
Nagaon :: Assam

Nowgong Girls' College
ESTD: 1962
Nagaon :: Assam

5. CONCLUSION

In conclusion, ITS2 DNA sequence variation among the taxa observed in the present study was partially able to establish their phylogenetic relationship as the monophyly of genus *Pethia* was established but the status of genus *Puntius* was found to be obscure. Our understanding of the study of phylogenetic relationships of fish taxa using ITS2 DNA marker is growing but much more studies are required to validate its potential. The present study paves a way for further studies in evaluating the potential of this DNA marker in fish phylogenetics.

7. ACKNOWLEDGEMENTS

The authors are thankful to Dr. Pranjan Barman, Dept. of Biotechnology, Gauhati University and Dr. Lingaraj Sahoo, Dept. of Biotechnology, Indian Institute of Technology - Guwahati for providing laboratory facilities and guidance.

6. AUTHOR CONTRIBUTIONS

All authors made substantial contributions to conception and design, acquisition of data, or analysis and interpretation of data; took part in drafting the article or revising it critically for important intellectual content; agreed to submit to the current journal; gave final approval of the version to be published; and agree to be accountable for all aspects of the work. All the authors are eligible to be an author as per the international committee of medical journal editors (ICMJE) requirements/guidelines.

7. FUNDING

There is no funding to report.

8. CONFLICTS OF INTEREST

The authors report no financial or any other conflicts of interest in this work.

9. ETHICAL APPROVALS

This study does not involve experiments on animals or human subjects.

10. PUBLISHER'S NOTE

This journal remains neutral with regard to jurisdictional claims in published institutional affiliation.

REFERENCES

1. Coleman AW. ITS2 is a double-edged tool for eukaryote evolutionary comparisons. Trends Genet 2003;19:370–5.
2. Schultz J, Müller T, Achtziger M, Seibel PN, Dandekar T, Wolf M. The internal transcribed spacer 2 database—a web server for (not only) low level phylogenetic analyses. Nucleic Acids Res 2006;34(suppl_2):704–7.
3. Porter CH, Collins FH. Species-diagnostic differences in a ribosomal DNA internal transcribed spacer from the sibling species *Anopheles freeborni* and *Anopheles hermsi* (Diptera: Culicidae). Am J Trop Med Hyg 1991;45:271–9.
4. Talwar PK, Jhingran AG. Inland fishes of India and adjacent countries. Oxford and IBH, New Delhi, India, vol. II, 1991.
5. Hora SL, Mukherji DD. Notes on fishes in the Indian Museum (xxiii). On a collection of fishes S. Shan states, Burma. Rec Indian Museum 1934;36:353–70.
6. Smith HM. The fresh-water fishes of Siam, or Thailand. Bulletin of U.S. National Museum i-xi, Washington, USA. 1945.
7. Myers GS. Preface to any future classification of the cyprinid fishes of the genus *Barbus*. Stanford Ichthyol Bull 1960;7:212–5.
8. Kullander SO, Fang F. Two new species of *Puntius* from Northern Myanmar (Teleostei: Cyprinidae). Copeia 2005;2005:290–302.
9. Kottelat M. Nomenclature of the genera *Barbodes, Cyclocheilichthys, Rasbora* and *Chonerhinos* (Teleostei: Cyprinidae and Tetraodontidae), with comments on the definition of the first reviser. Raffles Bull Zoo 1999;47:591–600.
10. Pethiyagoda R, Meegaskumbura M, Maduwage K. A synopsis of the South Asian fishes referred to *Puntius* (Pisces: Cyprinidae). Ichthyol Explor Freshwaters 2012;23:69–95.
11. Ren Q, Mayden RL. Comparative phylogenetics of the Asian genus "*Puntius*" and relatives (Cypriniformes; Cyprinidae): explorations into the potential impacts of taxon and character sampling. J3 Biodiversity 2019;3:1–19.
12. Jayaram KC. The freshwater fishes of the Indian region. Narendra Publishing House, New Delhi, India, 1999.
13. Vishwanath W. Fishes of North East India: a field guide to species identification. Manipur University, Imphal, India, 2002.
14. Frose R, Pauly D. FishBase. World Wide Web electronic publication. 2010. Available via http://www.fishbase.org. Version (11/2010)
15. Sambrook J, Fritsch EF, Maniatis T. Molecular cloning: a laboratory manual. 2nd edition, Cold Spring Harbor laboratory press, New York, NY, 1989.
16. Sambrook J, Russell DW. Molecular cloning: a laboratory manual. 3rd edition, Cold Spring Harbor laboratory press, New York, NY, 2001.
17. Carlos F, Barbas III, Dennis RB, Jamie KS, Gregg JS. Quantitation of DNA and RNA. Cold Spring Harbor laboratory press, New York, NY, 2007.
18. Hall TA. BioEdit: a user-friendly biological sequence alignment editor and analysis program for Windows 95/98/NT. Nucleic Acids Symp Ser 1999;41:95–8.
19. McGinnis S, Madden TL. BLAST: at the core of a powerful and diverse set of sequence analysis tools. Nucleic Acids Res 2004;32(suppl_2):W20–5.
20. Larkin MA, Blackshields G, Brown NP, Chenna R, McGettigan PA, McWilliam H, *et al.* Clustal W and Clustal X version 2.0. Bioinformatics 2007;23:2947–8.
21. Kimura M. A simple method for estimating evolutionary rates of base substitutions through comparative studies of nucleotide sequences. J Mol Evol 1980;16:111–20.
22. Felsenstein J. PHYLIP ver. 3.69. University of Washington, Seattle, WA, 2009.
23. Librado P, Rozas J. DnaSP v5: a software for comprehensive analysis of DNA polymorphism data. Bioinformatics 2009;25:1451–2.
24. Tamura K, Stecher G, Peterson D, Filipski A, Kumar S. MEGA6: molecular evolutionary genetics analysis version 6.0. Mol Biol Evol 2013;30(12):2725–9.
25. Felsenstein J. Confidence limits on phylogenies: an approach using the bootstrap. Evolution 1985;39:783–91.
26. Page RDM. TreeView version 1.6. 6. University of Glasgow, Glasgow, UK, 2001.
27. Presa P, Pardo BG, Martinez P, Bernatchez L. Phylogeographic congruence between mtDNA and rDNA ITS markers in brown trout. Mol Biol Evol 2002;19:2161–75.
28. He M, Huang L, Shi J, Jiang Y. Variability of ribosomal DNA ITS-2 and its utility in detecting genetic relatedness of pearl [illegible] Mol Biotechnol 2005;7:40–5.
29. Marinho MAT, Junqueira ACM, Azeredo-Espin AML. Evaluation of the internal transcribed spacer 2 (ITS2) as a [illegible] marker for phylogenetic inference using sequence and [illegible]

C.T.C.
Principal
Nowgong Girls' College
Nagaon :: Assam

Nowgong Girls' College
ESTD: 1962
Nagaon :: Assam

information in blow flies (Diptera: Calliphoridae). Genetica 2011;139:1189–207.
30. Orti G, Bell MA, Reimchen TE, Meyer A. Global survey of mitochondrial DNA sequences in the three spine stickleback: evidence for recent migrations. Evolution 1994;48:608–22.
31. Ashoktaru B, Ali S, Sati J, Sivaraman GK. Phylogenetic analysis of fishes of the subfamily Schizothoracinae (Teleostei: Cyprinidae) from Indian Himalayas using cytochrome b gene. Indian J Fish 2012;59:43–7.
32. Shantakumar M, Vishwanath W. Inter-relationship of *Puntius* Hamilton-Buchanan (Cyprinidae: cyprininae) found in Manipur, India. Zoo's Print J 2006;21:2279–83.
33. Pallavi, Goswami M, Nautiyal P, Malakar AK, Nagpure NS. Genetic divergence and molecular phylogenetics of *Puntius* spp. based on the mitochondrial cytochrome b gene. Mitochondrial DNA 2012;23: 77–483.
34. Saroniya RK, Nagpure NS, Saksena DN, Basdeo K, Ravindra K, Mahender S, *et al.* Phylogenetic analysis of some *Puntius* species based on 18S rDNA. Eur J Biotechnol Biosci 2016;4:42–7.
35. Gupta D, Dwivedi AK, Tripathi M. Taxonomic validation of five fish species of subfamily Barbinae from the Ganga river system of northern India using traditional and truss analyses. PLoS One 2018;13:1–21.
36. Yazdani MF, Aliabadian M, Khalijah DS, Seifali M. Molecular phylogeny of the *Puntius* (Hamilton, 1822) based on nuclear gene RAG2. Prog Biol Sci 2012;2:66–75.
37. Mayden RL, Chen WJ, Bart HL, Doosey MH, Simons AM, Tang KL, *et al.* Reconstructing the phylogenetic relationships of the earth's most diverse clade of freshwater fishes - order Cypriniformes (Actinopterygii: Ostariophysi): a case study using multiple nuclear loci and the mitochondrial genome. Mol Phylogenet Evol 2009;51:500–14.

How to cite this article:
Choudhury S, Kashyap B, Dutta K. The ITS2 DNA sequence analysis in six species of barbin fishes with phylogenetic insights. J Appl Biol Biotech 2022; 10(01):62–67.

Principal
Nowgong Girls' College
Nagaon :: Assam

Nowgong Girls' College
ESTD: 1962
Nagaon :: Assam

Plasma Chemistry and Plasma Processing
https://doi.org/10.1007/s11090-021-10215-1

ORIGINAL PAPER

Effects of Dielectric Barrier Discharge Plasma on Physicochemical Characteristics, Mechanical Properties and Biocompatibility of Silk/PVA Nanofibers

Namita Ojah[1] · Susmita Thakur[2] · Dolly Gogoi[3] · Gazi Ameen Ahmed[1] · Manabendra Mandal[2] · Robin Doley[2] · Arup Jyoti Choudhury[1,4]

Received: 13 January 2021 / Accepted: 21 October 2021
© The Author(s), under exclusive licence to Springer Science+Business Media, LLC, part of Springer Nature 2021

Abstract

This work reports an investigation of the discharge characteristics of atmospheric dielectric barrier discharge (DBD) plasma in terms of I-V curves and Lissajous figures and their effect on the surface functionalities of electrospun silk/PVA nanofibers. The results show that the filamentary discharge is predominant at lower electrode gap (3 mm) and then significantly reduces at higher electrode gaps of 6 mm and 10 mm, respectively and in the applied voltage range of 11–17 kV. The silk/PVA nanofibers which are treated with 6 mm electrode gap shows good wettability, higher surface energy, higher tensile strength, young's modulus values and improved anti-thrombogenic property. All these findings suggest that, although the silk/PVA nanofiber itself can be used in biomedical applications however, nanofibers plasma treated at 6 mm electrode gap shows better results in terms of physical and biological performances.

Keywords Dielectric barrier discharges (DBD) · Plasma treatment · Surface modification · Mechanical properties, cell viability

Introduction

Silk fibroin based nanofibers have rapidly emerged as potential biomaterials for various biomedical applications [1–3]. The advantages of silk fibroin based nanofibers include but not limited to their outstanding properties such as biocompatibity, flexibility, controlled microporous structure, large surface to volume ratio and morphology similar to that of native

✉ Arup Jyoti Choudhury
arupjchoudhury@gmail.com

1 Laboratory for Plasma Processing of Materials, Department of Physics, Tezpur University, Napaam, Tezpur, Assam 784028, India

2 Department of Molecular Biology and Biotechnology, Tezpur University, Napaam, Tezpur, Assam 784028, India

3 Central Instruments Facility, Indian Institute of Technology, Guwahati, Assam 781039, India

4 Department of Physics, Guwahati College, Bamunimaidam, Guwahati, Assam 781021, India

Principal
Nowgong Girls' College
Nagaon :: Assam

Nowgong Girls' College ESTD: 1962 Nagaon :: Assam

Published online: 03 November 2021
Springer

extracellular matrix [1–5]. Accordingly the silk fibroin based nanofibers have been widely explored as scaffolds for tissue engineering and wound dressing materials [4–6]. However, due to inherent hydrophobicity of silk fibroin and poor mechanical behavior of the nanofibers, preparation of silk fibroin based nanofibers and manipulation of their surface properties of still remains a challenge to fully explore their potential usage as biomaterials [7–10].

As a promising and versatile modification method, non-thermal plasma treatment has been extensively utilized in surface modification and functionalization of polymeric biomedical [11–14]. Due to its efficacy in controlling and reproducing the surface properties of polymers without affecting their bulk properties, versatility and environment friendly, selective treatment and sterilization of polymer surface in single step and improving surface biocompatibility for cell growth and proliferation and immobilization of bioactive proteins, non-thermal plasma treatment has drawn significant research interest in clinical applications and biomedical engineering [15–17]. Non-thermal plasma treatment further enables rapid processing of polymers with shorter treatment time without the use of any solvent and chemical as compared to wet surface modification [18–20].

Non-thermal plasma treatment has been used extensively to improve bioactivities of silk and silk-based biopolymers by modifying surface chemical composition and grafting specific functional groups onto the surface [16, 18, 20, 21]. Significant efforts have been made to investigate the effect of low pressure non-thermal plasma to enhance biocompatiblity and cellular interactions of silk and silk-based biopolymers whereas atmospheric pressure plasma is being less explored in this regard [16, 18, 20, 22]. Atmospheric pressure plasma has the advantage of processing and maintenance cost reduction and ease of operation without any need of sophisticated and expensive vacuum systems and therefore this technique can be utilized as an alternative to low pressure plasmas for surface modification of silk and silk-based biopolymers [15, 16]. In atmospheric pressure plasma, the efficiency of the plasma treatment is influenced by the processing parameters such as electrode gap, operating voltage, gas flow rate etc. and proper control of these parameters enables to sustain uniform glow discharges at atmospheric pressure which is important for effective and uniform surface treatment of silk and silk-based biopolymers [17, 19, 22–24]. Using optimized atmospheric pressure plasma treatment conditions, the potentialities of silk and silk-based biopolymers with improved hydrophilicity, mechanical robustness and biocompatibility can be explored in various biomedical and bioengineering applications [17–19, 22–24].

In this work, surface modification of silk/PVA nanofibers has been carried out using DBD plasma at atmospheric pressure. The operating plasma parameters are optimized to achieve uniform discharge for effective surface treatment of silk/PVA nanofibers. The effect of plasma treatment, at optimized discharge conditions, on physicochemical and mechanical properties and biocompatibility of silk/PVA nanofibers is further investigated. The untreated and plasma treated silk/PVA nanofibers are subjected to various characterization techniques and the observed properties are attempted to correlate with the optimized plasma discharge conditions.

Principal
Nowgong Girls' College
Nagaon :: Assam

Experimental

Materials

B. mori silk cocoons are collected from central silk board, Guwahati, Assam, India. Polyvinyl alcohol (PVA) of molecular weight 145 kDa is purchased from Merck, India. Sodium bicarbonate ($NaHCO_3$ > 99%) and Lithium bromide (LiBr > 99%) are supplied by Sigma

Nowgong Girls' College
ESTD: 1962
Nagaon :: Assam

Aldrich, USA and Tokyo Chemical Industries, Japan, respectively. All chemical reagents are analytical reagent grade and used as received. The cellulose dialysis membrane (12 kDa molecular weight cut off) is supplied by Himedia, India.

Preparation of Silk Fibroin/PVA Solutions

B. mori silk fibroin solution is prepared as per the protocol previously described [16]. Briefly the raw *B. mori* silk cocoons are cut into pieces and boiled for 30 min in aqueous 0.02 M Na_2CO_3 and then rinsed thoroughly with water to extract the glue-like sericin proteins by means of the process known as degumming. The degummed silk is then dissolved in 9.3 M LiBr solution at 60 °C for 4 h yielding a 7% (w/v) solution. The dissolved solution is dialyzed against deionized water using 12 kDa dialysis membrane for 3 days with frequent change in water to remove the LiBr. The resulting solution is then centrifuged at 5000 rpm for 10 min to remove aggregates and debris. The purified SF solution is stored at 4 °C for further use.

An 8% (w/v) PVA solution is prepared by dissolving PVA in distilled water at 80 °C with vigorous stirring for a period about 3 h [16]. After cooling to room temperature, the PVA solution is kept overnight to remove trapped air bubbles. Afterward, both silk and PVA solutions are mixed at a ratio of 2:1 (silk: PVA) with mild stirring for 15 min at room temperature [18]. The final blend solution is kept at 4 °C until further use.

Electrospinning of Silk/PVA Solution

The electrospinning of blend silk/PVA solution is performed at room temperature. The schematic diagram of the method of *B. mori* silk fibroin solution preparation and the electrospinning setup is shown in Fig. 1A. The silk/PVA mixed solution is loaded into a 5 ml syringe with a 22 gauge stainless steel needle having an inner diameter of 0.6 mm. The positive electrode of a high voltage power supply is connected to the needle using an alligator clip and the nanofibers are collected on a grounded aluminum foil which is used as the collector. The high voltage is set at 18 kV, tip-to-collector distance was fixed at 12 cm and flow rate of the solution is maintained at 0.5 ml/hr. Finally, the aluminum foil with the electrospun nanofibrous mat is dried in vacuum for 12 h.

DBD Plasma Treatment

The schematic diagram of the experimental DBD setup and measurement is shown in Fig. 1B. The discharge is generated between two square plane-parallel copper electrodes with an area of 250 mm × 250 mm and both of them are covered by quartz glass plate with a thickness of 3 mm and an area of 250 mm × 250 mm as dielectric barrier. The upper electrode is connected with a high voltage power supply (0–40 kV, 50 Hz) and the lower electrode is connected to ground. The samples are placed on the grounded electrode which can be moved mechanically to adjust the discharge gap. The O_2 (Assam Air Products, purity > 99.99%) gas is allowed to enter the discharge chamber and the gas flow rate (2 slpm) is controlled by a digital mass flow controller (Alicat Scintific, USA). In this work, surface treatment of silk/PVA nanofibers is carried out at different discharge gap (3 mm, 6 mm and 10 mm) [illegible] the applied voltage range [illegible] kV (rms). Figure 1A shows the typical images (Nikon DSLR, D5200) of as prepared and

Principal
Nowgong Girls' College
Nagaon :: Assam

Nowgong Girls' College
ESTD: 1962
Nagaon :: Assam

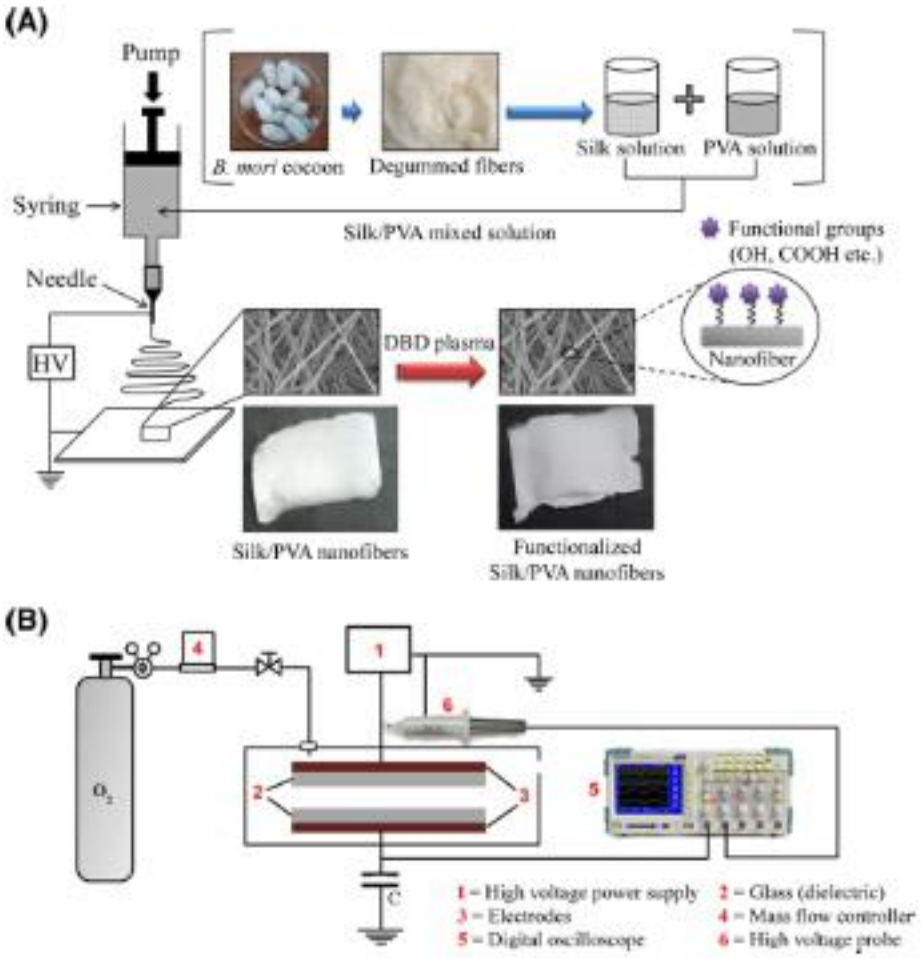

Fig. 1 **A** Schematic of the silk/PVA nanofibers preparation procedure. **B** Schematic diagram of the DBD plasma system and measurement set-up

plasma treated silk/PVA nanofibers obtained at discharge gap of 6 mm and applied voltage of 15 kV, where smooth and pinhole free surface with no morphological alteration due to plasma treatment can be observed.

The voltage applied to the upper electrode is measures using a high voltage probe (Tektronix P6015A, 1000:1) and the current–voltage waveforms are displayed in a dual channel digital oscilloscope (Tektronix TPS2024B, 200 MHz). The instantaneous charge, $Q(t)$ transported to the discharge is calculated by measuring the instantaneous voltage, $V_m(t)$ across capacitor (22 nF) that is connected in series to the ground electrode by applying the following relation [23].

$$Q(t) = C_m V_m(t)$$

where C_m is the capacitance of the capacitor.

Principal
Nowgong Girls' College
Nagaon :: Assam

Nowgong Girls' College
ESTD: 1962
Nagaon :: Assam

A charge–voltage (Q–V) diagram, or Lissajous figure, is obtained by plotting instantaneous charge across the capacitor and the applied voltage against each other [23]. The energy which is consumed during one half-cycle of the discharge is then obtained by measuring the area of the Lissajous figure [23].

Characterization Techniques

Morphological characterization of untreated and plasma treated silk/PVA nanofibers is investigated by field emission electron microscope (FESEM) at 10 kV after sputter-coating with ultrathin layer of gold/palladium alloy. The average diameter of the nanofibers is determined by measuring around 150 nanofibers selected randomly from the FESEM images using Image J software.

The chemical compositions of silk/PVA nanofibers are analyzed by attenuated total reflectance Fourier transform infrared (ATR-FTIR) spectrometer (IMPACT 410 NICOLET, USA). The spectra are obtained as the mean of 32 scans taken in transmittance mode in the range of 650–4000 cm^{-1} with resolution of 4 cm^{-1} at room temperature.

To determine the wettability of silk/PVA nanofibers, the contact angle is measured by a contact angle measurement system (dataphysics OCA 20, Germany). The droplet size is set at 1 µL and immediately after dropping, the image is taken and stored via a CCD video camera, using a PC based acquisition and data processing system. To confirm the uniformity of electrospun nanofibers, the contact angle is measured 15 times at random points on the surface and the result is reported as mean ± standard deviation (SD). The surface energy is calculated by OWRK method using three different liquids (deionized water, n-hexane and diiodomethane).

The mechanical properties of the silk/PVA nanofibers are evaluated using a tensile tester (INSTRON 4204) at a constant speed of 5 mm min^{-1} with a 10 N load. Each sample is cut into rectangular strip with a length of 30 mm and a width of 10 mm. For each sample, data is taken for five times and the average of Young's modulus of elasticity, tensile strength and elongation at break (%) are evaluated from stress–strain curves. The results are presented as average ± standard deviation (SD) [15, 18].

Hemocompatibility Studies

Fresh Venous blood is collected from a healthy human donor in heparinized tubes, stored at 4 °C and used immediately after collection. The plasma treated (at discharge gaps of 6 mm and 10 mm, respectively and applied voltage range of 11–17 kV) and untreated silk/PVA nanofibers (0.5 cm^2) are incubated with 150 µL of human blood with 10% RBC suspension (prepared with 0.9% NaCl) and volume is adjusted to 2 ml with 0.9% NaCl followed by incubation for 1 h at 37 °C. Blood incubated with 0.9% NaCl is considers as negative control as well as with distilled water without test material is considered as positive control for the test. After 1 h of incubation, the reaction mixture is centrifuged at 10,000 rpm for 10 min and the supernatant is carefully collected. The free hemoglobin present in the supernatant is measured using a UV–visible spectrophotometer at wavelength 540 nm. The percentage of hemolysis is calculated using the following relation,

Principal
Nowgong Girls' College
Nagaon :: Assam

Nowgong Girls' College
ESTD: 1962
Nagaon :: Assam

$$\text{Hemolysis}\ (\%) = \frac{Abs_{sample} - Abs_{-ve control}}{Abs_{+ve control} - Abs_{-ve control}} \times 100 \quad (2)$$

MTT Assay Test

The cell viability after growth on the silk/PVA nanofibers (untreated and plasma treated) are evaluated by the MTT (3-[4,5-dimethylthiazole- 2-yl]-2,5-diphenyltetrazolium bromide) assay in human embryonoc kidney (HEK293T) cells. Briefly, HEK293T cells are plated in 96 well plates and exposed with 1 mg/ml concentration of different samples for 24 h. MTT is added to each well and incubated for 4 h at 37 °C. On termination of incubations, formazan crystals formed in cells are dissolved in acidic isopropanol and incubated further for 30 min at 37 °C. Cytotoxicity is measured spectrophotometrically at 570 nm with Varioskan LUX Multimode Microplate Reader (Thermo Scientific, Finland). Absorbance values are blanked against acidic isopropanol and the absorbance of cells exposed to medium only (without any treatment) are taken as 100% cell viability (control). The percentage of cell viability is calculated by using the following formula.

$$\text{Cell viability}\ (\%) = \frac{N_t}{N_c} \times 100 \quad (3)$$

where N_t and N_c are absorbance of the treated and untreated cells. All experiments are performed in triplicate and data are expressed as mean ± standard deviation (SD).

In-Vitro Antithrombogenic Property

The antithrombogenic properties of these silk/PVA nanofibers are evaluated using an in-vitro kinetic method. 1 ml of anticoagulant citrate dextrose (ACD) blood is incubated in micro centrifuge tubes each containing the silk/PVA nanofibers (untreated and plasma treated) separately at 37 °C without shaking. After 1 h of incubation, 0.2 ml of blood is taken out from each tube and placed on a clean sterilized glass plate. Prior to the experiment, the glass plates are sterilized by autoclaving at high pressure saturated steam at 121 °C for 30 min. The clotting is initiated by addition of 0.02 ml 0.1 M $CaCl_2$ to the citrated blood. After 15 min and 60 min intervals respectively, the blood clot formed on each glass plate is scrapped and fixed in 2 ml formaldehyde solution (36% v/v) for 10 min, then washed with distilled water, blotted with tissue paper and weighed. The ACD blood alone, without any sample incubation, is considered as control. The experiment is carried out in triplicates and the results are reported as mean ± standard deviation (SD).

Statistical Analysis

All the data were statistically analyzed and expressed as the mean ± standard deviation (SD). The significance of the differences among the tested samples are determined by one-way analysis of variance (ANOVA) followed by Tukey test for multiple comparisons (Origin Lab OriginV8.6 Software). P values < 0.05 is considered statistically significant for hemocompatibility and MTT assay studies. $P < 0.05$ is considered statistically significant for water contact angle measurements.

Principal
Nowgong Girls' College
Nagaon :: Assam

Nowgong Girls' College
ESTD: 1962
Nagaon :: Assam

Results and Discussions

Electrical Characterization of DBD Plasma

The respective voltage and current waveform for the DBD plasma at three different electrode gaps (3 mm, 6 mm and 10 mm) and applied voltage range of 11–17 kV with an interval of 2 kV is shown in Fig. 2A–L. As seen from Fig. 2A–D, filamentary discharge is observed at electrode gap of 3 mm, characterized by the spikes that appear in the current waveform and is found to sustain in the entire voltage range of 11–17 kV. For electrode gaps of 6 mm and 10 mm (Fig. 2E–L), filamentary discharge is significantly reduced at all applied voltages (11–17 kV) as revealed by single current pulse per half-cycle of the applied voltage with the same periodicity. Furthermore, from visual observation it is seen that by increasing the electrode gap above 3 mm, the filaments diminish and the discharge uniformly spreads over the entire surface of the electrode. This possibly results in uniform surface treatment of silk/PVA nanofibers without any structural damage which is evident from Fig. 1A where smooth surface, free of pinholes, can be observed. As uniform surface treatment of polymer is more preferred for desirable properties, the characterization results of silk/PVA nanofibers treated at electrode gaps of 6 mm and 10 mm, respectively and applied voltage range of 11–17 kV are considered for further discussions in this work.

Figure 3A–C show the Lissajous figures of the DBD discharge at different electrode gaps and applied voltages. From the area of the respective Lissajous figure, the energy dissipated during one half-cycle of the discharge is calculated and the results are presented in Fig. 3D. It is evident that lowering in energy dissipation in the discharge is associated with decrease in electric field strength with increase in electrode discharge gap for a particular applied voltage. Although higher energy dissipation takes place at electrode gap of 3 mm and applied voltage range of 11–17 kV, the occurrence of high degree of filamentary discharge under these experimental conditions does not seemed to be appropriate for uniform surface treatment of silk/PVA nanofibers.

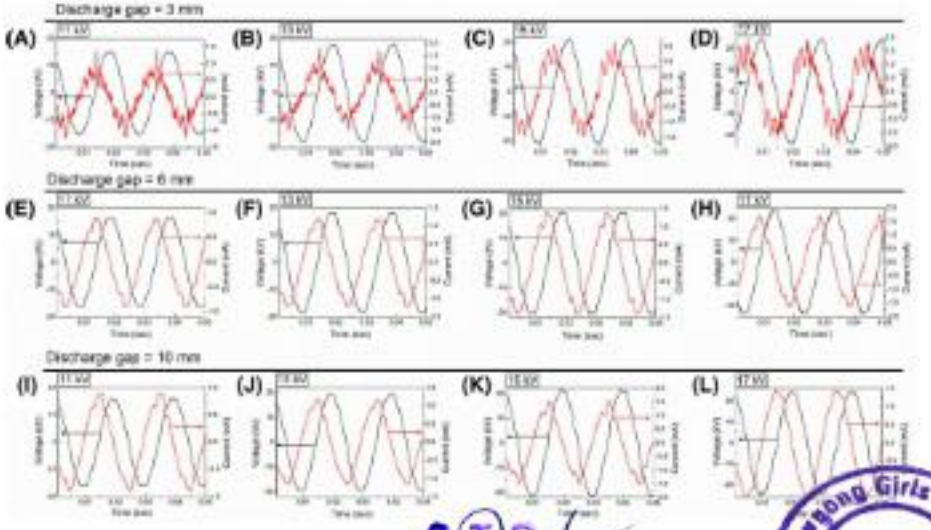

Fig. 2 A–L Voltage and current waveforms with different discharge gaps and applied voltages

Principal
Nowgong Girls' College
Nagaon :: Assam
Nowgong Girls' College ESTD: 1962 Nagaon :: Assam

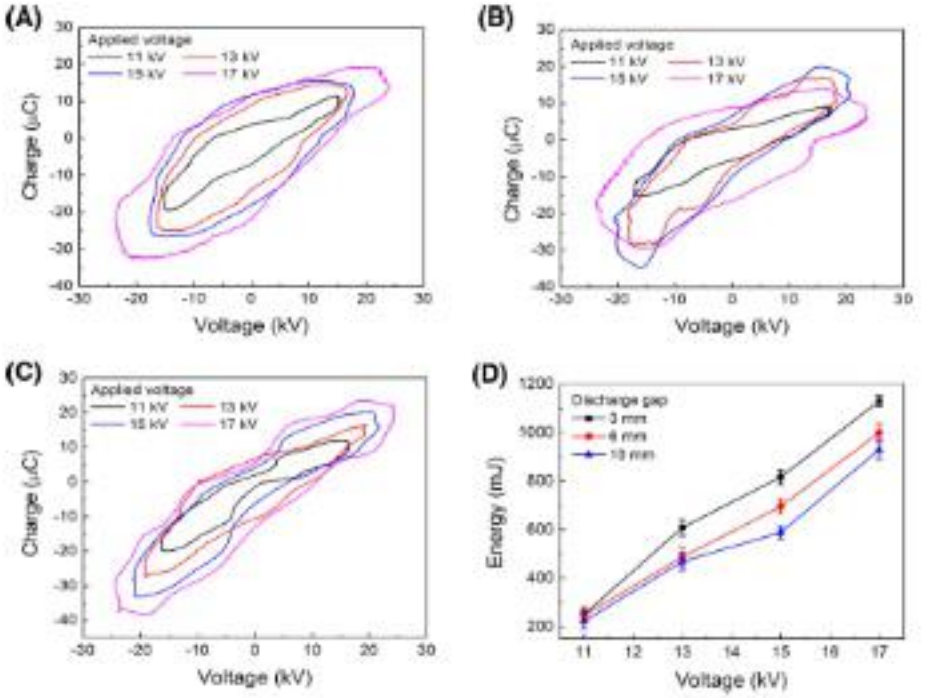

Fig. 3 Lissajous figures for discharge gaps at **A** 3 mm, **B** 6 mm and **C** 10 mm, respectively. **D** Variation of electric energy dissipation in the DBD discharge with applied voltage

From these experimental observations, it may be suggested that above discharge gap of 3 mm and in the voltage range of 11–17 kV, the discharge becomes more macroscopically homogeneous although complete elimination of filamentary discharge under the present investigation cannot be confirmed.

Surface Morphology of Silk/PVA Nanofibers

The FESEM images show morphology of untreated and plasma treated silk/PVA nanofibers with wide and uneven nanofiber diameter distribution (Fig. 4A–I). The nanofibers are obtained with smooth fiber morphology without the presence of beads. The average diameter of untreated silk/PVA nanofibers is evaluated to be 150 ± 23 nm. It is observed that DBD plasma treatment does not significantly alter the surface structure and morphology of silk/PVA nanofibers as the average fiber diameter, after plasma treatment, is found to be in the range of 149–153 nm. FESEM analyses clearly shows that in this present work, DBD plasma treatment applied under various discharge conditions causes no structural and morphological damage to the silk/PVA nanofibers and the DBD plasma can be utilized as an effective and non-destructive method for treating silk and silk-based polymeric surfaces [16, 31].

Principal
Nowgong Girls' College
Nagaon :: Assam

Nowgong Girls' College
ESTD: 1962
Nagaon :: Assam

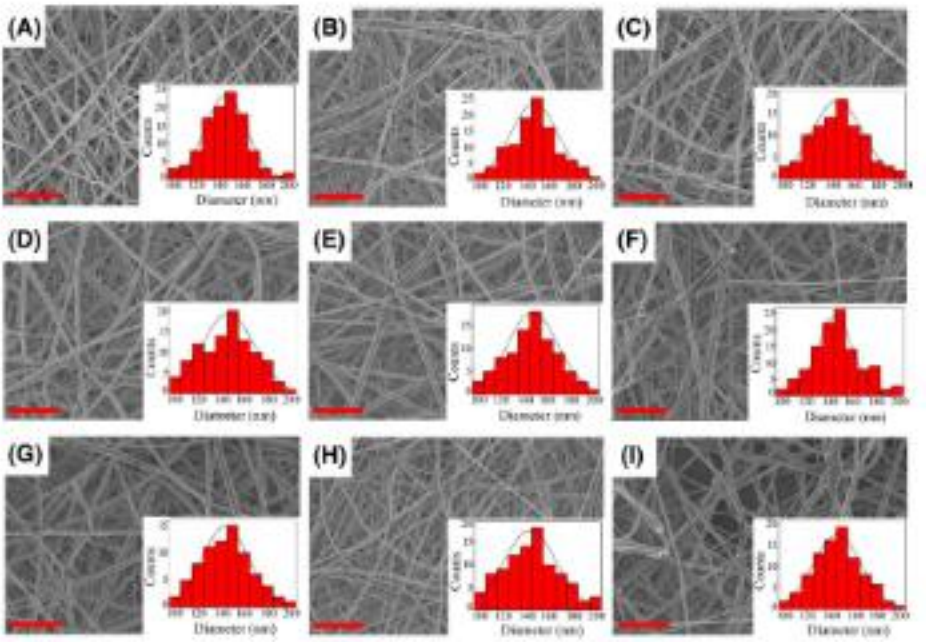

Fig. 4 FESEM images of **A** untreated silk/PVA nanofibers; plasma treated nanofibers at discharge gap of 6 mm and applied voltages of **B** 11 kV, **C** 13 kV, **D** 15 kV and **E** 17 kV, respectively and plasma treated nanofibers at discharge gap of 10 mm and applied voltages of **F** 11 kV, **G** 13 kV, **H** 15 kV and **I** 17 kV, respectively. The insets show the diameter distribution of untreated and plasma treated silk/PVA nanofibers, respectively. AMOX-BMSF/PVA and AMOX-BMSF/PVA/O_2 nanofibers, respectively (FESEM image, scale: 1 μm)

Water Contact Angle Measurement

In this work, the wettability of silk/PVA nanofibers, before and after plasma treatment is studied using water contact angle measurements and the results are presented in Table 1. It is evident that the plasma treatment results in lowering in water contact angle and subsequent increase in surface energy of silk/PVA nanofibers, which is attributed to surface functionalization of the nanofibers with oxygen containing functional groups such as –OH, –C=O, –O–C–O, COOH etc., [16, 18, 20]. An increase in the content of polar components onto the surface of silk/PVA nanofibers also corroborates the inference. It is further observed that surface hydrophilicity is more pronounced for silk/PVA nanofibers treated at discharge gap of 6 mm as compared to that of 10 mm discharge gap. Moreover, surface hydrophilicity of silk/PVA nanofibers is observed to be increased with applied voltage. These results are strongly related to the dissipation of more energy in the plasma at smaller discharge gap as well as increase of applied voltage at a particular discharge gap. This leads to high degree of dissociation and ionization of gas molecules and formation of reactive plasma species such as free radicals, excited metastable atoms/molecules and ions and subsequently facilitates more heterogeneous reactions between the surface of the nanofibers exposed to the plasma and the plasma species.

Principal
Nowgong Girls' College
Nagaon :: Assam

Nowgong Girls' College
ESTD: 1962
Nagaon :: Assam

Table 1 Contact angle and surface free energy of untreated and plasma treated silk/PVA nanofibers at different discharge parameters (mean ± standard deviation (SD))

Plasma treatment conditions		Water contact angle (°)	Polar component (mJm^{-2})	Dispersive component (mJm^{-2})	Total surface energy (mJm^{-2})
Untreated silk/PVA nanofibers		77.1 ± 1.7	4.8 ± 0.5	40.3 ± 1.4	45.1 ± 1.1
Plasma treated silk/PVA nanofibers					
Applied voltage (kV)	Electrode gap (mm)				
11	6	36.8 ± 1.2	27.4 ± 1.5	37.2 ± 1.2	64.6 ± 3.1
13		33.2 ± 1.1	26.4 ± 1.4	39.5 ± 1.8	65.9 ± 2.4
15		21.6 ± 1.6	33.4 ± 1.8	39.2 ± 1.7	72.6 ± 2.9
17		22.2 ± 1.5	34.5 ± 1.1	37.5 ± 1.4	72.0 ± 2.4
11	10	58.3 ± 1.8	12.1 ± 1.2	44.3 ± 2.1	56.4 ± 1.9
13		47.5 ± 1.4	17.2 ± 1.4	42.0 ± 2.5	59.2 ± 1.5
15		43.5 ± 2.0	25.1 ± 1.0	37.2 ± 1.7	62.3 ± 1.7
17		42.6 ± 1.6	24.4 ± 1.9	38.1 ± 1.5	62.5 ± 1.8

ATR-IR Spectra Analyses

Figure 5A shows the ATR-IR spectra of PVA, BMSF and silk/PVA nanofibers. In the spectrum of PVA, a broad band appears in the region, 3100–3650 cm^{-1}, which is assigned as the absorption due to the OH stretching vibration from intermolecular and intramolecular hydrogen bonds of PVA [16]. The peaks at 2940 cm^{-1} and 2907 cm^{-1} are assigned to the symmetric and asymmetric CH stretching vibrations of alkyl groups, respectively [16, 25]. The characteristics of carbonyl group of PVA are found at 1645 cm^{-1} and 1533 cm^{-1} which are attributed to the C–O stretching vibrations and C = C stretching vibrations, respectively [16, 25]. The peaks that are observed at 1410 cm^{-1}, 1323 cm^{-1}, 1227 cm^{-1} and 1085 cm^{-1} correspond to the CH_2 bending, CH deformation, CH wagging and C-O stretching vibrations of acetyl group, respectively [16, 25]. The ATR-IR spectrum shows the characteristics peaks of BMSF at 1622 cm^{-1}, 1515 cm^{-1} and 1224 cm^{-1} which correspond to amide I, amide II and amide III groups, respectively [16, 18, 25]. The broad band appeared in

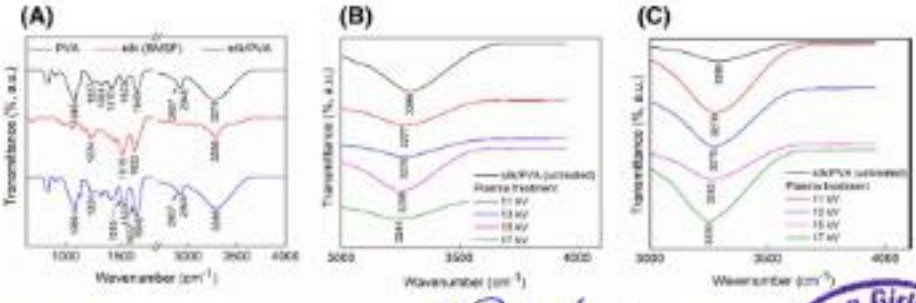

Fig. 5 ATR-IR spectra of **A** PVA, BMSF and silk/PVA nanofibers, untreated and plasma treated silk/PVA nanofibers at discharge gaps of **B** 6 mm and **C** 10 mm, respectively and applied voltage ranging from 11–17 kV

Principal
Nowgong Girls' College
Nagaon :: Assam
Nowgong Girls' College
ESTD: 1962
Nagaon :: Assam

the region, 3100–3650 cm^{-1}, is due to the overlapping of the stretching vibrations of primary amino group (NH) and hydrogen bonded OH groups [16, 20, 24]. Moreover, in the ATR-IR spectra of composite nanofiber of silk/PVA both the peaks of PVA as well as silk has appeared. The presence of the absorption bands/peaks of PVA and BMSF in the ATR-FTIR spectrum of silk/PVA nanofibers confirms the successful formation of the composite nanofibers.

The ATR-IR spectra of plasma treated silk/PVA nanofibers at discharge gaps of 6 mm and 10 mm, respectively and applied voltage range of 11–17 kV are plotted in the region of interest (3000–4000 cm^{-1}) and shown in Fig. 5B, C. The plasma treatment does not seem to induce any change in the characteristic peaks of PVA and BMSF in the lower wavenumber region (650–3000 cm^{-1}). However, the band positioned in the region 3100–3650 cm^{-1} is found to be shifted towards lower wavenumber with increase in applied voltage (11–17 kV) and at different electrode gaps, which indicates incorporation of polar functional groups (e.g. hydroxyl, carboxyl, carboxylate etc.) through formation of hydrogen bonds on to the surface of silk/PVA nanofibers [18]. The hydrogen bond formation is facilitated mainly by the different highly reactive plasma species that are generated during air/O_2 plasma treatment and their subsequent interaction with the surface of silk/PVA nanofibers [16]. These polar groups are responsible for enhancing surface free energy and wettability of silk/PVA nanofibers which is well evident from earlier discussions on contact angle measurement.

Mechanical Analysis

The tensile strength, Young's modulus and elongation at break (%) of silk/PVA nanofibers are investigated before and after plasma treatment and the results are presented in Table 2. It is observed that tensile strength and Young's modulus of plasma treated silk/PVA nanofibers are higher than the untreated nanofibers, which is contributed by the interaction of polar groups with the surface of silk/PVA nanofibers through formation of hydrogen bonds which subsequently results in efficient load transfer in the nanofibers [18, 20]. However, decrease in elongation at break indicates relatively higher degree of stiffness in

Table 2 Mechanical properties of untreated and plasma treated silk/PVA nanofibers at different discharge parameters (mean ± standard deviation (SD))

Mechanical properties	silk/PVA (untreated)	Applied voltage (kV)	Electrode gap	
			6 mm	10 mm
Tensile strength (MPa)	5.25 ± 0.33	11	5.40 ± 0.43	5.31 ± 0.52
		13	5.47 ± 0.51	5.40 ± 0.40
		15	6.11 ± 0.60	5.80 ± 0.62
		17	6.44 ± 0.55	6.02 ± 0.53
Young's modulus (MPa)	37.60 ± 2.25	11	39.23 ± 2.54	38.12 ± 2.44
		13	40.11 ± 2.61	38.50 ± 2.52
		15	44.52 ± 2.70	40.53 ± 2.80
		17	47.34 ± 2.81	42.44 ± 2.83
Elongation at break (%)	38.01 ± 2.01	11	35.20 ± 1.54	37.40 ± 1.64
		13	35.05 ± 2.05	36.00 ± 2.04
		15	33.02 ± 2.01	34.[illegible]
		17	30.10 ± 1.74	[illegible] ± 1.87

Principal
Nowgong Girls' College
Nagaon :: Assam

Nowgong Girls' College
ESTD: 1962
Nagaon :: Assam

plasma treated silk/PVA nanofibers compared to the untreated nanofibers [16, 18]. It is further observed that the increase in tensile strength and Young's modulus in plasma treated silk/PVA nanofibers is more prominent at and above applied voltage of 15 kV which suggest that plasma treatment up to the applied voltage of 13 kV may not be effective in modifying the surface properties of silk/PVA nanofibers. For silk/PVA nanofibers treated at discharge gap of 6 mm, the percentage increase in tensile strength and Young's modulus is observed to be 4.20% and 6.70% respectively. However, the tensile strength and Young's modulus increases to 16.40% and 18.42%, respectively at applied voltage of 15 kV and it reaches up to 22.70% and 26.00%, respectively with increase in applied voltage to 17 kV. Similar inference can be drawn for silk/PVA nanofibers treated at discharge gap of 10 mm and applied voltage range of 11–17 kV. Furthermore, silk/PVA nanofibers treated at discharge gap of 6 mm shows higher values of tensile strength and Young's modulus as compared to that treated at discharge gap of 10 mm. This is accounted for dissipation of higher electrical energy at discharge gap of 6 mm which eventually leads to high degree of hydrogen bonding interaction between the polar groups and the surface of silk/PVA nanofibers.

Hemocompatibility and Cell Viability Assays

Hemoysis study provides a useful tool for assessing blood compatibility of materials and can hold significant implications for biomedical use. As per the ASTM standards (F756-17), materials exhibiting percentage of hemolysis less than 2% is considered as non-hemolytic and suitable for use in biomedical application [18]. The hemolysis studies of untreated and plasma treated silk/PVA nanofibers are performed for the evaluation of hemocompatibility and the results are shown in Fig. 6A. The results show that the percentage of hemolysis for all the test samples is far below the permissible limit and thus indicate that no cytotoxic effects are caused by silk/PVA nanofibers and plasma treatment, regardless of change in applied voltage and discharge gap, does not affect the hemolytic activity of the nanofibers.

The results of in vitro cytotoxicity studies of the untreated and plasma treated silk/PVA nanofibers at various discharge parameters are shown in Fig. 6B, C. The cell viability of the untreated silk/PVA nanofibers is observed to be increased with higher incubation period which clearly indicates that the nanofibers do not have any toxic effect on the HEK293T cells, but rather increases the viability of cells. For silk/PVA nanofibers treated at discharge gap of 6 mm, noticeable increase in cell viability is observed at applied

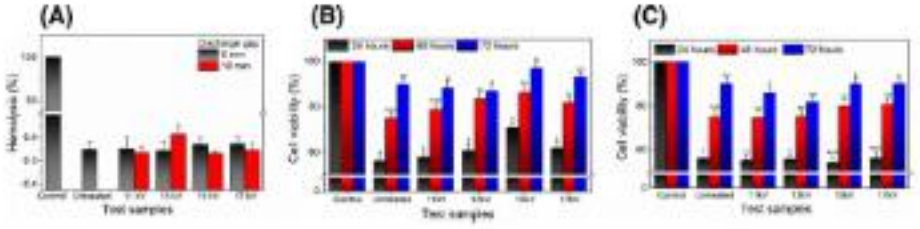

Fig. 6 **A** Hemocompatibility studies of the untreated and plasma treated silk/PVA nanofibers at discharge gaps of 6 mm and 10 mm, respectively and applied voltage range of 11–17 kV. Viability (%) of human embryonoc kidney (HEK293T) cells at different post incubation periods with untreated and plasma treated silk/PVA nanofibers at discharge gaps of **B** 6 mm and **C** 10 mm, respectively. (***, ** and * show significant difference from control at $p < 0.01$, $p < 0.02$ and $p < 0.05$, respectively). Values represent mean ± SD of three replicates. Control: cell with no treatment

Principal
Nowgong Girls' College
Nagaon :: Assam

Nowgong Girls' College
ESTD: 1962
Nagaon :: Assam

voltage of 15 kV, after incubation period of 24 h, as compared to the untreated one. After incubation period of 48 h, the cell viability of silk/PVA nanofibers moderately increases up to applied voltage of 15 kV while no significant change in cellular viability is observed in the nanofibers treated in the applied voltage range of 11–13 kV, as observed after 72 h of incubation period. During the entire incubation period, silk/PVA nanofibers treated at applied voltage of 15 kV displays better activity with regard to cell proliferation capability among the untreated and other plasma treated nanofibers. At applied voltage of 17 kV, a minor decrease in cellular viability is observed for silk/PVA nanofibers, although it still remains higher as compared to those treated at lower applied voltages (11–13 kV). The improvement in cell viability of silk/PVA nanofibers treated at applied voltage of 15 kV and 17 kV and after incubation period of 72 h is attributed to the enhanced hydrophilicity due to incorporation of more polar functional groups onto the surface.

At discharge gap of 10 mm and after incubation period of 24 h, cell viability of plasma treated silk/PVA nanofibers is similar to the untreated one and with increase in applied voltage (11–17 kV) no changes can be observed in cell viability of the nanofibers. After incubation period of 48 h, similar observations can be made for silk/PVA nanofibers treated at applied voltages of 11 kV and 13 kV although those treated at and above applied voltage of 15 kV shows improvement in cellular viability. At higher applied voltage of 15 kV and 17 kV, respectively, the silk/PVA nanofibers displays cell viability similar to the untreated one, as observed after incubation period of 72 h. The results suggest that at discharge gap of 10 mm and in the applied voltage range of 11–17 kV, the energy dissipated in the plasma may not be effective in altering the surface properties of silk/PVA nanofibers. The overall observations indicate that plasma treated silk/PVA nanofibers do not show any adverse effect on cell proliferation and viability and that these biomaterials can be considered suitable for tissue engineering [18].

In vitro Antithrombogenic Activity

The antithrombogenic activity of the untreated and plasma treated silk/PVA nanofibers are further evaluated in this work and the results are presented in Table 3. It is evident that weight of thrombus formation increases with increase in blood coagulation time. As observed from the data presented in Table 3, the untreated silk/PVA nanofibers alone do not show significant effect on antithrombogenic activity which suggests that the nanofibers are compatible with human erythrocytes. At discharge gap of 6 mm, the silk/PVA nanofibers treated at applied voltage of 11 kV and 13 kV respectively shows no change in antithrombogenic activity in comparison with the control. However, with further increase in applied voltage at and above 15 kV, silk/PVA nanofibers begin to show reduction in the weight of thrombus formation. The improvement in antithrombogenicity of plasma treated silk/PVA nanofibers at applied voltage of 15 kV and may be associated with their enhanced surface free energies due to incorporation of polar functional groups onto the surface.

At discharge gap of 10 mm and applied voltage range of 11–13 kV, the silk/PVA nanofibers show antithrombogenic activity similar to that of the control although an improvement in the observed property can be seen at and above applied voltage of 15 kV. At observation period of 60 min, no significant changes in antithrombogenicity of the silk/PVA nanofibers, treated at applied voltage range of 11–17 kV, can be observed which suggests that at these particular discharge conditions, the DBD plasma treatment [illegible] be [illegible] in improving the blood compatibility of the nanofibers.

C.T.C.
Principal
Nowgong Girls' College
Nagaon :: Assam

Nowgong Girls' College
ESTD: 1962
Nagaon :: Assam

Table 3 Measurement of thrombus (mg) formed after 15 and 60 min of observation period for untreated and plasma treated silk/PVA nanofibers at different discharge parameters (mean ± standard deviation (SD))

	Sample	Observation time (Minutes)	
		15	60
		Weight of thrombosis (mg)	
	Control	57.15 ± 2.33	110.75 ± 2.84
	Silk/PVA nanofibers (Untreated)	55.04 ± 2.14	108.35 ± 2.54
Electrode gap (mm)	Applied voltage (kV)		
6	11	56.25 ± 2.35	104.50 ± 2.53
	13	52.75 ± 2.33	102.20 ± 2.70
	15	31.04 ± 1.65	75.15 ± 2.75
	17	32.30 ± 1.70	74.70 ± 2.13
10	11	56.22 ± 2.61	105.54 ± 2.41
	13	57.51 ± 3.14	104.62 ± 3.25
	15	47.00 ± 1.82	106.60 ± 2.74
	17	44.25 ± 1.75	105.25 ± 3.17

Conclusions

The present study investigates the effect of atmospheric DBD plasma modification on surface properties and biocompatibility of silk/PVA nanofibers. For uniform surface modification of the nanofibers, the electrical characteristics of DBD plasma are investigated at different electrode gaps and applied voltages. At discharge gaps of 6 mm and 10 mm and applied voltage range of 11–17 kV, uniform and lower degree of filamentary glow discharge is observed and subsequently surface treatment of the silk/PVA nanofibers is carried out under these discharge conditions. It is observed that the silk/PVA nanofibers treated at discharge gap of 6 mm and applied voltage range of 11–17 kV shows high degree of surface wettability and mechanical strength as compared to the untreated one and those treated at discharge gap of 10 mm. It is apparent that dissipation of more energy in the plasma at smaller discharge gap which results in incorporation of more polar groups onto the surface and an increase in hydrogen bonding interaction between the polar groups and the surface of the silk/PVA nanofibers is mainly responsible for improvement in the observed properties of the nanofibers. The hemolysis and antithrombogenic studies reveal that DBD plasma treatment does not seemed to compromise but improve the blood compatibility of silk/PVA nanofibers. Furthermore, the silk/PVA nanofibers treated at optimized applied voltage of 15 kV and discharge gap of 6 mm, exhibit better ability of cell adhesion and proliferation onto the surface as compared to the untreated nanofibers. The results reported in this work clearly suggest that the DBD plasma treated silk/PVA nanofibers can be explored as wound dressing in clinical applications.

Acknowledgements This research work is supported by DST-SERB (Grant No. SR/FTP/ PS-147/2012 and EMR/2016/006146) funded by Department of Science and Technology (DST), India. Arup Jyoti Choudhury expresses his gratitude to the DST-INSPIRE Faculty Fellowship (Grant No. IFA14-PH-93) for the financial support to carry out this research work and the Tezpur University, Assam, India for hosting the fellowship. Nilmoy Ojah acknowledges the support provided by DST (India) in the form of fellowship under DST-INSPIRE Faculty program. The assistance of Mr. Kaushik Nath and Dr. Suman Dasgupta from the Department

Principal
Nowgong Girls' College
Nagaon :: Assam

Nowgong Girls' College
ESTD: 1962
Nagaon :: Assam

of Physics and Department of Molecular Biology and Biotechnology, Tezpur University, 784028, Assam, India in carrying out the antithrombogenic test and MTT cell viability study is sincerely acknowledged.

References

1. Zhang X, Tsukada M, Morikawa H, Aojima K, Zhang G, Miura M (2011) Production of silk sericin/silk fibroin blend nanofibers. Nanosc Res lett 6:510
2. Jeong L, Yeo IS, Kim HN, Yoon YI, Jang DH, Jung SY, Min BM, Park WH (2012) In vivo evaluation of porous hydroxyapatite/chitosan-alginate composite scaffolds for bone tissue engineering. Int J Biol Macrom 51:1079
3. Shao W, He J, Sang F, Ding B, Chen L, Cui S, Kejing L, Han Q, Tan W (2016) Coaxial electrospun aligned tussah silk fibroin nanostructured fiber scaffolds embedded with hydroxyapatite–tussah silk fibroin nanoparticles for bone tissue engineering. Mater Sci Engg C 58:342
4. Min K, Kim S, Kim S (2018) Silk protein nanofibers for highly efficient, eco-friendly, optically translucent, and multifunctional air filters. Sci Reports 8:9598
5. Yang W, Li R, Fang C, Hao W (2019) Surface modification of polyamide nanofiber membranes by polyurethane to simultaneously improve their mechanical strength and hydrophobicity for breathable and waterproof applications. Prog Org Coat 131:67
6. Kim HJ, Park SJ, Park CS, Le TH, Lee SH, Ha TH, Kim HI, Kim J, Lee CS, Yoon H, Kwon OS (2018) Surface-modified polymer nanofiber membrane for high-efficiency microdust capturing. Chem Engg J 339:204
7. Jin HJ, Fridrikh SV, Rutledge GC, Kaplan DL (2002) Electrospinning Bombyx mori silk with poly (ethylene oxide). Biomacromol 3:1233
8. Yao J, Bastiaansen CWM, Peijs T (2014) High strength and high modulus electrospun nanofibers. Fibers 2:158
9. Nakashima R, Watanabe K, Lee Y, Kim BS, Kim IS (2013) Mechanical properties of poly (vinylidene fluoride) nanofiber filaments prepared by electrospinning and twisting. Adv Polym Tech 32:44
10. Chaivan P, Pasaja N, Boonyawan D, Suanpoot P, Vilaithong T (2005) Low-temperature plasma treatment for hydrophobicity improvement of silk. Sur Coat Tech 193:356
11. Kingshott P, Andersson G, McArthur SL, Griesser HJ (2011) Surface modification and chemical surface analysis of biomaterials. Curr Opinion Chem Bio 15:667
12. Bhurke AS, Askeland PA, Drzal LT (2007) Surface modification of polycarbonate by ultraviolet radiation and ozone. J Adhesion 83:43
13. Kim SE, Wang J, Jordan AM, Korley LTJ, Baer E, Pokorski JK (2014) Surface modification of melt extruded poly (ε-caprolactone) nanofibers: toward a new scalable biomaterial scaffold. ACS Macro Lett 3:585
14. Yoo HS, Kim TG, Park TG (2009) Surface-functionalized electrospun nanofibers for tissue engineering and drug delivery. Adv Drug Deliv Rev 61:1033
15. Das P, Ojah N, Kandimalla R, Mohan K, Gogoi D, Dolui SK, Choudhury AJ (2018) Surface modification of electrospun PVA/chitosan nanofibers by dielectric barrier discharge plasma at atmospheric pressure and studies of their mechanical properties and biocompatibility. Int J Bio Macromol 114:1026
16. Ojah N, Saikia D, Gogoi D, Baishya P, Ahmed GA, Ramteke A, Choudhury AJ (2019) Surface modification of core-shell silk/PVA nanofibers by oxygen dielectric barrier discharge plasma: studies of physico-chemical properties and drug release behavior. App Sur Sci 475:219
17. Rajasekaran P, Mertmann P, Bibinov N, Wandke D, Viol W, Awakowicz P (2010) Filamentary and homogeneous modes of dielectric barrier discharge (DBD) in air: investigation through plasma characterization and simulation of surface irradiation. Plasma Process Polym 7:665
18. Ojah N, Borah R, Ahmed GA, Mandal M, Choudhury AJ (2020) Surface modification of electrospun silk/AMOX/PVA nanofibers by dielectric barrier discharge plasma: physiochemical properties, drug delivery and in-vitro biocompatibility. Prog In Biomater 9:219
19. Miao C, Liu F, Wang Q, Cai M, Fang Z (2018) Investigation on the influence of electrode geometry on characteristics of coaxial dielectric barrier discharge reactor driven by an oscillating microsecond pulsed power supply. Eur Phys J D 72:57
20. Ojah N, Deka J, Haloi S, Kandimalla R, Gogoi D, Medhi T, Mandal M, Ahmed GA, Choudhury AJ (2019) Chitosan coated silk fibroin surface modified by atmospheric dielectric-barrier discharge plasma: a mechanically robust drug release system. J Biomater Sci Polym Ed [illegible]
21. Zhu P, Xu W, Ma M, Zhou H (2010) Effect of plasma treatment of silk fibroin powder on the properties of silk fibroin powder/polyurethane blend film. Polym Eng Sci 50:1705

Principal
Nowgong Girls' College
Nagaon :: Assam

Nowgong Girls' College
ESTD: 1962
Nagaon :: Assam

22. Long JJ, Wang HW, Lu TQ, Tang RC, Zhu YW (2008) Application of low-pressure plasma pretreatment in silk fabric degumming process. Plasma Chem Plasma Process 28:701
23. Wang C, Zhang G, Wang X (2012) Comparisons of discharge characteristics of a dielectric barrier discharge with different electrode structures. Vacuum 86:960
24. Choo K, Ching YC, Chuah CH, Julai S, Li NS (2016) Preparation and characterization of polyvinyl alcohol-chitosan composite films reinforced with cellulose nanofiber. Mater 9:644
25. Zhou J, Cao C, Ma X (2009) A novel three-dimensional tubular scaffold prepared from silk fibroin by electrospinning. Int J Bio Macromol 45:504

Publisher's Note Springer Nature remains neutral with regard to jurisdictional claims in published maps and institutional affiliations.

Principal
Nowgong Girls' College
Nagaon :: Assam

Springer

Nowgong Girls' College
ESTD: 1962
Nagaon :: Assam

Principal
Nowgong Girls' College
Nagaon :: Assam

Nowgong Girls' College
ESTD: 1962
Nagaon :: Assam

Journal of Positive School Psychology
2022, Vol. 6, No. 4, 1230-1236
http://journalppw.com

A Study of Inward and Outward Migration of North-East India

Arundhuti Patangia[1], Bimal Kumar Kar[2], Ashish Saikia[3]

[1,2,3]*Department of Geography, Gauhati University, Guwahati, India*

Abstract

The process of migration which is a key feature of human history; can be considered as one of the most dynamic human activities. This work mainly focuses on the analysis of the causes of inward and outward migration in North-East India. Considering inter-state migration; North-East India which remained a net negative receiver in 2001, has become net positive during the 2011 Census. Most of the migrants coming to this region from other states/UTs of India are male and their prime cause of migration is recorded as employment and business. On the contrary, out-migration from North-East India to rest of the country is female dominated. Moved with household and marriage are the two major causes behind female-migration in this region as per Census of India, 2011.

Keywords—Inward migration, Outward migration, North-East India, Spatio-temporal Analysis

I. INTRODUCTION

Migration is a universal phenomenon. In simple words, migration which may be permanent, temporary or seasonal; is the process of movement of people from one place to another due to different causes. It is the most significant component of population growth and most sensitive to economic, political and cultural factors (Singh, 1998). As per the UN Migration Agency (IOM), any person who is moving or has moved across an international border or within a state away from his/her habitual place of residence, regardless of the person's legal status, causes of movement and the length of duration is known as Migrant. Indian Constitution provides basic freedom to move to any part of the country, right to reside and earn livelihood of their choices. That is why migrants are not needed to take permission or register at the place of origin as well as at the place of destination (Bhagat, 2018). The process of migration in India in general and North-East India in particular, is facilitated by the development of transport and communication. Industrialization and economic development have played a major role for large scale movement of people from rural to urban areas.

India; the second most populous country in the world; has a long history of internal migration. Around 3.6% of the total population in India was inter-state migrants in 1931 (Davis, 1951). In 2001; inter-state migration stood at 4.1% in India (Census of India, 2001). In India, around 4.6% of the total population is inter-state migrants as per Census of India, 2011. North-East India shares its borders with four foreign countries viz. China, Myanmar, Bangladesh and Bhutan. Thus states of North-East India are experiencing a higher influx of international migration. Apart from the international migrants; North-East India has been the receiver of migrants coming from other states and Union Territories of the country. Of the total migrants of North-East India, only 3.5% of migrants have come to this region from other states of India (Lusome&Bhagat, 2020). Analysis of the reasons for movement of people from one place to another is one of the most important aspects of a migration study. In India, Marriage is the main cause of female migration. It remains identical between 2001 to 2011. On the other hand, work/employment is stated as the major cause of male migration within the country. This paper is an attempt to analyse the causes of inward migration to North-East India from other parts of the country as well as the causes of outward migration from this region to other states/ UTs of India.

II. STUDY AREA

North-East India commonly called the land of 'Seven Sisters' is located between 20° N latitude and 29° 30′ N latitude and 89°

© 2021 JPPW. All rights reserved

Principal
Nowgong Girls' College
Nagaon :: Assam

Nowgong Girls' College
ESTD: 1962
Nagaon :: Assam

longitude and 97 ° 30′ E longitude. This easternmost region of India consists of seven states of India, viz. Arunachal Pradesh, Assam, Nagaland, Meghalaya, Mizoram, Manipur and Tripura. In the year 2014, Sikkim was also included in this region. In this study the early North-East India comprised of seven states is taken into consideration. It covers a total area of 2,55,036 Sq. Km representing about 7.3% of India's total geographical area. This region shares an international border of 5,182 km with its four neighboring foreign countries. More than 99% of its total geographical boundary of North-East India is international border (Gogoi et al., 2009).

North-East India lies in the regime of tropical monsoon climate. Soil of North-East India can be categorized into four major groups; viz. alluvial soil, red soil, laterite soil and mountain soil. North-East India is the home of various types of natural vegetation. The natural vegetation of this region can be classified as Tropical Evergreen forest, Tropical Deciduous forest, Tropical Grassland and Alpine Grassland. The total population of North-East India is 449,80,294 as per Census of India, 2011 which represents 3.7% of the total population of India (Taher& Ahmed, 1998). During the last decade (2001-2011) population of North-East India has increased by 6.8 million. Such a high rate of growth is due to a large influx of migrants from both within and outside the country, improvement in health and hygiene and failure of family planning measures. The population density of North-East India is 170 persons per Sq. km as per Census of India, 2011. Among the states of North-East India Assam is the most densely populated state with an average population density of 398 persons per Sq. km. With an average population density of 17 persons per Sq. km, Arunachal Pradesh is the most sparsely populated state in this region.

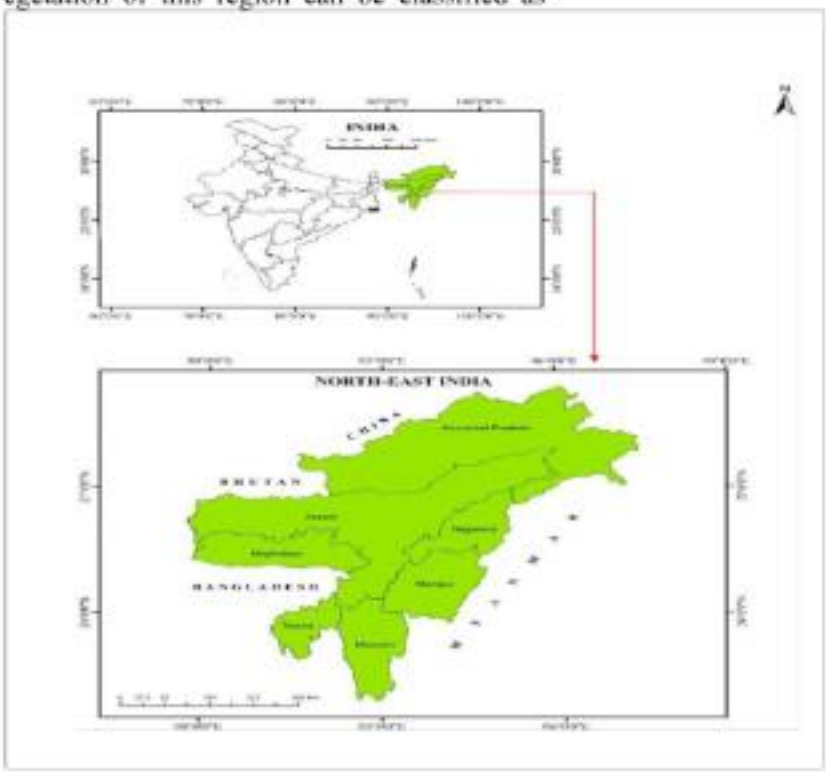

© 2021 JPPW. All rights reserved

Principal
Nowgong Girls' College
Nagaon :: Assam

Nowgong Girls' College
ESTD: 1962
Nagaon :: Assam

CATION MAP OF NORTH-EAST INDIA
Fig. 1: Location Map of the Study Area
Source: Authors' own work

III. OBJECTIVES OF THE STUDY

The major objectives of the present study are:

- To analyze the causes of inward migration to North-East India from other parts of the country.
- To find out the causes of outward migration from North-East India to other states/UTs of India.

IV. DATA BASE AND METHODOLOGY

In the contemporary period, the COVID-19 pandemic has created havoc across the globe. In this situation collection of field data is not possible. Thus this study is completely based on secondary sources of data. Data on migration of the study area are collected from the Census of India which is considered as one of the most reliable sources of population data. The collected data have been processed, analysed through quantitative techniques. Processed data are represented thorough simple cartograms. Conclusions of the study are merely based on the results derived from data analysis.

V. RESULTS AND DISCUSSION

Causes of Inward Migration to North-East India from Other Parts of India:

Migration is a response to the uneven distribution of opportunities over space. The place from where they move is called the place of origin and the place to which they move is called the place of destination. People tend to move from a place of low opportunity and low safety to a place of higher opportunity and better safety. Migration may either be voluntary or involuntary. Sometimes people are forced to move to a new place due to natural hazards, war etc. Causes of migration can broadly be categorised as pull factors and push factors. Less employment opportunities, low wages, lack of basic amenities, landlessness etc. act as push factors in rural areas. On the other hand, better employment opportunities, higher income, better wages act as pull factors towards the rural to urban migration (Sangappa, 2015).

As per place of birth; 5,91,212 people migrates to North-East India from the rest of the country in 2001. The number of in-migrants to this region from other states and Union Territories of India has slightly decreased to 5,90,939 which represents 1.31% of the total population of North-East India in the year 2011. On the other hand; the number of out-migrants from North-East India to other states and Union Territories of India was 6,91,234. But the number of out-migrants slightly falls to 5,10,353 in the year 2011. It is very important to analyze the reasons for the movement of people between the North-Eastern states and other parts of the country as it will be helpful in portraying the socio-economic conditions of the states of North-East India.

In this work, reasons for migration are categorized as employment and business, education, marriage, moved after birth, moved with households and others. For the sake of comparison; India has been divided into five regions viz. **1.North-India** comprising Jammu and Kashmir, Himachal Pradesh, Punjab, Uttaranchal, Haryana, Rajasthan, Delhi, Chandigarh, **2.West-India** comprising Gujarat, Maharashtra, Goa, Daman and Diu, Dadra and Nagar Haveli, Lakshadweep, **3.Central-India** comprising Chhattisgarh, Madhya Pradesh, Uttar Pradesh,**4. South-India** comprising Andhra Pradesh, Karnataka, Kerala, Tamil Nadu, Pondicherry, **5.East-India** comprising Bihar, Jharkhand, Orissa, Sikkim, West Bengal, Andaman and Nicobar Islands.

Table 1: Causes of Inward Migration to North-East India from Other Parts of India (as per Place of Last Residence), 2001.

Place of Origin	Causes (%)					
	Employment and Business	Education	Marriage	Moved after Birth	Moved with Household	Others
North-India	30.22	1.22	12.39	2.04	29.39	24.74
East-India	37.72	0.62	19.42	1.42	20.70	20.12
Central-India	32.17	0.97	15.02	1.45	27.34	23.05
West-India	18.36	1.69	6.74	2.03	34.60	36.58
South-India	33.11	1.27	10.54	1.92	27.66	25.5
[illegible]	35.45	0.79	17.27	1.54	23.29	21.67

Source: Migration Table D-3, Census of India, 2001

©2021 IJPPW. All rights reserved

Principal
Nowgong Girls' College
Nagaon :: Assam

Nowgong Girls' College ESTD: 1962 Nagaon :: Assam

In 2001, employment and business has emerged as the major causes of inter-state migration to North-East India. Around 35% of the total inter-state migrants have come to North-East India for the purpose of employment and business. Around 23% of the total inter-state migrants to North-East India have reported their reason for migration as moved with household. Around 22% of the inter-state migrants have stated 'others' as their reason for migration. It is followed by marriage. Around 17% of the total inter-state migration has come to this region due to marriage. Only a smaller portion of inter-state migrants (0.79%) have come to North-East India for educational purposes in 2001. Migrants from all parts of India except West-India; have come to North-East India mainly due to employment and business. East-India is the major source of migration to North-East India. Around 38% of the total migrants have come to this region for the purpose of employment and business. On the other hand; less than one-fifth of the migrants from West-India have reported their cause of migration as employment and business.

Table 2: Causes of Inward Migration to North-East India from Other Parts of India (as per Place of Last Residence), 2011

Place of Origin	Causes (%)					
	Employment and Business	Education	Marriage	Moved after Birth	Moved with Household	Others
North-India	27.82	1.59	18.25	2.77	25.62	23.92
East-India	37.15	0.81	25.40	1.68	19.82	15.14
Central-India	32.7	0.97	24.23	1.42	24.05	16.63
West-India	22.32	2.92	13.77	2.40	32.69	25.9
South-India	33.42	3.9	15.39	1.94	25.59	19.76
Total	35.29	1.06	24.30	1.69	21.04	16.62

Source: Migration Table D-3, Census of India, 2011

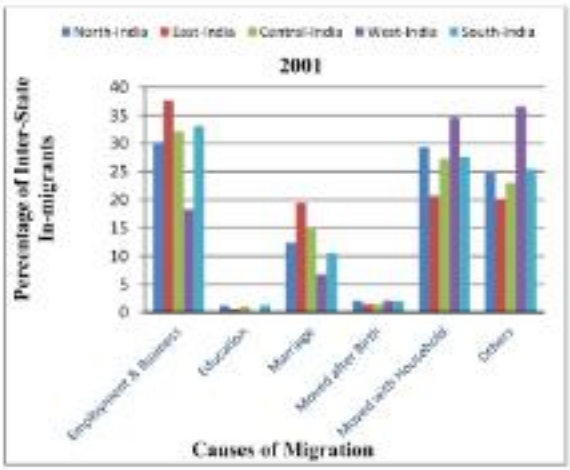

© 2022 All rights reserved

Principal
Nowgong Girls' College
Nagaon :: Assam

Nowgong Girls' College
ESTD: 1962
Nagaon :: Assam

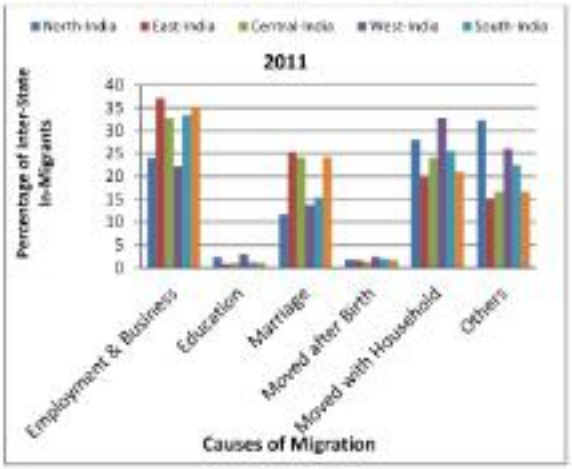

Fig. 2: Causes of Inward Migration to North-East India from Other Parts of India (as per Place of Last Residence), 2001 and 2011

Around 35% of the total inter-state migrants have come to North-East India for the purpose of employment and business in 2011. The second most important cause of inter-state migration to this region is marriage. Around 24% of the total inter-state migration has come to this reason due to marriage. Around 21% of the total inter-state migrants to this region have reported their reason for migration as moved with household. Around 17% of the inter-state migrants have stated 'others' as the reason for migration. Only a smaller portion of inter-state migrants (1.06%) have come to North-East India for educational purpose in the year 2011. It indicates the poor educational infrastructure and limited choice of education in North-East India. The major cause of migration from North-India, East-India, Central-India and South-India to this region is recorded as employment and business. More than one-fourth of the migrants from East-India have come to North-East India due to marriage. On the other hand; most of the migrants coming to North-East India from West-India have stated their cause of migration as moved with household.

4.2 Causes of Outward Migration from North-East India to Other Parts of India:

Table 3: Causes of Outward Migration From North-East India to Other Parts of India (as per Place of Last Residence), 2001.

Place of Destination	Causes (%)					
	Employment and Business	Education	Marriage	Movedafter Birth	Movedwith Household	Others
North-India	26.79	4.95	15.48	1.84	37.55	13.39
East-India	7.12	1.09	55.92	0.93	18.32	16.62
Central-India	9.45	1.91	52.74	0.64	16.94	18.32
West-India	30.67	11.65	7.46	2.67	37.12	10.43
South-India	22.02	16.36	8.09	3.08	28.67	21.78
Total	12.35	2.85	44.84	1.18	22.49	16.29

Source: Migration Table D-3, Census of India, 2001

The major cause of inter-state migration from North-East India to other parts of the country is marriage. Around 45% of the total inter-state migrants move to other parts of India from this region due to marriage. It is followed by moved with household. Reasons for migration of around 16% of the total out-migrants can be included in the category of others. Around 12% of the inter-state migrants from this region have moved to other parts of India for employment and business purposes. Less than 3% of the inter-state migrants have moved to other parts of India for educational purposes. Reasons for migration of around 1% of the total out-migrants can be included in the category of moved after birth in the year 2001.

Table 4: Causes of Outward Migration From North-East India to Other Parts of India (as p... Place of Last Residence), 2011.

© 2023 IJSDW. All rights reserved

Principal
Nowgong Girls' College
Nagaon :: Assam

Nowgong Girls' College
ESTD: 1962
Nagaon :: Assam

Place of Destination	Causes (%)					
	Employment and Business	Education	Marriage	Moved after Birth	Moved with Household	Others
North-India	24.46	6.30	17.65	1.95	34.82	14.82
East-India	13.94	1.69	32.41	2.61	30.77	18.58
Central-India	18.68	5.38	28.11	1.34	33.00	13.49
West-India	42.49	6.76	8.06	2.41	26.08	14.2
South-India	42.50	14.67	5.50	1.84	19.31	16.18
Total	23.64	5.30	22.56	2.23	29.75	16.52

Source: Migration Table D-3, Census of India, 2011

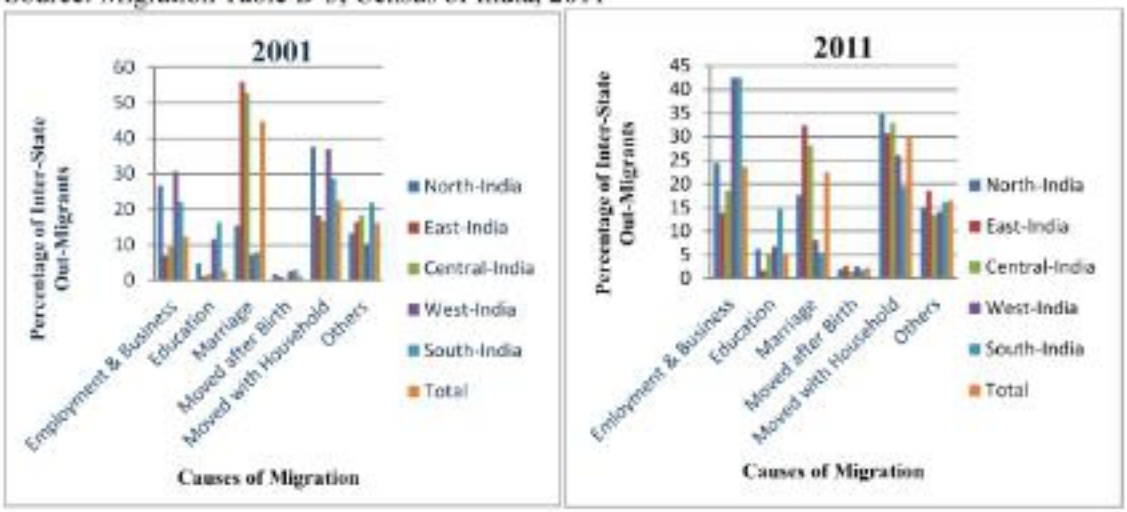

Fig. 3: Causes of Outward Migration From North-East India to Other Parts of India (as per Place of Last Residence), 2001 and 2011

The dominant cause of inter-state migration from North-East India to other parts of the country has shifted to 'moved with household' from marriage in the year 2011 as shown in table. The second most important cause of inter-state out-migration from his region is recorded as employment and business. Around 24% of the total inter-state out-migration from this region has moved to other parts of the country due to employment and business purpose. Marriage is the third important cause of inter-state out-migration from North-East India. Causes of migration of around 17% of the total inter-state out-migrants have been included in the category of others. The movement of people from this region to other parts of India for the purpose of education is very less (5.30%) in the year 2011 (Table 4).

VI. CONCLUSION

This work aims to analyse the causes of migration between the states of North-East India and other parts of the country. The major cause of inter-state migration to North-East India is recorded as employment (work) and business. Around 35% of the total inter-state migrants have come to North-East India for the purpose of employment and business in 2011 and majority of them are from the states of East India. Marriage is another significant reason for inter-state migration to North-East India. The major cause of inter-state outward migration from North-East India to other parts of the country is recorded as marriage in 2001. Around 45% of the total inter-state migrants move to other parts of India from this region due to marriage. The dominant cause of inter-state migration from North-East India to other parts of the country has shifted to 'moved with household' from marriage in the year 2011. The region receives only 1.06% of the inter-state in-migrants coming duo to educational purposes. It indicates the poor level of development in the educational sector of North-East India. On the other hand, around 12% of total inter-state out-migrants of the region moved to the rest of India for work-related purposes in 2001. It has increased to around 24% in the year 2011 indicating the alarming picture of unemployment in North-East India.

REFERENCES

© 2021 JPPW. All rights reserved

Principal
Nowgong Girls' College
Nagaon :: Assam

Nowgong Girls' College
ESTD: 1962
Nagaon :: Assam

1. Bernard, A., Bell, M. and Charles-Edwards, E. (2014). Life-course transitions and the age
2. profile of internal migration. *Population and Development Review*, Vol. 40, pp. 213- 239.
3. Bhagat, R. B. (2018). *Migration Situation in North-east India Citation : R . Lusome and R . B . Bhagat (2010) " Migration D . W . Bansod and Lekha Subaiya (eds) Population , Gender and Health in India : methods , Processes and Policies , Academic Foundation , New Delhi , 2, July*.
4. Bhagat, R., Keshri, K., & Ansary, R. (2018). Internal Migration in India: Intensity, Flows and Impact. *Migration Letters*, *15*(July 2018), 347–360.
5. Bhati, R. K. (2015). A study of Rural To Urban Migration In India. *ASM's International E-Journal on Ongoing Research in Management and IT, January 2015*, 371–379. Devi, P. (2017). Analysis of Factors Affecting Internal Migration in India. *Amity Journal of Economics*, *1*(2), 2017.
6. Gogoi, J. K., Goswami, H., & Borah, K. C. (2009). *Project report on Problems of border areas in North East India : implications for the Thirteenth Finance Commission*. 376 p.
7. Lingam, L. (1998). Locating women in migration studies: An overview. *Indian Journal of Social Work*, *59*(3), 723–727.
8. Lusome, R., & Bhagat, R. B. (2020). Migration in Northeast India: Inflows, Outflows and Reverse Flows during Pandemic. *Indian Journal of Labour Economics*, *63*(4), 1125–1141.
9. Mahapatro, S. (2010). Patterns and determinants of female migration in India : insights from census. *Working Papers*, 19.
10. Mahapatro, S. (2013). Contemporary Patterns & Issues of Internal Migration in India: Evidence from NSSO. *Journal of Chemical Information and Modeling*, *53*(9), 1689–1699.
11. Peneder, M., & Resch, A. (2021). Causes and consequences. *Schumpeter's Venture Money*, 246–262.
12. Sali Rajakumar Sangappa, & Shanta. B. Astig. (2015). Causes and Consequences of Migration in India: a Sociological Perspective. *Golden Research Thoughts*, *4*(7), 1–7.
13. Singh, H. (2016). Increasing rural to urban migration in India: A challenge or an opportunity. *International Journal of Applied Research*, *2*(4), 447–450.

© 2021 JPPW. All rights reserved

Principal
Nowgong Girls' College
Nagaon :: Assam

Nowgong Girls' College ESTD: 1962 Nagaon :: Assam